frontiers | Research Topics

Nitrogen use efficiency: Plant biology to crop improvement

Edited by
Nandula Raghuram, Surya Kant and Fabien Chardon

Published in
Frontiers in Plant Science

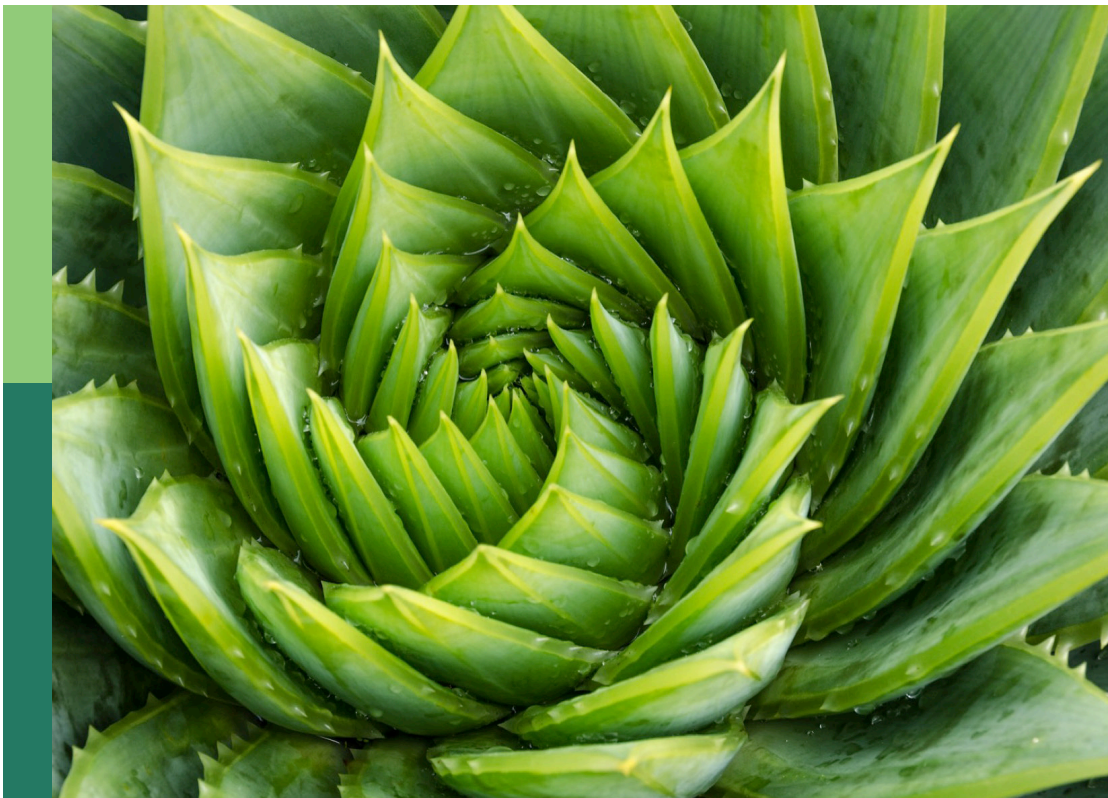

ISSN 1664-8714
ISBN 978-2-8325-5222-3
DOI 10.3389/978-2-8325-5222-3

About Frontiers

Frontiers is more than just an open access publisher of scholarly articles: it is a pioneering approach to the world of academia, radically improving the way scholarly research is managed. The grand vision of Frontiers is a world where all people have an equal opportunity to seek, share and generate knowledge. Frontiers provides immediate and permanent online open access to all its publications, but this alone is not enough to realize our grand goals.

Frontiers journal series

The Frontiers journal series is a multi-tier and interdisciplinary set of open-access, online journals, promising a paradigm shift from the current review, selection and dissemination processes in academic publishing. All Frontiers journals are driven by researchers for researchers; therefore, they constitute a service to the scholarly community. At the same time, the *Frontiers journal series* operates on a revolutionary invention, the tiered publishing system, initially addressing specific communities of scholars, and gradually climbing up to broader public understanding, thus serving the interests of the lay society, too.

Dedication to quality

Each Frontiers article is a landmark of the highest quality, thanks to genuinely collaborative interactions between authors and review editors, who include some of the world's best academicians. Research must be certified by peers before entering a stream of knowledge that may eventually reach the public - and shape society; therefore, Frontiers only applies the most rigorous and unbiased reviews. Frontiers revolutionizes research publishing by freely delivering the most outstanding research, evaluated with no bias from both the academic and social point of view. By applying the most advanced information technologies, Frontiers is catapulting scholarly publishing into a new generation.

What are Frontiers Research Topics?

Frontiers Research Topics are very popular trademarks of the *Frontiers journals series*: they are collections of at least ten articles, all centered on a particular subject. With their unique mix of varied contributions from Original Research to Review Articles, Frontiers Research Topics unify the most influential researchers, the latest key findings and historical advances in a hot research area.

Find out more on how to host your own Frontiers Research Topic or contribute to one as an author by contacting the Frontiers editorial office: frontiersin.org/about/contact

Nitrogen use efficiency: Plant biology to crop improvement

Topic editors

Nandula Raghuram — Guru Gobind Singh Indraprastha University, India
Surya Kant — La Trobe University, Australia
Fabien Chardon — Université Paris-Saclay, France

Citation

Raghuram, N., Kant, S., Chardon, F., eds. (2024). *Nitrogen use efficiency: Plant biology to crop improvement*. Lausanne: Frontiers Media SA.
doi: 10.3389/978-2-8325-5222-3

Table of contents

frontiers in Plant Science

ORIGINAL RESEARCH
published: 04 February 2022
doi: 10.3389/fpls.2021.807798

Genotypic Variation of Nitrogen Use Efficiency and Amino Acid Metabolism in Barley

*Bérengère Decouard[1†], Marlène Bailly[1†], Martine Rigault[1], Anne Marmagne[1], Mustapha Arkoun[2], Fabienne Soulay[1], José Caïus[3,4], Christine Paysant-Le Roux[3,4], Said Louahlia[5], Cédric Jacquard[6], Qassim Esmaeel[6], Fabien Chardon[1], Céline Masclaux-Daubresse[1] and Alia Dellagi[1]**

[1] Université Paris-Saclay, INRAE, AgroParisTech, Institut Jean-Pierre Bourgin (IJPB), Versailles, France, [2] Agro Innovation International - Laboratoire Nutrition Végétale, TIMAC AGRO International SAS, Saint Malo, France, [3] Université Paris-Saclay, CNRS, INRAE, University of Évry Val d'Essonne, Institute of Plant Sciences Paris-Saclay (IPS2), Orsay, France, [4] Université de Paris, CNRS, INRAE, Institute of Plant Sciences Paris-Saclay (IPS2), Orsay, France, [5] Natural Resources and Environment Lab, Faculté Polydisciplinaire de Taza, Université Sidi Mohamed Ben Abdellah, Taza, Morocco, [6] Université de Reims Champagne Ardenne, RIBP EA 4707 USC INRAE 1488, SFR Condorcet FR CNRS 3417, Reims, France

OPEN ACCESS

Edited by:
Li-Qing Chen,
University of Illinois at Urbana-Champaign, United States

Reviewed by:
Shengguan Cai,
Zhejiang University, China
Yong Han,
Department of Primary Industries and Regional Development of Western Australia (DPIRD), Australia

***Correspondence:**
Alia Dellagi
dellagi@agroparistech.fr

† These authors have contributed equally to this work

Specialty section:
This article was submitted to Plant Physiology, a section of the journal Frontiers in Plant Science

Received: *02 November 2021*
Accepted: *02 December 2021*
Published: *04 February 2022*

Citation:
Decouard B, Bailly M, Rigault M, Marmagne A, Arkoun M, Soulay F, Caïus J, Paysant-Le Roux C, Louahlia S, Jacquard C, Esmaeel Q, Chardon F, Masclaux-Daubresse C and Dellagi A (2022) Genotypic Variation of Nitrogen Use Efficiency and Amino Acid Metabolism in Barley. Front. Plant Sci. 12:807798. doi: 10.3389/fpls.2021.807798

Owing to the large genetic diversity of barley and its resilience under harsh environments, this crop is of great value for agroecological transition and the need for reduction of nitrogen (N) fertilizers inputs. In the present work, we investigated the diversity of a North African barley genotype collection in terms of growth under limiting N (LN) or ample N (HN) supply and in terms of physiological traits including amino acid content in young seedlings. We identified a Moroccan variety, Laanaceur, accumulating five times more lysine in its leaves than the others under both N nutritional regimes. Physiological characterization of the barley collection showed the genetic diversity of barley adaptation strategies to LN and highlighted a genotype x environment interaction. In all genotypes, N limitation resulted in global biomass reduction, an increase in C concentration, and a higher resource allocation to the roots, indicating that this organ undergoes important adaptive metabolic activity. The most important diversity concerned leaf nitrogen use efficiency (LNUE), root nitrogen use efficiency (RNUE), root nitrogen uptake efficiency (RNUpE), and leaf nitrogen uptake efficiency (LNUpE). Using LNUE as a target trait reflecting barley capacity to deal with N limitation, this trait was positively correlated with plant nitrogen uptake efficiency (PNUpE) and RNUpE. Based on the LNUE trait, we determined three classes showing high, moderate, or low tolerance to N limitation. The transcriptomic approach showed that signaling, ionic transport, immunity, and stress response were the major functions affected by N supply. A candidate gene encoding the HvNRT2.10 transporter was commonly up-regulated under LN in the three barley genotypes investigated. Genes encoding key enzymes required for lysine biosynthesis in plants, dihydrodipicolinate synthase (DHPS) and the catabolic enzyme, the bifunctional Lys-ketoglutarate reductase/saccharopine dehydrogenase are up-regulated in Laanaceur and likely account for a hyperaccumulation of lysine in this genotype. Our work provides key physiological markers of North African barley response to low N availability in the early developmental stages.

Keywords: NUE (nitrogen use efficiency), crop/stress physiology, barley, natural variability, lysine (amino acids)

INTRODUCTION

Barley is a staple crop known for its great adaptability to harsh environments. It was one of the first domesticated crops and is the fourth most productive cereal crop after rice, wheat, and maize (FAOSTAT). Barley (*Hordeum vulgare* L.) shows a very large genetic diversity and is grown under a large array of environmental and soil conditions with areas of production at high altitudes and latitudes as well as in desert regions (Ryan and Sommer, 2012; Muñoz-Amatriaín et al., 2014; Dawson et al., 2015).

Barley is mainly used for animal feed, human consumption, and malting. Today, barley is gaining value in the field of nutrition, not only for its original flavor but also for its nutritional value especially because of its high content in β-glucans and low gluten (Baik and Ullrich, 2008; Chutimanitsakun et al., 2013). Barley is considered for several benefits to human health, such as reduction of blood cholesterol and glucose levels as well as weight loss by increased satiety, control of heart disease, and type-2 diabetes (Baik and Ullrich, 2008). In some parts of the world, such as Ethiopia, North Africa, and Asia, it is used in human food more frequently than in the rest of the world (Baik and Ullrich, 2008).

Mediterranean climate and soils impose drastic constraints on agriculture. Barley is one of the best-adapted species to the Mediterranean conditions (Pswarayi et al., 2008). Climate change and the growing Mediterranean population will further increase environmental constraints on barley culture in a near future (Cammarano et al., 2019). Fortunately, barley shows great potential for biomass production under Mediterranean climates. As is the case for most cereals, barley yields are strongly dependent on nitrogen fertilization (Oscarsson et al., 1998; Sedlář et al., 2011; Stupar et al., 2017). Importantly, nitrogen fertilization impacts plant tolerance to abiotic and biotic stresses (Fagard et al., 2014; Abid et al., 2016; Mur et al., 2017; Ding et al., 2018; Verly et al., 2020). The genetic diversity in terms of barley tolerance to nitrogen starvation has been explored (Oscarsson et al., 1998; Górny, 2001; Sinebo et al., 2004; Quan et al., 2016, 2019; Karunarathne et al., 2020). However few data are available concerning the diversity of molecular responses of barley to nitrogen limitation (Møller et al., 2011; Quan et al., 2016, 2019; Karunarathne et al., 2020, 2021).

World agriculture benefited from unprecedented changes in agronomic practices during the "Green Revolution" due to technological progress after Second World War. Major crop yields doubled per capita over a 50 year period in some regions of the world, such as Asia and South America (Lassaletta et al., 2016; Pretty, 2018). During that period, new crop varieties were bred, and inorganic fertilizers and chemically synthesized pesticides and herbicides were produced and used. Their application was combined with the modernization of agricultural machinery (Lassaletta et al., 2016; Pretty, 2018). In particular, it is estimated that the use of synthetic inorganic nitrogen (N) fertilizers has increased 8- during the last 50 years (Lassaletta et al., 2016; Pretty, 2018). Nowadays, the industrial Haber-Bosch process uses 1–2% of the world's fossil-fuel energy output for the synthesis of ammonia that is the basis for the production of the other N fertilizers as nitrate salts, ammonium-nitrate, and urea (Chen et al., 2018). However, because crops do not take up more than 30–50% of the N available in the soil (Wang et al., 2018), the extensive use of N fertilizers caused major detriments to ecosystems and animal health (Schlesinger, 2009; Withers et al., 2014).

In the context of a growing population and shrinking farmlands, cereals yields and nutritional quality is fundamental because cereal grains provide 60% of the food necessary to feed the world population, either directly as part of the human diet or indirectly as animal feed (Hirel et al., 2007; Lafiandra et al., 2014; Landberg et al., 2019). Nitrogen is one of the key elements that determine plant growth and yield formation (Hirel et al., 2007; Masclaux-Daubresse et al., 2010). It is thus essential to optimize N use efficiency (NUE) in crops. NUE is most commonly defined as the grain or biomass yields obtained per unit of available N in the soil (Xu et al., 2012; Han et al., 2015; Li et al., 2017; Hawkesford and Griffiths, 2019). Nitrogen uptake refers to processes involved in the acquisition of nitrogen compounds from the soil. Nitrogen assimilation refers to processes associated with the N utilization and N metabolism that transform inorganic nitrogen into organic nitrogen *in planta*. Nitrogen remobilization refers to processes associated with the recycling and reuse of organic nitrogen within the plant and its transfer from organs to organs. Nitrogen uptake, assimilation, and remobilization contribute to plant NUE (Hirel et al., 2007; Lea and Miflin, 2018) that can be also estimated considering the three components that are N uptake efficiency (NupE), N utilization efficiency (NutE), and nitrogen remobilization efficiency (NRE) (Han et al., 2015; Li et al., 2017).

Nitrogen (N) is present in the soil in the form of nitrate (NO_3^-), ammonium (NH_4^+), or amino acids, with their availability depending upon physical factors, such as pH and temperature. Most plants adapted to alkaline pH in aerobic soils, which is the case for most arable lands, use mostly NO_3^- as their N source (Hirel et al., 2007; Masclaux-Daubresse et al., 2010; O'Brien et al., 2016; Xu, 2018). Nitrate is taken up by the roots and then transported in the plant via plasma membrane located transporters that are either low-affinity transporters (LATs) or high-affinity transporters (HATs) (Léran et al., 2014; O'Brien et al., 2016; Kant, 2018; Wang et al., 2018; Zhang et al., 2018). Following uptake, NO_3^- is reduced to nitrite (NO_2^-) by the cytosolic enzyme nitrate reductase (NR). Then, NO_2^- is further reduced to ammonium by the plastid nitrite reductase (NiR). Ammonium derived from direct uptake or NO_3^- reduction is finally incorporated into amino acids *via* the combined activity of the two enzymes glutamine synthase (GS) and glutamate synthase (GOGAT) (Masclaux-Daubresse et al., 2010; Wang et al., 2018; Hirel and Krapp, 2020).

Although barley is a major crop requiring N fertilization in poor soils, such as those of North Africa, and despite functional and evolutionary genomics tools developed on this species, little is known about the diversity of physiological and molecular mechanisms in barley responses to N limitation.

In the present work, we investigated the diversity of a collection of north African barley genotypes in terms of growth under limiting N conditions and in terms of N nutrition physiological traits related to N nutrition including amino acid content that led to the identification of a barley genotype

accumulating five times more lysine than the others. To gain further insight into the molecular mechanisms involved in barley adaptation to N limitation, a transcriptomics approach revealed that N supply has an impact on ionic transport, signaling, stress responses, and immunity. We identified candidate genes controlling N deficiency response and lysine biosynthesis in barley.

MATERIALS AND METHODS

Plant Material and Growth Conditions

The origin of barley genotypes is indicated in **Table 1**. Seeds were provided by M. Bennaceur from the National Gene Bank of Tunisia and by Université Sidi Mohamed Ben Abdellah. The barley North African collection used in this study contains nine Moroccan genotypes that correspond to commercialized varieties (herein named M1 to M9), one Tunisian variety (herein named T6), and one Egyptian variety (herein named E6) **Table 1**. The North African barley collection used in this study displays different characteristics in particular, with regard to their yield and tolerance to drought (Hellal et al., 2019) and it was recently described for its response to Cd (Ayachi et al., 2021). The European cultivar Golden Promise (herein named GP), which is a reference genotype since its genome is fully sequenced and for which Agrobacterium-mediated transformation is possible (Schreiber et al., 2020), was included in the analyses as a reference line. Seeds were surface-sterilized then sown on the sand under long days 16 h day (23°C)/8 h night (18°C). They were watered three times a week with the same nutrient solution containing either 0.5 mM nitrate (Low N, LN) or 5 mM ample nitrate (High N, HN). Reducing tenfold nitrate concentration involves necessarily compensation of counterion changes. Although this is not a perfect method, there is no other way for that and

TABLE 1 | Names and characteristics of the barley collection genotypes used in this study.

Code in this work	Official name	Country of origin	References describing the genotype	Row type	Spring/ winter type	Hulled/ hulless	Earliness of maturity (Badraoui et al., 2009; Noaman et al., 2007; Mlaouhi et al., 2020; Saidi et al., 2005)	Disease resistance (Badraoui et al., 2009; Noaman et al., 2007; Saidi et al., 2005)	Year of release
M1	Adrar	Morocco	Hellal et al., 2019	2 rows	Spring type	Hulled	Medium type	Resistant to powdery mildew, susceptible to Rhynchosporium, moderately resistant to rust	1998
M2	Taffa	Morocco	Hellal et al., 2019	6 rows	Winter type	Hulled	Medium type	Moderately resistant to powder mildew and rust; susceptible to Rhynchosporium	1994
M3	Massine	Morocco	Hellal et al., 2019	6 rows	Winter type	Hulled	Medium type	Moderately resistant to powdery mildew and yellow rust, susceptible to Rhynchosporium and moderately susceptible to brown rust	1994
M4	Laannaceur	Morocco	Hellal et al., 2019	6 rows	Winter type	Hulled	Medium type	Moderately susceptible to powdery mildew and Rhynchosporium, susceptible to rust	1991
M5	Oussama	Morocco	Hellal et al., 2019	6 rows	Winter type	Hulled	Medium type	Susceptible to powdery mildew and Rhynchosporium, susceptible to yellow and brown rust	1995
M6	Firdaws	Morocco	Hellal et al., 2019	6 rows	Winter type	Hulled	Medium type	Resistant to powdery mildew	1998
M7	Tamellalt	Morocco	Hellal et al., 2019	2 rows	Spring type	Hulled	Medium type	Moderately susceptible to powdery mildew, susceptible to Rhynchosporium, moderately resistant to yellow and brown rust	1984
M8	Amalou	Morocco	Hellal et al., 2019	6 rows	Winter type	Hulled	Early type	Moderately resistant to powdery mildew, susceptible to Rhynchosporium, moderately resistant to yellow and brown rust	1997
M9	Amira	Morocco	Hellal et al., 2019	6 rows	Winter type	Hulled	Medium type	Resistant to powdery mildew, susceptible to Rhynchosporium and rust	1996
T6	Manel	Tunisia	Ben Naceur et al., 2012	6 rows	Spring type	Hulled	Early type	Moderately resistant to powdery mildew and Rhynchosporium, moderately resistant to net blotch	1996
E6	Giza 2000	Egypt	Ben Naceur et al., 2012	6 rows	Spring type	Hulled	Early type	Moderately resistant to leaf Rust. Resistant to powdery mildew and net blotch	2003
GP	Golden Promise	Europe	Avila-Ospina et al., 2015	2 rows	Spring type	Hulled	Early type	Susceptible to net blotch and powdery mildew	1968

most care was taken to design the mineral composition of the nutritional solution so that there is no other major deficiency or toxicity. Most importantly, the K levels are not limiting both under LN and HN (Epstein et al., 1963; Gierth and Mäser, 2007; Genies et al., 2021). Watering was applied by sub-irrigation of the pots and maintained for 2 h before nutritive solutions were discarded. The nutrient solution composition is described in **Supplementary Table 1**. Plants were harvested 14 days after sowing by separating shoot and root which were weighed separately. The experiments were performed four times with eight plants in each biological replicate.

Determination of Nitrate Uptake Into the Shoots and Roots Using ^{15}N Labeling During 24 h

To determine ^{15}N uptake over 24 h before harvesting, thus on day 13 after sowing, a ^{15}N labeling was performed. On day 13 after sowing, the unlabeled watering solution was replaced by a ^{15}N-containing solution that had the same nutrient composition as the Low N and High N solutions except that the natural $^{14}NO_3^-$ was replaced by nitrate with 10% $^{15}NO_3^-$ enrichment (w/w). All the pots were watered for 24 h, using an equal volume of labeled solutions. Cutting the shoots stopped ^{15}N uptake in the shoots. Roots were extracted from sand and carefully rinsed before freezing in liquid nitrogen. Shoot and root tissues were harvested, weighed for fresh weight quantification, then ground in liquid nitrogen and stored at -80°C for further experiments.

Dry weight was calculated based on the weight of lyophilized tissues for amino acid analysis (see below). This allowed the calculation of the percentage of dry matter in each sample.

Quantification of Total Nitrogen, Total Carbon, and ^{15}N Enrichment

The experiment dried again 50 mg of ground frozen plant material before weighting 5,000 μg of dry material in tin capsules to determine the total N and C concentrations using the FLASH 2000 Organic Elemental Analyzer (Thermo Fisher Scientific Villebon, France) and the ^{15}N enrichment using the Delta V Advantage isotope ratio mass spectrometer (Thermo Fisher Scientific, France). The data obtained are N% (g of N per 100 g of DW), C% (g of C per 100 g of DW), and A% (Atom percent) that represent the^{15}N enrichment in the sample [^{15}N/(total N)]. Since the natural ^{15}N abundance in N labeled samples was 0.3663 (A% control), specific enrichments due to the ^{15}N uptake were calculated as E% = (A% - 0.3363).

Amino Acid Analysis

For amino acid determination, 10 mg of lyophilized dry matter was extracted with a solution containing 400 μl of MeOH and 0.25 nmol/μl of Norvaline, which was used as the internal standard (Sigma Aldrich, St. Louis, MO, United States). The extract was stirred for 15 min, and it was then re-suspended with 200 μl of chloroform (agitation for 5 min) and 400 μl of double-distilled water (ddH_2O). After centrifugation (12,000 rpm, 10°C, 5 min), the supernatant was recovered, evaporated, and dissolved in 100 μl of ddH_2O. Derivatization was performed using an Ultra Derivatization Kit AccQ tag (Waters Corp, Milford, MA, United States), following the protocol of the manufacturer (Waters Corp, Milford, MA, United States). The amino acid profile was determined by ultra-performance liquid chromatography coupled with a photodiode array detector (UPLC/PDA) H-Class system (Waters Corp, Milford, MA, United States) with an ethylene bridge hybrid (BEH) C18 100 × 2.1 mm column (pore size: 1.7 μm).

Plant Growth and N Nutrition Trait Indicators

The plant phenotypic traits and indicators were measured or calculated based on the formula detailed in **Supplementary Table 2**.

Inoculum Preparation and Pathogen Infection

For each of the three barley cultivars M4, M5, and GP, seeds were sown at a rate of 10 seeds/pot in plastic pots 7 cm in diameter filled with 300 g of sand. They were watered three times a week with either LN or HN solutions. Plants were grown in a growth chamber (Aralab) at 23°C under white fluorescent light (130 μmol m^{-2} s^{-1}), with a 14- and 10-h photoperiod and 80% relative humidity as previously described by Backes et al. (2021b). A detached leave assay was carried out to evaluate the susceptibility of the three genotypes to the pathogen *Pyrenophora teres*. For each condition, 30 plants were inoculated and recorded. Three independent biological replicates were performed. Briefly, leaves of 10-day-old barley plants were excised and placed on Petri dishes containing 1% of agar. Leaves were then injured with a wooden pick and then a volume of 10 μl of suspensions containing *P. teres* spores at a concentration of 10^5 spores/mL was deposited at the leaf wound area. The incidences of net blotch disease symptoms, represented by the presence of necrosis on barley leaves, were recorded at 10 days post-infection.

RNA-Seq Analysis

Furthermore, three independent biological replicates were produced. Leaves were collected on plants at three leaf developmental growth stages corresponding to 14 days after sowing, cultivated in two conditions, LN or HN. Each sample is composed of the leaf (tissue) of 1–2 plants. Total RNA was extracted using the Nucleosol extraction kit according to the supplier's instructions and was further purified using the RNA Clean & Concentrator Kits (Zymo Research®, California, United States). RNA-seq libraries were constructed by the POPS platform (IPS2) using the TruSeq Stranded mRNA library prep kit (Illumina®, California, United States) according to the supplier's instructions. The libraries were sequenced in Single end (SE) mode with 75 bases for each read on a NextSeq500 to generate between 5 and 62 million SE reads per sample.

Adapter sequences and bases with a Q-Score below 20 were trimmed out from reads using Trimmomatic (version 0.36; Bolger et al., 2014) and reads shorter than 30 bases after trimming were discarded. Reads corresponding to rRNA sequences were removed using sortMeRNA (version 2.1; Kopylova et al., 2012)

against the silva-bac-16s-id90, silva-bac-23s-id98, silva-euk-18s-id95, and silva-euk-28s-id98 databases.

Filtered reads were then mapped and counted using STAR (version 2.7.3a; Dobin et al., 2013) with the following parameters –alignIntronMin 5 –alignIntronMax 60000 –outSAMprimaryFlag AllBestScore –outFilterMultimapScoreRange 0 –outFilterMultimapNmax 20 on the Hordeum_vulgare.IBSC_v2.48.gtf and its associated GTF annotation file.

Between 76.28 and 77.7% of the reads were associated with annotated genes (a mean of 76.9, 76.6, and 76.7%, respectively for GP, M4, and M5 barley cultivars). Statistical analysis was performed with Wilcoxon's test (**Supplementary Figure 7**). When comparing the percentages of assigned read samples per cultivar, the difference between the means is not statistically significant. The three cultivars mapped similarly onto Morex reference. Morex reference has a higher version (v2) than GP reference (v1). The reference annotation should be better for Morex.

A gene is analyzed if it is present at more than 1 read per million in several samples greater than or equal to the minimum number of replicates. The resulting raw count matrix was fed into edgeR (Robinson et al., 2010) for differential expression testing by fitting a negative binomial generalized log-linear model (GLM) including a condition factor and a replicate factor to the TMM-normalized read counts for each gene. We performed pairwise comparisons of each of the depleted conditions to the control condition. The distribution of the resulting *p*-values followed the quality criterion described by Rigaill et al. (2018). Genes with an adjusted *p*-value (FDR; Benjamini and Hochberg, 1995) below 0.05 were considered as differentially expressed.

Statistical Analysis

Analysis of variance followed by Tukey's honestly significant difference (HSD) test, as well as two-sample *t*-tests, were used in this study. All statistical analyses were performed using the free software environment R Version 4.0.2.1. The least-square means were calculated using the R package emmeans.

RESULTS

Global Trends of the Impact of Nitrogen Nutrition on Barley Physiological Traits

Although barley is commonly grown in North Africa, little is known about the mechanisms involved in its tolerance to low N availability, a common feature in this cultivation area. Global changes for N nutrition physiological indicators in the barley species were determined depending on nitrogen availability by considering the entire barley collection (**Table 2**). Nitrogen limitation resulted in the reduction of plant DW mainly due to a decrease in leaf DW. By contrast, root DW was higher under LN compared to HN, which globally resulted in a decrease of the shoot/root ratio (SR) under LN. As expected, barley nitrogen concentration was strongly reduced under LN irrespective of a plant organ. In contrast, carbon concentration was higher under LN. As expected, the global trend of the collection indicates that nitrogen uptake efficiencies (LNUpE, RNUpE, and PNUpE) were lower under LN in both shoots and roots, certainly due to the fact that nitrate was less available under LN. The biomass produced per unit of N reflects nitrogen use efficiency (NUE) in plants at the vegetative stage. As such NUE, in our case, can be calculated as the ratio between biomass and N concentration (Chardon et al., 2010). As expected, NUE was higher under LN than under HN. It is interesting to notice that leaf NUE (LNUE) was slightly lower under N limitation than under HN, while root NUE (RNUE) was sharply higher under LN than HN (**Table 2**). Partitioning of dry matter and N was different under LN and HN. Dry matter and N partitioning in roots, RP%DW and RP%N, respectively, were higher under LN than under HN (**Table 2**), thus reflecting the fact that shoot/root was decreased under LN relative to HN. Similarly, under LN, nitrogen was taken up more efficiently to the roots than to the shoots. This is illustrated by

TABLE 2 | Comparison of global trends of physiological traits within the barley collection under HN and LN.

Short-name	Trait name and unit	HN	*> or *<	LN
PDW	Plant dry weight (mg/plant)	78.18	ns	59.47
LDW	Leaf dry weight (mg/plant)	58.57	*>	39.56
RDW	Root dry weight (mg/plant)	19.07	*<	19.82
PN%	Nitrogen concentration in the whole plant (gN/100 gDW)	5.17	*>	3.32
LN%	Nitrogen concentration in shoot (gN/100 gDW)	5.67	*>	3.83
RN%	Nitrogen concentration in root (gN/100 gDW)	3.69	*>	2.32
PC%	Carbon concentration in the whole plant (gC/100 gDW)	35.2	*<	37.19
LC%	Carbon concentration in shoot (gC/100 gDW)	35.92	*<	37.85
RC%	Carbon concentration in root (gC/100 gDW)	32.99	*<	36.28
PNUE	Plant NUE (mg DW/%N)	15.3	*<	16.9
LNUE	Leaf NUE (mg DW/%N)	10.72	*>	9.92
RNUE	Root NUE (mg DW/%N)	5.38	*<	7.33
PNUpE	Plant N uptake efficiency mg ^{15}N/100 mg DW	4.11	*>	3.63
LNUpE	Leaf N uptake efficiency mg ^{15}N/ 100 mg DW	3.77	*>	3.26
RNUpE	Root N uptake efficiency mg ^{15}N/100 mg DW	4.92	*>	4.46
LP%DW	Biomass partitioning in shoot	0.75	*>	0.67
RP%DW	Biomass partitioning in root	0.25	*<	0.33
SR	Shoot DW to root DW ratio	3.08	*>	1.96
LP%N	Nitrogen partitioning in shoot	0.83	*>	0.75
RP%N	Nitrogen partitioning in root	0.17	*<	0.25
LP%15N	^{15}N partitioning in shoot	0.7	*>	0.6
RP%15N	^{15}N partitioning in root	0.3	*<	0.4
PNUp	Plant N uptake (Total _Nitrogen.Uptake) (mg ^{15}N per plant/h)	4.11	*>	3.62

*HN and LN indicate the mean of the considered trait over the whole individuals of the collection under high or low N, respectively. *> or *< indicates that the mean is significantly different between HN and LN, t student $p < 0.05$.*
SE, standard error for the variable over the whole individuals of the collection; ns, non-significant.

the higher partitioning of ^{15}N in roots (RP%15N) under LN compared to HN (**Table 2**).

Altogether these data indicate that barley responds to nitrogen limitation by a global biomass reduction, an increase in C concentration, and a higher resource allocation (DW, N, and C) to the roots.

Exploring Natural Variation for N and C Management Within the Barley Collection

To determine the effect of genotype (G) and N nutrition on the nitrogen-related physiological indicators, a three-way ANOVA was applied. We also checked the interaction between these factors (GXN) and the effect of biological replicates (E). ANOVA results in concerned traits related to (i) biomass and elemental (C, N) distribution in aerial parts and roots presented in **Table 3A**; (ii) plant capacity to take up and use N for biomass production (**Table 3B**); (iii) relative partitioning of biomass, C and N between leaves and roots (**Table 3C**).

These data show that nitrate nutrition significantly affects all traits except root dry weight.

The genotypic effect was also significant for most physiological traits, except the shoot/root (SR) ratio. Interestingly, the N-uptake (PNUp) and NUE (LNUE and PNUE) related traits are more impacted by the genotype effect than by the nutrition effect, as indicated by the sum of squares for the genotype effect which is larger than that of the nutrition effect (**Table 3**). Thus, in barley,

TABLE 3 | Level of significance of the variance sources for biomass and C and N concentrations in barley cultivated under limiting or ample nitrate.

A:	**Level of significance**									**Sum of squares**								
	LDW	**RDW**	**PDW**	**LN%**	**RN%**	**PN%**	**LC%**	**RC%**	**PC%**	**LDW**	**RDW**	**PDW**	**LN%**	**RN%**	**PN%**	**LC%**	**RC%**	**PC%**
G	***	***	***	***	**	***	***	***	***	25.0	29.1	23.4	2.1	3.0	1.0	3.8	9.0	6.5
N	***		***	***	***	***	***	***	***	**40.9**	0.6	29.1	**82.4**	**58.7**	**76.7**	**77.5**	29.5	**50.2**
E	***	***	***	***	***	***	***	***	***	7.9	8.4	8.5	5.5	12.0	10.7	1.5	6.4	6.4
GXN	***	***	***	***		***	***	*		8.0	13.4	3.8	2.1	1.2	1.1	3.0	5.0	1.6
GXE	**		***	**		***	***		**	4.6	10.5	7.7	1.4	3.8	1.9	6.2	7.0	8.6
NXE			***	***	***	***		***	***	0.3	0.8	1.8	2.6	2.9	4.1	0.1	4.3	4.7
GXNXE	*		***	*		*				3.5	6.6	7.4	1.0	2.1	1.0	1.0	5.9	3.1
R										9.8	**30.6**	18.2	2.9	16.4	3.4	6.9	**32.9**	18.9

B:	**Level of significance**							**Sum of squares**						
	LNUE	**RNUE**	**PNUE**	**LNUpE**	**RNUpE**	**PNUpE**	**PNUp**	**LNUE**	**RNUE**	**PNUE**	**LNUpE**	**RNUpE**	**PNUpE**	**PNUp**
G	***	***	***	***	***	***	***	**40.0**	14.1	**33.2**	15.1	14.8	12.8	**23.7**
N	***	***	***	***	***	***	***	2.6	12.0	5.8	9.1	3.8	3.5	23.1
E	***	***	***	***	***	***	***	2.7	19.0	4.2	20.9	21.5	**32.7**	14.5
GXN	***		**	**	**		**	12.6	3.5	6.1	4.9	7.3	3.0	3.0
GXE	**	*	*	**			**	8.7	9.7	10.1	10.1	4.6	5.4	6.5
NXE	*	***	**	***	***	***	***	1.4	4.4	2.5	8.3	7.0	9.7	4.2
GXNXE	***	*	**	**			***	11.4	9.3	10.3	9.5	8.7	7.1	8.3
R								20.6	**28.0**	27.8	**22.0**	**32.4**	25.8	16.6

C:	**Level of significance**							**Sum of squares**						
	LP%DW	**RP%DW**	**SR**	**LP%N**	**RP%N**	**LP%15N**	**RP%15N**	**LP%DW**	**RP%DW**	**SR**	**LP%N**	**RP%N**	**LP%15N**	**RP%15N**
G	**	***		***	***	***	***	5.0	6.1	2.1	5.4	5.8	7.0	6.8
N	***	***	***	***	***	***	***	**32.1**	**37.1**	**41.9**	**51.9**	**52.2**	**50.4**	**54.0**
E	***	***	***	***	***	***	***	14.9	15.8	24.1	8.4	8.7	4.4	3.5
GXN	**	***	***	***	***	***	***	5.3	6.0	3.9	4.7	4.6	6.0	6.6
GXE	*							9.0	5.6	4.7	5.9	6.1	4.7	4.3
NXE		**		***	***	**	**	1.2	1.7	0.8	2.6	2.2	1.9	2.1
GXNXE	*	*						6.7	6.1	5.1	2.7	3.0	3.0	3.2
R								25.8	21.5	17.5	18.3	17.4	22.5	19.5

G, N, and E stand for the following factors respectively: "Barley genotype," "N nutrition," and "experiment replicate." The significance of the interaction between these factors is indicated as follows GXN, NXE, GXE, and GXNXE. R: residuals. The highest sum of squares for each trait is in bold. Three-way ANOVA was applied to the data set. Sub-tables represent A: biomasses, C and N content; B: Nitrogen uptake and use efficiency, C: partitioning of biomass, C and N.

**Significant at 0.05 probability level.*

***Significant at 0.01 probability level.*

****Significant at 0.001 probability level.*

NUE can be improved via breeding since the genetic factor plays a significant role in this trait.

The genotypic by nutrition (GxN) interaction effect is significant for several traits for which the plant response to the nutrition depends on the genotype (**Table 3**). For example, the total N uptake (PNUp) is higher under HN than LN for all genotypes and we can clearly distinguish two groups of genotypes with different PNUp under HN and LN. The GP, M2, M4, M9, T6 genotypes exhibit the lowest PNUp scores whereas the PNUp of M1, M3, M5, M6, M7, M8, and E6 reached higher scores (**Figure 1A**). The clustering of these genotypes follows the same trend for leaf DW (LDW) but only under HN (**Figure 1B**) indicating that these traits are correlated as shown in **Supplementary Figure 1**. For plant NUE (PNUE), it is not possible to cluster genotypes in different groups. We can notice five genotypes (GP, M6, M8), showing similar PNUE values under HN and LN, while all the others present lower PNUE under HN than LN (**Figure 1C**). This suggests that for the five genotypes mentioned above, low N does not affect NUE. Last, for root N partitioning (RP%N), all genotypes show lower values under HN than under LN, but the T6 genotype clearly behaves as an outlier with significantly lower RP%N under LN compared to other accessions (**Figure 1D**).

These four examples illustrate the diversity of the pattern of GxN responses in the barley collection. Thus, depending on the trait we observe, nutrition may cause different modifications according to the genotypes. Interestingly, GP, M6, and M8 are resilient for PNUE whatever the N supply.

Deciphering Groups of Barley Genotype Displaying Similar GxN Responses to N Supply

To compare the traits between the barley genotypes and determine common patterns shared within the collection under LN and HN, a hierarchical clustering analysis (HCA) was applied to key physiological variables. This allowed us to identify the traits that displayed the most conserved trends and those that showed the highest variation among the genotypes. Genotypes presenting similar profiles could then be clustered (**Figure 2**).

Clustering clearly separated the two nutritional conditions (clusters A and B) indicating that nitrate supply is the main factor affecting barley physiological traits. Several traits displayed opposite trends in LN and HN for the whole barley collection. This clustering shows that most traits related to the roots reached higher values under LN than under HN, and the

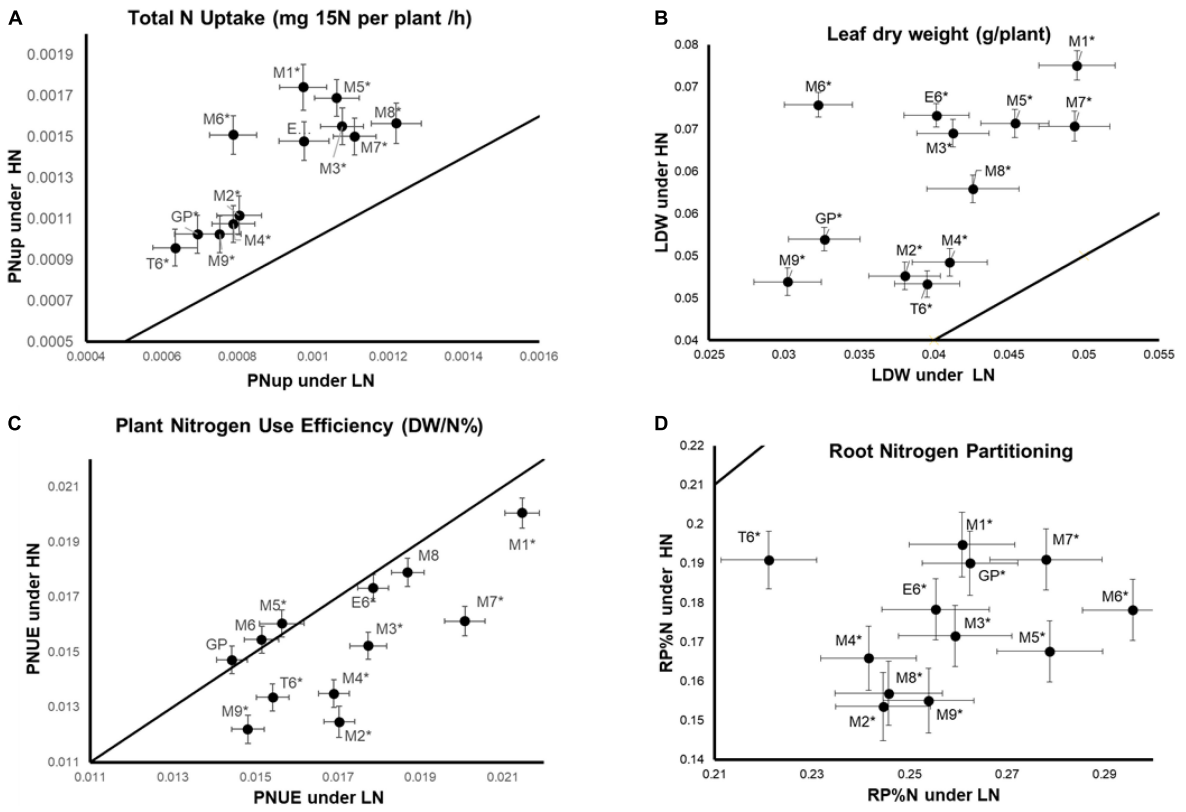

FIGURE 1 | Different genotypes by N supply interactions within the barley North African collection. Plants were grown for 14 days under LN or HN then leaves and roots were harvested separately and frozen under liquid nitrogen. The physiological parameters were measured as indicated in the "Materials and Methods" section. Traits displaying GXN interactions are illustrated by different GXN patterns. **(A)** Total plant N uptake (PNUpE). **(B)** Leaf dry weight (LDW). **(C)** Plant nitrogen use efficiency (PNUE). **(D)** Root nitrogen partitioning (RP%N). Mean values under HN are plotted against mean values under LN. Four independent experiments were performed. Stars indicate a significant difference between LN and HN (Student's test, $13 \leq n \leq 16$, $p < 0.05$). Bars represent SE.

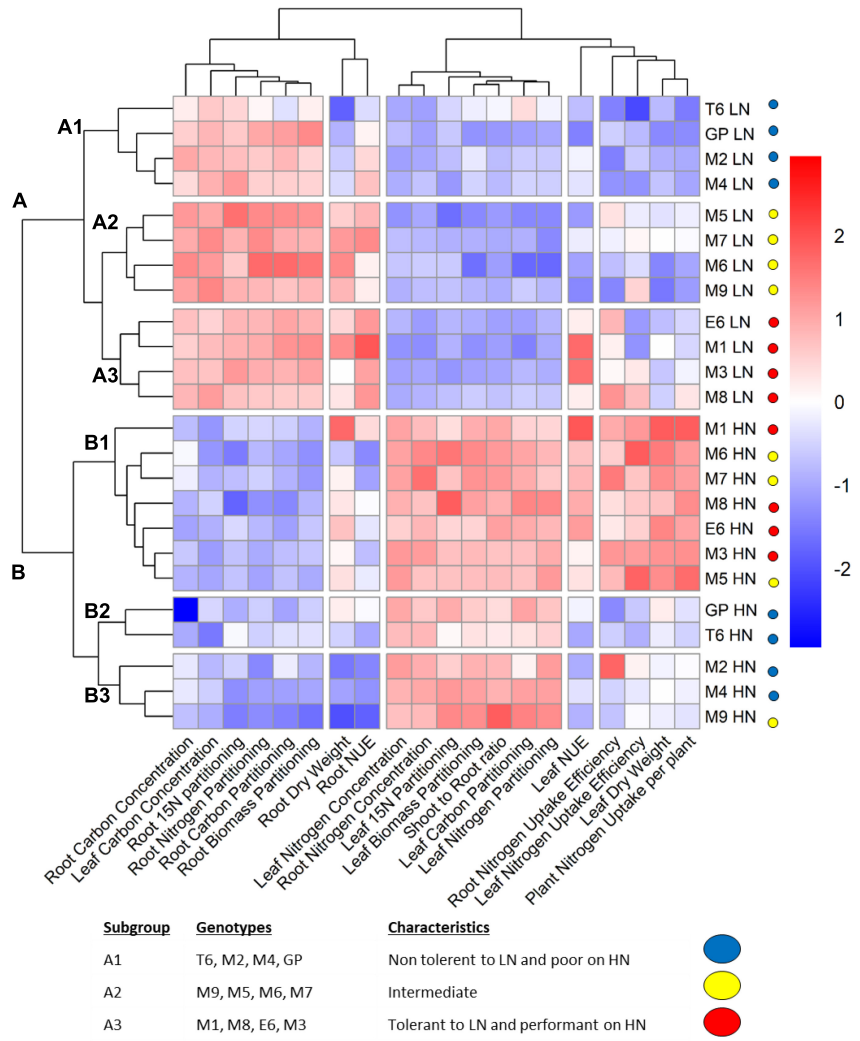

FIGURE 2 | Hierarchical clustering analysis (HCA) showing groups of genotypes sharing similar physiological traits. Plants were grown for 14 days under LN or HN then leaves and roots were harvested separately and frozen under liquid nitrogen. The physiological parameters were measured as indicated in the "Materials and Methods" section. The color scale is based on the value of the normalized mean for each trait. Normalization was made for the LN and HN conditions separately. The clustering under LN was chosen to determine three subgroups (A1, A2, and A3) labeled with the indicated colors. HCA was constructed with the R package.

opposite is observed for the shoots. Interestingly, the traits that displayed genetic variation among the collection and reflected different responses to nitrate supply of the barley genotypes are essentially related to N uptake (leaf and root nitrogen uptake efficiency and total nitrogen uptake), leaf and root DW, and nitrogen use efficiency (leaf and root NUE) (**Figure 2**).

Under low N conditions (cluster A), genotypes are distributed into three groups. The A3 group is clearly the most efficient because it displays the best leaf NUE amongst the entire collection. The A3 genotypes have a bigger root system and higher root N uptake efficiency than the others. The A1 group is the less efficient based on leaf NUE which coincided with lower total N uptake per plant, lower leaf dry weight as well as lower leaf and root N uptake efficiencies. The A2 group displays intermediate characteristics with reduced capacity to use nitrogen resources to produce biomass. Indeed, what clearly distinguishes A2 from A3 is the leaf NUE.

Data from A group (plants under LN) highlight the different strategies of barley genotypes to deal with limiting nitrate as previously suspected from ANOVA (**Figure 2** and **Supplementary Figure 2**). In the most performant genotypes (A3 group), the highest leaf NUE is associated with the highest root nitrogen uptake efficiency, root biomass, and root NUE. Taken together, the data from barley grown under low nitrate show that performance in N use is linked to high root biomass and high N uptake.

Under the HN condition (cluster B), three groups, B1, B2, and B3, display different behaviors. The B1 genotypes are characterized by high leaf and root N uptake, high leaf NUE, and higher leaf and root DW. These B1 genotypes are more

performant than the others for nitrogen uptake, translocation, and assimilation; they efficiently use their N resources to produce biomass. The B2 and B3 genotypes are less performant. Indeed, in contrast with B1 genotypes, they exhibit lower N uptake, lower leaf NUE, and lower root dry weight. It is then interesting to focus on what distinguishes B2 from B3. In the B2 group, root biomass is more important than in the B3 group. However, in B2, N uptake in the root is lower than in B3, and as a consequence, there is a lack of N uptake in the shoots that display *per se* low leaf NUE. Then, B3 seems more performant than B2 since, with less root biomass, it can take up nitrogen more efficiently in both root and shoot. Taken together, data from the B group (plants under HN) highlight the different strategies developed by plants to use nitrate when it is not limiting. Performance for N utilization in the shoot is linked to larger roots and higher plant N uptake capacity. Some genotypes (M2, M4, M9) are able to fine-tune their leaf NUE with reduced root biomass.

Interestingly, genotypes with poor performance under LN (sub-cluster A1) also displayed poor performance under HN (B2/B3), and genotypes with high performances under LN (sub-cluster A3) also kept high performances under HN (B1). With the exception of GP and M9, all the other intermediate genotypes from sub-cluster A2 performed relatively better under HN indicating that these genotypes are less tolerant to low nitrate availability than the others. The A1 sub-cluster contains the T6, GP, M2, and M4 genotypes. Interestingly, M2 and M4 belong to B3 and GP and T6 to B2, indicating that they are poorly performant under both LN and HN.

We were able to identify four genotypes M1, M8, E6, and M3 that displayed good performance in both LN and HN. Genotypes that perform poorly under both LN and HN are T6, M2, and M4 due to their reduced root biomass and low N uptake.

Taken together, our data indicate that an increase in the root nitrogen sink strength and of global C content are the most conserved responses to nitrogen limitation among the studied genotypes. The most heterogeneous responses are related to N uptake efficiency and NUE, which highlight different metabolic adaptation strategies to N limitation. Dissecting the molecular mechanisms building such a diversity deserves further attention for a better comprehension of the genetic diversity of plant strategies for adaptation to nitrate limitation.

Diversity of Amino Acid Concentrations in the Barley Collection Grown Under Low or Ample N Supply

Nitrogen metabolism is strictly related to amino acid composition, which can play diverse roles in plant physiology and tolerance to stress (Rai, 2002; Zeier, 2013; Galili et al., 2016). Thus, to better characterize the nitrogen metabolism in the barley collection, amino acid concentrations were determined in leaves and roots under LN and HN using HPLC.

As expected, total free amino acid concentration was significantly higher under HN than under LN in both shoot and root (**Supplementary Figure 3**). To know how amino acid distribution between aerial parts and roots is controlled in response to N supply, we compared total amino acid contents in leaves and roots for each genotype. All the genotypes accumulated higher amounts of amino acids in shoot than root under LN except M3 (**Figure 3A**). The contrast between root and shoot was less important under ample N supply and only four genotypes (GP, M1, M2, M8) contained significantly higher amounts of amino acids under HN.

Since amino acids have different roles in plant metabolism (Häusler et al., 2014), we investigated the influence of N supply on the concentration of individual amino acids. The relative proportion of each amino acid was calculated as % of total amino acids. Globally, the percentages of individual amino acids depended on the organ and the N nutrition (**Figure 3B**). For instance, in both shoot and root, accumulations of GABA branched-chain amino acids (BCAA: isoleucine, leucine, valine), phenylalanine, serine, tyrosine, and lysine under N limitation was paralleled with a decrease of the percentage of glutamine and threonine. Aspartate and glutamate percentage was also decreased under LN but only in leaves.

Hierarchical clustering based on the relative proportions of individual amino acids was performed independently for the shoot (**Figure 4A**) and root (**Figure 4B**). In leaves, clustering clearly separated LN and HN. In the root, there was no HN or LN-dependent clustering.

Interestingly, HCA facilitated the identification of two genotypes (M4 and T6) that did not cluster with any other genotype irrespective of nutrition or organs (**Figure 4**). The M4 genotype indeed accumulated five times more lysine in shoot than any other genotype, irrespective of N conditions (**Figure 4C**). Under low N, M4 also displayed higher proportions of branched-chain amino acids (isoleucine, leucine, and valine) and proline in shoots compared to all the other genotypes (**Figure 4A** and **Supplementary Figure 4**). Under high N, in addition to lysine, proportions of glutamine, isoleucine, and leucine were also higher in the M4 shoot compared to other genotypes (**Figure 4A** and **Supplementary Figure 5**). The percentage of glutamate and aspartate in the M4 shoot were among the lowest irrespective of N nutrition. Interestingly, the M4 genotype displayed an early senescing phenotype on leaves 12 days after sowing under LN (**Figure 4D**) that may explain the special amino acid profile of this barley genotype.

The T6 genotype was also quite different from others. It exhibited low glutamate and aspartate percentage in shoot under LN and higher isoleucine, phenylalanine, proline, and leucine percentages (**Figure 4A** and **Supplementary Figure 3**). In the root, T6 is characterized by a higher percentage for most of the minor amino acids except lysine and aspartate under HN (**Figure 4B** and **Supplementary Figure 4**). Under LN, the T6 root did not distinguish itself from other genotypes. The most prominent amino acid feature of T6 is a higher percentage of serine and proline.

Clustering of the barley genotypes according to their amino acid profiles in roots or leaves (**Figure 4**) was different from clustering based on physiological traits (**Figure 2**). This suggests

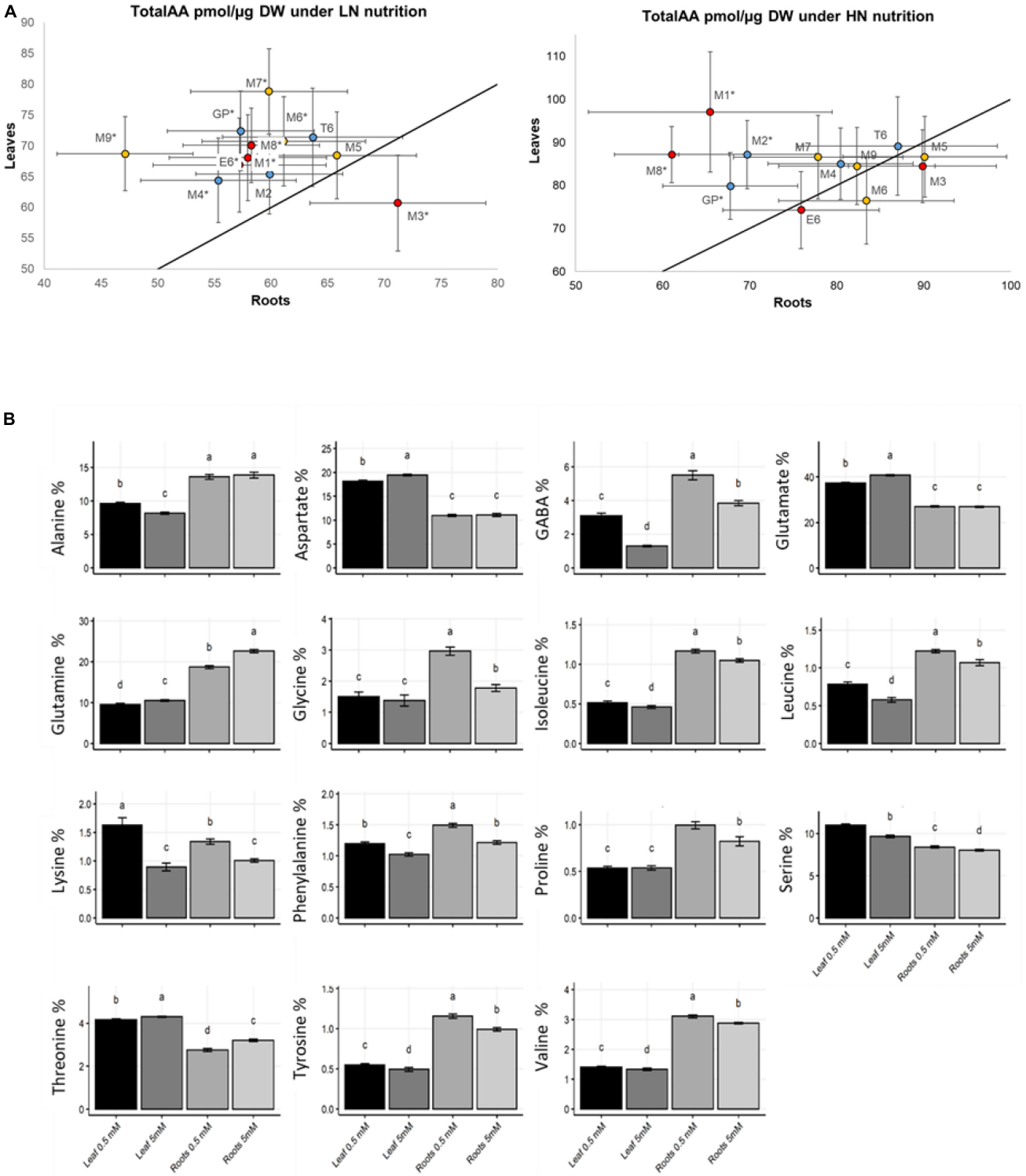

FIGURE 3 | Amino acid distribution in barley leaves and roots under LN and HN. Plants were grown for 14 days under LN or HN then leaves and roots were harvested separately and frozen under liquid nitrogen. Following freezing in liquid nitrogen, AA were quantified by HPLC as indicated in the "Material and Methods." **(A)** Comparison of total amino acids levels in leaves were plotted against levels in roots of barley genotypes under LN and HN as indicated. The strait line represents the Y = X curve. Bars represent SE. Stars indicate a significant difference between LN and HN for each barley genotype (Student's test, $13 \leq n \leq 16$, $p < 0.05$). Colors of the dots correspond to the classes defined in **Figure 1**. **(B)** Individual amino acid % in the barley collection under LN or HN. Four independent experiments were performed. Stars indicate significant difference between LN and HN (Student's test, $13 \leq n \leq 16$, $p < 0.05$). Bars represent SE.

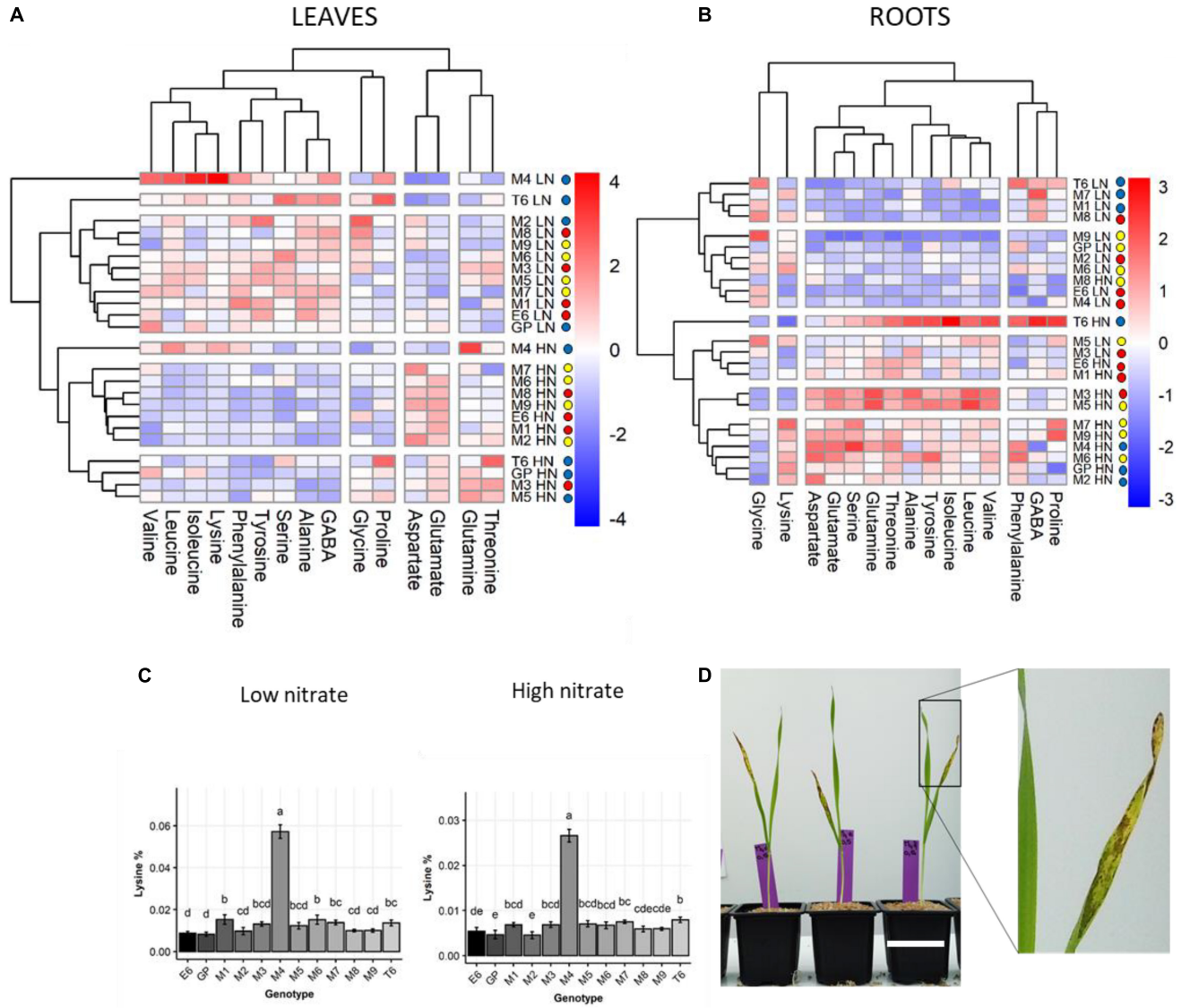

FIGURE 4 | Genetic diversity of amino acid composition in barley leaves and roots under LN and HN. Plants were grown for 14 days under LN or HN then leaves and roots were harvested separately and frozen under liquid nitrogen. The following freezing in liquid nitrogen AA was quantified by HPLC as indicated in the Material and methods. **(A,B)** Hierarchical clustering analysis of the amino acid % under LN or HN in leaves and roots, respectively, showing genotypes sharing similar amino acid profiles. The color scale is based on the value of the normalized mean for each trait. Normalization was made for the LN and HN conditions separately. The colored circles in front of each genotype label represent the above-mentioned group A, B, C in **Figure 2**. HCA was constructed with the R package. **(C)** Level of lysine in leaves of each genotype under HN or LN. The different letters indicate values significantly different at $P < 0.05$ as determined using R-ANOVA Newman–Keuls (SNK) comparisons. **(D)** Picture showing the senescing phenotype of M4 leaves under LN. An enlargement of the senescing leaf is shown on the right. White scale bar = 5 cm.

complex relationships between N assimilation and amino acid homeostasis.

Transcriptional Changes in Limiting N Relative to Ample N Conditions

To further characterize the molecular processes taking place in barley in response to nitrate limitation, an RNAseq transcriptomic approach was undertaken on leaves of three barley genotypes displaying different physiological responses to N supply: GP, M4, and M5. This approach is aimed at identifying genes that are related to barley adaptation to nitrate limitation. The rationale behind the choice of these three genotypes was the following. First, the M4 genotype displays very poor adaptation to low N with early senescing leaves under LN while the M5 genotype had intermediate N adaptation traits under LN with high leaf and root N uptake efficiencies and leaf and root biomass under LN as shown in HCA (**Figures 2**, **4**). The GP genotype was included since it is one of the most used genotypes in barley genomics studies. In addition, the poor response of GP PNUE to

N availability is a shared feature with M5 (**Figure 1**). Significant GO overrepresented functions encoded by genes differentially expressed in the three genotypes were found to be related to stress responses, defense, signaling, and cytoskeleton remodeling (**Figure 5**). The differential regulation of defense-related genes prompted us to test the impact of N on barley tolerance to *Pyrenophora teres* Drechsler (anamorph *Drechslera teres*) one of the major pathogens affecting barley especially in Morocco (Jebbouj and El Yousfi, 2009; Backes et al., 2021a). Disease severity was higher under HN compared to LN in M5 and GP (**Supplementary Figure 6**).

In order to determine genes differentially expressed in the three genotypes and that could be candidate markers for nitrate limitation, we looked for genes commonly regulated in the three genotypes in LN vs. HN. There were no common genes with similar expression profiles in the three genotypes. However, 12 genes were up-regulated both in GP and M4 (**Supplementary Table 4**). They encode functions related to senescence, stress response, and ionic transport. Interestingly, the nitrate transporter encoding gene annotated *HvNRT2.10* (HORVUHr098550 orthologous to *AtNRT2.7*) is up-regulated in GP and M4. Although not statistically significant, we could observe an up-regulation of this gene in M5 LN compared to HN with a *p*-value close to the level of significance ($p = 0.06$). These data suggest that *HvNRT2.10* is commonly up-regulated in the three genotypes further supporting this gene as a candidate involved in nitrate nutrition under N limitation. Six genes were found to be commonly down-regulated in GP and M5, three of them encode transcription factors, and the three others encode iron-containing proteins (**Supplementary Table 5**).

Together, these data indicate that functions related to stress, immunity, signaling, senescence, and ionic transport are affected by N limitation in barley.

Genotypic Diversity of Barley Transcriptome Supports Amino-Acid Profiles

Since we found that lysine was highly accumulated in M4 leaves compared to the other genotypes, we investigated genes involved in the lysine metabolic pathway in the transcriptome of M4 compared to the two other genotypes M5 and GP. For this purpose, the transcriptomic profile of M4 was compared to the average of the transcript levels of each gene in GP and M5 (hereafter referred to as "GP+M5") under HN because of the variance of the transcriptome under HN was lower than under LN (data not shown). Lysine is synthesized through a branch of the Asp family pathway. The first reactions leading to lysine biosynthesis (Jander and Joshi, 2009) are catalyzed by aspartate kinase, dihydrodipicolinate synthase, and reductase. At least eight genes putatively involved in lysine biosynthesis, degradation, and transport were differentially expressed in M4 compared to M5+GP. Two genes encoding putative dihydrodipicolinate reductase (*HORVU1Hr1G078290* and *HORVU7Hr1G117980*) are up-regulated in M4 and a third one putatively encoding the same enzyme (*HORVU4Hr1G086020*) was down-regulated (**Figure 6**). A gene encoding a putative aspartate kinase (*HORVU7Hr1G085930*) and three genes encoding putative lysine histidine transporter 1 (*HORVU2Hr1G123160*, *HORVU7Hr1G074640*, and *HORVU7Hr1G074660*) were

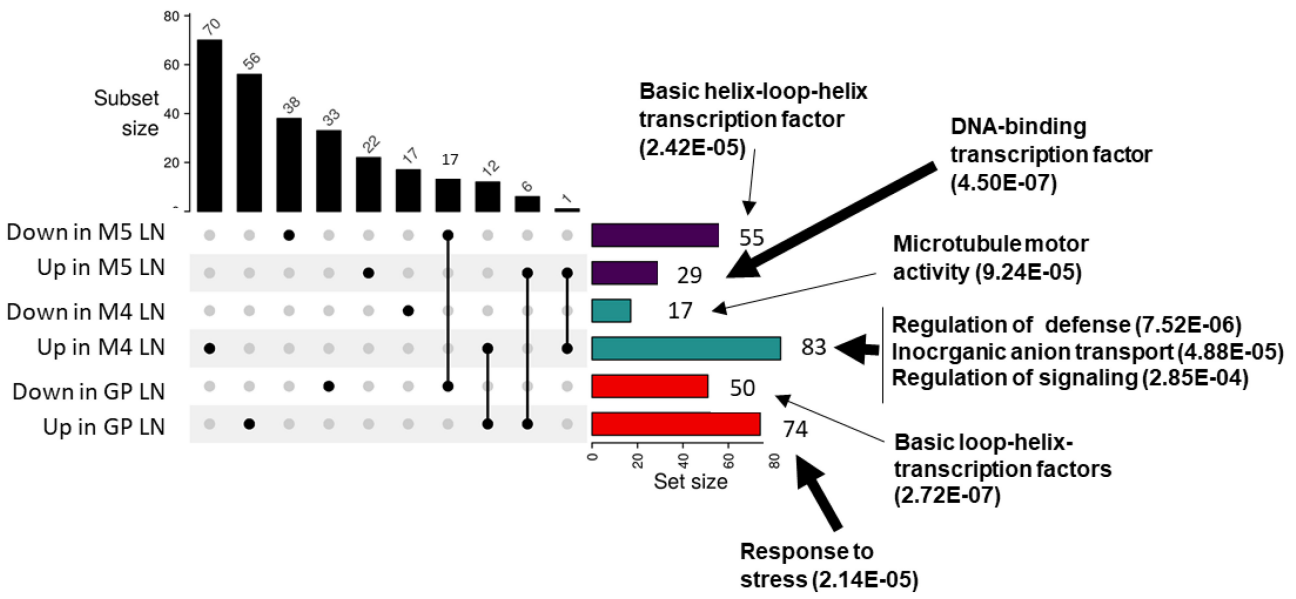

FIGURE 5 | Differentially regulated genes under LN and HN in GP, M4, and M5. Plants were grown for 14 days under LN or HN then leaves were frozen under liquid nitrogen. RNA was extracted from leaves and RNAseq was performed as indicated in "Materials and Methods" section. Upset plot for overlapping up and down differentially expressed genes in M4, M5, and GP barley genotypes under LN or HN. The number of genes in each category is indicated on top of each bar. Functional categories overrepresented in the set of genes are indicated next to the arrows (geneontology.org). Thick arrows indicate up-regulated genes, thin arrows indicate down-regulated genes.

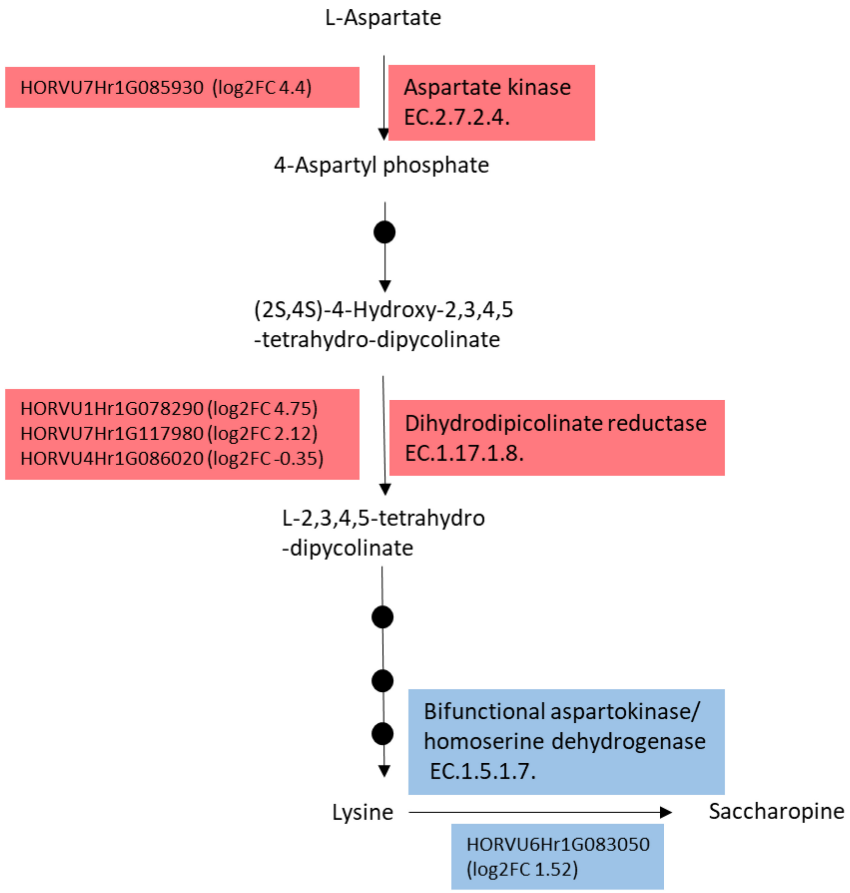

FIGURE 6 | Simplified Lysine biosynthesis and catabolism pathways were found to be differentially expressed in M4 compared to GP and M5. Genes encoding enzymes of these pathways are indicated with their accession numbers in front of the corresponding enzyme. For each gene, the log2 of the fold change (log2FC) corresponds to the expression in M4 compared to the mean of the gene expression level in M5 and GP. Red and blue boxes correspond to biosynthesis and catabolism of lysine, respectively. Black dots represent intermediate enzymatic steps that were omitted for simplification.

found to be up-regulated in M4 (see RNAseq data). In addition, a gene encoding the bifunctional Lys-ketoglutarate reductase/saccharopine dehydrogenase was found to be upregulated in M4 compared to GP+M5 (*HORVU61G083050*). In addition to lysine accumulation, M4 leaves accumulate higher levels of BCAA (leucine, isoleucine, and valine, **Figure 4** and **Supplementary Figures 4, 5**). Consistently, genes encoding three key steps involved in BCAA biosynthesis were found to be differentially expressed in M4 compared to GP+M5 as follows (Binder et al., 2007; Binder, 2010). The branched-chain amino acid transaminase encoding genes *HORVU2Hr1G096380*, *HORVU3Hr1G032400* are upregulated in M4 by a log2 fold change (log2 FC) of 1 and 1.4, respectively. The threonine aldolase encoding genes *HORVU2Hr1G097910* and *HORVU4Hr1G085690* are down-regulated in M4 by a log2 FC of -.53 and -.6, while *HORVU1Hr1G046630* is up-regulated by a log2 FC of 1.26. The isopropylmalate dehydrogenase encoding genes *HORVU2Hr1G124400*, *HORVU3Hr1G059060*, *HORVU3Hr1G000570* are up-regulated in M4 by a log2 FC of 0.35, 3.35, and 0.54, respectively while *HORVU7Hr1G066450* is down-regulated in M4 by a log2 FC of -6.58.

Thus, transcriptomic data are consistent with the M4 phenotype and its amino acid composition profile.

DISCUSSION

Owing to the large genetic diversity of barley and its resilience under harsh environments, this crop is of great value for agroecological transition under global change and the need for reduction of nitrogen fertilizers inputs. Barley culture in north Africa is mainly performed under rainfall conditions and nitrogen input is a limiting factor to the same extent as water availability (Ryan et al., 2008; Ryan and Sommer, 2012). Indeed, North African soils are calcareous with low organic matter content thus requiring N fertilization (Ryan and Sommer, 2012). However, for economic and environmental reasons, it is crucial to improve the management of N fertilization. Therefore, it is crucial to characterize the Mediterranean varieties with respect to their adaptation to different nitrogen supplies. We worked on a panel of north African barley genotypes thus, adapting to the Mediterranean climate and environment.

Our goal was to focus on the response of these genotypes to low N and to decipher the diversity of their physiological and molecular responses to N supply at early stages of development. Here, we have considered that the most performant genotypes are those displaying higher leaf NUE under LN.

Traits affected by N supply at the level of the whole barley collection are an increase in C content in the whole plant and increased root biomass. Partitioning of root C, N, and biomass was increased in roots compared to leaves under LN. These are well-known responses of plants to LN and the major role of root in this response is well-known (Lea and Miflin, 2018; Sun X. et al., 2020). Interestingly, leaf carbon concentration was positively correlated with several root traits (root NUE, root ^{15}N partitioning, root carbon partitioning, and root biomass partitioning) (**Supplementary Figure 1**). Similarly, positive correlations were observed between leaf and root N uptake efficiencies indicating coordination of both processes. In addition, leaf biomass was positively correlated with plant nitrogen uptake and leaf NUE indicating an important role of N uptake and utilization in building the aerial biomass of barley plants (**Supplementary Figure 1**). Root allocation of C and N is generally observed as a general response to N deficiency (Zhang et al., 2007; Kobe et al., 2010; Krapp et al., 2011). Root DW was higher under LN compared to HN, which globally resulted in a decrease of the shoot/root ratio (SR) under LN, in good accordance with previous reports (Van Der Werf and Nagel, 1996; Lea and Azevedo, 2007). In contrast, carbon concentration was higher under LN which is consistent with the fact that under N deficiency, plants usually accumulate sugars, starch, or fructan (Wang et al., 2000; Lemaître et al., 2008). Here we verified that NUE was higher under LN than under HN which is a shared feature with other plant species (Chardon et al., 2010; Masclaux-Daubresse and Chardon, 2011; Lammerts van Bueren and Struik, 2017). Higher NUE in LN-grown plants is explained by the fact that low N supply results in a tradeoff that favors the use of metabolic resources to support growth and survival. Conversely, when nitrogen is not limiting, a proportion can be stored under the form of nitrate in vacuoles and is not directly metabolized. These data show that nitrate nutrition significantly affects all traits except root dry weight, in good accordance with the physiological responses to N limitation previously reported (Van Der Werf and Nagel, 1996; Lea and Azevedo, 2007). These data make sense since the capacity of larger root systems to better explore the soil allows a higher nitrate uptake and a more efficient translocation of inorganic nitrogen to the shoot available for growth and biomass production (Gastal and Lemaire, 2002).

Other traits display different variations depending on the barley genotype in response to nitrogen supply highlighting a GxN interaction: root development and nitrogen uptake processes. For instance, root dry weight increased under LN for some genotypes while it was lower under LN for other genotypes. Similar trends were observed for maize where LN affected shoot biomass negatively but had different impacts on root biomass indicating that root plasticity allows a reliable marker of adaptation to LN (Chun et al., 2005). Root growth under LN is known to be mainly due to increased auxin levels in the root but this may be counteracted by the action of other hormones mainly abscisic acid, ethylene, and cytokinin (Sakakibara et al., 2006; Sun X. et al., 2020). Thus, different root developments in the barley genotypes in response to N limitation may reflect different hormonal regulatory mechanisms. The diversity of physiological responses allowed us to classify the barley genotypes into three categories; tolerant, moderately tolerant, and poorly tolerant to LN based on their leaf NUE. Interestingly the two genotypes GP and T6 originating from Europe and Tunisia, respectively, exhibited lower root biomass under LN and low leaf NUE. It remains to be determined whether this classification is also observed in the field.

The investigation of the impact of N supply on the transcriptome of three barley genotypes led to the identification of a low number of differentially expressed genes compared to other studies (Comadira et al., 2015; Quan et al., 2019). Nevertheless, significant GO overrepresented functions encoded by genes differentially expressed in the three genotypes were found to be related to stress responses and to signaling (**Figure 5**). Down-regulated genes in M4 under LN were related to microtubule-binding motor protein suggesting a down-regulation of cell vesicular trafficking and/or an arrest in cell development. Signaling, ionic transport, and metal enzymes are common over-represented functional categories in our study and in the aforementioned transcriptomic analyses. The differential expression of genes related to defense in the RNAseq is in agreement with the observed impact of N supply on barley susceptibility to one of the major pathogens affecting barley especially in Morocco (Jebbouj and El Yousfi, 2009; Backes et al., 2021a). It is known that N nutrition can affect plant tolerance to pathogens but positive and negative correlations have been observed depending on the plant-pathogen interaction considered (Fagard et al., 2014; Mur et al., 2017; Sun Y. et al., 2020). In the case of the barley-*P. teres* interaction, N enhances susceptibility.

The low number of differentially expressed genes found in the present study may be due to the long-lasting stressful conditions experienced by the plants from seed sowing to harvest under LN. Indeed, at the time of harvest, i.e., 14 days after sowing, most of the metabolic processes may have been adjusted and stabilized under LN and HN. Among the genes found to be commonly up-regulated, the putative nitrate transporter coding gene *HvNRT2.10* (HORVUHrG098550) orthologous to the Arabidopsis *AtNRT2.7* gene, is of particular interest since it was found in a QTL mapping study as involved in barley tolerance to low N (Karunarathne et al., 2020). This gene is closely related to *OsNRT2.4* (Guo et al., 2020) which encodes a dual affinity nitrate transporter and was found to be involved in rice N nutrition although no phenotype was found for the knockout mutant (Wei et al., 2018). Further investigation of the function *of HvNRT2.10* in barley nitrogen nutrition deserves attention.

Nitrogen limitation altered amino acid composition in leaves and roots. The overall soluble amino acid concentration decreased under LN. While roots appeared as C and N metabolic sinks under LN for most genotypes, partitioning of soluble amino acids in roots varied depending on the genotype. Most genotypes concentrated amino acids in leaves under LN while this

partitioning was more diverse under HN suggesting variability for the role of amino acids in barley coping with N deficiency.

Interestingly, leaf amino acid composition was correlated with nitrogen supply. Indeed, we found that the profiles of amino acids under LN were strictly different from the profiles under HN. Thus, an important impact of nitrogen nutrition can be observed in the aerial part of the plant. Notwithstanding the nutritional effect, an important genetic diversity of relative amino acid composition was observed between barley genotypes.

Nitrate limitation resulted in elevated levels of the amino acids GABA, Tyr, Leu, Ileu, Val, Phe, Ser, Lys in roots and leaves of the barley plants. In addition to being vital components of proteins, these amino acids display additional properties, such as signaling, stress tolerance or provide precursors for other compounds. For instance, GABA is known to be involved in plant stress tolerance to biotic and abiotic stresses (Ramesh et al., 2017; Xu et al., 2021). More specifically, GABA was described as triggering a better N uptake under stress conditions, such as salt stress or N limitation (Chen et al., 2020; Khanna et al., 2021). BCAA (Leu, Ileu, Val) are known to accumulate in response to abiotic stresses presumably to serve as a substrate for biosynthesis of stress proteins (Joshi et al., 2010). They are also known to serve as substrates in the biosynthesis of lipids and glucosinolates (Binder et al., 2007). Tyrosine accumulation in barley genotypes in response to LN may be linked to the role of this amino acid as a precursor for several products that could be involved in response to low N, such a tocopherol providing an antioxidant effect, or electron carrier or defense compounds (Schenck and Maeda, 2018; Xu et al., 2020). Phenylalanine is the precursor of phenylpropanoids known to be involved in tolerance to biotic stresses (Lynch and Dudareva, 2020). Accumulation of stress-related amino acids is consistent with the RNAseq data showing enhanced stress response signatures in LN barley leaves compared to HN. Interestingly, serine accumulation is mainly produced via increased photorespiration rate which is known to be able to provide ammonia under nitrogen deficiency (Shi and Bloom, 2021).

The investigation of amino acid content in this barley collection revealed that M4 stood out with a high lysine content. Interestingly, lysine was part of the amino acids accumulating in all genotypes under LN but reached five times higher levels in M4. In another study investigating amino acid content in four barley varieties, the authors found diversity in the lysine content of grains (Jood and Singh, 2001). In maize, the opaque mutant was identified as accumulating 69% more lysine in its endosperm compared to the parental line (Mertz et al., 1964; Wang et al., 2019). Interestingly, lysine accumulation in the endosperm is related to reduced levels of endosperm proteins like alpha-zein in maize (Wang et al., 2019) and hordein in barley (Schmidt et al., 2015). The level of lysine in M4 grains was not higher than that of M5 or GP (data not shown).

Lysine biosynthetic and catabolic pathways were extensively studied in plants because this is amino acid cannot be synthesized by human or monogastric bodies and it is present in low amounts in cereals (Galili, 2002; Galili et al., 2016). The key enzymes required for its biosynthesis in plants have been identified: dihydrodipicolinate synthase (DHPS) and the catabolic enzyme bifunctional Lys-ketoglutarate reductase/saccharopine dehydrogenase (LKR/SDH) (Galili et al., 2016). To increase the level of lysine, several approaches using DHPS overexpression or down-regulation of LKR/SDH or both were successful (Galili et al., 2016). Mutant forms of DHPS from *Nicotiana sylvestris* protoplasts resulted in lysine accumulation due to the loss of DHPS negative feedback regulation by lysine (Negrutiu et al., 1984). Strikingly, M4 transcript levels of genes encoding the two limiting steps in lysine biosynthesis and turnover, DHPS and LKR/SDH, are up-regulated compared to M5 and GP, suggesting that these genes are responsible for high lysine levels in M4. Thus, the accumulation of lysine in M4 might be due to altered negative feedback regulation of the DHPS enzyme. In addition, BCAA (leucine, isoleucine, and valine) accumulate to higher levels in M4 in agreement with the upregulation in the genotype M4 of genes encoding key enzymes involved in the biosynthesis of BCAA, the branched-chain amino acid transaminase, and the isopropylmalate dehydrogenase (Binder et al., 2007; Binder, 2010). One gene encoding a putative isopropylmalate dehydrogenase (*HORVU3Hr1G069300*) is down-regulated in M4 suggesting a fine-tuned regulation of this biosynthetic pathway depending on the isoforms. Interestingly, two genes encoding the threonine aldolase are downregulated. This is consistent with the reports indicating that this enzyme competes for threonine, the first amino acid in the BCAA biosynthesis pathway (Joshi et al., 2006).

Our work provides key physiological markers of North African barley adaptation to low N availability in the early developmental stages, in particular the *HvNRT2.10* gene. Candidate genes involved in key steps of lysine metabolism were identified with a potential link with immunity. Further investigation of the role of these genes in barley nitrogen metabolism and immunity would provide valuable data for sustainable barley production under harsh conditions.

DATA AVAILABILITY STATEMENT

RNA-Seq projects were deposited [Gene Expression Omnibus (Edgar et al., 2002)]: http://www.ncbi.nlm.nih.gov/geo/; accession no. GEO GSE188216. All steps of the experiment, from growth conditions to bioinformatic analyses, were detailed in CATdb (Gagnot et al., 2008): http://tools.ips2.universite-paris-saclay.fr/CATdb/project.html?project_id=493; project: NGS2020_19_ARIMNet according to the MINSEQE "minimum information about a high-throughput sequencing experiment".

AUTHOR CONTRIBUTIONS

CM-D and AD: supervision of this work. FS, MB, and MR: plant growth, ^{15}N labeling, and sampling. MB, MR, and SL: plant material preparation for all measurements. AM: ^{15}N, N, and C quantification. MA and MB: amino acid determination. CP-L and JC: RNAseq. CJ and QE: pathogenicity tests. AD, BD, CM-D, FC, and MB: data computing and statistical analyses. AD, CM-D, and FC: project supervision and writing. All authors contributed to the article and approved the submitted version.

FUNDING

This work was supported by ARIMNET 2 project entitled "Exploring genotypic diversity to optimize barley grain and straw quality under marginal/stressful growth conditions," BEST ANR-15-ARM2-0007. IJPB benefits from the support of the LABEX Saclay Plant Sciences-SPS (ANR-10-LABX-0040-SPS).

ACKNOWLEDGMENTS

We thank the research analytical platforms of Agro Innovation International—TIMAC AGRO, Saint-Malo, France and the National Institute of Agronomic Research (INRA), Morocco. The POPS platform benefits from the support of Saclay Plant Sciences-SPS (ANR-17-EUR-0007). We thank Chedly Abdelly, Tahar Gnaya (Laboratory of Extremophile Plants, Biotechnology Center of Borj Cedria, Tunisia), Mbarek Bennaceur (National Gene Bank of Tunisia), and Mejda Cherif (Institut National Agronomique de Tunisie) for interesting discussions about the project. We thank Hervé Ferry for managing plant growth chambers and Laurence Bill for helping with plant harvesting. We thank Etienne Delannoy INRAE for discussions about the transcriptomics approach.

SUPPLEMENTARY MATERIAL

The Supplementary Material for this article can be found online at: https://www.frontiersin.org/articles/10.3389/fpls.2021.807798/full#supplementary-material

REFERENCES

Abid, M., Tian, Z., Ata-Ul-Karim, S. T., Cui, Y., Liu, Y., Zahoor, R., et al. (2016). Nitrogen nutrition improves the potential of wheat (*Triticum aestivum* L.) to alleviate the effects of drought stress during vegetative growth periods. *Front. Plant Sci.* 7:981. doi: 10.3389/fpls.2016.00981

Avila-Ospina, L., Marmagne, A., Talbotec, J., Krupinska, K., and Masclaux-Daubresse, C. (2015). The identification of new cytosolic glutamine synthetase and asparagine synthetase genes in barley (*Hordeum vulgare* L.), and their expression during leaf senescence. *J. Exp. Bot.* 66, 2013–2026. doi: 10.1093/jxb/erv003

Ayachi, I., Ghabriche, R., Kourouma, Y., Ben Naceur, M., Abdelly, C., Thomine, S., et al. (2021). Cd tolerance and accumulation in barley: screening of 36 North African cultivars on Cd-contaminated soil. *Environ. Sci. Pollut. Res.* 28, 42722–42736. doi: 10.1007/s11356-021-13768-y

Backes, A., Guerriero, G., Ait Barka, E., and Jacquard, C. (2021a). Pyrenophora teres: taxonomy, morphology, interaction with barley, and mode of control. *Front. Plant Sci.* 12:509. doi: 10.3389/fpls.2021.614951

Backes, A., Vaillant-Gaveau, N., Esmaeel, Q., Ait Barka, E., and Jacquard, C. (2021b). A biological agent modulates the physiology of barley infected with *Drechslera teres*. *Sci. Rep.* 11:8330. doi: 10.1038/s41598-021-87853-0

Badraoui, M., Rachid Dahan, R., and Balaghi, R. (2009). "Acquis de l'INRA en Matière de Recherche Scientifique et Technologique pour L'amélioration de la Production Agricole au Maroc," in *Bulletin D'information de l'Académie Hassan II des Sciences et Techniques*, N°5, 50–65.

Baik, B.-K., and Ullrich, S. E. (2008). Barley for food: characteristics, improvement, and renewed interest. *J. Cereal Sci.* 48, 233–242. doi: 10.1016/j.jcs.2008.02.002

Benjamini, Y., and Hochberg, Y. (1995). Controlling the false discovery rate: a practical and powerful approach to multiple testing. *J. R. Stat. Soc. Ser. B* 57, 289–300. doi: 10.1111/j.2517-6161.1995.tb02031.x

Ben Naceur, A., Chaabane, R., El-Faleh, M., Abdelly, C., Ramla, D., Nada, A., et al., (2012). Genetic diversity analysis of North Africa's barley using SSR markers. *J. Genet. Eng. Biotechnol.* 10, 13–21. doi: 10.1016/j.jgeb.2011.12.003

Binder, S. (2010). Branched-chain amino acid metabolism in *Arabidopsis thaliana*. *Arabidopsis Book* 8, e0137–e0137. doi: 10.1199/tab.0137

Binder, S., Knill, T., and Schuster, J. (2007). Branched-chain amino acid metabolism in higher plants. *Physiol. Plant.* 129, 68–78. doi: 10.1111/j.1399-3054.2006.00800.x

Bolger, A. M., Lohse, M., and Usadel, B. (2014). Trimmomatic: a flexible trimmer for Illumina sequence data. *Bioinformatics* 30, 2114–2120. doi: 10.1093/bioinformatics/btu170

Cammarano, D., Ceccarelli, S., Grando, S., Romagosa, I., Benbelkacem, A., Akar, T., et al. (2019). The impact of climate change on barley yield in the *Mediterranean basin*. *Eur. J. Agron.* 106, 1–11. doi: 10.1016/j.eja.2019.03.002

Chardon, F., Barthélémy, J., Daniel-Vedele, F., and Masclaux-Daubresse, C. (2010). Natural variation of nitrate uptake and nitrogen use efficiency in *Arabidopsis thaliana* cultivated with limiting and ample nitrogen supply. *J. Exp. Bot.* 61, 2293–2302. doi: 10.1093/jxb/erq059

Chen, J. G., Crooks, R. M., Seefeldt, L. C., Bren, K. L., Bullock, R. M., Darensbourg, M. Y., et al. (2018). Beyond fossil fuel–driven nitrogen transformations. *Science* 360:eaar6611. doi: 10.1126/science.aar6611

Chen, W., Meng, C., Ji, J., Li, M.-H., Zhang, X., Wu, Y., et al. (2020). Exogenous GABA promotes adaptation and growth by altering the carbon and nitrogen metabolic flux in poplar seedlings under low nitrogen conditions. *Tree Physiol.* 40, 1744–1761. doi: 10.1093/treephys/tpaa101

Chun, L., Mi, G., Li, J., Chen, F., and Zhang, F. (2005). genetic analysis of maize root characteristics in response to low nitrogen stress. *Plant Soil* 276, 369–382. doi: 10.1007/s11104-005-5876-2

Chutimanitsakun, Y., Cuesta-Marcos, A., Chao, S., Corey, A., Filichkin, T., Fisk, S., et al. (2013). Application of marker-assisted selection and genome-wide association scanning to the development of winter food barley germplasm resources. *Plant Breed.* 132, 563–570. doi: 10.1111/pbr.12086

Comadira, G., Rasool, B., Karpinska, B., Morris, J., Verrall, S. R., Hedley, P. E., et al. (2015). Nitrogen deficiency in barley (*Hordeum vulgare*) seedlings induces molecular and metabolic adjustments that trigger aphid resistance. *J. Exp. Bot.* 66, 3639–3655. doi: 10.1093/jxb/erv276

Dawson, I. K., Russell, J., Powell, W., Steffenson, B., Thomas, W. T. B., and Waugh, R. (2015). Barley: a translational model for adaptation to climate change. *New Phytol.* 206, 913–931. doi: 10.1111/nph.13266

Ding, L., Lu, Z., Gao, L., Guo, S., and Shen, Q. (2018). Is nitrogen a key determinant of water transport and photosynthesis in higher plants upon drought stress? *Front. Plant Sci.* 9:1143. doi: 10.3389/fpls.2018.01143

Dobin, A., Davis, C. A., Schlesinger, F., Drenkow, J., Zaleski, C., Jha, S., et al. (2013). STAR: ultrafast universal RNA-seq aligner. *Bioinformatics* 29, 15–21. doi: 10.1093/bioinformatics/bts635

Edgar, R., Domrachev, M., and Lash, A. E. (2002). Gene expression omnibus: NCBI gene expression and hybridization array data repository. *Nucleic Acids Res.* 30, 207–210. doi: 10.1093/nar/30.1.207

Epstein, E., Rains, D. W., and Elzam, O. E. (1963). Resolution of dual mechanisms of potassium absorption by barley roots. *Proc. Natl. Acad. Sci. U.S.A.* 49, 684–692. doi: 10.1073/pnas.49.5.684

Fagard, M., Launay, A., Clément, G., Courtial, J., Dellagi, A., Farjad, M., et al. (2014). Nitrogen metabolism meets phytopathology. *J. Exp. Bot.* 65, 5643–5656. doi: 10.1093/jxb/eru323

Gagnot, S., Tamby, J.-P., Martin-Magniette, M.-L., Bitton, F., Taconnat, L., Balzergue, S., et al. (2008). CATdb: a public access to *Arabidopsis transcriptome*

data from the URGV-CATMA platform. *Nucleic Acids Res.* 36, D986–D990. doi: 10.1093/nar/gkm757

Galili, G. (2002). New insights into the regulation and functional significance of lysine metabolism in plants. *Annu. Rev. Plant Biol.* 53, 27–43. doi: 10.1146/annurev.arplant.53.091401.110929

Galili, G., Amir, R., and Fernie, A. R. (2016). The regulation of essential amino acid synthesis and accumulation in plants. *Annu. Rev. Plant Biol.* 67, 153–178. doi: 10.1146/annurev-arplant-043015-112213

Gastal, F., and Lemaire, G. (2002). N uptake and distribution in crops: an agronomical and ecophysiological perspective. *J. Exp. Bot.* 53, 789–799. doi: 10.1093/jexbot/53.370.789

Genies, L., Martin, L., Kanno, S., Chiarenza, S., Carasco, L., Camilleri, V., et al. (2021). Disruption of AtHAK/KT/KUP9 enhances plant cesium accumulation under low potassium supply. *Physiol. Plant* 173, 1230–1243. doi: 10.1111/ppl.13518

Gierth, M., and Mäser, P. (2007). Potassium transporters in plants – Involvement in K+ acquisition, redistribution and homeostasis. *FEBS Lett.* 581, 2348–2356. doi: 10.1016/j.febslet.2007.03.035

Górny, A. G. (2001). Variation in utilization efficiency and tolerance to reduced water and nitrogen supply among wild and cultivated barleys. *Euphytica* 117, 59–66. doi: 10.1023/A:1004061709964

Guo, B., Li, Y., Wang, S., Li, D., Lv, C., and Xu, R. (2020). Characterization of the nitrate transporter gene family and functional identification of HvNRT2.1 in barley (*Hordeum vulgare* L.). *PLoS One* 15:e0232056. doi: 10.1371/journal.pone.0232056

Han, M., Okamoto, M., Beatty, P. H., Rothstein, S. J., and Good, A. G. (2015). The genetics of nitrogen use efficiency in crop plants. *Annu. Rev. Genet.* 49, 269–289. doi: 10.1146/annurev-genet-112414-055037

Häusler, R. E., Ludewig, F., and Krueger, S. (2014). Amino acids – a life between metabolism and signaling. *Plant Sci.* 229, 225–237. doi: 10.1016/j.plantsci.2014.09.011

Hawkesford, M. J., and Griffiths, S. (2019). Exploiting genetic variation in nitrogen use efficiency for cereal crop improvement. *Curr. Opin. Plant Biol.* 49, 35–42. doi: 10.1016/j.pbi.2019.05.003

Hellal, F., Abdel-Hady, M., Khatab, I., El-Sayed, S., and Abdelly, C. (2019). Yield characterization of mediterranean barley under drought stress condition. *AIMS Agric. Food* 3, 518–533. doi: 10.3934/agrfood.2019.3.518

Hirel, B., and Krapp, A. B. T.-R. M. (2020). "Nitrogen utilization in plants i biological and agronomic importance," in *Encyclopedia of Biological Chemistry*, 3rd Edn, ed. J. Jez (Amsterdam: Elsevier), doi: 10.1016/B978-0-12-809633-8.21265-X

Hirel, B., Le Gouis, J., Ney, B., and Gallais, A. (2007). The challenge of improving nitrogen use efficiency in crop plants: towards a more central role for genetic variability and quantitative genetics within integrated approaches. *J. Exp. Bot.* 58, 2369–2387. doi: 10.1093/jxb/erm097

Jander, G., and Joshi, V. (2009). Aspartate-derived amino acid biosynthesis in *Arabidopsis thaliana*. *Arabidopsis Book* 2009, e0121. doi: 10.1199/tab.0121

Jebbouj, R., and El Yousfi, B. (2009). Barley yield losses due to defoliation of upper three leaves either healthy or infected at boot stage by *Pyrenophora teres* f. teres. *Eur. J. Plant Pathol.* 125, 303–315. doi: 10.1007/s10658-009-9483-6

Jood, S., and Singh, M. (2001). Amino acid composition and biological evaluation of the protein quality of high lysine barley genotypes. *Plant Foods Hum. Nutr.* 56, 145–155. doi: 10.1023/A:1011114604008

Joshi, V., Joung, J.-G., Fei, Z., and Jander, G. (2010). Interdependence of threonine, methionine and isoleucine metabolism in plants: accumulation and transcriptional regulation under abiotic stress. *Amino Acids* 39, 933–947. doi: 10.1007/s00726-010-0505-7

Joshi, V., Laubengayer, K. M., Schauer, N., Fernie, A. R., and Jander, G. (2006). Two *Arabidopsis threonine* aldolases are nonredundant and compete with threonine deaminase for a common substrate pool. *Plant Cell* 18, 3564–3575. doi: 10.1105/tpc.106.044958

Kant, S. (2018). Understanding nitrate uptake, signaling and remobilisation for improving plant nitrogen use efficiency. *Semin. Cell Dev. Biol.* 74, 89–96. doi: 10.1016/j.semcdb.2017.08.034

Karunarathne, S. D., Han, Y., Zhang, X.-Q., Dang, V. H., Angessa, T. T., and Li, C. (2021). Using chlorate as an analogue to nitrate to identify candidate genes for nitrogen use efficiency in barley. *Mol. Breed.* 41:47. doi: 10.1007/s11032-021-01239-8

Karunarathne, S. D., Han, Y., Zhang, X.-Q., Zhou, G., Hill, C. B., Chen, K., et al. (2020). Genome-wide association study and identification of candidate genes for nitrogen use efficiency in barley (*Hordeum vulgare* L.). *Front. Plant Sci.* 11:1361. doi: 10.3389/fpls.2020.571912

Khanna, R. R., Jahan, B., Iqbal, N., Khan, N. A., AlAjmi, M. F., Tabish Rehman, M., et al. (2021). GABA reverses salt-inhibited photosynthetic and growth responses through its influence on NO-mediated nitrogen-sulfur assimilation and antioxidant system in wheat. *J. Biotechnol.* 325, 73–82. doi: 10.1016/j.jbiotec.2020.11.015

Kobe, R. K., Iyer, M., and Walters, M. B. (2010). Optimal partitioning theory revisited: nonstructural carbohydrates dominate root mass responses to nitrogen. *Ecology* 91, 166–179. doi: 10.1890/09-0027.1

Kopylova, E., Noé, L., and Touzet, H. (2012). SortMeRNA: fast and accurate filtering of ribosomal RNAs in metatranscriptomic data. *Bioinformatics* 28, 3211–3217. doi: 10.1093/bioinformatics/bts611

Krapp, A., Berthomé, R., Orsel, M., Mercey-Boutet, S., Yu, A., Castaings, L., et al. (2011). *Arabidopsis* roots and shoots show distinct temporal adaptation patterns toward nitrogen starvation. *Plant Physiol.* 157, 1255L–1282. doi: 10.1104/pp.111.179838

Lafiandra, D., Riccardi, G., and Shewry, P. R. (2014). Improving cereal grain carbohydrates for diet and health. *J. Cereal Sci.* 59, 312–326. doi: 10.1016/j.jcs.2014.01.001

Lammerts van Bueren, E. T., and Struik, P. C. (2017). Diverse concepts of breeding for nitrogen use efficiency. *Rev. Agron. Sustain. Dev.* 37:50. doi: 10.1007/s13593-017-0457-3

Landberg, R., Hanhineva, K., Tuohy, K., Garcia-Aloy, M., Biskup, I., Llorach, R., et al. (2019). Biomarkers of cereal food intake. *Genes Nutr.* 14:28. doi: 10.1186/s12263-019-0651-9

Lassaletta, L., Billen, G., Garnier, J., Bouwman, L., Velazquez, E., Mueller, N. D., et al. (2016). Nitrogen use in the global food system: past trends and future trajectories of agronomic performance, pollution, trade, and dietary demand. *Environ. Res. Lett.* 11:095007. doi: 10.1088/1748-9326/11/9/095007

Lea, P. J., and Azevedo, R. A. (2007). Nitrogen use efficiency. 2. Amino acid metabolism. *Ann. Appl. Biol.* 151, 269–275. doi: 10.1111/j.1744-7348.2007.00200.x

Lea, P. J., and Miflin, B. J. (2018). Nitrogen assimilation and its relevance to crop improvement. *Annu. Plant Rev.* 1–40. doi: 10.1002/9781119312994.apr0448

Lemaître, T., Gaufichon, L., Boutet-Mercey, S., Christ, A., and Masclaux-Daubresse, C. (2008). Enzymatic and metabolic diagnostic of nitrogen deficiency in *Arabidopsis thaliana Wassileskija* accession. *Plant Cell Physiol.* 49, 1056–1065. doi: 10.1093/pcp/pcn081

Léran, S., Varala, K., Boyer, J.-C., Chiurazzi, M., Crawford, N., Daniel-Vedele, F., et al. (2014). A unified nomenclature of Nitrate transporter 1/peptide transporter family members in plants. *Trends Plant Sci.* 19, 5–9. doi: 10.1016/j.tplants.2013.08.008

Li, H., Hu, B., and Chu, C. (2017). Nitrogen use efficiency in crops: lessons from *Arabidopsis* and rice. *J. Exp. Bot.* 68, 2477–2488. doi: 10.1093/jxb/erx101

Lynch, J. H., and Dudareva, N. (2020). Aromatic amino acids: a complex network ripe for future exploration. *Trends Plant Sci.* 25, 670–681. doi: 10.1016/j.tplants.2020.02.005

Masclaux-Daubresse, C., and Chardon, F. (2011). Exploring nitrogen remobilization for seed filling using natural variation in *Arabidopsis thaliana*. *J. Exp. Bot.* 62, 2131–2142. doi: 10.1093/jxb/erq405

Masclaux-Daubresse, C., Daniel-Vedele, F., Dechorgnat, J., Chardon, F., Gaufichon, L., and Suzuki, A. (2010). Nitrogen uptake, assimilation and remobilization in plants: challenges for sustainable and productive agriculture. *Ann. Bot.* 105, 1141–1157. doi: 10.1093/aob/mcq028

Mertz, E. T., Bates, L. S., and Nelson, O. E. (1964). Mutant gene that changes protein composition and increases lysine content of maize endosperm. *Science* 145, 279–280. doi: 10.1126/science.145.3629.279

Mlaouhi, S., Ghanem, H., and Najar, A. (2020). Potential climate change impacts on imen barley BYDV resistant variety yields in tunisia. *Agron. Agric. Sci.* 3, 1–8. doi: 10.24966/AAS-8292/100025

Møller, A. L. B., Pedas, P. A. I., Andersen, B., Svensson, B., Schjoerring, J. A. N. K., and Finnie, C. (2011). Responses of barley root and shoot proteomes to long-term nitrogen deficiency, short-term nitrogen starvation and ammonium. *Plant Cell Environ.* 34, 2024–2037. doi: 10.1111/j.1365-3040.2011.02396.x

Muñoz-Amatriaín, M., Cuesta-Marcos, A., Hayes, P. M., and Muehlbauer, G. J. (2014). Barley genetic variation: implications for crop improvement. *Briefings Funct. Genomics Proteomics* 13, 341–350. doi: 10.1093/bfgp/elu006

Mur, L. A. J., Simpson, C., Kumari, A., Gupta, A. K., and Gupta, K. J. (2017). Moving nitrogen to the centre of plant defence against pathogens. *Ann. Bot.* 119, 703–709. doi: 10.1093/aob/mcw179

Negrutiu, I., Cattoir-Reynearts, A., Verbruggen, I., and Jacobs, M. (1984). Lysine overproducer mutants with an altered dihydrodipicolinate synthase from protoplast culture of *Nicotiana sylvestris* (Spegazzini and Comes). *Theor. Appl. Genet.* 68, 11–20. doi: 10.1007/BF00252303

Noaman, M. M., Ahmed, I. A., El-Sayed, A. A., Abo-El-Enin, R. A., El-Gamal, A. S., El-Sherbiny, A. M., et al. (2007). Registration of 'giza 2000' drought-tolerant six-rowed barley for rainfed and new reclaimed areas in egypt. *Crop Sci.* 47:440. doi: 10.2135/cropsci2006.05.0350

O'Brien, J. A., Vega, A., Bouguyon, E., Krouk, G., Gojon, A., Coruzzi, G., et al. (2016). Nitrate transport, sensing, and responses in plants. *Mol. Plant* 9, 837–856. doi: 10.1016/j.molp.2016.05.004

Oscarsson, M., Andersson, R., Åman, P., Olofsson, S., and Jonsson, A. (1998). Effects of cultivar, nitrogen fertilization rate and environment on yield and grain quality of barley. *J. Sci. Food Agric.* 78, 359–366.

Pretty, J. (2018). Intensification for redesigned and sustainable agricultural systems. *Science* 362:eaav0294. doi: 10.1126/science.aav0294

Pswarayi, A., Van Eeuwijk, F. A., Ceccarelli, S., Grando, S., Comadran, J., Russell, J. R., et al. (2008). Barley adaptation and improvement in the *Mediterranean basin*. *Plant Breed.* 127, 554–560. doi: 10.1111/j.1439-0523.2008.01522.x

Quan, X., Zeng, J., Chen, G., and Zhang, G. (2019). Transcriptomic analysis reveals adaptive strategies to chronic low nitrogen in Tibetan wild barley. *BMC Plant Biol.* 19:68. doi: 10.1186/s12870-019-1668-3

Quan, X., Zeng, J., Ye, L., Chen, G., Han, Z., Shah, J. M., et al. (2016). Transcriptome profiling analysis for two Tibetan wild barley genotypes in responses to low nitrogen. *BMC Plant Biol.* 16:30. doi: 10.1186/s12870-016-0721-8

Rai, V. K. (2002). Role of amino acids in plant responses to stresses. *Biol. Plant.* 45, 481–487. doi: 10.1023/A:1022308229759

Ramesh, S. A., Tyerman, S. D., Gilliham, M., and Xu, B. (2017). γ-Aminobutyric acid (GABA) signalling in plants. *Cell Mol. Life Sci.* 74, 1577–1603. doi: 10.1007/s00018-016-2415-7

Rigaill, G., Balzergue, S., Brunaud, V., Blondet, E., Rau, A., Rogier, O., et al. (2018). Synthetic data sets for the identification of key ingredients for RNA-seq differential analysis. *Brief. Bioinform.* 19, 65–76. doi: 10.1093/bib/bbw092

Robinson, M. D., McCarthy, D. J., and Smyth, G. K. (2010). edgeR: a bioconductor package for differential expression analysis of digital gene expression data. *Bioinformatics* 26, 139–140. doi: 10.1093/bioinformatics/btp616

Ryan, J., and Sommer, R. (2012). Soil fertility and crop nutrition research at an international center in the Mediterranean region: achievements and future perspective. *Arch. Agron. Soil Sci.* 58, S41–S54. doi: 10.1080/03650340.2012.693601

Ryan, J., Masri, S., Ceccarelli, S., Grando, S., and Ibrikci, H. (2008). Differential responses of barley landraces and improved barley cultivars to nitrogen-phosphorus fertilizer. *J. Plant Nutr.* 31, 381–393. doi: 10.1080/01904160801894939

Saidi, S., Jilal, A., Amri, A., Grondo, S., and Ceccarelli, S. (2005). "Amélioration Génétique de L'orge," in *La création Variétale á l'INRA. Méthodologie, Acquis et Perspectives*, eds F. A. Andaloussi and A. Chahbar (INRA).

Sakakibara, H., Takei, K., and Hirose, N. (2006). Interactions between nitrogen and cytokinin in the regulation of metabolism and development. *Trends Plant Sci.* 11, 440–448. doi: 10.1016/j.tplants.2006.07.004

Schenck, C. A., and Maeda, H. A. (2018). Tyrosine biosynthesis, metabolism, and catabolism in plants. *Phytochemistry* 149, 82–102. doi: 10.1016/j.phytochem.2018.02.003

Schlesinger, W. H. (2009). On the fate of anthropogenic nitrogen. *Proc. Natl. Acad. Sci. U.S.A.* 106, 203L–208. doi: 10.1073/pnas.0810193105

Schmidt, D., Rizzi, V., Gaziola, S. A., Medici, L. O., Vincze, E., Kozak, M., et al. (2015). Lysine metabolism in antisense C-hordein barley grains. *Plant Physiol. Biochem.* 87, 73–83. doi: 10.1016/j.plaphy.2014.12.017

Schreiber, M., Mascher, M., Wright, J., Padmarasu, S., Himmelbach, A., Heavens, D., et al. (2020). A genome assembly of the barley 'transformation reference' cultivar golden promise. *G3 Genes Genomes Genet.* 10, 1823L–1827. doi: 10.1534/g3.119.401010

Sedlář, O., Balík, J., Kozlovský, O., Peklová, L., and Kubešová, K. (2011). Impact of nitrogen fertilizer injection on grain yieldand yield formation of spring barley (*Hordeum vulgare* L.). *Plant Soil Environ.* 57, 547–552. doi: 10.17221/429/2011-pse

Shi, X., and Bloom, A. (2021). Photorespiration: the futile cycle? *Plants* 10:908. doi: 10.3390/plants10050908

Sinebo, W., Gretzmacher, R., and Edelbauer, A. (2004). Genotypic variation for nitrogen use efficiency in Ethiopian barley. *Field Crop. Res.* 85, 43–60. doi: 10.1016/S0378-4290(03)00135-7

Stupar, V., Paunoviæ, A., Madiæ, M., and Kneževiæ, D. (2017). Influence of genotype and nitrogen nutrition on grain size variability in spring malting barley. *Genetika* 49, 1095–1104. doi: 10.2298/GENSR1703095S

Sun, X., Chen, F., Yuan, L., and Mi, G. (2020). The physiological mechanism underlying root elongation in response to nitrogen deficiency in crop plants. *Planta* 251:84. doi: 10.1007/s00425-020-03376-4

Sun, Y., Wang, M., Mur, L. A. J., Shen, Q., and Guo, S. (2020). Unravelling the roles of nitrogen nutrition in plant disease defences. *Int. J. Mol. Sci.* 21:572. doi: 10.3390/ijms21020572

Van Der Werf, A., and Nagel, O. W. (1996). Carbon allocation to shoots and roots in relation to nitrogen supply is mediated by cytokinins and sucrose: opinion. *Plant Soil* 185, 21–32. doi: 10.1007/BF02257562

Verly, C., Djoman, A. C. R., Rigault, M., Giraud, F., Rajjou, L., Saint-Macary, M. E., et al. (2020). Plant defense stimulator mediated defense activation is affected by nitrate fertilization and developmental stage in *Arabidopsis thaliana*. *Front. Plant Sci.* 11:583. doi: 10.3389/fpls.2020.00583

Wang, C., Van den Ende, W., and Tillberg, J. E. (2000). Fructan accumulation induced by nitrogen deficiency in barley leaves correlates with the level of sucrose:fructan 6-fructosyltransferase mRNA. *Planta* 211, 701–707. doi: 10.1007/s004250000335

Wang, W., Niu, S., Dai, Y., Wang, M., Li, Y., Yang, W., et al. (2019). The Zea mays mutants opaque2 and opaque16 disclose lysine change in waxy maize as revealed by RNA-Seq. *Sci. Rep.* 9:12265. doi: 10.1038/s41598-019-48478-6

Wang, Y.-Y., Cheng, Y.-H., Chen, K.-E., and Tsay, Y.-F. (2018). Nitrate transport, signaling, and use efficiency. *Annu. Rev. Plant Biol.* 69, 85–122. doi: 10.1146/annurev-arplant-042817-040056

Wei, J., Zheng, Y., Feng, H., Qu, H., Fan, X., Yamaji, N., et al. (2018). OsNRT2.4 encodes a dual-affinity nitrate transporter and functions in nitrate-regulated root growth and nitrate distribution in rice. *J. Exp. Bot.* 69, 1095–1107. doi: 10.1093/jxb/erx486

Withers, P. J. A., Neal, C., Jarvie, H. P., and Doody, D. G. (2014). Agriculture and eutrophication: where do we go from here? *Sustainability* 6, 5853–5875. doi: 10.3390/su6095853

Xu, B., Sai, N., and Gilliham, M. (2021). The emerging role of GABA as a transport regulator and physiological signal. *Plant Physiol.* 187, 2005–2016. doi: 10.1093/plphys/kiab347

Xu, G. (2018). Sensing and transport of nutrients in plants. *Semin. Cell Dev. Biol.* 74, 78–79. doi: 10.1016/j.semcdb.2017.09.020

Xu, G., Fan, X., and Miller, A. J. (2012). Plant nitrogen assimilation and use efficiency. *Annu. Rev. Plant Biol.* 63, 153–182. doi: 10.1146/annurev-arplant-042811-105532

Xu, J.-J., Fang, X., Li, C.-Y., Yang, L., and Chen, X.-Y. (2020). General and specialized tyrosine metabolism pathways in plants. *aBIOTECH* 1, 97–105. doi: 10.1007/s42994-019-00006-w

Zeier, J. (2013). New insights into the regulation of plant immunity by amino acid metabolic pathways. *Plant Cell Environ.* 36, 2085–2103. doi: 10.1111/pce.12122

Zhang, G.-B., Meng, S., and Gong, J.-M. (2018). The expected and unexpected roles of nitrate transporters in plant abiotic stress resistance and their regulation. *Int. J. Mol. Sci.* 19:3535. doi: 10.3390/ijms19113535

Zhang, H., Rong, H., and Pilbeam, D. (2007). Signalling mechanisms underlying the morphological responses of the root system to nitrogen in *Arabidopsis thaliana*. *J. Exp. Bot.* 58, 2329–2338. doi: 10.1093/jxb/erm114

Conflict of Interest: MA was employed by company TIMAC AGRO International SAS.

The remaining authors declare that the research was conducted in the absence of any commercial or financial relationships that could be construed as a potential conflict of interest.

Publisher's Note: All claims expressed in this article are solely those of the authors and do not necessarily represent those of their affiliated organizations, or those of the publisher, the editors and the reviewers. Any product that may be evaluated in this article, or claim that may be made by its manufacturer, is not guaranteed or endorsed by the publisher.

frontiers | Frontiers in Plant Science

ORIGINAL RESEARCH
published: 02 May 2022
doi: 10.3389/fpls.2022.893610

The Genetic Architecture of Nitrogen Use Efficiency in Switchgrass (*Panicum virgatum* L.)

Vivek Shrestha[1,2], Hari B. Chhetri[2], David Kainer[2], Yaping Xu[1,2], Lance Hamilton[1,2], Cristiano Piasecki[3], Ben Wolfe[1,2], Xueyan Wang[2,4], Malay Saha[2,4], Daniel Jacobson[2], Reginald J. Millwood[1,2], Mitra Mazarei[1,2]* and C. Neal Stewart Jr.[1,2]**

[1] Department of Plant Sciences, The University of Tennessee, Knoxville, Knoxville, TN, United States, [2] Center for Bioenergy Innovation, Oak Ridge National Laboratory, Oak Ridge, TN, United States, [3] ATSI Brazil Pesquisa e Consultoria, Passo Fundo, Brazil, [4] Noble Research Institute, Ardmore, OK, United States

OPEN ACCESS

Edited by:
Surya Kant,
La Trobe University, Australia

Reviewed by:
Bin Xu,
Nanjing Agricultural University, China
Sakura Dilhani Karunarathne,
Murdoch University, Australia
Joseph Evans,
DuPont Pioneer, United States

***Correspondence:**
Reginald J. Millwood
rmillwood@utk.edu
Mitra Mazarei
mmazarei@utk.edu
C. Neal Stewart Jr.
nealstewart@utk.edu

Specialty section:
This article was submitted to Plant Physiology, a section of the journal Frontiers in Plant Science

Received: *10 March 2022*
Accepted: *01 April 2022*
Published: *02 May 2022*

Citation:
Shrestha V, Chhetri HB, Kainer D, Xu Y, Hamilton L, Piasecki C, Wolfe B, Wang X, Saha M, Jacobson D, Millwood RJ, Mazarei M and Stewart CN Jr (2022) The Genetic Architecture of Nitrogen Use Efficiency in Switchgrass (Panicum virgatum L.). Front. Plant Sci. 13:893610. doi: 10.3389/fpls.2022.893610

Switchgrass (*Panicum virgatum* L.) has immense potential as a bioenergy crop with the aim of producing biofuel as an end goal. Nitrogen (N)-related sustainability traits, such as nitrogen use efficiency (NUE) and nitrogen remobilization efficiency (NRE), are important factors affecting switchgrass quality and productivity. Hence, it is imperative to develop nitrogen use-efficient switchgrass accessions by exploring the genetic basis of NUE in switchgrass. For that, we used 331 diverse field-grown switchgrass accessions planted under low and moderate N fertility treatments. We performed a genome wide association study (GWAS) in a holistic manner where we not only considered NUE as a single trait but also used its related phenotypic traits, such as total dry biomass at low N and moderate N, and nitrogen use index, such as NRE. We have evaluated the phenotypic characterization of the NUE and the related traits, highlighted their relationship using correlation analysis, and identified the top ten nitrogen use-efficient switchgrass accessions. Our GWAS analysis identified 19 unique single nucleotide polymorphisms (SNPs) and 32 candidate genes. Two promising GWAS candidate genes, *caffeoyl-CoA O-methyltransferase* (*CCoAOMT*) and *alfin-like 6* (*AL6*), were further supported by linkage disequilibrium (LD) analysis. Finally, we discussed the potential role of nitrogen in modulating the expression of these two genes. Our findings have opened avenues for the development of improved nitrogen use-efficient switchgrass lines.

Keywords: nitrogen use efficiency, nitrogen remobilization efficiency, switchgrass, accessions, genome wide association study

INTRODUCTION

Nitrogen (N) is a major macronutrient, which is essential for plant biomass and yield production. In the past 50 years, the application of synthetic N fertilizer to farmland has resulted in a dramatic increase in crop yields but with considerable negative impacts on the environment (Han et al., 2015). A large proportion of the applied N (50–70%) is lost from the plant-soil framework (Lam et al., 1996; Ranjan and Yadav, 2019). Excessive use of N fertilizer degrades the natural resources, such as air, soil, underground water, and contributes to global warming (Byrnes, 1990; Glass et al., 2002; Chien et al., 2016). Synthetic nitrogen fertilizer production and N_2O from use of synthetic

N fertilizers contribute to 0.8 and 1.3% of global greenhouse gas emissions, respectively (Jensen and Schjoerring, 2011; Langholtz et al., 2021). Therefore, new solutions are needed to decrease applied N without yield penalty to maximize the nitrogen use efficiency (NUE) of crops. A study conducted on simulating 20% increase in NUE in row crops has shown to reduce N requirements by 1.27 metric tons per year and increase farmers' net profits by 1.6% per year by 2026 over the base simulation for the same period (Langholtz et al., 2021).

Switchgrass (*Panicum virgatum* L.) is a perennial grass native to North America and developed as a potential bioenergy crop due to its high biomass production, ability to grow in marginal land, low input requirements for maintenance, and high cellulose content (Sanderson et al., 1996; Adler et al., 2006). It has been reported that a substantial proportion of nutritive elements are removed with each biomass harvest from switchgrass, although it remobilizes nutrients from shoots to roots, each growing cycle during senescence (Yang et al., 2009). Studies have shown that the total N removed with one-cut fall biomass harvest ranges from 31 to 63 kg N per ha per year, while, for two-cut system, it ranges from 90 to 144 kg per ha per year over the 5 years of measurement (Reynolds et al., 2000). With such high nutrient withdrawal, it is inevitable that N depletion from soil will occur over time and necessitate the addition of N fertilizer to maintain sustainable switchgrass production. Therefore, the development of nitrogen-use-efficient switchgrass cultivars is imperative for the sustainable production of biofuel. To develop nitrogen-use-efficient switchgrass cultivars, we need to have a better understanding of the NUE and its genetic architecture.

Several definitions and calculations of NUE have been published, which encompass a wide range of NUE calculations, as well as acknowledge that different NUE indices have distinctive functions (Good et al., 2004; Ladha et al., 2005; Dobermann, 2007; Sadeghpour et al., 2014; Ernst et al., 2020; Congreves et al., 2021). Hence, it is recommended to use multiple NUE approaches or NUE-related indices to ensure the better representation of different insights (Van, 2007; Fixen et al., 2015; Congreves et al., 2021). NUE is complex and possesses several components. Nitrogen remobilization efficiency (NRE) is one of the important components of NUE in switchgrass. For perennial grass, such as switchgrass, improving NRE from aboveground to underground organs during yearly shoot senescence is equally important for sustainable production of switchgrass (Yang et al., 2016) and should be considered for developing nitrogen use-efficient switchgrass varieties. NRE has been investigated intensively at the agronomic level (Lemus et al., 2008; Yang et al., 2009; Strullu et al., 2011; Dohleman et al., 2012; o Di Nasso et al., 2013) but very limited at the genetic level. Therefore, the present study will add a foundational understanding of the genetic basis of NRE in switchgrass.

Nitrogen use efficiency is a quantitative trait and governed by polygenes. A quantitative genetics approach, such as genome wide association study (GWAS), has been a powerful tool to dissect the genetic architecture of complex traits (Lander and Schork, 1994; Mackay, 2001; Doerge, 2002). GWAS for NUE has been used in several crops, such as barley (Karunarathne et al., 2020), maize (Morosini et al., 2017; He et al., 2020), rice (Xin et al., 2021), wheat (Cormier et al., 2014; Hitz et al., 2017), and mustard (Gupta et al., 2021). Several genes were highlighted in the previous studies, regulating the genetic basis of NUE. Previous studies showed ammonium (AMT) and nitrate transporters (NRT1/NRT2) play important roles in the N uptake and transport in rice (Huang et al., 2017; Wang et al., 2018) and barley (Karunarathne et al., 2020). Several transcription factors and protein kinases were reported in a plant N regulatory network of *Brassicajuncea* (Goel et al., 2018). Studies also reported on manipulation of genes, regulating primary and secondary N assimilatory pathways to improve NUE (Pathak et al., 2008; Karunarathne et al., 2020). GWAS and downstream genomic analysis was found to be effective in understanding the genetic basis of NUE in several of these crops, but the genetic basis of NUE in switchgrass is not studied yet.

It has been reported that the most fundamental approach to enhanced NUE cultivar development necessitates plant evaluation under both low and high N conditions (Han et al., 2015). This helps in comparative evaluation of performance of a genotype at both low and high N conditions and facilitates the identification of the NUE-efficient genotype (Han et al., 2015). In the present study, our switchgrass experimental population is also grown at a contrasting N fertility condition—low N and moderate N conditions. Since NUE is regulated by biological, physiological, environmental, genetic, agronomic, and developmental factors (Congreves et al., 2021), no single measure of NUE could unravel the complexity of its genetic basis. Therefore, in the present study, we have used a holistic approach to target the genetic basis of NUE by using GWAS of not only the absolute dry biomass trait at low and moderate N but also the different NUE indices, such as NUE and NRE. We performed GWAS analysis on total dry biomass and NUE using 331 diverse switchgrass accessions as well as NRE using 150 diverse accessions that were field grown under two different N treatments. These traits are closely related to NUE in plants and have been widely used in the physiological, agronomical, and genetic studies of NUE (Ball Coelho et al., 2006; Lemus et al., 2008; Yang et al., 2009; Sadeghpour et al., 2014; Karunarathne et al., 2020). Our assumption is that the genes and the biological process uncovered from the GWAS analysis of the NUE and related traits should depict the genetic basis to improve the NUE. Here, we highlighted the several SNPs and candidate genes for NUE and related traits in switchgrass. We used linkage disequilibrium analysis to further support the GWAS-derived candidate genes and, finally, put forward an interesting discussion on the role of N in modulating the expression of these GWAS candidate genes. To our knowledge, this is the first report on the genetic basis of NUE of field-grown switchgrass.

MATERIALS AND METHODS

Field Experimental Design

A highly diverse panel of 331 switchgrass accessions (Lovell et al., 2021) was planted in May 2019 in a 75.2 m × 122.5 m dimension at The University of Tennessee Plant Sciences Unit of the East Tennessee Research and Education Center (ETREC) (latitude: 35°54′11.14″N; longitude: 83°57′33.31″W;

and elevation: 255.7 m.). Planting details and experimental design can be found in Li et al. (2020) and Xu et al. (2021). Briefly, the 331 accessions were planted under two nitrogen (N) fertility treatments: one with moderate nitrogen (135 kg of N ha^{-1}), while the other with low (0 kg of N ha^{-1}) supplementation in 2019 and 2020. Each of the 330 accessions has four replicates in the field (2 replicates per N treatment), totaling 1,320 switchgrass plants, plusone control AP13 ("Alamo") grown with 40 replicates (20 at low and 20 at moderate nitrogen), which were arranged in honeycomb design with ∼2.5 m interplant spacing. AP13 is the reference sequenced lowland cultivar, which is broadly used as a reference genome for switchgrass (Lovell et al., 2021). The field is equipped with a weather station (HOBO, RX3000, Bourne, MA, United States). The average temperature was 23.8°C, and the average precipitation was 0.03 mm during the period of July 2020 to December 2020.

Biomass Quantification

The dry biomass for each switchgrass accession was quantified as previously described (Li et al., 2020). Briefly, the biomass for each plant was quantified at the end of season after plant senescence. The aboveground biomass of individual plants was harvested and weighed. Subsequently, ten random tillers were harvested from each plant and oven-dried at 45°C for 72 h. Weight of the 10 tillers before and after drying was used to determine the ratio of dry-to-fresh weight. Total dry biomass was determined by calculating the percentage of water loss recorded for each subsample and subsequently applying the water loss percentage to the respective total wet biomass weight for individual plants.

Nitrogen Use Efficiency Index Calculation

The following equations were adopted from Ball Coelho et al. (2006), Lemus et al. (2008), Sadeghpour et al. (2014) to calculate NUE.

$$NUE\ (KgKg/m^2) = (BMY_f - BMY_u)/N_s \quad (1)$$

BMY_f = Biomass yield (BMY) of the fertilized plant.
BMY_u = Biomass yield of the unfertilized plant.
N_s = Nitrogen fertilizer at the given rate.

Nitrogen Quantification

The detail of the nitrogen quantification was previously described in Xu et al. (2021). Briefly, nitrogen content of the aboveground biomass was measured *via* near-infrared spectroscopy (NIRS) using a FOSS 6500 NIR system (Silver Spring, MD, United States). Nitrogen content was measured at two developmental time points during the field-growing season: one in August 2020 at mid-season (M) and the other in December 2020 at the end of season (S). A total of 150 accessions in two replicates in two N treatments and two time points (150 × 2 × 2 × 2 = 1,200 samples) were used, i.e., 300 plants at mid-season at low N, 300 plants at mid-season at moderate N, 300 plants at the end of season at low N, and 300 plants at the end of season at moderate N were used. The 150 accessions were chosen based on biomass yield data of the 2019 growing season (Li et al., 2020). Two tillers containing both stems and leaves were collected from each plant, and the samples were oven dried at 45°C for 72 h. The dried tillers were then chipped into 5–8 pieces, each around 4–6 inch long, prior to milling. The chipped samples were milled with a Wiley Mill (Thomas Scientific, Model 4, Swedesboro, NJ, United States) through a 20-mesh screen (1.0-mm particle size).

Nitrogen Remobilization Efficiency Index Calculation

Nitrogen remobilization efficiency index calculation was performed by adopting the equation from Yang et al. (2009).

$$NRE = (M - S)/M \quad (2)$$

where M and S represent nitrogen content at the green/mature (mid-season) and senescent (the end of season) stages, respectively. Since we took N samples at two different time points (M and S) from each of the 150 accessions grown at low N condition and moderate N condition, we calculated NRE for low N and NRE for moderate N condition separately.

Phenotypic Data

We evaluated five NUE-related traits. All traits were treated independently. NUE ratio/indices traits were derived prior to calculation of the best linear unbiased predictions (BLUP) to minimize noise. We removed outliers using the median absolute deviation (MAD) method such that any phenotypic values with MAD > 4 from the population median for a particular trait were removed. Variance components were estimated from a mixed linear model where accession and replication were fitted as random effects and were used to estimate broad sense heritability on a line-mean basis as previously described (Holland et al., 2003).

Genome Wide Association Study and Linkage Disequilibrium Analysis

Methods for SNP variant calling were described previously (Lovell et al., 2021). Briefly, whole-genome resequencing data for 331 genotypes were obtained using Illumina genetic analyzers at the DOE Joint Genome Institute. After removing SNPs with more than 10% missing genotypes, the genotypes with more than 10% missing SNPs, the SNPs with severe departure from Hardy Weinberg Equilibrium (SNPs with HWE > 1E-50 removed), and the SNPs with minor allele frequency (MAF < 0.01), the SNPs with $r^2 \geq 0.95$, a total of 11,976,627 SNPs were available for the downstream analysis.

Genome-wide association tests for all phenotypic traits were performed using the genome-wide complex trait analysis (GCTA) software using the following linear model (Yang et al., 2011). Phenotypic BLUPs, a genetic relationship matrix, and 11,976,627 SNPs were used for the association test. Univariate GWAS was run for six phenotypic traits using the following model:

$$y = X\beta + Wu + \alpha + \varepsilon \quad (3)$$

where y is a phenotypic vector of size n x 1, with n representing sample size, β is a q x 1 vector of fixed effect that includes the

first three eigenvectors from the PCA analysis of the genomic data with its incidence matrix X (an n x q matrix of covariates), u is the p x 1 vector of additive SNP effects with its incidence matrix W (an n x p genotype matrix), α is the n x 1 vector of random effects that include the genetic relationship matrix (GRM), and ε is the n x 1 vector of residual random effects.

Since the Bonferroni threshold for multiple hypothesis correction is too stringent for significant SNPs, the genome-wide threshold of significance in this study was set to $8. \times 10^{-8}$ (1/N, with N = 11,976,627 SNPs). Bonferroni assumes each tested SNP is independent, but the presence of LD between SNPs makes that assumption incorrect and overly stringent. Previously, a similar threshold set was being widely used in other species, such as maize and Arabidopsis (Wen et al., 2014; Wu et al., 2021; Zhu et al., 2021). Candidate gene lists were obtained from the 10-kb interval of the peak GWAS SNP. However, if the gene was not found within that range, we chose the nearest gene left and right from the peak GWAS SNPs. Gene annotations of the candidate genes were based on the orthologs of *Arabidopsis thaliana* and rice (*Oryza sativa*).

Pairwise LD values between peak GWAS SNPs and SNPs within 20-kb interval SNPs (10 kb up and downstream) of peak GWAS SNPs were calculated using squared allele-frequency correlations (r^2) using plink version 1.9 (Chang et al., 2015). All SNPs were filtered at a 1% minor allele frequency. We also computed the proportion of variance in phenotype explained (PVE), as previously described in Shim et al. (2015), for those GWAS peak SNPs that were in moderate-to-strong LD with the SNPs underlying associated candidate genes.

RESULTS

Characterization of the Phenotypic Variability of Nitrogen Use Efficiency and the Related Traits

The extent of the phenotypic variability of dry biomass at low and moderate N and NUE was assessed using the 331-switchgrass diversity panel, while the N content at mid-season and the end of season, NRE at low N and NRE at moderate N were assessed using 150 switchgrass accessions grown at low and moderate N conditions. The full data used to perform the phenotypic variability of NUE and the related traits can be found in **Supplementary Tables 1, 2**. A descriptive statistical summary of the absolute traits (dry biomass at low and moderate N, and N content at mid-season and the end of season), as well as derived NUE indices (NUE and NRE), is presented in **Table 1**.

We found that the mean dry biomass at the end of season for both low and moderate N conditions in the switchgrass GWAS panel to be similar; however, the range for dry biomass at moderate N (0.03–9.11 Kg) was larger compared to dry biomass at low N (0.08–7.77 Kg) (**Table 1**). The heritability of dry biomass at both low and moderate N is high (low-0.94 and moderate-0.93) (**Table 1**), indicating the trait is highly heritable and, therefore, provides the basis for further genetic improvement.

Using the absolute dry biomass traits at low and moderate N, we also calculated NUE as derived traits using Equation 1 (see Section "Materials and Methods"). The mean NUE was found to be 0.67 kgkg/m^2. We found a broad range of NUE in our diversity panel, including negative values. The negative values indicate that the dry biomass at low N is higher compared to the dry biomass at moderate N, and, as such, those lines could be even more effective to explore further as nitrogen use efficient lines. While the heritability of absolute dry biomass at low and moderate traits was found to be high, the heritability of NUE was found to be low (0.39), indicating derived indices, such as NUE, are much more complex and should be influenced much more by the environment and governed by multiple genes (**Table 1**).

Regarding the N content in tillers, we found that the mean N content of the switchgrass accessions at the end of season for both low and moderate N conditions (0.72 and 0.76%, respectively) is lower than the mean N content at the mid-season (1.04 and 1.14%, respectively) (**Table 1**), indicating the plant during senescence lowers the N content in tillers regardless of N fertilizers treatment. Also, the mean N content at moderate N condition was found to be relatively higher than the mean N content at low N at both mid-season and end-of-season harvests (**Table 1**). Overall, the heritability of the N content for the end of season was found to be higher as compared to mid-season N content; however, the heritability was found to be consistent for mid-season low and moderate N conditions (0.59 for low N and 0.54 for moderate N), as well as the end-of-season low and moderate N conditions (0.74 for low N and 0.78 for moderate N) (**Table 1**). In addition to the absolute N content in tillers at mid-season and the end of season, we also calculated NRE as a derived trait at low N and moderate N conditions. The mean NRE for moderate N (0.32) was found to be higher compared to mean NRE for low N (0.29), indicating that moderate nitrogen treatment has potentially enhanced the remobilization use efficiency compared to low-nitrogen treatment. The heritability of NRE at moderate N (0.64) is higher than at low N (0.54) (**Table 1**).

Top 10 Nitrogen Use Efficiency Accessions in the Switchgrass Genome Wide Association Study Panel

We used two different perspectives to identify the top 10 NUE lines (**Table 2**); (1) accessions ranked based on the NUE negative value (highest fold change of low N/moderate nitrogen) and (2) accessions ranked based on the NUE positive value (highest fold change of moderate N/low nitrogen). Category 1 indicates those accessions that were highly N use efficient even under the low-N condition, while Category 2 indicates those accessions that showed highest performance when supplemented with moderate N but do poor with low-N treatment. Our analysis identified J504.C as the most efficient NUE accession in Category 1 with fold change of (10.28), followed by J612.C (3.79), J008.C (3.66), Performer TCL-32 (3.09), and J226.A (2.48) (**Table 2**.1). J504.C, J612.C, J008.C, and J226.A are all lowland tetraploid accessions collected from Missisipppi, Rhode Island, Arkansas, and Texas, United States, respectively. Performer TCL-32 was collected from

TABLE 1 | A descriptive statistical summary [mean, standard error (SE), and range] of NUE and related traits and their estimated heritability at low- and moderate-N conditions on a switchgrass diversity panel.

Treatment	Trait	Unit	Trait category	No. lines	Mean	SE	Range	Heritability
Low N	Dry biomass end-of-season	Kg	Absolute	676	2.27	0.06	0.08–7.77	0.94
Moderate N	Dry biomass end-of-season	Kg	Absolute	674	2.29	0.06	0.03–9.11	0.93
	NUE	$KgKg/m^2$	Derived	670	0.67	1.45	(−242.36)–178.51	0.39
	Midseason nitrogen	%	Absolute	295	1.04	0.01	0.48–1.65	0.59
Low N	End-of-season nitrogen	%	Absolute	297	0.72	0.01	0.26–1.63	0.74
	NRE	%	Derived	294	0.29	0.01	(−1.24)–0.74	0.54
	Midseason nitrogen	%	Absolute	293	1.14	0.01	0.62–1.74	0.54
Moderate N	End-of-season nitrogen	%	Absolute	256	0.76	0.01	0.09–1.50	0.78
	NRE	%	Derived	252	0.32	0.02	(−1.06)–0.92	0.64

The traits were categorized as absolute and derived traits. The derived traits, such as nitrogen use efficiency (NUE), were calculated from the absolute dry biomass at low and moderate N, while NRE was derived from N content on tillers at midseason and end-of-season growth stages. More details of calculation of these derived traits can be found in Section "Materials and Methods." Dry biomass was measured in a full panel (330 accessions), with two replications each in low- and moderate-N treatments plus AP13 as control with 20 replications in low N and 20 replications in moderate N, while N content in tillers was measured using 150 accessions, with two replications each of low- and moderate-N treatments.

TABLE 2 | Top 10 nitrogen use-efficient switchgrass accessions.

2.1	Switchgrass accession	Mean total dry Biomass_Moderate N (Kg)	Mean total dry Biomass_Low N (Kg)	NUE ($KgKg/m^2$)	Fold change (Low N/Moderate N)
	J504.C	0.62	6.37	−195.61	10.28
	J612.C	0.17	0.66	−16.57	3.79
	J008.C	0.90	3.31	−81.74	3.66
	Performer TCL-32	0.88	2.72	−62.63	3.09
	J226.A	2.26	5.61	−113.70	2.48
2.2	**Switchgrass accession**	**Mean total dry Biomass_Moderate N (Kg)**	**Mean total dry biomass_Low N (Kg)**	**NUE ($KgKg/m^2$)**	**Fold change (Moderate N/Low N)**
	J477.B	3.24	0.70	86.34	4.61
	J500.B	2.24	0.52	58.52	4.33
	J006.C	1.80	0.52	43.72	3.49
	J466.B	5.42	1.97	117.31	2.75
	J516.C	2.51	0.95	53.08	2.65

The top 10 accessions were categorized into two categories. 2.1 shows the top five NUE accessions based on the fold change (low N/moderate N), while 2.2 shows the top five NUE accessions based on the fold change (moderate N/low N). The essence of these two categories is mentioned in text. The means from the two replicates from each of low-N and moderate-N accessions were taken from untransformed data to calculate the NUE. The NUE was calculated based on the Equation 1 in Section "Materials and Methods".

North Caroline, NC, United States, but the information on its ploidy level was not found.

In Category 2, Accession J477.B was found to be the most efficient NUE accession with fold change of 4.61, followed by J500.B (4.33), J006.C (3.49), J466.B (2.75), and J516.C (2.65) (**Table 2**.2). J500.B, J006.C, and J516.C are all lowland tetraploid accessions collected from Mississippi, North Carolina, and New York, United States, respectively. J477.B is tetraploid and collected from Arkansas, United States, but the information on lowland or upland was not found. Similar information was not found for Accession J466.B. All the NUE-ranked accessions from the switchgrass GWAS panel can be found in **Supplementary Table 3**.

Correlation Analysis Among the Nitrogen Use Efficiency and the Related Traits

We performed a pairwise Pearson correlation analysis to access the relationship between NUE and the related traits. The pairwise correlation that was significant at false discovery rate (*qFDR-values* < 0.05) was only included for further explanation (**Figure 1** and **Supplementary Tables 4A,B**). Dry biomass at low N had a strong positive correlation with dry biomass at moderate N (*r*, 0.88) (**Figure 1** and **Supplementary Tables 4A,B**). NUE had a significant positive correlation with dry biomass at moderate N (*r*, 0.35; *qFDR-value*, 0.00013), while an insignificant negative correlation with dry biomass at low N (*r*, −0.14; *qFDR-value*, 0.22), inferring strong contribution from moderate N toward the plant biomass (**Figure 1** and **Supplementary Tables 4A,B**).

It is surprising to not see any significant correlation between any of the absolute dry biomass traits or their derivative traits (NUE) with that of absolute N content at mid-season and at the end of season, as well as their derivative traits (NRE) (**Figure 1** and **Supplementary Tables 4A,B**). This might be due to the low sample size of N content at mid-season and the end of season at both low and moderate N conditions. It is interesting to observe that NRE is negatively correlated with the

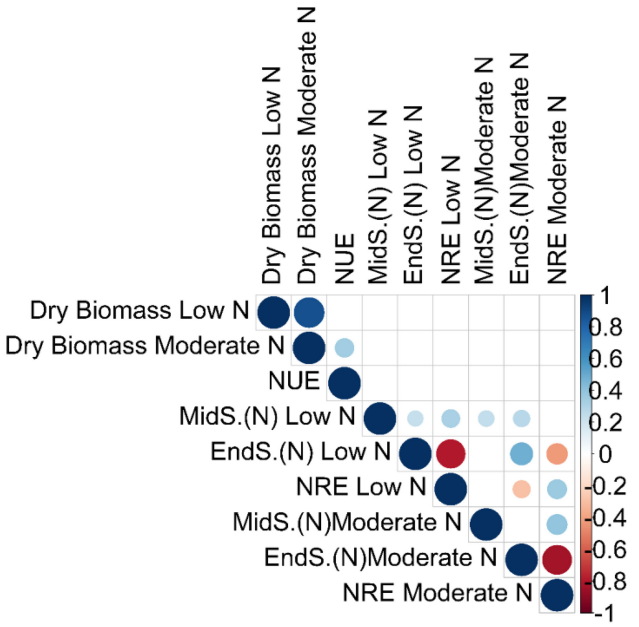

FIGURE 1 | Correlation analysis among the NUE and the related traits. Pairwise Pearson correlation analysis between NUE and related traits was performed using the best linear unbiased predictions (BLUPs) of the switchgrass diversity panel. The correlation matrix was visualized in R v.3.4.3 (R Core Team). Each dot represents a significant correlation coefficient (r) at false discovery rate (qFDR) values < 0.05. Blue dots indicate a strong positive correlation, while light blue indicates a moderate positive correlation. Similarly, red dots indicate a strong negative correlation, while orange indicates a moderate negative correlation. The stronger the correlation (positive or negative), the bigger are the blue and red dots, respectively, and *vice versa*. MidS.(N) and EndS.(N) indicate the % of N content in tillers at the mid season and the end of season, respectively. The unit of dry biomass is Kg; NUE (nitrogen use efficiency) is Kg Kg/m2; and NRE (nitrogen remobilization efficiency) is % (percent of total).

end of season (N) while positively correlated with mid-season (N) regardless of two N treatment conditions (**Figure 1** and **Supplementary Tables 4A,B**). The strongest significant negative correlation was found between NRE at moderate N and end-of-season N content at moderate N (*r*, −0.83) (**Figure 1** and **Supplementary Tables 4A,B**)

Potential Candidate Genes in the Switchgrass Genome Wide Association Study Panel

To uncover the genetic architecture of NUE, dry biomass at moderate N and dry biomass at low N, we explored the natural variation in the 331-switchgrass diversity panel genotyped with 11,976,627 SNP markers. The SNP numbers are after the minor allele frequency (MAF) filtration at 1%. For NRE at low N and NRE at moderate N, we explored the natural variation in 150 switchgrass accessions. We used the mixed linear model using GCTA (Yang et al., 2011) to perform the GWAS. At the specified threshold, overall, we obtained 19 unique (i.e., non-redundant) SNPs across Chromosome 2 (2K), 3 (3K), 4 (4K), 6 (6K), 7 (7K), 8 (8K), 13 (4N), 14 (5N), 15 (6N), and 18 (9N) (**Figure 2** and **Supplementary Table 5**).

We identified 32 unique candidate genes from the 10-kb interval, as well as from the nearest left and right from each unique GWAS peak SNPs (**Supplementary Table 5**). The GWAS candidate gene list of NUE and the related traits in switchgrass, along with its Arabidopsis and rice orthologous gene description, can be found in **Supplementary Table 5**.

Linkage Disequilibrium Analysis Supports Genome Wide Association Study Candidate Genes

We found the GWAS peak SNP Chr06N_45879490 (located in Chromosome 06N at 45879490 bp) being significantly associated with the dry biomass at moderate N (*p*-value, 5.43E-10), which led to two candidate genes: Pavir.6NG264600 and Pavir.6NG264700 (**Supplementary Table 5**). Gene Pavir.6NG264600 was found to be 7703 bp away from SNP Chr06N_45879490, while Pavir.6NG264700 was just 9 bp away from the SNP Chr06N_45879490 (**Supplementary Table 5**).

We also performed the pairwise LD analysis using the squared allele-frequency correlations (r^2) between the GWAS peak SNP and the SNPs across 20 kb (10 kb up/downstream) of the peak SNPs. Emphasis was given between the GWAS peak SNPs and SNPs, residing within the candidate genes within the 20 kb region to better understand the LD association between them. Our LD analysis strongly supported the Pavir.6NG264700 to be a strong candidate gene for dry biomass at the moderate-N condition (**Figure 3A**). The peak SNP Chr06N_45879490 (**Figure 3A**—a purple arrow) was found to be in moderate to strong LD with the top 4 SNPs (**Figure 3A**—a red arrow, **Supplementary Table 6**), residing within gene Pavir.6NG264700, i.e., Chr06N _45879322 (r^2, 0.57), Chr06N _45879172 (r^2, 0.55), Chr06N _45879369 (r^2, 0.52), Chr06N _45879412 (r^2, 0.43) (**Figure 3A** and **Supplementary Table 6**). The SNPs residing within gene Pavir.6NG264600 had low LD (r^2, 0.1), with the GWAS peak SNP Chr06N_45879490, suggesting gene Pavir.6NG264700 is worthwhile to explore for downstream analysis as compared to gene Pavir.6NG264600 (**Figure 3A**). We computed PVE for SNP Chr06N_45879490 and was found to be 0.104.

Next, we identified another interesting GWAS peak SNP Chr08K_12432787, which was significantly associated with the NUE (*p*-value, 4.07E-8) that led to the candidate gene Pavir.8KG136200 (**Supplementary Table 5**). Interestingly, the gene was found to be residing within the GWAS peak SNP Chr08K_12432787 (**Figure 3B** and **Supplementary Table 5**).

We again performed the pairwise LD analysis using the squared allele-frequency correlations (r^2) between the GWAS peak SNPChr08K_12432787 and the SNPs residing within the candidate genes within the 20 kb region (10 kb up/down stream of GWAS peak SNP) to better understand the LD association between them. Our LD analysis strongly supported Pavir.8KG136200 to be a strong candidate gene for NUE (**Figure 3B**). The peak SNP Chr08K_12432787 (**Figure 3B**—a purple arrow) was found to be in strong LD with the SNPs Chr08K_12432786 (r^2, 0.78) (**Figure 3**—a red arrow just below

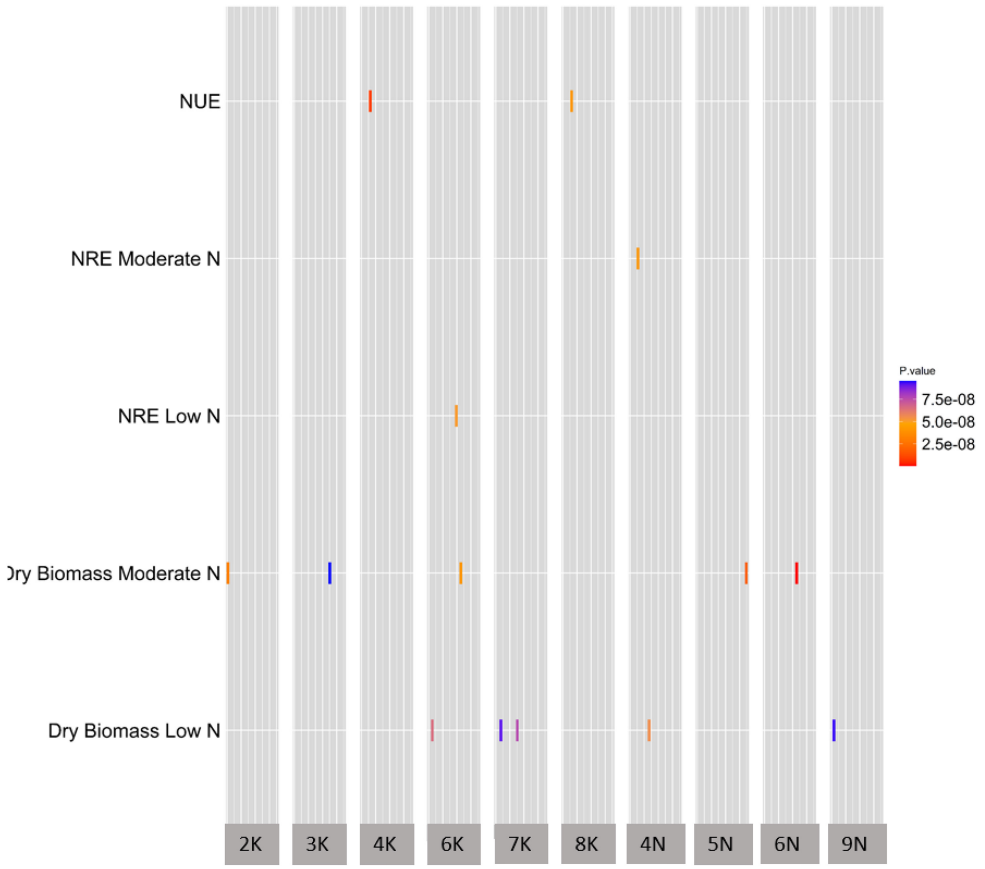

FIGURE 2 | A summary of GWAS of NUE and the related traits. The heatmap of GWAS of NUE and the related traits demonstrating significant SNP distribution across chromosomes. All five traits on y-axis were significant at the genome-wide threshold level of significance at 8.0×10^{-8} (1/N, with N = 11,976,628, where N is the total number of SNP markers used in this GWAS study). The x-axis shows the chromosome number for significant SNPs, while the y-axis shows all traits with significant SNP-trait associations. The width of the gray bar of a given chromosome number on the x-axis indicates the chromosomal position of that chromosome. The units of traits in y-axis; NUE (nitrogen use efficiency) is Kg Kg/m^2; NRE at moderate and low N is %; dry biomass for low and moderate N is Kg; rectangles represent SNPs that are color coded based on *p*-value.

the purple arrow, **Supplementary Table 7**) residing within gene Pavir.8KG136200, supporting our candidate gene for NUE. On the other hand, GWAS peak SNPChr08K_12432787was found to be in low LD with SNP residing within gene Pavir.8KG136001 (**Figure 3B** and **Supplementary Tables 5, 7**). We also computed the PVE for SNP Chr08K_12432787 and was found to be 0.083.

DISCUSSION

Understanding the genetic basis of NUE is the key for developing nitrogen use-efficient switchgrass lines. To our knowledge, there is no documented study on the genetic basis of NUE in field-grown switchgrass at two contrasting nitrogen fertility treatments. Here, we studied the genetic basis of NUE in switchgrass. Our results provide interesting insights into the genetic architecture of NUE and its relationship among the various NUE-related traits. We highlighted *CCoAOMT* and *AL6* as important candidate genes to regulate NUE and the potential role of N treatments in modulating the expression of these genes.

Response of N Fertilization to Switchgrass Accessions May Not Be Immediate and Requires Longer Establishment Time

We found the mean dry biomass for the switchgrass diversity panel grown in low- and moderate-N conditions to be similar (**Table 1**). One of the potential reasons to have a similar dry biomass mean for low- and moderate-N-grown switchgrass may be due to the early establishment of the switchgrass panel (Wolf and Fiske, 2009; Fike et al., 2017). The dry biomass data presented here were collected in the 2nd year of the switchgrass field trial. It has been reported that the time required to reach switchgrass full productivity can vary widely. The production guides often suggest that switchgrass stands may not be fully established (i.e., not fully productive) until the third growing season (Wolf and Fiske, 2009; Fike et al., 2017), which might be one of the reasons that the response to N fertilization could not be fully seen. Switchgrass productivity in response to N depends on several factors that include genotype; location;

environmental conditions, such as precipitation and soil; and managements, such as harvest frequency and timing (Fike et al., 2017). Interestingly, our analysis on the mean N content at moderate N was found to be relatively higher than the mean N content at low N at both the mid-season and the end of season (**Table 1**). This indicates that the response to N treatment has started to show up but may need longer duration to significantly impact other phenotypic traits, such as dry biomass yield.

Accessions Having Negative Nitrogen Use Efficiency Values Should Be Considered Acceptable, While Negative Nitrogen Remobilization Efficiency Values Should Be Considered Unacceptable for Breeding Switchgrass

We have found a range of both positive and negative values when calculating NUE and NRE in our study (**Tables 1**, **2**). These positive and negative signs would play important roles in subsequent selection of switchgrass accessions for improving their NUEs. Positive NUE values of a switchgrass accession indicate the performance of the accession improved by the application of N fertility treatment as compared to the unfertilized condition (higher N responsiveness), and, hence, breeders could select these lines for the areas where there is ample abundance of N fertilizers (Han et al., 2015). However, care should be taken in applying the recommended dose of fertilizers to gain the benefit while, at the same time, mitigating the unwanted environmental consequences. Negative NUE values of a switchgrass accession indicate that the accession performs best even under low N and does not need to be supplemented with N fertilizers (high-genetic N efficiency) (Han et al., 2015). These accessions will be best to use from an NUE point of view and can be suitable to those areas with low-fertility soil status (Han et al., 2015). Hence, both categories of NUE could help breeders produce nitrogen use-efficient switchgrass accessions based on the choice of availability of N fertilization, response of accessions to N fertilizers, and with respect to protect the environment due to heavy use of N fertilizers. We identified the top 10 switchgrass accessions ranked based on the most positive and negative NUE values (**Table 2**); however, we want to emphasize that this result is based on a single location here at Knoxville, TN. Additional experiments are needed to evaluate these top accessions at different locations and at multiple time points to check the stability and consistency for both high-genetic N efficiency and high-N responsiveness. Therefore, these experiments warrant additional future evaluations. These selected accessions open the avenues to further breed for nitrogen use-efficient switchgrass accessions. It further explores the differential genes and the gene network to understand the underlying biological mechanism for the nitrogen use-efficient lines under contrasting N fertility conditions. Similar to NUE, we found NRE also had both positive and negative values in its distribution (**Table 1**). Positive NRE of a switchgrass accession indicates the N content in the tillers of the mid-season is higher than the N content in tillers at the end of season (Yang et al., 2016), which is an acceptable trait for breeding nitrogen remobilization efficiency. However, negative NRE values indicate N content in tillers of the end of season is higher than the N content in tillers at the mid-season, indicating these accessions are not favorable to breed further as they are inefficient to remobilize the N content (Yang et al., 2009). This information will be important for breeders to select the switchgrass accession that has the highest N content at the mid-season growth but lowest at the end-of-season growth.

Gene Related to the Lignin Biosynthesis (*CCoAOMT*) Was Found to Be Associated With Nitrogen Use Efficiency-Related Traits

We found GWAS peak SNPChr06N_45879490 significantly associated with dry biomass at moderate N that led to candidate gene Pavir.6NG264700 (**Supplementary Table 5**). Pavir.6NG264700 was predicted to best hit the orthologous gene *caffeoyl-CoA O-methyltransferase* (*CCoAOMT*) in rice (LOC_Os08g38900) and S-adenosyl-L-methionine-dependent methyltransferases superfamily protein in Arabidopsis (AT4G34050) (**Supplementary Table 5**).

CCoAOMT is one of the key enzymes reported to be involved in the biosynthesis of monolignols (Wagner et al., 2011; Shen et al., 2013; Liu et al., 2016). In angiosperms, this enzyme is required for the biosynthesis of G- and S-type lignins (Meyermans et al., 2000; Wagner et al., 2011). Evidence has shown that the downregulation of *CCoAOMT* in *Pinus rediata*, *Medicago sativa*, and *Populustremula* × *Populus alba* leads to significant decrease of the G-type lignin but not the S-type lignin, inferring that *CCoAOMT* is mainly required for the biosynthesis of the G-type lignin (Zhong et al., 2000; Guo et al., 2001; Wagner et al., 2011; Liu et al., 2016). Previous studies in several species, such as maize (Li et al., 2013), pine (Wagner et al., 2011), and poplar (Lu et al., 2004), have reported that the suppression of *CCoAOMT* causes lignin reductions. Most of the *CCoAOMT* studies were conducted to understand its direct functional role; however, there are limited studies shown on the response of *CCoAOMT* on the environmental alternation, such as stress or change in plant or soil nutritional status.

A study conducted by Camargo et al. (2014) in *Eucalyptus* shows that the nitrogen fertilization could modulate the expression of *CCoAOMT* expression and its impact on the lignin and total biomass of the plant. Consequently, this would be important to improve the quality and composition of lignocellulosic feedstock, such as switchgrass. The study reported *Eucalyptus* (another bioenergy crop potential of producing lignocellulosic biofuels) grown at contrasting N treatments could be identified with significant differential expression levels of *CCoAOMT* between the two N contrasting treatments, supporting the dynamic role of N in regulating the expression of *CCoAOMT* (Camargo et al., 2014). Camargo et al. (2014) also reported that the expression of phenylpropanoid and lignin biosynthesis genes, such as *phenylalanine ammonia lyase (PAL)*, *Cinnamate-4-hydroxylase* (*C4H*), *4-coumarate CoA ligase* (*4CL*), *caffeic acid O-methyltransferase* (*COMT*), and

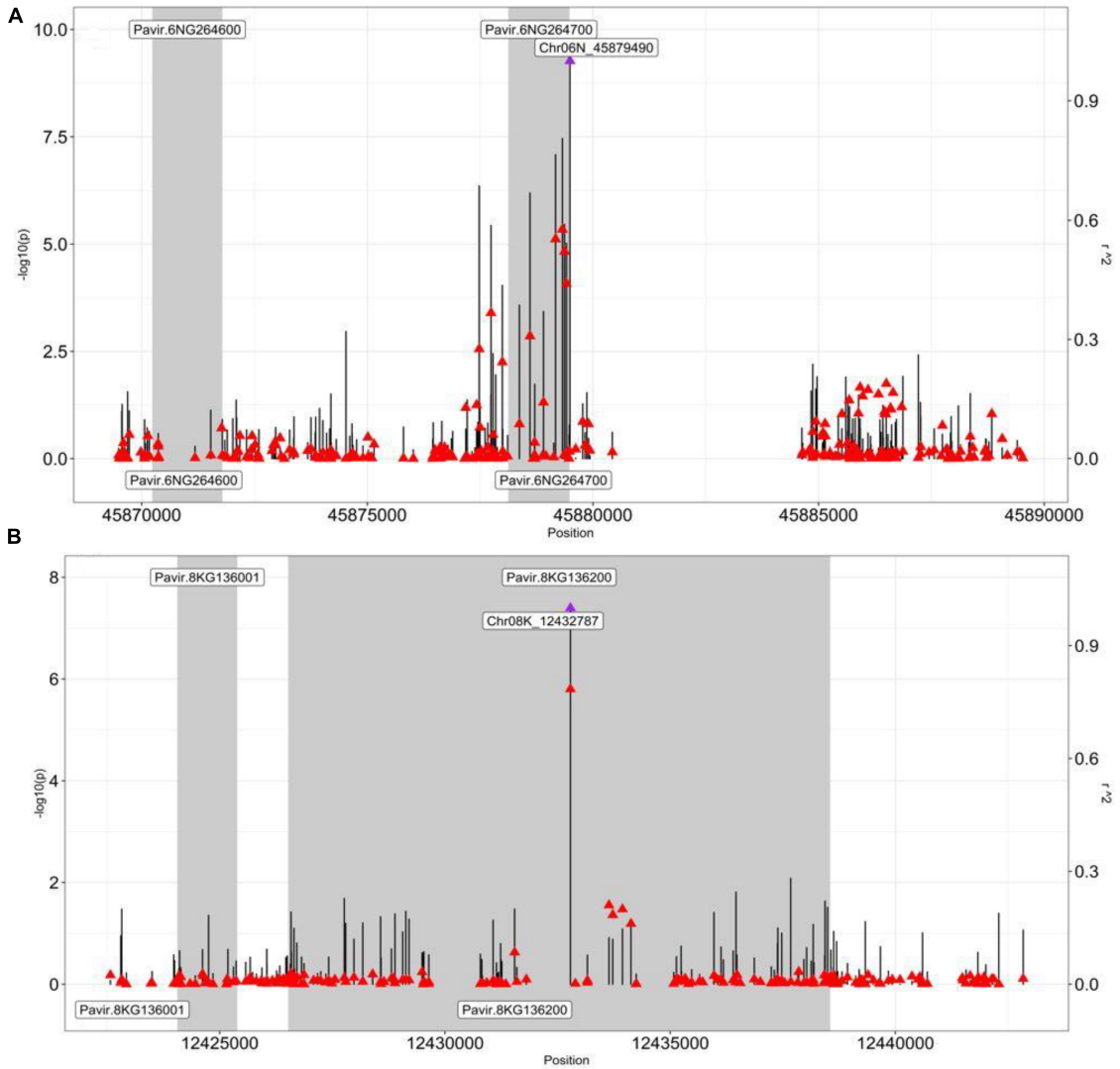

FIGURE 3 | Pairwise LD analysis between the peak SNP and the SNP underlying genes. Pairwise LD estimates (*r2*) of the GWAS peak SNP with SNPs spanning a 20-kb (±10 kb) interval from the GWAS peak SNP. A scatterplot of the association results and LD estimates with the GWAS peak SNP **(A)** Chr06N_45879490 (dry biomass moderate N) and **(B)** Chr08K_12432787 (NUE), with SNPs spanning a 20-kb interval from their respective positions (bp). The negative log10-transformed *p*-values (left, y-axis) and r^2 (right, y-axis) from the GWAS analysis are plotted against the genomic physical position. Vertical lines are the negative –log10 transformed *p*-values for individual SNPs from the GWAS results. Red triangles are pairwise LD r^2 estimates of SNPs with the GWAS peak SNP (a purple triangle). Shaded bars designate genes. Gene Pavir.6NG264700 in panel **(A)** is *caffeoyl-CoA O-methyltransferase* (*CCoAOMT*), and gene Pavir.8KG136200 in panel **(B)** is *alfin-like 6* (*AL6*).

CCoAOMT were downregulated in response to high N fertilization while upregulated in the N-limiting condition (Camargo et al., 2014).

CCoAOMT was mainly described as a key gene in the lignin biosynthesis pathway. Yet, with our GWAS result (**Supplementary Table 5**) and support from our LD analysis (**Figure 3A** and **Supplementary Table 6**), as well as from a previous study (Camargo et al., 2014), we propose *CCoAOMT* as a strong candidate gene for NUE in switchgrass. It is possible that N fertilization could affect the composition and quality of switchgrass lignocellulosic feedstock by modulating the expression of a lignin biosynthesis gene, such as *CCoAOMT* (Camargo et al., 2014). The future study should consider investigating the gene expression study of the *CCoAOMT* at two different N fertilization conditions in switchgrass.

AL6-a Transcription Factor and a Strong Candidate for Nitrogen Use Efficiency in Switchgrass

Genome wide association study peak SNP Chr08K_12432787, which was significantly associated with the NUE, led to the candidate gene Pavir.8KG136200 and was predicted to best hit the orthologous PHD finger protein in rice (LOC_Os11g14010) and *AL6* in Arabidopsis (AT2G02470) (**Supplementary Table 5**). A limited study is found in the literature for the functional

analysis of *AL6*. However, one study showed that *AL6* is involved in the root hair elongation during phosphate deficiency in Arabidopsis (Chandrika et al., 2013). The study identified a T-DNA mutant line from a large-scale genetic screen and found that it has a defect in root hair elongation, specifically under the low-phosphate condition. It was also shown that the mutant phenotype was caused by a mutation in the homeodomain protein *AL6* (Chandrika et al., 2013). The study further concluded that the *AL6* controls the transcription of a suite of genes (*ETC1*, *NPC4*, *SQD2*, and *PS2*); all of which are critical to root hair elongation (Chandrika et al., 2013). Up to now, to our knowledge, there has been no report on the possible role of the *AL6* gene in the N-deficient condition in the literature.

Since we identified *AL6* as a candidate gene associated for the NUE trait (**Supplementary Table 5**) and this gene is also supported by LD analysis (**Figure 3B** and **Supplementary Table 7**), our hypothesis is that, like the phosphate-deficiency condition, *AL6* may also regulate root hair elongation genes in the N-deficient condition. Hence, the variable expression of *AL6* in different switchgrass lines at different N conditions might be the reason for the natural variation of nitrogen use-efficient lines in our diversity GWAS panel. The roles of root hair elongation and growth are critical to nutrient absorption, uptake, and utilization and would be strong factors to contribute directly to the NUE. Gaudin et al. (2011) reported a decrease in root hair length under N stress in maize (Gaudin et al., 2011), while Foehse and Jungk (1983) found that tomato, rape, and spinach significantly increase root hair length when the nitrate concentration was decreased from 1,000 to 2 mM (Foehse and Jungk, 1983), suggesting the response to root hair in response to N availability may be species specific. For a future study, we will be exploring the functional role of *AL6* in switchgrass root hair in response to two N treatments, low and moderate. We will also perform the differential gene expression analysis of *AL6* at low and moderate N conditions using RNAseq analysis. It would be interesting to observe either of our hypothesis is supported or rejected.

CONCLUSION

We have shown here that, by targeting NUE using a holistic approach, we can dissect its genetic architecture to identify novel SNPs and genes. We found genes related to lignin biosynthesis (*CCoAOMT)* and gene encoding root hair elongation (*AL6*), regulating the natural variation of NUE and related traits in switchgrass. We also highlighted the N fertilizer application potentially plays a role in modulating not only the biomass quantity but, more importantly, the biomass quality and composition. We identified the top ten nitrogen-efficient switchgrass accessions and uncovered the relationship among the various NUE-related traits. Our findings provide exciting possibilities to explore the underlying biological mechanism of NUE and to use marker-assisted selection and GWAS-assisted genomic selection in developing nitrogen use-efficient switchgrass cultivars.

DATA AVAILABILITY STATEMENT

The original contributions presented in the study are included in the article/**Supplementary Material**, further inquiries can be directed to the corresponding authors.

AUTHOR CONTRIBUTIONS

VS performed the experiments, processed and analyzed the data, and wrote the manuscript. HC performed the BLUP and GWAS analysis and assisted in writing the methodology. DK performed GWAS model optimization. YX assisted in writing and revisions to the manuscript. LH, CP, and BW participated in the field experiments and data collection. XW and MS performed nitrogen quantification analysis. DJ performed statistical and computational analysis. RM and MM designed the experiments, participated in result interpretation, supervised the work, and assisted in writing and revisions to the manuscript. CS conceived the study and its coordination, acquired funding, and assisted in interpretation of the results and the revisions to the manuscript. All authors contributed to the text and approved the final manuscript.

FUNDING

This work was supported by funding from the Center for Bioenergy Innovation. The Center for Bioenergy Innovation is a U.S. Department of Energy Bioenergy Research Center supported by the Office of Biological and Environmental Research in the Department of Energy Office of Science (DE-AC05-000R22725).

ACKNOWLEDGMENTS

We thank Thomas Juenger, University of Texas—Austin, for providing the switchgrass GWAS panel. We wish to acknowledge Joint Genome Institute (JGI) for providing genome sequences for the switchgrass GWAS accessions. We also thank Sujan Mamidi and Jeremy Schmutz from Hudson Alpha Institute for their contribution to sequence alignment and variant calling of the genotypic dataset. We also wish to acknowledge Bryce Trull, Eric Stuart, and Kamryn Cregger for their assistance in harvesting and postharvest processing of the switchgrass diversity panel and the East Tennessee Research and Education Center (ETREC)—Plant Sciences Unit for their assistance in field experiments.

SUPPLEMENTARY MATERIAL

The Supplementary Material for this article can be found online at: https://www.frontiersin.org/articles/10.3389/fpls.2022.893610/full#supplementary-material

REFERENCES

Adler, P. R., Sanderson, M. A., Boateng, A. A., Weimer, P. J., and Jung, H.-J. G. (2006). Biomass yield and biofuel quality of switchgrass harvested in fall or spring. *Agron J.* 98, 1518–1525. doi: 10.2134/agronj2005.0351

Ball Coelho, B., Roy, R., and Bruin, A. (2006). Nitrogen recovery and partitioning with different rates and methods of sidedressed manure. *Soil Sci. Soc. Am. J.* 70, 464–473. doi: 10.2136/sssaj2005.0122

Byrnes, B. (1990). Environmental effects of N fertilizer use—An overview. *Fertil. Res.* 26, 209–215. doi: 10.1007/BF01048758

Camargo, E. L. O., Nascimento, L. C., Soler, M., Salazar, M. M., Lepikson-Neto, J., Marques, W. L., et al. (2014). Contrasting nitrogen fertilization treatments impact xylem gene expression and secondary cell wall lignification in Eucalyptus. *BMC Plant Biol.* 14:256. doi: 10.1186/s12870-014-0256-9

Chandrika, N. N. P., Sundaravelpandian, K., Yu, S. M., and Schmidt, W. (2013). Alfin-Like 6 is involved in root hair elongation during phosphate deficiency in *Arabidopsis*. *New Phytol.* 198, 709–720. doi: 10.1111/nph.12194

Chang, C. C., Chow, C. C., Tellier, L. C., Vattikuti, S., Purcell, S. M., and Lee, J. J. (2015). Second-generation PLINK: rising to the challenge of larger and richer datasets. *Gigascience* 4:7. doi: 10.1186/s13742-015-0047-8

Chien, S. H., Teixeira, L. A., Cantarella, H., Rehm, G. W., Grant, C. A., and Gearhart, M. M. (2016). Agronomic effectiveness of granular nitrogen/phosphorus fertilizers containing elemental sulfur with and without ammonium sulfate: a review. *Agron J.* 108, 1203–1213. doi: 10.2134/agronj2015.0276

Congreves, K. A., Otchere, O., Ferland, D., Farzadfar, S., Williams, S., and Arcand, M. M. (2021). Nitrogen use efficiency definitions of today and tomorrow. *Front. Plant Sci.* 12:637108. doi: 10.3389/fpls.2021.637108

Cormier, F., Le Gouis, J., Dubreuil, P., Lafarge, S., and Praud, S. (2014). A genome-wide identification of chromosomal regions determining nitrogen use efficiency components in wheat (*Triticum aestivum* L.). *Theor. Appl. Genet.* 127, 2679–2693. doi: 10.1007/s00122-014-2407-7

Dobermann, A. (2007). "Nutrient use efficiency–measurement and management," in *General Principles of FBMPs, IFA International Workshop on Fertilizer Best Management Practices*, ed. IFA (Paris: International Fertilizer Industry Association(IFA)), 1–30.

Doerge, R. W. (2002). Multifactorial genetics: mapping and analysis of quantitative trait loci in experimental populations. *Nat. Rev. Genet.* 3:43. doi: 10.1038/nrg703

Dohleman, F. G., Heaton, E. A., Arundale, R. A., and Long, S. P. (2012). Seasonal dynamics of above-and below-ground biomass and nitrogen partitioning in M iscanthus× giganteus and P anicum virgatum across three growing seasons. *GCB Bioenergy* 4, 534–544. doi: 10.1111/j.1757-1707.2011.01153.x

Ernst, O. R., Kemanian, A. R., Mazzilli, S., Siri-Prieto, G., and Dogliotti, S. (2020). The dos and don'ts of no-till continuous cropping: evidence from wheat yield and nitrogen use efficiency. *Field Crops Res.* 257:107934. doi: 10.1016/j.fcr.2020.107934

Fike, J. H., Pease, J. W., Owens, V. N., Farris, R. L., Hansen, J. L., Heaton, E. A., et al. (2017). Switchgrass nitrogen response and estimated production costs on diverse sites. *GCB Bioenergy* 9, 1526–1542. doi: 10.1111/gcbb.12444

Fixen, P., Brentrup, F., Bruulsema, T., Garcia, F., Norton, R., and Zingore, S. (2015). "Nutrient/fertilizer use efficiency: measurement, current situation and trends," in *Managing Water and Fertilizer for Sustainable Agricultural Intensification*, eds P. Drechsel, P. Heffer, H. Magen, R. Mikkelsen, and D. Wichelns (Paris: International Fertilizer Industry Association (IFA)), 270.

Foehse, D., and Jungk, A. (1983). Influence of phosphate and nitrate supply on root hair formation of rape, spinach and tomato plants. *Plant Soil* 74, 359–368. doi: 10.1007/BF02181353

Gaudin, A. C., Mcclymont, S. A., Holmes, B. M., Lyons, E., and Raizada, M. N. (2011). Novel temporal, fine-scale and growth variation phenotypes in roots of adult-stage maize (Zea mays L.) in response to low nitrogen stress. *Plant Cell Environ.* 34, 2122–2137. doi: 10.1111/j.1365-3040.2011.02409.x

Glass, A. D., Britto, D. T., Kaiser, B. N., Kinghorn, J. R., Kronzucker, H. J., Kumar, A., et al. (2002). The regulation of nitrate and ammonium transport systems in plants. *J. Exp. Bot.* 53, 855–864. doi: 10.1093/jexbot/53.370.855

Goel, P., Sharma, N. K., Bhuria, M., Sharma, V., Chauhan, R., Pathania, S., et al. (2018). Transcriptome and co-expression network analyses identify key genes regulating nitrogen use efficiency in *Brassica juncea* L. *Sci. Rep.* 8:7451. doi: 10.1038/s41598-018-25826-6

Good, A. G., Shrawat, A. K., and Muench, D. G. (2004). Can less yield more? Is reducing nutrient input into the environment compatible with maintaining crop production? *Trends Plant Sci.* 9, 597–605. doi: 10.1016/j.tplants.2004.10.008

Guo, D., Chen, F., Inoue, K., Blount, J. W., and Dixon, R. A. (2001). Downregulation of caffeic acid 3-O-methyltransferase and caffeoyl CoA 3-O-methyltransferase in transgenic alfalfa: impacts on lignin structure and implications for the biosynthesis of G and S lignin. *Plant Cell* 13, 73–88. doi: 10.1105/tpc.13.1.73

Gupta, N., Gupta, M., Akhatar, J., Goyal, A., Kaur, R., Sharma, S., et al. (2021). Association genetics of the parameters related to nitrogen use efficiency in *Brassica juncea* L. *Plant Mol. Biol.* 105, 161–175. doi: 10.1007/s11103-020-01076-x

Han, M., Okamoto, M., Beatty, P. H., Rothstein, S. J., and Good, A. G. (2015). The genetics of nitrogen use efficiency in crop plants. *Annu. Rev. Genet.* 49, 269–289. doi: 10.1146/annurev-genet-112414-055037

He, K., Xu, S., Zhang, X., Li, Y., Chang, L., Wang, Y., et al. (2020). Mining of candidate genes for nitrogen use efficiency in maize based on genome-wide association study. *Mol. Breeding* 40:83. doi: 10.1007/s11032-020-01163-3

Hitz, K., Clark, A. J., and Van Sanford, D. A. (2017). Identifying nitrogen-use efficient soft red winter wheat lines in high and low nitrogen environments. *Field Crops Res.* 200, 1–9. doi: 10.1371/journal.pone.0228775

Holland, J. B., Nyquist, W. E., and Cervantes-Martínez, C. T. (2003). Estimating and interpreting heritability for plant breeding: an update. *Plant Breed. Rev.* 22, 9–112 doi: 10.1002/9780470650202.ch2

Huang, S., Zhao, C., Zhang, Y., and Wang, C. (2017). "Nitrogen use efficiency in rice," in *Nitrogen in Agriculture-Updates*, eds K. Amanullah and S. Fahad (London: IntechOpen), 188–208.

Jensen, L., and Schjoerring, J. (2011). "Benefits of nitrogen for food, fibre and industrial production," in *The European Nitrogen Assessment*, eds M. A. Sutton, C. M. Howard, and J. W. Erisman (Cambridge: Cambridge University Press), 32–61. doi: 10.1017/cbo9780511976988.006

Karunarathne, S. D., Han, Y., Zhang, X.-Q., Zhou, G., Hill, C. B., Chen, K., et al. (2020). Genome-wide association study and identification of candidate genes for nitrogen use efficiency in barley (*Hordeum vulgare* L.). *Front. Plant Sci.* 11:1361. doi: 10.3389/fpls.2020.571912

Ladha, J. K., Pathak, H., Krupnik, T. J., Six, J., and van Kessel, C. (2005). Efficiency of fertilizer nitrogen in cereal production: retrospects and prospects. *Adv. Agron.* 87, 85–156. doi: 10.1016/S0065-2113(05)87003-8

Lam, H. M., Coschigano, K., Oliveira, I., Melo-Oliveira, R., and Coruzzi, G. (1996). The molecular-genetics of nitrogen assimilation into amino acids in higher plants. *Annu. Rev. Plant Biol.* 47, 569–593. doi: 10.1146/annurev.arplant.47.1.569

Lander, E. S., and Schork, N. J. (1994). Genetic dissection of complex traits. *Science* 265, 2037–2048. doi: 10.1126/science.8091226

Langholtz, M., Davison, B. H., Jager, H. I., Eaton, L., Baskaran, L. M., Davis, M., et al. (2021). Increased nitrogen use efficiency in crop production can provide economic and environmental benefits. *Sci. Total Environ.* 758:143602. doi: 10.1016/j.scitotenv.2020.143602

Lemus, R., Parrish, D. J., and Abaye, O. (2008). Nitrogen-use dynamics in switchgrass grown for biomass. *Bioenergy Res.* 1, 153–162. doi: 10.1007/s12155-008-9014-x

Li, F., Piasecki, C., Millwood, R. J., Wolfe, B., Mazarei, M., and Stewart, C. N. Jr. (2020). High-throughput switchgrass phenotyping and biomass modeling by UAV. *Front. Plant Sci.* 1: 574073. doi: 10.3389/fpls.2020.574073

Li, X., Chen, W., Zhao, Y., Xiang, Y., Jiang, H., Zhu, S., et al. (2013). Downregulation of caffeoyl-CoA O-methyltransferase (CCoAOMT) by RNA interference leads to reduced lignin production in maize straw. *Genet. Mol.Biol.* 36, 540–546. doi: 10.1590/S1415-47572013005000039

Liu, S. J., Huang, Y. H., He, C. J., Cheng, F., and Zhang, Y. W. (2016). Cloning, bioinformatics and transcriptional analysis of caffeoyl-coenzyme A 3-O-methyltransferase in switchgrass under abiotic stress. *J. Integr. Agric.* 15, 636–649. doi: 10.1016/S2095-3119(16)61363-1

Lovell, J. T., MacQueen, A. H., Mamidi, S., Bonnette, J., Jenkins, J., Napier, J. D., et al. (2021). Genomic mechanisms of climate adaptation in polyploid bioenergy switchgrass. *Nature* 590, 438–444. doi: 10.1038/s41586-020-03127-1

Lu, J., Zhao, H., Wei, J., He, Y., Shi, C., Wang, H., et al. (2004). Lignin reduction in transgenic poplars by expressing antisense CCoAOMT gene. *Prog. Nat. Sci.* 14, 1060–1063. doi: 10.1080/10020070412331344801

Mackay, T. F. (2001). The genetic architecture of quantitative traits. *Annu. Rev. Genet.* 35, 303–339. doi: 10.1146/annurev.genet.35.102401.090633

Meyermans, H., Morreel, K., Lapierre, C., Pollet, B., De Bruyn, A., Busson, R., et al. (2000). Modifications in lignin and accumulation of phenolic glucosides in poplar xylem upon down-regulation of caffeoyl-coenzyme A O-methyltransferase, an enzyme involved in lignin biosynthesis. *J. Biol. Chem.* 275, 36899–36909. doi: 10.1074/jbc.M006915200

Morosini, J. S., de Freitas Mendonça, L., Lyra, D. H., Galli, G., Vidotti, M. S., and Fritsche-Neto, R. (2017). Association mapping for traits related to nitrogen use efficiency in tropical maize lines under field conditions. *Plant Soil* 421, 453–463. doi: 10.1007/s11104-017-3479-3

o Di Nasso, N. N., Roncucci, N., and Bonari, E. (2013). Seasonal dynamics of aboveground and belowground biomass and nutrient accumulation and remobilization in giant reed (*Arundo donax* L.): a three-year study on marginal land. *Bioenergy Res.* 6, 725–736. doi: 10.1007/s12155-012-9289-9

Pathak, R. R., Ahmad, A., Lochab, S., and Raghuram, N. (2008). Molecular physiology of plant nitrogen use efficiency and biotechnological options for its enhancement. *Curr. Sci.* 94, 1394–1403.

Ranjan, R., and Yadav, R. (2019). Targeting nitrogen use efficiency for sustained production of cereal crops. *J. Plant Nutr.* 42, 1086–1113. doi: 10.1080/01904167.2019.1589497

Reynolds, J., Walker, C., and Kirchner, M. (2000). Nitrogen removal in switchgrass biomass under two harvest systems. *Biomass Bioenergy* 19, 281–286. doi: 10.1016/S0961-9534(00)00042-8

Sadeghpour, A., Gorlitsky, L., Hashemi, M., Weis, S., and Herbert, S. (2014). Response of switchgrass yield and quality to harvest season and nitrogen fertilizer. *Agron. J.* 106, 290–296. doi: 10.2134/agronj2013.0183

Sanderson, M., Reed, R., McLaughlin, S., Wullschleger, S., Conger, B., Parrish, D., et al. (1996). Switchgrass as a sustainable bioenergy crop. *Bioresour. Technol.* 56, 83–93. doi: 10.1016/0960-8524(95)00176-X

Shen, H., Mazarei, M., Hisano, H., Escamilla-Trevino, L., Fu, C., Pu, Y., et al. (2013). A genomics approach to deciphering lignin biosynthesis in switchgrass. *Plant Cell* 25, 4342–4361. doi: 10.1105/tpc.113.118828

Shim, H., Chasman, D. I., Smith, J. D., Mora, S., Ridker, P. M., Nickerson, D. A., et al. (2015). A multivariate genome-wide association analysis of 10 LDL subfractions, and their response to statin treatment, in 1868 Caucasians. *PLoS One* 10:e0120758. doi: 10.1371/journal.pone.0120758

Strullu, L., Cadoux, S., Preudhomme, M., Jeuffroy, M.-H., and Beaudoin, N. (2011). Biomass production and nitrogen accumulation and remobilisation by Miscanthus× giganteus as influenced by nitrogen stocks in belowground organs. *Field Crops Res.* 121, 381–391. doi: 10.1016/j.fcr.2011.01.005

Van, L. L. (2007). Evaluation of different nitrogen use efficiency indices using field-grown green bell peppers (*Capsicum annuum* L.). *Can. J. Plant Sci.* 87, 565–569. doi: 10.4141/P06-116

Wagner, A., Tobimatsu, Y., Phillips, L., Flint, H., Torr, K., Donaldson, L., et al. (2011). CCoAOMT suppression modifies lignin composition in *Pinus radiata*. *Plant J.* 67, 119–129. doi: 10.1111/j.1365-313X.2011.04580.x

Wang, W., Hu, B., Yuan, D., Liu, Y., Che, R., Hu, Y., et al. (2018). Expression of the nitrate transporter gene OsNRT1. 1A/OsNPF6. 3 confers high yield and early maturation in rice. *Plant Cell* 30, 638–651. doi: 10.1105/tpc.17.00809

Wen, W., Li, D., Li, X., Gao, Y., Li, W., Li, H., et al. (2014). Metabolome-based genome-wide association study of maize kernel leads to novel biochemical insights. *Nat. Commun.* 5:3438. doi: 10.1038/ncomms4438

Wolf, D. D., and Fiske, D. A. (2009). *Planting and Managing Switchgrass for Forage, Wildlife, and Conservation. Virginia Cooperative Extension, 418-013*. Blacksburg, VA: Virginia Polytechnic Institute and State University.

Wu, X., Feng, H., Wu, D., Yan, S., Zhang, P., Wang, W., et al. (2021). Using high-throughput multiple optical phenotyping to decipher the genetic architecture of maize drought tolerance. *Genome Biol.* 22:185. doi: 10.1186/s13059-021-02377-0

Xin, W., Wang, J., Li, J., Zhao, H., Liu, H., Zheng, H., et al. (2021). Candidate gene analysis for nitrogen absorption and utilization in japonica rice at the seedling stage based on a genome-wide association study. *Front. Plant Sci.* 12:670861. doi: 10.3389/fpls.2021.670861

Xu, Y., Shrestha, V., Piasecki, C., Wolfe, B., Hamilton, L., Millwood, R. J., et al. (2021). Sustainability trait modeling of field-grown switchgrass (*Panicum virgatum*) using UAV-based imagery. *Plants* 10:2726. doi: 10.3390/plants10122726

Yang, J., Lee, S. H., Goddard, M. E., and Visscher, P. M. (2011). GCTA: a tool for genome-wide complex trait analysis. *Am. J. Hum. Genet.* 88, 76–82. doi: 10.1016/j.ajhg.2010.11.011

Yang, J., Worley, E., Ma, Q., Li, J., Torres-Jerez, I., Li, G., et al. (2016). Nitrogen remobilization and conservation, and underlying senescence-associated gene expression in the perennial switchgrass *Panicum virgatum*. *New Phytol.* 211, 75–89. doi: 10.1111/nph.13898

Yang, J., Worley, E., Wang, M., Lahner, B., Salt, D. E., Saha, M., et al. (2009). Natural variation for nutrient use and remobilization efficiencies in switchgrass. *Bioenergy Res.* 2, 257–266. doi: 10.1007/s12155-009-9055-9

Zhong, R., Morrison, W. H. III, Himmelsbach, D. S., Poole, F. L., and Ye, Z.-H. (2000). Essential role of caffeoyl coenzyme AO-methyltransferase in lignin biosynthesis in woody poplar plants. *Plant Physiol.* 124, 563–578. doi: 10.1104/pp.124.2.563

Zhu, F., Alseekh, S., Koper, K., Tong, H., Nikoloski, Z., Naake, T., et al. (2021). Genome-wide association of the metabolic shifts underpinning dark-induced senescence in *Arabidopsis*. *Plant Cell* 34, 557–578. doi: 10.1093/plcell/koab251

Conflict of Interest: The authors declare that the research was conducted in the absence of any commercial or financial relationships that could be construed as a potential conflict of interest.

Publisher's Note: All claims expressed in this article are solely those of the authors and do not necessarily represent those of their affiliated organizations, or those of the publisher, the editors and the reviewers. Any product that may be evaluated in this article, or claim that may be made by its manufacturer, is not guaranteed or endorsed by the publisher.

frontiers | Frontiers in Plant Science

ORIGINAL RESEARCH
published: 14 June 2022
doi: 10.3389/fpls.2022.881204

Comparative Transcriptomic Analyses of Nitrate-Response in Rice Genotypes With Contrasting Nitrogen Use Efficiency Reveals Common and Genotype-Specific Processes, Molecular Targets and Nitrogen Use Efficiency-Candidates

*Narendra Sharma, Supriya Kumari†, Dinesh Kumar Jaiswal† and Nandula Raghuram**

University School of Biotechnology, Guru Gobind Singh Indraprastha University, New Delhi, India

OPEN ACCESS

Edited by:
Khurram Bashir, Lahore University of Management Sciences, Pakistan

Reviewed by:
M. Z. Abdin, Jamia Hamdard, India
Aysha Kiran, University of Agriculture, Faisalabad, Pakistan

***Correspondence:**
Nandula Raghuram
raghuram@ipu.ac.in

† These authors have contributed equally to this work

Specialty section:
This article was submitted to Plant Physiology, a section of the journal Frontiers in Plant Science

Received: *01 March 2022*
Accepted: *26 April 2022*
Published: *14 June 2022*

Citation:
Sharma N, Kumari S, Jaiswal DK and Raghuram N (2022) Comparative Transcriptomic Analyses of Nitrate-Response in Rice Genotypes With Contrasting Nitrogen Use Efficiency Reveals Common and Genotype-Specific Processes, Molecular Targets and Nitrogen Use Efficiency-Candidates. Front. Plant Sci. 13:881204. doi: 10.3389/fpls.2022.881204

The genetic basis for nitrogen (N)-response and N use efficiency (NUE) must be found in N-responsive gene expression or protein regulation. Our transcriptomic analysis of nitrate response in two contrasting rice genotypes of *Oryza sativa* ssp. *Indica* (Nidhi with low NUE and Panvel1 with high NUE) revealed the processes/functions underlying differential N-response/NUE. The microarray analysis of low nitrate response (1.5 mM) relative to normal nitrate control (15 mM) used potted 21-days old whole plants. It revealed 1,327 differentially expressed genes (DEGs) exclusive to Nidhi and 666 exclusive to Panvel1, apart from 70 common DEGs, of which 10 were either oppositely expressed or regulated to different extents. Gene ontology analyses revealed that photosynthetic processes were among the very few processes common to both the genotypes in low N response. Those unique to Nidhi include cell division, nitrogen utilization, cytoskeleton, etc. in low N-response, whereas those unique to Panvel1 include signal transduction, protein import into the nucleus, and mitochondria. This trend of a few common but mostly unique categories was also true for transporters, transcription factors, microRNAs, and post-translational modifications, indicating their differential involvement in Nidhi and Panvel1. Protein-protein interaction networks constructed using DEG-associated experimentally validated interactors revealed subnetworks involved in cytoskeleton organization, cell wall, etc. in Nidhi, whereas in Panvel1, it was chloroplast development. NUE genes were identified by selecting yield-related genes from N-responsive DEGs and their co-localization on NUE-QTLs revealed the differential distribution of NUE-genes between genotypes but on the same chromosomes 1 and 3. Such hotspots are important for NUE breeders.

Keywords: networks, nitrate, nitrogen use efficiency, QTLs, rice, transcriptome

INTRODUCTION

Reactive nitrogen (N) impacts all 17 sustainable development goals including food security. It is quantitatively the most important nutritional requirement for plant growth and agricultural productivity and is therefore supplied in various organic and inorganic forms including urea, ammonium salts, and nitrates. However, poor nitrogen use efficiency (NUE) in agriculture is one of the major reasons for anthropogenic nitrogen pollution that affects soil, air, water, health, biodiversity, and climate change (Sutton et al., 2019). It has already crossed our planetary boundaries, in addition to the loss of fertilizers worth billions of dollars (Sutton et al., 2019). The advocacy of the International Nitrogen Initiative and others over the last two decades led to the UNEP resolution on Sustainable Nitrogen Management in 2019 (Raghuram et al., 2021). Improving agricultural NUE is critical to meet the emerging calls to halve the nitrogen waste (Sutton et al., 2021), especially in agrarian countries.

Plant biology has a central role in understanding and improving crop NUE (Raghuram and Sharma, 2019; Udvardi et al., 2021; Madan et al., 2022). This has to begin with cereals that dominate global crop production and fertilizer demand, of which rice is predominant, due to its lowest NUE (Norton et al., 2015). It is the third most-produced and second most consumed crop in the world, apart from being a post-genomic model crop. This is evidenced by genome sequences of 3000 rice genotypes (Li et al., 2014) and growing functional genomics of N (Li et al., 2018; Pathak et al., 2020; Mandal et al., 2022). Further, the recent NUE phenotype (Sharma et al., 2018, 2021; Pathak et al., 2021) growing quantitative trait loci (QTL) and genotyping (Kumari et al., 2021) make rice an ideal target crop for NUE improvement. A recent simulation showed that $743 million per year could be saved by a 20% increase in rice NUE (Langholtz et al., 2021), while the global expenditure in that direction is not even a tiny fraction of it. Therefore, improving rice NUE is a highly desirable economic and environmental goal.

Nitrogen use efficiency can be understood in terms of uptake/utilization or remobilization efficiencies but is agronomically best expressed as yield or harvested N per unit N input (Raghuram and Sharma, 2019). Among the various N-fertilizers used as inputs, urea is the most predominant form of N-fertilizer used in the rice-growing and developing countries, whereas nitrates and ammonium salts are predominant in cropping in the developed world. However, soil microbial conversions ensure that nitrate is the predominant form of N available to all crops including rice, regardless of the form of N-supply (Coskun et al., 2017). This is one of the reasons why nitrate-transcriptomes are predominant even in the rice functional genomics literature (listed in Kumari et al., 2021). They are also available for subspecies Indica (Pathak et al., 2020) and Japonica (Mandal et al., 2022).

Nitrate uptake is mediated by nitrate transporters followed by intracellular conversion into ammonium ions by the sequential action of nitrate reductase (*NR*) and nitrite reductase (*NiR*) and assimilated into amino acids by the glutamine synthetase and glutamate synthase (*GS-GOGAT*) cycle (Raghuram and Sharma, 2019). All other metabolites containing N are generated by transamination of amino acids, which also provide the main organic N-pool for translocation and secondary remobilization during senescence, which is particularly important in cereals (Snyder and Tegeder, 2021). All these processes have been targeted for understanding and improving NUE with varying results (Mandal et al., 2018; Raghuram and Sharma, 2019; Sinha et al., 2016, 2020; Madan et al., 2022).

In rice, several genes such as *OsGRF4, OsDof1, NADH-GOGAT, OsNPF6.1, OsNRT2.3b, OsNRT2.1, OsPTR9, OsNPF8.20, OsNRT1.1A, OsFBP1* have been reported to increase NUE (Kumari et al., 2021 and references cited therein) including alanine aminotransferase (Good et al., 2007), *OsPTR9* (Fang et al., 2013), and *DEP1* (Sun et al., 2014). In addition to these genes, some interesting QTLs have been identified as linked to NUE (Sinha et al., 2018; Waqas et al., 2018; Kumari et al., 2021). Transcriptomic studies in rice revealed thousands of nitrate-responsive genes totaling 23,626 numbers (Mandal et al., 2022) but they were all limited to single genotypes. This limits the utility of functional genomic studies in the genetic dissection of NUE. The only studies that compared the transcriptomes of two genotypes for NUE were in the context of ammonium nitrate (Sinha et al., 2018; Subudhi et al., 2020). Therefore, in the present study, we undertook a comparative transcriptome analysis for NUE in two Indica rice genotypes with contrasting NUE, Nidhi and Panvel1, as identified earlier (Sharma et al., 2018, Sharma et al., 2021) to understand the genes/processes underlying NUE.

MATERIALS AND METHODS

Plant Material, Growth Conditions, and Nitrate-Treatments

Two genotypes of rice (*Oryza sativa* ssp. *Indica*), namely, Nidhi and Panvel1 were chosen, based on contrasting germination, yield, and NUE (Sharma et al., 2018, Sharma et al., 2021). Seeds of Nidhi were procured from the Indian Institute of Rice Research, Hyderabad, India, whereas seeds of Panvel1 were from Panvel, Maharashtra, India. Seeds of modal weight were selected (Sharma et al., 2018) and surface sterilized using 0.1% mercuric chloride for 50 s followed by several washes with ultrapure water and allowed to soak in it for 2 h. They were sown in pots filled with nutrient-depleted sand (Sharma et al., 2019) saturated with Arnon-Hoagland medium (Hoagland and Arnon, 1950) with normal (15 mM) or low nitrate concentration (1.5 mM) as control and test conditions as described earlier (Sharma et al., 2021). The pots were replenished with media to saturation every few days and plants were grown for 21 days in the greenhouse at 28°C and 70% relative humidity with 270 μmol m^{-2} s^{-1} light intensity and 12/12 h photoperiod. For microarray the treated and control tissues from three independent biological replicates were frozen in liquid N_2 and stored at −80°C till further use.

Total RNA Extraction and Microarray

The total RNA was isolated from 21-day whole plants using TRIzol reagent (Invitrogen, Carlsbad, CA, United States) as per the manufacturer's instructions. Microarray analyses were performed under MIAME compliant conditions using independent biological triplicates. Microarray analysis was performed at Genotypic Technologies (Bengaluru, India). RNA was quantified using a NanoDrop spectrophotometer (ND2000, Thermo Fisher Scientific, Waltham, MA, United States). The integrity of the isolated RNA samples was determined by the Agilent 2100 Bioanalyzer (Agilent Technologies, Palo Alto, CA, United States) as per the manufacturer's instructions. The ratio of 18S and 28S rRNA was obtained from 2100 Expert software (Agilent Technologies, Palo Alto, CA, United States) and the RNA integrity number was obtained from RIN Beta Version Software (Agilent Technologies, Palo Alto, CA, United States). The RNA samples used for microarray hybridization had RIN values above 6. They were reverse transcribed using 500 ng of each RNA sample into double-stranded cDNA using MMLV-RT enzyme and random primer tagged to a T7 polymerase promoter. The double-stranded cDNA was then used as a template to generate Cy3-labeled cRNA by *in vitro* transcription using RNaseOUT (Invitrogen, United States), inorganic pyrophosphatase, and T7 RNA polymerase at 40°C as per the manufacturer's instructions [Agilent Quick Amp labeling kit (p/n:5190-0444, United States)]. Labeled cRNA was purified using Qiagen RNeasy columns (Qiagen, Cat No: Cat#74104) and assessed for yields and specific activity. Agilent Rice Gene Expression 8 × 60 K (AMADID 48014) microarrays were customized to include nuclear and organellar gene probes. Labeled cRNA samples of 600 ng each were fragmented and hybridized onto microarrays using the gene expression hybridization kit (Agilent's *in situ* Hybridization kit 5188-5242) in an Agilent's Surehyb hybridization chamber at 65°C for 16 h. The hybridized slides were washed and scanned using an Agilent microarray scanner.

Microarray Data Analysis

Scanned images were processed using Agilent Feature Extraction Software (Version-11.5, United States) to obtain raw data, which were analyzed using Agilent Gene-Spring GX software (Version-12.6.1, United States). The data were normalized using the 75th percentile shift method of global normalization that adjusts the locations of all the spot intensities and provides fold expression values relative to controls. The raw and processed data were deposited in the NCBI-GEO database (GSE140257). The transcripts showing geometric mean fold change value ± 1 ($\log_2$FC) with statistically significant cut-of ($P \leq 0.05$) were considered as differentially expressed genes (DEGs) in the low nitrate-treated samples relative to the normal nitrate controls. The Student's *t*-test was used to calculate the *P*-value among the replicates. During the data analysis using R studio (Version 1.2.5042, Boston, ME, United States), we observed that one of the three biological replicates was a consistent outlier, causing either non-significant or negative correlation with the other two biological replicates and affecting the robust identification of DEGs. This problem persisted despite quantile normalization and Data-Driven Haar-Fisz for Microarrays (DDHFm) transformation and therefore, the data were re-analyzed with R studio (Version 1.2.5042, Boston, ME, United States) using raw intensity values of the best two significantly correlated replicates and used for the rest of the downstream analysis.

Functional Classification, Subcellular Localization of Differentially Expressed Genes, and Data Analysis

Gene Ontology (GO) based functional annotation was performed using EXPath 2.0. Protein subcellular localization was predicted using the cropPAL database (Hooper et al., 2016) using default parameters for rice plants. MS Excel was used for filtering the data and the Student's *t*-test. Venn selection[1] was used to make Venn diagrams.

Construction of Protein-Protein Interaction Network

The experimentally validated interactors associated with DEGs were retrieved from BioGRID,[2] STRING,[3] PRIN,[4] and MCDRP[5] databases. They were used to construct protein-protein interaction (PPI) networks in Cytoscape 3.9.0 (Shannon et al., 2003) and the expression values of DEGs were mapped onto networks. PPI subnetworks/molecular complexes were obtained using the molecular complex detection (MCODE) plugin in Cytoscape. Transcriptional regulatory networks (TRN) were developed using Cytoscape for DEG-encoded transcription factors based on rice ortholog information retrieved from Arabidopsis (Gaudinier et al., 2018). The expression values of DEGs were used to label the nodes in the networks. Expath was used for GO analysis of DEGs.

Physiological Measurements

Potted plants grown for 21 days were used to measure photosynthesis, stomatal conductance, and transpiration rate using the LI-6400XT Portable Photosynthesis System (LI-COR Biosciences, Lincoln, NE, United States). The net photosynthetic rate was measured in terms of CO_2 assimilated as μmol (CO_2) m^{-2} s^{-1}; transpiration was measured in terms of mol (H_2O) m^{-2} s^{-1}; stomatal conductance was measured in terms of mmol (H_2O) m^{-2} sec^{-1}; internal water use efficiency was measured in terms of μmol CO_2/mol (H_2O) and transpiration efficiency was measured in terms of μmol (CO_2)/mmol (H_2O) m^{-2} s^{-1}. The Student's *t*-test was performed on test *vs.* control data. The reference CO_2 concentration was 410 ± 20 μmol mol^{-1} during the measurements. All

[1]https://bioinfogp.cnb.csic.es/tools/venny/
[2]https://thebiogrid.org/
[3]https://string-db.org/
[4]http://bis.zju.edu.cn/
[5]http://www.genomeindia.org/biocuration/

LICOR measurements were carried out at the time of maximal photosynthetic activity between 12:00 p.m. and 5:00 p.m. IST. All the measurements were done in five independent replicates.

RT-qPCR Validation of Nitrate-Responsive Expression of Differentially Expressed Genes

Total RNAs were isolated from 21 days old whole potted plants grown in normal and low nitrate concentrations (15 mM as control and 1.5 mM as a test). 3 μg each of total RNA was reverse transcribed into cDNA using PrimeScript 1st strand cDNA synthesis kit (Takara, Kusatsu, Shiga, Japan). To avoid amplification from genomic DNA, primers spanning exon-exon junctions were designed using the Quant Prime tool.[6] The primer sequences are provided in **Supplementary Table S4**. Quantitative reverse transcription polymerase chain reaction (RT-qPCR) reactions were carried out in three technical replicates and two independent biological replicates in an Agilent Aria-Mx Real-Time PCR System. Each 10 μl reaction mix contained 1 μl of undiluted cDNA, 1.0 μl of forward and 1.0 μl of reverse primers (10 μM), and 5 μl of KAPA SYBR FAST Master Mix (2×) Universal (Kapa Biosystems, Wilmington, MA, United States). The relative changes in gene expression were quantified by the $2^{-\Delta\Delta CT}$ method (Livak and Schmittgen, 2001) using actin genes (*BGIOSGA013463*) as internal controls. Melting curve analyses of the amplicons were used to determine the specificity of RT-qPCR reactions. The data were statistically analyzed by unpaired *t*-test using the software MS Excel.

Retrieval of Molecular Functions and Identification of MicroRNAs and Their Targets

Transcription factors (TFs) encoded by DEGs were retrieved from the databases PlantPAN3.[7]

For transcription factor binding sites (TFBS) prediction, 2 kb promoter upstream sequences of the translational start site of the TFs were downloaded from RAPDB and subjected to Regulatory Sequence Analysis Tools (RSAT).[8] To find out the motif sequences 6,7 and 8 mer sequences with a significance level ($P < 0.05$) were obtained from transcription factor binding sites (TFBS). Tomtom v 5.1.1 tool[9] (Gupta et al., 2007) with default settings was used to filter redundant motifs and define known conserved regulatory elements (CREs) based on the Arabidopsis DAP motifs database. GoMo tool[10] was used for the identification of detection of possible biological and molecular functions (Buske et al., 2010). Transporters encoded by DEGs were retrieved from the Rice transporters database[11] and Transport DB 2.0.[12] Plant microRNA (miRNA) database was used to retrieve the miRNAs that target NUE-related genes (PMRD[13]). The database Plant PTM Viewer was used to finding the products of DEGs associated with post-translational modifications (PTM).[14]

Identification of Nitrogen Use Efficiency-Genes and Their Co-localization Onto Nitrogen Use Efficiency-QTLs

Nitrogen use efficiency genes were defined as N-responsive and yield-related genes, as reported by Kumari et al. (2021). The yield-related genes reported therein were further updated from literature and databases and used for Venn selection with the N-responsive DEGs identified in the genotypes Nidhi and Panvel1 to obtain the NUE genes in them. Similarly, NUE-QTLs reported therein were further updated from literature and the NUE genes identified in Nidhi and Panvel1 were co-localized onto NUE-QTLs as described by Kumari et al. (2021).

RESULTS

Nitrate-Responsive Transcriptomes of Rice Genotypes With Contrasting Nitrogen Use Efficiency

In this study, we used two Indica rice genotypes Nidhi and Panvel1 identified previously (Sharma et al., 2018, Sharma et al., 2021) as a contrast for their nitrate response and NUE (**Figures 1A,B**). They were grown in pots with low nitrate (1.5 mM for the test) and normal nitrate (15 mM for control) and total RNAs were isolated from 21 days old whole plants and used for whole transcriptome microarray analysis. Nitrate metabolism marker enzymes genes, viz., nitrate reductase (*NR*), and nitrite reductase (*NiR*) were used to assess the effects of low nitrate in both the genotypes. In both the genotypes, *NR* and *NiR* transcripts were significantly reduced in low nitrate compared with normal nitrate (**Figures 1C,D**). The raw microarray data were deposited in GEO at NCBI under the accession number GSE140257. After comparing the data from three independent replicates, the best two replicates with higher correlation coefficients were selected. Their scatter plots showed good correlations between the two replicates (**Supplementary Figure S1**). Transcripts showing geometric mean fold change value ± 1.0 ($\log_2$FC) with statistically significant cut-off (*p*-value ≤ 0.05) were used to identify the differentially expressed genes (DEGs). As visualized in the volcano plot (**Figure 1E**), 1,397 DEGs were detected in Nidhi, out of which 712 were upregulated and 685 DEGs were downregulated in response to low nitrate (**Figure 1E** and **Supplementary Table S1**). Similarly, a total of 735 DEGs were detected in Panvel1, of which 376 were upregulated while 359 were downregulated (**Figure 1F** and **Supplementary Table S1**). Many of the well-known N-regulated genes figured

[6]https://quantprime.mpimp-golm.mpg.de/?page=about

[7]http://plantpan.itps.ncku.edu.tw/

[8]http://plants.rsat.eu

[9]http://meme-suite.org/tools/tomtom

[10]http://meme-suite.org/tools/gomo

[11]https://ricephylogenomics.ucdavis.edu/transporter/genInfo.shtml

[12]http://www.membranetransport.org/transportDB2/index.html

[13]Zhang, Z., Yu, J., Li, D., Zhang, Z., Liu, F., Zhou, X., et al. (2010). PMRD: plant microRNA database. *Nucleic Acids Res.* 38, D806–D813. doi: 10.1093/nar/gkp818

[14]https://www.psb.ugent.be/webtools/ptm-viewer/experiment.php

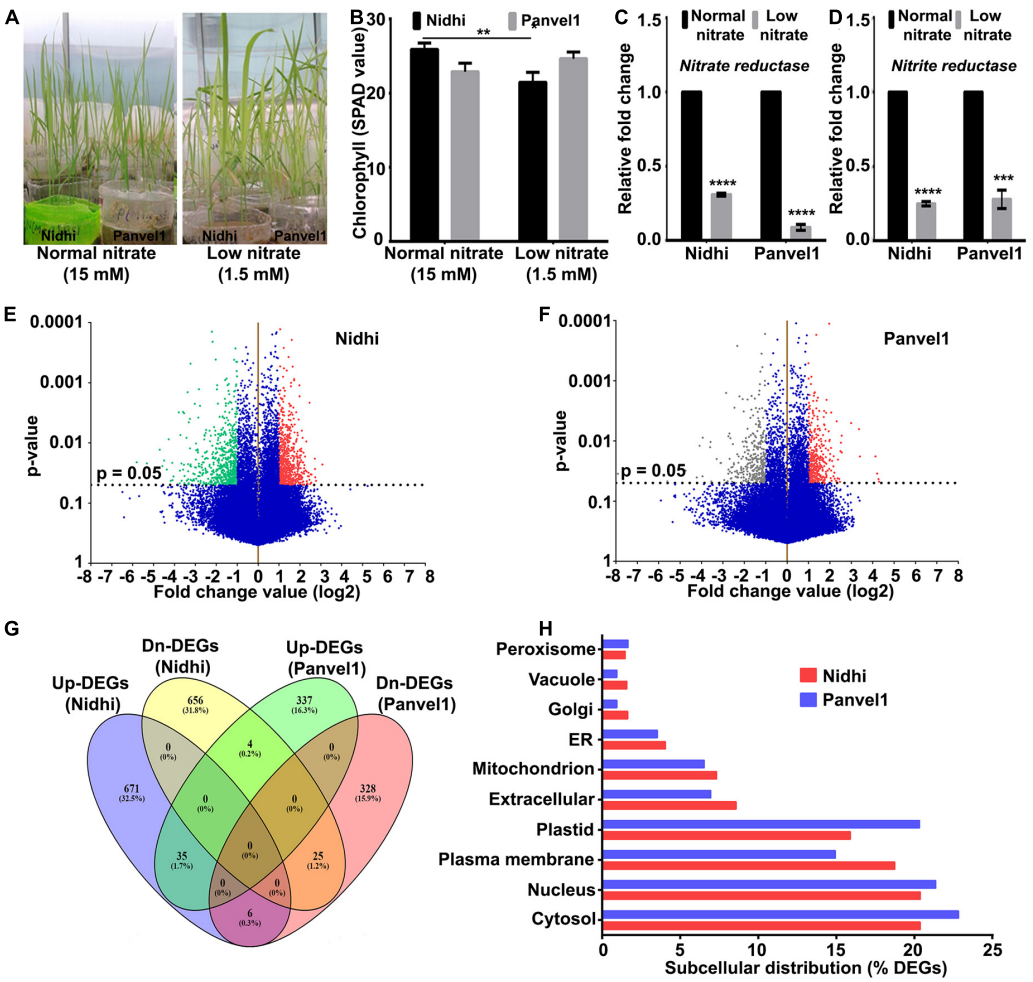

FIGURE 1 | Nitrate-responsive transcriptomes in Nidhi and Panvel1. **(A)** Representative image of 21 days old Nidhi and Panvel1 plants grown in nutrient-depleted soil supplemented with AH media containing normal (15 mM) and low (1.5 mM) nitrate. **(B)** Leaf chlorophyll content (SPAD value) was estimated earlier in Nidhi and Panvel1 (Sharma et al., 2021). Quantitative RT-PCR was used to calculate the relative mRNA expression of nitrate reductase **(C)** and nitrite reductase **(D)** genes in 21 days old Nidhi and Panvel1 plants. Test samples were low nitrate, whereas normal nitrate samples were used as control. The actin gene was used as a reference gene to normalize the expression data. Data represent the mean ± SE of three technical replicates. An unpaired *t*-test was performed in GraphPad Prism. Experiments were performed repeatedly with two independent biological replicates. Volcano plots for differential gene regulation are shown for Nidhi **(E)** and Panvel1 **(F)**. Scattered dots represent different transcripts and the horizontal dashed line corresponds to the *P*-value cut-off ($P = 0.05$). Red scattered dots represent the mapping of upregulated genes, whereas downregulated genes are by green dots. **(G)** Venn diagram shows commonly and uniquely up or downregulated DEGs between Nidhi and Panvel1. **(H)** Predicted subcellular localization of DEGs encoded proteins in Nidhi and Panvel1. $^{**}P < 0.01$, $^{***}P < 0.001$, $^{****}P < 0.0001$.

among the DEGs identified in this study, confirming the overall reliability of our transcriptome data (**Supplementary Table S2**). Interestingly, only 70 DEGs were common between these two genotypes, of which 41 were upregulated, while 29 DEGs were downregulated (**Figure 1G** and **Supplementary Table S1**). Further, Nidhi showed differential expression of many more genes than Panvel1, clearly indicating a more extensive genome-wide nitrate response in the genotype Nidhi. The sequences of proteins encoded by the DEGs were retrieved from RAP-DB and their subcellular localizations were predicted by the CropPAL2 tool (Hooper et al., 2016) using default parameters and rice as the reference organism. In the case of multiple predicted localizations, the first hit was considered. In both the cultivars, DEG-encoded proteins were predominantly located in the cytosol, followed by nucleus and plasma membranes among others (**Figure 1H**). Interestingly, plasma membrane-associated protein-encoding DEGs were comparatively higher in Nidhi, whereas plastid localized proteins were predominant in Panvel1 (**Figure 1H**).

Nitrate Induces Common and Distinct Processes/Pathways in Contrasting Genotypes

An important purpose of comparatively analyzing contrasting genotypes is to identify the key cellular processes involved in NUE. For this purpose, Gene Ontology (GO)-based functional annotation of DEGs was performed using EXPath

2.0 tool (Chien et al., 2015). It revealed photosynthesis, response to light stimulus, protein-chromophore linkage, and carbohydrate metabolism among others, as enriched biological processes regulated by nitrate that are common to both the genotypes (**Figure 2** and **Supplementary Table S3**). Cell cycle/division, nitrogen utilization, ammonium transport, ammonia assimilation cycle, and processes related to cytoskeleton among others were highly enriched only in Nidhi under low nitrate conditions (**Supplementary Table S3**). However, biological processes related to signal transduction, protein import into the nucleus and mitochondria, phosphorelay signal transduction, chromatin organization, transport of ions, water, and carbohydrate, and response to heat and ozone among others were enriched only in Panvel1 (**Supplementary Table S3**).

Validation of Selected Differentially Expressed Genes by RT-qPCR

The expression pattern of DEGs associated with photosynthesis, transport, and flowering time were validayted by RT-qPCR (**Figure 3**). One of them that is common to both the genotypes codes for B-Box-Containing Protein 19 (*OsBBX19, Os06g0298200*) and was upregulated. Two DEGs light-harvesting protein CP29 (*OsCP29, Os07g0558400*) and Chloroplast Signal Recognition Particle 43 (*SRP43, Os03g0131900*) exclusive to Nidhi were downregulated. Three DEGs were exclusive to Panvel1, two of which were upregulated: Big Grain Like 1 (*BGL1, Os03g0414900*) and Phytoclock 1 (*OsPCL1, Os01g0971800*) while sulfate transporter 3;2 (*Ossultr3;2, Os03g0161200)* was downregulated. The list of primers used in this study is provided in **Supplementary Table S4**.

Differential Regulation of Transporters May Contribute to Nitrogen Use Efficiency in Contrasting Genotypes

Nitrate-responsive transporters have been implicated in source-sink dynamics (Tegeder and Masclaux-Daubresse, 2018) and NUE (Wang et al., 2018; Zhang Z. et al., 2020; Kumari et al., 2021). To discriminate the effects of nitrate on different transporters in Nidhi and Panvel1, DEGs were searched in Transport DB (see text footnote 12) and Rice

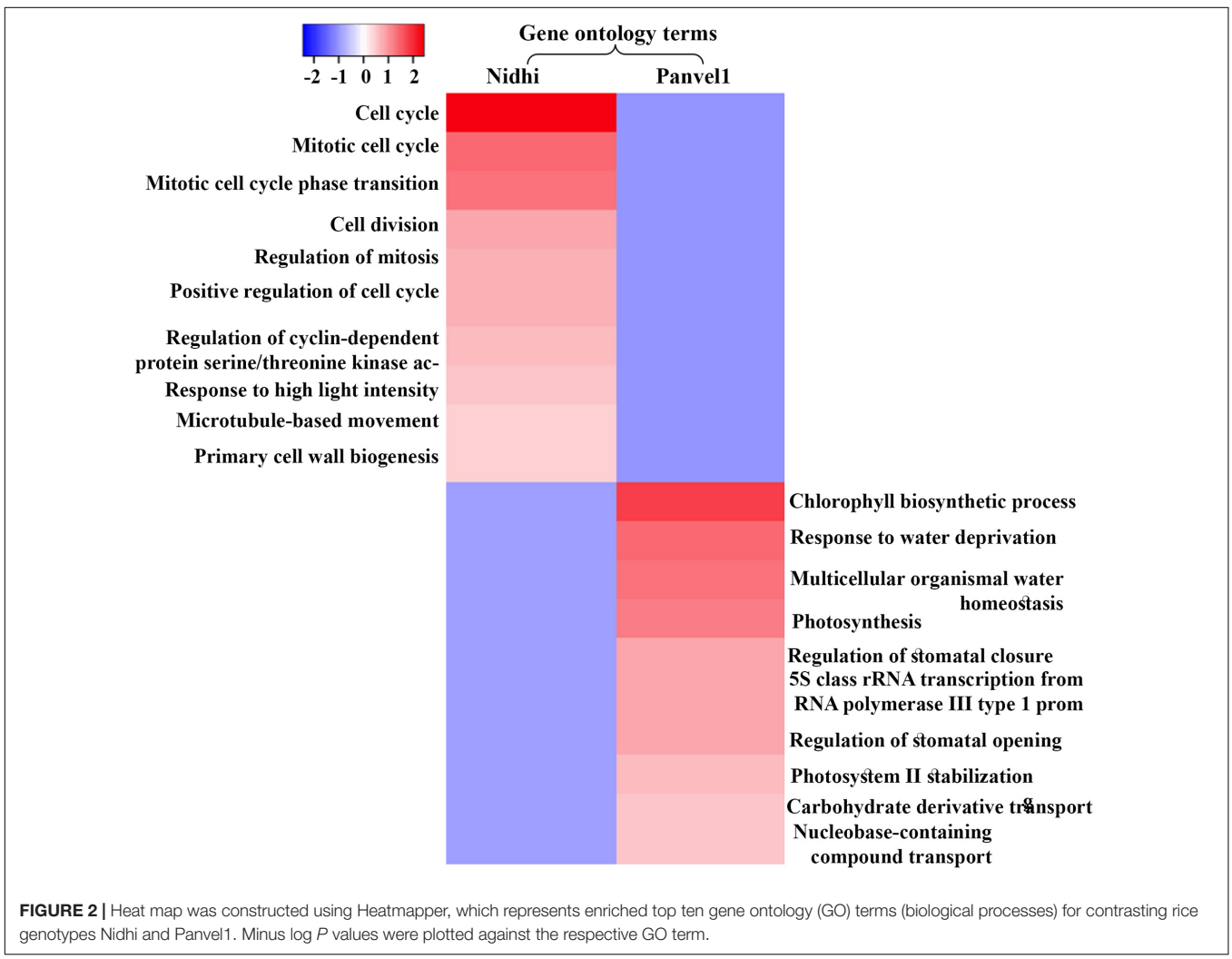

FIGURE 2 | Heat map was constructed using Heatmapper, which represents enriched top ten gene ontology (GO) terms (biological processes) for contrasting rice genotypes Nidhi and Panvel1. Minus log *P* values were plotted against the respective GO term.

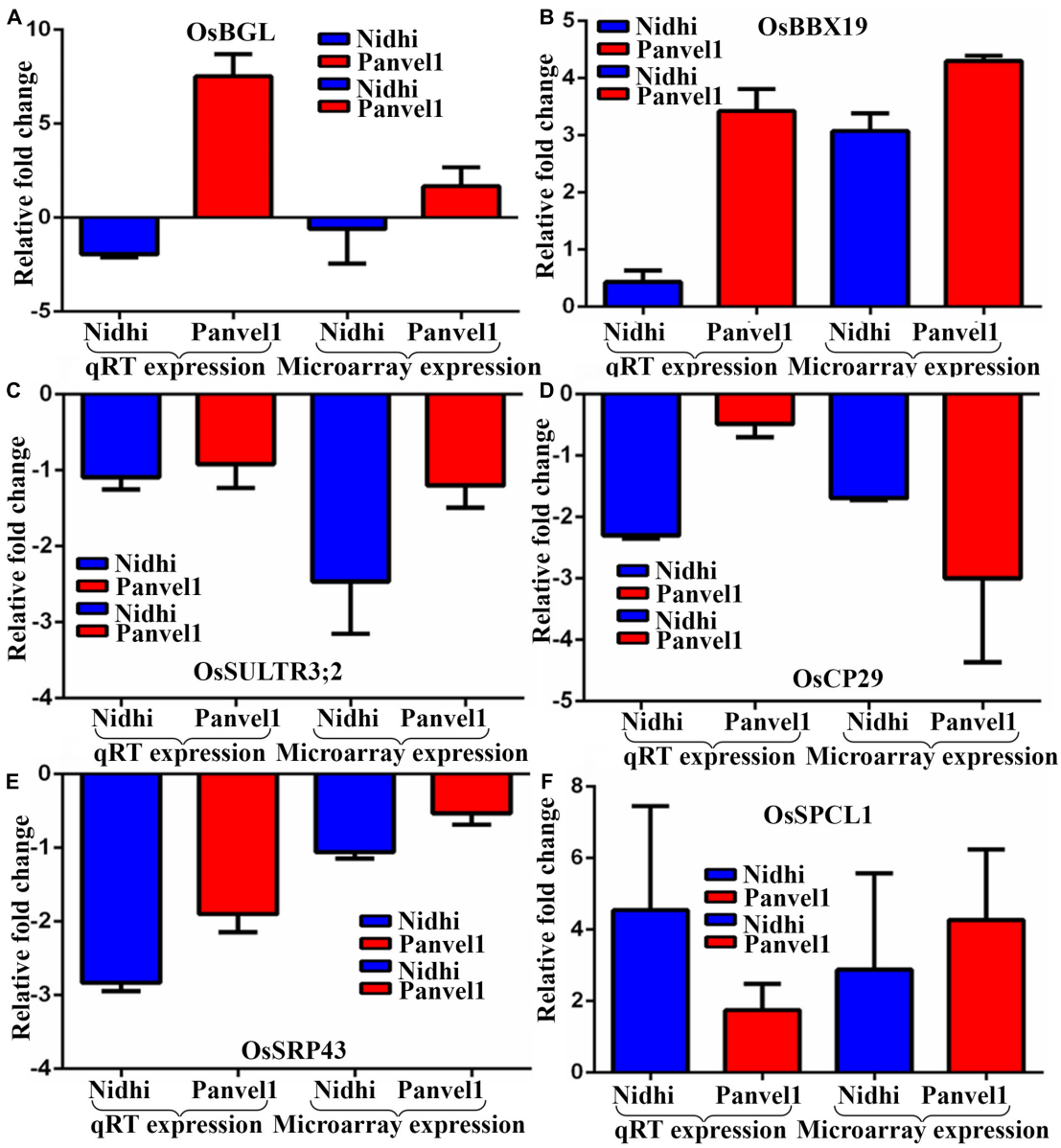

FIGURE 3 | Validation of expression profile of nitrate responsive genes by RT-qPCR. Relative change in the gene expression was calculated by the comparative *Ct* value method and the actin gene was used for data normalization. The control values were taken as zero and the test values are shown as the average of three technical and two independent biological replicates (±SE) except gene *BGL1* for which the calculations were done based on three technical replicates of a biological replicate. Each sub-figure compares gene expression of RT-qPCR and microarray for Nidhi versus Panvel1 for gene *OsBGl1* **(A)**, *OSBBX19* **(B)**, *OsSULTR3;2* **(C)**, *OsCP29* **(D)**, *OsSRP43* **(E)**, and *OsPCL1* **(F)**.

Transporter database and associated transporters were retrieved. Sixty-six and twenty-seven nitrate-responsive transporters belonging to 22 and 18 families, respectively, were detected in Nidhi and Panvel1 (**Figure 4A** and **Supplementary Table S5**). Two transporters belonging to distinct families, a potassium permease (*KUP; Os12g0515400*) and a sodium symporter (*DASS; Os03g0575200*), were similarly regulated in both the genotypes, whereas 64 transporters were exclusive to Nidhi and 25 were exclusive to Panvel1. Nidhi revealed a higher number of downregulated transporters than upregulated, while approximately equal numbers of up- and downregulated transporters were detected in Panvel1.

This clearly shows that nitrate differentially regulates various transporters in contrasting genotypes. The extent to which this may contribute to their differences in NUE needs to be examined, in order to consider such transporters as targets for NUE improvement. Venn analyses of these transporters found in Nidhi with NUE-related genes in rice predicted by Kumari et al. (2021) revealed nine transporters, viz. *OsCAX1a,*

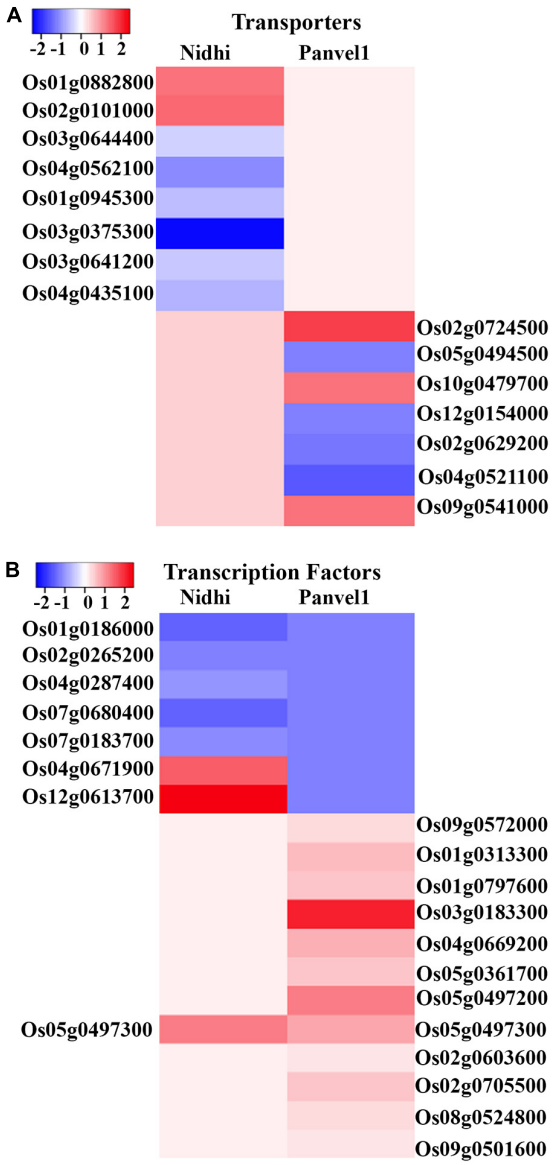

FIGURE 4 | (A) Heat map was constructed using Heatmapper, which represents the expression pattern of nitrate regulated differentially expressed genes (DEGs) of the top two transporters' families for Nidhi and Panvel1 rice contrasting genotypes. For Nidhi, the top two transporter families are Amino Acid/Auxin Permease (AAAP) Family and Amino Acid-Polyamine-Organocation (APC) Family, while for Panvel1 they are Drug/Metabolite Transporter (DMT) Superfamily and Major Intrinsic Protein (MIP) Family. **(B)** Expression pattern of nitrate regulated DEGs of top two transcription factors' families for Nidhi and Panvel1 rice contrasting genotypes. For Nidhi, the top two TFs families are WRKY and ARF, while for Panvel1 they are AP2 and bHLH.

OsTPC1, OsMGT1, OsYSL15, OsMST4, OsHAK1, OsAMT1;1, OsYSL16 and OsMATE2 as related to NUE. Seventeen of the 66 transporters identified in Nidhi in this study were associated with biotic/abiotic stress, root, hormones, etc., whereas 40 of them are completely novel and functionally unvalidated (**Supplementary Table S5**). In the case of Panvel1, three transporters, viz. *OsSUT1, NPF7.1,* and *Lsi3* are associated with NUE (Kumari et al., 2021), nine were linked with other functions such as abiotic stress, micro and macronutrient transport, photosynthesis, pollen germination, etc., and 15 are completely novel and functionally unvalidated (**Supplementary Table S5**). Hence, our analysis identified 12 transporters as potential targets to improve NUE in rice for the first time on the basis of their differential regulation in contrasting genotypes, including 53 novel candidates (**Supplementary Table S5**).

Differential Involvement of Transcription Factors and Their Binding Sites in Nitrogen Use Efficiency

To identify any differential transcriptional regulation in the contrasting genotypes for N-response/NUE, DEGs from both genotypes were searched in the rice transcription factors database PlantPAN3 (see text footnote 7). We identified 37 transcription factors (TFs) in the genotype Nidhi and 27 TFs in the genotype Panvel1, with only two TFs common to both (**Figure 4B** and **Supplementary Table S6**). In Nidhi, they belonged to 20 TF classes including 9 major classes ($\geq$2 genes) totaling 26 genes and 11 minor classes (<2 genes) totaling 11 genes. In Panvel1 the TFs belonged to 11 classes, including 5 major classes ($\geq$2 genes) totaling 21 genes and 6 minor classes (<2 genes) totaling 6 genes.

In Nidhi, all the identified members of TCP and AP2 TF families were upregulated, while the members of WRKY, bHLH, bZIP, NAC, and NAM TF families were downregulated under low nitrate. In Panvel1, AP2 and bHLH TF family members were upregulated, while only HSF TF family members were downregulated. Among the other major TF families, Myb/SANT more members were upregulated than downregulated in both the genotypes, but this was true for the ARF family only in Nidhi. In the C2H2 family, there were more members of downregulated than upregulated TFs in the genotype Nidhi, while in the genotype Panvel1, there were an equal number of up and downregulated TFs of the Homeodomain/HD-ZIP family.

Venn selection of these TFs found in Nidhi with the predicted NUE-related genes in rice (Kumari et al., 2021) revealed four TFs, viz. *OsAP2/ERF-40, OsMYB102, OsDREB1,* and *OsNAC5* as differentially regulated by nitrate, relative to Panvel1. Among them, twenty-two were associated with biotic/abiotic stress, root/leaf development, panicle architecture, hormones, etc., whereas nine of them are completely novel and functionally unvalidated (**Supplementary Table S6**). In Panvel1, six TFs, viz., *OsPCL1, OsBLR1, HSfA2d, R2R3-MYB, OsEPR1,* and *OsNAC3* figure among the predicted NUE-related genes (Kumari et al., 2021), while fifteen TFs were linked with other functions such as abiotic stress, spikelet meristem, stamen development, chloroplast development, and hormone metabolism, etc. Four other TFs are completely novel and functionally unvalidated (**Supplementary Table S6**).

These results clearly indicate that nitrate regulates common and exclusive TFs, which may control different N-response/NUE in Nidhi and Panvel1. Further, in addition to our validation of some of the predicted NUE-related TFs as differentially regulated by nitrate among contrasting rice genotypes, we identified

13 TFs as novel candidates in contrasting rice genotypes (**Supplementary Table S6**) to improve NUE.

Transcription factors are known to regulate target genes by binding the *cis*-acting motifs present in their promoter regions. To further discriminate the distinct N-response/NUE in the contrasting genotypes Nidhi and Panvel1, TF binding sites (TFBS) were predicted/searched using Regulatory Sequence Analysis Tools (RSAT) (see text footnote 8). Transcription factor binding sites for the transcription factors exclusively N-responsive in the genotype Nidhi revealed the majority of binding sites for AP2-EREBP and Cys2His2 (C2H2) followed by TCP, G2 like, and FAR1. This indicates that the NUE-related TFs are themselves regulated by nitrate through these families of TFs. Annotation analysis of these motifs revealed various interesting biological and molecular functions, which include regulation of transcription, translation, ATPase activity, and structural constituent of ribosome, while two motifs were not annotated. All *cis*-regulatory sites (CREs) are novel NUE-related CREs in rice (**Supplementary Table S7**).

In Panvel1, promoter regions for the transcription factors exclusively N-responsive in this genotype contain binding sites for GRF, AP2-EREBP followed by bzip, MYB, HSF, TCP, and Cys2His2 (C2H2). This indicates that these NUE-related TFs are themselves regulated by these families of TFs in Panvel1 as well. Annotation analysis of these motifs revealed many interesting biological and molecular functions, which include regulation of transcription, translation, response to auxin stimulus, kinase activity, and peroxidase activity, while three motifs were not annotated. All CREs identified in the present study are novel NUE-related CREs in rice (**Supplementary Table S7**).

To further delineate the contrasting N-response/NUE of Nidhi and Panvel1 in the context of global regulation of TFs, we predicted a DEG-associated transcriptional regulatory network (TRN). For this purpose, we used ortholog information available in Arabidopsis (Gaudinier et al., 2018) to retrieve the corresponding rice DEGs from the PlantGDB database as described earlier (Pathak et al., 2020). Then, we constructed DEG-associated TRN for Nidhi and Panvel1 in Cytoscape and mapped the expression value of DEGs onto the networks (**Figure 5**). Venn analysis was performed to identify the common and unique genes associated with the TRNs developed in Nidhi and Panvel1. It revealed 51 genes common to both the genotypes, whereas 42 and 15 genes were exclusive to Nidhi and Panvel1 TRNs, respectively (**Supplementary Table S8**). High-affinity nitrate transporter, glutamine synthetase, nodulin MtN3 family protein, and NIN protein among others were common to both the genotypes. MADS-box family gene (*OsMADS18*), auxin-regulated gene involved in organ size (*ARGOS*), and Ser/Thr protein phosphatase family protein among others were exclusive to N-response in Nidhi, whereas heat stress transcription factor B-1 and TCP family transcription factor among others were exclusively N-responsive in Panvel1 (**Supplementary Table S8**). Further, GO-based functional annotation of TRNs using the EXPath tool revealed response to nitrate and auxin and regulation of transcription as common GO terms in both the cultivars, whereas exclusive GO terms in Nidhi were cell differentiation, carbohydrate transport, and protein dephosphorylation, among others. Those exclusive to Panvel1 were responses to salicylic acid and cold and root development (**Supplementary Table S9**).

MicroRNA-Mediated Post-transcriptional Regulation of N-Response in Contrasting Genotypes

MicroRNA are involved in the post-transcriptional regulation of gene expression in plants (Michlewski and Cáceres, 2019). To understand the possible role of post-transcriptional regulation in contrasting NUE rice genotypes, DEG-associated microRNAs were retrieved from the Plant miRNA database (see text footnote 13). A subset of nitrate-regulated genes in contrasting rice genotypes comprised 35 miRNAs targets in Nidhi and 21 in Panvel1 (**Supplementary Table S10**). Out of the 35 miRNA targets found in Nidhi, 22 were upregulated whereas 13 were downregulated. Similarly, out of 21 targets in Panvel1, 11 were upregulated and 10 were downregulated. Two miRNAs osa-miR167c and osa-miR441a were common between Nidhi and Panvel1. Venn analyses of these miRNAs with those targeting reported NUE-related genes in rice (Kumari et al., 2021) revealed three miRNAs osa-miR1440, osa-miR170a, and osa-miR399e exclusively in Nidhi. Overall, our analysis in contrasting genotypes identified 54 miRNAs as novel candidates (**Supplementary Table S10**) to be validated further for their role in improving NUE in rice.

Gene ontology analysis of target genes of miRNA in Nidhi using ExPath 2.0 revealed the role of post-translational modifications, viz., phosphorylation, de-phosphorylation, hydrolase activity, and phosphatase activity (**Supplementary Table S10**). Some other associated GO terms were metal ion binding, sequence-specific DNA binding, protein dimerization activity, oxidoreductase activity regulation of transcription, and DNA-template. Gene ontology for target genes of miRNA in Panvel1 showed processes such as cytosol, metal ion binding, plasma membrane, oxidation-reduction process, and protein binding. The details of their genes, functions, and gene ontology analysis along with references are provided in **Supplementary Table S10**. This gene ontology analysis indicates differential regulation of miRNA targets in contrasting rice genotypes and predominant post-transcriptional regulation by nitrate in the genotype Nidhi than in Panvel1.

Genotype-Specific N-Responsive Protein-Protein Interaction Networks

To understand the contrasting N-response/NUE of Nidhi and Panvel1 in terms of the underlying pathways, we developed DEG-associated PPI networks (**Supplementary Figures S2, S3**). Experimentally validated interactors associated with DEGs were retrieved from STING, BioGRID, MCDRP, and PRIN databases for this purpose. Nitrate-responsive PPI networks were constructed in Cytoscape and the expression value of DEGs was mapped onto the network for each genotype (**Supplementary Figures S2, S3**). In the case of Nidhi, the PPI network consisted of 528 nodes and 1622 edges, whereas 215 nodes and 368 edges were present in Panvel1. Venn analysis showed that 29 interactors were common in both the genotypes,

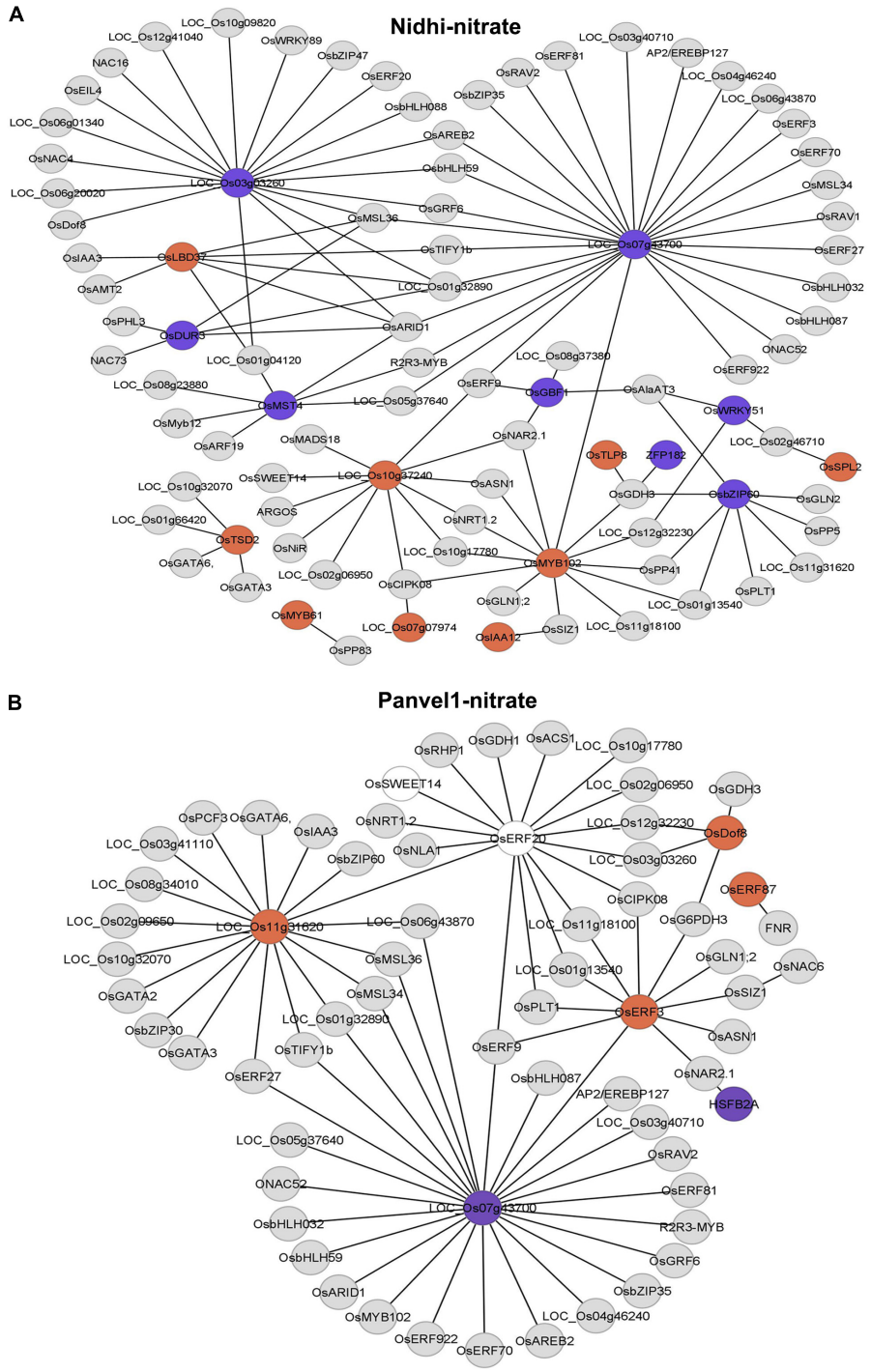

FIGURE 5 | Predicated nitrate-responsive transcriptional regulatory network (TRN) in Nidhi **(A)** and Panvel1 **(B)**. Nitrate-regulated Arabidopsis TRNs (Gaudinier et al., 2018) were used to identify the DEGs-associated interactors in rice. Orthologous information was retrieved from the PlantGDB database and networks were constructed in Cytoscape ver 3.9.0. Expression values of DEGs were mapped onto the networks where red color nodes represent upregulated DEGs and blue color nodes correspond to downregulated DEGs. Light gray color nodes represent interactors but not DEGs in Nidhi and Panvel1.

whereas 500 and 186 exclusive interactors were detected in Nidhi and Panvel1, respectively (**Supplementary Table S11**). GO annotation of interactors involved in the PPI network revealed signal transduction, phosphorylation, cell cycle, and post-translational protein modification among others, as highly enriched exclusive GO terms in Nidhi. In Panvel1, highly

enriched GO terms were a response to heat, protein refolding, water homeostasis, cell redox homeostasis, specification of floral organ identity, and protein import into mitochondrial matrix among others (**Supplementary Table S12**). To reduce the network complexity for better interpretation, MCODE algorithm-based sub-clustering of networks was performed in Cytoscape. We detected 13 network subclusters/molecular complexes in Nidhi, and 6 subclusters in Panvel1 (**Figure 6** and **Supplementary Table S4**). Those with MCODE score > 3 and node number > 3 were considered for further analyses (**Supplementary Table S13**). In Nidhi, subcluster 1 with the highest MCODE score consisted of 23 nodes and 242 edges, whereas 11 nodes and 48 edges were present in cluster 1 in Panvel1. EXPath-based GO enrichment analyses revealed that important sub-clusters in Nidhi were primarily involved in cytoskeleton organization, cell wall, and related processes, whereas in Panvel1, they were chloroplast development and related processes (**Supplementary Table S13**).

Nitrate-Regulated Differential Post-translational Modifications in Contrasting Genotypes

Initial gene ontology analysis of N-responsive DEGs in Nidhi using ExPath 2.0 revealed terms associated with post-translational modifications (PTM), viz., phosphorylation,

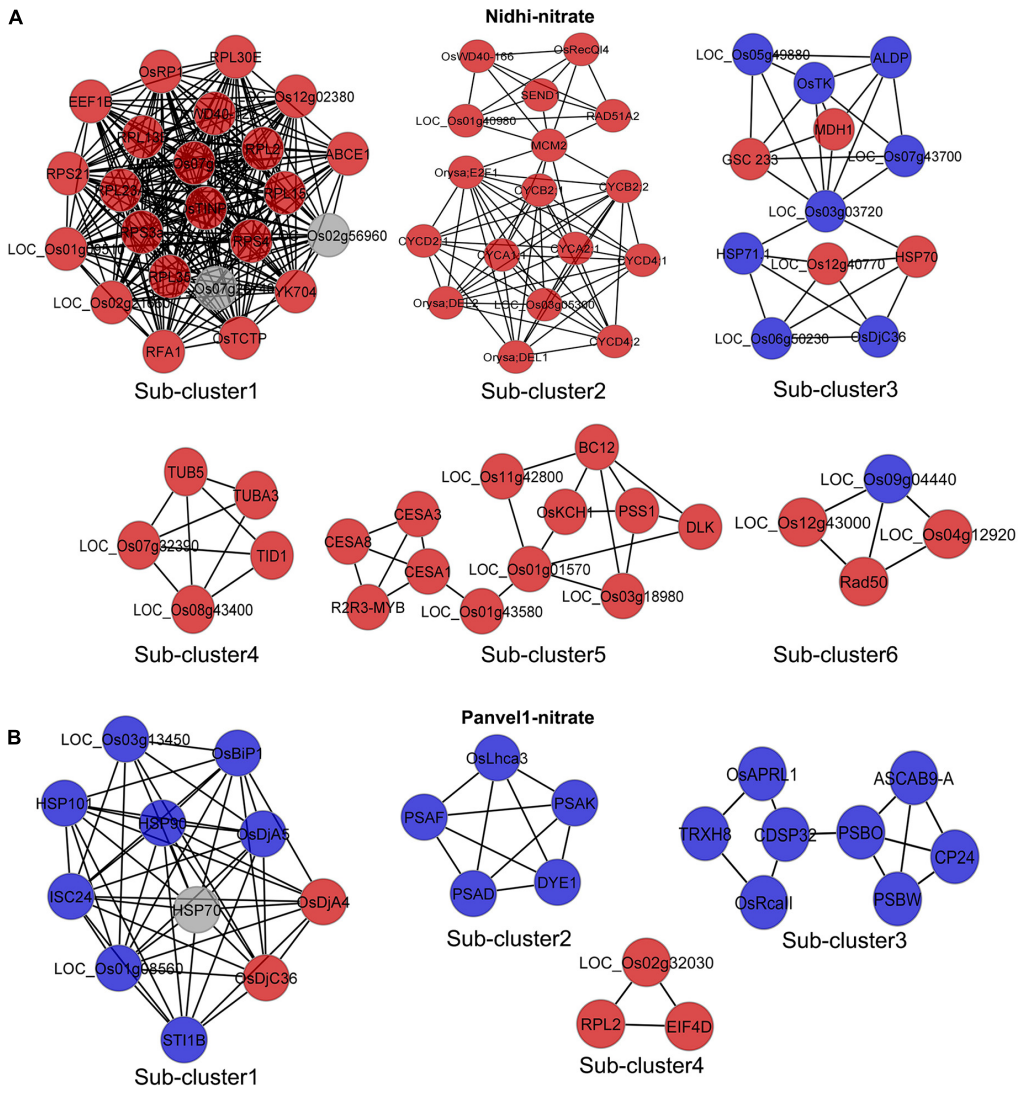

FIGURE 6 | Nitrate-responsive protein-protein interaction (PPI) sub-clusters/molecular complexes in Nidhi and Panvel1. DEGs-associated interactors were retrieved by STRING, BioGRID, PRIN, and MCDRP databases. Experimentally validated interaction pairs were used to construct the PPI networks in Cytoscape (**Supplementary Figures S2, S3**). Molecular complexes/sub-clusters of PPI networks were identified using the MCODE plugin in Cytoscape. Thirteen and six sub-clusters/molecular complexes were detected in Nidhi and Panvel1, respectively. Important nitrate-responsive sub-clusters/molecular complexes identified in Nidhi and Panvel1 are shown **(A,B)** and the remaining are given in **Supplementary Figure S4**. Red and blue color nodes correspond to the up and downregulated DEGs, respectively. Light gray color nodes represent the interactors, which are not DEGs.

de-phosphorylation, hydrolase activity, and phosphatase activity (**Supplementary Table S14**). In order to find out the N-responsive DEG-encoded proteins that can be modified post-translationally, gene ids were searched in the PTM viewer database (see text footnote 14). We found 475 IDs for Nidhi, of which a maximum number of PTMs (258) were found for phosphorylation followed by Hydroxyisobutyrylation (156), Acetylation (50), Carbonylation (20), Glycosylation (6), and one each of Malonylation, Succinylation, and Ubiquitinylation. Similarly, out of the 185 IDs for PTMs in Panvel1, the majority were Phosphorylation (85), followed by Hydroxyisobutyrylation (65), Acetylation (23), Carbonylation (9), N-glycosylation (2), and 1 for Ubiquitinylation (**Supplementary Table S14**). Venn analyses of these PTM genes with predicted NUE-related transporters and transcription factors in rice (Kumari et al., 2021) revealed post-translational modifications in the products of 7 DEGs of Nidhi and 3 DEGs of Panvel1. Out of these 7 genes, five were transporters and two were TFs. Out of the five transporters, four transporters, namely, *OsCAX1a, OsMGT1, OsHAK1,* and *AMT1.1* were modified post-translationally by phosphorylation, while *OsTPC1* was modified by acetylation. Out of the two TFs, *OsCOL4* was modified by acetylation while *OsAP2/ERF-40* by phosphorylation. Out of the 3 genes in Panvel1, two encoding TFs *OsPCL1* and *OsBBX26,* and one encoding transporter *OsSUT1* were modified by phosphorylation. Overall, our analysis identified 660 post-translationally modified proteins differentially regulated by nitrate in contrasting genotypes, of which the nature of PTM was known for only ten of them. The remaining 650 are novel and need detailed characterization and shortlisting for their role in NUE (**Supplementary Table S14**).

Yield Association and QTL Co-localization of N-Responsive Differentially Expressed Genes Reveals Nitrogen Use Efficiency Candidates

We have earlier shown that yield association is the most important distinction between N-response and NUE, whether for the phenotype (Sharma et al., 2021) or genotype (Kumari et al., 2021). Using an updated and expanded list of 3,532 yield-related genes in rice from literature and databases and the N-responsive DEGs identified in each of the contrasting genotypes, Venn Selection was performed and the resulting common genes are termed NUE-genes. This exercise with 1,327 DEGs exclusive to Nidhi revealed 188 NUE-genes (**Figure 7A**). Among these, 36 NUE- related genes (Nidhi nitrate) co-localized onto 9 NUE-QTLs regulating 7 phenotypic traits including grain yield response (GR), plant height (PH), panicle length, (PL) root length (RL), relative shoot dry weight (RSW), thousand-grain weight (TGW), spikelet per primary panicle (SPY). The maximum number of 18 NUE-genes co-localized onto chromosome 3, followed by 8 on chromosomes 1, 3 on chromosome 11, and two each on chromosomes 6 and 11 (**Figure 7B** and **Supplementary Table S15**). GO analysis of these 36 NUE- genes revealed Cyano-amino acid metabolism, starch, and sucrose metabolism as important pathways at FDR $\leq$ 0.05 (**Supplementary Table S16**).

Similar Venn selection using 665 N-responsive DEGs exclusive to Panvel1 and 3532 yield-related rice genes from literature resulted in 98 NUE-genes. Among these, 26 were co-localized onto 16 NUE-QTLs regulating 11 phenotypic traits including a number of productive tillers (PTN), grain yield response (GR), harvest index (HI), nitrogen use efficiency (NUE), panicle length (PL), plant height (PH), relative biomass (RBM), relative shoot dry weight (RSW), spikelet fertility percentage (SFP), spikelet per primary panicle (SPY), and thousand-grain weight (TGW). The maximum number of 9 genes were co-localized onto chromosome 3, 8 genes on chromosome 1, 2 genes each on chromosomes 2 and 7, and one gene each co-localized onto chromosomes 4, 5, 6, 8, and 11 (**Figure 7** and **Supplementary Table S15**). GO analysis of these 36 NUE - genes revealed photosynthesis, carbon metabolism, and pyruvate metabolism along with others as important pathways at FDR $\leq$ 0.05 (**Supplementary Table S16**).

Nitrate Influences Photosynthetic and Water Use Efficiencies in Contrasting Genotypes

To experimentally validate some of the common physiological processes, viz. photosynthesis, transpiration, water stress, and stomatal conductance in the contrasting rice genotypes Nidhi and Panvel1, they were grown in the greenhouse for 21 days as described in materials and methods. They were used to measure photosynthesis, transpiration, stomatal conductance, photosynthetic efficiency, transpiration efficiency, and internal water use efficiency. For the purpose of better understanding of NUE, the relative percentage was calculated in low nitrate over normal nitrate for each of the measured parameters. All three relative efficiencies in low nitrate (1.5 mM) over normal nitrate (15 mM) were found to be significantly higher ($P < 0.05$) for the high NUE genotype Panvel1 than for low NUE genotype Nidhi (**Figure 8**). These results are in line with our earlier results (Kumari et al., 2021). The relative rate of transpiration and stomatal conductance were significantly higher ($P < 0.05$) in the genotype Nidhi than in Panvel1, while the opposite pattern was found in the high NUE genotype Panvel1 (**Figure 8**). Interestingly, relative photosynthesis was significantly higher in low nitrate in genotype Panvel1 while it was not found significant in the genotype Nidhi (**Figure 8**).

DISCUSSION

Understanding the genetic determinants of NUE is crucial for crop improvement toward NUE and much remains to be done despite the rapid recent progress in this direction (Raghuram and Sharma, 2019). This study used comparative microarray analysis of nitrate response in two Indica rice genotypes, viz. Nidhi and Panvel1 with contrasting NUE toward dissection of the genetic basis for NUE, as well as to identify its underlying biological processes. The two genotypes, namely, Nidhi and Panvel1 were previously characterized as contrasting for NUE (Sharma et al., 2018, Sharma et al., 2021). Their potted whole plants were grown in nutrient-depleted sand as described earlier

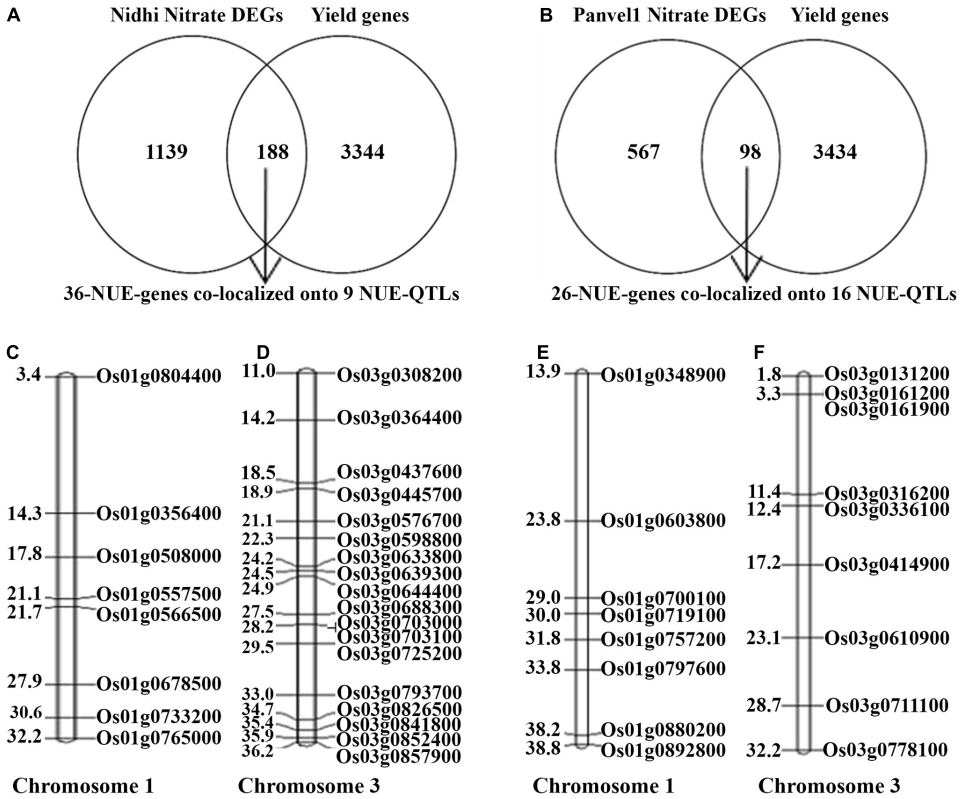

FIGURE 7 | (A) Venn selection of yield-related and Nidhi nitrate genes revealed 188 NUE-genes. Among them, only 36 NUE-genes colocalized onto 9 NUE-QTLs. **(B)** Venn selection of yield-related and Panvel nitrate genes revealed 98 NUE-genes. Among them, only 26 NUE-genes colocalized to 16 NUE-QTLs. **(C,D)** Representative figure of Nidhi nitrate NUE genes colocalized on chromosomes 1 and 3. **(E,F)** Representative figure of Panvel nitrate NUE genes colocalized on chromosomes 1 and 3. Gene id is given on the right side of the map and the physical location of genes is given on the left side of the map (in mb).

(Sharma et al., 2019) to ensure precise control of the N-form (nitrate) and N-dose (1.5 or 15 mM) and avoid uncertainties typical in the field soils. The differential N-response and NUE of both the genotypes (**Figures 1A,B**) was confirmed by RT-qPCR analysis of the expression of nitrate reductase and nitrite reductase (**Figures 1C,D**). Following microarray analysis, some genes/processes that could explain the differences in NUE were identified and validated, apart from localizing them in QTLs known to be associated with NUE as discussed below.

Our previous transcriptomic analyses revealed many unreported genes/processes involved in nitrate-response in Indica rice (Pathak et al., 2020) as well as in Japonica (Mandal et al., 2022). Further, a meta-analysis of all N-responsive transcriptomes together with yield-related genes predicted and shortlisted some NUE-related genes (Kumari et al., 2021). Comparative transcriptomic analyses of contrasting genotypes are expected to take these studies to the next level, but they were confined to ammonium nitrate response so far (Sinha et al., 2018; Subudhi et al., 2020), hence the current comparative study was conducted with nitrate.

We hypothesized that contrasting NUE between genotypes can be traced to the differential expression of genes and can reveal the underlying biological processes/pathways. We found that the majority of the DEGs were unique or genotype-specific, while a small but significant fraction of the 70 common DEGs were either oppositely regulated between the genotypes, or differed in their extent of up or downregulation.

Another interesting finding was that among the 10 nitrate-responsive DEGs that were common to both the genotypes but were oppositely regulated, there was one gene that was predicted to be NUE related by Kumari et al. (2021). This gene is associated with GDP-mannose 3,5-epimerase activity (*OsGME1*, GO:0047918) and is related to both grain yield (Oryzabase) and N-response (Kumari et al., 2021). In our study, it was downregulated in the low NUE genotype Nidhi and upregulated in the high NUE genotype Panvel1, making it another attractive candidate for further validation of its role in NUE.

Photosynthesis is considered to be a key process that determines N response and NUE in crops (Long, 2020), through the regulation of associated genes in rice (Kumari et al., 2021; Sharma et al., 2021; Mandal et al., 2022). We sought to further validate these findings using contrasting genotypes in this study. Our gene ontology (GO) analyses of the nitrate-responsive biological processes (**Supplementary Table S3**) revealed photosynthesis/photosystem, response to light, and translation as prominently regulated by nitrate in both contrasting rice genotypes. Our physiological data validated this finding (**Figure 8**), with increased carbon fixation, photosynthetic

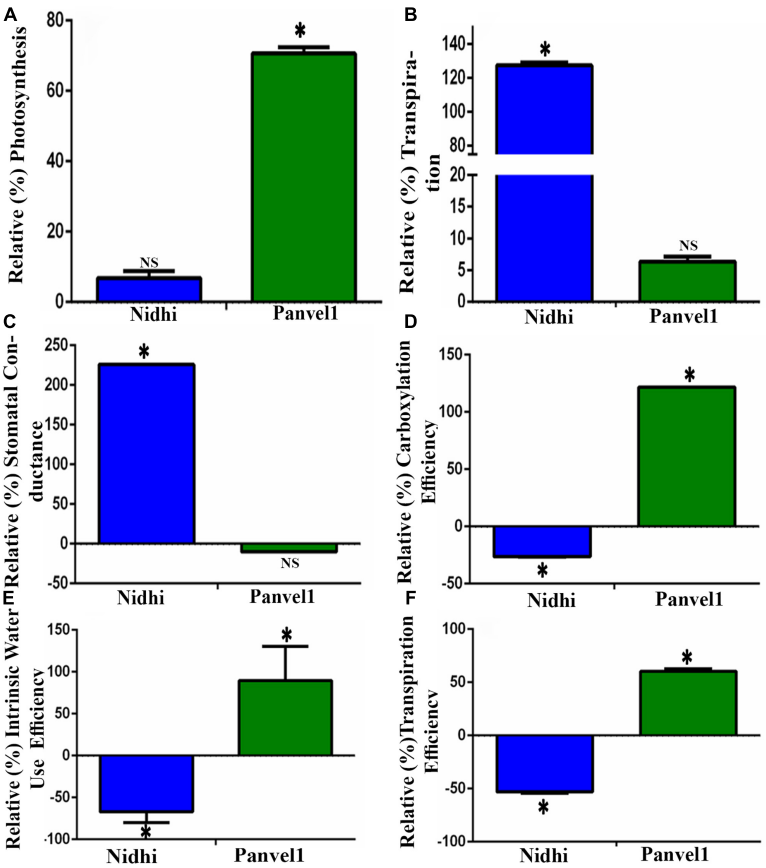

FIGURE 8 | Validation of biological processes: Validation was done using Licor instrument 6400XT (LI-COR, Lincoln, NE, United States) on 21 old days grown plants. Plants were grown in nutrient-depleted soil and fertilized with Arnon Hoagland medium having nitrate as the sole source of N with 15 mM concentration as control while 1.5 mM, was used as a test. Measurement was done in five biological replicates. Percent increase or decrease (relative measurement) for each of the measurements was calculated in low nitrate over normal nitrate. **(A)** Relative photosynthesis was measured in terms of μmol (CO_2) m^{-2} s^{-1}. **(B)** Relative transpiration was measured in terms of mol (H_2O) m^{-2} s^{-1}, and **(C)** Relative stomatal conductance was measured in terms of mol (H_2O) m^{-2} sec^{-1}). **(D)** Relative carboxylation efficiency was measured in terms of μmol (CO_2)/m^2 s^1/Ci as the ratio of photosynthesis and internal CO_2 concentration, **(E)** Relative internal water use efficiency was measured in terms of μmol (CO_2)/mol (H_2O), and **(F)** Relative transpiration efficiency was measured in terms of μmol (CO_2)/mmol H_2O m^{-2} s^{-1}. The test of significance for low nitrate over normal nitrate for each of the individual bars has been shown as star ($P < 0.05$), while NS represents non-significance.

efficiency, and internal water use efficiency in low nitrate relative to normal nitrate in the genotype Panvel1 compared to Nidhi. Therefore, these processes might explain, at least in part, the superior NUE of the genotype Panvel1 over Nidhi.

Similarly, our RT-qPCR data revealed differential regulation of CP29 (*LHCB4*) by nitrate in a genotype-specific manner. It has been established that along with other light-harvesting proteins, this gene is involved in energy dissipation in *Arabidopsis thaliana* (De Bianchi et al., 2008). Our results indicate the involvement of light-harvesting in NUE, in addition to carbon fixation discussed above. Interestingly, PPI networks of proteins encoded by DEGs in Nidhi and Panvel1 revealed a sub-cluster/molecular complex associated with chloroplast development/processes in Panvel1, but not in Nidhi (**Supplementary Figure S3**). Chloroplast development and associated processes such as N-assimilation are considered hotspots for NUE improvement in plants (Sandhu et al., 2021). Our earlier greenhouse/field experiments demonstrated that Panvel1 had higher chlorophyll contents (Sharma et al., 2021), which may in part explain its higher NUE *via* better management of N-related cellular homeostasis.

Transporters are known to regulate N-response/NUE in many crops (Mandal et al., 2018; Raghuram and Sharma, 2019; Madan et al., 2022), including rice (Pathak et al., 2020; Kumari et al., 2021; Nazish et al., 2021; Mandal et al., 2022). But they were not validated in contrasting genotypes to the best of our knowledge. In our present study, Nidhi revealed nine N-responsive transporters among many known to be associated with NUE, apart from an additional 17 linked with other functions and 40 others that are completely novel and functionally unvalidated (Kumari et al., 2021). In Panvel1, we found three nitrate-responsive transporters previously associated with NUE, nine linked with other functions, and 15 others that are completely novel and functionally unvalidated (**Supplementary Table S5**). Hence, our results validate the genotype-dependent expression of 55 transporters and aid in shortlisting them from many more transporters predicted to be associated with NUE by

Kumari et al. (2021). Eleven of them have been independently validated for their role in NUE in rice (Katayama et al., 2009; Fang et al., 2013, 2017; Fan et al., 2014, 2016; Ranathunge et al., 2014; Chen et al., 2016, 2017; Wang et al., 2018; Gao et al., 2019; Tang et al., 2019) making the rest of our shortlisted transporters attractive candidates in future efforts to improve NUE.

Transcription factors (TFs) are known to regulate N-response/NUE in many crops and cereals (Mandal et al., 2018; Raghuram and Sharma, 2019; Pathak et al., 2020; Kumari et al., 2021; Madan et al., 2022). But they were not validated in contrasting genotypes to the best of our knowledge. In our present study, Nidhi transcriptome revealed four N-responsive transcription factors among many known to be associated with NUE, apart from an additional 22 linked with other functions and 11 others that are completely novel and functionally unvalidated (Kumari et al., 2021). In Panvel1, we found six nitrate-responsive TFs previously associated with NUE, 15 linked with other functions, and six others that are completely novel and functionally unvalidated (**Supplementary Table S5**). Hence, our results validate the genotype-dependent expression of 17 transcription factors and aid in shortlisting them from many more TFs predicted to be associated with NUE by Kumari et al. (2021). Seven of them have been independently validated for their role in NUE in rice (Lijavetzky et al., 2003; Kurai et al., 2011; Sun et al., 2016; Tang et al., 2019; Alfatih et al., 2020; Gao et al., 2020; Wu et al., 2021), making the rest of our shortlisted TFs attractive candidates for future efforts toward improving NUE. We also identified many enriched binding motifs for NUE-associated N-responsive TFs in the present study for the first time for further validation of their role in NUE and shortlisting the targets for crop improvement.

Transcriptional regulatory networks can be used to predict the underlying interactions in pathways that regulate various responses. They were used to construct transcription regulatory networks and study N-response/NUE in rice (Pathak et al., 2020; Mandal et al., 2022). But they were not examined in contrasting genotypes to the best of our knowledge. We used Arabidopsis orthologs information to construct nitrate-responsive TRN in both the genotypes (**Figure 5** and **Supplementary Table S8**). The TF classes common to both the genotypes include AP2 domain-containing protein, no apical meristem protein, bZIP, and NAC domain-containing protein, and their target genes such as high-affinity nitrate transporter, glutamine synthetase, NIN protein, calcium/calmodulin-dependent protein kinases. Lactate/malate dehydrogenase was identified as a common expression of downregulated DEG in both the genotypes, whereas 16 and 7 DEGs were exclusive to TRN developed in Nidhi and Panvel1, respectively. Interestingly, the TRN captures some of the already validated individual targets in rice NUE such as nitrate reductase (Gao et al., 2019), glutamine synthetase1 (Brauer et al., 2011), and urea transporter (Beier et al., 2018), make the rest of the interactors in the TRN as attractive candidates in future efforts to improve NUE.

MicroRNAs are known to regulate N-response/NUE in a few crops (Zuluaga and Sonnante, 2019; Kumari et al., 2021). But they were not validated in contrasting genotypes to the best of our knowledge. In our present study, three N-responsive miRNAs among many known to be associated with NUE in Nidhi, apart from an additional 32 that are completely novel and functionally unvalidated (Kumari et al., 2021). In Panvel1, none of the miRNAs was found to be linked with NUE thus all 21 are completely novel and functionally unvalidated (**Supplementary Table S10**). Five of them have been independently reported for their role in yield (osa-miR1440; Liu et al., 2020, MIR396e and MIR396f; Zhang J. et al., 2020), phosphate starvation, and root traits (osa-miR399e; Dai et al., 2012) and NUE also including osa-miR170a (Kumari et al., 2021).

Our RT-qPCR validation of higher expression of the N-responsive DEG, big grain like1 (*BGL1*) in Panvel1 under low nitrate (relative to Nidhi), indicates its role in yield and NUE, as ectopic expression of *BGL1* leads to high yield through cell division and organ development enhancement (Lo et al., 2020). Similarly, a mutation in Phytoclock1 has been reported for early flowering in wheat (Mizuno et al., 2016) and our RT-qPCR results show lower expression of this N-responsive gene in Panvel1 relative to Nidhi. We earlier showed that flowering time is an important phenotypic trait for NUE (Sharma et al., 2021), indicating that the Phytoclock gene could also be one of the attractive candidates to manipulate NUE. Our RT-qPCR validation of the N-responsive upregulation of B-Box-Containing Protein 19 revealed far higher expression in Panvel1 relative to Nidhi. This gene has been reported for various kinds of stresses (Shalmani et al., 2019) and our results on its differential N-regulation in contrasting genotypes show the first indication of convergence between NUE and stress pathways. This is an underexplored area with considerable potential (Jangam et al., 2016).

An important caveat of transcriptome-based inferences is that they often ignore the role of post-translational modifications (PTMs). Recently, PTMs have been reported to play roles in nitrogen utilization, signal transduction, and response to sudden changes in nitrogen availability (Kumari and Raghuram, 2020). Our study revealed PTMs related to phosphorylation and ubiquitination among others, which could play their role in NUE. This is in line with the reported regulation of the ubiquitination pathway in controlling source-to-sink nitrate remobilization in Arabidopsis (Liu et al., 2017). We identified 475 N-responsive PTMs in Nidhi and 185 PTMs in Panvel1, demonstrating large differences between genotypes and opening an underexplored avenue to be tested for the role of specific PTMs in NUE.

Identification and characterization of QTL is a major driver of genetic improvement for any trait. But its progress for NUE has been slow, largely due to the poor characterization of the NUE phenotype, which became available recently for rice (Sharma et al., 2021). It was also pointed out recently that even though several QTL studies exist for NUE in rice, there is inadequate convergence between QTL and functional genomics (Kumari et al., 2021 and references cited therein). Earlier only N-responsive genes were co-localized on NUE-QTLs or yield QTLs (Chandran et al., 2016; Sinha et al., 2018) irrespective of their role in yield or NUE. But in the present study, we co-localized NUE genes (N-responsive and yield-related genes) to NUE-QTLs to identify NUE-candidates. On that basis, we found the

maximum number of 18 NUE-genes in Nidhi and 9 NUE genes in Panvel1 co-localized with NUE- QTLs on chromosome 3. In addition, there were 8 NUE-genes each on chromosome 1 in both Nidhi and Panvel1. These results advance the findings of Kumari et al. (2021), who reported these two chromosomes as the hotspots for NUE-QTLs in rice. This information could be of great value to breeders. Finally, GO analysis of those NUE-related DEGs co-localized onto NUE-QTLs revealed that carbon fixation, carbon metabolism, and photosynthesis as important processes for NUE in Panvel1 relative to Nidhi, revalidating our findings based on gene expression and physiological data described in the earlier sections.

CONCLUSION

Transcriptomic analysis of nitrate-response in two rice genotypes contrasting for NUE revealed differential involvement of biological processes, transporters, transcription factors and their networks, miRNAs, post-translational modifications, and NUE-candidates co-localized onto NUE QTLs in a genotype-dependent manner.

DATA AVAILABILITY STATEMENT

The datasets presented in this study can be found in online repositories. The names of the repository/repositories and accession number(s) can be found below: https://www.ncbi.nlm.nih.gov/geo/, accession number: GSE140257.

AUTHOR CONTRIBUTIONS

NS performed most of the experiments, analyzed the data, and wrote the first draft. SK performed NUE-gene identification and their co-localization to NUE-QTLs and TFBS ontology analysis, and helped in raising and harvesting plant tissues, RNA isolation, and RT-qPCR. DJ performed statistical and network analysis, and helped in RT-qPCR and manuscript drafting. NR helped in the planning, mentoring, and supervision of the experiments, data interpretation, edited, and finalizing of the manuscript. All authors read and approved the submitted version.

FUNDING

We thank research grants from NICRA-ICAR [F. No. 2-2(60)/10-11/NICRA], DBT-NEWS-India-UK (BT/IN/UK-VNC/44/NR/2015-531 16), and UKRI-GCRF South Asian Nitrogen Hub (SANH) (NE/S009019/1), including a fellowship to NS, apart from his earlier UGC-NET Fellowship. SK and DJ thank UKRI GCRF South Asian Nitrogen Hub for their fellowship (UKRI GCRF South Asian Nitrogen Hub (SANH) [NE/S009019/1]).

ACKNOWLEDGMENTS

We thank Kuljeet S. Sandhu for training in data transformations, ICAR Indian Institute of Rice Research for providing seeds, Vikas Kumar Mandal for his help in preparatory work, and Pradeep Kumar for his technical and administrative support.

SUPPLEMENTARY MATERIAL

The Supplementary Material for this article can be found online at: https://www.frontiersin.org/articles/10.3389/fpls.2022.881204/full#supplementary-material

REFERENCES

Alfatih, A., Wu, J., Zhang, Z. S., Xia, J. Q., Jan, S. U., Yu, L. H., et al. (2020). Rice NIN-LIKE PROTEIN 1 rapidly responds to nitrogen deficiency and improves yield and nitrogen use efficiency. *J. Exp. Bot.* 71, 6032–6042. doi: 10.1093/jxb/eraa292

Beier, M. P., Obara, M., Taniai, A., Sawa, Y., Ishizawa, J., Yoshida, H., et al. (2018). Lack of ACTPK 1, an STY kinase, enhances ammonium uptake and use, and promotes growth of rice seedlings under sufficient external ammonium. *Plant J.* 93, 992–1006. doi: 10.1111/tpj.13824

Brauer, E. K., Rochon, A., Bi, Y. M., Bozzo, G. G., Rothstein, S. J., and Shelp, B. J. (2011). Reappraisal of nitrogen use efficiency in rice overexpressing glutamine synthetase1. *Physiol. Plant.* 141, 361–372. doi: 10.1111/j.1399-3054.2011.01443.x

Buske, F. A., Bodén, M., Bauer, D. C., and Bailey, T. L. (2010). Assigning roles to DNA regulatory motifs using comparative genomics. *Bioinformatics* 26, 860–866. doi: 10.1093/bioinformatics/btq049

Chandran, A. K. N., Priatama, R. A., Kumar, V., Xuan, Y., Je, B. I., Kim, C. M., et al. (2016). Genome-wide transcriptome analysis of expression in rice seedling roots in response to supplemental nitrogen. *J. Plant Physiol.* 200, 62–75. doi: 10.1016/j.jplph.2016.06.005

Chen, J., Fan, X., Qian, K., Zhang, Y., Song, M., Liu, Y., et al. (2017). pOsNAR 2.1: Os NAR 2.1 expression enhances nitrogen uptake efficiency and grain yield in transgenic rice plants. *Plant Biotechnol. J.* 15, 1273–1283. doi: 10.1111/pbi.12714

Chen, J. G., Zhang, Y., Tan, Y., Zhang, M., Zhu, L., Xu, G., et al. (2016). Agronomic nitrogen-use efficiency of rice can be increased by driving OsNRT2.1 expression with the OsNAR2.1 promoter. *Plant Biotechnol. J.* 14, 1705–1715. doi: 10.1111/pbi.12531

Chien, C. H., Chow, C. N., Wu, N. Y., Chiang-Hsieh, Y. F., Hou, P. F., and Chang, W. C. (2015). EXPath: a database of comparative expression analysis inferring metabolic pathways for plants. *BMC Genomics* 16(Suppl. 2):S6. doi: 10.1186/1471-2164-16-S2-S6

Coskun, D., Britto, D. T., Shi, W., and Kronzucker, H. J. (2017). Nitrogen transformations in modern agriculture and the role of biological nitrification inhibition. *Nat. Plants* 3, 1–10. doi: 10.1038/nplants.2017.74

Dai, X., Wang, Y., Yang, A., and Zhang, W. H. (2012). OsMYB2P-1, an R2R3 MYB transcription factor, is involved in the regulation of phosphate-starvation responses and root architecture in rice. *Plant Physiol.* 159, 169–183. doi: 10.1104/pp.112.194217

De Bianchi, S., Dall'Osto, L., Tognon, G., Morosinotto, T., and Bassi, R. (2008). Minor antenna proteins CP24 and CP26 affect the interactions between photosystem II subunits and the electron transport rate in grana membranes of *Arabidopsis*. *Plant Cell* 20, 1012–1028. doi: 10.1105/tpc.107.055749

Fan, X., Tang, Z., Tan, Y., Zhang, Y., Luo, B., Yang, M., et al. (2016). Overexpression of a pH-sensitive nitrate transporter in rice increases crop yields. *Proc. Natl. Acad. Sci. U.S.A.* 113, 7118–7123.

Fan, X., Xie, D., Chen, J., Lu, H., Xu, Y., Ma, C., et al. (2014). Over-expression of OsPTR6 in rice increased plant growth at different nitrogen supplies but decreased nitrogen use efficiency at high ammonium supply. *Plant Sci.* 227, 1–11. doi: 10.1016/j.plantsci.2014.05.013

Fang, Z., Bai, G., Huang, W., Wang, Z., Wang, X., and Zhang, M. (2017). The rice peptide transporter OsNPF7. 3 is induced by organic nitrogen, and contributes to nitrogen allocation and grain yield. *Front. Plant Sci.Sci.* 8:1338. doi: 10.3389/fpls.2017.01338

Fang, Z., Xia, K., Yang, X., Grotemeyer, M. S., Meier, S., Rentsch, D., et al. (2013). Altered expression of the PTR/NRT 1 homologue Os PTR 9 affects nitrogen utilization efficiency, growth and grain yield in rice. *Plant Biotechnol. J.* 11, 446–458. doi: 10.1111/pbi.12031

Gao, Y., Xu, Z., Zhang, L., Li, S., Wang, S., Yang, H., et al. (2020). MYB61 is regulated by GRF4 and promotes nitrogen utilization and biomass production in rice. *Nat. Commun.* 11:5219.

Gao, Z., Wang, Y., Chen, G., Zhang, A., Yang, S., Shang, L., et al. (2019). The indica nitrate reductase gene OsNR2 allele enhances rice yield potential and nitrogen use efficiency. *Nat. Commun* 10, 1–10. doi: 10.1038/s41467-019-13110-8

Gaudinier, A., Rodriguez-Medina, J., Zhang, L., Olson, A., Liseron-Monfils, C., Bågman, A. M., et al. (2018). Transcriptional regulation of nitrogen-associated metabolism and growth. *Nature* 563, 259–264. doi: 10.1038/s41586-018-0656-3

Good, A. G., Johnson, S. J., De Pauw, M., Carroll, R. T., Savidov, N., Vidmar, J., et al. (2007). Engineering nitrogen use efficiency with alanine aminotransferase. *Botany* 85, 252–262.

Gupta, S., Stamatoyannopoulos, J. A., Bailey, T. L., and Noble, W. S. (2007). Quantifying similarity between motifs. *Genome Biol.* 8:R24. doi: 10.1186/gb-2007-8-2-r24

Hoagland, D. R., and Arnon, D. I. (eds) (1950). "The water culture method for growing plants without soil," in *California Agricultural Experimental Station Circular No. 347* (Berkeley, CA: University of California), 1–32.

Hooper, C. M., Castleden, I. R., Aryamanesh, N., Jacoby, R. P., and Millar, A. H. (2016). Finding the subcellular location of barley, wheat, rice and maize proteins: the compendium of crop proteins with annotated locations (cropPAL). *Plant Cell Physiol.* 57:e9. doi: 10.1093/pcp/pcv170

Jangam, A. P., Pathak, R. R., and Raghuram, N. (2016). Microarray analysis of rice d1 (RGA1) mutant reveals the potential role of G-protein alpha subunit in regulating multiple abiotic stresses such as drought, salinity, heat, and cold. *Front. Plant Sci.* 7:11. doi: 10.3389/fpls.2016.00011

Katayama, H., Mori, M., Kawamura, Y., Tanaka, T., Mori, M., and Hasegawa, H. (2009). Production and characterization of transgenic rice plants carrying a high-affinity nitrate transporter gene (OsNRT2. 1). *Breed. Sci.* 59, 237–243.

Kumari, S., and Raghuram, N. (2020). "Protein phosphatases in N response and NUE in crops," in *Protein Phosphatases and Stress Management in Plants*, ed. G. K. Pandey (Switzerland: Springer), 233–244.

Kumari, S., Sharma, N., and Raghuram, N. (2021). Meta-analysis of yield-related and N-responsive genes reveals chromosomal hotspots, key processes and candidate genes for nitrogen-use efficiency in rice. *Front. Plant Sci.* 12:627955. doi: 10.3389/fpls.2021.627955

Kurai, T., Wakayama, M., Abiko, T., Yanagisawa, S., Aoki, N., and Ohsugi, R. (2011). Introduction of the ZmDof1 gene into rice enhances carbon and nitrogen assimilation under low-nitrogen conditions. *Plant Biotechnol. J.* 9, 826–837. doi: 10.1111/j.1467-7652.2011.00592.x

Langholtz, M., Davison, B. H., Jager, H. I., Eaton, L., Baskaran, L. M., Davis, M., et al. (2021). Increased nitrogen use efficiency in crop production can provide economic and environmental benefits. *Sci. Total Environ.* 758:143602. doi: 10.1016/j.scitotenv.2020.143602

Li, J. Y., Wang, J., and Zeigler, R. S. (2014). The 3,000 rice genomes project: new opportunities and challenges for future rice research. *Gigascience* 3, 2047–2117. doi: 10.1186/2047-217X-3-8

Li, Y., Xiao, J., Chen, L., Huang, X., Cheng, Z., Han, B., et al. (2018). Rice functional genomics research: past decade and future. *Mol. Plant* 11, 359–380. doi: 10.1016/j.molp.2018.01.007

Lijavetzky, D., Carbonero, P., and Vicente-Carbajosa, J. (2003). Genome-wide comparative phylogenetic analysis of the rice and *Arabidopsis* Dof gene families. *BMC Evol. Biol.* 3:17. doi: 10.1186/1471-2148-3-17

Liu, A., Zhou, Z., Yi, Y., and Chen, G. (2020). Transcriptome analysis reveals the roles of stem nodes in cadmium transport to rice grain. *BMC Genom.* 21:127. doi: 10.1186/s12864-020-6474-7

Liu, W., Sun, Q., Wang, K., Du, Q., and Li, W. X. (2017). Nitrogen Limitation Adaptation (NLA) is involved in source-to-sink remobilization of nitrate by mediating the degradation of NRT 1.7 in *Arabidopsis*. *New Phytol.* 214, 734–744. doi: 10.1111/nph.14396

Livak, K. J., and Schmittgen, T. D. (2001). Analysis of relative gene expression data using real-time quantitative PCR and the 2− ΔΔCT method. *Methods* 25, 402–408.

Lo, S. F., Cheng, M. L., Hsing, Y. I. C., Chen, Y. S., Lee, K. W., Hong, Y. F., et al. (2020). Rice Big Grain 1 promotes cell division to enhance organ development, stress tolerance and grain yield. *Plant Biotechnol. J.* 18, 1969–1983. doi: 10.1111/pbi.13357

Long, S. P. (2020). Photosynthesis engineered to increase rice yield. *Nat. Food* 1, 105–105.

Madan, B., Malik, A., and Raghuram, N. (2022). "Crop nitrogen use efficiency for sustainable food security and climate change mitigation," in *Plant Nutrition and Food Security in the Era of Climate Change*, eds V. Kumar, A. K. Srivastava, and P. Suprasanna (Amsterdam: Elsevier), 44–72.

Mandal, V., Sharma, N., and Raghuram, N. (2018). "Molecular targets for improvement of crop nitrogen-use efficiency: current and emerging options," in *Engineering Nitrogen Utilization in Crop Plants*, eds A. Shrawat, A. Zayed, and D. A. Lightfoot (Cham: Springer).

Mandal, V. K., Jangam, A. P., Chakraborty, N., and Raghuram, N. (2022). Nitrate-responsive transcriptome analysis reveals additional genes/processes and associated traits viz. height, tillering, heading date, stomatal density and yield in japonica rice. *Planta* 255, 1–19. doi: 10.1007/s00425-021-03816-9

Michlewski, G., and Cáceres, J. F. (2019). Post-transcriptional control of miRNA biogenesis. *RNA* 25, 1–16. doi: 10.1261/rna.068692.118

Mizuno, N., Kinoshita, M., Kinoshita, S., Nishida, H., Fujita, M., Kato, K., et al. (2016). Loss-of-function mutations in three homoeologous PHYTOCLOCK 1 genes in common wheat are associated with the extra-early flowering phenotype. *PLoS One* 11:e0165618. doi: 10.1371/journal.pone.0165618

Nazish, T., Arshad, M., Jan, S. U., Javaid, A., Khan, M. H., Naeem, M. A., et al. (2021). Transporters and transcription factors gene families involved in improving nitrogen use efficiency (NUE) and assimilation in rice (*Oryza sativa* L.). *Transgen. Res.* 31, 23–42. doi: 10.1007/s11248-021-00284-5

Norton, R., Davidson, E., and Roberts, T. (2015). *Nitrogen Use Efficiency and Nutrient Performance Indicators*. Washington, DC: GPNM.

Pathak, R. R., Jangam, A. P., Malik, A., Sharma, N., Jaiswal, D. K., and Raghuram, N. (2020). Transcriptomic and network analyses reveal distinct nitrate responses in light and dark in rice leaves (*Oryza sativa* indica var. Panvel1). *Sci. Rep.* 10, 1–17. doi: 10.1038/s41598-020-68917-z

Pathak, R. R., Mandal, V. K., Jangam, A. P., Sharma, N., Madan, B., Jaiswal, D. K., et al. (2021). Heterotrimeric G-protein α subunit (RGA1) regulates tiller development, yield, cell wall, nitrogen response and biotic stress in rice. *Sci. Rep.* 11, 1–19. doi: 10.1038/s41598-021-81824-1

Raghuram, N., and Sharma, N. (2019). "Improving crop nitrogen use efficiency," in *Comprehensive Biotechnology*, ed. M. Moo-Young (Pergamon: Elsevier), 211–220.

Raghuram, N., Sutton, M. A., Jeffery, R., Ramachandran, R., and Adhya, T. K. (2021). From South Asia to the world: embracing the challenge of global sustainable nitrogen management. *One Earth* 4, 22–27.

Ranathunge, K., El-Kereamy, A., Gidda, S., Bi, Y. M., and Rothstein, S. J. (2014). AMT1; 1 transgenic rice plants with enhanced NH4+ permeability show superior growth and higher yield under optimal and suboptimal NH4+ conditions. *J. Exp. Bot.* 65, 965–979. doi: 10.1093/jxb/ert458

Sandhu, N., Sethi, M., Kumar, A., Dang, D., Singh, J., and Chhuneja, P. (2021). Biochemical and genetic approaches improving nitrogen use efficiency in cereal crops: a review. *Front. Plant Sci.* 12:757. doi: 10.3389/fpls.2021.657629

Shalmani, A., Jing, X. Q., Shi, Y., Muhammad, I., Zhou, M. R., Wei, X. Y., et al. (2019). Characterization of B-BOX gene family and their expression profiles under hormonal, abiotic and metal stresses in Poaceae plants. *BMC Genom.* 20:27. doi: 10.1186/s12864-018-5336-z

Shannon, P., Markiel, A., Ozier, O., Baliga, N. S., Wang, J. T., Ramage, D., et al. (2003). Cytoscape: a software environment for integrated models of biomolecular interaction networks. *Genome Res.* 13, 2498–2504. doi: 10.1101/gr.1239303

Sharma, N., Sinha, V. B., Gupta, N., Rajpal, S., Kuchi, S., Sitaramam, V., et al. (2018). Phenotyping for nitrogen use efficiency (NUE): rice genotypes differ in N-responsive germination, oxygen consumption, seed urease activities, root growth, crop duration and yield at low N. *Front. Plant. Sci.* 9:1452. doi: 10.3389/fpls.2018.01452

Sharma, N., Kuchi, S., Singh, V., and Raghuram, N. (2019). Method for preparation of nutrient-depleted soil for determination of plant nutrient requirements. *Comm. Soil Sci. Plant Anal.* 50, 1878–1886.

Sharma, N., Sinha, V. B., Prem Kumar, N. A., Subrahmanyam, D., Neeraja, C. N., Kuchi, S., et al. (2021). Nitrogen use efficiency phenotype and associated genes: roles of germination, flowering, root growth, crop duration and yield at low N. *Front. Plant Sci.* 11:587464. doi: 10.3389/fpls.2020.587464

Sinha, S. K., Sevanthi V, A. M., Chaudhary, S., Tyagi, P., Venkadesan, S., Rani, M., et al. (2018). Transcriptome analysis of two rice varieties contrasting for nitrogen use efficiency under chronic N starvation reveals differences in chloroplast and starch metabolism-related genes. *Genes* 9:206. doi: 10.3390/genes9040206

Sinha, V. B., Jangam, A. P., and Raghuram, N. (2016). "Biological determinants of crop N use efficiency and biotechnological avenues for improvement," in *Proceedings of the N 2013*, eds C. Masso, A. Bleeker, N. Raghuram, M. Bekunda, and M. Sutton (Berlin: Springer).

Sinha, V. B., Jangam, A. P., and Raghuram, N. (2020). "Biological determinants of crop nitrogen use efficiency and biotechnological avenues for improvement," in *Just Enough Nitrogen*, eds M. A. Sutton, K. E. Mason, A. Bleeker, W. K. Hicks, C. Masso, N. Raghuram, et al. (Cham: Springer), 157–171.

Snyder, R., and Tegeder, M. (2021). Targeting nitrogen metabolism and transport processes to improve plant nitrogen use efficiency. *Front. Plant Sci.* 11:628366. doi: 10.3389/fpls.2020.628366

Subudhi, P. K., Garcia, R. S., Coronejo, S., and Tapia, R. (2020). Comparative Transcriptomics of Rice genotypes with contrasting responses to nitrogen stress reveals genes influencing nitrogen uptake through the regulation of root architecture. *Int. J. Mol. Sci.* 21:5759. doi: 10.3390/ijms21165759

Sun, H., Qian, Q., Wu, K., Luo, J., Wang, S., Zhang, C., et al. (2014). Heterotrimeric G proteins regulate nitrogen-use efficiency in rice. *Nat. Genet.* 46, 652–656. doi: 10.1038/ng.2958

Sun, P., Zhang, W., Wang, Y., He, Q., Shu, F., Liu, H., et al. (2016). OsGRF4 controls grain shape, panicle length and seed shattering in rice. *J. Integr. Plant Biol.* 58, 836–847. doi: 10.1111/jipb.12473

Sutton, M., Raghuram, N., and Adhya, T. K. (2019). "The nitrogen fix: from nitrogen cycle pollution to nitrogen circular economy," in *Frontiers Emerging Issues of Environmental Concern*, ed. S. Pinya (Nairobi: United Nations Environment Programme), 52–64.

Sutton, M. A., Howard, C. M., Kanter, D. R., Lassaletta, L., Móring, A., Raghuram, N., et al. (2021). The nitrogen decade: mobilizing global action on nitrogen to 2030 and beyond. *One Earth* 4, 10–14.

Tang, W., Ye, J., Yao, X., Zhao, P., Xuan, W., Tian, Y., et al. (2019). Genome-wide associated study identifies NAC42-activated nitrate transporter conferring high nitrogen use efficiency in rice. *Nat. Commun.* 10, 1–11. doi: 10.1038/s41467-019-13187-1

Tegeder, M., and Masclaux-Daubresse, C. (2018). Source and sink mechanisms of nitrogen transport and use. *New Phytol.* 217, 35–53.

Udvardi, M., Below, F. E., Castellano, M. J., Eagle, A. J., Giller, K. E., Ladha, J. K., et al. (2021). A research road map for responsible use of agricultural nitrogen. *Front. Sustain. Food Syst.* 5:660155. doi: 10.3389/fsufs.2021.660155

Wang, W., Hu, B., Yuan, D., Liu, Y., Che, R., Hu, Y., et al. (2018). Expression of the nitrate transporter gene OsNRT1. 1A/OsNPF6. 3 confers high yield and early maturation in rice. *Plant Cell* 30, 638–651. doi: 10.1105/tpc.17.00809

Waqas, M., Feng, S., Amjad, H., Letuma, P., Zhan, W., Li, Z., et al. (2018). Protein phosphatase (PP2C9) induces protein expression differentially to mediate nitrogen utilization efficiency in rice under nitrogen-deficient condition. *Int. J. Mol. Sci.* 19:2827. doi: 10.3390/ijms19092827

Wu, J., Zhang, Z. S., Xia, J. Q., Alfatih, A., Song, Y., Huang, Y. J., et al. (2021). Rice NIN-LIKE PROTEIN 4 plays a pivotal role in nitrogen use efficiency. *Plant Biotechnol. J.* 19, 448–461. doi: 10.1111/pbi.13475

Zhang, J., Zhou, Z., Bai, J., Tao, X., Wang, L., Zhang, H., et al. (2020). Disruption of MIR396e and MIR396f improves rice yield under nitrogen-deficient conditions. *Natl. Sci. Rev.* 7, 102–112. doi: 10.1093/nsr/nwz142

Zhang, Z., Gao, S., and Chu, C. (2020). Improvement of nutrient use efficiency in rice: current toolbox and future perspectives. *Theor. Appl. Genet.* 133, 1365–1384. doi: 10.1007/s00122-019-03527-6

Zuluaga, D. L., and Sonnante, G. (2019). The use of nitrogen and its regulation in cereals: structural genes, transcription factors, and the role of miRNAs. *Plants* 8:294. doi: 10.3390/plants8080294

Conflict of Interest: The authors declare that the research was conducted in the absence of any commercial or financial relationships that could be construed as a potential conflict of interest.

Publisher's Note: All claims expressed in this article are solely those of the authors and do not necessarily represent those of their affiliated organizations, or those of the publisher, the editors and the reviewers. Any product that may be evaluated in this article, or claim that may be made by its manufacturer, is not guaranteed or endorsed by the publisher.

frontiers | Frontiers in Plant Science

TYPE Original Research
PUBLISHED 25 November 2022
DOI 10.3389/fpls.2022.1006044

OPEN ACCESS

EDITED BY
Nandula Raghuram,
Guru Gobind Singh Indraprastha University, India

REVIEWED BY
Antonio Lupini,
Mediterranea University of Reggio Calabria, Italy
Fabien Chardon,
INRA UMR1318 Institut Jean Pierre Bourgin, France

*CORRESPONDENCE
Gloria M. Coruzzi
gloria.coruzzi@nyu.edu

SPECIALTY SECTION
This article was submitted to Plant Physiology, a section of the journal Frontiers in Plant Science

RECEIVED 28 July 2022
ACCEPTED 01 November 2022
PUBLISHED 25 November 2022

CITATION
Shanks CM, Huang J, Cheng C-Y, Shih H-JS, Brooks MD, Alvarez JM, Araus V, Swift J, Henry A and Coruzzi GM (2022) Validation of a high-confidence regulatory network for gene-to-NUE phenotype in field-grown rice.
Front. Plant Sci. 13:1006044.
doi: 10.3389/fpls.2022.1006044

Validation of a high-confidence regulatory network for gene-to-NUE phenotype in field-grown rice

Carly M. Shanks[1], Ji Huang[1], Chia-Yi Cheng[1,2], Hung-Jui S. Shih[1], Matthew D. Brooks[1,3], José M. Alvarez[1,4,5], Viviana Araus[1,5,6], Joseph Swift[1,7], Amelia Henry[8] and Gloria M. Coruzzi[1]*

[1]Department of Biology, Center for Genomics and Systems Biology, New York University, New York, NY, United States, [2]Department of Life Science, College of Life Science, National Taiwan University, Taipei, Taiwan, [3]Global Change and Photosynthesis Research Unit, United States Department of Agriculture (USDA) Agricultural Research Service (ARS), Urbana, IL, United States, [4]Centro de Biotecnología Vegetal, Facultad de Ciencias de la Vida, Universidad Andrés Bello, Santiago, Chile, [5]Agencia Nacional de Investigación y Desarrollo–Millennium Science Initiative Program, Millennium Institute for Integrative Biology (iBio), Santiago, Chile, [6]Departamento de Genética Molecular y Microbiología, Pontificia Universidad Católica de Chile, Santiago, Chile, [7]Plant Biology Laboratory, The Salk Institute for Biological Studies, La Jolla, CA, United States, [8]Rice Breeding Innovations Platform, International Rice Research Institute, Los Baños, Laguna, Philippines

Nitrogen (N) and Water (W) - two resources critical for crop productivity – are becoming increasingly limited in soils globally. To address this issue, we aim to uncover the gene regulatory networks (GRNs) that regulate nitrogen use efficiency (NUE) - as a function of water availability - in Oryza sativa, a staple for 3.5 billion people. In this study, we infer and validate GRNs that correlate with rice NUE phenotypes affected by N-by-W availability in the field. We did this by exploiting RNA-seq and crop phenotype data from 19 rice varieties grown in a 2x2 N-by-W matrix in the field. First, to identify gene-to-NUE field phenotypes, we analyzed these datasets using weighted gene co-expression network analysis (WGCNA). This identified two network modules ("skyblue" & "grey60") highly correlated with NUE grain yield (NUEg). Next, we focused on 90 TFs contained in these two NUEg modules and predicted their genome-wide targets using the N-and/or-W response datasets using a random forest network inference approach (GENIE3). Next, to validate the GENIE3 TF→target gene predictions, we performed Precision/Recall Analysis (AUPR) using nine datasets for three TFs validated *in planta*. This analysis sets a precision threshold of 0.31, used to "prune" the GENIE3 network for high-confidence TF→target gene edges, comprising 88 TFs and 5,716 N-and/or-W response genes. Next, we ranked these 88 TFs based on their significant influence on NUEg target genes responsive to N and/or W signaling. This resulted in a list of 18 prioritized TFs that regulate 551 NUEg target genes responsive to N and/or W signals. We validated the direct regulated targets of two of these candidate NUEg TFs in a plant cell-based TF assay called TARGET, for which we also had *in planta* data for comparison. Gene ontology analysis revealed that 6/18 NUEg TFs - OsbZIP23 (LOC_Os02g52780), Oshox22 (LOC_Os04g45810), LOB39

(LOC_Os03g41330), Oshox13 (LOC_Os03g08960), LOC_Os11g38870, and LOC_Os06g14670 - regulate genes annotated for N and/or W signaling. Our results show that OsbZIP23 and Oshox22, known regulators of drought tolerance, also coordinate W-responses with NUEg. This validated network can aid in developing/breeding rice with improved yield on marginal, low N-input, drought-prone soils.

KEYWORDS

rice, drought, nitrogen, gene regulatory network, network validation, NUE, GENIE3, WGCNA

Introduction

Nitrogen (N) and water (W) are essential resources for plant productivity that are becoming increasingly limited in marginal soils world-wide (Gibbs and Salmon, 2015; Hsieh et al., 2018). Moreover, applications of N and W in agriculture are costly resources to society (Williamson, 2011; Keeler et al., 2016; D'Odorico et al., 2020). Most studies in major crops like rice, examine the effects of N and drought separately (Anantha et al., 2016; Li et al., 2017; Volante et al., 2017; Zhao et al., 2017). More recently, studies that examine how the interaction between N and W availability affects rice phenotypes and gene regulation have been examined (Swift et al., 2019; Araus et al., 2020; Plett et al., 2020; Sevanthi et al., 2021).

Several studies have shown that genes critical to N-uptake, sensing and metabolism have been associated with a drought phenotype. For example, NRT1.1/CHL1/NPF6.3 the a dual-affinity nitrate transporter (Liu et al., 1999) is expressed in the guard cells in Arabidopsis. Moreover, *nrt1.1/chl1* mutant is more drought tolerant compared to wild-type. The loss of NRT1.1/CHL1 reduced the stomatal opening and transpiration rates which contribute to its drought-tolerant phenotype (Guo et al., 2003). Next, mutants in nitrate reductase in both Arabidopsis (NIA1 and NIA2) and rice (OsNR1.2) exhibit a drought-tolerant phenotype with reduced water loss (Lozano-Juste and Leon, 2010; Han et al., 2022). Transcription factors (TFs) are also at the center of N-by-W response. NLP7 is a master regulator of nitrogen signaling in Arabidopsis (Alvarez et al., 2020). The *nlp7* mutant shows drought resistant phenotype, similar to *nrt1.1/chl1* (Castaings et al., 2009). Putting these findings together, it has been hypothesized that NLP7 regulates NRT1.1/CHL1 expression in guard cells and further controls stomatal opening and hence drought tolerance. Another TF in rice, drought and salt tolerance (DST), also bridges between N-assimilation and stomata movement that provides a path to crop improvement under marginal soil (lowN-lowW) (Han et al., 2022).

On the genome-wide level, our current manuscript explores on the gene regulatory networks (GRN) involved in N-by-W interactions by mining the N-by-W response RNA-seq and phenotype dataset from field grown rice (Swift et al., 2019). In our previous Swift et al 2019 study, we used linear models to discover that N-by-W signaling (N/W, molarity and/or NxW synergistic interactions) significantly correlate with rice field phenotypes, compared to genes that respond *only* to W-dose or N-moles (Swift et al., 2019). That dataset – which we use in our current analysis includes transcriptomic and phenotypic data for 19 rice varieties that vary in their drought and N-response. These 19 rice varieties were treated in a 2x2 N-by-W matrix of two N-doses (fertilized vs. without N) and W-doses (high vs. low water) in field experiments conducted at the International Rice Research Institute (IRRI) in the Philippines (Swift et al., 2019) (Figure 1). While our Swift et al., 2019 study determined the importance of the N-by-W gene responses (e.g., N/W and NxW) to phenotypic field outcomes in rice, the goal of our present study is to determine the GRNs underlying TF→target gene→phenotype interactions that correlate with NUE phenotypes in the rice N-by-W field study.

To develop sustainable agricultural solutions to feed a growing population, in this study we exploit a systems biology approach to uncover and validate the gene regulatory networks (GRNs) by which rice (*Oryza sativa*) plants sense and respond to the combination of N- and W- availability to promote crop productivity. To this end, we connected gene-to-NUE phenotype using weighted gene correlation analysis (WGCNA) (Langfelder and Horvath, 2008). Next, for the target genes that correlate with NUE phenotypes, we identified TF-to-target gene relationships in a gene regulatory network (GRN) using GENIE3 (Huynh-Thu et al., 2010). We then validated the TF-to-target gene network predictions via precision/recall (AUPR) analysis using validated TF-target gene data obtained *in planta* using the ConnecTF platform (https://rice.connectf.org). Additionally, we applied the plant cell-based Transient Assay Reporting Genome-wide Effects of Transcription factors (TARGET) system

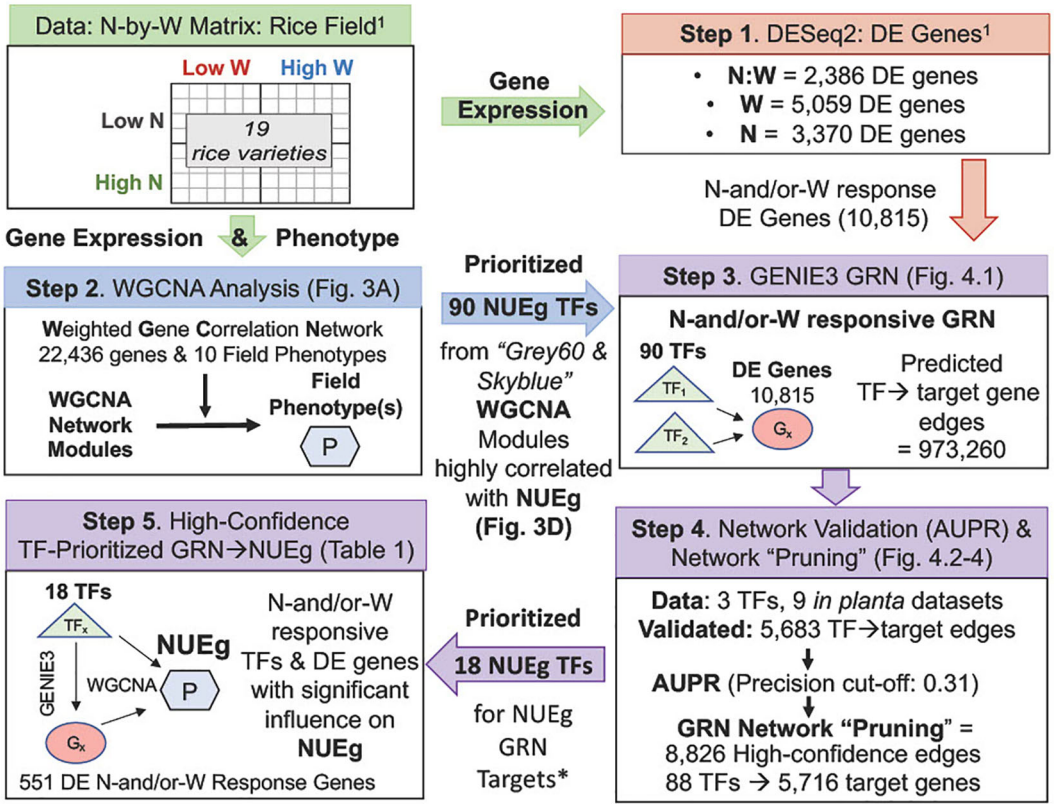

FIGURE 1
Flow-chart for generation of a high-confidence GRN of TF→target gene→NUEg phenotype from rice field data. Gene expression and phenotype data from field grown rice used to generate the WGCNA modules and GRN were obtained from 19 rice varieties of varying drought resistance, grown under a 2x2 N-by-W matrix with four combinations of N and W conditions (Low vs High) from Swift et al., 2019 (Swift et al., 2019)[1]. Step 1. N-by-W matrix: RNA-seq and field phenotype data: The differentially expressed (DE) rice genes that respond exclusively to either N:W, W and N were identified using DESeq2 analysis from field gene expression data (Swift et al., 2019). Step 2. WGCNA analysis: network modules-to-phenotype: The genes/TFs highly correlated with field phenotypes were identified using the field gene expression counts of the 22,436 normalized genes and 10 field phenotypes as inputs into weighted gene co-expression network analysis (WGCNA). Step 3. GENIE3 analysis: TF→target gene predictions: The TF→target gene predictions between 90 TFs highly correlated with the NUE grain yield (NUEg) from WGCNA analysis (Step 2) and the total 10,815 N-and/or-W response genes from Swift et al., 2019 (Step 1) determined using the network inference program GENIE3 resulted in ((90 TFs*10,815 DE genes) - 90 TFs) = 973,260 edges or TF→target gene predictions) Step 4. Network validation (AUPR) and "pruning": Validation data for 3 TFs in the GENIE3 network was located using rice.connectf.org (Brooks et al., 2020), which consisted of 9 RNA-seq/ChIP-seq *in planta* datasets. This rice validation data confirmed 5,683 predicted edges for the 3 TFs was used to calculate the area under the precision/recall curve (AUPR) using automated functions in ConnecTF (Brooks et al., 2020). This AUPR was then used to select a precision cut-off and "prune" the network for high-confidence edges of the GENIE3 gene regulatory network (GRN), again using automated functions in ConnecTF. The "pruned" GENIE3 network consists of 8,826 high-confidence edge predictions for 88 TFs and 5,716 genes linked to the NUEg phenotype from WGCNA. Step 5. High-confidence GRN: There are 18/88 TFs in the pruned network that regulated a significant number of the genes highly correlated with NUEg as identified in the WGCNA modules, for a total of 551 DE N-and/or-W Response Genes (Step 2).*See Table 1 and Supplementary Figure 3 for TF prioritization results and pipeline.

(Bargmann et al., 2013; Brooks et al., 2019), which we adapted in rice to validate the high-confidence TF-to-gene network for the N-by-W response genes whose expression level correlate with NUE.

Overall, we identified six TFs that regulate genes involved in both N and/or W signaling: OsbZIP23 (LOC_Os02g52780), Oshox22 (LOC_Os04g45810), LOB39 (LOC_Os03g41330), Oshox13 (LOC_Os03g08960), LOC_Os11g38870, LOC_Os06g14670. Two of these TFs are known regulators of drought tolerance - OsbZIP23 and Oshox22 – (Xiang et al., 2008; Zhang et al., 2012; Dey et al., 2016; Zong et al., 2016). Our present study shows that these TFs involved in drought responses are also responsive to N-by-W interactions. Moreover, we show that these six TFs control N-and/or-W response genes that correlate with NUEg. This information can now be applied to develop/breed rice plants with improved yield, on marginal, low N-input, drought-prone soils and on fields where water and N are limited due to climate change.

TABLE 1 Ranked list of 18 prioritized TFs that correlate with NUEg based on high-confidence edges to N-and/or-W DE genes in WGCNA modules (grey60 and skyblue).

Rank. TF Name	Significant overlap of pruned GENIE3 target genes w/ 1,099 N-and/or-W DE genes in WGCNA modules (grey60&skyblue) #TF_2s / #genes (Z score)	Relevant N and/or W GO terms associated with TF-target genes that overlap with N-and/or-W DE genes in WGCNA modules (grey60&skyblue)	TFs with High GS and MM for NUEg &/or WUE in WGCNA	Published TF Function (Reference)
1. OsbZIP23	17 TF_2s/159 genes (52.2)	"Response to water deprivation"	NUEg & WUE	Drought tolerance (Xiang 2008; Dey 2016; Zong 2016)
2. Oshox22	11 TF_2s/93 genes (39.3)	"Response to water deprivation" & "Response to abscisic acid"	NUEg & WUE	Drought tolerance (Zhang et al., 2012)
3. LOB39	5 TF_2s/53 genes (30.9)	"Nitrate assimilation"	NUEg & WUE	N-responsive gene (Obertello 2015; Yang 2017)
4. Oshox13	5 TF_2s/52 genes (27.6)	"Response to water deprivation"	NUEg & WUE	Unknown/Novel
5. LOC_Os11g38870	0 TF_2s/37 genes (25.9)	"Nitrate assimilation"	NUEg & WUE	Unknown/Novel
6. LOC_Os06g14670	4 TF_2s/49 genes (24.2)	"Response to water deprivation" & "Ammonia assimilation cycle"	NUEg & WUE	Unknown/Novel
7. ERF65	7 TF_2s/53 genes (32.1)	No N and/or W GO terms found	NUEg & WUE	Unknown/Novel
8. OsERF48	6 TF_2s/57 genes (27.3)	No N and/or W GO terms found	NUEg & WUE	Drought tolerance (Jung 2017)
9. OsIRO3	2 TF_2s/24 genes (16.4)	No N and/or W GO terms found	NUEg & WUE	Iron homeostasis (Wang 2020)
10. LOC_Os03g08470	1 TF_2/20 gene (15.2)	No N and/or W GO terms found	NUEg & WUE	Unknown
11. OsERF1	4 TF_2s/25 genes (15.2)	No N and/or W GO terms found	NUEg & WUE	Ethylene response (Hu 2008)
12. OsABF1	5 TF_2s/61 genes (13.6)	No N and/or W GO terms found	NUEg & WUE	Drought tolerance (Zhang 2017)
13. OsIRO2	1 TF_2/15 genes (13.3)	No N and/or W GO terms found	NUEg & WUE	Iron homeostasis/ N-signaling (Ogo 2007; Ueda 2020)
14. OSBZ8	1 TF_2/19 genes (12.8)	No N and/or W GO terms found	NUEg & WUE	ABA response (RoyChoudhury 2008)
15. RSR1	4 TF_2s/18 genes (10.2)	No N and/or W GO terms found	NUEg & WUE	Starch biosynthesis (Fu 2010)

(Continued)

10.3389/fpls.2022.1006044

10.3389/fpls.2022.1006044

TABLE 1 Continued

Rank. TF Name	Significant overlap of pruned GENIE3 target genes w/ 1,099 N-and/or-W DE genes in WGCNA modules (grey60&skyblue) #TF_2s / #genes (Z score)	Relevant N and/or W GO terms associated with TF-target genes that overlap with N-and/or-W DE genes in WGCNA modules (grey60&skyblue)	TFs with High GS and MM for NUEg &/or WUE in WGCNA	Published TF Function (Reference)
16. OsSPL9	0 TF_2s/15 genes (10.0)	No N and/or W GO terms found	NUEg & WUE	Grain yield (Hu 2021)
17. EIL4	4 TF_2s/40 genes (18.4)	No N and/or W GO terms found	NUEg	Unknown/Novel
18. IDEF2	5 TF_2s/96 genes (10.7)	No N and/or W GO terms found	NUEg	Iron homeostasis (Ogo 2008)
	Total 52 TF_2s/551 genes	"Response to water deprivation" & "Response to abscisic acid"		

First the TFs were ranked by the Z score for the overlap between the TF—target genes and the 1,099 N and/or W DE genes in WGCNA modules (grey60 & skyblue) associated with NUEg; second, for if the overlapping target genes for each TF were enriched for nitrogen and/or water GO terms; and third, for if the TF was highly associated with both NUEg and WUE.

Materials and methods

Source of N-by-W response data (transcriptome and phenotype) for 19 rice varieties

Field phenotypic data collection and conditions for 19 rice varieties (Indica and Japonica) can be found in Swift et al., 2019 (Swift et al., 2019). The details of the treatments are in Swift et al., 2019, but as an overview: For the +N treatment, 150 kg/ha dose of (NH4)2SO4 was applied at 23 days after sowing (DAS). The -N treatment had no addition of fertilizer. Plants in the -W condition were covered from rain with a rainout shelter (intermittent watering was applied to ensure growth), while plants in the +W condition received rainfall and normal watering. Water-use-efficiency (WUE) was determined from leaves with carbon isotope discrimination as outlined in Swift et al., 2019 (Swift et al., 2019). The nitrogen usage data was calculated using the Kjeldahl N (KJ N) method which determined the nitrogen content from 1 gram of leaf samples. The total KJ N is determined as in (Bremner and Mulvaney, 1982; Bremner, 1996) by converting organic nitrogen forms to NH_4^{3+} and then measuring the concentration. To calculate N-uptake, we used the Kjeldahl N percent (KJ N%) and vegetative shoot dry weight (SDW) measurements from Swift et al., 2019 collected from leaf samples. We then used the N uptake measurement to calculate NUEg and NUE biomass (NUEb).

$$N\ \ uptake\ \ (g/m2) = (KJ\ \ N\,\% * SDWg/plant) * plants/m2$$

$$NUEg = \frac{Grain\ \ yield\ \ g/m2}{N\ \ uptake\ \ g/m2}$$

$$NUEb = \frac{Biomass\ \ g/m2}{N\ \ uptake\ \ g/m2}$$

The field transcriptomic data consisted of 19 rice varieties (*Indica* and *Japonica*) of varying drought tolerant phenotypes, grown under four N-by-W treatment conditions, with three replicate leaf samples for RNA-seq for a total of 228 RNA-seq samples. Expression counts for 228 RNA-seq samples were normalized with the DESeq2 package (Love et al., 2014). The TFs and TF families from the N-and/or-W DE gene lists were identified based on the Plant Transcription Factor Database v4.0 categorization (Jin et al., 2017). See data availability in Swift et al., 2019 (Swift et al., 2019) for source phenotypes and transcriptome data.

Potential index (I_{PO}) calculation of NUE under low vs. high N and W conditions

To compare NUEg among the 19 rice varieties, we calculated the potential index (I_{PO}) as similar to Ndiaye et al, 2019

(Ndiaye et al., 2019). For the calculation, each variety's NUEg was compared with the conditional average, using the formula below.

$$I_{PO} = \frac{Y_{ij} - \underline{Y_j}}{\underline{Y_j}}$$

The I_{PO} is the potential index of variety *i*; Y_{ij} is the NUEg of variety *i* for the condition *j* where *j* is HWHN, HWLN, LWHN or LWLN; $\underline{Y_j}$ is the conditional mean of all 19 varieties under condition *j*. The I_{PO} is a relative value that shows the increase or decrease of a specific variety's NUEg, over the mean values. An $I_{PO} > 0$ indicates better NUEg, whereas $I_{PO} < 0$ indicates worse NUEg (Figure 2). The NUEg phenotype data was downloaded from Swift et al, 2019 (Swift et al., 2019).

WGCNA analysis: Gene-to-field phenotype correlation

The normalized counts files for each treatment and genotype were averaged as inputs into WGCNA to match the averaged field phenotypes for each biological replicate. This resulted in 76 transcriptomic and phenotypic values (19 varieties and 4 treatments) as inputs into WGCNA. The transcriptome counts file consists of counts for 22,436 genes in 76 samples. The R package, WGCNA, was used to perform the weighted correlation network analysis using step-by-step network construction and module detection (Langfelder and Horvath, 2008). We selected a MEDissThres of 0.5 to combine modules correlated with each other. We averaged the absolute value of the NUEg GS, WUE GS, and module membership (MM) scores for the genes in each module to select a cut-off value for highly correlated genes. (Figure 3C and Supplemental Figure 1). Overlapping module gene lists and N-and/or-W DE gene lists were made with Venny 2.1 web tool (Oliveros, 2015). To determine the Z score and p-value of the NUEg and WUE genes that overlap with N-and/or-responsive DE gene lists, we used the Genesect function in Virtual Plant 1.3 (Katari et al., 2010) (Figures 3B, D and Supplementary Figure 1).

GENIE3 analysis of GRNs and validation of TF→ target gene predictions by AUPR and "network pruning"

The GENIE3 package in R (Huynh-Thu et al., 2010) was used for network inference analysis. The gene expression data used to make the GENIE3 network consisted of the normalized counts of 228 RNA-seq samples for 10,815 N-and/or-W DE genes from Swift et al., 2019 (Swift et al., 2019) (Figure 1 Step 3). The 90 TFs for GENIE3 were selected from the two WGCNA modules (grey60 and skyblue) that are highly correlated with NUEg and are also N-and/or-W responsive (Figure 3D and Supplementary Data 4). The total unpruned network of 973,260 edges were uploaded to ConnecTF-Rice (rice.connectf.org) for network pruning and AUPR analysis (Brooks et al., 2020). This analysis is based on the *in planta* TF-target gene validation data

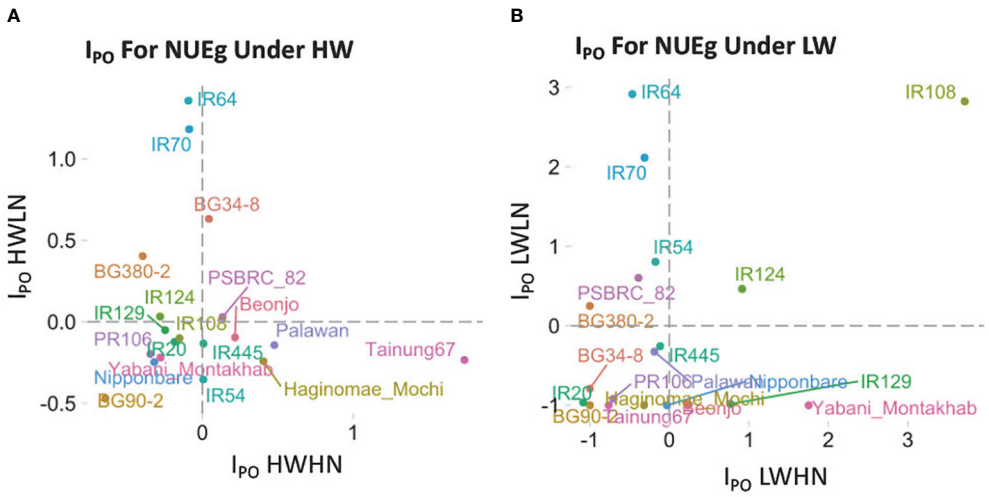

FIGURE 2
The NUEg phenotype for 19 rice varieties measured under four N-by-W conditions. We used the Potential index (I_{PO}) (Ndiaye et al., 2019) on 19 rice varieties which differ in their drought resistance to assess the NUEg values under **(A)** high water and **(B)** low water conditions with varying N-doses. **(A)** DHWHN, high-W/high-N; HWLN, high-W/low N; **(B)** LWHN, low-W/high N; LWLN, low-W/low-N.

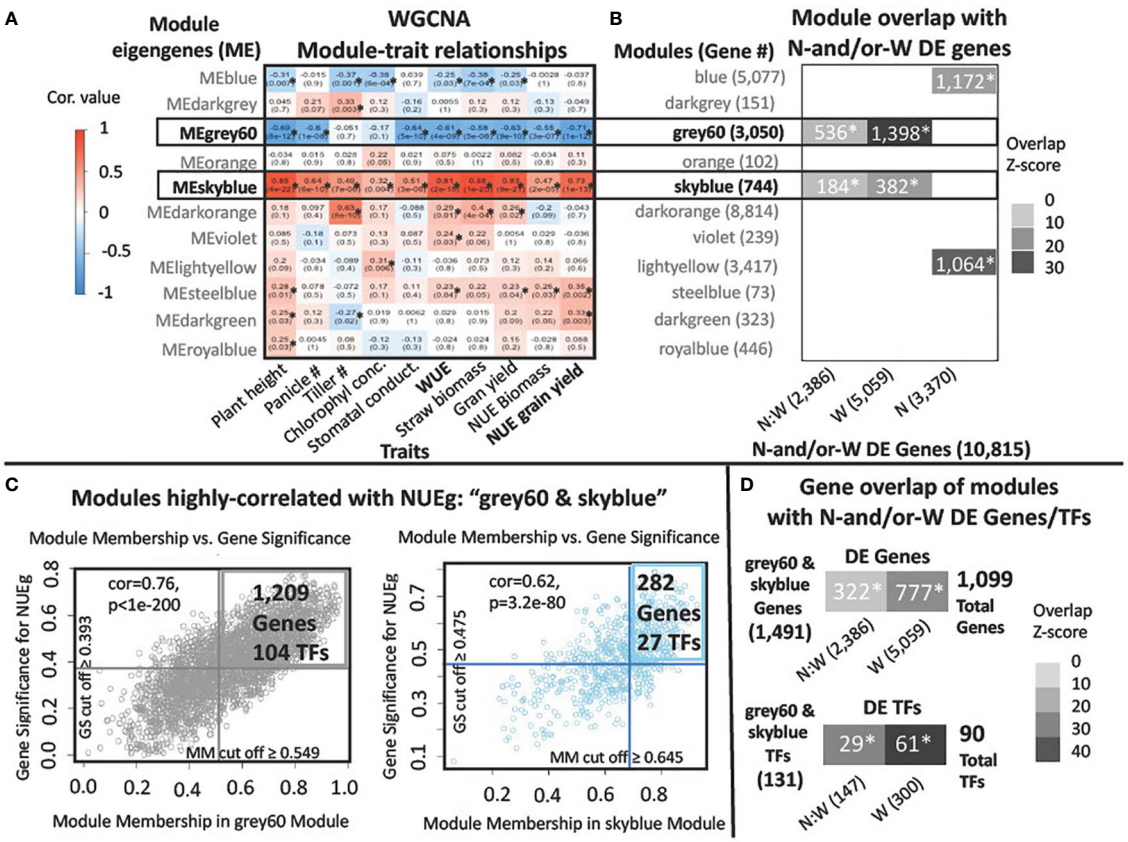

FIGURE 3
WGCNA modules named "grey60" and "skyblue" are highly correlated with NUEg in field grown rice. **(A)** Heatmap of the correlation values for the Module Eigengene (ME) values with field phenotypes from WGCNA. Red and blue colors note positive and negative correlation, respectively, for the ME for each module of co-expressed genes. Modules significantly associated with traits have a p value< 0.05, denoted by an asterisk*. **(B, D)** N-and/or-W DE genes and TFs for N:W, W and N -response genes derived from ANOVA analysis in Swift et al., 2019 (Swift et al., 2019). Heatmap of the Z-score for each overlap (Z-score ≥ 10). The p-value< 0.001 is denoted with an asterisk*. Z-score and p-values were calculated using the Geneset function in VirtualPlant 1.3 (Katari et al., 2010). **(B)** Significance of intersection between the genes in each co-expression module from WGCNA (Supplementary Data 1) and the N, W, and N:W DE genes, identified using Geneset function in VirtualPlant 1.3. **(C)** Scatterplots of the WGCNA Gene Significance (GS) for NUEg, versus the Module Membership (MM) for the grey60 and skyblue modules exhibit a significant correlation p-value< 0.001 with NUEg. The genes with a GS and MM cut-off scores above the average score for the genes in each module were selected for further analysis (1,209 grey60 + 282 skyblue genes = 1,491 genes). **(D)** Significance of gene intersection (using Geneset) between the union of the genes and TFs with an above-average GS and MM score from the WGCNA grey60 and skyblue modules (grey60∂skyblue) and the N:W, W, or N- responsive DE genes. Union of the genes in grey60 and skyblue modules: N-and/or-W response DE TFs (29 + 61 = 90 total) used for GENIE3 network analysis and N-and/or-W response DE genes (322 + 777 = 1,099 total) used to prioritize TFs from the pruned GENIE3 network (Supplementary Data 2).

for OsbZIP23, OsABF1, and OsNAC14 that is housed in the ConnecTF database (Brooks et al., 2020) (Figure 4 and Supplementary Figure 2). Gene Ontology (GO) biological process analysis was conducted using g:Profiler (https://biit.cs.ut.ee/gprofiler/gost) with settings for only annotated genes and a significance threshold of 0.05 calculated with Benjamini-Hochberg FDR (Raudvere et al., 2019) (Table 1). For this analysis the gene IDs for target genes and genes associated with GO terms were converted between MSU7 and RAPDB gene designations. Cytoscape v3.9.1 was used for network visualization (Paul Shannon et al., 1971) (Figure 5).

Plasmid construction for TF-perturbation experiments using *TARGET* assay in plant cells

The coding sequences of OsABF1 and OsbZIP23 were determined as listed in Phytozome 13 (Goodstein et al., 2012) and were synthesized by GENEWIZ (South Plainfield, NJ) with the GATEWAY cassette for cloning into the p1107 destination plasmid (Supplementary Figure 4). Entry vectors were cloned into the p1107 plasmid using the LR Clonase II reaction according to manufacturer's instructions (Invitrogen).

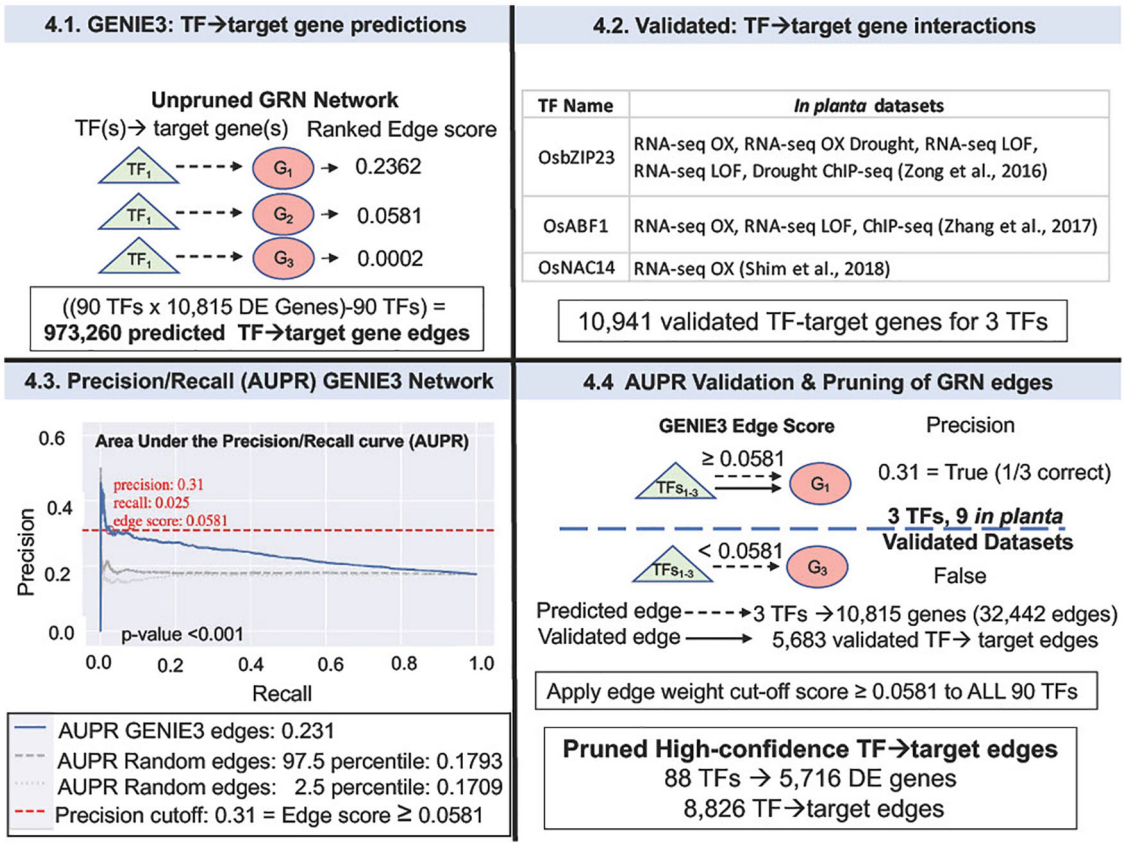

FIGURE 4
Validation of GENIE3 network using rice TF-perturbation datasets in Area Under the Precision Recall (AUPR) curve analysis. 4.1. GENIE3: The GENIE3 network ranked TF→target gene predictions for 90 N-and/or-W DE TFs (from the grey60 and the skyblue modules, Figure 3D), and 10,815 DE genes - each TF→target gene edge is given a weight. 4.2 The validated TF→target gene data used to "prune" the network predictions was identified using the rice TF data housed in the ConnecTF database (https://rice.connectf.org) (Brooks et al., 2020) (Supplementary Figure 2). Data for three TFs, OsbZIP23, OsABF1, and OsNAC14 were then used to validate the predicted GENIE3 edges with a total of 10,941 validated edges between all three TFs. 4.3. Area Under the Precision-Recall (AUPR) curve was calculated with the rice shoot *in planta* validation data for the three TFs. AUPR analysis shows that the ranking for the validated TF→target gene edges of the GENIE3 network (blue line) is significantly better (p-value<0.001, permutation test), than a set of randomly validated edges (Note: gray dashed lines are for the highest and lowest AUPR that resulted from random validated edges). A precision cut-off of 0.31 (red dashed line) was selected as the highest precision value before the curve flattens, and the "pruned" network edges were exported as an automated function in ConnecTF (Brooks et al., 2020). 4.4 The pruned GENIE3 network consists of 8,826 edges for 88 TFs and 5,716 genes that pass an edge score threshold of 0.0581. Source data of the original GENIE3 network vs. the high-confidence "pruned" GENIE3 network are supplied as Supplemental Data 4 and 5. Precision and Recall are calculated as in Brooks et al., 2019, 2020 (Brooks et al., 2019, 2020).

The p1107 plasmid for rice TARGET has a pBeaconRFP_GR (Bargmann et al., 2013) backbone with the following modification. The 35S promoters were replaced with maize Ubiquitin promoter subcloned from pTDM-C (Wu et al., 2016). A biotin ligase recognition peptide (BLRP) was fused at the N-terminal of the GATEWAY cassette, which is followed by the GR protein. All junctions were sequenced and verified for in frame TF-GR fusion proteins. The plasmid map and sequence (.FASTA) are provided in Supplemental Data File 1.

TARGET temporal TF perturbation experiment in rice leaf cells and RNA-sequencing

The rice protocol was adapted from our Arabidopsis *TARGET* protocol (Bargmann et al., 2013; Brooks et al., 2019) with some modifications. Rice seeds (Nipponbare) were sterilized by 70% ethanol for 3 mins followed by 50% commercial bleach for 30 min with rotation. The rice seeds were germinated in the dark for 4 days. The germinated rice

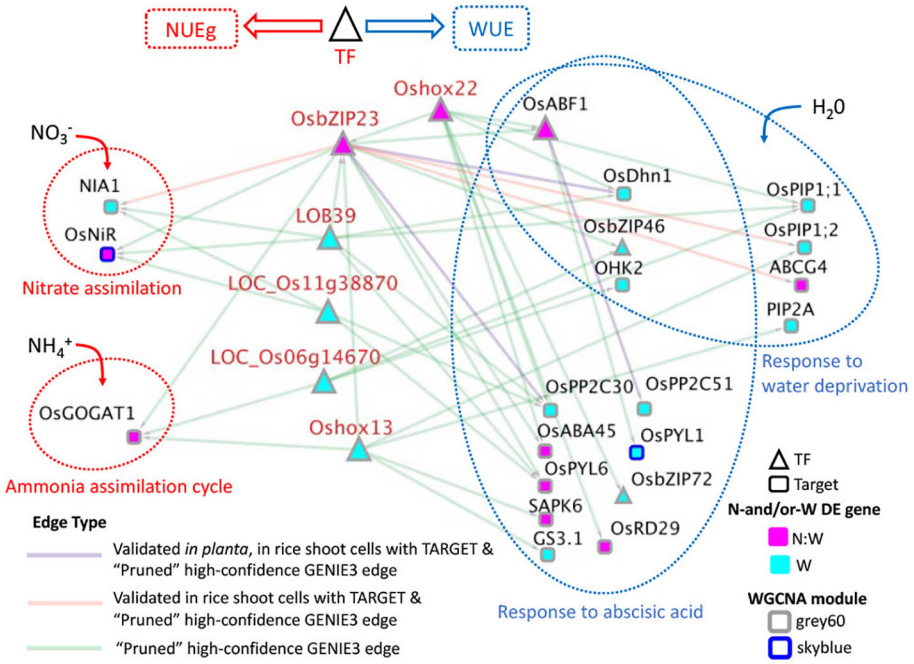

FIGURE 5
High-confidence GRN of rice TFs Targeting N-and/or W response DE genes correlated with NUEg connected to nitrogen and drought GO terms. This network consists of the TFs from Table 1 that regulate target genes associated with the gene ontology (GO) terms, "nitrate assimilation" (GO:0042128), "ammonia assimilation cycle" (GO:0019676), "response to water deprivation" (GO:0009414), and "response to abscisic acid" (GO:0009737). These GO terms were selected based upon the enrichment of these terms in the TF-target genes for each TF candidate from Table 1 using g:Profiler (Raudvere et al., 2019). The full list of GO terms for each TF is in Supplementary Data 8. To create this network the 551 total target genes from Table 1 were examined for the genes associated with the selected GO terms. This left 23/551 target genes and 14/18 TFs from Table 1 that regulate them. For simplicity and significance, we highlight the 6 TFs in red and their target genes because they regulate genes related to both nitrogen and water, either directly or indirectly. All 6 TFs were also associated highly with NUEg and WUE (Table 1). Edges for this network include either high-confidence GENIE3 edges, or validated GENIE3 edges for OsbZIP23 and OsABF1 for which we had TARGET data, and *in planta* data. The total network is in list in Supplemental Data 7.

seeds were transferred to ½ MS plates without sugar for 13 days in the growth chamber, under 16 h light/8 h dark diurnal cycle, at temperatures 27 and 25°C respectively and 70% humidity. On the day of the TARGET experiment, rice shoot tissue was cut into small (1 mm) pieces and stirred with cell-wall digestion solution (1.5% cellulase RS, 0.3% macerozyme R10 (Yakult Honsha), 0.6M mannitol, 10 mM MES (pH 5.7), 1 mM $CaCl_2$, 5 mM b-mercaptoethanol, and 0.1% BSA) in a flask. The flask was vacuumed infiltrated for 20 minutes and shaken at 50 rpm in the dark for 4 hours. Rice shoot protoplasts were filtered through a 40 µm cell strainer (BD Falcon, USA) and spun down for 5 min at 500 g. The rice shoot protoplasts were then washed with 10 mL W5 solution (150 mM NaCl, 1M $CaCl_2$, 1M KCl, 200 mM MES pH 5.7) three times, then resuspended in MMG solution (400 mM D-mannitol, 10 mM $MgCl_2$, 4 mM MES pH 5.7) to $1.0x10^6$ cells/mL. For protoplast transfection with vector, $1.0x10^5$ cells were mixed with 40 µg plasmid DNA and 110 µL 40% PEG solution (40% 4000 PEG (Sigma, 81242), 400 mM D-mannitol, 50 mM $CaCl_2$). The mixture was incubated at room temperature for 10 minutes. After incubation, the protoplasts were washed with W5 solution three times and resuspended in 1 mL WI solution (400 mM D-mannitol, 1M KCl, 200 mM MES pH 5.7). The transfected protoplasts were stored in the dark overnight. The next day, transfected protoplasts were treated with 30 µM cycloheximide (CHX) for 20 minutes (to block translation of secondary TF_2 targets genes), before a three-hour 10 mM dexamethasone (DEX) treatment (to induce TF-GR nuclear import). After 3 hours, TF vector and control empty vector transfected protoplasts were FACS sorted for RFP signals into 150 µL TRI regent for RNA extraction (Zymo, R2061) (Supplementary Figure 5). We used Lexogen QuantSeq 3' mRNA-Seq Library Prep Kit FWD for Illumina (Lexogen, 015.2x96) for making RNA-Seq libraries. The libraries were pooled and sequenced on the Illumina NextSeq 500 platform at NYU-CGSB Genomics Core facility.

RNA-seq analysis of TARGET assay for validation of TF-target direct regulated genes

The UMI-incorporated RNA-Seq libraries of TF-transfected and empty vector control were analyzed following Lexogen's guidance (https://www.lexogen.com/quantseq-3mrna-sequencing/). The reads' UMI were extracted from raw fastq files using `*extract*` command from UMI-tools v1.1.1 (Smith et al., 2017). Then the fastq files were trimmed by fastp 0.21.0 (Chen et al., 2018). The clean fastq files were aligned to MSU7 (Kawahara et al., 2013) genome using STAR 2.7.6a (Dobin et al., 2013). The aligned reads with the identical UMI were deduplicated using `*dedup*` command from UMI-tools v1.1.1 (Smith et al., 2017). The gene counts matrix was generated by featureCounts v2.0.1 (Liao et al., 2014) from the deduplicated bam files. The TARGET DE genes for OsABF1 and OsbZIP23 were identified using DESeq2 package (Love et al., 2014) by comparing TF vs Empty Vector with a Benjamin & Hochberg adjusted p-values< 0.05. Differentially expressed (DE) genes identified for OsABF1 and OsbZIP23 are listed in Supplementary Data 9. Overlap between *in planta* and TARGET data was conducted with Venny 2.1 (Oliveros, 2015) and the significance was determined with Genesect in Virtual Plant 1.3 (Katari et al., 2010). The calculations for precisions, recall and F-score for the GENIE3 network was the same as in Brooks et al., 2019 (Brooks et al., 2019) (Supplementary Figure 6).

Results

Phenotypic variation in NUEg in 19 rice varieties grown in N-by-W matrix field

The N-by-W response field data set used in our current study consisted of 19 rice varieties treated in a 2x2 matrix of four N-and/or-W treatment conditions (Figure 1) (Swift et al., 2019), comprising: well-watered (HW) with low-or-high N (HWLN, HWHN) (Figure 2A) vs. Low-W (LW) with low-or-high N (LWHN, LWLN) (Figure 2B) (For treatment details see Materials & Methods, and Swift et al., 2019. To refine our focus to NUEg, we examined how each of the 19 rice varieties performed for NUEg in the field (Figure 2). To identify the rice varieties with higher NUEg in the four different N-by-W field conditions, we adapted the Potential Index (I_{PO}) (Ndiaye et al., 2019) of NUEg for our N-by-W field dataset (Figure 2). The I_{PO} for NUEg indicated the relative performance of each of the 19 rice varieties, compared to the conditional average (dotted lines). Under the well-watered (HW) condition, none of the rice varieties performed well under *both* LN *and* HN conditions (Figure 2A). For example, IR64 showed the highest NUEg values under HWLN, but only average NUEg values under HWHN conditions (Figure 2A). By contrast, Tainung67 showed the highest NUEg values under HWHN, but only average NUEg values under HWLN conditions (Figure 2A). However, under LW treatments, there was one variety, IR108, that performed well under *both* LWLN *and* LWHN conditions, with the highest I_{PO}-NUEg compared to the other 18 varieties (Figure 2B). In line with this finding, the IR108 variety has been released under the variety name "Sukha dhan 5" to be used in the drought-prone regions of Nepal (Anantha et al., 2016). The I_{PO} analysis reveals that this phenotypic dataset covers a range of rice NUEg values. Therefore, we used this NUEg phenotype data from the 2016 growing season data and the corresponding transcriptome data of Swift et al 2019, for the ensuing network-to-NUE phenotype analysis (Figure 1).

Identification of N-and/or-W responsive DE genes highly correlated with NUEg

To discover the relationships between genes and field phenotypes including NUEg, we used WGCNA (Langfelder and Horvath, 2008) (Figure 1, Step 2, and Figure 3). The WGCNA analysis identified 11 co-expression modules for the 22,436 genes from the rice transcriptome data from the N-by-W field plot (Figure 1, Step 2, Figure 3A, Data in Supplemental Data 1). The genes in each of the WGCNA co-expression modules contribute to a Module Eigengene (ME) value based upon their Module Membership (MM) score. The MM score is the contribution of the individual gene to the ME value of the module (Langfelder and Horvath, 2008). We used the ME value to determine module correlation with each of the rice phenotypes from the N-by-W field plots (Figure 3A). The ME score for two WGCNA modules, grey60 (3,050 genes) and skyblue (744 genes) was significantly and highly correlated with the NUEg and WUE phenotype data in the N-by-W plot (Figure 3A). The ME value of the grey60 module was negatively correlated with NUEg (-0.71), while the ME value of the skyblue module was positively correlated with NUEg (+0.73) (Figure 3A). However, each WGCNA module contains subsets of genes that can be either positively or negatively correlated with NUEg. In WGCNA, this gene expression-to-phenotype correlation is called Gene Significance (GS), as shown for the plot of MM vs. GS in Figure 3C.

To identify which WGCNA modules had a significant representation of genes responding to N-and/or-W signals, the genes comprising each module were overlapped with the N-and/or-W responsive DE genes from Swift et al 2019 (Swift et al., 2019) (Figure 3B). This analysis uncovered a significant overlap of the N:W- and W- responsive gene lists with the genes in the WGCNA modules - grey60 and skyblue - which are each highly correlated with NUEg and WUE (Figure 3A). This demonstrates that the genes in the WGCNA modules - grey60 and skyblue - not only correlate with the NUEg phenotypes from the N-by-W

matrix field plots but are *also* enriched in genes responsive to N-and/or-W signals (Figure 3B). Additionally, the blue and lightyellow WGCNA modules are enriched in genes that respond to N-moles, but not to the interaction of N and W. While the WGCNA modules - blue and lightyellow - do not correlate significantly with NUEg, each of these modules correlates significantly with chlorophyll concentration (Figure 3A), a trait known to be regulated by N and used to determine N-status and the need for fertilizer in the field (Fageria et al., 2010).

Next, we performed two analyses that enabled us to prioritize the N-and/or-W response DE TFs and genes within each of the two WGCNA modules - grey60 and skyblue - that are most highly correlated with the NUEg phenotype (Figures 3C, D). The genes with MM scores closes to -1 or 1 are highly connected to their WGCNA module. In addition, genes with GS scores that have a high absolute value for a specific trait are also more biologically significant (Langfelder and Horvath, 2008). Therefore, to filter genes in each module that were highly correlated with NUEg, we identified genes with high absolute values for both their MM and GS scores. To do this, we first plotted the absolute values of the MM vs. GS scores for each gene in the WGCNA modules - grey60 and skyblue - which are highly correlated with NUEg (Figure 3C). Next, we calculated the average MM and GS scores for the genes in each of these two modules. This enabled us to set a cut-off and identify genes whose absolute MM and GS values were great than or equal to the average of the genes in each module (Figure 3C, upper right quadrant).

This analysis identified a combined total of 131 TFs and 1,491 genes highly relevant to NUEg in the two WGCNA modules: grey60 (104 TFs & 1,209 genes) and skyblue (27 TFs & 282 genes) (Figure 3C). Next, to identify whether genes highly relevant to NUEg are significantly enriched in N-and/or-W response gene, we performed a Genesect analysis (Katari et al., 2010) (Figure 3D). This analysis revealed significant overlaps between the N:W and W responsive gene lists from Swift et al 2019 (Swift et al., 2019), with the genes highly correlated with NUEg (131 TFs and 1,491 genes) from the combined grey60 and skyblue WGCNA modules (Figure 3D). The resulting overlap consisted of 90 TFs and 1,099 genes that are highly associated with NUEg and N-and/or-W responsive (Supplementary Data 2). Next, we determined which of these TFs and genes correlated NUEg were also highly associated with the WUE phenotype. To do this, we conducted the same analysis pipeline as described above for NUEg, in which we determine a new GS cut off value for WUE (Supplementary Figure 1A). This resulted in 79 TFs and 976 genes that are highly correlated with WUE and are N-and/or-W responsive (Supplementary Figure 1B, Supplementary Data 3). We find that 72 (80%) NUEg TFs and 815 (74%) NUEg genes are also highly correlated with WUE, thus suggesting a dual role for these genes/TFs in regulating both N and W responses.

For further analysis, we prioritized 90 TFs from the GENIE3 analysis that are; i) N-and/or-W responsive and ii) highly correlated to NUEg from the combined WGCNA modules - grey60 and skyblue. This analysis resulted in 29 TFs that are N:W-responsive and 61 TFs that are W-responsive (Figures 3C, D).

Validation of TF→target GRN predictions in WGCNA modules associated with NUEg

To predict TF→target gene interactions in GRNs important for NUEg, we used GENIE3, a random forest network inference method (Huynh-Thu et al., 2010). This analysis will identify potential master TF regulators of the NUEg response amongst the 90 TFs (29 TFs N:W-responsive and 61 TFs W-responsive) (Figure 3D) that are highly correlated with NUEg (e.g., members of WGCNA grey60 and skyblue models) (Figures 3A, C). To identify and rank these 90 TFs from these NUEg modules, we generated a GRN using 90 potential TF-regulators of 10,815 DE (N-and/or-W response genes) from the field N-by-W matrix (Figure 1, Step 1). The output of GENIE3 ranks the TF→target gene predictions in the order of confidence for each of the 90 TFs and the 10,815 DE genes N-and/or-W responsive (Figure 4). In total, the resulting GENIE3 inferred network ranks numerical confidence scores for each TF and target gene, excluding self-regulation of the TF ((90 TF x 10,815 genes) - 90 TFs) = 973,260 TF-target edges (Figure 4 and Supplemental Data 4).

Our next goal was to validate the TF-target gene interactions in our predicted GRN, using TF-target gene data validated *in planta*. To this end, we used experimentally validated TF-target gene interactions from TF perturbation data in rice, housed in the ConnecTF platform (https://rice.connectf.org) (Brooks et al., 2020) (Figure 4 and Supplementary Figure 2). The ConnecTF database includes published rice RNA-seq and ChIP-seq data available as of June 2020. To validate the GRN, we uploaded the TF→target gene interactions predicted by the GENIE3 network into ConnecTF and filtered for validated TF-regulation (RNA-seq) and TF-binding (ChIP-seq) data from rice *in planta* datasets (Figure 4 and Supplementary Figure 2, Supplementary Data 4). We focused our analysis on validated TF-target gene datasets from rice leaf tissue, given that the source RNA-seq data used to make the GENIE3 network was from rice leaves (Supplementary Figure 2).

Our query of the ConnecTF rice TF database identified experimental TF-target gene validation datasets for three TFs in rice leaf tissue from our GENIE3 network (Figure 4 and Supplemental Figure 2). The three validated rice TFs are OsABF1 (Zhang et al., 2017), OsbZIP23 (Zong et al., 2016), and OsNAC14 (Shim et al., 2018). These three validated rice TFs include a total of nine datasets with 10,941 validated target genes from TF-regulation and/or TF-binding data (Figure 4 and Supplementary Figure 2). We then used this *in planta* data as

"gold-standard" data to validate the TF→target gene predictions from our GENIE3 network using Area Under the Precision Recall (AUPR) curve analysis, which is an automated function in the ConnecTF platform (Figure 4). The results show that the AUPR for the TF→target gene predictions (edges) in the rice GENIE3 network were significantly higher than the random TF-target gene edges (P-value<0.001, permutation test) (Figure 4). Given the AUPR curve, we were able to select a precision threshold of 0.31 (e.g., TF→target gene edge score ≥ 0.0581). This cut-off score is equivalent to the TF→target gene predictions being accurate 1/3 of the time and this level of accuracy is comparable to other similar network validation AUPR studies (Varala et al., 2018; Brooks et al., 2019). The GENIE3 network was then pruned for only the high-confidence TF→target gene predictions using this precision cut-off score. This network pruning for precision, resulted in a GRN containing 8,826 high confidence edges connecting 88 TFs and 5,716 target N-and/or-W response DE genes (Figure 4 and Supplementary Data 5).

Prioritization of master TFs that regulate NUEg in response to N-and /or-W signaling

Our next goal was to prioritize candidate N-and/or-W response TFs with a significant influence on NUEg from the pruned GENIE3 network. To this end, we overlapped the pruned high confidence TF→target edges for the 88 TFs in the GENIE3 network with the 1,099 genes from the two WGCNA modules that are highly correlated with NUEg - grey60 & skyblue - N-and/or-W DE genes = 322 N:W response genes + 777 W-response genes) (Supplementary Figure 3). We calculated the significance of the overlapping TF→target genes with the 1,099 NUEg genes. To prioritize the 88 TFs, we ranked them by the Z-score for the overlap (Supplementary Data 6). We found 18 TFs whose high confidence TF→targets gene edges had the highest significant overlap (P-value<0.001, Z score ≥ 10) with the 1,099 genes in the NUEg WGCNA modules – grey60 and skyblue (Table 1). This analysis links 18 TFs→ 551 N-and/or-W response target genes→NUEg. Among the 18 TFs, OsbZIP23 is predicted to regulate the most of the NUEg correlated genes, compared to the other 17 TFs (Table 1). Additionally, we find that 16/18 TFs (all except EIL4 and IDEF4) are also highly corelated with WUE (Table 1 and Supplemental Data 3).

Of these 18 TFs, multiple TFs have published functions in drought tolerance including, OsABF1 (Zhang et al., 2017), OsbZIP23 (Xiang et al., 2008; Dey et al., 2016; Zong et al., 2016), Oshox22 (Zhang et al., 2012), and OsERF48 (Jung et al., 2017). Of note, OsABF1, OsbZIP23, and Oshox22 are N:W-responsive genes based on the N-and/or-W response DE gene lists from Swift et al 2019 (Supplemental Data 6), suggesting their new function in regulating N:W responses, in addition to drought (Table 1). Published functions for other candidate TFs in the 18 TF list include, N-signaling (LOB39) (Obertello et al., 2015; Yang et al., 2017), ABA signaling (OSBZ8) (RoyChoudhury et al., 2008), ethylene signaling (OsERF1) (Hu et al., 2008), iron homeostasis (IDEF2, OsIRO3, and OsIRO2) (Ogo et al., 2007, 2008; Masuda et al., 2019; Wang et al., 2020), starch biosynthesis (RSR1) (Fu and Xue, 2010), and grain yield (OsSPL9) (Hu et al., 2021) (Table 1). OsIRO2 was also found to regulate NUE in a N-response gene network in rice (Ueda et al., 2020).

Gene ontology for target genes for prioritized TFs

To further determine the mechanism of the prioritized TFs in regulating NUEg, we performed Gene Ontology (GO) analysis on the NUEg target genes from Table 1 regulated by each TF using g:Profiler (Table 1 and Supplemental Data 7) (Raudvere et al., 2019). For each TF, we focused on the relevant biological process GO terms related to water and nitrogen signaling. We found that the target genes of the TFs, LOB39, LOC_Os11g38870, and LOC_Os06g14670, were enriched for GO terms related to nitrogen including, "nitrate assimilation," and "ammonia assimilation cycle" (Table 1). Further, we found that the target genes of the TFs, OsbZIP23, Oshox22, Oshox13, LOC_Os06g14670, were enriched for GO terms related to drought including, "response to water deprivation," and "response to abscisic acid" (Table 1). LOC_Os06g14670 was the only TF enriched for nitrogen and drought-related GO terms. We did not identify any GO enrichment for the TF-target genes of OsERF48, OsIRO3, LOC_Os03g08470, OSBZ8, RSR1 and IDEF2. However, we did identify some other GO terms of interest for the remaining TFs including, "sulfur compound metabolic process" for EIL4, "cell communication" ERF65, "response to temperature stimulus" for OsABF1, "phosphorus metabolic process" for OsERF1, "iron ion homeostasis" for OsIRO2, and "zinc ion homeostasis" for OsSPL9 (Supplemental Data 8). While these enriched GO terms suggest the relevance of these TFs in other cell processes, we focus on the TFs that regulate the target genes associated with the nitrogen and water related GO terms.

High-confidence GRN of TFs that target nitrogen and drought-related genes

To identify the TFs that regulate both nitrogen and water response from our list of prioritized TFs, we took the subset of the GENIE3 network that includes 18 TFs→ 551 N-and/or-W response target genes associated with NUEg, and identified the target genes from this list of 551 that were part of the GO terms "nitrate assimilation", "ammonia assimilation cycle", "response to

water deprivation," and "response to abscisic acid" (Supplemental Data 7). This resulted in a list of 23 target genes regulated by 14 TFs (Supplemental Data 7). We found six TFs that regulated both nitrogen and water related target genes either directly (OsbZIP23, LOB39, LOC_Os11g38870, LOC_Os06g14670, and Oshox13) or indirectly (Oshox22 via regulation of OsbZIP23) (Figure 5). While OsABF1 did not regulate genes related to nitrogen, it is included in the network visualization because it is annotated for the water-related GO terms and is regulated by OsbZIP23 and Oshox22 (Figure 5).

The target genes involved in nitrate and ammonia assimilation that are regulated by the TFs in our high-confidence GRN include validated regulators of NUE, glutamate synthetase 1 (OsGOGAT), and nitrite reductase (OsNiR) (Lee et al., 2020; Yu et al., 2021) (Figure 5). We also find regulation of the putatively expressed nitrate reductase 1 (NIA1) gene, which is necessary for nitrate assimilation (Subudhi et al., 2020). The TFs, OsbZIP23, LOB39 and LOC_Os11g38870 regulate nitrate assimilation genes, while OsbZIP23, Oshox13, and LOC_Os06g14670 regulate the ammonia assimilation gene. OsbZIP23 is the only TF that regulates genes in both nitrate and ammonia assimilation genes (Figure 5).

Furthermore, each TF regulates genes involved in water deprivation and/or ABA signaling (Figure 5). These genes include the TFs OsbZIP46 and OsbZIP72, which are known positive regulators of drought tolerance and function in coordination with OsbZIP23 and OsABF1, two other prioritized TFs in our network (Lu et al., 2009; Chang et al., 2017; Zhang et al., 2017; Song et al., 2020). We also find regulation of the rice aquaporins, OsPIP1;1, OsPIP1;2, and PIP2A that facilitate water transport (Sakurai et al., 2005; Xu et al., 2019). In addition, there are genes that regulate multiple components involved in the ABA signaling pathway including, the ABA drought receptors, OsPYL1, OsPYL6 (Li et al., 2015; Santosh Kumar et al., 2021a), the clade A type 2C protein phosphatases, OsPP2C51, OsPP2C30 (Zong et al., 2016; Santosh Kumar et al., 2021a), and the ABA-activated protein kinase, SAPK6 (Chang et al., 2017). Overall, this result demonstrates that a subset of our prioritized candidate TFs regulates both nitrogen and water genes.

Network validation with *in vivo* TARGET assay

To further validate the nitrogen and drought-related edges in our high-confidence GRN (Figure 5), we performed *in vivo* Transient Assay Reporting Genome-wide Effects of Transcription factors (*TARGET*) assays to identify the *direct* TF-target genes for these TFs. We selected OsbZIP23 and OsABF1 for TARGET assays because we could compare the accuracy of our TARGET results with the available *in planta* data for these TFs in ConnecTF (Brooks et al., 2020). The *TARGET* TF-perturbation assay in isolated plant cells has been previously used to identify direct TF→regulated target genes in Arabidopsis (Bargmann et al., 2013; Varala et al., 2018; Brooks et al., 2019). In this paper, we adapt the vectors and the *TARGET* temporal TF-perturbation assay to rice shoot cells (Supplementary Figure 4).

The *TARGET* TF-perturbation assay identifies the direct TF→ regulated target gene interactions because; i) there is timed nuclear entry of the TF, and ii) translation of regulated secondary (TF_2) transcription factors is blocked by cycloheximide treatment. TF-regulated DE genes are identified by comparison to an empty vector control. The *TARGET* assay identifies direct TF→target genes as follows: i) the TF is fused to the glucocorticoid receptor (GR) protein that when expressed in the plant cells, ii) the TF-GR fusion is retained in the cytoplasm by HSP90 binding, iii) upon dexamethasone (DEX) treatment, the GR binding is released and the TF is imported into the nucleus where it can regulate expression (Bargmann et al., 2013; Brooks et al., 2019) (Supplementary Figure 5). iv) Additionally, cycloheximide + DEX treatment inhibits translation of mRNA for TF_2s. Therefore only the target genes of the over-expressed TF are identified, when compared to the empty vector control (Brooks et al., 2019).

Based on our TARGET assay, OsbZIP23 directly regulates 3,095 target genes, while OsABF1 directly regulates 2,151 target genes in rice shoot protoplasts (Supplementary Figure 6 and Supplemental Data 9). To determine the accuracy of our TARGET results, we took the overlap between the TARGET results and the *in planta* binding and expression data for each TF from ConnecTF (Zong et al., 2016; Zhang et al., 2017; Brooks et al., 2020). We found a significant overlap between the TARGET and *in planta* DE genes (Supplemental Figure 6A). This significant overlap suggests that the plant cell-based TF-target data can accurately identify *in planta* TF-regulated genes. Additionally, we find the *TARGET* data is as accurate, if not even better, than the *in planta* data at validating the predicted TF→target genes in the GENIE3 network, with a higher F-score and similar precision and recall values (Supplementary Figure 6B).

Given that the TARGET data was accurate in identifying OsbZIP23 and OsABF1 target genes, we used the TARGET and *in planta* data to validate the nitrogen and drought-related edges in our high-confidence GRN (Figure 5). We confirm with TARGET that OsbZIP23 directly regulates genes involved in nitrogen and drought responses including, NIA1 involved in nitrate assimilation (Subudhi et al., 2020), ABCG4 involved in abiotic stress responses (Matsuda et al., 2012), and the rice aquaporin, OsPIP1;2, that improves yield in rice (Xu et al., 2019). Additionally, we confirm with OsbZIP23 TARGET and *in planta* data that OsbZIP23 regulates drought associated genes OsDhn1 and OsPP2C30 (Lee et al., 2013; Santosh Kumar et al., 2021b). Furthermore, we confirm the role of OsABF1 in regulating drought signaling, as it regulates the drought-associated gene OsPP2C51 in both TARGET and in planta datasets (Figure 5) (Zong et al., 2016).

Overall, our TARGET results show that the high-confidence edges inferred in our GENIE3 network accurately predict TF→target genes, thus further confirming the role of OsbZIP23 in regulating both NUEg and WUE. In addition, we find a new function for OsbZIP23 in mediating NUEg phenotypes, as previous studies show its role in drought responses (Xiang et al., 2008; Dey et al., 2016; Zong et al., 2016). Thus, our combined network inference and validation approach reveals new TFs in regulating NUEg (Table 1).

Discussion

In this study, we sought to identify GRNs that control NUEg in response to two key interacting components that regulate rice productivity: N and W. By exploiting transcriptomic and phenotypic data collected from 19 rice varieties grown in a 2x2 N-by-W matrix in the field (Swift et al., 2019), we identified and validated the role GRNs comprised of N-and/or-W response genes for their role in TF→target gene→ NUEg phenotype relationships. The TF to N-by-W response gene information now encoded in this high-confidence GRN correlated to NUEg, can now be applied to develop/breed rice plants with improved yield marginal, low N-input, drought-prone soils – which are increasing in the face of climate change.

High-confidence GRN identifying master regulators of NUEg responsive to N-and/or-W signals

We were able to link the TF→target gene→NUEg phenotype using a combination of four approaches (*i*) WGCNA-based gene-to-trait co-expression network (Langfelder and Horvath, 2008), (*ii*) GENIE3, a random forest machine learning approach to GRN inference for predicting TF-target interactions (Huynh-Thu et al., 2010), (iii) Experimental validation of GRN predictions and Network "pruning" by AUPR (Varala et al., 2018; Brooks et al., 2019), and (iv) Network validation using TARGET, an approach which uses plant cells to identify *direct* TF→target gene interactions (Bargmann et al., 2013; Brooks et al., 2019). Using this pipeline (Figure 1), the WGCNA approach identified two network modules that were highly correlated to NUEg called "grey" and "skyblue". Next, we constructed a GRN for the genes in this module, based on their N-and/or-W response DE genes. Finally, we used experimental data for TF-target genes validated *in planta* (Zong et al., 2016; Zhang et al., 2017; Shim et al., 2018) as well as ones we generated in rice leaf cells for this study. These validated rice TF datasets were used to conduct precision/recall analysis of our GRN. This enabled us to set a precision cut-off score to prune the network for high confidence TF-target predictions for *all* TFs in the GRN.

Overall, our GRN analysis and validation identified OsbZIP23 and Oshox22 as top candidate master regulators of NUEg in response to N and W signaling. These two TFs are network hubs, as they regulate the largest number of DE genes (N-and/or-W responsive) that are highly correlated with NUEg in the grey60 and skyblue WGCNA modules (Table 1 and Supplemental Data 6). Further validating their known role in drought, these two TFs have published functions in regulating drought tolerance through the plant hormone abscisic acid (ABA) signaling responses (Xiang et al., 2008; Zhang et al., 2012, 2017; Park et al., 2015) (Table 1). Our current study, now links these two well-known drought TFs to regulation by N-and/or-W signaling and NUEg. Our results are also in line with previous studies that show OsbZIP23 activity to be dependent upon phosphorylation by SAPK2 (Zong et al., 2016), an osmotic stress/ABA-activated protein kinase, which promotes nitrate uptake and assimilation under drought stress (Lou et al., 2020).

In addition to the TF hubs (OsbZIP23 and Oshox22), we identify four TFs with novel functions NUEg and WUE gene regulation in our GRN. We identified four TFs (LOB39, Oshox13, LOC_Os11g38870, and LOC_Os06g14670), that regulate genes involved in both N and/or W responses using GO analysis of their predicted TARGET genes in the high-confidence GRN (Table 1 and Figure 5). Unlike OsbZIP23 and Oshox22, the TFs Oshox13, LOC_Os11g38870, and LOC_Os06g14670TFs had until now unknown functions in both nitrogen and drought regulation (Table 1). LOB39 expression is regulated by nitrogen, however it was previously not known to be involved in drought (Obertello et al., 2015). OsbZIP23, LOB39 and LOC_Os11g38870 regulate nitrate assimilation genes NIA1 and OsNiR, which is a known to promote nitrogen assimilation and NUE in coordination with OsNLP4 (Figure 5) (Yu et al., 2021). Furthermore, OsbZIP23, Oshox13 and LOC_Os06g14670 regulate the ammonia assimilation gene OsGOGAT1, which improves NUE in low N conditions in coordination with the ammonium transporter OsAMT1;2 (Lee et al., 2020). While it is known that rice prefers ammonia uptake compared to nitrate (Sasakawa and Yamamoto, 1978; Hachiya and Sakakibara, 2017), we find the TFs in this network regulate both pathways, with OsbZIP23 regulating genes involved in both.

We also examined the mechanism of transcriptional regulation between these master TFs in the NUEg GRN by validating TF→target gene interactions using TARGET, a plant cell-based assay that identifies *direct* TF→TARGET gene interactions (Bargmann et al., 2013; Varala et al., 2018; Brooks et al., 2019). We find that Oshox22 regulates nitrogen and water responses indirectly via candidate TFs OsbZIP23, and OsABF1 (Figure 5). We then validate the TF→target gene interactions for OsbZIP23 and OsABF1 TFs with the TARGET assay. We confirm that OsbZIP23 regulates both nitrogen and drought response genes, and OsABF1 regulated drought response genes, with TARGET and *in planta* data.

Overall, these finding supports previous studies that show the regulation of these two essential signals N-and-W are linked (Swift et al., 2019; Araus et al., 2020; Plett et al., 2020). Our work presents a path of how ABA/drought induced signaling regulates both N and W responses which ultimately affect crop phenotypes, such as NUEg, the trait of focus in our study.

Validation of GRNs in rice using ConnecTF as a platform to validate and prune for high-confidence networks

In our study, we demonstrate the usefulness of ConnecTF as a platform - now applied to rice - to integrate published TF-binding and TF-expression datasets to identify and validate target genes in GRNs (Brooks et al., 2020) (Figure 4 and Supplementary Figure 2). While some GRN studies use an arbitrary cut-off value for network pruning as in other network studies (Ueda et al., 2020), we show how TF-perturbation data can be used as a "gold-standard" for GRN validation and "network pruning", using automated AUPR functions in ConnecTF (Brooks et al., 2020) (Figure 4). We performed Precision/Recall analysis of the GRN for NUEg – using the TF-target gene validation sets for rice housed in the ConnecTF database. This enabled us to empirically select a TF→target precision cut-off value of 0.31 from the AUPR curve. This AUPR cut-off represents that approximately 1/3 of our GENIE3 network predictions are validated (Figure 4). This precision cut-off is comparable to what we find in other network studies in Arabidopsis that use AUPR analysis (Varala et al., 2018; Brooks et al., 2019). Overall, the automated AUPR function in ConnecTF provides an accurate, and facile means to validate GRN predictions in any rice GRN that researchers can load onto the site. Importantly, these cut-off values for TF→target gene validated edges established a cut-off score that can be applied to all TF→target gene edges in the network – including TFs which have not been validated. This enables the generation of a high-confidence network for all TFs in the GRN.

bZIP family TFs as regulators of N and W signaling

In our high-confidence GRN we identify nine bZIP TFs as regulators in our "pruned" network (Supplementary Data 6). Members of the bZIP family of TFs are known to regulate drought stress responses in multiple crops species in addition to rice, including *Glycine max*, *Zea mays* and *Hordeum vulgare* (Joshi et al., 2016). Additionally, bZIP family TFs regulate ABA hormone responses, which play a crucial role in regulating the drought response in plants in general (Joshi et al., 2016; Zong et al., 2016; Zhang et al., 2017; Araus et al., 2020). In our high-confidence GRN studies that focus on genes correlated with NUEg, we find that bZIP TFs regulate N-signaling as well as drought responses in rice. In line with our finding, previous studies examining N-responses in rice, identified bZIP transcription factors that regulate NUE (Ueda et al., 2020).

We identified three bZIP family members - OsABF1, OsbZIP23, and OSBZ8 - as top-regulators of N-and/or-W signaling in regulating NUEg (Table 1). Additionally, we find regulation of two other bZIP TFs, OsbZIP72 and OsbZIP46, in our NUEg GRN regulated by Oshox22 and OsbZIP23, respectively (Figure 5). This finding is significant, as OsbZIP23, OsbZIP46, OsbZIP72 are part of the same subgroup-III of bZIP TFs and are known to be coordinated in their regulation of ABA signaling and drought responses (Lu et al., 2009; Hossain et al., 2010; Song et al., 2020). Additionally, ObZIP46 improves drought tolerance in coordination with the ABA-activated protein kinase, SAPK6, which is another target gene in our NUEg GRN (Figure 5) (Chang et al., 2017). Overall, our NUEg GRN results link bZIP TFs in rice as mediating N-and/or-W response genes that control NUEg. We validate the TF→target genes predictions in our high-confidence GRN for NUEg for two bZIP TFs, OsbZIP23 and OsABF1, using the TARGET assay.

Functional validation of TFs in rice: TARGET assay to identify direct TF→target gene interactions in rice cells

The TARGET system allows researchers to identify the validated TF-target gene interactions for any TF of interest using a rapid plant cell based temporal TF perturbation assay (Bargmann et al., 2013; Brooks et al., 2019). The key to this assay is the inducible TF nuclear localization and its ability to identify *direct* TF-target genes based on RNA-seq data (Bargmann et al., 2013). Previously, the TARGET assay has been used to identify direct TF→target gene interactions in Arabidopsis root or shoot cells (Bargmann et al., 2013; Varala et al., 2018; Brooks et al., 2019). In this study we establish the TARGET system in rice leaf protoplasts (see Methods). We then used the rice TARGET assay to identify the direct regulated target genes of the rice TFs OsbZIP23 and OsABF1 (Supplementary Data 9). Our analysis shows that the TF target genes identified in rice leaf protoplasts using TARGET, are comparable and show a significant overlap with genes identified *in planta* (Supplementary Figure 6A). Additionally, in this study, we demonstrate that the accuracy of rice TARGET data is comparable to *in planta* data at validating network predictions (Supplementary Figure 6B). This finding suggests that rice TARGET data can be used to validate GRN predictions in rice, as was shown in Arabidopsis (Varala et al., 2018; Brooks et al., 2019; Brooks et al.,2020; Cirrone et al., 2020). In our study, we validated that OsbZIP23 regulates both nitrogen and water-related genes including, NIA1 which is involved in nitrate assimilation (Subudhi et al., 2020),

OsDhn1 which is induced by drought (Lee et al., 2013), OsPIP1;2 which is an aquaporin that improves yield (Xu et al., 2019), ABCG4 which is involved in abiotic stress responses (Matsuda et al., 2012), and OsPP2C30 which a core regulator in the ABA signaling pathway (Zong et al., 2016). Overall, our study supports that the TARGET assay is a fast and reliable approach to identify the direct TF→target genes in rice, bypassing the time-consuming process of developing transgenic rice. Importantly, the rapid rice TARGET TF-perturbation assay, can be used to prioritize rice TFs for more laborious studies *in planta*.

Our network approach is transferrable to any phenotype in any organisms

The method we applied in this study relies on two inputs: a transcriptome-wide gene expression table and collected phenotypes from the same samples. With the reduced cost of RNA-Seq, especially with the 3′ RNA-sequencing (Weih, 2014; Groen et al., 2020; Weng and Juenger, 2022), it is much more feasible for researchers to obtain transcriptome expression data from many samples. Moreover, the software we used are all open-source and publicly available. This includes WGCNA (Langfelder and Horvath, 2008) for gene-to-phenotype correlation, GENIE3 (Huynh-Thu et al., 2010) for GRN inference and ConnecTF (Brooks et al., 2020) for network pruning. Putting these together, our network approach is not limited in rice research, but can be applied to any organism for any phenotype or trait.

Conclusions

By using a combination of WGCNA and GENIE3 network methods, we present a gene regulatory network that links TF→target gene→NUEg phenotype to determine the mechanism of N-and/or-W signaling to the regulation of NUEg (Figure 1). We also show how to use TF-validation datasets from rice to validate inferred networks using ConnecTF (https://rice.connectf.org) (Brooks et al., 2020). In addition, we apply the cell-based TARGET temporal TF-perturbation system to rice to identify direct TF→target genes interactions and validate inferred gene networks. Overall, we identify a new role for OsbZIP23 and Oshox22 as regulators of the N-and/or-W signaling and regulation of NUEg, in addition to ABA/drought signaling. More broadly, we have identified 18 prioritized TFs and their targets that correlate with NUEg, and results from this network approach can potentially be used to optimize rice varieties to thrive in marginal low-N/arid soils, which are increasing in the face of global climate change.

Data availability statement

The data presented in the study are deposited in NCBI repository, BioProject: PRJNA828338.

Author contributions

CS, JH, C-YC, and GC designed the research experiments. CS, JH, C-YC, and H-JS, performed research experiments. JS, AH, MB, VA, and JA contributed data and analysis. CS, JH, C-YC, JS, AH, and GC wrote and edited the paper. All authors contributed to the article and approved the submitted version.

Funding

This work is supported by NSF-PGRP IOS-1840761 to GC, a Grant from the Zegar Family Foundation (A16-0051) to GC, an NIH Grant RO1-GM121753 to GC, an NIH NIGMS Fellowship F32GM139299 to CS, and JS is an Open Philanthropy Awardee of the Life Sciences Research Foundation.

Acknowledgments

We thank the staff at IRRI for their work on the field studies. We would also like to thank Dr. Manpreet Katari and Will Hinkley for their advice and sharing code for data analysis.

Conflict of interest

The authors declare that the research was conducted in the absence of any commercial or financial relationships that could be construed as a potential conflict of interest.

Publisher's note

Supplementary material

The Supplementary Material for this article can be found online at: https://www.frontiersin.org/articles/10.3389/fpls.2022.1006044/full#supplementary-material

References

Alvarez, J. M., Schinke, A.-L., Brooks, M. D., Pasquino, A., Leonelli, L., Varala, K., et al. (2020). Transient genome-wide interactions of the master transcription factor NLP7 initiate a rapid nitrogen-response cascade. *Nat. Commun.* 11, 1–13. doi: 10.1038/s41467-020-14979-6

Anantha, M. S., Patel, D., Quintana, M., Swain, P., Dwivedi, J. L., Torres, R. O., et al. (2016). Trait combinations that improve rice yield under drought: Sahbhagi dhan and new drought-tolerant varieties in south Asia. *Crop Sci.* 56, 408–421. doi: 10.2135/cropsci2015.06.0344

Araus, V., Swift, J., Alvarez, J. M., Henry, A., and Coruzzi, G. M. (2020). A balancing act: how plants integrate nitrogen and water signals. *J. Exp. Botany* 71 (15), 4442–445. doi: 10.1093/jxb/eraa054

Bargmann, B. O. R., Marshall-Colon, A., Efroni, I., Ruffel, S., Birnbaum, K. D., Coruzzi, G. M., et al. (2013). TARGET: A transient transformation system for genome-wide transcription factor target discovery. *Mol. Plant* 6, 978–980. doi: 10.1093/mp/sst010

Bremner, J. M. (1996). *Nitrogen-total* In D. Sparks, A. Page, P. Helmke, R. Loeppert, P.N. Soltanpour, M.A. Tabatabai, C.T. Johnston, et al Eds. *Methods of Soil Analysis*. (Sparks, DL). doi: 10.2136/sssabookser5.3.c37

Bremner, J., and Mulvaney, C. (1982). "Nitrogen-total," in A. L. Miller, R.H. Keeney and D. R. Eds. *Methods of soil analysis. part 2. chemical and microbiological properties* Madison, Wisconsin: American Society of Agronomy, Soil Science Society of America, 595–624.

Brooks, M. D., Cirrone, J., Pasquino, A. V., Alvarez, J. M., Swift, J., Mittal, S., et al. (2019). Network walking charts transcriptional dynamics of nitrogen signaling by integrating validated and predicted genome-wide interactions. *Nat. Commun.* 10, 1–13. doi: 10.1038/s41467-019-09522-1

Brooks, M. D., Juang, C.-L., Katari, M. S., Alvarez, J. M., Pasquino, A. V., Shih, H.-J., et al. (2020). ConnecTF: A platform to build gene networks by integrating transcription factor-target gene interactions. *bioRxiv* 2020, 191627. doi: 10.1101/2020.07.07.191627

Castaings, L., Camargo, A., Pocholle, D., Gaudon, V., Texier, Y., Boutet-Mercey, S., et al. (2009). The nodule inception-like protein 7 modulates nitrate sensing and metabolism in arabidopsis. *Plant J.* 57, 426–435. doi: 10.1111/j.1365-313X.2008.03695.x

Chang, Y., Nguyen, B. H., Xie, Y., Xiao, B., Tang, N., Zhu, W., et al. (2017). Co-Overexpression of the constitutively active form of OsbZIP46 and ABA-activated protein kinase SAPK6 improves drought and temperature stress resistance in rice. *Front. Plant Sci.* 8. doi: 10.3389/fpls.2017.01102

Chen, S., Zhou, Y., Chen, Y., and Gu, J. (2018). Fastp: an ultra-fast all-in-one FASTQ preprocessor. *Bioinformatics* 34, i884–i890. doi: 10.1093/bioinformatics/bty560

Cirrone, J., Brooks, M. D., Bonneau, R., Coruzzi, G. M., and Shasha, D. E. (2020). OutPredict: multiple datasets can improve prediction of expression and inference of causality. *Sci. Rep* 10 (1), 6804. doi: 10.1038/s41598-020-63347-3

Dey, A., Samanta, M. K., Gayen, S., Sen, S. K., and Maiti, M. K. (2016). Enhanced gene expression rather than natural polymorphism in coding sequence of the OsbZIP23 determines drought tolerance and. *PLoS One* 11, 1–26. doi: 10.1371/journal.pone.0150763

Dobin, A., Davis, C. A., Schlesinger, F., Drenkow, J., Zaleski, C., Jha, S., et al. (2013). STAR: Ultrafast universal RNA-seq aligner. *Bioinformatics* 29, 15–21. doi: 10.1093/bioinformatics/bts635

D'Odorico, P., Chiarelli, D. D., Rosa, L., Bini, A., Zilberman, D., and Rulli, M. C. (2020). The global value of water in agriculture. *Proc. Natl. Acad. Sci. United States America* 117, 21985–21993. doi: 10.1073/pnas.2005835117

Fageria, N. K., Baligar, V. C., and Jones, C. A. (2010). *Growth and mineral nutrition of field crops* (*3rd ed.*). (CRC Press). doi: 10.1201/b10160

Fu, F. F., and Xue, H. W. (2010). Coexpression analysis identifies rice starch regulator1, a rice AP2/EREBP family transcription factor, as a novel rice starch biosynthesis regulator. *Plant Physiol.* 154, 927–938. doi: 10.1104/pp.110.159517

Gibbs, H. K., and Salmon, J. M. (2015). Mapping the world's degraded lands. *Appl. Geogr.* 57, 12–21. doi: 10.1016/j.apgeog.2014.11.024

Goodstein, D. M., Shu, S., Howson, R., Neupane, R., Hayes, R. D., Fazo, J., et al. (2012). Phytozome: A comparative platform for green plant genomics. *Nucleic Acids Res.* 40, 1178–1186. doi: 10.1093/nar/gkr944

Groen, SC, Ćalić, I, Joly-Lopez, Z, Platts, AE, Choi, JY, Natividad, M, et al. The strength and pattern of natural selection on gene expression in rice. *Nature* (2020) 578(7796):572–6. doi: 10.1038/s41586-020-1997-2

Guo, F.-Q., Young, J., and Crawford, N. M. (2003). The nitrate transporter AtNRT1. 1 (CHL1) functions in stomatal opening and contributes to drought susceptibility in arabidopsis. *Plant Cell* 15, 107–117. doi: 10.1105/tpc.006312

Hachiya, T., and Sakakibara, H. (2017). Interactions between nitrate and ammonium in their uptake, allocation, assimilation, and signaling in plants. *J. Exp. Bot.* 68, 2501–2512. doi: 10.1093/jxb/erw449

Han, M.-L., Lv, Q.-Y., Zhang, J., Wang, T., Zhang, C.-X., Tan, R.-J., et al. (2022). Decreasing nitrogen assimilation under drought stress by suppressing DST-mediated activation of nitrate reductase 1.2 in rice. *Mol. Plant* 15, 167–178. doi: 10.1016/j.molp.2021.09.005

Hossain, M. A., Lee, Y., Cho, J., Ahn, C. H., Lee, S. K., Jeon, J. S., et al. (2010). The bZIP transcription factor OsABF1 is an ABA responsive element binding factor that enhances abiotic stress signaling in rice. *Plant Mol. Biol.* 72, 557–566. doi: 10.1007/s11103-009-9592-9

Hsieh, P. H., Kan, C. C., Wu, H. Y., Yang, H. C., and Hsieh, M. H. (2018). Early molecular events associated with nitrogen deficiency in rice seedling roots. *Sci. Rep.* 8, 1–23. doi: 10.1038/s41598-018-30632-1

Hu, L., Chen, W., Yang, W., Li, X., Zhang, C., Zhang, X., et al. (2021). OsSPL9 regulates grain number and grain yield in rice. *Front. Plant Sci.* 12. doi: 10.3389/fpls.2021.682018

Huynh-Thu, V. A., Irrthum, A., Wehenkel, L., and Geurts, P. (2010). Inferring regulatory networks from expression data using tree-based methods. *PLoS One* 5, 1–10. doi: 10.1371/journal.pone.0012776

Hu, Y., Zhao, L., Chong, K., and Wang, T. (2008). Overexpression of OsERF1, a novel rice ERF gene, up-regulates ethylene-responsive genes expression besides affects growth and development in arabidopsis. *J. Plant Physiol.* 165, 1717–1725. doi: 10.1016/j.jplph.2007.12.006

Jin, J., Tian, F., Yang, D. C., Meng, Y. Q., Kong, L., Luo, J., et al. (2017). PlantTFDB 4.0: Toward a central hub for transcription factors and regulatory interactions in plants. *Nucleic Acids Res.* 45, D1040–D1045. doi: 10.1093/nar/gkw982

Joshi, R., Wani, S. H., Singh, B., Bohra, A., Dar, Z. A., Lone, A. A., et al. (2016). Transcription factors and plants response to drought stress: Current understanding and future directions. *Front. Plant Sci.* 7. doi: 10.3389/fpls.2016.01029

Jung, H., Chung, P. J., Park, S. H., Redillas, M. C. F. R., Kim, Y. S., Suh, J. W., et al. (2017). Overexpression of OsERF48 causes regulation of OsCML16, a calmodulin-like protein gene that enhances root growth and drought tolerance. *Plant Biotechnol. J.* 15, 1295–1308. doi: 10.1111/pbi.12716

Katari, M. S., Nowicki, S. D., Aceituno, F. F., Nero, D., Kelfer, J., Thompson, L. P., et al. (2010). VirtualPlant: A software platform to support systems biology research. *Plant Physiol.* 152, 500–515. doi: 10.1104/pp.109.147025

Keeler, B. L., Gourevitch, J. D., Polasky, S., Isbell, F., Tessum, C. W., Hill, J. D., et al. (2016). The social costs of nitrogen. *Sci. Adv.* 2(10):e1600219. doi: 10.1126/sciadv.1600219

Langfelder, P., and Horvath, S. (2008). WGCNA: An r package for weighted correlation network analysis. *BMC Bioinf.* 9, 559. doi: 10.1186/1471-2105-9-559

Lee, S. C., Kim, S. H., and Kim, S. R. (2013). Drought inducible OsDhn1 promoter is activated by OsDREB1A and OsDREB1D. *J. Plant Biol.* 56, 115–121. doi: 10.1007/s12374-012-0377-3

Lee, S., Marmagne, A., Park, J., Fabien, C., Yim, Y., Kim, S., et al. (2020). Concurrent activation of OsAMT1;2 and OsGOGAT1 in rice leads to enhanced nitrogen use efficiency under nitrogen limitation. *Plant J.* 103, 7–20. doi: 10.1111/tpj.14794

Liao, Y., Smyth, G. K., and Shi, W. (2014). FeatureCounts: An efficient general purpose program for assigning sequence reads to genomic features. *Bioinformatics* 30, 923–930. doi: 10.1093/bioinformatics/btt656

Li, H., Hu, B., and Chu, C. (2017). Nitrogen use efficiency in crops: Lessons from arabidopsis and rice. *J. Exp. Bot.* 68, 2477–2488. doi: 10.1093/jxb/erx101

Li, C., Shen, H., Wang, T., and Wang, X. (2015). ABA regulates subcellular redistribution of OsABI-LIKE2, a negative regulator in ABA signaling, to control root architecture and drought resistance in oryza sativa. *Plant Cell Physiol.* 56, 2396–2408. doi: 10.1093/pcp/pcv154

Liu, K.-H., Huang, C.-Y., and Tsay, Y.-F. (1999). CHL1 is a dual-affinity nitrate transporter of arabidopsis involved in multiple phases of nitrate uptake. *Plant Cell* 11, 865–874. doi: 10.1105/tpc.11.5.865

Lou, D., Chen, Z., Yu, D., and Yang, X. (2020). SAPK2 contributes to rice yield by modulating nitrogen metabolic processes under reproductive stage drought stress. *Rice* 13, 35. doi: 10.1186/s12284-020-00395-3

Love, M. I., Huber, W., and Anders, S. (2014). Moderated estimation of fold change and dispersion for RNA-seq data with DESeq2. *Genome Biol.* 15, 1–21. doi: 10.1186/s13059-014-0550-8

Lozano-Juste, J., and Leon, J. (2010). Enhanced abscisic acid-mediated responses in nia1nia2noa1-2 triple mutant impaired in NIA/NR-and AtNOA1-dependent nitric oxide biosynthesis in arabidopsis. *Plant Physiol.* 152, 891–903. doi: 10.1104/pp.109.148023

Lu, G., Gao, C., Zheng, X., and Han, B. (2009). Identification of OsbZIP72 as a positive regulator of ABA response and drought tolerance in rice. *Planta* 229, 605–615. doi: 10.1007/s00425-008-0857-3

Masuda, H., Aung, M. S., Kobayashi, T., Hamada, T., and Nishizawa, N. K. (2019). Enhancement of iron acquisition in rice by the mugineic acid synthase gene with ferric iron reductase gene and OsIRO2 confers tolerance in submerged and nonsubmerged calcareous soils. *Front. Plant Sci.* 10. doi: 10.3389/fpls.2019.01179

Matsuda, S., Funabiki, A., Furukawa, K., Komori, N., Koike, M., Tokuji, Y., et al. (2012). Genome-wide analysis and expression profiling of half-size ABC protein subgroup G in rice in response to abiotic stress and phytohormone treatments. *Mol. Genet. Genomics* 287, 819–835. doi: 10.1007/s00438-012-0719-3

Ndiaye, M., Adam, M., Ganyo, K. K., Guissé, A., Cissé, N., and Muller, B. (2019). Genotype-environment interaction: Trade-offs between the agronomic performance and stability of dual-purpose sorghum (Sorghum bicolor l. moench) genotypes in Senegal. *Agronomy* 9, 867. doi: 10.3390/agronomy9120867

Obertello, M., Shrivastava, S., Katari, M. S., and Coruzzi, G. M. (2015). Cross-species network analysis uncovers conserved nitrogen-regulated network modules in rice. *Plant Physiol.* 168, 1830–1843. doi: 10.1104/pp.114.255877

Ogo, Y., Kobayashi, T., Itai, R. N., Nakanishi, H., Kakei, Y., Takahashi, M., et al. (2008). A novel NAC transcription factor, IDEF2, that recognizes the iron deficiency-responsive element 2 regulates the genes involved in iron homeostasis in plants. *J. Biol. Chem.* 283, 13407–13417. doi: 10.1074/jbc.M708732200

Ogo, Y., Nakanishi Itai, R., Nakanishi, H., Kobayashi, T., Takahashi, M., Mori, S., et al. (2007). The rice bHLH protein OsIRO2 is an essential regulator of the genes involved in fe uptake under fe-deficient conditions. *Plant J.* 51, 366–377. doi: 10.1111/j.1365-313X.2007.03149.x

Oliveros, J. C. (2015) *Venny. an interactive tool for comparing lists with venn's diagrams*. Available at: https://bioinfogp.cnb.csic.es/tools/venny/index.html.

Park, S. H., Jeong, J. S., Lee, K. H., Kim, Y. S., Do Choi, Y., and Kim, J. K. (2015). OsbZIP23 and OsbZIP45, members of the rice basic leucine zipper transcription factor family, are involved in drought tolerance. *Plant Biotechnol. Rep.* 9, 89–96. doi: 10.1007/s11816-015-0346-7

Plett, D. C., Ranathunge, K., Melino, V. J., Kuya, N., Uga, Y., and Kronzucker, H. J. (2020). The intersection of nitrogen nutrition and water use in plants: New paths toward improved crop productivity. *J. Exp. Bot.* 71, 4452–4468. doi: 10.1093/jxb/eraa049

Raudvere, U., Kolberg, L., Kuzmin, I., Arak, T., Adler, P., Peterson, H., et al. (2019). G:Profiler: A web server for functional enrichment analysis and conversions of gene lists (2019 Update). *Nucleic Acids Res.* 47, W191–W198. doi: 10.1093/nar/gkz369

RoyChoudhury, A., Gupta, B., and Sengupta, D. N. (2008). Trans-acting factor designated OSBZ8 interacts with both typical abscisic acid responsive elements as well as abscisic acid responsive element-like sequences in the vegetative tissues of indica rice cultivars. *Plant Cell Rep.* 27, 779–794. doi: 10.1007/s00299-007-0498-1

Sakurai, J., Ishikawa, F., Yamaguchi, T., Uemura, M., and Maeshima, M. (2005). Identification of 33 rice aquaporin genes and analysis of their expression and function. *Plant Cell Physiol.* 46, 1568–1577. doi: 10.1093/pcp/pci172

Santosh Kumar, V. V., Yadav, S. K., Verma, R. K., Shrivastava, S., Ghimire, O., Pushkar, S., et al. (2021a). The abscisic acid receptor OsPYL6 confers drought tolerance to indica rice through dehydration avoidance and tolerance mechanisms. *J. Exp. Bot.* 72, 1411–1431. doi: 10.1093/jxb/eraa509

Santosh Kumar, V. V., Yadav, S. K., Verma, R. K., Shrivastava, S., Ghimire, O., Pushkar, S., et al. (2021b). The abscisic acid receptor OsPYL6 confers drought tolerance to indica rice through dehydration avoidance and tolerance mechanisms. *J. Exp. Bot.* 72, 1411–1431. doi: 10.1093/jxb/eraa509

Sasakawa, H., and Yamamoto, Y. (1978). Comparison of the uptake of nitrate and ammonium by rice seedlings. *Plant Physiol.* 62, 665–669. doi: 10.1104/pp.62.4.665

Sevanthi, A. M., Sinha, S. K., Rani, M., Saini, M. R., Kumari, S., et al. (2021). Integration of dual stress transcriptomes and major QTLs from a pair of genotypes contrasting for drought and chronic nitrogen starvation identifies key stress responsive genes in rice. *Rice* 14(1):49. doi: 10.1186/s12284-021-00487-8

Shannon, P., Markiel, A., Ozier, O., Baliga, N., Wang, J., Ramage, D., et al. (1971). Cytoscape: A software environment for integrated models. *Genome Res.* 13, 426. doi: 10.1101/gr.1239303.metabolite. 山本隆久.

Shim, J. S., Oh, N., Chung, P. J., Kim, Y. S., Choi, Y., and Kim, J. K. (2018). Overexpression of OsNAC14 improves drought tolerance in rice. *Front. Plant Sci.* 9. doi: 10.3389/fpls.2018.00310

Smith, T., Heger, A., and Sudbery, I. (2017). UMI-tools: modeling sequencing errors in unique molecular identifiers to improve quantification accuracy. *Genome Res.* 27, 491–499. doi: 10.1101/gr.209601.116

Song, S., Wang, G., Wu, H., Fan, X., Liang, L., Zhao, H., et al. (2020). OsMFT2 is involved in the regulation of ABA signaling-mediated seed germination through interacting with OsbZIP23/66/72 in rice. *Plant J.* 103, 532–546. doi: 10.1111/tpj.14748

Subudhi, P. K., Garcia, R. S., Coronejo, S., and Tapia, R. (2020). Comparative transcriptomics of rice genotypes with contrasting responses to nitrogen stress reveals genes influencing nitrogen uptake through the regulation of root architecture. *Int. J. Mol. Sci.* 21, 1–23. doi: 10.3390/ijms21165759

Swift, J., Adame, M., Tranchina, D., Henry, A., and Coruzzi, G. M. (2019). Water impacts nutrient dose responses genome-wide to affect crop production. *Nat. Commun.* 10(1):1374. doi: 10.1038/s41467-019-09287-7

Ueda, Y., Ohtsuki, N., Kadota, K., Tezuka, A., Nagano, A. J., Kadowaki, T., et al. (2020). Gene regulatory network and its constituent transcription factors that control nitrogen-deficiency responses in rice. *New Phytol.* 227, 1434–1452. doi: 10.1111/nph.16627

Varala, K., Marshall-Colón, A., Cirrone, J., Brooks, M. D., Pasquino, A. V., Léran, S., et al. (2018). Temporal transcriptional logic of dynamic regulatory networks underlying nitrogen signaling and use in plants. *Proc. Natl. Acad. Sci. United States America* 115, 6494–6499. doi: 10.1073/pnas.1721487115

Volante, A., Desiderio, F., Tondelli, A., Perrini, R., Orasen, G., Biselli, C., et al. (2017). Genome-wide analysis of japonica rice performance under limited water and permanent flooding conditions. *Front. Plant Sci.* 8. doi: 10.3389/fpls.2017.01862

Wang, Q., Zeng, X., Song, Q., Sun, Y., Feng, Y., and Lai, Y. (2020). Identification of key genes and modules in response to cadmium stress in different rice varieties and stem nodes by weighted gene co-expression network analysis. *Sci. Rep.* 10, 1–13. doi: 10.1038/s41598-020-66132-4

Weih, M. (2014). A calculation tool for analyzing nitrogen use efficiency in annual and perennial crops. *Agronomy* 4, 470–477. doi: 10.3390/agronomy4040470

Weng, X, and Juenger, TE. A High-throughput 3'-tag RNA sequencing for large-scale time-series transcriptome studies. *Methods Mol Biol* (2022) 2398:151–72. doi: 10.1007/978-1-0716-1912-4_13

Williamson, J. M. (2011). The role of information and prices in the nitrogen fertilizer management decision: New evidence from the agricultural resource management survey. *J. Agric. Resource Economics* 36, 552–572. doi: 10.22004/ag.econ.119180

Wu, T. M., Lin, K. C., Liau, W. S., Chao, Y. Y., Yang, L. H., Chen, S. Y., et al. (2016). A set of GFP-based organelle marker lines combined with DsRed-based gateway vectors for subcellular localization study in rice (Oryza sativa l.). *Plant Mol. Biol.* 90, 107–115. doi: 10.1007/s11103-015-0397-8

Xiang, Y., Tang, N., Du, H., Ye, H., and Xiong, L. (2008). Characterization of OsbZIP23 as a key player of the basic leucine zipper transcription factor family for conferring abscisic acid sensitivity and salinity and drought tolerance in rice. *Plant Physiol.* 148, 1938–1952. doi: 10.1104/pp.108.128199

Xu, F., Wang, K., Yuan, W., Xu, W., Liu, S., Kronzucker, H. J., et al. (2019). Overexpression of rice aquaporin OsPIP1;2 improves yield by enhancing mesophyll CO2 conductance and phloem sucrose transport. *J. Exp. Bot.* 70, 671–681. doi: 10.1093/jxb/ery386

Yang, H. C., Kan, C. C., Hung, T. H., Hsieh, P. H., Wang, S. Y., Hsieh, W. Y., et al. (2017). Identification of early ammonium nitrate-responsive genes in rice roots. *Sci. Rep.* 7, 1–16. doi: 10.1038/s41598-017-17173-9

Yu, J., Xuan, W., Tian, Y., Fan, L., Sun, J., Tang, W., et al. (2021). Enhanced OsNLP4-OsNiR cascade confers nitrogen use efficiency by promoting tiller number in rice. *Plant Biotechnol. J.* 19, 167–176. doi: 10.1111/pbi.13450

Zhang, S., Haider, I., Kohlen, W., Jiang, L., Bouwmeester, H., Meijer, A. H., et al. (2012). Function of the HD-zip I gene Oshox22 in ABA-mediated drought and salt tolerances in rice. *Plant Mol. Biol.* 80, 571–585. doi: 10.1007/s11103-012-9967-1

Zhang, C., Li, C., Liu, J., Lv, Y., Yu, C., Li, H., et al. (2017). The OsABF1 transcription factor improves drought tolerance by activating the transcription of COR413-TM1 in rice. *J. Exp. Bot.* 68, 4695–4707. doi: 10.1093/jxb/erx260

Zhao, H., Wu, D., Kong, F., Lin, K., Zhang, H., and Li, G. (2017). The arabidopsis thaliana nuclear factor y transcription factors. *Front. Plant Sci.* 7. doi: 10.3389/fpls.2016.02045

Zong, W., Tang, N., Yang, J., Peng, L., Ma, S., Xu, Y., et al. (2016). Feedback regulation of ABA signaling and biosynthesis by a bZIP transcription factor targets drought-resistance-related genes. *Plant Physiol.* 171, 2810–2825. doi: 10.1104/pp.16.00469

frontiers | Frontiers in Plant Science

TYPE Original Research
PUBLISHED 13 January 2023
DOI 10.3389/fpls.2022.1099701

OPEN ACCESS

EDITED BY
Surya Kant,
La Trobe University, Australia

REVIEWED BY
Swapna M,
Indian Institute of Sugarcane Research (ICAR), India
Jianwen Chen,
South China Agricultural University, China

*CORRESPONDENCE
Prakash Lakshmanan
plakshmanan2018@outlook.com
Xiao-Yan Liu
652639625@qq.com

SPECIALTY SECTION
This article was submitted to Plant Physiology, a section of the journal Frontiers in Plant Science

RECEIVED 16 November 2022
ACCEPTED 20 December 2022
PUBLISHED 13 January 2023

CITATION
Luo T, Li C-N, Yan R, Huang K, Li Y-R, Liu X-Y and Lakshmanan P (2023) Physiological and molecular insights into the resilience of biological nitrogen fixation to applied nitrogen in *Saccharum spontaneum*, wild progenitor of sugarcane. *Front. Plant Sci.* 13:1099701. doi: 10.3389/fpls.2022.1099701

Physiological and molecular insights into the resilience of biological nitrogen fixation to applied nitrogen in *Saccharum spontaneum*, wild progenitor of sugarcane

Ting Luo[1], Chang-Ning Li[1], Rui Yan[1], Kejun Huang[1], Yang-Rui Li[1], Xiao-Yan Liu[1*] and Prakash Lakshmanan[1,2,3*]

[1]Sugarcane Research Institute; Key Laboratory of Sugarcane Biotechnology and Genetic Improvement (Guangxi), Ministry of Agriculture and Rural Affairs, Guangxi Academy of Agricultural Sciences, Nanning, China, [2]Interdisciplinary Research Center for Agriculture Green Development in Yangtze River Basin, College of Resources and Environment, Southwest University, Chongqing, China, [3]Queensland Alliance for Agriculture and Food Innovation, University of Queensland, St Lucia, QLD, Australia

Excessive use of nitrogen (N) fertilizer for sugarcane cultivation is a significant cause of greenhouse gas emission. N use-efficiency (NUE) of sugarcane is relatively low, and considerable effort is now directed to exploit biological nitrogen fixation (BNF) in sugarcane. We hypothesize that genetic base-broadening of sugarcane using high-BNF *Saccharum spontaneum*, a wild progenitor of sugarcane, will help develop N-efficient varieties. We found remarkable genetic variation for BNF and growth in *S. spontaneum* accessions, and BNF in some accessions remained highly resilient to inorganic N application. Physiological and molecular analyses of two *S. spontaneum* accessions with high-BNF capacity and growth, namely G152 and G3, grown under N replete and low N conditions showed considerable similarity for total N, NH_4-N, soluble sugar, indoleacetic acid, gibberellic acid, zeatin and abscisic acid content; yet, they were strikingly different at molecular level. Global gene expression analysis of G152 and G3 grown under contrasting N supply showed genotype effect explaining much of the gene expression variation observed. Differential gene expression analysis found an over-representation of carbohydrate and amino acid metabolism and transmembrane transport genes in G152 and an enrichment of lipid metabolism and single-organism processes genes in G3, suggesting that distinctly divergent metabolic strategies are driving N-related processes in these accessions. This was attested by the remarkable variation in carbon, N,

amino acid and hormone metabolism-related gene expression in G152 and G3 under high- and low-N supply. We conclude that both accessions may be achieving similar BNF and growth phenotypes through overlapping but distinctly different biochemical and molecular mechanisms.

KEYWORDS

hormone, nitrogen, fixation, *Saccharum spontaneum*, sugarcane

1 Introduction

Nitrogen (N) is one of the major essential elements for plant growth and development. Both carbon fixation and sugar production are directly affected by N deficiency in sugarcane (Robinson et al., 2008). In natural ecosystems, mineralization of organic pools provides the N used by the plants, and thus the growth of natural vegetation in general remains relatively low compared to those in managed agricultural ecosystems. Yet, to feed the growing world population, agriculture intensification through continuous high-input cropping became the norm for many crop production regions (Kopittke et al., 2019). This paradigm shift in crop cultivation driven by Green Revolution has made remarkable achievements in food production and food security. However, it also resulted in overuse of agro-chemicals causing severe unintended adverse impacts on environment and human health (Yang et al., 2021). Excessive use of agrochemicals, particularly inorganic N fertiliser, led to soil acidification, reduced soil fertility and crop productivity, ground water and air pollution, eutrophication and increased agriculture carbon footprint (Guo et al., 2010). Currently, about 120 Tg (million metric tonnes) of inorganic N is used annually worldwide (FAO, 2019) with 60-80% of it is lost to the environment due to a combination of excessive inorganic N fertiliser input and the low crop nitrogen use efficiency (NUE) (Robinson et al., 2014; Luo et al., 2022). The need for reduced N fertiliser input for sustainable crop production is now well recognised globally (Udvardi et al., 2021). To realise this outcome, it is also recognised that a multi-pronged crop production strategy involving transformational innovations in agronomy, increased use of organic sources of N including biologically fixed N, and improved crop genetics is needed (Rossetto et al., 2022; Luo et al., 2022).

Sugarcane is a fast-growing high-biomass crop cultivated in both tropical and sub-tropical countries. It provides most of the sugar and about 35% of ethanol produced globally (FAO, 2020; Yang et al., 2021). Sugarcane is mostly cultivated under rainfed condition, often in low fertile N-limited soils. It is highly responsive to N supply and, consequently, overuse of inorganic N fertiliser to boost cane yield is widespread (Robinson et al., 2011; Yang et al., 2022). For instance, N application rate for sugarcane ranges from 400 kg ha^{-1} in certain production regions in India to 1381 kg ha^{-1} in some areas of China, the two major sugarcane producing countries (Robinson et al., 2011; Yang et al., 2022). As with most other crops, NUE of sugarcane is relatively low, with crop recovering 20-40% of N applied even in well-managed production systems following best crop management practices (Luo et al., 2022). The substantial loss of applied N fertiliser to ground water, run off and atmosphere, and the attended environmental costs prompted considerable effort to improve sugarcane crop NUE in many cane producing countries. This include exploring the use of enhanced efficiency fertilisers, and increasing the soil organic N pool through crop residue retention, organic amendments such as sugar mill by-products and legume intercropping (Bell, 2014; Moreira et al., 2021). Also, considerable effort is now underway in researching and exploiting biological N fixation (BNF) to reduce inorganic N use for sustainable production of sugarcane and other crops (Solanki et al., 2020; Soumare et al., 2020).

Biological N fixation by diazotrophs, a diverse group of bacteria and archaea capable of fixing atmospheric N_2 to NH_3, is a significant source of N used by plants in different ecosystems, including agro-ecosystems (Solanki et al., 2020; Imran et al., 2021). Diazotrophs can be symbiotic endophytes as nodulating and non-nodulating bacteria or it can be associative diazotrophs inhabiting on rhizosphere and the bulk soil surrounding the root system, or on above-ground plant body (Imran et al., 2021). Growth improvement by rhizospheric and endophytic diazotrophs has been reported in sugarcane (Shastri et al., 2020; Singh et al., 2021a; Singh et al., 2021b). Under field condition, diazotrophs contribute up to 15% of crop N demand (Imran et al., 2021). In addition, they possess a number of plant growth promoting properties such as phytohormone production, solubilisation of minerals, control of pathogens, abiotic stress tolerance and siderophore formation in many crops including sugarcane (Singh et al., 2021b; Singh et al., 2021c). Reports from Brazil suggest that BNF accounts for a significant proportion, 60-80% in some cases, of N used by commercial sugarcane crops (Boddey et al., 1991). There are numerous reports of sugarcane BNF by associative diazotrophs from Brazil, China and India but attempts to detect sugarcane

BNF in some other countries were unsuccessful. The reasons for the conflicting results are unclear, but strong host genotype specificity and soil environmental sensitivity of diazotrophs are now well-recognised (Imran et al., 2021). Considering the remarkable variation for host genotypic compatibility of diazotrophs (Malviya et al., 2022) and the inherent narrow genetic base of current commercial sugarcane varieties in general (Hemaprabha et al., 2022), we studied the abundance and diversity of rhizosphere diazotrophs in sugarcane ancestral species and found large rhizospheric microbial diversity in the analysed species (Malviya et al., 2022). Of the five wild *Saccharum* species analysed, *Saccharum spontaneum* is the most crossable, highly genetically diverse and ubiquitous in distribution. Being a versatile sugarcane progenitor with remarkable genetic diversity, we were interested in identifying accessions with high BNF capacity and desirable growth features useful for introgression breeding. As part of this research, we studied a population of 33 *S. spontaneum* accessions representing Chinese *Saccharum* spp germplasm collection covering very diverse tropical and sub-tropical ecological regions for their BNF property to identify accessions with high N fixing capacity. In most sugarcane production systems external N input is necessary for achieving economic yield. Because of this inevitability, we were interested in understanding the impact of externally applied inorganic N fertiliser on *S. spontaneum* BNF and how it affects carbon, N, amino acid and hormone metabolism at the molecular level. Hence, two *S. spontaneum* accessions with high BNF, well-developed stalk, high brix and flowering propensity were selected for further physiological and molecular studies to gain more insights into BNF and carbon, N, amino acid and hormone metabolism in this species, and the results are presented here.

2 Materials and methods

2.1 Plant materials and growing conditions

Wild accessions of sugarcane (*Saccharum* spp. interspecific hybrids) progenitor *Saccharum spontaneum* L. were used for this study. They were sourced from the Chinese *S. spontaneum* collection maintained in the germplasm garden of Sugarcane Research Institute, Guangxi Academy of Agricultural Sciences (SRI), Nanning, Guangxi, China. Nanning has a hot humid subtropical climate with annual temperatures ranging between 2°C and 35°C. It receives, on average, 1300 mm rainfall yearly with an annual mean humidity of 79%. For this study, thirty-three *S. spontaneum* accessions collected from very diverse tropical and sub-tropical agroclimatic conditions of Southern China, where sugarcane is grown commercially, were selected. All the selected accessions were free of pests and diseases, never fertilised, and grew well in the garden.

2.2 Screening of *S. spontaneum* population for BNF and growth attributes

Ten-month-old *S. spontaneum* plants were used for population screening experiment. Plants selected for the screening experiment were grown individually in large pots with soil collected from SRI germplasm garden in a naturally-lit glasshouse. They were not fertilised or sprayed with any chemicals prior to and during the screening experiment. The soil was irrigated as and when needed. The plants of all 33 accessions were divided equally into three blocks (six to eight plants of each accession in one replicate block), and in each block, they were arranged randomly. These accessions were screened for BNF activity using nitrogenase assay, and plant height (from soil surface to the dewlap of the youngest fully expanded leaf), stalk number and brix (using juice expressed from 10 cm of the basal part of stem) were also determined. Brix of expressed juice was measured by refractometry using ATR-P Refractometer (Schmidt and Haensch, Germany). For each accession there were six independent measurements from plants randomly selected from 3 replicate blocks.

2.2.1 BNF assay: Nitrogenase activity of *S. spontaneum* accessions

Nitrogen fixation ability of *S. spontaneum* test clones was determined by assaying *in vivo* nitrogenase activity in nitrogen-free medium as described previously (Hardy et al., 1968). Lamina (1 g) of the youngest fully expanded leaf from each plant was sampled, cut into 0.5 cm long pieces and immediately transferred to 50 mL Erlenmeyer flask containing 10 mL of nitrogen-free assay medium. Then, under sterile condition, flask headspace air was removed and replaced with acetylene gas (10% v/v) and the flasks were incubated at 28 ^{0}C for 48 h on a gyratory shaker set at 120 rpm. At the end of the incubation, 0.5 mL of headspace gas was removed from each flask and analyzed in a GC-17A gas chromatograph (Shimadzu, Japan) with DB-1,701 column (Agilent, Santa Clara, United States) using the flame ionization detector (FID) at 80 ^{0}C and the injector at 110 ^{0}C, with 35 mL min^{-1} flow rate of carrier gas. For each accession, nitrogenase activity of six individual plants selected randomly from 2 replicated blocks were determined. The amount of ethylene (C_2H_4) produced by each accession was calculated and presented as nmol C_2H_4 produced g^{-1} fresh weight h^{-1}.

2.3 Impact of inorganic N fertiliser application on BNF in high-BNF *S. spontaneum* accessions

Six accessions with high BNF activity identified in the BNF screening experiment, namely G03, G152, G177, G720, G824

and G1926, were selected for studying the sensitivity of N fixation to high N condition. Single node cuttings from 12-month-old healthy plants were planted in unfertilized moist garden soil in plastic trays with perforated bottom and kept in a naturally-lit glasshouse for sprouting and plantlet development. One month after planting the cuttings, plantlets of uniform size were transplanted into 30 lit pots with unfertilized soil. All pots were watered regularly to avoid moisture stress. Two weeks after transplanting, potted plants were divided into two equal groups; one for high nitrogen (HN) and the other for low nitrogen (LN) treatments. All HN plants were supplied with Murashige and Skoog (MS) mineral nutrients (2 lit pot-1) (Murashige and Skoog, 1962), which contained 18.8 mM KNO_3 and 20.6 mM NH_4NO_3, while those in LN received MS mineral nutrients without N (2 lit pot-1) once every three weeks. This N treatment was continued during the 5-month experimental period. The experiment followed a completely randomized block design with three replicated blocks. For both treatments, there were 5 plants of each accession in a single block (replicate). At the end of the experiment, middle portion of the youngest fully-expanded leaf was sampled and nitrogenase activity was determined as described above. For each accession, three biological replicates from each block were used for the enzyme assay.

2.4 Physiological and molecular responses of selected high-BNF *S. spontaneum* accessions G3 and G152 to inorganic N application

Two high-BNF *S. spontaneum* accessions with high brix, good stalk development, high stalk number, high propensity for flowering and a relatively low impact of applied inorganic N on their N fixation activity, namely G152 and G3, were selected for further physiological and molecular characterization. Plants were raised and the experiment was conducted as described in section 2.2. except for the following conditions. Experiment was continued for 7 months. The experiment followed a completely randomized block design with three replicated blocks for each treatment. Each block had 6-8 plants of each accession for HN and LN treatments.

At the end of the experiment, leaf tissue from the youngest fully expanded leaf and root samples were harvested for measuring nitrate reductase (NR) and glutamine synthetase (GS) activity, and total N, NH_4-N, soluble protein and soluble sugars content. Leaf tissue was also used for BNF assay and transcriptome analysis. For NR and GS activity, lamina (1 gm) from the youngest fully-expanded leaf and root tips (10 mm from the tip) were collected and immediately snap-frozen in liquid nitrogen. The tissue samples were collected between 09.30 and 13.00 hours to minimise the effect of diurnal variation.

2.5 Shoot growth and content of total N, NH_4-N and soluble sugars in G3 and G152 grown under externally supplied inorganic N

At the end of seven months of growth, shoot height and stalk number of experimental plants were measured. For chemical analyses, oven dried (80 ^{0}C for 5 days) leaf and root tissues were finely powdered and used for total N, NH_4-N and soluble sugars content measurement. Total N was determined by acid digestion of samples following Kjeldahl method. NH_4-N and soluble sugars content were measured using Plant Ammonium Nitrogen Activity Assay Kit (# BC1520, Solarbio, China), and Plant Soluble Sugar Content Assay Kit (# BC0035, Solarbio, China), respectively, following manufacture's instruction. For each treatment, eight independent plants (measurements) randomly selected from different replicated blocks were used for analysis.

2.5.1 BNF activity of *S. spontaneum* accessions G3 and G152 grown under externally supplied inorganic N

Nitrogen fixation ability of *S. spontaneum* test clones supplied with and without N was determined by measuring *in vivo* nitrogenase activity of youngest fully expanded leaf tissue of seven-month-old plants in N-free medium as described in section 2.2.1.

2.5.2 Nitrate reductase and glutamine synthetase activity of *S. spontaneum* accessions G3 and G152 grown under externally supplied inorganic N

Frozen leaf and root tissue samples were ground to a fine powder and used for nitrate reductase (NR, EC 1.7.1.1) and glutamine synthetase (GS, EC 6.3.1.2) activity assays. Five ml of the extraction buffer (50 mM Tris HCl, 1 mM MgSO4, 1 mM EDTA, 10 mM cysteine, 1% insoluble PVP) was mixed with 1 g of tissue and the homogenate was kept for 30 min on ice with occasional stirring. The homogenate was then centrifuged at 4°C at 12000 rpm for 10 min and the supernatant was used for enzyme activity measurement. The NR activity was measured by methods developed by Bories and Bories (1995), and expressed as the amount of NO_2 produced g^{-1} fresh weight of tissue. The GS activity was measured according to Bressler and Ahmed (Bressler and Ahmed, 1984), and expressed as nmol γ-glutamyl-monohydroxamate (GHA) produced mg^{-1} protein min^{-1}. Soluble protein content of sampled tissues was determined with bicinchoninic acid (BCA) method using bovine serum albumin as standard. For each treatment, eight independent plants randomly selected from different replicated blocks were used for analysis.

2.5.3 Changes in endogenous level of plant hormones in G3 and G152 grown under externally supplied inorganic N

The frozen leaf samples of G3 and G152 plants grown with and without external N were finely powdered in liquid nitrogen. The powdered tissue (1 g) was extracted with cold methanol (10 ml) containing 1 mM butylated hydroxytoluene at 4°C for 16 h in dark as described previously (Gong et al., 2017). These samples were then centrifuged at 2000 rpm for 20 min at 4°C and the pH of supernatants collected was adjusted to 2.8, then extracted thrice with an equal volume of ethyl acetate, and the extract was evaporated to dryness in a vacuum centrifuge (RVC 2-25 CDplus, Christ, Germany). The dried samples were redissolved in 0.5 ml of methanol with 0.1M glacial acetic acid as the mobile phase for high performance liquid chromatography (HPLC) analysis. Hormones were quantified using RIGOL L-3000 HPLC system (RIGOL, Beijing, China) as described previously (Yang et al., 2014). Analysis was done using a Kromasil C18 column (250 mm*4.6 mm, 5 µm; EKA chemical Inc) with 100% methanol (A) and 0.1M acetic acid (B) as mobile phases and a flow rate set at 1 mL/min. Extracted samples (10 µL) were injected into column and gibberellic acid (GA_3), abscisic acid (ABA), zeatin riboside (ZR) and indole-3-acetic acid (IAA) were detected at wavelengths 210 nm, 254 nm, and 275 nm, respectively. Plant hormone standards with known concentration were used for establishing calibration curves, which were used for quantifying hormones in the test samples.

2.6 Statistical analysis

All data presented here are analysed using analysis of variance (ANOVA) in Genstat statistical system, 19th Edition (VSNI, 2017).

2.7 Molecular analysis of high-BNF *S. spontaneum* accessions to understand carbon, N, amino acid and hormone metabolism-related gene expression

2.7.1 Plant materials and RNA isolation

Youngest fully expanded leaves harvested from G152HN, G152LN, G3HN and G3LN plants (see section 2.4. for experimental details) were immediately snap-frozen in liquid nitrogen. Total RNA was isolated using TRIzol™ Reagent (Thermo Fisher Scientific, Wilmington, USA) and the RNA quality was monitored on 1% agarose gel. RNA purity was determined using the NanoPhotometer® (IMPLEN, CA, USA). RNA samples were quantified spectrophotometrically using Qubit® RNA Assay Kit in Qubit® 2.0 Flurometer (Life Technologies, CA, USA) and RNA integrity was assessed using the RNA Nano 6000 Assay Kit of the Bioanalyzer 2100 system (Agilent Technologies, CA, USA). Two biological replicates were used for each treatment for molecular analyses.

2.7.2 cDNA library construction and sequencing

A total of 1.5 µg RNA per sample was used for preparing the RNA for sequencing. Sequencing libraries were prepared using MGIEasy RNA library preparation kit (MGI, Shenzhen, China) and index codes were added to attribute sequences to each sample. PCR products were purified (MGIEasy DNA purification magnetic bead Kit) and the library quality was determined using the Agilent Bioanalyzer 2100 system. After purification, the double stranded PCR library was unzipped and then looped to form single stranded circular DNA. The rolling circle amplification (RCA) technology is used to form DNA nanoball (DNB), the DNB is loaded into the chip through the automatic sample loading system and fixed. The chip loaded with DNB was put into DNBSEQ-T7 for sequencing, and 150 bp double-ended sequencing reads was obtained. The transcriptome sequencing data are deposited into the National Center for Biotechnology Information (NCBI) SRA database under accession number PRJNA847754 and can be accessible with the following link https://www.ncbi.nlm.nih.gov/sra/PRJNA847754

2.7.3 Data processing, transcriptome assembly and functional annotation

The raw reads in fastq format were initially processed through Perl scripts. After removing reads containing adapter and ploy-N, and low-quality reads, the clean reads obtained were used for Q20, Q30 and GC content. These high-quality clean reads were used for all the downstream analyses.

Clean reads were *de novo* assembled into transcriptome using Trinity v2.11.0 (Grabherr et al., 2011). Non-redundant unigenes were determined through sequence splicing and redundancy removal from all sample unigenes. The unigenes with lengths >200 bp were used for further analyses. All the assembled unigenes were searched and annotated using NCBI non-redundant protein sequences (Nr; https://www.ncbi.nlm.nih.gov/guide/), NCBI non-redundant nucleotide sequences (Nt; https://www.ncbi.nlm.nih.gov/guide/), Protein family (Pfam; http://www.pfam.org/), Gene Ontology (GO; http://geneontology.org/), Kyoto Encyclopedia of Genes and Genomes (KEGG) Orthology database (KO; https://www.genome.jp/kegg/ko.html), Swiss-Prot (https://web.expasy.org/docs/swiss-prot_guideline.html), and Clusters of Orthologous Groups of proteins (KOG/COG; ftp://ftp.ncbi.nih.gov/pub/COG/KOG), with an E-value cut-off of 1E-5.

2.7.4 Analysis of differential gene expression in response to inorganic nitrogen application

The unigenes obtained were assembled into a Ref and the clean data for each sample were aligned back into the assembled Ref. Gene expression of all samples were calculated using RSEM v1.2.8. For the gene read counts of each library, DESeq2 v3.11 was used to estimate the transcripts per million values for each gene. Differential gene expression analysis of different comparative groups was performed using DESeq R package (1.18.0). DESeq provides statistical routines for determining differential expression in digital gene expression data using a model based on the negative binomial distribution. The resulting p -values were adjusted using the Benjamini and Hochberg's approach for controlling the false discovery. Genes with an adjusted p-value < 0.05 and an absolute value of log2ratio (treatment/control) ≥ 1 were considered as differentially expressed genes (DEGs).

2.7.5 GO and KEGG enrichment analysis

Gene Ontology (GO) enrichment analysis of differentially expressed genes was implemented by the GOseq R package, following gene length bias correction. GO terms with corrected p-value < 0.05 were considered significantly enriched by differential expressed genes. For KEGG pathway analysis we used KOBAS software to test the statistical enrichment of differential gene expression genes in KEGG pathways.

2.7.6 Analysis of differential expression of genes involved in amino acids, nitrogen, carbon and hormone metabolism in response to N application

To expand our understanding how high N supply affects key metabolic pathways that regulate growth in *S. spontaneum* with BNF capacity we generated gene expression heatmaps and clustering of DEGs involved in carbon, nitrogen, amino acid and hormone metabolism of G3 and G152 accessions grown under external N supply. This analysis was performed with pheatmap R package using the FPKM value.

2.7.7 Quantitative real time RT-PCR analysis

The RNA-Seq data was validated by quantitative real time RT-PCR analysis (qRT-PCR) using ten genes. The expression of eight selected genes were normalized using three reference genes, namely, glyceraldehyde-3-phosphate dehydrogenase (GAPDH); acyl-CoA dehydrogenase (ACAD);clathrin adaptor complex (CAC). The primers used for each gene are given in Table S9. The RNA for qRT-PCR was prepared as described in the section 2.7.1. cDNA was synthesized with HiScript II Q RT SuperMix (Vazyme, China) according to the manufacturer's instructions. The qPCR reaction mixture (20 µL) consisted of 1 µL cDNA, 10 µL ChamQ Universal SYBR qPCR Master Mix (Vazyme, China), 0.4 µL forward primer, 0.4 µL reverse primer and 8.2 µL H20. The qPCR reaction followed a pre-denaturing step (95 °C for 3 min), amplification steps (95 °C for 20 s, 58 °C for 20 s, 72 °C for 25 s, and fluorescence acquisition) of 40 cycles, and a melting curves step (continue capturing fluorescence from 60°C to 95°C). The qPCR was performed on A qTOWER Real-Time Thermal Cyclers (Analytik Jena, Germany) was used for qPCR. The 2−ΔΔct method was used to calculate the relative gene expression.

3 Results

3.1 Substantial genetic variation for BNF, shoot growth, stalk number and brix exist in *S. spontaneum* accessions

Analysis of nitrogenase activity in *S. spontaneum* accessions showed remarkable variation for BNF capacity among the clones tested (Figure 1). For example, accession G152, the clone with the highest BNF activity, recorded 72-fold greater enzyme activity than the poorest performer, G103. Among the 33 clones tested, 15 had a relatively high BNF activity (>50 nmol C2H4 mg-1 protein h-1). A similar trend was also evident for plant height, stalk number and brix (Figures 2, 3) although the range of variation for these traits was much smaller than that of BNF (Figure 2). On average, a six-fold variation was evident for plant height, stalk number and brix at the end of the experiment.

3.2 Sensitivity of BNF to inorganic nitrogen varies greatly among high-BNF *S. spontaneum* accessions

Analysis of nitrogenase activity in six high BNF accessions grown under externally supplied inorganic N showed remarkable genotypic variation for BNF activity (Figure 3). External application of inorganic N had a relatively low impact on the nitrogenase activity (20-25% reduction) of accessions G152 and G3, whereas the activity was reduced by 42-53% in other four accessions tested. The N-induced reduction in nitrogenase activity was significant for all accessions ($p<0.01$)

3.3 External nitrogen supply boosted shoot growth and content of total N, NH_4-N and soluble sugars but reduced BNF in *S. spontaneum* accessions

External application of inorganic N significantly ($p<0.01$) increased shoot length and stalk number in both accessions (Table 1). Under external N supply, stalk length was increased by 19% in G3 and 22% in G152, whereas a more remarkable rise in stalk number, 46 – 50%, was observed in both accessions. Similar to shoot growth, total N and NH4-N content of leaf and root tissues of G152 and G3 accessions also showed a substantial

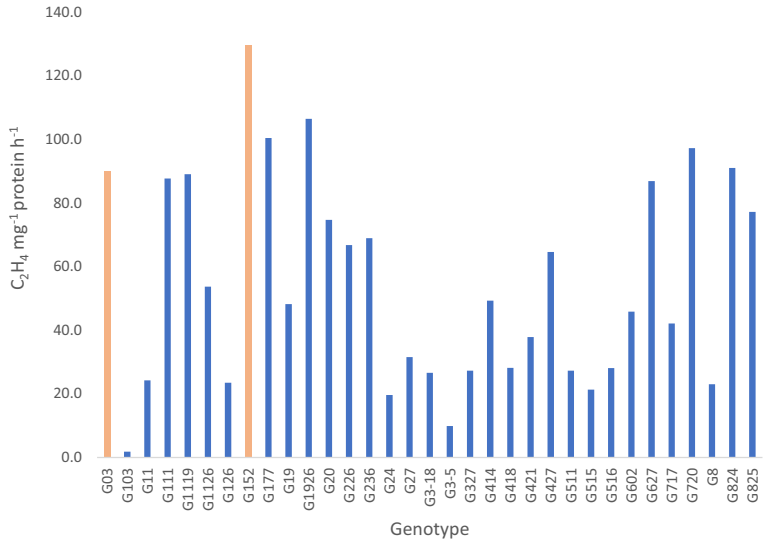

FIGURE 1
Nitrogenase activity measured by acetylene reduction assay of 33 *S. spontaneum* accessions showing large variation in their BNF activity. Values are mean of 6 independent measurements; l.s.d. 9.8, $p < 0.001$.

increase when plants received external N supply (Figures 4A, B). Total N content variation was more pronounced in roots than in leaf tissue for both accessions, but that was not the case for NH4-N; there was very little variation for root NH4-N in G152 and G3plants. Compared with total N content, N-induced increase in soluble sugar was markedly lower in leaf and root tissues except for G3 leaf tissue (Figure 4C).

From the six high-BNF accessions tested for their BNF-response to externally applied inorganic N (Figure 3), two accessions with BNF least affected by external N and desirable

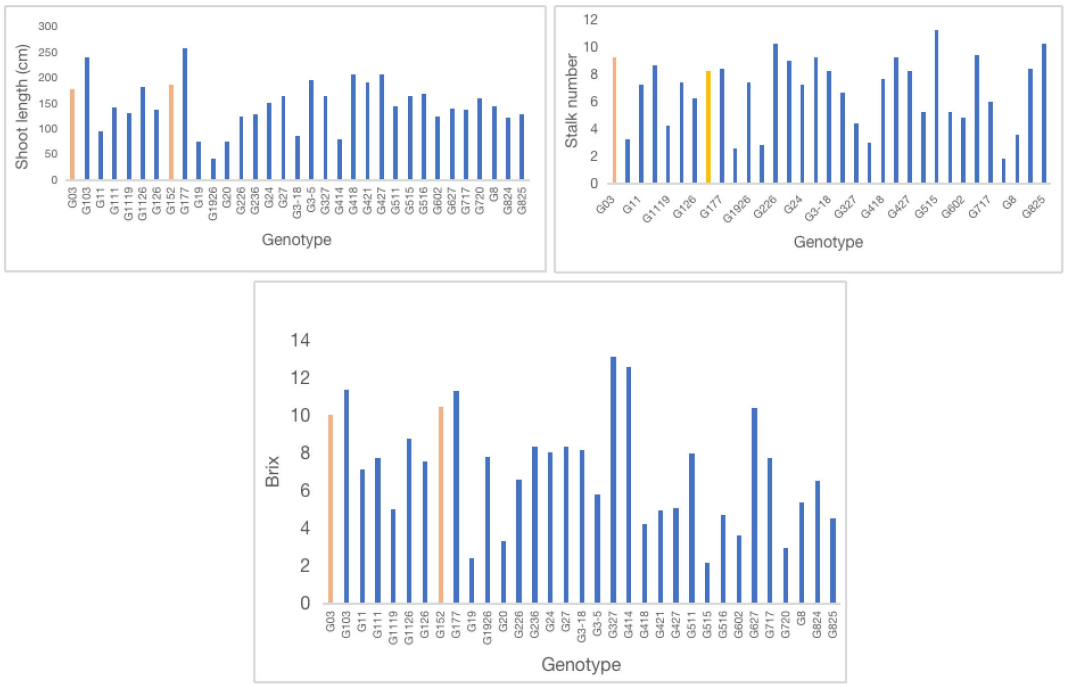

FIGURE 2
Variation in shoot length, stalk number per stool and brix (%) of *S. spontaneum* accessions Values are mean of 6 independent measurements; shoot length l.s.d. 15.4, $p < 0.001$; shoot number l.s.d. 1.2, $p < 0.001$; brix l.s.d. 1.09, $p < 0.001$.

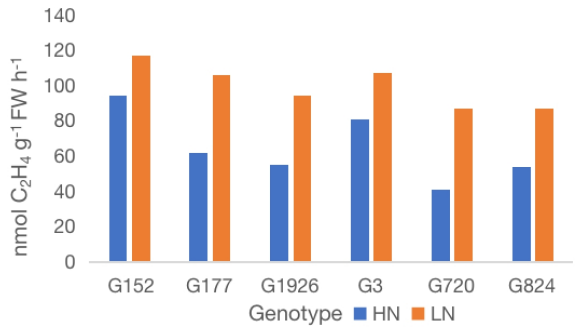

FIGURE 3
Effect of external application of inorganic N on nitrogenase activity of six high-BNF *S. spontaneum* accessions. Values are mean of 6 independent measurements; l.s.d. 12.4, p < 0.001. HN, high N; LN, low N.

agronomic features as well as flowering propensity, G152 and G3, were selected for more detailed physiological and molecular analyses. Consistent with the results of the previous experiment (Figure 3), external application of N significantly reduced (19-23%; P<0.001) the nitrogenase activity in both accessions (Figure 5).

Activity of NR in both leaf and root tissues of G152 and G3 accessions was substantially increased with the application of inorganic N (Figure 6A; p<0.001). The percentage increase in roots was much greater (2.4 to 3.5-fold) than that of leaf, and in both accessions rate of enzyme induction in leaf tissue was somewhat similar (~1.5 fold) (Figure 6A). As with NR, GS activity also showed an increasing trend in leaf and root tissues though the N-induced enzyme induction was not as pronounced as in NR, except for the G3 leaf tissue (Figure 6B).

3.4 Nitrogen supply increased auxin, gibberellin and cytokinin content and nitrate reductase activity remarkably, but not so for abscisic acid and glutamine synthetase

Inorganic N application had a remarkable effect on endogenous hormones in both G152 and G3 accessions (Table 2). The endogenous level of growth promoting hormones IAA, GA3 and ZR in both accessions increased by 60-80%, except for a doubling of ZR in G152. No consistent and significant change in ABA content was noticed with N application.

3.5 RNA sequencing, *de novo* assembly of reads and functional annotation of unigenes

In the RNA-Seq experiment, the number of clean reads obtained from each library after trimming and filtering ranged between 44725188 and 481766948, with average 6.83 (range 6.09-7.07) gigabases, 93.6% Q30 (range 91.82-94.4%) and 53.5% GC (range 50.48-55.07%) content. Out of 266228 transcripts obtained, 110947 unigenes with a mean length of 1087 bp (range 201- 17867 bp) were identified (Table S1).

The function of all unigenes obtained were annotated using seven databases. (Table S2–S4). In this analysis, transcriptome assembled from RNA-Seq data was used as reference. Out of a total of 110947 unigenes identified, 64.9% (72056), the largest proportion of unigenes, were annotated from NT, followed by 67404 (60.8%) in NR. The lowest number of genes annotated, 8435 (7.6%), was in KOG. It is important to note that 76.6% (84986) of all the unigenes identified were annotated at least in one of the seven databases used in this study.

3.6 Differential gene expression in high-BNF *S. spontaneum* accessions grown under external N supply: Genotype effect far outweighed treatment effect

In the gene expression study, the impact of external application of N on the expression of genes associated with carbon, N, amino acids and hormones in leaf tissues of two high-BNF *S. spontaneum* accessions, G152 and G3, was analysed. Four different pair-wise comparisons, i.e., same accession with contrasting N treatments, high N and low N, comparison (G152 HN *vs* G152 LN; G3HN *vs* G3 LN) and different accessions with

TABLE 1 Effect of external application of inorganic N on stalk length and stalk number of *S. spontaneum* accessions G3 and G152.

Treatments	Stalk length (cm)	Stalk number $stool^{-1}$
G3HN	214	12
G3LN	177	9.2
G152HN	231	14
G152LN	186	8.2
l.s.d.	19.6	2.4
	P<0.01	P<0.01

Values are mean of 6 independent measurements. HN, high N; LN, low N.

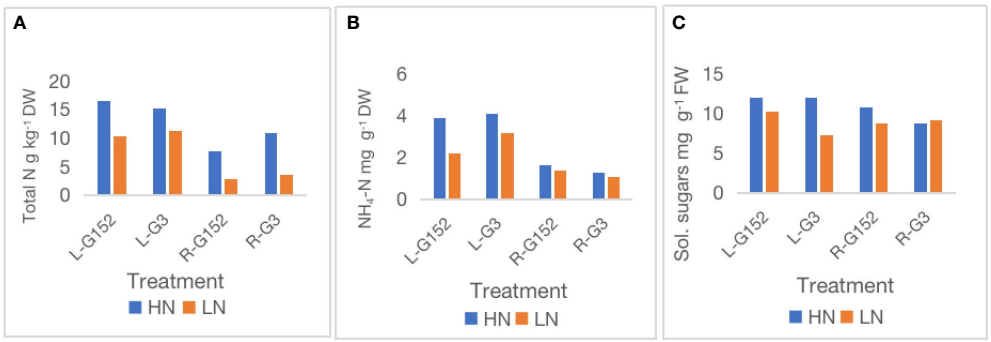

FIGURE 4
Effect of external application of inorganic N on leaf and root nitrogen **(A)**, NH4-N **(B)** and soluble sugars **(C)** content in *S. spontaneum* accessions G152 and G3. Values are mean of 6 independent measurements; L, leaf; R, root; HN, high N, low N, LN; total N l.s.d. 1.02, $p < 0.001$; NH4-N l.s.d. 0.52, $p < 0.01$; soluble sugars l.s.d. 0.64, $p < 0.01$.

the same N treatment comparison (G152 HN *vs* G3 HN; G152 LN *vs* G3 LN), were performed to identify DEGs (Figure S1). In the initial global analysis of differential gene expression using the threshold of an adjusted p value of <0.05 and log2FoldChange >1 based on DESeq2 method, 864 genes were found to be differentially expressed between G152HN and G152LN with 360 genes downregulated and 504 upregulated (Figure S1). For the same comparison (HN *vs* LN) in G3, the number of DEGs was less than half of what was found in G152 (HN *vs* LN), and more genes were downregulated (155) than upregulated (87). In contrast to treatment comparison (HN *vs* LN for the same genotype), the genotype comparison (G152HN *vs* G3HN, G152LN *vs* G3LN) showed a substantially large number of DEGs, >2000 in each comparison, irrespective of the treatment (Figure S2). However, the pattern of gene expression in genotype comparison under high N treatment (G152HN *vs* G3HN) was just opposite of low N treatment (G152 LN *vs* G3 LN) with more downregulated DEGs under HN while the opposite was true for LN.

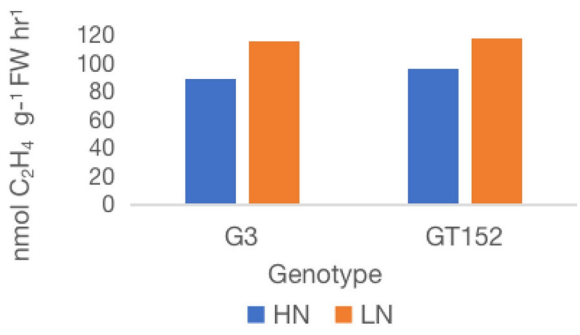

FIGURE 5
Effect of external application of inorganic N on nitrogenase activity of *S. spontaneum* accessions G152 and G3. Values are mean of 6 independent measurements; l.s.d. 7.3, $p < 0.01$. HN, high N; LN, low N.

In order to identify common and unique genes that expressed differentially in response to N application in G152 and G3 accessions, Venn diagrams of DEGs were prepared (Figure S2). There were 28 common DEGs among G152 and G3 for treatment (HN *vs* LN) comparisons (Figure S2A), In this comparison (HN *vs* LN), G152 accession showed four-fold greater DEGs than that of G3 (Figure S2A). However, when G152 and G3 accessions were grown under similar soil N condition (Figure S2B), 1101 common DEGs were found. And, a similar number of DEGs was also found for genotype comparison under HN and LN conditions (Figure S2B). Interestingly, there were no common DEGs across all pair-wise comparisons (Figure S2C).

3.7 Carbohydrate, amino acid and energy metabolism DEGs over-represented in G152 in response to external N, while lipid, secondary metabolites and carbohydrate metabolism dominated in G3

To determine the potential functions of DEGs identified in this study, we performed gene ontology (GO) enrichment analysis and they were grouped into two main GO functional categories- biological processes and molecular functions. There was large variation for functional classes between all four pair-wise comparisons (Figure 7). For instance, DEGs identified in G152 HN *vs* LN comparison were mostly mapped to regulation of proteolysis, peptidases, catalytic activity, amino acid, protein and carboxylic acid metabolism and membrane transport GO terms in biological process and molecular functions categories combined (Figure 7A). Most of the DEGs in this comparison were upregulated with transmembrane transport and amino acid biosynthesis being the most enriched ones. In contrast, DEGs found in G3HN *vs* LN comparison were enriched for single-

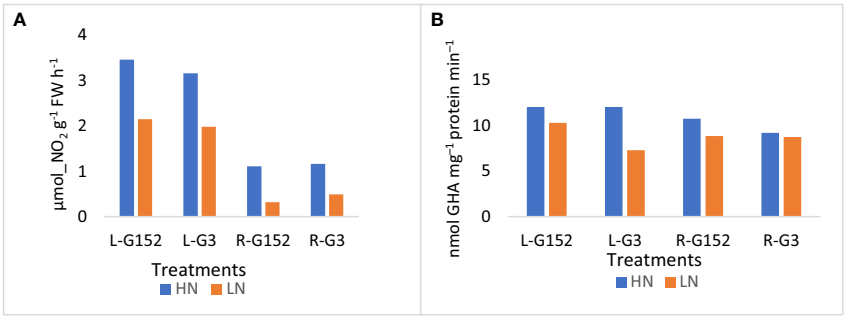

FIGURE 6
Effect of external application of inorganic N on leaf and root nitrogenase **(A)** and glutamine synthetase **(B)** activity in *S. spontaneum* accessions G152 and G3. Values are mean of 6 independent measurements; NR Ls.d. 0.58, $p < 0.01$; GS l.s.d. 1.29, $p < 0.001$; L, leaf; R, root; HN, high N; LN, low N.

organism process, fatty acid, lipid and carboxylic acid metabolism, and anion homeostasis for biological processes, and fatty acid and iron binding for molecular functions (Figure 7B). Another interesting observation noted in this analysis was that when both accessions grown under the same N supply conditions (HN or LN) were compared, a substantially greater number of DEGs was highly enriched in samples from HN than those from LN (Figures 7C, D). Also, in the genotype comparison under HN condition, DEGs were mostly up-regulated whereas an opposite trend was true for LN plants (Figures 7C, D). Under LN condition, highly enriched DEGs were attributed to phosphorylation and metabolism of phosphorous-containing compounds GO terms in biological processes category, while protein kinase, transferases form the most enriched GO terms in molecular functions category. In the comparison of genotypes grown under HN, highly enriched DEGs identified were mapped to phosphorylation and DNA metabolic processes for biological processes, and nucleotide binding, kinases, carbohydrate derivative-binding, phosphotransferases, and anion binding, for molecular processes (Figures 7C, D). Also, it is interesting to note that under LN growth condition, though only minimally enriched, cytokinin biosynthesis was up-regulated (Figure 7C).

In order to gain more insights into the potential metabolic roles of genes differentially expressed in G152 and G3 accessions, they were mapped to various metabolic pathways in KEGG database (Figure 8). The genes differentially expressed in G152 in response to external N supply were mostly mapped to metabolism category with amino acid metabolism and carbohydrate metabolism being the most enriched pathways followed by lipid, energy, other amino acids, terpenoids and polyketides metabolism and biosynthesis of secondary metabolites (Figure 8A). Transport and catabolism, and signal transduction in cellular processes and environmental information processing categories, respectively, were the other significant pathways identified in G152 HN *vs* G152 LN comparison (Figure 8A). As with G152, DEGs identified in G3 HN *vs* LN comparison were mostly over-represented in metabolism category (Figure 8B). However, in G3, DEGs were most enriched for lipid metabolism pathway followed by biosynthesis of secondary metabolites and carbohydrate and amino acid metabolism pathways. Transport and catabolism, membrane transport and signal transduction pathways were also significantly enriched.

Unlike the large variation in representation of DEGs in various KEGG metabolic pathways seen between G152 and G3 grown under contrasting N supply (HN *vs* LN comparison)

TABLE 2 Effect of external application of inorganic N on endogenous levels of hormones in the leaf tissue of *S. spontaneum* accessions G152 and G3.

Treatment	IAA (ng/g FW)	GA3(µg/g FW)	ABA (µg/g FW)	ZR (µg/g FW)
GSM152 HN	73.1	1.83	0.19	1.23
GSM152 LN	41.1	1.1	0.24	0.58
GSM3 HN	126.5	1.34	0.26	1.09
GSM3 LN	73.3	0.79	0.22	0.68
l.s.d. (5% level)	7.1	0.2	0.01	0.11
p	<0.01	<0.01	<0.004	0.001

Values are mean of 6 independent measurements. IAA, indole-3-acetic acid; GA3, gibberellic acid; ABA, abscisic acid; ZR, zeatin riboside.

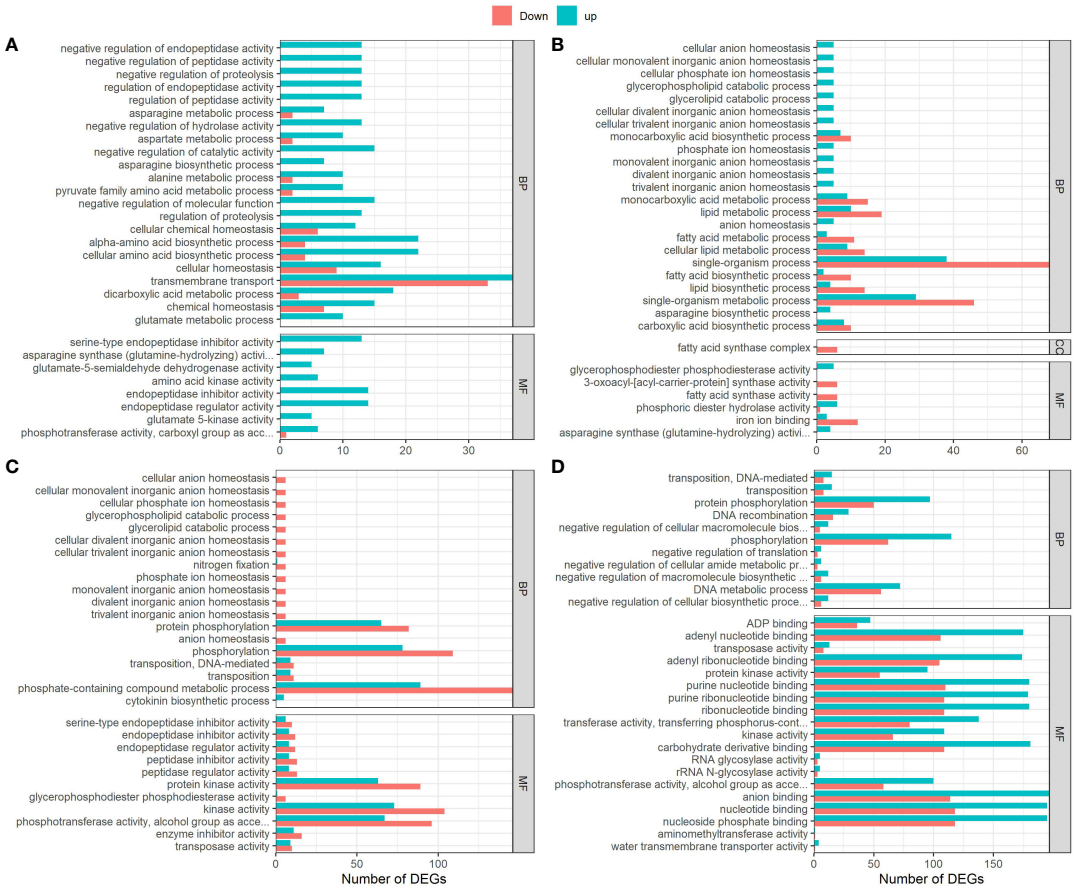

FIGURE 7
Gene ontology (GO) annotation of DEGs in *S. spontaneum* accessions G152 and G3 grown in high and low N treatments. The DEGs used here were identified by pairwise comparisons between high N and low N treatments and between genotypes (p-value < 0.05). **(A)**, G152HN vs G152LN; **(B)**, G3HN vs G3LN; **(C)**, G152 LN vs G3 LN; **(D)**, G152 HN vs G3 HN.

(Figures 8A, B), there were remarkable similarity for enrichment of DEGs in G152 and G3 grown under same N level (HN or LN) (Figures 8C, D). Carbohydrate metabolism was the most over-represented category in this genotype comparison, followed by amino acid, energy, lipid and nucleotide metabolism, and biosynthesis of secondary metabolites. Significantly, DEGs mapped to component pathways of genetic information processing category and that of transport and catabolism, and environmental adaptation, showed greater representation in genotype comparison (Figures 8C, D) than in treatment comparison (Figures 8A, B).

3.8 Distinct genotype- and N-dependent differential expression of genes involved in amino acids, carbon, nitrogen and hormones metabolism

Expression of DEGs involved in amino acid, carbon, N and hormones were further studied to gain more insights into metabolic responses of G152 and G3 accessions to inorganic N fertiliser application (Figure 9). A large number of amino acid metabolism-related genes were differentially expressed in response to external N supply in both accessions (Figure 9; Table S5). Also, there was substantial genotypic variation for this gene expression response. For instance, many amino acid metabolism-related genes that are up-regulated in G152 under high N condition were either down-regulated or remained unchanged under low N, and vice versa (Figure 9). This include glutamine synthetase, asparagine synthase, alanine transaminase, glutamate synthase, tryptophane synthase, etc. A similar result was also found for G3 grown under HN and LN conditions (Figure 9; Table S5). Several genes up-regulated in G3 under HN, such as alanine transaminase, glutamate dehydrogenase, glutamate synthase, asparagine synthase and serine acetyltransferase were either down-regulated or remained unchanged under LN condition. A similar notable result was the substantial variation in amino acid gene expression observed between G152 and G3 grown under same N condition (HN or LN). For instance, caffeoyl-CoA O-

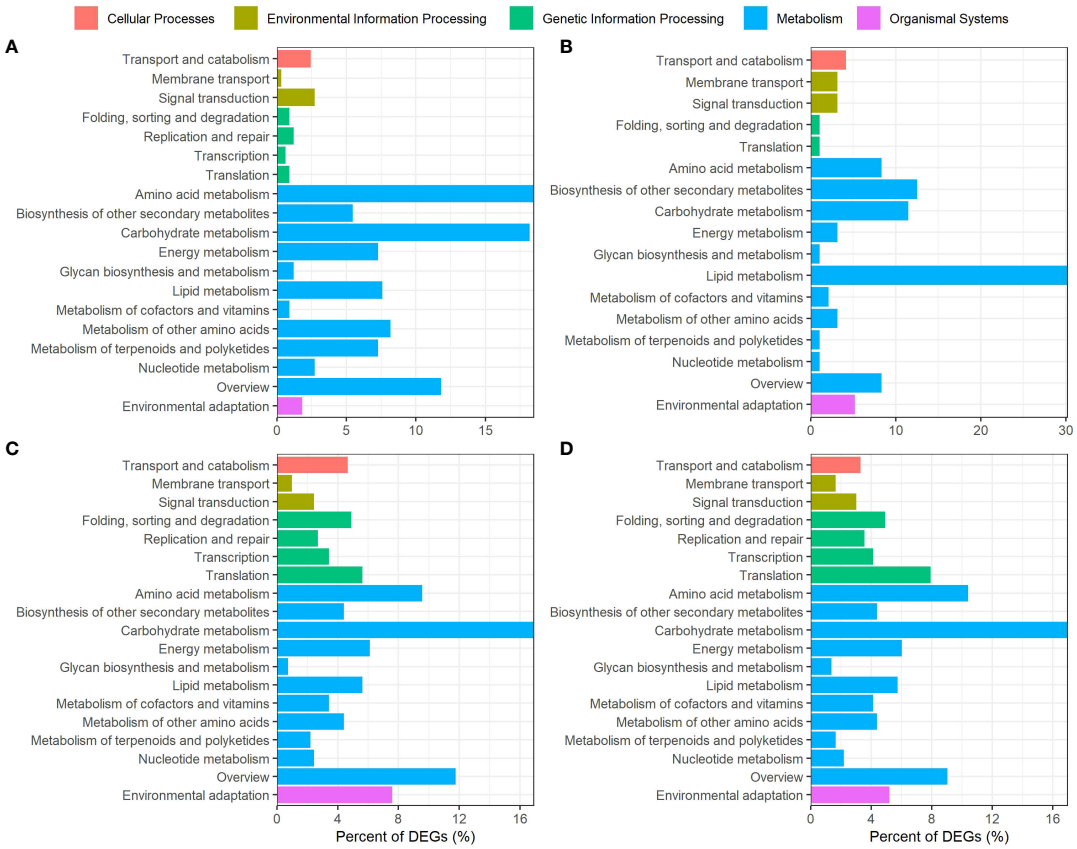

FIGURE 8
Kyoto Encyclopedia of Genes and Genomes (KEGG) pathways analysis of *S. spontaneum* accessions G152 and G3 grown under high N and low N conditions. The DEGs used here were identified by pairwise comparisons between high N and low N treatments and between genotypes (p-value < 0.05). **(A)**, G152HN vs G152LN; **(B)**, G3HN vs G3LN; **(B)**, G152 LN vs G3 LN; **(D)**, G152 HN vs G3 HN.

methyltransferase gene activity did not change in G152HN but it was down-regulated in G3HN. Proline dehydrogenase gene was up-regulated in G152 LN but its activity hardly changed in G3 LN (Figure 9). There was little change in the expression of serine O-acetyltransferase in G152HN but was over-expressed in G3HN, and it was down-regulated in G152LN with little change in G3LN. Collectively, these results show large N-induced and genotype-dependent variation for amino acid metabolism in the *S. spontaneum* accessions tested.

As with amino acid metabolism, expression of DEGs involved in carbon metabolism changed significantly in G152 and G3 accessions in response to inorganic N fertiliser application (Figure 9, Table S6). For example, in both G152 and G3, genes encoding fructose-bisphosphate aldolase, phosphoglycerate kinase and pyruvate dehydrogenase were down-regulated under HN condition whereas, under LN condition, they were over-expressed in G152 but remained unchanged in G3 (Figure 9, Table S6). In contrast, phosphenolpyruvate carboxylase, 6-phosphofructokinase 1 and ribulose phosphate 3-epimerase were over-expressed in G152HN but its expression did not change under LN condition. However, all these three enzymes were down-regulated in G3 irrespective of its soil N condition. Similar to amino acid metabolism, remarkably opposite expression patterns of DEGs were observed between G152 and G3 grown under HN or LN condition. This further attests the fact that genotypic variation is remarkably greater than treatment effect for carbon metabolism in the test accessions.

Consistent with the activity of amino acid and carbohydrate metabolism genes, expression of DEGs involved in N metabolism also showed remarkable variation under contrasting N supply in G152 and G3 accessions (Figure 9, Table S7). As an example, expression of nitrate and nitrite transporters and nitrate reductase genes was mostly inhibited in G152 and G3 grown under high N condition whereas their activity under low N was strongly up-regulated in G152 but remained mostly unaffected in G3. Contrarily, glutamate synthase expression was not affected in G152HN but was down-regulated in G3HN.The gene activity was either down-

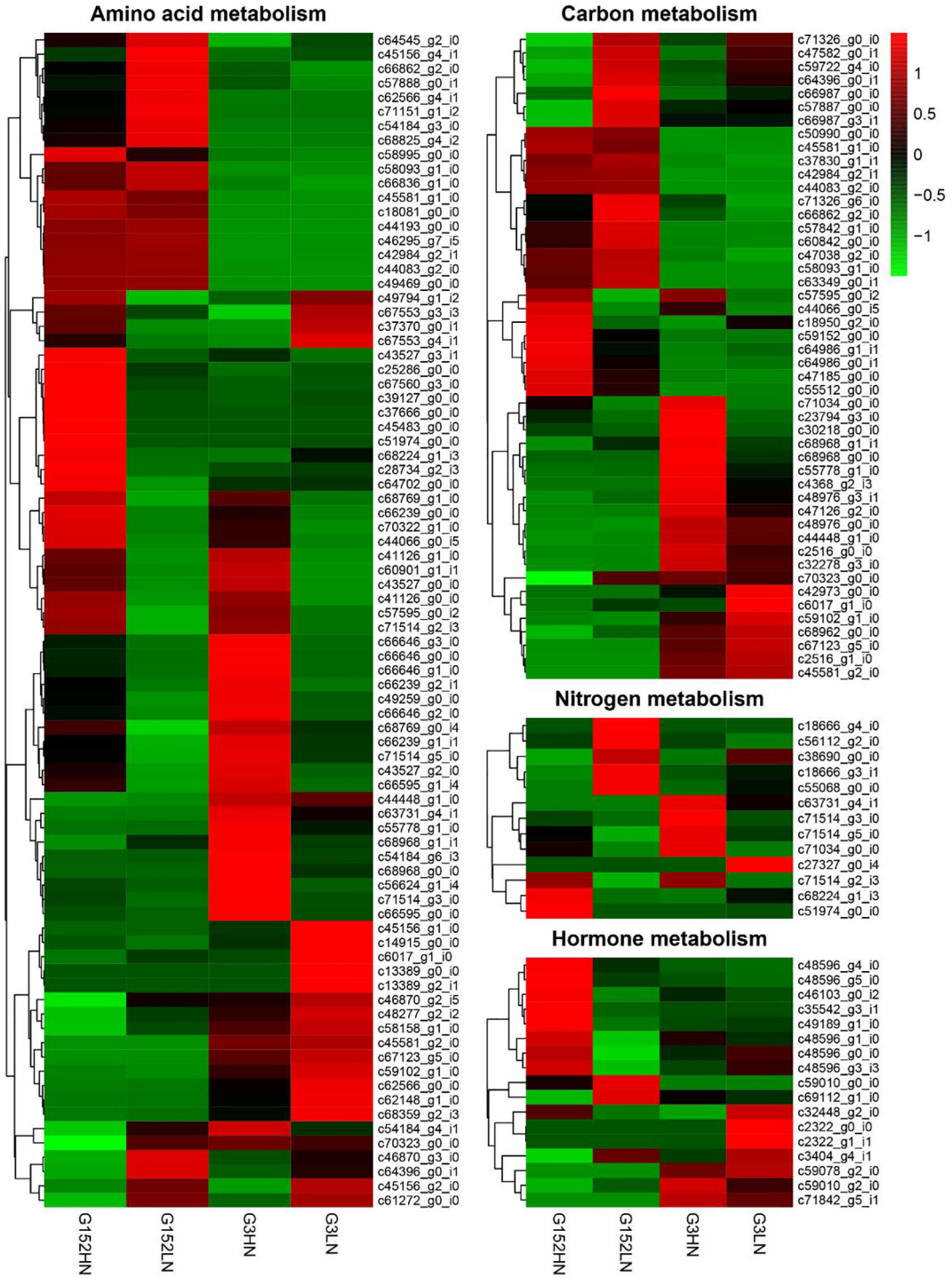

FIGURE 9
Expression of genes of involved in amino acids, carbon, nitrogen and hormones in response to external N application in *S. spontaneum* accessions G152 and G3.

regulated or unaffected under LN condition in both accessions. In general, N metabolism gene expression showed remarkable variation in different genetic background and contrasting soil N conditions.

Genes involved in plant hormones auxin, gibberellin, cytokinin, abscisic acid and brassinosteroid metabolism were substantially altered by externally applied inorganic N in high-BNF *S. spontaneum* accessions G152 and G3 (Figure 9, Table

S8). Under high N supply condition, (+)-abscisic acid 8'-hydroxylase gene expression was up-regulated conspicuously in G152 but it remained unchanged or down-regulated under low N supply in G152, and in G3 in both soil N conditions. A similar observation was also evident for GA2-oxidase except for G152LN plants where the gene activity was down-regulated. With regard to auxin metabolism, auxin-responsive GH3 genes involved in auxin homeostasis were slightly down-regulated in G152HN, G152 LN and G3HN plants but were up-regulated in G3LN (Figure 9, Table S8). A somewhat similar trend was also observed for transcripts of cytokinin dehydrogenase, a gene regulating cytokinin homeostasis. In contrast, a cytochrome P450 gene involved in brassinosteroid biosynthesis was strongly up-regulated in G152HN plants but not in plants from the other three treatments. In brief, as with external N treatment, genotype also had a pronounced effect on hormone metabolism in the test plants.

3.9 Expression of DEGs tallied well with qRT-PCR results

The reliability of RNA-Seq data was confirmed by qRT-PCR analysis of 8 randomly selected unigenes involved in amino acid (c43527_g3_i1; c45156_g2_i0), carbon (c47126_g2_i0; c59722_g4_i0; c66987_g0_i0) and nitrogen metabolism (c51974_g0_i0; c55068_g0_i0; c56112_g2_i0) (Figure 10). The expression data from RNA-Seq was consistent with qRT-PCR except for a few minor quantitative variations.

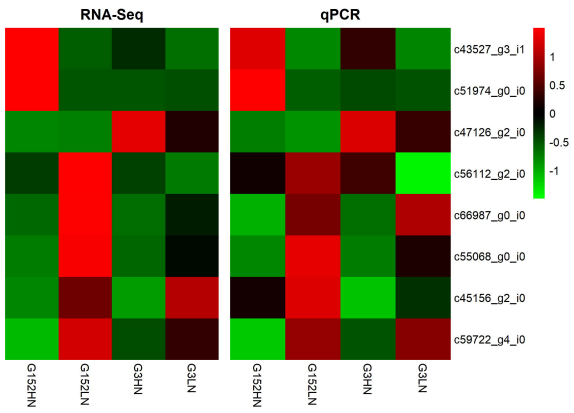

FIGURE 10
Validation of RNA-Seq data by analysing the expression of nine genes involved in amino acid, carbon and nitrogen metabolism by qRT-PCR.

4 Discussion

One of the important and novel results of this study is the finding that large genetic variation for BNF and brix exists in *S. spontaneum* accessions (Figures 1 - 3). And, some of the accessions have remarkably high capacity for BNF and favourable stalk traits including brix content (~10%). This result has considerable practical significance in that the native N fixing property of *S. spontaneum* could be introgressed into commercial sugarcane breeding population, similar to disease resistance, abiotic stress tolerance, vigour, ratooning, stalk population traits previously introduced (Lakshmanan et al., 2022). There are very few reports on BNF in *S. spontaneum* (Dong et al., 2018; Malviya et al., 2022), and extensive screening of geographically diverse accessions for BNF has not been reported. The data presented here forms the first evidence that high-BNF *S. spontaneum* with desirable agronomic attributes could be a potentially valuable genetic source for sugarcane BNF improvement through breeding. This is particularly relevant at present as sugarcane is touted as a sustainable food and energy crop (Yang et al., 2021; Camargo et al., 2022). However, its sustainability and carbon neutrality remain unclear (Yang et al., 2021; Camargo et al., 2022; Luo et al., 2022). As an example, China is a major sugarcane producing country and the excessive use of N fertiliser in sugarcane crop for a long period of time led to extensive soil degradation, soil and water pollution and crop productivity plateau (Luo et al., 2022). Thus, minimising fertiliser input, particularly N fertiliser use, for sugarcane production is critical for controlling soil degradation, improving crop NUE and regaining soil health and crop productivity.

While the large genetic variation for BNF in Chinese *S. spontaneum* is promising, little is known about its sensitivity to external N. This knowledge is very important for *S. spontaneum* introgression to improve NUE because significant quantities of inorganic N supply is needed to sustain economic yield in almost all sugarcane growing countries and any change in N input reduction is likely to be gradual. Also, BNF alone cannot meet crop N demand and sustain economic yield as observed in Brazilian sugarcane production. Hence, we studied the sensitivity of N fixation to externally applied inorganic N in high-BNF *S. spontaneum* accessions. The results showed remarkable resilience of BNF to relatively high externally supplied inorganic N in two (G152 and G3) out of six accessions grown in soil (Figure 4), demonstrating the potential of *S. spontaneum* for reducing external N requirement for sugarcane production through variety improvement (Liu et al., 2020; Udvardi et al., 2021).

Externally applied N is known to inhibit BNF even in high-N fixers like legumes (Liu et al., 2020; Imran et al., 2021; Udvardi et al., 2021). This is not surprising in that ready availability of fixed N inhibits N fixation (Udvardi et al., 2021). Hence, more experiments were conducted to further understand the physiological and molecular aspects of external N effect on

BNF in *S. spontaneum* accessions G152 and G3. It appears that external N supply affects N and carbon metabolism differently in different accessions and even in different tissues. For example, external N supply inhibited BNF in both accessions but it greatly increased total N content of leaf and root tissues (Figure 5A). However, a different pattern was evident for NH4-N and soluble sugars with external N increasing their contents in leaf tissues of G152 and G3 but not so in the roots. This indicates that the effect of external N supply on carbon and N metabolism in *S. spontaneum* is organ-specific with a remarkable effect on leaves but has a minimal impact on roots (Figure 5). Such organ- and tissue-specific variation on carbon and N metabolism has been reported previously (Lawlor, 2002). Here, it is also interesting to note that different N metabolic enzymes responded differently to external N supply. For instance, NR activity was upregulated markedly in leaf and root tissues in response to external N in both varieties but GS activity was not much affected (Figure 6). Differential organ-specific expression of NR and GS enzymes in response to external N supply has been reported in other crops (Prinsi and Espen, 2015; Iqbal et al., 2020). Further, it is worth noting that the upregulation of N metabolism enzymes in leaf tissues of G152 and G3 was opposite of BNF activity. Collectively, these results suggest that external N supply may be regulating N and carbon metabolism differently in different organs and genotypes, and key N metabolism enzymes within each organ, in *S. spontaneum*.

Hormones regulate all aspects of plant growth and development. And, it is well established that nutrient availability, particularly macro-nutrients, determine plant growth and development (Krouk et al., 2011). It is also now well-established that plant growth, hormones and plant nutrition are finely coordinated through a network of hormonal and nutritional signal (Krouk et al., 2011). Since carbon and N are very central to growth and development of every organism, it is not surprising that its uptake, use and storage in plants are under hormonal regulation (Krouk et al., 2011; Yu et al., 2016). From the results of our study, it is clear that external N supply markedly increased plant growth promoting hormones such as auxin (IAA), gibberellin (GA3), and cytokinin (ZR) with little effect on abscisic acid in the leaf tissues of both varieties (Table 2). These results are corresponding well with the increased shoot elongation growth and shoot number observed in plants grown with external N supply (Table 1). Modulation of nutrient uptake, its use and remobilization, and plant grown by externally applied hormones, especially plant growth promoters, has been observed in many plant species (Lu et al., 1992; Krouk et al., 2011).

Regulation of carbon and nitrogen is tightly linked to plant-environment interactions and it determine plant growth and development (Raven et al., 2004). Thus, to gain more insights into the modulation of shoot growth, BNF, N and carbon metabolism and tissue composition elicited by externally applied N in *S. spontaneum* accessions G152 and G3, we analysed the expression of genes involved in carbon, N, amino acid and hormone metabolism in both accessions grown under externally supplied N (Figure 9). Here, we first discuss some of the general but important trends in gene expression as affected by N application, followed by more specific findings related to the inter-linked processes of carbon, N, amino acids and hormone metabolism. Overall, N application significantly altered >2000 genes in both accessions combined, with genotype accounting for most of the variation (Figure S1, S2). This suggests that large genetic variation in gene expression exists between G152 and G3, and that G152 is relatively more sensitive to applied N. This contention is further corroborated by the very small number of common DEGs (28) found between the two accessions when their N treatment effects were compared (Figure S2). However, in contrast to treatment effect (LN *vs* HN for each accession) where G152 had almost thrice the number of DEGs detected in G3, the number of DEGs were similar when both accessions grown under same N condition (HN or LN) were compared (Figure S1, S2). Also, there was remarkable similarity of classes of DEGs associated with different cellular activities under LN and HN as shown in Figures 8C, D. However, it is interesting to note that more genes were found to be up-regulated under low N whereas high N had an opposite effect (Figure S1). Contrasting expression of genes involved in plant nutrition under different nutrient availability has been reported previously. For instance, under low N growth condition high- affinity N transporters are strongly up-regulated whereas they are down-regulated when N is replete (Dreyer and Michard, 2020). An opposite expression pattern occurs for low-affinity N transporters.

External application of inorganic N markedly up- and down-regulated genes in all metabolic pathways studied (Figures 7–9). More specifically, the set of genes involved in N, carbon, amino acid and hormone metabolism showed remarkably varied expression patten in different genotypes and N supply condition (Figure 9), giving further evidence of the complexity and variation in molecular mechanism regulating these pathways in different genetic background. A clearer picture of differential gene expression has emerged with GO and KEGG analyses. GO analysis of DEGs revealed very large difference in gene expression pattern between G152 and G3 (Figure 7). In G152, applied N caused remarkable effect on carbon and N metabolism and transport processes with more up-regulation than down-regulation, while single organism processes and lipid and carboxylic acid metabolism were the most affected (more down- than up-regulation) in G3. It appears that under low N, activity of genes associated with phosphorylation, kinase activity and metabolism of phosphate-containing compounds are more affected (more down- than up-regulation). In contrast, under HN, expression of genes involved in nucleotide binding, kinase activity, DNA metabolism are more altered (more up- than down-regulation) (Figure 7). These results were further corroborated by the KEGG analysis of DEGs, with amino acid, carbohydrate and N metabolism dominating in G152 in response to N and DEGs of lipid metabolism enriching far in excess than others in G3 (Figure 8).

The overall picture arising from the molecular analysis is that the two accessions may be achieving the same outcome of relatively high shoot growth (Table 1) and remarkable resilience of BNF (Figure 3) possibly through different metabolic strategies (Figures 7, 8). Uptake, transport and use of N and other minerals needed for plant growth involve considerable energy. It appears that G152 may be directly utilising photosynthate to drive N assimilation and use (Figure 8) whereas G3 may be relying more on lipids for the same (Figure 8). Further, the molecular evidence points towards a remarkable difference in expression of a large number of same genes or their alleles associated with carbon, N, amino acid and hormone metabolism in different genetic background and contrasting N supply conditions.

5 Conclusion

Reducing N fertiliser use for sugarcane production is critical for reducing soil acidification and carbon footprint. While optimisation of cropping system will help improve the environmental sustainability of sugarcane production, replicating the Brazilian experience of low N input farming using varieties with BNF capacity that complement improved cropping system would be a very desirable outcome. Until now, efforts to breed or select N-efficient sugarcane varieties proved unsuccessful, suggesting the genetic complexity of sugarcane NUE and possibly the limited BNF capacity in the current breeding pool. In this context, exploring sugarcane progenitor *S. spontaneum*, the species with very large eco-climatic adaptability including very low-fertile marginal soils, to breed for N-efficient clones would be a logical approach. Our *S. spontaneum* screening experiments provided the first evidence of large genetic variation for BNF capacity existing in this species. Further, BNF property of a small number of clones proved to be quite resilient to external inorganic N application, without which economic crop production remains unattainable. Molecular characterization of high-BNF accessions unraveled the diversity of gene activity and metabolic pathways associated with carbon, N, amino acid and hormone metabolism operating in different *S. spontaneum* accessions. Understanding the genetic elements and the molecular mechanism(s) underpinning BNF in *S. spontaneum* would be the next logical step for research. It is concluded that *S. spontaneum* accessions with high BNF capacity could be a valuable tool to improve N-efficiency in sugarcane.

Data availability statement

The datasets presented in this study can be found in online repositories. The names of the repository/repositories and accession number(s) can be found in the article/Supplementary Material.

Author contributions

TL conceived, designed, and conducted research, analysed data and wrote the original manuscript. PL and C-NL contributed methodology. PL, TL, RY and X-YL analysed data and wrote the final manuscript. KH conducted experimental work. Y-RL contributed to original manuscript writing. X-YL revised the manuscript. PL and Y-RL reviewed and edited original manuscript. All authors contributed to the article and approved the submitted version.

Funding

This study was supported by the grant from National Natural Science Foundation of China (Project No.32001484 and 32201910) by the Ministry of Science and Technology of the People's Republic of China, and Major Research Program Fund, (Project numbers 2021AB19026; AA22117009; AA22117004) by the Department of Science and Technology, Guangxi Provincial Government, Guangxi, and Guangxi Academy of Agricultural Sciences.

Acknowledgments

We thank all our colleagues from Guangxi Academy of Agricultural Sciences who have supported this study. We also thank Nanning Goldtech Biotech Ltd., Co., Nanning, Guangxi for analysis and related technical services.

Conflict of interest

The authors declare that the research was conducted in the absence of any commercial or financial relationships that could be construed as a potential conflict of interest.

Publisher's note

Supplementary material

The Supplementary Material for this article can be found online at: https://www.frontiersin.org/articles/10.3389/fpls.2022.1099701/full#supplementary-material

References

Bell, M. J. (2014). *A review of nitrogen use efficiency in sugarcane* (Brisbane, Australia: Sugar Research Australia).

Boddey, R. M., Urquiaga, S., Reis, V., and J Dobereiner, J. (1991). Biological nitrogen fixation associated with sugar cane. *Plant Soil* 137, 111–117. doi: 10.1007/BF02187441

Bories, P. N., and Bories, C. (1995). Nitrate determination in biological fluids by an enzymatic one-step assay with nitrate reductase. *Clin. Chem.* 41, 904–907. doi: 10.1093/clinchem/41.6.904

Bressler, S. L., and Ahmed, S. I. (1984). Detection of glutamine synthetase activity in marine phytoplankton: Optimization of the biosynthetic assay. *Mari Ecol. Progr* 14, 207–217. doi: 10.3354/meps014207

Camargo, L. R., Castro, G., Gruber, K., Jewell, J., Klingler, M., Turkovska, O., et al. (2022). Pathway to a land-neutral expansion of Brazilian renewable fuel production. *Nat. Commun.* 13, 3157. doi: 10.1038/s41467-022-30850-2

Dong, M., Yang, Z., Cheng, G., Peng, L., Xu, Q., and Xu, J. (2018). Diversity of the bacterial microbiome in the roots of four saccharum species: S. spontaneum, *S. robustum, s. barberi and s. officinarum*. *Front. Microbiol.* 9. doi: 10.3389/fmicb.2018.00267

Dreyer, I., and Michard, E. (2020). High- and low-affinity transport in plants from a thermodynamic point of view. *Front. Plant Sci.* 10, 1797. doi: 10.3389/fpls.2019.01797

FAO (2019). *World fertilizer trends and outlook to 2022* (Rome, Italy: Food and Agriculture Organisation of the United Nations).

FAO (2020). *FAOSTAT database* (Rome: Food and Agriculture Organisation of the United Nations).

Gong, M., Luo, H., Wang, A., Zhou, Y., Huang, W., Zhu, P., et al. (2017). Phytohormone profiling during tuber development of chinese yam by ultra-high performance liquid chromatography–triple quadrupole tandem mass spectrometry. *J. Plant Grow Regul.* 36, 362–373. doi: 10.1007/s00344-016-9644-8

Grabherr, M. G., Hass, B. J., Yassour, M., Levin, J. Z., Thompson, D. A., Amit, I., et al. (2011). Full-length transcriptome assembly from RNA-Seq data without a reference genome. *Nature Biotechnol.* 29, 644–52. doi: 10.1038/nbt.1883

Guo, J. H., Liu, X. J., Zhang, Y., Shen, J. L., Han, W. X., Zhang, W. F., et al. (2010). Significant acidification in major Chinese croplands. *Science* 327, 1008–1010. doi: 10.1126/science.1182570

Hardy, R. W. F., Holsten, R. D., Jackson, E. K., and Burns, R. C. (1968). The acetylene-ethylene assay for N2 fixation: laboratory and field evaluation. *Plant Physiol.* 43, 1185–1207. doi: 10.1104/pp.43.8.1185

Hemaprabha, G., Mohanraj, K., Jackson, P. A., Lakshmanan, P., Ali, G. S., Li, A. M., et al. (2022). Sugarcane genetic diversity and major germplasm collections. *Sugar Tech* 24, 279–297. doi: 10.1007/s12355-021-01084-1

Imran, A., Hakkim, S., Tariq, M., Nawaz, M. S., Laraib, I., Gulzar, U., et al. (2021). Diazotrophs for lowering nitrogen pollution crises: Looking deep into the roots. *Front. Microbiol.* 12. doi: 10.3389/fmicb.2021.637815

Iqbal, A., Dong, Q., Wang, X., Gui, H., Zhang, H., Zhang, X., et al. (2020). Transcriptome analysis reveals differences in key genes and pathways regulating carbon and nitrogen metabolism in cotton genotypes under n starvation and resupply. *Int. J. Mol. Sci.* 21, 1500. doi: 10.3390/ijms21041500

Kopittke, P. M., Menzies, N. W., Wang, P., McKenna, B. A., and Lombic, E. (2019). Soil and the intensification of agriculture for global food security. *Environ. Int.* 132, 105078. doi: 10.1016/j.envint.2019.105078

Krouk, G., Ruffel, S., Gutiérrez, R. A., Gojon, A., Crawford, N. M., Coruzzi, G. M., et al. (2011). A framework integrating plant growth with hormones and nutrients. *Trends Plant Sci.* 16, 178–182. doi: 10.1016/j.tplants.2011.02.004

Lakshmanan, P., Jackson, P., Hemaprabha, G., and Yang, R. L. (2022). Sugar tech special issue: History of sugarcane breeding, germplasm development and related molecular research. *Sugar Tech* 24, 1–3. doi: 10.1007/s12355-021-01080-5

Lawlor, D. W. (2002). Carbon and nitrogen assimilation in relation to yield: mechanisms are the key to understanding production systems. *J. Exp. Bot.* 53, 773–787. doi: 10.1093/jexbot/53.370.773

Liu, J., Yu, X., Qin, Q., Dinkins, R. D., and Zhu, H. (2020). The impacts of domestication and breeding on nitrogen fixation symbiosis in legumes. *Front. Genet.* 11. doi: 10.3389/fgene.2020.00973

Lu, J. L., Ertl, J. R., and Chen, C. M. (1992). Transcriptional regulation of nitrate reductase mRNA levels by cytokinin-abscisic acid interactions in etiolated barley leaves 1. *Plant Physiol.* 98, 1255–1260. doi: 10.1104/pp.98.4.1255

Luo, T., Lakshmanan, P., Zhou, Z. F., Deng, Y., Deng, Y., Yang, L., et al. (2022). Sustainable sugarcane cropping in China. *Front. Agri Sci. Eng.* 9, 272–283. doi: 10.15302/J-FASE-2022442

Malviya, M. K., Li, C.-N., Lakshmanan, P., Solanki, M. K., Wang, Z., Solanki, A. C., et al. (2022). High-throughput sequencing-based analysis of rhizosphere and diazotrophic bacterial diversity among wild progenitor and closely related species of sugarcane (Saccharum spp. inter-specific hybrids). *Front. Plant Sci.* 13. doi: 10.3389/fpls.2022.829337

Moreira, L. A., Otto, R., Cantarella, H., Junior, J. L., Azevedo, R. A., and de Mira, A. B. (2021). Urea- versus ammonium nitrate–based fertilizers for green sugarcane cultivation. *J. Soil Sci. Plant Nutr.* 21, 1329–1338. doi: 10.1007/s42729-021-00443-x

Murashige, T., and Skoog, F. (1962). A revised medium for rapid growth and bioassays with tobacco tissue cultures. *Physiol. Planta* 15, 473–497. doi: 10.1111/j.1399-3054.1962.tb08052.x

Prinsi, B., and Espen, L. (2015). Mineral nitrogen sources differently affect root glutamine synthetase isoforms and amino acid balance among organs in maize. *BMC Plant Biol.* 15, 96. doi: 10.1186/s12870-015-0482-9

Raven, J. A., Handley, L. L., and Andrews, M. (2004). Global aspects of C/N interactions determining plant–environment interactions. *J. Exp. Bot.* 55, 11–25. doi: 10.1093/jxb/erh011

Robinson, N., Brackin, R., Vinall, K., Soper, F., Holst, J., Gamage, H., et al. (2011). Nitrate paradigm does not hold up for sugarcane. *PloS One* 6, e19045. doi: 10.1371/journal.pone.0019045

Robinson, N., Fletcher, A., Whan, A., Critchley, C., von Wirén, N., Lakshmanan, P., et al. (2008). Sugarcane genotypes differ in internal nitrogen use efficiency. *Funct. Plant Biol.* 34, 1122–1129. doi: 10.1071/FP07183

Robinson, N., Schmidt, S., and Lakshmanan, P. (2014). "Genetic improvement of nitrogen use efficiency in sugarcane," in *A review of nitrogen use efficiency in sugarcane*. Ed. M. J. Bell (Brisbane, Australia: Sugar Research Australia), 125–155.

Rossetto, R., Ramos, N. P., de Matos Pires, N. P., Xavier, R. C., Cantarella, M. A., de Andrade, H. G., et al. (2022). Sustainability in sugarcane supply chain in Brazil: Issues and way forward. *Sugar Tech* 24, 941–966. doi: 10.1007/s12355-022-01170-y

Shastri, B., Kumar, R., and Lal, R. J. (2020). Isolation, characterization and identification of indigenous endophytic bacteria exhibiting PGP and antifungal traits from the internal tissue of sugarcane crop. *Sugar Tech* 22, 563–573. doi: 10.1007/s12355-020-00824-z

Singh, R. K., Singh, P., Guo, D. J., Sharma, A., Li, D. P., Li, X., et al. (2021a). Root-derived endophytic diazotrophic bacteria pantoea cypripedii AF1 and kosakonia arachidis EF1 promote nitrogen assimilation and growth in sugarcane. *Front. Microbiol.* 12. doi: 10.3389/fmicb.2021.774707

Singh, P., Singh, R. K., Guo, D. J., Sharma, A., Singh, R. N., Li, D. P., et al. (2021c). Whole genome analysis of sugarcane root-associated endophyte pseudomonas aeruginosa B18- a plant growth-promoting bacterium with antagonistic potential against sporisorium scitamineum. *Front. Microbiol.* 12. doi: 10.3389/fmicb.2021.628376

Singh, P., Singh, R. K., Li, H.-B., Guo, D.-J., Sharma, A., Lakshmanan, P., et al. (2021b). Diazotrophic bacteria pantoea dispersa and enterobacter asburiae promote sugarcane growth by inducing nitrogen uptake and defense-related gene expression. *Front. Microbiol.* 11. doi: 10.3389/fmicb.2020.600417

Solanki, M. K., Wang, F.-Y., Li, C.-N., Wang, Z., Lan, T.-J., Singh, R. K., et al. (2020). Impact of sugarcane–legume intercropping on diazotrophic microbiome. *Sugar Tech* 22, 52–64. doi: 10.1007/s12355-019-00755-4

Soumare, A., Diedhiou, A. G., Thuita, M., Hafidi, M., Ouhdouch, Y., Gopalakrishnan, S., et al. (2020). Exploiting biological nitrogen fixation: A route towards a sustainable agriculture. *Plants* 9, 1011. doi: 10.3390/plants9081011

Udvardi, M., Below, F., Castellano, M. J., Eagle, A. J., Giller, K. E., Ladha, J. K., et al. (2021). A research road map for responsible use of agricultural nitrogen. *Front. Sust Food Syst.* 5, 660155. doi: 10.3389/fsufs.2021.660155

VSNI (2017). *Genstat for windows 19th edition* (Hemel Hempstead, United Kingdom: VSN International).

Yang, L., Deng, Y., Wang, X., Zhang, W., Shi, X., Chen, X., et al. (2021). Global direct nitrous oxide emissions from the bioenergy crop sugarcane (Saccharum spp. inter-specific hybrids). *Sci. Total Environ.* 752, 141795. doi: 10.1016/j.scitotenv.2020.141795

Yang, R. C., Yang, T., Zhang, H., Qi, Y., Xing, Y., Zhang, N., et al. (2014). Hormone profiling and transcription analysis reveal a major role of ABA in tomato salt tolerance. *Plant Physiol. Biochem.* 77, 23–34. doi: 10.1016/j.plaphy.2014.01.015

Yang, L., Zhou, Y., Meng, B., Li, H., Zhan, J., Xiong, H., et al. (2022). Reconciling productivity, profitability and sustainability of small-holder sugarcane farms: A combined life cycle and data envelopment analysis. *Agri Syst.* 199, 103392. doi: 10.1016/j.agsy.2022.103392

Yu, J., Han, J., Wang, R., and Li, X. (2016). Down-regulation of nitrogen/carbon metabolism coupled with coordinative hormone modulation contributes to developmental inhibition of the maize ear under nitrogen limitation. *Planta* 244, 111–124. doi: 10.1007/s00425-016-2499-1

frontiers | Frontiers in Plant Science

TYPE Original Research
PUBLISHED 02 February 2023
DOI 10.3389/fpls.2023.1098175

OPEN ACCESS

EDITED BY
Nandula Raghuram,
Guru Gobind Singh Indraprastha University, India

REVIEWED BY
Maharajan Theivanayagam,
Rajagiri College of Social Sciences, India
Anandan Annamalai,
Indian Institute of Seed Science, India

*CORRESPONDENCE
Matthew J. Milner
matthew.milner@niab.com

SPECIALTY SECTION
This article was submitted to Plant Physiology, a section of the journal Frontiers in Plant Science

RECEIVED 14 November 2022
ACCEPTED 23 January 2023
PUBLISHED 02 February 2023

CITATION
Milner MJ, Bowden S, Craze M and Wallington EJ (2023) *OsPSTOL* but not *TaPSTOL* can play a role in nutrient use efficiency and works through conserved pathways in both wheat and rice. *Front. Plant Sci.* 14:1098175. doi: 10.3389/fpls.2023.1098175

OsPSTOL but not *TaPSTOL* can play a role in nutrient use efficiency and works through conserved pathways in both wheat and rice

Matthew J. Milner*, Sarah Bowden, Melanie Craze and Emma J. Wallington

NIAB, Cambridge, United Kingdom

There is a large demand to reduce inputs for current crop production, particularly phosphate and nitrogen inputs which are the two most frequently added supplements to agricultural production. Gene characterization is often limited to the native species from which it was identified, but may offer benefits to other species. To understand if the rice gene Phosphate Starvation Tolerance 1 (PSTOL) *OsPSTOL*, a gene identified from rice which improves tolerance to low P growth conditions, might improve performance and provide the same benefit in wheat, *OsPSTOL* was transformed into wheat and expressed from a constitutive promoter. The ability of *OsPSTOL* to improve nutrient acquisition under low phosphate or low nitrogen was evaluated. Here we show that *OsPSTOL* works through a conserved pathway in wheat and rice to improve yields under both low phosphate and low nitrogen. This increase is yield is mainly driven by improved uptake from the soil driving increased biomass and ultimately increased seed number, but does not change the concentration of N in the straw or grain. Overexpression of *OsPSTOL* in wheat modifies N regulated genes to aid in this uptake whereas the putative homolog *TaPSTOL* does not suggesting that expression of *OsPSTOL* in wheat can help to improve yields under low input agriculture.

KEYWORDS

PSTOL, phosphate, nitrogen, wheat, uptake, N15, nitrogen use efficiency, phosphate use efficiency

Introduction

There is a strong desire to reduce inputs in agriculture to make large scale farming more sustainable and lessen our impact on the surrounding environment. Phosphorous (P) and nitrogen (N) are added in large quantities as chemical fertilizers in modern agricultural practices. Both elements are essential macronutrients which are required for all major developmental processes in plants and are key for both completing the life cycle and

maintaining food production. Their mobility within the soil, mechanisms of uptake and the plant scavenge response to their limitation differ (Marschner, 1995).

Recent advances in our understanding of the molecular mechanisms by which different plant species adapt to different abiotic stresses, including the regulation and expression of key genes and growth habits have enabled the design of more effective breeding strategies to produce highly resilient crops (Xu et al., 2006; Magalhaes et al., 2007; Gamuyao et al., 2012; Milner et al., 2022). A number of the underlying genes involved in the response of plants to low P and N are highly conserved and play similar roles in a number of diverse plant species including both model system and crop species (Borah et al., 2018; Milner et al., 2022). Thus, a greater understanding of the pathways involved, the key genes involved in P and N acquisition and signaling will allow breeders and plant molecular biologists to develop more efficient crops. Identification of these conserved pathways and genes from "model" organisms, and the subsequent transfer of this knowledge to crop species, would therefore allow farmers to optimize fertilizer use worldwide, resulting in increased efficiency of food production with lower environmental cost.

One such gene, believed to be important in increased nutrient use efficiency, is the recent identification of a key gene under the PUP1 locus from rice. The gene has been shown to be a serine/threonine receptor-like kinase, named Phosphate Starvation Tolerance 1 (PSTOL), is a major gene involved in tolerance to growth on low P soils (Heuer et al., 2009; Chin et al., 2011; Gamuyao et al., 2012; Vigueira et al., 2016). The PUP1 locus was originally identified in an upland variety of rice, Kasalath, yet is absent from most rice cultivars including the current reference japonica variety Nipponbare and indica variety 93-11 (Wissuwa et al., 2002; Vigueira et al., 2016). Rice varieties which have this genomic introgression containing a functional *PSTOL* gene, show greater biomass, larger root systems leading to increased tiller number and yield increases of up to 30% when grown under low P conditions whereas no deleterious consequences were seen when grown under normal soil fertility conditions (Chin et al., 2011; Gamuyao et al., 2012). The identification of *OsPSTOL* and its role in helping rice tolerate low P conditions has led to the belief that one could increase the PUE by incorporation of *PSTOL* type genes into many crop species. However when *OsPSTOL* was first identified the authors also suggested that other elements may also benefit from in increased root growth and make the plant more efficient to low nitrogen (N) conditions and drought (Gamuyao et al., 2012), but as yet no data been presented to substantiate the possibility of a role outside of PUE.

Others have identified homologous *PSTOL*-like genes in both maize and sorghum, based upon QTL analysis and sequence homology (Hufnagel et al., 2014; Azevedo et al., 2015; Bernardino et al., 2019). Further evidence of the role of *PSTOL*-like genes in PUE has been supported through QTL mapping rather than direct molecular characterization of candidate genes. Criteria to identify other potential *PSTOL* like genes has included identification of protein domains such as ATP kinase domains and on DNA sequence conservation meeting certain bioinformatic cut-offs for genes underlying these QTL. Some of these homologues appear to have differences in their gene structure such as number and length of introns and UTRs. Despite the lack of a highly conserved gene in most plant species, it is critical to understand whether other *PSTOL* genes exist in other important crop species and if they can be exploited. Our previous study identified a putative wheat *PSTOL* gene (*TaPSTOL*) and characterized its role in PUE and other important agronomic phenotypes (Milner et al., 2018). As the overexpression of *TaPSTOL* was not able to replicate the yield increase seen with overexpression of *OsPSTOL* in rice, we suggested that either wheat lacked the other genes downstream of *PSTOL* to increase yields or a critical domain within the coding sequence itself was the reason for the lack of increased yields.

Here, we set out to test whether the differences seen in a plants ability to maintain yield on low P is due to the presence of the *OsPSTOL* or *TaPSTOL* genes *per se* or if other parts of an unknown pathway underlie the differences seen in yield increases. We also test whether expression of *OsPSTOL* can overcome other nutrient deficiencies to see if the presence of *OsPSTOL* is only beneficial to low phosphate conditions.

Methods

Cloning: The *OsPSTOL* coding sequence from European Molecular Biology Laboratory (EMBL) (AB458444.1) was synthesized with a ribosomal binding site, CCACC, immediately upstream of the ATG start codon and flanked with gateway attL1/attL2 sites (Genewiz). The synthesized sequence was then recombined into the binary vector pSc4ActR1R2 using a Gateway LR Clonase II kit (Thermofisher) to create the plasmid pMM007 for stable wheat transformation. In pMM007 *OsPSTOL* is driven by the OsActin promoter and terminated by the *Agrobacterium tumefaciens* nopaline synthase terminator (tNOS).

Wheat Transformation: Wheat cv. Fielder plants were grown in controlled environment chambers (Conviron) at 20°C day/15°C night with a 16 h day photoperiod (approximately 400 µE m^{-2} s^{-1}). Immature seeds were harvested for transformation experiments at 14–20 days post-anthesis. Isolated immature wheat embryos were co-cultivated with *A. tumefaciens* for 2 days in the dark [35]. Subsequent removal of the embryonic axis and tissue culture was performed as previously described [36]. Individual plantlets were hardened off following transfer to Jiffy-7 pellets (LBS Horticulture), potted up into 9 cm plant pots containing M2 compost plus 5 g/l slow-release fertilizer (Osmocote Exact 15:9:9) and grown on to maturity and seed harvest in controlled environment chambers. *TaPSTOL* overexpression line OE-1 was also grown for comparison (Milner et al., 2018).

DNA analysis of transformed wheat plants: Wheat plantlets which regenerated under G418 selection in tissue culture were transferred to Jiffy-7 pellets and validated using an nptII copy number assay relative to a single copy wheat gene amplicon, GAMyb for wheat, normalized to a known single copy wheat (Milner et al., 2018). Primers and Taqman probes were used at a concentration of 10 µM in a 10 µl multiplexed reaction using ABsolute Blue qPCR ROX mix (Thermofisher) with the standard run conditions for the ABI 7900 HT for wheat. The relative quantification, $\Delta\Delta^{Ct}$, values were calculated to determine nptII copy number in the T_0 and subsequent generations. Primers for the copy number determination are listed in Suppl. Table 1. Homozygous and

null transgenic lines were identified on the basis of copy number for the selection gene and segregation analysis in the T_1 generation. Null segregates were used for further study and referred to as WT Fielder.

Plant growth conditions: Plants were grown in a controlled growth chamber under 16 h light with 20°C/15°C day/night temperatures for all conditions tested. To study low P conditions WT and transgenic wheat lines were grown under in sand and fertilized twice a week with nutrient solution (Magnavaca et al., 1987) containing 3 µM KH_2PO_4, 1.3 mM NH_4NO_3, 3.52 mM Ca $(NO_3)_2$, 0.58 mM, KCl, 0.58 mM K_2SO_4, 0.56 mM KNO_3, 0.86 mM $Mg(NO_3)_2$ 0.13 mM H_3BO_3, 5 µM $MnCl_2$, 0.4 µM Na_2MoO_4, 10 µM $ZnSO_4$, 0.3 µM $CuSO_4$, $Fe(NO_3)_3$ and 2 mM MES (pH 5.5) twice a week until maturity. For low N conditions wheat and plants were grown on TS5 low fertility soil to control total nitrogen with a starting nitrogen level of 0.1 mg/l (Bourne Amenity, Kent, UK). Ammonium nitrate was then added to reach a final concentration in the pots equivalent to field fertilizer application of 70, 140 or 210 kg N/ha which equates to 23.3, 46.6, or 70 mg/1 L pot. Each pot also received 4.2 mg Ca, 2.7 mg K, 0.62 mg Mg, 0.04 mg P, 0.56 mg S, 0.008 mg B, 0.13 mg Fe, 0.015 mg Mn, 0.0012 mg Cu, 0.0024 Mo, 0.0045 Zn, 0.00 mg Na, and 0.63 mg Cl per pot added as Magnavaca solution which was added 10 days after sowing.

Whole plant measurements: Total above ground biomass, which is the leaves stems without the grain, seed weight (yield per plant), seed number, seed size, tiller number. Biological replicates each contained at least 14 plants per line and were grown until seed maturation. Tissues were allowed to dry for a further two weeks before harvesting and sampling or measurements were taken.

N tissue measurements: Samples were measured using the Dumas method. The samples were dried for 17 hours at 100°C and then milled on a 1mm hammer mill. Prior to testing the sample were dried at 104°C for 3 hours and 1g of sample was loaded on the instrument (Leco TruMacN Dumas gas analyser), following the manufacturer's instructions. Samples were converted to gases by heating in a combustion tube at 1150°C. Interfering components are removed from the resulting gas mixture. The nitrogen compounds in the gas mixture or a representative part of the mixture, are converted to molecular nitrogen which is quantitatively determined by a thermal conductivity detector. The nitrogen content is then calculated by a microprocessor.

RNA isolation and cDNA synthesis for gene expression analysis: Wheat seedlings were grown for seven days in 2.2 L pots containing Magnavaca solution as listed above and amended with 3 µM KH_2PO_4 for low P treatments or omitting 1.3 mM NH_4NO_3, and 3.52 mM Ca $(NO_3)_2$ for low N treatment. Plants were grown for an additional 7 days before harvesting tissue and separating the samples into root and shoot tissues for analysis. Total RNA was isolated from both roots and shoots for each treatment using a RNeasy Kit (Qiagen) and treated with DNaseI (Thermofisher) prior to cDNA synthesis from 500 ng of total RNA using Omniscript RT Kit (Qiagen). The cDNA was diluted 1:2 with water and 0.5 µL was used as template in each RT-PCR reaction. Expression levels were quantified by quantitative PCR in triplicate reactions from three biological replications using SYBR Green JumpStartTaq ReadyMix (SIGMA) with the standard run conditions for the ABI 7900 HT. OsPSTOL expression was compared to TaUbi. Primers used for amplification of transcripts are listed in Suppl. Table 1.

^{15}N uptake: To measure N uptake a similar protocol as previously reported (Milner et al., 2022), briefly roots from 2 week old seedlings were exposed to $^{15}NH_4^{15}NO_3$ for 10 min, then washed in 0.1 mM $CaSO_4$ for 2 min, harvested separated into root and shoot tissue, and dried at 70°C for 48 h before grinding. Dried tissue was then placed in 2mL microfuge tubes with 2 x 5mm diameter stainless steel beads and shaken in a genogrinder until a fine powder was obtained. Dried and ground samples were carefully weighed (0.5 mg) into tin capsules, sealed and loaded into the auto-sampler. Samples were analyzed for percentage carbon, percentage nitrogen, $^{12}C/^{13}C$ ($\delta^{13}C$) and $^{14}N/^{15}N$ ($\delta^{15}N$) using a Costech Elemental Analyzer attached to a Thermo DELTA V mass spectrometer in continuous flow mode. The excess ^{15}N was calculated based on measurements of $\delta^{15}N$ and tissue N%. The absolute isotope ratio (R) was calculated for labelled samples and controls, using $R_{standard}$ (the absolute value of the natural abundance of ^{15}N in atmospheric N_2; 1).

(1) $R_{sample\ or\ control} = [(\delta^{15}N/1000)+1] \times R_{standard}$

Then, molar factional abundance (F) and mass-based factional abundance (MF) were calculated (2,3,4)

(2) $F= R_{sample\ or\ control}/(R_{sample\ or\ control}+1)$

(3) $MF= (F \times 15)\ x/[(F \times 15)+ ((1-F)x\ 14)]$

(4) $\Delta MF = MF_{sample} - MF_{control}$

The excess ^{15}N in mg in a total tissue was calculated as in (5)

(5) Excess ^{15}N (g)= ΔMF x Tissue DW (g) x Tissue N%/100

Chlorophyll measurements: Leaf chlorophyll content was determined using the method developed by Hiscox et al. (Hiscox and Israelstam, 1979). Chlorophyll was extracted from 100mg of fresh leaf tissue from six plants into 20mL DMSO, mixed for on a rotary shaker for 30 mins and then placed at 4°C overnight. Chlorophyll measurements were taken at 645 and 663 nm (spectrophotometer Jenway model 7315, Staffordshire, UK).

Carbon assimilation measurements: An LI-6800 portable photosynthesis infrared gas analyzer system (LI-COR) equipped with a multiphase flash fluorimeter was used to assess physiological differences for photosynthetic parameters between transgenic and WT wheat plants. Measurements were taken on the fourth leaf of plants grown on TS5 low fertility soil (Bourne Amenity, Kent, UK). Ammonium nitrate or K_2PO_4 was then added to reach a final concentration in the pots equivalent to field fertilizer application of 70 kg N/ha for low N or 50 kg P/ha for Phosphate deficiency. Plants were grown in a climate-controlled chamber with supplemented light (250 $\mu mol.m^{-2}/s^{-1}$) for a 16hr day and 20°C/15°C day night temperatures for wheat. All measurements were also normalized for the amount of area of the measuring disk. Measurements were carried out on consecutive days between 1 and 8 h post dawn, measuring three plants total selected at random from each treatment per day.

Results

Growth on low P

To understand if the lack of a response of plants expressing *TaPSTOL* was due to some other mitigating factor other than OsPSTOL wheat plants were transformed with *OsPSTOL* driven by the OsActin promoter as described previously for *TaPSTOL* (Milner

10.3389/fpls.2023.1098175

et al., 2018). Three highly expressing *OsPSTOL* wheat transgenic lines were compared to the previously created *TaPSTOL* overexpressing line (OE-1), and WT Fielder for their ability to improve growth under low P conditions (Milner et al., 2018). As seen in Figure 1, the three transgenic wheat lines expressing *OsPSTOL* showed increased biomass and increased yield compared to either TaOE-1 or WT wheat plants when grown under low P conditions (p val 0). When compared to a null segregant, lines expressing *OsPSTOL* but not *TaPSTOL* showed increased biomass and yields when grown on low P soil (Figure 1). This includes increased yields of 29 to 47% compared with the null segregant. The yield increase is most likely due to higher biomass production leading to higher seed set as the number of seeds per plant was significantly higher in wheat lines expressing *OsPSTOL* (Figure 1C). There was a significant difference found in yields between TaOE-1 and WT wheat lines in their yield on low P grown plants, but above ground biomass produced per plant was not significantly different, similar to previous reports (Milner et al., 2018). Similar to previous reports not significant differences were seen in either the root or shoot P concentration relative to WT wheat plants (Suppl. Figure 1) (Pariasca-Tanaka et al., 2009).

Growth on low N

To determine if expression of *OsPSTOL* can lead to increased yield under other nutrient limiting conditions such a low N, the three transgenic wheat lines were grown under three N levels to study the transgenes effect on growth. The three levels of N were equivalent to 70, 140 and 210 kg/ha N levels in soil. As shown with growth in low P growth conditions, increases in both biomass and yield were seen in plants expressing *OsPSTOL*, but not *TaPSTOL* (Figure 2). This difference is mainly driven by growth under the higher N levels as no significant differences were seen in OsOE-1 or OsOE-2, either in above ground biomass or per plant yield at the lowest N level (p vals, 0.07 and 0.33). At higher N levels (140 and 210) significant differences were seen in OE-2 and OE-3 for both traits. As seen previously with growth on low P, the gains in yield were mainly driven by increased biomass leading to increased seed set and consequently higher yields.

N levels in the grain and leaf tissue were measured by DUMAS to determine whether many of the same phenotypes of overexpression of *OsPSTOL* were seen under low N as when grown under low P conditions. No significant differences were seen in the straw N

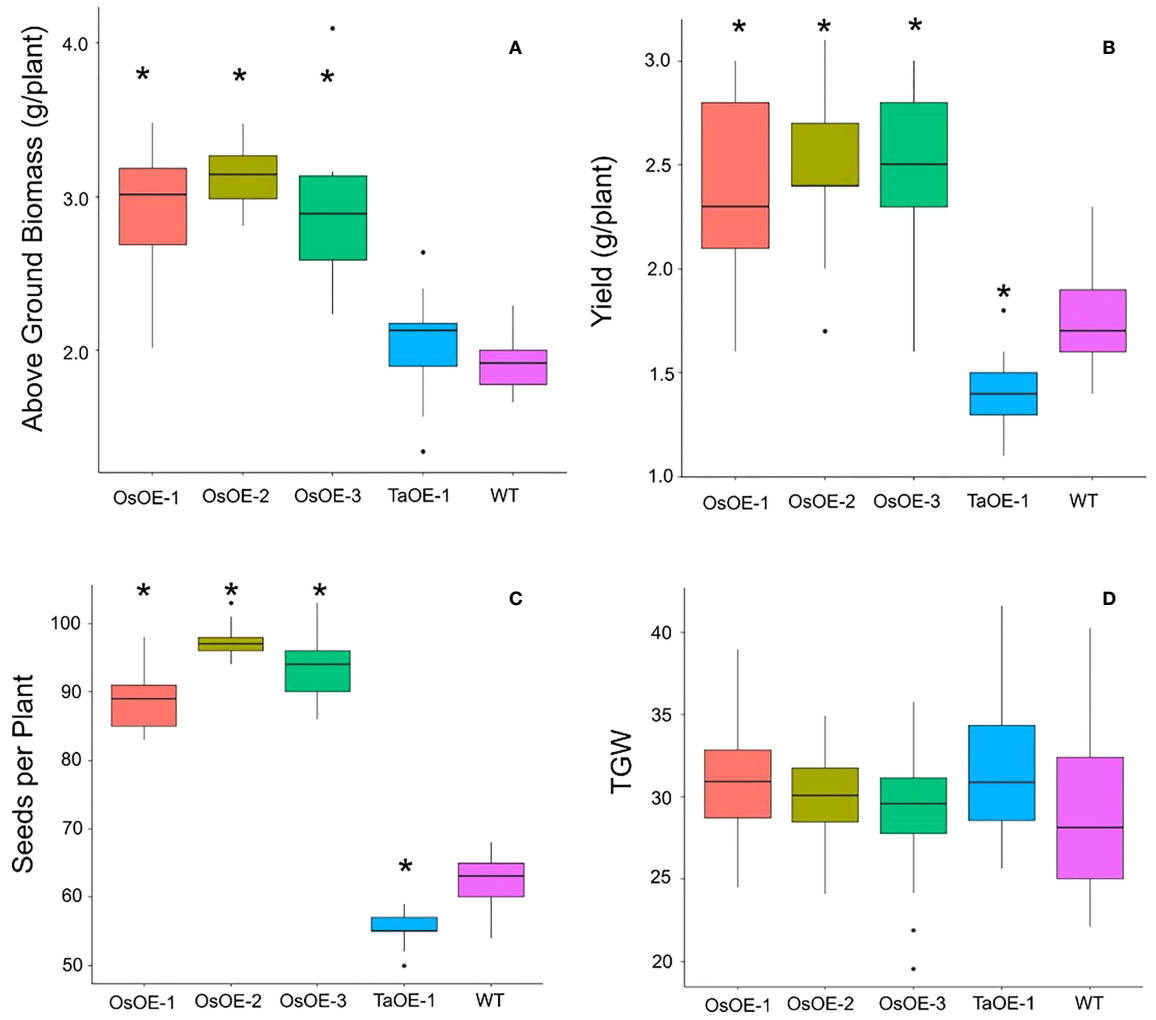

FIGURE 1
Agronomic traits of transgenic wheat plants expressing either OsPSTOL or TaPSTOL grown under low P conditions. **(A)** Above ground biomass **(B)** yield per plant **(C)** seeds per plant **(D)** thousand grain weight (TGW). A star indicates a significant difference (p val <0.05) between an overexpression line and WT.

10.3389/fpls.2023.1098175

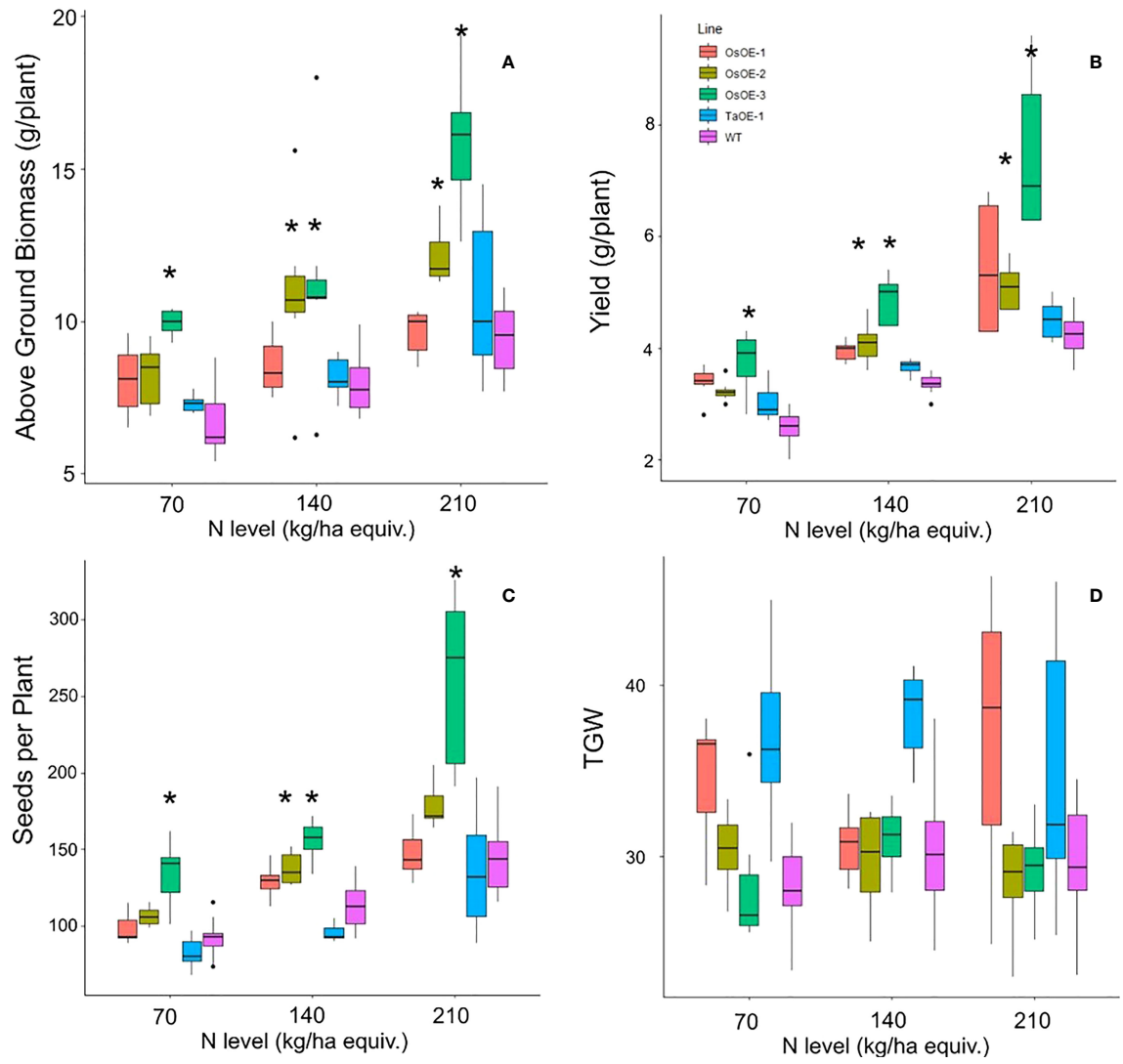

FIGURE 2
Agronomics of Os and TaPSTOL lines grown under a range of N levels. **(A)** Above ground biomass **(B)** Yield per plant **(C)** seeds per plant **(D)** Thousand Grain Weight (TGW). A star indicates a significant difference between an overexpression line and WT (pval < 0.05).

levels for any of the OsOE lines or TaOE line compared to WT (Figure 3). In the grain a significant difference in N content could be seen with significant differences in N concentrations for two of three OsPSTOL overexpression lines, OsOE-1 and OsOE-3, with OsOE-2 was just outside the 0.05 cutoff for significance relative to WT (p vals 0.03, 0.0005, 0.07). No significant difference was observed in N content of the TaOE-1 lines relative to WT wheat in the grain under any N level tested (p val. 0.31). Only OsOE-3 had significantly more N in the grain under 210 kg/ha treatments (p val 0.02) and no other direct comparison between a line at the same treatment was significantly different.

To understand if the N deficiency increased transcript levels of *OsPSTOL* or if transcript levels are higher only in response to low P, we tested expression of both *OsPSTOL* in the rice variety Kasalth by qPCR and *TaPSTOL* expression in Fielder. As seen in Figure 4, *OsPSTOL* can be activated by low N growth conditions although this change in transcript level is lower than that of low P conditions (Figure 4A). But both low N and low P growth conditions significantly increased *OsPSTOL* expression in the roots of Kasalath rice plants. *TaPSTOL* expression was also measured in Roots of wheat cv. Fielder *via* qPCR and no change in transcript levels could be seen in response to N level relative to replete, although low P did significantly increase *TaPSTOL* expression (Figure 4B).

LICOR

To understand how *OsPSTOL* activates enhanced biomass we measured the rate at which plants were able to fix carbon under low P or low N conditions. When measuring C assimilation rates under low N and low P no significant differences could be seen the levels of C being fixed under the given growth conditions or replete conditions (Figure 5A). This was further supported by the levels of chlorophyll in the leaves of the treated plants as again no significant differences were seen between lines under each condition tested (Figure 5B).

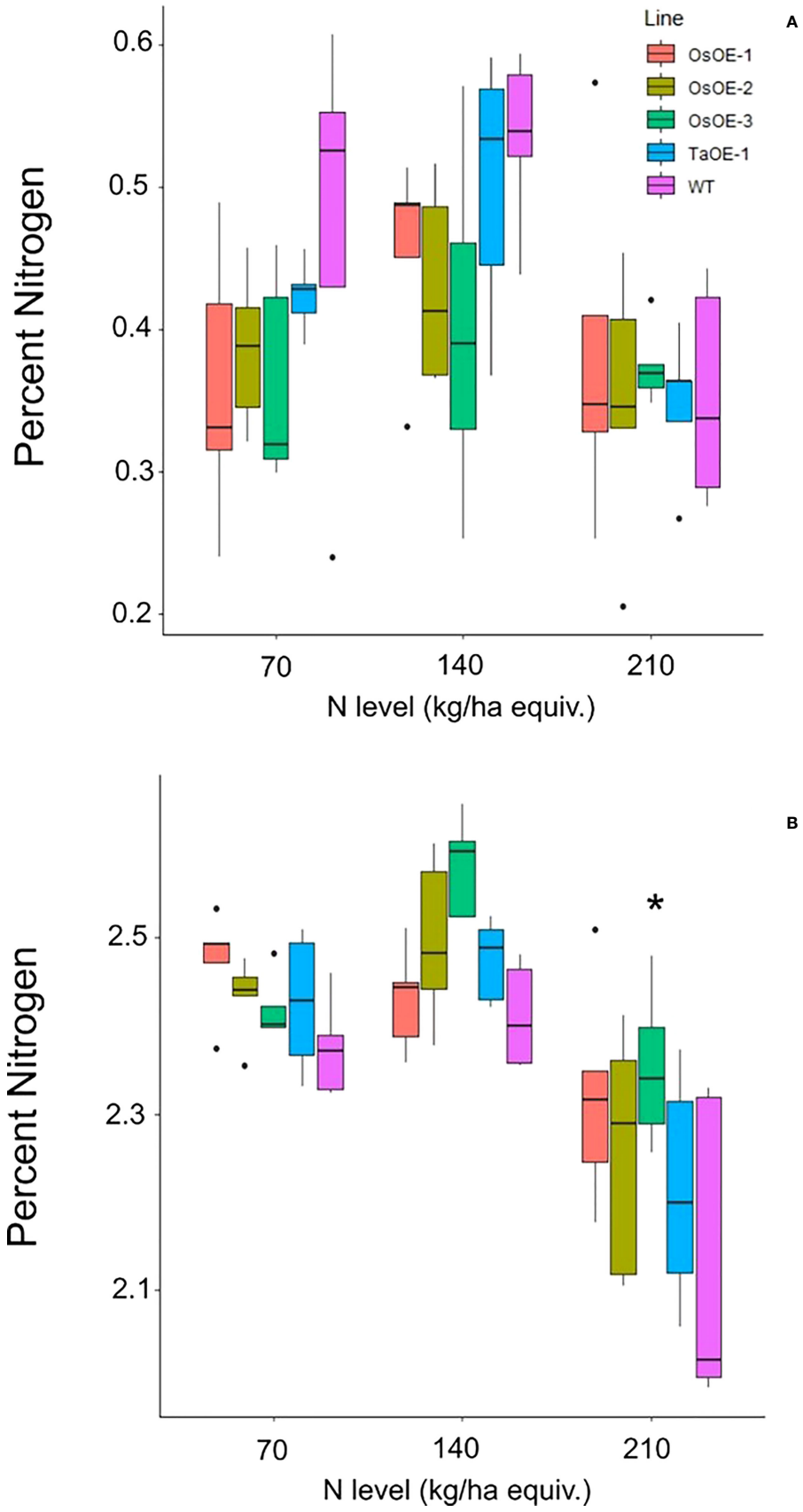

FIGURE 3
N content of Os and TaPSTOL lines grown under a range of N levels. **(A)** Percent nitrogen in the flag leaf **(B)** Percent nitrogen in the grain. A star indicates a significant difference between an overexpression line and WT (pval < 0.05).

10.3389/fpls.2023.1098175

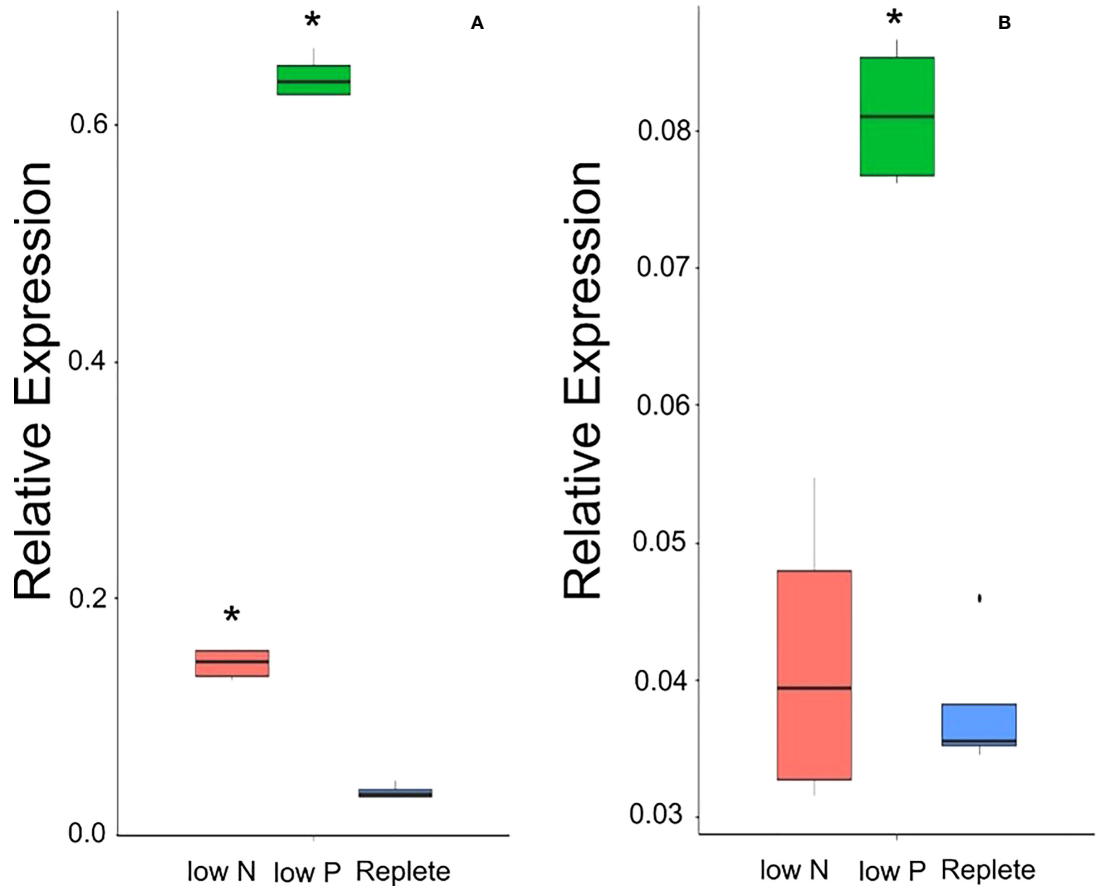

FIGURE 4
Transcript levels of OsPSTOL or TaPSTOL in the roots under different nutrient levels in rice and wheat. Expression values shown are PSTOL transcript levels relative to transcript levels of *OsUbi* for rice **(A)** and *TaUbi* for wheat **(B)** plants grown under low nitrogen (low N), low phosphate (low P) and replete nutrient levels in hydroponic solution. Data shown as the mean values (central line), lower and upper quartiles (box), minimum and maximum values (whiskers), and outliers as individual points. The statistical analysis was performed with ANOVA and *post hoc* Tukey test, * correspond to significant differences between transcript levels of either line under either treatment ($p < 0.05$).

N Uptake and Expression of N related genes

To further understand how expression of *OsPSTOL* in wheat is allowing for increased growth under a range of N conditions we studied direct uptake of N in the form of ammonium nitrate, with each N atom labeled as ^{15}N. When comparing rates of uptake in the roots of N deprived plants a significant difference in the amount of N being taken up per g of tissue was observed (Figure 6). This was found only in plants overexpressing *OsPSTOL* as no significant differences in uptake were seen in the roots of plants overexpressing *TaPSTOL* relative to WT roots (p val 0.13).

The expression of four genes known to be differentially regulated under low N conditions in wheat were selected to test the N-responsiveness at the transcript level of the OsOE line (OE-3), TaOE-1 relative to WT (Figure 7) (Buchner and Hawkesford, 2014). The genes selected encode the high and low-affinity N uptake transporters (*TaNRT2.1* and *TaNRT1*), an N transporter involved in N translocation through the plant (*TaNPF7.1*), and glutamate dehydrogenase (*TaGDH2*), an enzyme involved in N remobilization in response to limiting carbon. Expression of a number of the genes were differentially expressed in the transgenic lines relative to WT Fielder. Measurements of *TaGDH2* transcript levels showed no significant differences in the roots of OsOE-3, TaOE-1 or WT. There was a significant increase in *TaGDH2* transcript levels seen in shoots of OsOE-3 compared to WT (pval <0.001). For *TaNRT1*, transcripts in roots of OsOE-3 showed significantly lower expression under replete conditions (p val < 0.001). Both OsOE3-3 and TaOE-1 showed higher transcript levels of *TaNRT1* in the shoots under both low N and replete conditions (pval <0.001). Analysis of *TaNPF7.1* transcript levels in the roots showed similar expression to that of *TaNRT1* with only OsOE-3 showing significantly lower expression than WT (p val <0.001). In the shoots *TaNPF7.1* transcript levels were higher under low N growth conditions in OsOE-3 and TaOE-1 relative to WT, but no difference in expression was seen in plants grown under replete N levels (p val <0.001). The high affinity uptake transporter *TaNRT2.1* showed significantly higher transcript levels in the roots of both OsOE-3 and TaOE-1 under both low N and replete growth conditions (p val <0.01). No significant difference in the transcript levels of *TaNRT2.1* was seen

10.3389/fpls.2023.1098175

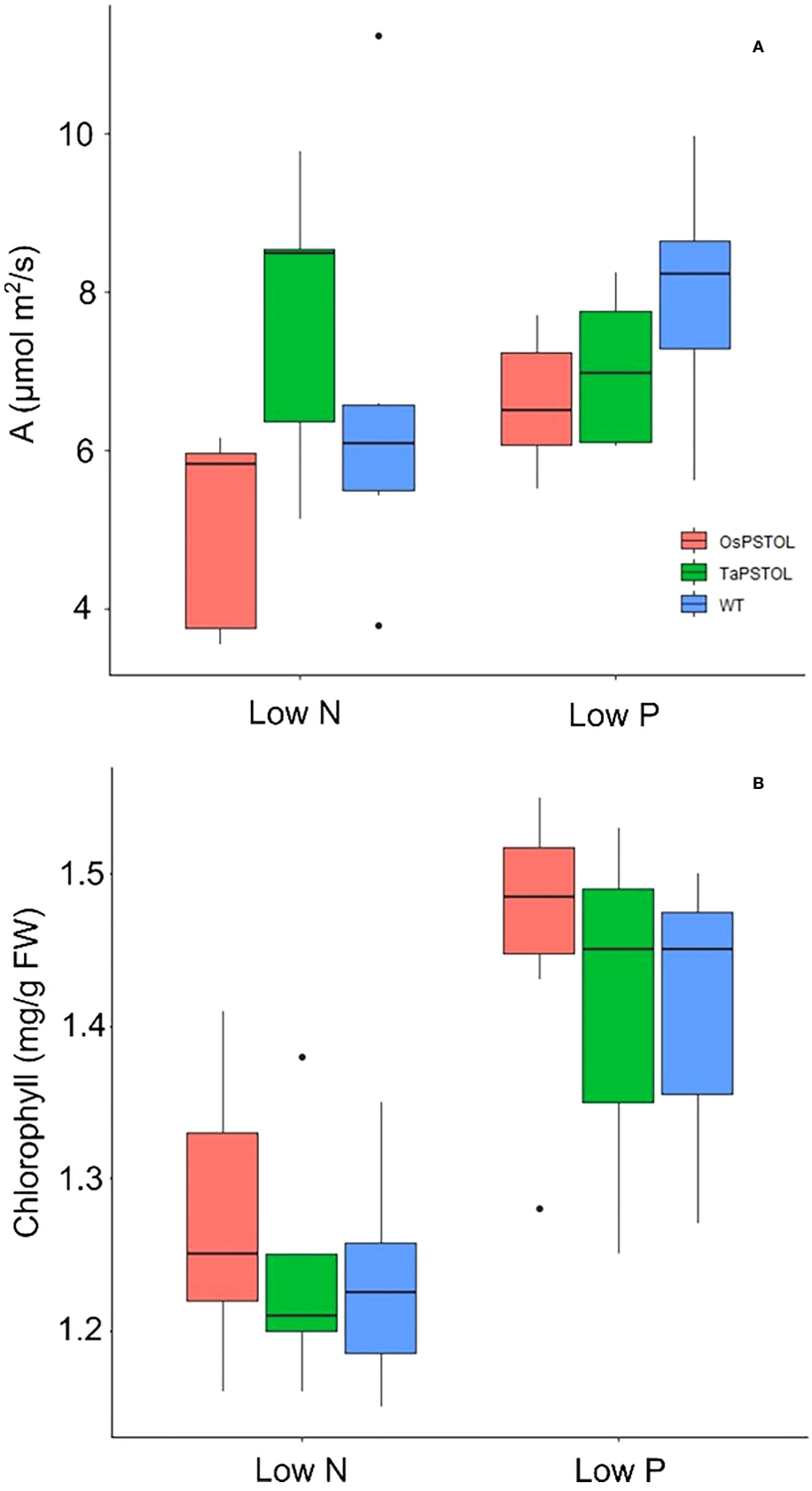

FIGURE 5
Spot measurements of C assimilation and chlorophyll content in plants overexpressing either OsPSTOL or TaPSTOLOE-1 relative to WT grown under low nitrogen (low N) or low phosphate (low P) conditions. **(A)** Spot measurements of C assimilation grown in growth chamber conditions which include a light intensity of 250 µmol m^2 /s and CO_2 level of 400 ppm. **(B)** Chlorophyll content of plants grown under low nitrogen (low N) or low phosphate (low P) conditions.

10.3389/fpls.2023.1098175

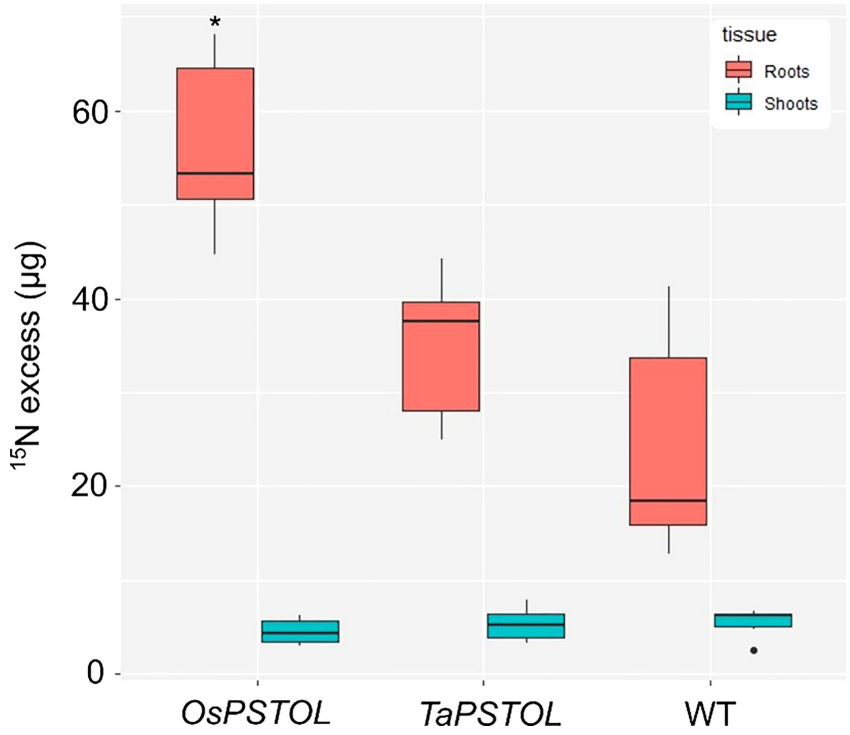

FIGURE 6
Uptake of ^{15}N in the roots and shoots of overexpression lines expressing either *OsPSTOL* (OsOE-3) or *TaPSTOL* (TaOE-1) relative to WT. Data are shown as mean values (central line), lower and upper quartiles (box), minimum and maximum values (whiskers), and outliers as individual points. The statistical analysis was performed with ANOVA and *post hoc* Tukey test. Asterisks indicate a significant difference ($p < 0.05$) between WT and an OE line in the same tissue.

in the shoots of either overexpression line relative to WT under either N growth conditions.

Discussion

To be able to translate our understanding of how plants tolerate various abiotic conditions it is important to understand if orthologous genes are present in various species or if the gene is part of a wider pathway. In this work we set out to understand why differences in the expression of *TaPSTOL* relative to *OsPSTOL* were seen (Gamuyao et al., 2012; Milner et al., 2018). To do this we created new transgenic material to make direct comparisons in a consistent genetic background and observe the transgene's effects. From this we have learned that OsPSTOL can activate a conserved pathway in other cereal species and increase biomass production and ultimately yield under P limiting growth conditions (Figure 1). This suggests that wheat lacks a fully functional *PSTOL* type gene and that *TaPSTOL* is not the functional ortholog of OsPSTOL in wheat even though it is 92.7% similar (Milner et al., 2018). This is not that surprising as many different rice varieties including both reference varieties of japonica and indica also do not contain a functional *OsPSTOL* gene (Vigueira et al., 2016). The presence of a *PSTOL* type gene may have been selected in rice for under conditions for which wheat is not widely grown or has lost, as further mutations the near the N terminus of TaPSTOL locus reduced the N terminus of the protein. Or perhaps it was a chance event in rice and has never been present in wheat. This would fit with why no other direct ortholog of PSTOL has been found in any other species in the past decade (Milner et al., 2018; Bernardino et al., 2019).

It was found however that the benefits of overexpressing *OsPSTOL* in wheat conferred increased yields under a range of N conditions. This includes under N levels approximately 1/3 that of what current best practices in the UK for some transgenic lines (Figure 2). This mechanism of action seems to be by increasing biomass which leads to greater seed set. This was seen under both low P growth conditions as well as low N growth conditions (Figures 1 and 2). To further understand how *OsPSTOL* expression conferred tolerance to low N measurements of uptake, tissue concentrations and expression of N related genes were undertaken. From this it was found that *OsPSTOL* expression increased N uptake from the soil but did not change overall levels of N in the above ground tissues including the grain. This increased uptake of N was seen *via* differences in N regulated genes such as the high affinity uptake transporter *NRT2.1* the low affinity and N sensor *NRT1* and genes involved in N translocation *NPF7.1* (Figure 7) (Ho et al., 2009; Buchner and Hawkesford, 2014). This direct measurement of increased N uptake in plant overexpressing *OsPSTOL* is the first direct evidence that *OsPSTOL* increases uptake of nutrients to help aid growth.

This increased uptake did not change other physiological parameters including carbon assimilation or increased chlorophyll content suggesting that *OsPSTOL* helps plants take up or acquire more nutrients and does not alter perception of those nutrients

10.3389/fpls.2023.1098175

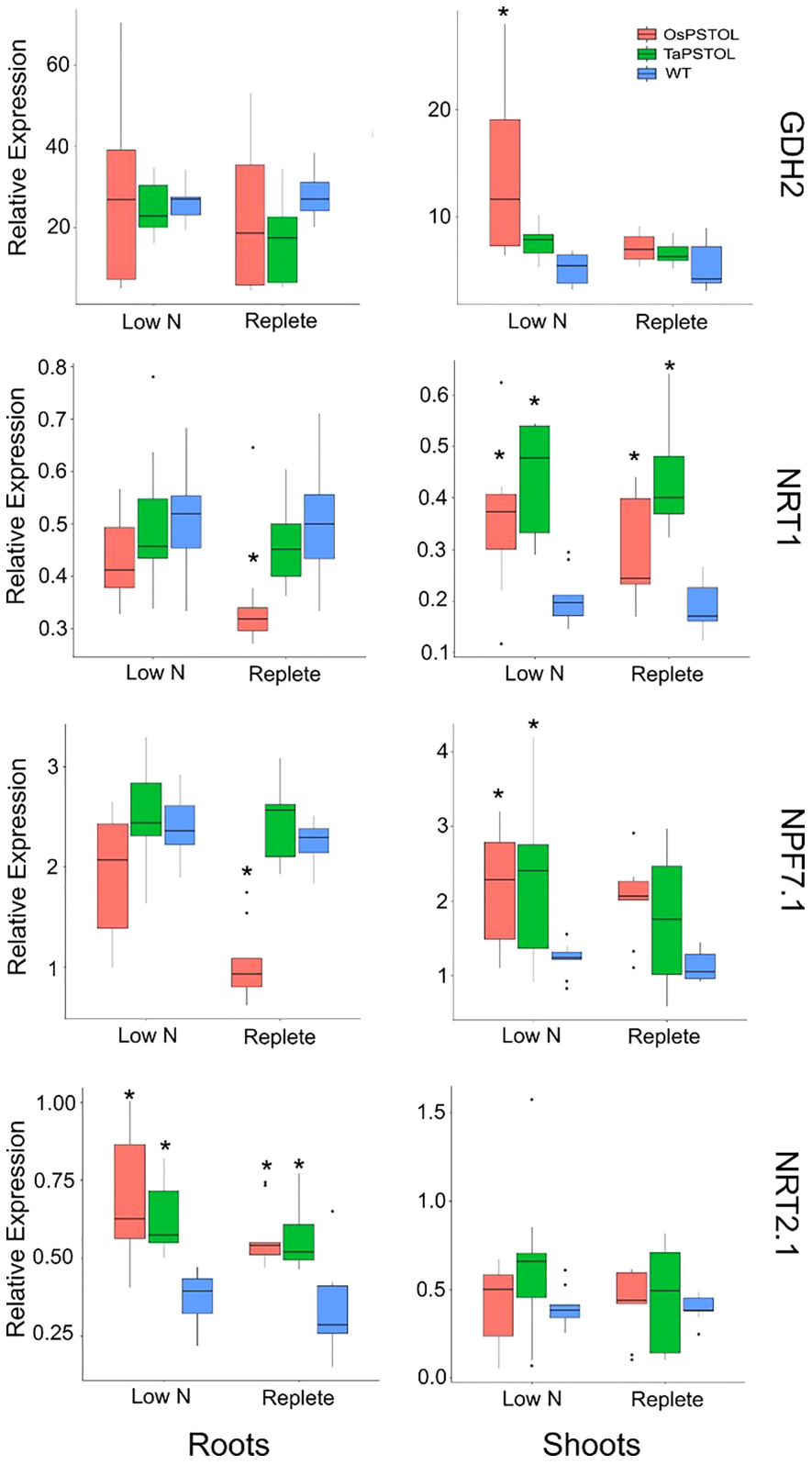

FIGURE 7
Transcript levels for N regulated genes *TaNRT1*, *TaNRT2.1*, *TaNPF7.1*, and *TaGDH2* in transgenic wheat plants expressing either *OsPSTOL* (OsOE-3) or *TaPSTOL* (TaOE-1). Expression values shown are relative to the expression of *TaUbi* under in wheat plants grown under low nitrogen (low N) and replete nitrogen (replete) levels in hydroponic solution. Root specific expression is in the panels on the left and shoots specific expression in panels on the right for each gene. Data shown as the mean values (central line), lower and upper quartiles (box), minimum and maximum values (whiskers), and outliers as individual points. The statistical analysis was performed with ANOVA and *post hoc* Tukey test, * correspond to significant differences between transcript levels of either line under either treatment ($p < 0.05$).

unlike more recent reports involving altered brassinosteroid genes (Milner et al., 2022). We also show that *OsPSTOL* transcript levels can be seen under low N levels further supporting a role for *OsPSTOL* in nutrient uptake rather than just P directly. However this increase in transcript levels might be due to the cross talk of N and P in plants and not a direct activation of *OsPSTOL* by a N sensing transcription factor per se (Hong et al., 2012; Borah et al., 2018; Medici et al., 2019; Zhu et al., 2021).

Overall, it appears that *OsPSTOL* is able to aid in multiple nutrient deficiencies in different plant species by helping acquire the nutrients which are limiting growth. It is tempting to wonder if a combination of genes such as the recently cloned *OsNRT2.3b* or *SPDT* in combination with *OsPSTOL* could dramatically increase grain production under lower inputs (Fan et al., 2016; Yamaji et al., 2016).

Data availability statement

The raw data supporting the conclusions of this article will be made available by the authors, without undue reservation.

Author contributions

MM and EW conceived the research. MM, MC and SB. performed experiments and MM wrote the manuscript and it was edited by EW. All authors contributed to the article and approved the submitted version.

Funding

This work was supported by the UK Biotechnology and Biological Sciences Research Council grant BB/N013441/1 and BB/N013484/1.

Conflict of interest

The authors declare that the research was conducted in the absence of any commercial or financial relationships that could be construed as a potential conflict of interest.

Publisher's note

Supplementary material

The Supplementary Material for this article can be found online at: https://www.frontiersin.org/articles/10.3389/fpls.2023.1098175/full#supplementary-material

References

Azevedo, G. C., Cheavegatti-Gianotto, A., Negri, B. F., Hufnagel, B., da Costa E Silva, L., Magalhaes, J. V., et al. (2015). Multiple interval QTL mapping and searching for PSTOL1 homologs associated with root morphology, biomass accumulation and phosphorus content in maize seedlings under low-p. *BMC Plant Biol.* 15, 172. doi: 10.1186/s12870-015-0561-y

Bernardino, K. C., Pastina, M. M., Menezes, C. B., De Sousa, S. M., MacIel, L. S., Geraldo Carvalho, G. C., et al. (2019). The genetic architecture of phosphorus efficiency in sorghum involves pleiotropic QTL for root morphology and grain yield under low phosphorus availability in the soil. *BMC Plant Biol.* 19, 87. doi: 10.1186/s12870-019-1689-y

Borah, P., Das, A., Milner, M. J., Ali, A., Bentley, A. R., and Pandey, R. (2018). Long non-coding rnas as endogenous target mimics and exploration of their role in low nutrient stress tolerance in plants. *Genes (Basel)* 9, 1. doi: 10.3390/genes9090459

Buchner, P., and Hawkesford, M. J. (2014). Complex phylogeny and gene expression patterns of members of the NITRATE TRANSPORTER 1/PEPTIDE TRANSPORTER family (NPF) in wheat. *J. Exp. Bot.* 65, 5697–5710. doi: 10.1093/jxb/eru231

Chin, J. H., Gamuyao, R., Dalid, C., Bustamam, M., Prasetiyono, J., Moeljopawiro, S., et al. (2011). Developing rice with high yield under phosphorus deficiency: Pup1 sequence to application. *Plant Physiol.* 156, 1202–1216. doi: 10.1104/pp.111.175471

Fan, X., Tang, Z., Tan, Y., Zhang, Y., Luo, B., Yang, M., et al. (2016). Overexpression of a pH-sensitive nitrate transporter in rice increases crop yields. *Proc. Natl. Acad. Sci. U.S.A.* 113, 7118–7123. doi: 10.1073/pnas.1525184113

Gamuyao, R., Chin, J. H., Pariasca-Tanaka, J., Pesaresi, P., Catausan, S., Dalid, C., et al. (2012). The protein kinase Pstol1 from traditional rice confers tolerance of phosphorus deficiency. *Nature* 488, 535–539. doi: 10.1038/nature11346

Heuer, S., Lu, X., Chin, J. H., Tanaka, J. P., Kanamori, H., Matsumoto, T., et al. (2009). Comparative sequence analyses of the major quantitative trait locus p hosphorus up take 1 (Pup1) reveal a complex genetic structure. *Plant Biotechnol. J.* 7, 456–471. doi: 10.1111/j.1467-7652.2009.00415.x

Hiscox, J. D., and Israelstam, G. F. (1979). A method for the extraction of chlorophyll from leaf tissue without maceration. *Can. J. Bot.* 57, 1332–1334. doi: 10.1139/b79-163

Ho, C. H., Lin, S. H., Hu, H. C., and Tsay, Y. F. (2009). CHL1 functions as a nitrate sensor in plants. *Cell* 138, 1184–1194. doi: 10.1016/J.CELL.2009.07.004

Hong, Y. F., Ho, T. H. D., Wu, C. F., Ho, S. L., Yeh, R. H., Lu, C. A., et al. (2012). Convergent starvation signals and hormone crosstalk in regulating nutrient mobilization upon germination in cereals. *Plant Cell* 24, 2857–2873. doi: 10.1105/TPC.112.097741

Hufnagel, B., de Sousa, S. M., Assis, L., Guimaraes, C. T., Leiser, W., Azevedo, G. C., et al. (2014). Duplicate and conquer: Multiple homologs of PHOSPHORUS-STARVATION TOLERANCE1 enhance phosphorus acquisition and sorghum performance on low-phosphorus soils. *Plant Physiol.* 166, 659–677. doi: 10.1104/pp.114.243949

Magalhaes, J. V., Liu, J., Guimarães, C. T., Lana, U. G. P., Alves, V. M. C., Wang, Y. H., et al. (2007). A gene in the multidrug and toxic compound extrusion (MATE) family confers aluminum tolerance in sorghum. *Nat. Genet.* 39, 1156–1161. doi: 10.1038/ng2074

Magnavaca, R., Gardner, C. O., and Clark, R. B. (1987). "Evaluation of inbred maize lines for aluminum tolerance in nutrient solution," in *Genetic aspects of plant mineral nutrition* (Dordrecht: Springer Netherlands), 255–265. doi: 10.1007/978-94-009-3581-5_23

Marschner, H. (1995). *Mineral nutrition of higher plants. 2nd edition* 889 pp. (London: Academic Press).

Medici, A., Szponarski, W., Dangeville, P., Safi, A., Dissanayake, I. M., Saenchai, C., et al. (2019). Identification of molecular integrators shows that nitrogen actively controls the phosphate starvation response in plants. *Plant Cell* 31, 1171–1184. doi: 10.1105/TPC.18.00656

Milner, M. J., Howells, R. M., Craze, M., Bowden, S., Graham, N., and Wallington, E. J. (2018). A PSTOL-like gene, TaPSTOL, controls a number of agronomically important traits in wheat. *BMC Plant Biol.* 18, 115. doi: 10.1186/s12870-018-1331-4

Milner, M. J., Swarbreck, S. M., Craze, M., Bowden, S., Griffiths, H., Bentley, A. R., et al. (2022). Over-expression of TaDWF4 increases wheat productivity under low and sufficient nitrogen through enhanced carbon assimilation. *Commun. Biol.* 5 (1), 1–12. doi: 10.1038/s42003-022-03139-9

Pariasca-Tanaka, J., Satoh, K., Rose, T., Mauleon, R., and Wissuwa, M. (2009). Stress response versus stress tolerance: A transcriptome analysis of two rice lines contrasting in tolerance to phosphorus deficiency. *Rice* 2, 167–185. doi: 10.1007/S12284-009-9032-0/FIGURES/3

Vigueira, C. C., Small, L. L., and Olsen, K. M. (2016). Long-term balancing selection at the phosphorus starvation tolerance 1 (PSTOL1) locus in wild, domesticated and weedy rice (Oryza). *BMC Plant Biol.* 16, 101. doi: 10.1186/s12870-016-0783-7

Wissuwa, M., Wegner, J., Ae, N., and Yano, M. (2002). Substitution mapping of Pup1 : a major QTL increasing phosphorus uptake of rice from a phosphorus-deficient soil. *TAG Theor. Appl. Genet.* 105, 890–897. doi: 10.1007/s00122-002-1051-9

Xu, K., Xu, X., Fukao, T., Canlas, P., Maghirang-Rodriguez, R., Heuer, S., et al. (2006). Sub1A is an ethylene-response-factor-like gene that confers submergence tolerance to rice. *Nature* 442, 705–708. doi: 10.1038/nature04920

Yamaji, N., Takemoto, Y., Miyaji, T., Mitani-Ueno, N., Yoshida, K. T., and Ma, J. F. (2016). Reducing phosphorus accumulation in rice grains with an impaired transporter in the node. *Nature* 541 (7635), 92–95. doi: 10.1038/nature20610

Zhu, Z., Li, D., Cong, L., and Lu, X. (2021). Identification of microRNAs involved in crosstalk between nitrogen, phosphorus and potassium under multiple nutrient deficiency in sorghum. *Crop J.* 9, 465–475. doi: 10.1016/J.CJ.2020.07.005

frontiers | Frontiers in Plant Science

TYPE Review
PUBLISHED 21 February 2023
DOI 10.3389/fpls.2023.1074839

OPEN ACCESS

EDITED BY
Mamoru Okamoto,
University of Adelaide, Australia

REVIEWED BY
Hongmei Cai,
Huazhong Agricultural University, China
Mingyong Zhang,
South China Botanical Garden (CAS), China

*CORRESPONDENCE
Haobao Liu
liuhaobao@caas.cn
Qian Wang
wangqian01@caas.cn

†PRESENT ADDRESS
Oluwaseun Olayemi Aluko,
State Key Laboratory of Cotton Biology,
Key Laboratory of Plant Stress Biology,
School of Life Sciences, Henan University,
Kaifeng, China

SPECIALTY SECTION
This article was submitted to Plant Physiology, a section of the journal Frontiers in Plant Science

RECEIVED 20 October 2022
ACCEPTED 16 January 2023
PUBLISHED 21 February 2023

CITATION
Aluko OO, Kant S, Adedire OM, Li C, Yuan G, Liu H and Wang Q (2023) Unlocking the potentials of nitrate transporters at improving plant nitrogen use efficiency.
Front. Plant Sci. 14:1074839.
doi: 10.3389/fpls.2023.1074839

Unlocking the potentials of nitrate transporters at improving plant nitrogen use efficiency

Oluwaseun Olayemi Aluko[1,2†], Surya Kant[3,4], Oluwafemi Michael Adedire[5], Chuanzong Li[1,2], Guang Yuan[1,2], Haobao Liu[1*] and Qian Wang[1*]

[1]Tobacco Research Institute of Chinese Academy of Agricultural Sciences, Qingdao, China, [2]Graduate School of Chinese Academy of Agricultural Sciences, Beijing, China, [3]Agriculture Victoria, Grains Innovation Park, Horsham, VIC, Australia, [4]School of Applied Systems Biology, La Trobe University, Bundoora, VIC, Australia, [5]School of Agriculture, Federal College of Agriculture, Ibadan, Nigeria

Nitrate (NO_3^-) transporters have been identified as the primary targets involved in plant nitrogen (N) uptake, transport, assimilation, and remobilization, all of which are key determinants of nitrogen use efficiency (NUE). However, less attention has been directed toward the influence of plant nutrients and environmental cues on the expression and activities of NO_3^- transporters. To better understand how these transporters function in improving plant NUE, this review critically examined the roles of NO_3^- transporters in N uptake, transport, and distribution processes. It also described their influence on crop productivity and NUE, especially when co-expressed with other transcription factors, and discussed these transporters' functional roles in helping plants cope with adverse environmental conditions. We equally established the possible impacts of NO_3^- transporters on the uptake and utilization efficiency of other plant nutrients while suggesting possible strategic approaches to improving NUE in plants. Understanding the specificity of these determinants is crucial to achieving better N utilization efficiency in crops within a given environment.

KEYWORDS

nitrate transporters, nitrate uptake, nitrate transport and signaling, nitrate remobilization, nitrogen use efficiency, environmental stress

1 Introduction

Nitrogen (N) is an essential element required for plant growth and overall yield; hence, the demand and use of N-based chemical fertilizers have consistently increased over the years. Approximately 60-70% of the applied N fertilizers are lost to the environment (Mohanty et al., 2020), causing severe environmental havoc such as pollution, global warming, biodiversity loss, and major plant physiological disorders. Since the increasing rate of N application is becoming increasingly alarming, minimizing fertilizer use while maintaining a high crop yield would be imperative. Thus, improving plants' nitrogen use efficiency (NUE) is one of the inherent ways of

overcoming these crises associated with crop production. Efficient N utilization is a critical factor in crop yield improvement, and research has shown that over 1.0 billion US dollars might be saved with a one percent NUE increment (Kant et al., 2011a).

Crop NUE is the measure of seed yield, grain, or fruit corresponding to a unit of soil N supplied, depending on the individual species of plant. NUE can also be expressed in terms of N uptake efficiency (NUpE), N transport efficiency (NTE), N remobilization efficiency (NRE), and N utilization (assimilation) efficiency (NUtE) (Bharati and Mandal, 2019), all of which are key determinant factors of NUE in plants. N is made available to plants in organic and inorganic forms; nitrate (NO_3^-) and ammonium. Due to the mobility nature of NO_3^-, it gets easily leached; thus, its availability to plants becomes limiting (Jin et al., 2015). NO_3^- functions as a signaling molecule, inducing the expression of NO_3^--related genes involved in its uptake, transport, assimilation, vegetative and reproductive development. Plants take up NO_3^- from the root, assimilate NO_3^-, and subsequently transport it to the shoot, where it can be remobilized to sink organs (Iqbal et al., 2020). NO_3^- transporters are the main drivers involved in the uptake of NO_3^- to the remobilization stage.

Indeed, several studies have discussed the relationship between NO_3^- uptake transport activities in plants while addressing the mechanisms involved in transport, sensing, and signaling processes (Fan et al., 2017; Zuluaga and Sonnante, 2019; Vidal et al., 2020). Therefore, optimizing the activities of NO_3^- transporters is a prerequisite for plants to utilize N supplies. Some studies have elucidated the functional roles of these NO_3^- transporters in plant NUE improvement. However, less is known about the influence of essential nutrients and environmental cues on the expression and activities of NO_3^- transporters. To better understand the extent to which these transporters can function in improving plant NUE, an illustration of their response to changes in plant environmental cues, including salinity, pathogenic and drought stress, and contamination from heavy metals, becomes expedient. Even if these conditions are being optimized, it is crucial to explore the possible aftermath effect of these NO_3^- transporters on the efficiency of other plant nutrient elements and related factors. These necessities ignite a few questions: 1) Does stress affect NO_3^- transporter activities directly or indirectly? and 2) Do the activities of these NO_3^- transporters exert a positive or negative effect on the uptake of other nutrients? To resolve these issues, this review critically summarized the roles of NO_3^- transporters in N uptake, transport, and distribution processes and their functions in crop productivity and NUE, especially when coexpressed with other transcription factors. This review focuses on the functional roles of these nitrate transporters in assisting plants in adverse environmental conditions. We also discussed the impact of these NO_3^- transporters on the uptake and utilization efficiency of other plant nutrients while describing possible strategic approaches to improving NUE in plants. The contribution of nitrate transporters in nitrate and auxin crosstalk for root growth and NUE is also reviewed. Understanding the specificity of all these factors is crucial for better N utilization efficiency of crops.

2 Nitrate uptake and transport systems

Most agricultural fields, especially, those used for commercial crop production, are NO_3^- deficient with significant spatiotemporal fluctuations, inhibiting N utilization (Kant, 2018). Plants have evolved two major NO_3^- uptake mechanisms to survive. The first is the low-affinity transport system (LATS), which facilitates nitrate uptake under high soil-N (millimolar concentration; > 0.5 mM), while the other is the high-affinity transport system (HATS), which drives nitrate under insufficient soil-N (micromolar range) (Léran et al., 2014; Iqbal et al., 2020; Raddatz et al., 2020). Four families of NO_3^- transporters have been widely known to participate in plant nitrate uptake and transport: nitrate transporter 1/or peptide transporter NPF (NRT1), nitrate transporter 2/nitrate-nitrite-porter NRT2/NNP, slow anion channel-associated homologs (SLAC/SLAH), and chloride channel (CLC) (Tsay et al., 1993; Bergsdorf et al., 2009; Maierhofer et al., 2014; Von Wittgenstein et al., 2014). Among them, NPF (NRT1) and NRT2 and homologs have been identified as the major channels actively involved in root nitrate uptake and long-distance transport between and within plant organs (Hsu and Tsay, 2013; Wang et al., 2021b). In this review, proteins or genes void of prefixes connote Arabidopsis plant species.

Phylogenetic studies revealed that the NPF family comprises 53 identified Arabidopsis genes, and over 130 genes exist in higher plants (Zhang et al., 2020). Generally, NPF transporter genes have low affinity for NO_3^-, except for Chlorate resistant 1/nitrate transporter 1 (*CHL1*/*NRT1.1*), also called *NPF6.3*, a dual-affinity nitrate transporter that operates as both a low- and high-affinity transporter (Liu and Tsay, 2003). The regulatory mechanism involved in the dual-affinity system enables the rapid switch between these two affinity modes. Under a low external supply of NO_3^-, *NPF6.3* (*CHL1*/*NRT1.1*) functions as a high-affinity NO_3^- transporter and is phosphorylated, whereas it becomes dephosphorylated under a high NO_3^- supply to perform a low-affinity transporter role (Liu and Tsay, 2003; Noguero et al., 2018). Thus, the affinity of the *NPF6.3* transporter for NO_3^- uptake depends on the phosphorylation state at the T101 residue, which is subject to the status of N in the medium *NPF6.3* (*CHL1*/*NRT1.1*) is expressed in various plant tissues, including younger leaves, flower buds, and roots, where it participates in root NO_3^- uptake and translocation (Noguero et al., 2018). In addition to *NPF6.3* (*CHL1*/*NRT1.1*), *NPF4.6* (*NRT1.2*) and *NPF2.7* (*NAXT1*) are the two putative NPF genes that coordinate NO_3^- influx and efflux in plant roots, respectively (Figure 1). *NPF4.6* (*NRT1.2*) is primarily expressed at the root tip where it takes up NO_3^- (Huang et al., 1999), whereas *NPF2.7* (*NAXT1*), is expressed in the root zone but in the cortex, performs NO_3^--efflux functions (Segonzac et al., 2007). A considerable amount of NRT1 family members have been identified in other crops, including wheat (*Triticum aestivum*) (Kumar et al., 2022), rice (*Oryza sativa*) (Yang et al., 2020), cucumber (*Cucumis sativus*) (Migocka et al., 2013), potato (*Solanum tuberosum*) (Zhang et al., 2021a), and apple (*Malus* × *domestica Borkh.*) (Wang et al., 2018b), with their unique expression at either the root or shoot of plants. The expression pattern of these transporters is a clear indication of their active involvement in uptake and long-distance NO_3^- transport.

Unlike the NRT1 family, NRT2 family members are high-affinity NO_3^- transporters (HATs). There are eight identified NRT2 family members, of which seven have been characterized (Von Wittgenstein et al., 2014). Four (*NRT2.1*, *NRT2.2*, *NRT2.4*, and *NRT2.5*) out of the seven characterized NRT2 transporters have been actively involved in the influx of NO_3^- into Arabidopsis root cells (O'Brien et al., 2016).

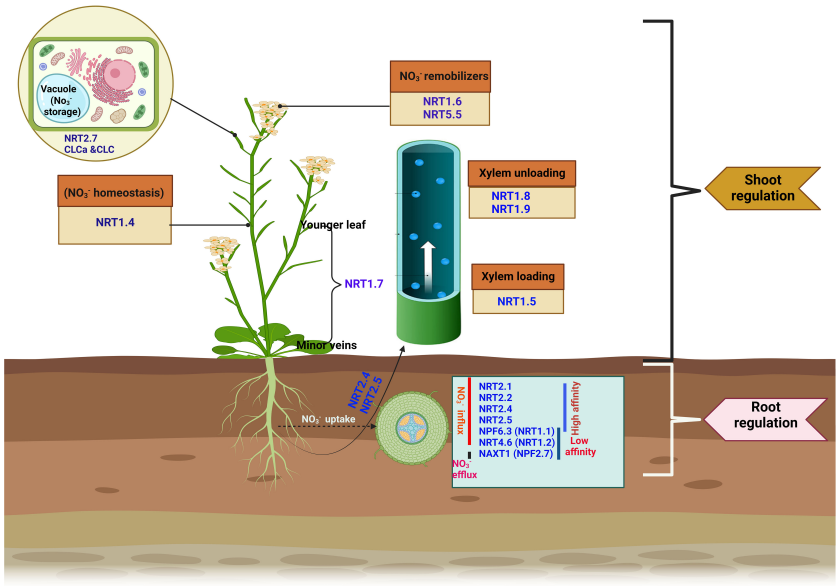

FIGURE 1
Key nitrate transporters involved in nitrate uptake, transport, and remobilization in plants. Nitrate transporters involved in NO_3^- acquisition from the root include *NRT2.1*, *NRT2.2*, *NPF4.6* (*NRT1.2*), *NRT2.4*, *NRT2.5*, and *NPF6.3* (*NRT1.1*). *NPF2.7* performs the NO_3^- efflux function. In addition to the uptake function, *NRT2.4* and *NRT2.5* facilitates root-to-shoot NO_3^- transport. *NRT1.5* is responsible for xylem loading, while *NRT1.8* and *NRT1.9* functions to unload NO_3^- from the xylem. *NRT1.4* regulates NO_3^- homeostasis, and the expression of *NRT1.7* in the phloem of the minor vein promotes nitrate remobilization from mature to younger leaves. At shoot, *NRT1.6* and *NPF5.5* act as a NO_3^- remobilizer, remobilizing NO_3^- in the embryo. *NRT2.7* enhances NO_3^- storage in the seed vacuole.

Detailed functions of these transporters in uptake of NO_3^- are presented in (Figure 1).

Nitrate transporters are the major channels mediating root-to-shoot NO_3^- transport. Transport is predominantly mediated by NRT1 and NRT2 transporters, such as *NPF7.3* (*NRT1.5*), *NPF7.2* (*NRT1.8*), *NPF2.3*, and *NPF2.9* (*NRT1.9*). *NPF7.3* (*NRT1.5*) is expressed in pericycle cells, where it facilitates xylem loading of NO_3^- (Figure 1). Knockout *nrt1.5* mutant plants had reduced amounts of NO_3^- translocated from the roots to the shoots. However, when *NRT1.5* was reduced in *nrt1.5*, no NO_3^- translocation defect was observed, suggesting the existence of another mechanism facilitating nitrate xylem loading (Lin et al., 2008). The low-affinity nitrate transporters *NRT1.8* and *NRT1.9* perform similar roles of unloading NO_3^- from the xylem (Figure 1), consequently reducing NO_3^- concentration within the xylem. Knockout mutants of such transporters *(NRT1.8* and *NRT 1.9)* exhibited increased amounts of NO_3^- in the xylem and, by implication, accelerated root-shoot transport of nitrate (Li et al., 2010; Wang and Tsay, 2011). In addition, the uptake and transport function of the NRT1 and NRT2 homologs have also been revealed in rice (*OsNRT1.1B* and *OsNRT2.3*, respectively) (Tang et al., 2012; Hu et al., 2015; Fan et al., 2017), and tomato, *LeNRT2.3* (Fu et al., 2015).

While NO_3^- is relocated to the shoot, a larger proportion of N is delivered to the sink organs (e.g., seeds, fruits, roots, and younger leaves), especially for the anabolic development of new tissues, prioritized by the growth stage or physiological condition of individual plants, a process called N remobilization (Snyder and Tegeder, 2021). NRT1.4, localized in the leaf petiole, regulates NO_3^- accumulation within the petiole while maintaining the homeostasis of available NO_3^- between the leaf lamina and petiole (Figure 1). The *nrt1.4* mutant had a low NO_3^- content in its petiole, a major NO_3^- storage organ, indicating the involvement of *NRT1.4* in nitrate homeostasis and leaf development (Chiu et al., 2004). Another NO_3^- transporter, *NRT1.7*, predominantly expressed in the phloem of minor veins, enhances nitrate relocation from older to younger leaves (Figure 1) (Fan et al., 2009). However, the extent of NO_3^- transfer and the proportion of NO_3^- remobilized to the sink organ remain unclear. NO_3^- storage in seeds is mediated by specific NO_3^- transporters that remobilize NO_3^- into embryos during seed formation. The expression of *NRT1.6* within the host embryo and seed coat demonstrates a potential role of this transporter in mediating embryonic NO_3^- relocation at the reproductive phase of the parent plant (Figure 1) (Almagro et al., 2008). Similar to *NRT1.6*, *NPF5.5* also mediates NO_3^- transport into the embryo (Figure 1) (Léran et al., 2015; Iqbal et al., 2020). *NRT2.7*, a high-affinity NO_3^- transporter in the tonoplast, plays specific NO_3^- storage roles in the seed vacuole (Chopin et al., 2007). In the tonoplast, CLCa and CLCb were observed to perform a similar localization pattern, where they also participate in NO_3^- storage (Von Der Fecht-Bartenbach et al., 2010). While NO_3^- accumulation in seed vacuoles has been well documented, relatively less is understood about the characterization of transporter genes involved in NO_3^- efflux out of the vacuole. An in-depth understanding of the specificity of these N transporters, from chronological studies, is the first step toward exploiting and optimizing NUE in plants.

3 Nitrogen assimilation in relation to NUE

For efficient NO_3^- assimilation, a larger proportion of NO_3^- assimilated after root uptake is diverted back to the cytosol, where it is

converted to nitrite by nitrate reductase (NR). The nitrite obtained is relocated to plastids for subsequent reduction. At this stage, nitrite is converted to ammonium (NH_4^+) by the nitrite-reducing enzyme nitrite reductase (NiR) and then finally incorporated as an amino acid through the glutamine synthetase (GS) and glutamate synthase (GOGAT) cycle (Wilkinson and Crawford, 1993; Li et al., 2017a). Nitrogenous compounds incorporated *via* glutamine (free amino acid) and glutamate serve as a major checkpoint for regulating N utilization efficiency and are further enhanced by the synergetic expression of NR and NO_3^- transporters (Li et al., 2020; Snyder and Tegeder, 2021). However, a recent study opined an improved grain yield and NUE on concurrent coexpression of *OsNRT1.1B* and indica *OsNR2*, indicating the positive regulatory roles of *OsNR2* and *OsNRT1.1B* in uptake of N in rice (Gao et al., 2019b).

The two functionally similar forms of GS, cytosolic GS1, and plastidic GS2, encoded by single or multiple gene families, have been reported to significantly influence N assimilation (Miflin and Habash, 2002). While cytosolic GS1 facilitates root N reassimilation and remobilization during protein turnover, GS2 isoforms primarily assimilate NH_4^+ produced during chloroplast photorespiration (Ferreira et al., 2019). Although GS1 is responsible for NH_4^+ reassimilation, some GS family members drive N assimilation when NO_3^- is abundant. A good example is *GLN1;2* in Arabidopsis, which drives N assimilation when NO_3^- is abundant, compared to the *gln1;2* mutant, which exhibits reduced GS activity, rosette biomass, and higher NH_4^+ concentration under such conditions. Due to the principal roles of GS in N assimilation, specific focus has been directed toward overexpressing GS family members to improve N assimilation in different plant species, such as *Triticum aestivum* (Hu et al., 2018), and *Oryza sativa* (Bao et al., 2014).

Despite the fundamental roles of GS in improving NH_4^+ assimilation, seed yield, and NUE (Hu et al., 2018; Gao et al., 2019a), attempts to improve NUE by overexpressing *GS1* have yielded inconsistent results (Check Table 1 for details). For instance, *TaGS2-2Ab*-overexpressing lines in wheat had increased spike number, seed yield, and NUE under poor and rich N supply compared to their wild type, due to an increased root N uptake and remobilization capacity (Hu et al., 2018). Following a similar trend, overexpressing *HvGS1-1* using its promoter confers improved grain yield and NUE on barley subjected to low and high N conditions (Gao et al., 2019a). In contrast, Bao et al. (2014) opined a drastic reduction in fresh and dry weight of *OsGS1;1*- and *OsGS1;2*-overexpressing lines in rice seedlings, with a further poor growth phenotype at the tillering and heading stages under limited and sufficient N conditions. The results suggest that the GS-overexpressing lines and plant biomass are negatively correlated. Further research is required to understand the underlying mechanisms of GS activity to improve NUE in plants.

Unlike GS, relatively few studies have addressed alterations in the expression of genes encoding NADH-dependent GOGAT (a key enzyme in N assimilation) and plastid-localized ferredoxin-dependent (Fd-GOGAT) (Good et al., 2004; Xu et al., 2012). The two kinds of GOGAT differ in their electron donor specificity. Fd-GOGAT is predominantly involved in the reassimilation of photorespiratory NH_4^+. In contrast, NADH-GOGAT participates in the assimilation of non-photorespiratory NH_4^+ and the synthesis of glutamate needed for plant development (Lee et al., 2020). Many attempts have been devoted to studies on the fundamental roles of both NADH-GOGAT and Fd-GOGAT in the growth and seed development of Arabidopsis (Somerville and Ogren, 1980), *Hordeum vulgare* L. (Kendall et al., 1986), and *Oryza sativa* (Zeng et al., 2017). However, few research studies have altered the genetic expression of GOGAT to promote seed yield and NUE, while those that focused on NADH-GOGAT had rather limiting outcomes. For example, overexpression of *ZmNADH-GOGAT* in maize confers drastic reduction on shoot biomass with no considerable alterations in kernel yield when N is abundant (Cañas et al., 2020). Meanwhile, the overexpression lines of *OsNADH-GOGAT* resulted in an increase

TABLE 1 Nitrogen assimilatory genes involved in nitrogen use efficiency.

S/N	Genes	Host species	Transgenic approach	Effects	References
1	*OsGS1;2*	Rice	Overexpression	• Improves N utilization efficiency	(Brauer et al., 2011)
				• Enhances N harvest index	
				• May not lead to less N input under field condition	
2	*GS1;1, GS1;2*	Rice	Overexpression	Poor yield and growth phenotypes under different N conditions.	(Bao et al., 2014)
3	*OsNADH-GOGAT*	Rice	Overexpression	Enhances N utilization and grain filling	(Yamaya et al., 2002)
4	*OsAlaAT*	Rice	Overexpression	Increases nitrate uptake efficiency, tiller number, and grain yield	(Shrawat et al., 2008; Beatty et al., 2009)
5	*OsAAT1-3*	Rice	Overexpression	Increases protein and amino acids in seeds	(Zhou et al., 2009)
6	*ASN1*	Arabidopsis	Overexpression	• Increases seedlings' tolerance to low N supply	(Lam et al., 2003)
				• Improves protein content in the seeds	
7	*HvGS1.1*	Barley	Cisgenic expression	Increased grain yields and NUE	(Gao et al., 2019a)
8	*TaGS2-2Ab*	Wheat	Transgenic expression	Improves grain yields and NUE under different N conditions	(Hu et al., 2018)
9	*ZmGln1-3*/ *ZmGln1-4*	Maize	Mutation	Exhibits reduced kernel size and number	(Martin et al., 2006)

in rice grain weight under limited N (Yamaya et al., 2002). Interestingly, Lee et al. (2020) recently revealed that the synergetic expression of *OsNADH-GOGAT1* and *OsAMT1;2* confers an increase in NUE under both high and low N supply. While transgenic lines had improved seed protein levels without any yield alteration under N-sufficient conditions, seed quality and overall yield increased under N starvation. These observations imply that the combined expression of N-transporters and GOGAT improves N uptake, N assimilation, and NUE rather than the negative effect of the expression of AMT or GOGAT alone. Consequently, understanding the factors involved in the synergetic expression of NO_3^- transporters and GOGAT under rich and poor N conditions in plants is imperative to augment NUE.

4 Nitrate sensing and signaling

In addition to its nutritional roles, NO_3^- functions as a major signaling element regulating several plant physiological processes, such as leaf expansion (Walch-Liu et al., 2000), induction of root architectural changes (Walch-Liu and Forde, 2008), regulation of root development, and regulation of floral induction (Marín et al., 2011). The first step in signaling is through external nitrate perception by the dual affinity NO_3^- transporter *NPF6.3* (*NRT1.1*), induced immediately after NO_3^- treatment. *NRT1.1* switches between two states of nitrate conditions (low and high NO_3^- conditions) (Wang et al., 1998; Bouguyon et al., 2015; Hu et al., 2015).

4.1 Roles of transcription factors in N use regulation

Several transcription factors (TFs) have been reported to play critical roles in NUE regulation by modulating the expression of NO_3^- responsive genes. Detailed functions of TFs involved in NUE improvements are outlined in Table 2. DNA binding with one finger (*Dof1*) TFs increases N use in plants. The transgenic expression *of ZmDof1* in *A. thaliana* (Yanagisawa et al., 2004), *TaDof1* in wheat (Hasnain et al., 2020), *ZmDof1* in rice (Kurai et al., 2011), wheat and sorghum (Peña et al., 2017) improve N assimilation and plant growth under N starvation.

The key regulators of nitrate assimilatory genes, teosinte branched1-cycloidea-proliferating cell factor1-20 (TCP20) and NIN-like protein

TABLE 2 Transcription factors (Tfs) involved plant nitrogen use efficiency.

Family	Tfs	Host species	Transgenic approach	Summary of findings	Reference
MADS-box	*ANR1*	Arabidopsis	Overexpression	Rapid early seedling developments	(Gan et al., 2012)
	AGL21	Arabidopsis	Overexpression	Increases lateral root (LR) density and length	(Yu et al., 2014)
	OsMADS25	Rice	Overexpression	• Promotes nitrate accumulation and upregulates other NO_3^- responsive genes • Positively regulates primary and LR development	(Yu et al., 2015)
	OsMADS57	Rice	Overexpression	• Regulates nitrate root-to-shoot transport • Upregulates *OsNRT2.1/2.2/2.4* and *OsNRT2.3a.*	(Huang et al., 2019)
	CmANR1	Arabidopsis	Overexpression	• Improves lateral root growth and development under moderate NO_3^- regime • 7.5%-116.2% increase in root auxin level	(Sun et al., 2018)
	ZmTMM1	Arabidopsis	Overexpression	Increases NR, GS, and PEPC activity and LR elongation	(Liu et al., 2020)
Dof	*ZmDof1*	Rice	Constitutive expression	Improves N assimilation and growth under N-deficient condition	(Yanagisawa et al., 2004; Kurai et al., 2011)
	Dof1(Dof1.7)	Tobacco	Overexpression	Increases plant length, total protein, and N assimilation under low N	(Wang et al., 2013)
	ZmDof1	Wheat and Sorghum	Constitutive expression	• Negatively affects photosynthesis, plant height, and biomass under poor-N • Reduces the expression of photosynthetic-regulatory genes	(Peña et al., 2017)
	TaDof1	Wheat	Overexpression	• Regulates Carbon and N metabolism under N-limiting conditions. • Improves different agronomic traits	(Hasnain et al., 2020)
bZIP	*TGA4*	Arabidopsis	Overexpression	• Alleviates N-starvation • Enhances nitrate transport and assimilation capacity.	(Zhong et al., 2015)
	TabZIP60	Wheat	Downregulation (RNAi)	• Stimulates lateral root branching, spike number and increases N uptake •; Accelerates NADH-dependent glutamate synthase (NA–H - GOGAT) activity	(Yang et al., 2019)

(Continued)

TABLE 2 Continued

Family	Tfs	Host species	Transgenic approach	Summary of findings	Reference
				• Improves grain yield by more than 25% under field-based conditions	
	HY5/HYH	Arabidopsis	Knockout	Upregulates *NRT1.1* and improves N-uptake	(Jonassen et al., 2009)
	TGA1/4	Arabidopsis	Mutation based	• Increases the expression of *NRT1.1*, *NRT2.1*, represses *NIA2* • Decreases LR growth and root hair density	(Canales et al., 2017)
NLP	*OsNLP1*	Rice	Overexpression	Increases plant growth, yield, and NUE under diverse N supplies.	(Alfatih et al., 2020)
	OsNLP4	Rice	Overexpression	Improves plant biomass, yield, and NUE under moderate N	(Wang et al., 2021a)
	ZmNLP6 and ZmNLP8	Arabidopsis	Overexpression	• Increases biomass and yield by 15% and 45% under low N • Contributes to NUE	(Cao et al., 2017)
	ZmNLP5	Maize	Mutation based	• Decreases in root NO_3- accumulation • Reduces ear, seed kernels, and leaves N contents • Suppresses shoot NH_4^+ content.	(Ge et al., 2020)
	NLP7	Arabidopsis	Overexpression	Increases plant growth under low and high-N conditions	(Yu et al., 2016)
MYB	*OsMYB305*	Rice	Overexpression	• Improves nitrate uptake, N assimilation, and growth • Improve NUE	(Wang et al., 2020a)
	SiMYB3	Arabidopsis/ and rice	Overexpression	• Improves seed N, grain weight, total N, and root growth • Upregulates *OsNRT2.1*, *OsNRT2.2*, *OsNiR2*, and *OsNAR2.1*	(Ge et al., 2019)
	MYB59	Arabidopsis	Mutation based	• Reduces K^+/NO_3^- root-to-shoot transport • Represses *NRT1.1* expression.	(Du et al., 2019)
Lateral organ boundary domain (LBD)	*LBD37* *LBD38* *LBD39*	Arabidopsis	Overexpression	Downregulates several N-related genes	(Rubin et al., 2009)
Zinc-finger proteins	*GATA4*	Arabidopsis	Downregulation	• Higher shoot biomass and root hair density • Fewer LRs, and shorter PRs	(Shin et al., 2017)
NAC	*TaNAC2-5A*	Wheat	Overexpression	• Increases tiller number and dry weight under low NO_3^- starvation • Improved grain and shoot N, harvest index, and grain yield	(He et al., 2015)
	NAM-B1	wheat	Downregulation (RNAi)	• Enhances leaf N to grain remobilization	(Uauy et al., 2006)
NF-Y	*TaNFYA-B1*	Wheat	Overexpression	Increases root growth, N uptake, and grain yield	(Qu et al., 2015)
ZYF	*TaZFP593;l*	Wheat	Overexpression	• Improves root system architecture, N uptake, and grain yield under low N	(Chen et al., 2017)

PR, Primary roots; PEPC, Phosphoenolpyruvate carboxylas.

(NLP), NLP6 and NLP7 interact with each other under N sufficient and N–starved condition to control NO_3^- response to root growth (Guan et al., 2017), a strong indication of NLP's involvement in NO_3^- signaling-related responses. Moreover, overexpression of *NLP7* results in positive regulation of key nitrate metabolites, total N contents, NO_3^- uptake, and signaling-related genes while improving plant biomass under poor and rich N conditions in Arabidopsis. This peculiar function suggests *NLP7* as a master regulator of the primary nitrate response and its importance in plant N use (Yu et al., 2016). Further research on NLP family members reveals that overexpressing *ZmNLP6* and *ZmNLP8* in Arabidopsis replaces the roles of *NLP7* in NO_3^- signaling, and metabolism (Cao et al., 2017). In a recent study by Wu et al. (2021), overexpression of *OsNLP4* in rice increased grain yield and NUE by 30% and 47%, respectively, under moderate N conditions. Contrary to NLP, three lateral organ boundary domain TFs (LBD37, LBD38, and LBD39) negatively regulate nitrate uptake and assimilatory genes, and thus could be candidates for improving NUE in plants (Rubin et al., 2009).

A putative MADS-box TF, *ANR1*, associated with lateral root growth and elongation (Zhang and Forde, 1998), functions as a downstream regulator of NRT1 in response to nitrate

(Remans et al., 2006). In addition, *AGL21* (AGAMOUS-Like 21) functions in lateral root initiation and growth by regulating auxin biosynthetic genes under N-deficient conditions (Yu et al., 2014). Although, other TFs efficiently utilizing N in Arabidopsis and cereal crops (especially rice) have been identified, the focus on identifying these genes in other crops has been minimal.

4.2 Nitrate-induced MicroRNA regulation

MicroRNAs (miRNAs) are small noncoding RNAs containing approximately 20-24 nucleotides with diverse regulatory potentials (Zhou et al., 2020). Studies have shown that miRNAs regulate gene expression pathways related to plant growth and developmental processes in response to nitrate (check Table 3 for further details) (Zuluaga and Sonnante, 2019). The upregulation or downregulation of miRNAs primarily anchors on their capacity to regulate key target N-related genes (Zhao et al., 2011). Research has also examined the crucial roles of miR169 family members in cereal crops. A drastic reduction in the expression level of miR169 was observed in N-starved maize (Zhao et al., 2012) and wheat (Qu et al., 2015), upregulating *TaNFYA-Bi* under such conditions. Despite the numerous miRNA-related NUE phenotypes identified, little is known about the regulatory mechanisms involved. Thus, further research is required to fully understand how N use can be optimized in plants.

5 Nitrate transporters involved in NUE and yield improvement

Nitrate transporters have been shown to play diverse NUE and yield improvement roles in plants (Check Table 4 for details). In Arabidopsis, *NRT1.1* transgenic lines habouring *Cauliflower Mosaic Virus* (CaMV) 35S promoter were observed to increase the uptake of NO_3^-, however, this did not necessarily improve seed yield (Liu et al., 1999). In contrast, the expression of the *NRT1.1* homolog *OsNRT1.1B* driven by the CaMV-35S promoter or its native promoter increased NUE and grain yield in rice. The key regulatory roles in NO_3^- nitrate signaling, absorption, and assimilation enable *OsNRT1.1B* to be a major contributor of rice NUE (Hu et al., 2015). Although, the crucial roles of *OsNRT1.1B* in NUE and yield improvement have been well studied, the underlying regulatory mechanism has not been elucidated. Similar to *OsNRT1.1B*, overexpression of the spliced form *OsNRT1.1A* also exhibits an approximately 50% grain yield and NUE increase, coupled with shortened maturation times (Wang et al., 2018c). The observations of this latter experiment could be successfully used to develop early maturing and high-yielding varieties in some other crops. The elevated expression of *OsNPF8.20* (*OsPTR9*) leads to increased NH_4^+ uptake, better root formation, and ultimately, an increased tiller and panicle number, indicating that *OsNPF8.20* improves grain yield and NUE in rice breeding (Fang et al., 2013). Similarly, *OsNPF7.20*-overexpressing lines exhibited a drastic increase in rice tiller number, fresh weight, dry weight, and grain yield. In contrast, an opposite effect was conferred on the RNA interference (Ri) lines and *osnpf7.2* mutant line under mixed nitrate supply (0.5-8 mM NO_3^-) (Wang et al., 2018a). In their experiment on the modification of NO_3^- transporters in Arabidopsis and rice, Liu et al. (1999) and Hu et al. (2015) reported some discrepancies in the response of these plants to the modified transporters. This may be due to the tolerance and sensitivity of both crops to NH_4^+ and NO_3^-. *Arabiodopsis* thrives under aerobic conditions where the NO_3^- transport system is well optimized, whereas rice thrives best in anaerobic environments where the NH_4^+ transport system is optimized. Hence, manipulating NO_3^- and NH_4^+ transporters for improved efficiency in Arabidopsis and rice, respectively, would generate little or no effect on their NUE. Several NO_3^- transporter genes in plants whose expression and subcellular localization pattern greatly determine the gene's function are essential in genetic manipulations of plant traits. As such, deep insight into the function of a gene and the environment to which plants are better adapted can encourage precise manipulation of NUE in crops. The influence of nitrate transporters on crop yield was also reported in tomatoes, where overexpression of *LeNRT2.3* improved NO_3^- uptake, root-to-shoot NO_3^- transport, plant biomass, and fruit weight (Fu et al., 2015).

The expression of several NRT2 transporters has also been found to influence yield and NUE under N-starved conditions. *NRT2.2* was upregulated to improve N uptake, assimilation, and plant growth under low NO_3^- conditions (Li et al., 2007). Under the same NO_3^- stressed conditions, *TaNRT2.5*, highly expressed in wheat, increases NO_3^- uptake and root growth (Guo et al., 2014). Chen et al. (2016) conducted a study on transgenic rice and observed that *OsNRT2.1*, which has the OsNAR2.1 promoter (*pOsNAR2.1: OsNRT2.1*), was upregulated in the roots and culms. This upregulation significantly increases the overall yield, biomass, and NUE in transgenic lines harboring *OsNAR2.1* (*pOsNAR2.1: OsNRT2.1*). However, the reverse (decrease in NUE) was obtained with the constitutive promoter of

TABLE 3 MicroRNAs involved in nitrogen use efficiency.

S/N	Genes	Host species	Transgenic approach	Summary of findings	Reference
1	*OsmiR393*	Rice	Mutation	Represses N-promoted tillering	(Li et al., 2016b)
2	*Osa-miR528*	Creeping Bentgrass	Overexpression	Increases total N, chlorophyll synthesis, and biomass accumulation	(Yuan et al., 2015)
3	*TaMIR444a*	Tobacco	Overexpression	Increases N uptake and plant biomass under N- limitation	(Gao et al., 2016)
4	*TaMIR2275*	Tobacco	Overexpression	Improves N and biomass accumulation under N starvation.	(Qiao et al., 2018)
5	*RDD1*	Rice	Overexpression	Increases N-uptake and grain yield under low N	(Iwamoto and Tagiri, 2016)

TABLE 4 Nitrate transporter genes involved in plant nitrogen use efficiency.

S/N	Gene	Host plants	Expression pattern	Promoter region	Summary of findings	Reference
1	*OsNPF8.20* (*OsPTR9*)	Rice	Root tips, leaves, stems, and panicles	Ubi promoter	Increases NH_4^+ uptake, lateral root, and grain yield.	(Fang et al., 2013)
2	*OsNPF6.5* (*NRT1.1B*)	Rice	Root epidermis, root hairs, and vascular tissues	CaMV 35S or native promoter	Improves NUE and grain yield	(Hu et al., 2015)
3	*OsNPF8.9* (*OsNRT1.1a* and *OsNRT1.1b*)	Rice	Roots	Ubi promoter	• Increases shoot biomass under the hydroponic system • Under low N conditions, *OsNRT1.1b* enhances N content and growth, but loss of function in *OsNRT1.1a*	(Fan et al., 2016a)
4	*OsNRT2.1*	Rice	Root, leaf sheaths, and leaf blades	Ubi and NAR2.1 promoter	• *pUbi*: *OsNRT2.1* exhibits decreased NUE • p*OsNAR2.1*:*OsNRT2.1* exhibits increased NUE	(Chen et al., 2016)
5	*OsNPF7.3* (*OsPTR6*)	Rice	Roots and shoots	Ubi promoter	Improved growth under various N supplies but decreased NUE on excessive NH_4^+ supply	(Fan et al., 2014)
6	*OsNRT2.3a*	Rice	Culms	p35S:NRT2.3a p35S:OsNAR2.1-p35S: OsNRT2.3a	• *p35S*: *NRT2.3a* exhibits no improvement yield and NUE • *p35S*:*OsNAR2.1-p35S*: *OsNRT2.3a* increases rice yield and NUE	(Fan et al., 2016b; Chen et al., 2020a)
7	*OsNRT2.3b*	Rice	Phloem	CaMV 35S/Ubi promoter	• Increases the uptake of other mineral nutrients • Improves grain yield and NUE by 40%	(Fan et al., 2016a)
8	*NRT1.7*	Arabidopsis, tobacco, and rice	Old leaves	NRT1.7 promoter (NRT1.7p::NC4N::3′)	• NO_3- accumulation at the younger leaves • Enhances NO_3- remobilization to the sink, • Improves plant growth and yield under low and high NO_3- supply	(Chen et al., 2020b)
9	*OsNPF6.1HapB*	Rice	Root cells	Transactivation of OsNPF6.1HapB by OsNAC42	• Improves N uptake and signaling pathway under N starvation • Improves NUE and yield	(Tang et al., 2019)
10	*OsNRT1.1A* (*OsNPF6.3)*	Rice	Epidermis, Root vascular tissues, parenchyma cells of both culms and leaf sheaths	CaMV 35S promoter	• Enhances N-utilization and flowering, and grain yield • Shortens maturation time • Increases the expression of N-utilization and flowering-related genes.	(Wang et al., 2018c)
11	*OsNPF2.4*	Rice	Root epidermis, phloem companion cells, and xylem parenchyma	Ubiquitin promoter	Enhances N acquisition and long-distance transport	(Xia et al., 2015)
13	OsNPF2.2	Rice	Leaves and branches	OsNPF2.2 promoter-β-glucuronidase	Affects root-to-shoot NO_3^- transport and plant growth.	(Li et al., 2015)
14	*LeNRT2.3*	Tomato	Rhizodermal and pericycle cells in roots.	CaMV 35S promoter	Enhances NO_3^- uptake, and transport to the shoot	(Fu et al., 2015)
15	*NRT2.7*	Arabidopsis	Seeds and siliques	CaMV 35S promoter	Regulates nitrate content in mature seeds	(David et al., 2014)
16	NPF3	Arabidopsis	Root epidermis	CaMV 35S promoter	Partly regulates gibberellin distribution	(Tal et al., 2016
17	*OsNPF7.9*	Rice	Xylem parenchyma cells	CaMV 35S promoter	Regulates NO_3^- allocation Coordinates growth and stress tolerance	(Guan et al., 2022)
18	*OsNPF5.16*	Rice	Roots, leaf sheaths, and tiller basal parts	Ubiquitin promoter	Improves sheath NO_3^- content, tiller number, and biomass	(Wang et al., 2022)
19	*OsNPF3.1*	Rice	Culms, panicle and, aerial parts of the roots	pYLCRISPR/Cas9 vector	• Enhances NUE • May participate in shoot N allocation	(Yang et al., 2023)

(Continued)

TABLE 4 Continued

S/N	Gene	Host plants	Expression pattern	Promoter region	Summary of findings	Reference
20	*MeNPF4.5*	Cassava	Root	CaMV35S promoter	• Regulates N uptake and utilization, thus improving NUE in cassava. • Improves photosynthesis and N-enzymatic activities.	(Liang et al., 2022)

OsNRT2.1 (*pUbi: OsNRT2.1*). These variations could be accrued to alterations in the localization and abundance of *OsNRT2.1* in the plant tissue (Chen et al., 2016). Further investigations regarding the importance of the NRT2 gene in NUE showed that two variants, *OsNRT2.3a* and *OsNRT2.3b*, were identified in rice. The elevated expression of *OsNRT2.3b* enhances intracellular pH balance under the synergetic supply of NH_4^+ and NO_3^-, thereby increasing the uptake capacity of other nutrients (P, N, and Fe) and ultimately increasing grain yield and NUE by 40% (Fan et al., 2016b). This result demonstrates the importance of pH sensing by *OsNRT2.3b* in improving plant NUE and adaptation of rice to changes due to different NH_4^+-NO_3^- supplies. However, this N uptake and transport function observed in *OsNRT2.3b* was lost in *OsNRT2.3a* (Fan et al., 2016b; Chen et al., 2020a). *OsNRT2.3a* cannot independently improve crop yield and NUE due to its inability to increase the expression of *OsNAR2.1* (Chen et al., 2020a). Thus, the coexpression of *OsNRT2.3a* with the OsNAR2.1 promoter becomes imperative to enhance rice N use. The literature reviewed thus far has demonstrated a need for most NRT family members to be coexpressed with specific promoters to effectively enhance plant growth, biomass, and NUE, especially in Arabidopsis and rice; however less in known in other crop species.

6 Nitrate transporters and environmental cues: Influence of environmental stress factors and inducers on nitrate allocation to roots

Numerous studies have investigated the crucial roles of NO_3^- transporters in mediating the uptake and long-distance transport of NO_3^-; however, less is known towards understanding transport systems involved in NO_3^- reallocation under biotic and abiotic stresses. NO_3^- transporters play crucial roles in the plants' response to adverse environmental conditions. Indeed, plants acclimatize better to environmental stress when less NO_3^- is allocated to the shoot. Thus, this section examines the contribution of NO_3^- transporters in assisting plants to strive in adverse environmental conditions.

The quantity of NO_3^- translocated from roots to shoots varies under diverse environmental conditions, as this could positively or negatively affect plant NUE. Hence, NO_3^- redistribution in plants is a prerequisite to improved plant growth under N shortages and adverse conditions (Fan et al., 2017). Stressed plants tend to uptake and transport less NO_3^- to the shoot while retaining more nitrate in its root than required (Figure 2). Such NO_3^- allocation to the root as induced by environmental fluctuations (including biotic and abiotic stress) is referred to as "stress-initiated nitrate allocation to roots" (SINAR) (Zhang et al., 2018). Over two decades ago, Hernandez et al. (1997) investigated the inherent effects of cadmium (Cd^{2+}) on NO_3^- uptake, and distribution in pea plants. They found that NO_3^- was increasingly retained at the plant root, and fewer NO_3^- were reallocated to the shoot of Cd-treated pea compared with the control, thereby disrupting the NUE of plants (Figure 2). However, the study could not elucidate the mechanism underlying the fluctuation in the root-to-shoot transport of NO_3^-. Many years later, several research investigations have shown the active involvement of NO_3^- transporters in regulating Cd^{2+} uptake and other SINAR-related stress conditions (Lin et al., 2008; Zhang et al., 2014). Mao et al. (2014) reported *NRT1.1* as a potential regulator of Cd^{2+} uptake in plants. They observed that plants exposed to Cd^{2+} stress exhibit repression of *NRT1.1* and, as such, exert a negative influence on plant N nutrition (Figure 2). Thus, the loss of *NRT1.1* function reduced Cd^{2+} in the roots and shoots, improving plant biomass production under Cd^{2+} stress (Figure 2). Although the disruption of *NRT1.1* activity induced by Cd^{2+} stress negates NO_3^- uptake, it enhances plant tolerance to Cd^{2+} stress by reducing Cd^{2+} influx into the root. A recent study by Jian et al. (2019) opined that overexpression of NRG2 (which functions downstream of *NRT1.1*) in wild-type and *nrt1.1* increased root NO_3^- over shoot nitrate, thus alleviating Cd^{2+} toxicity. These findings demonstrate the involvement of *NRT1.1* in regulating cadmium uptake while coordinating nitrate allocation to the root. *NRT1.1* also regulates Zn accumulation in Arabidopsis by improving NO_3^- uptake in the wild type through a NO_3^-dependent pathway under Zn stress (Figure 2) (Pan et al., 2020).

In addition to *NRT1.1*, *NRT1.5* and *NRT1.8* regulate the acropetal reallocation of NO_3^- to shoots under cadmium and salinity stress (Fan et al., 2017a). Such stresses activate antagonistic expression of the two latter genes (*NRT1.5* and *NRT1.8*), with reduced expression of *NRT1.5/NPF7.3* (Chen et al., 2012) and increased expression of *NRT1.8/NPF7.2* (Figure 2) (Li et al., 2010). From the study conducted by Li et al. (2010), loss of *NRT1.8* function displays greater sensitivity to Cd^{2+} stress than wild-type plants under high NO_3^- conditions. However, an opposite effect was observed, with *nrt1.5* mutants having greater Cd^{2+} tolerance in relation to the control. The Cd^{2+} sensitivity observed with the *ntr1.8* mutants could be due to Cd^{2+} translocation to its shoots, thus counteracting the plant adaptive strategy that supports Cd^{2+} accumulation in plant roots. The upregulation of *NRT1.8* expression triggers nitrate removal from the xylem under Cd^{2+}-stressed conditions. This result suggests a strong link between Cd^{2+} tolerance and NO_3^- allocation.

In addition to *NRT1.5* and *NRT1.8*, *NPF2.3* also contributes to the SINAR response under salt stress. Nitrate allocation to the shoot was drastically reduced under salt-stressed conditions due to the unaltered expression of *NPF2.3* and partial expression of the *NPF7.3* gene in the root stele. However, the loss of *NPF2.3* function led to the reduced root-

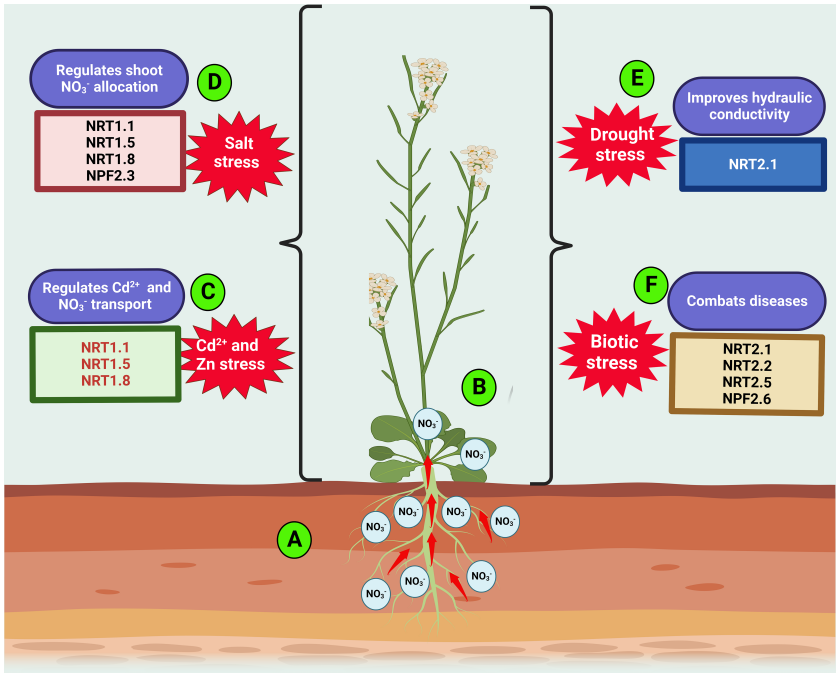

FIGURE 2
Roles of nitrate transporters in plant response to adverse environmental conditions. Environmental cues including heavy metals (Cd^{2+} and Zn), salinity, drought, and pathogenic stress engender reduction in plant growth and NUE. The resulting stressed plants accumulate more NO_3^- at the root **(A)** while retaining less in the shoot **(B)**. Under Cd^{2+} or Zn stress, nitrate transporters, *NRT1.1*, *NRT1.5* and *NRT1.8* concurrently regulates Cd^{2+} or Zn uptake and NO_3^- allocation to the root **(C)**. The transporters involved in root-to-shoot allocation of NO_3^- under salinity include *NPF2.3*, *NRT1.1*, *NRT1.5*, and *NRT1.8* **(D)**. *NRT2.1* promotes plants' tolerance to drought stress **(E)**. In addition to *NRT2.1*, *NRT2.2*, *NRT2.5* and *NRT2.6* are involved in biotic stress regulation **(F)**.

to-shoot allocation of NO_3^- (Figure 2) (Taochy et al., 2015). These data demonstrate the quantitative and physiological contribution of the NO_3^- efflux transporter *NPF2.3* to NO_3^- allocation to the shoot under salinity (Taochy et al., 2015; Chao et al., 2021). Alvarez-Aragon and Rodriguez-Navarro (2017) also found Na^+ accumulation to be partially defective in the *nrt1.1* mutant, demonstrating the partial contribution of *NRT1.1* to NO_3^-dependent Na^+ transport (Figure 2). Plants expressing these NO_3^- related genes in response to heavy metal or salt stress exhibit enhanced NO_3^- uptake, plant growth, and tolerance to heavy metal- or salt-stressed environments.

Previous physiological research investigations have shown varying impacts of NO_3^- and NH_4^+ availability on water uptake and transport in plants subjected to water stress (Guo et al., 2007). They found that the assimilation rate and stomatal conductance of NH_4^+-fed plants surpassed those of NO_3^--fed plants; thus, NH_4^+ nutrition improves rice seedling tolerance to drought (Guo et al., 2007). Li et al. (2016a) revealed that the high-affinity NO_3- transporter *NRT2.1* alters NO_3^- accumulation to regulate root hydraulic conductivity (Figure 2). They found *NRT2.1* to be a positive regulator of plasma membrane intrinsic protein PIPs. This latter study unraveled the link between NO_3^- use, water stress, and *NRT2.1* expression, indicating the potential roles of *NRT2.1* in drought tolerance (Li et al., 2016a). However, a more recent investigation has shown how the high-affinity NO_3^- transporter partner protein *OsNAR2.1* positively regulates drought-related responses to stress and enhances drought tolerance in rice (Figure 2) (Chen et al., 2019).

Ample agronomic evidence exists regarding the impact of excessive N fertilizer use on the incidence rate of plant diseases (Fagard et al., 2014; Fan et al., 2017). For example, excessive N fertilizer application triggers the severity of powdery mildew caused by a biotrophic pathogen that saps plant nutrients. Interestingly, a reduction in N fertilizer application has been found to reduce Arabidopsis tolerance to *Erwinia amylovora*. These findings indicate a complex relationship between N uptake, metabolism, and disease infection processes. Thus, it is evident that N status affects plant tolerance or susceptibility to diseases under specific environmental conditions (Fagard et al., 2014). Unfortunately, the molecular mechanism underlying the impact of NO_3^- transporters on fungal infection or pathogenic attack is not fully understood. To investigate the possible mechanisms involved in N uptake by the biotrophic pathogen, Pike et al. (2014) characterized the low-affinity transporter *VvNPF3.2* (in grapevine) and cloned Arabidopsis ortholog *NPF3.1*. In this study, powdery mildew pathogen infection was shown to upregulate the expression of *VvNPF3.2* and *NPF3.1* in vascular tissues, major and minor veins of leaves. The loss of *NRT2.1* and *NRT2.2* under N-deficient conditions resulted in increased resistance to *Pseudomonas syringae* pv tomato DC3000 infection (Figure 2) (Li et al., 2007; Camanes et al., 2012). Additionally, in the NRT2 family, the roles of two putative high-affinity NO_3^- transporters, *NRT2.5* and *NRT2.6*, were investigated in response to rhizospheric bacterium STM196 using single and double Arabidopsis mutants (Kechid et al., 2013). The study revealed that mutations in *NRT2.5* and *NRT2.6* inhibited plant growth and abolished root system architecture in response to STM196. Hence, Arabidopsis leaves expressing *NRT2.5* and *NRT2.6* appear to play crucial roles in the plant response to STM196 in a NO_3^- uptake-independent manner (Figure 2). The expression of both genes (*NRT2.5* and *NRT2.6*) is also crucial for promoting plant growth mediated by STM196

(Kechidet al., 2013). Recently, T-DNA mutants of *NRT2.5* showed stronger resistance to *Pseudomonas syringae* pv. tomato DC3000 inoculation compared to its wild-type counterpart, an indication of *NRT2.5* role in plant biotic defense (Du Toit et al., 2020; Devanna et al., 2021). These research findings have demonstrated the functional roles of NO_3^- transporters in the plant response to biotic stress, while suggesting safe, innovative, and sustainable means of controlling crop pathogens.Mycorrhizal colonization of rice root also appears to promote the expression of a putative nitrate transporter, *OsNPF4.5*. This result improved growth and yield properties in host plant (Wang et al., 2020c). However, inactivation of *OsNPF4.5* resulted in the reduction of arbuscule incidence, as well as a depletion in symbiotic nitrogen uptake in rice (Wang et al., 2020c).

Another member of the nitrate and peptide transporters family (NPF), *OsNPF8.1* (*OsPTR7*), a putative peptide transporter in rice (localized in the cell plasma membrane), has been reported as permeable to methylated arsenic species, especially, dimethylarsenate (DMA). *OsNPF8.1* is involved in long-distance transport of arsenic in rice (Tang et al., 2017). However, the peptide-mediated transport of arsenic species has been linked with imbalance nutrient (especially, phosphate) supply in plants (Finnegan and Chen, 2012). Consequently, it is imperative to investigate the activity of *OsNPF8.1* on N uptake, as well as the collateral accumulation of DMA, its clinical significance and nutrient imbalance in economically significant crops.

7 Could nitrate uptake and utilization affect the efficiency of other plant nutrients?

Balanced nutrition is paramount to maintaining good human health, and this is achievable by eating a balanced diet. In plants, maintaining an appropriate nutrient balance is also required because excessive accumulation of a specific nutrient might affect the uptake of the other and vice versa (Aluko et al., 2021). This nutritional balance ultimately affects crop growth and plant nutrient use efficiency (Bouain et al., 2019). Such nutritional crosstalk coexists between phosphorus (P) and N, the most limiting nutrient element required for crop growth and development. Phosphorus starvation reduces nitrate uptake capacity in tobacco (Rufty et al., 1990), maize (De Magalhães et al., 1998), and barley (Lee, 1982). These phenomena demonstrate the mechanisms involved in optimizing nutrient uptake and utilization to maintain plant homeostatic balance. Molecular evidence indicates that nitrogen limitation adaptation (NLA) ubiquitin offsets NO_3^- deficiency induced by excessive P *via* degradation of *PHT1*, the phosphate transporter (Kant et al., 2011b). The phenotypic analysis illustrated the functional role of nitrate-inducible garp-type transcriptional repressor 1.2 (*NIGT1.2*) in integrating N and P signals. Under sufficient P supply, *NIGT1.2* was not activated due to the coexpression of *PHR1* and SPXs, which are P-sensor proteins and repressors of *PHR1*, respectively (Medici et al., 2015). However, *PHR1* was detached from the inhibitors SPX1/2/3/4 to promote the expression of NIGT1 clade genes under P-starved conditions. Thus, nitrate uptake is suppressed due to P deficiency through the PHR1-NIGT1-NRT2.1 pathway (Maeda et al., 2018). With such development, N uptake regulation *via* the PHR1-NIGT1 path could be a good adaptative mechanism under P starvation (Maeda et al., 2018). Another recent study found that *NIGT1.2* increased the expression of phosphate transporters (PHT1;1 and PHT1;4) but repressed the nitrate transporter *NRT1.1*, an indication that *NIGT1.2* could maintain a balance between N and P to improve N uptake and utilization under (phosphorus) P starvation (Wang et al., 2020b).

The highly NO_3^- inducible NRT1.1-controlled GARP transcription factor, *HRS1*, and its closest homolog, *HHO1*, function downstream of NRT1.1, NLP6, and NLP7. However, *HRS1* and *HHO1* act as major primary root growth inhibitors only when the media is P-starved in the presence of NO_3^-, indicating extensive integration of the N and P signaling networks (Medici et al., 2015). Following the previous discussion on how HRS1 mediates N and P crosstalk, Medici et al. (2019) found that PSR marker gene responses depend on the N supplied. Indeed, transcript levels of *PHO2* were coordinated by nitrate availability accumulated during both high and low supplies of nitrate. Notably, this nitrate-induced strategy of PSR regulation is conserved in plants. However, several *PSR* genes were not regulated by NO_3^- in a *pho2* mutant, indicating that *PHO2* incorporates nitrate signals into PSR (Medici et al., 2019). Upon P starvation, *NRT1.1* is downregulated, while *PHO2* functions to positively regulate *NRT1.1*. In rice, the genes induced by P starvation *OsIPS1*, *OsSPX1*, and the P transporter *OsPT1* only respond to P starvation when nitrate is present (Medici et al., 2019). On the overall assessment, these findings elucidate the complexity of nitrate and phosphorus responses while emphasizing the principal roles of *NRT1.1* in regulating the interaction.

Another macronutrient required for plant health is potassium (K^+), as it strongly coordinates nitrate (NO_3^-). Previous reports indicated that *NRT1.5* facilitates the long-distance transport of NO_3^- and K^+ in a nitrate-dependent manner (Meng et al., 2016; Zheng et al., 2016). *NRT1.5*, expressed in the pericycle of root cells, participates in the xylem loading of nitrate. When there is a K deficit, *NRT1.5* directly triggers the movement of K^+ to the root xylem for root-to-shoot transport. This investigation demonstrates the crucial role of *NRT1.5* in root-to-shoot K^+ transport and its involvement in the synergetic regulation of NO_3^-/K^+ distribution in plants (Li et al., 2017b). Another study reported that MYB59 activates the expression of *NRT1.5* and binds directly to its promoter to ensure a controlled nutrient distribution from root to shoot. When plants become deficient in NO_3^-/K^+, the expression of MYB59 and *NRT1.5* is repressed to maintain a balanced NO_3^-/K^+ distribution between the roots and shoots (Du et al., 2019).

8 Nitrate transporter regulates nitrate and auxin crosstalk for root growth and nitrogen uptake

Evidence has shown the impact of changes in N status on auxin distribution in plants (Hou et al., 2021). Compared with moderate N supply, limited NO_3^- supply engenders auxin deposition in the roots of Arabidopsis, wheat, soybean, maize, and rapeseed (Caba et al., 2000; Tian et al., 2008; Asim et al., 2020), indicating the importance of *in situ* auxin synthesis in the root (Yang et al., 2022). Thus, the *in situ*

auxin synthesis and the shoot-to-root polar transport jointly contributes to auxin deposition in the root under N limitation (Yang et al., 2022). In contrast, a 30% reduction in root indole-3-acetic acid (the putative among natural auxins) content was observed when the amount of NO_3^- supplied to rice dropped from 2.5mM to 0.01mM (Sun et al., 2014b). Perhaps, the discrepancies in N induced auxin response stems from varying plant growth conditions and the species involved. Nevertheless, all these findings demonstrate the importance of nitrate and auxin crosstalk in root development, and the mechanism of such responses are triggered by the activities of NO_3^- transporters.

In addition to the NO_3^- transport and signaling function, *NRT1.1*, among other transporters, facilitates basipetal transport of auxin and negatively regulates auxin biosynthetic genes, *TAR2* and *LAX3*, under NO_3^- deficiency (Maghiaoui et al., 2020). As a consequence, *NRT1.1* removes auxin (required for lateral root growth) deposited at the lateral root primordia, inhibiting lateral root growth under such condition. All these inhibitory effects of *NRT1.1*, including root growth reduction and patchy auxins are alleviated in response to high NO_3^- supply (Maghiaoui et al., 2020). Thus, *NRT1.1*-mediated auxin transport was disrupted and its (*NRT 1.1*) expression repressed, to facilitate lateral root growth and auxin accumulation at the root tip under increasing NO_3^- supply (Remans et al., 2006). These findings indicated that *NRT1.1* functions in reprogramming root system architecture in response to NO_3^- availability. However, the integrated function of this molecular circuit is yet unraveled.

Although, it is understood that external N status regulates auxin biosynthetic genes and signaling pathways. However, less is known about the identities of auxin-related genes that are N-responsive, and whether these genes reprogram plant N metabolism to improve crop NUE is yet unexplored. To this end, Zhang et al. (2021b) identified DULL NITROGEN RESPONSE1 (DNR1) as an intriguing QTL regulating auxin and N crosstalk for NUE improvement in rice. DNR1 mediates plant N metabolism by counteracting the auxin deposited in response to N availability. This process enhances auxin biosynthesis and induces AUXIN RESPONSE FACTOR, a major regulator of N-responsive genes to improve NUE and grain yield.

Out of the identified NO_3^- transporters, the functions of the NO_3^- transceptor's (*NRT1.1*) in auxin regulation has been the most investigated. However, less is known about the versatile functions of other NO_3^- related proteins in regulating other plant developmental traits.

9 Integrated approaches to improve plant NUE

Genetic modification of crops has been a promising strategy for improving plant N use through diverse breeding techniques during the past few decades. Indeed, several NO_3^- transporter genes, their regulators, and other NO_3^--responsive genes regulating NUE have been well studied. However, mechanisms involved in this regulation, which specifically describes the strategies involved in NUE improvement, have been overlooked due to difficulties in identifying N-specific phenotypes. (Hu et al., 2015) revealed that genetic variation of the major quantitative trait locus (QTL) *NRT1.1B* (*OsNPF6.8*) promotes NUE divergence between *Indica* and *Japonica* rice subspecies. They found that *NRT1.1B* from indica improved the tiller number, NUE, and grain yield of *Japonica* rice. Several other QTL-based approaches have generated signaling proteins, transcriptional regulators, and components of hormonal pathways that regulate plant NUE. One of these is a QTL study that used positional cloning and genetic complementation to map out DEP1 (Dense and erect panicles 1), a heterotrimeric G protein that confers a significant yield increase (Sun et al., 2014a). Under moderate N fertilization, plants harboring the dominant allele *DEP1-1* display N-insensitive vegetative growth, as well as improved N uptake and assimilation, thereby increasing yield (Sun et al., 2014a). This result implies that modulating the activity of DEP1 could provide a lasting strategy for grain yield increases in rice. Another QTL study showed that the accumulation of the growth inhibitor DELLA confers semi-dwarfism and reduces NUE in rice (Li et al., 2018). However, the NUE and grain yield of green revolution varieties are restored by tilting the GRF4–DELLA stability toward an increased abundance of GRF4. This study indicated that regulating physiological activities and plant growth induced by efficient N use could open up innovative breeding ideas for sustainable food security (Li et al., 2018). Although QTL analysis has also informed the recent NUE gene identification strategy in crop species such as maize (Zhang et al., 2019), the importance of QTL analysis is yet unknown in some other higher plants.

In addition to QTL analysis, other analytical studies involving genome-wide association studies (GWAS) could be used to identify an array of NUE candidate genes in Arabidopsis (Atwell et al., 2010), maize (Li et al., 2013), rice (Si et al., 2016), and other crop species (Korte and Farlow, 2013; Ogura and Busch, 2015). An elite haplotype of the nitrate transporter *OsNPF6.1HapB* was recently identified using GWAS (Tang et al., 2019). This allele improved nitrate uptake, NUE, and grain yield under N-deficient conditions. In the same study, the NUE-related transcription factor OsNAC4 was used to transactivate $OsNPF6.1^{HapB}$, thereby increasing plant NUE and grain yield. This result suggests that the NAC42-NPF6.1 signaling cascade is a promising strategy for improving NUE and rice yield (Tang et al., 2019).

To further identify the genes enhancing NUE, Clustered Regularly Interspaced Palindromic Repeats (CRISPR)/Cas9 along with the Cas9 nuclease (CRISPR/CAS9) system was developed. CRISPR/CAS9 has been deployed to facilitate easy and robust technology to edit genes for improved plant N use. Multiple applications of CRISPR/CAS9 technology have been demonstrated in major crops, including sorghum, rice, and tomatoes (Ito et al., 2015; Ma et al., 2015). Notably, CRISPR/CAS9 mostly mutates negative growth regulators instead of overexpressing positive regulators, thereby providing prospects for crop breeding (Tiwari et al., 2020). A related strategy described one of the Bric-a-Brac/Tramtrack/Broad gene family members, *BT2*, that downregulates the *NRT2.1* and *NRT2.4* genes (Araus et al., 2016), thus reducing NO_3^- uptake and NUE under low NO_3^- conditions. When this *BT2* gene was mutated in Arabidopsis, a 65% increment in nitrate uptake was observed, while mutation of *OsBT2* yielded a 20% increase in NUE compared to wild-type under poor NO_3^- supply (Araus et al., 2016). To date, the functions and features of a significant number of negative regulators or inhibitors of nitrate transporters have yet to be functionally characterized in plants. Hence, it is plausible that gene editing or mutating their expression by CRISPR/Cas9 appears to be a promising strategy for achieving future breeding goals (Tiwari et al., 2020).

It is essential to note that incorporating transcriptomics, proteomics, and metabolomics, which characterize the expression profile, could facilitate the identification of agronomically induced genes or pathways. Moreover, computational and system biology could aid in identifying candidate genes during domestication.

10 Conclusion and future perspectives

Nitrate transporters have not only been shown to function in plant uptake and transport capacity; their vital roles and potential in improving plant N use have also guaranteed the possibility of meeting future global food demands. Indeed, improved NO_3^- uptake and utilization (NO_3^- transport, remobilization, and assimilation) through transporter activity is a prerequisite to attaining increased NUE and overall plant growth. With the understanding that the activities of these NO_3^- transporters are enhanced when co-expressed with their specific promoters or Tfs, it becomes imperative to select and integrate NO_3^-specific promoters with their transporters for efficient plant N utilization. An excellent way to improve NO_3^- utilization could be to carefully select senescence-specific promoters (primarily expressed in source organs or leaves) to facilitate phloem-expressed nitrate transporters. Most research works have successfully established the impact of nitrate transporters on adverse environmental conditions (biotic and abiotic stress). They have also addressed their relationships with other plant nutrients only under controlled conditions; however, field-based studies affirming these functions are scarce.

Moreover, relatively few NO_3^- transporters performing complex interplay functions have been identified, while the established ones were found to play multiple physiological roles in environmental and nutritional stresses. The underlying mechanisms behind these multipurpose functions are unknown, and the extent to which these transporters can mitigate abiotic stress is unresolved. Thus, to understand and manipulate the functional roles of nitrate transporters in enhancing plant NUE under diverse conditions, future research should address some critical questions, including the following, but not limited to:

- How do the combined effects of biotic/abiotic stressors influence nitrate transporter activities, and to what extent?
- Does the uptake of other macro- and micronutrients alter the expression or impair the prospective function of nitrate transporters and vice versa?
- Is there a possibility of having nutrient imbalance feedback due to alterations in the expression of either nitrate transporters or the transporters of other nutrients (macro- and micronutrients)?
- If the activities of nitrate transporters are eventually established to significantly affect the uptake of other nutrients and vice versa, what molecular techniques could be factored in to recuperate such imbalance?
- Could the crosstalk between N-responsive and auxin biosynthesis genes affect the uptake of other essential nutrients by plants?
- Could specific NO_3^- transporters or related genes function or be expressed differently in diverse crop species?
- Could models be developed to project or predict the possible influence of biotic and abiotic environmental parameters, as well as their complex interplay on the NUE of individual plant species?

Developing profound resolutions to these questions will afford us a better understanding of how nitrate transporters could be maximized to enhance plant NUE under adverse environmental conditions. Knowledge of these factors will also help settle crises related to plant nutritional imbalance and cross-talk, thereby achieving plant breeding goals for quality and sustainable food production.

Author contributions

Conceptualization, OOA, QW, and HL; writing-original draft, OOA; review and editing; SK and OMA; visualization, OOA, GY, and CL; validation, SK, OMA, QW, and HL; supervision, QW and HL; funding acquisition, QW and HL. All authors contributed to the article and approved the submitted version.

Funding

This work was supported by the Agricultural Science and Technology Innovation Program (ASTIP-TRIC03), the National Natural Science Foundation of China (32170387); the International Foundation of Tobacco Research Institute of Chinese Academy of Agricultural Sciences (IFT202102), the Key Funding of CNTC (No. 110202101035(JY-12)) and YNTI (No. 2022JY03).

Acknowledgments

The authors would like to appreciate E. Sanganyado, and O. Ohore for carefully proofreading the manuscript. We also appreciate V. Ninkuu for helping out with the graphics. Thanks to A. Adegbite, F. Akinde, H. Kaiyan, and T. Nong for their support and encouragement.

Conflict of interest

The authors declare that the research was conducted in the absence of any commercial or financial relationships that could be construed as a potential conflict of interest.

Publisher's note

References

Alfatih, A., Wu, J., Zhang, Z.-S., Xia, J.-Q., Jan, S. U., Yu, L.-H., et al. (2020). Rice NIN-LIKE PROTEIN 1 rapidly responds to nitrogen deficiency and improves yield and nitrogen use efficiency. *J. Exp. Bot.* 71, 6032–6042. doi: 10.1093/jxb/eraa292

Almagro, A., Lin, S. H., and Tsay, Y. F. (2008). Characterization of the arabidopsis nitrate transporter NRT1. 6 reveals a role of nitrate in early embryo development. *Plant Cell* 20, 3289–3299. doi: 10.1105/tpc.107.056788

Aluko, O. O., Li, C., Wang, Q., and Liu, H. (2021). Sucrose utilization for improved crop yields: A review article. *Int. J. Mol. Sci.* 22 (9), 4704. doi: 10.3390/ijms22094704

Alvarez-Aragon, R., and Rodriguez-Navarro, A. (2017). Nitrate-dependent shoot sodium accumulation and osmotic functions of sodium in arabidopsis under saline conditions. *Plant J.* 91, 208–219. doi: 10.1111/tpj.13556

Araus, V., Vidal, E. A., Puelma, T., Alamos, S., Mieulet, D., Guiderdoni, E., et al. (2016). Members of BTB gene family of scaffold proteins suppress nitrate uptake and nitrogen use efficiency. *Plant Physiol.* 171, 1523–1532. doi: 10.1104/pp.15.01731

Asim, M., Ullah, Z., Oluwaseun, A., Wang, Q., and Liu, H. (2020). Signalling overlaps between nitrate and auxin in regulation of the root system architecture: Insights from the arabidopsis thaliana. *Int. J. Mol. Sci.* 21(8):2880. doi: 10.3390/ijms21082880

Atwell, S., Huang, Y. S., Vilhjálmsson, B. J., Willems, G., Horton, M., Li, Y., et al. (2010). Genome-wide association study of 107 phenotypes in arabidopsis thaliana inbred lines. *Nature* 465, 627–631. doi: 10.1038/nature08800

Bao, A., Zhao, Z., Ding, G., Shi, L., Xu, F., and Cai, H. (2014). Accumulated expression level of cytosolic glutamine synthetase 1 gene (OsGS1; 1 or OsGS1; 2) alter plant development and the carbon-nitrogen metabolic status in rice. *PloS One* 9, e95581. doi: 10.1371/journal.pone.0095581

Beatty, P. H., Shrawat, A. K., Carroll, R. T., Zhu, T., and Good, A. G. (2009). Transcriptome analysis of nitrogen-efficient rice over-expressing alanine aminotransferase. *Plant Biotechnol. J.* 7, 562–576. doi: 10.1111/j.1467-7652.2009.00424.x

Bergsdorf, E.-Y., Zdebik, A. A., and Jentsch, T. J. (2009). Residues important for nitrate/proton coupling in plant and mammalian CLC transporters. *J. Biol. Chem.* 284, 11184–11193. doi: 10.1074/jbc.M901170200

Bharati, A., and Mandal, P. K. (2019). Strategies for identification of genes toward enhancing nitrogen utilization. *Nutrient Dynamics Sustain. Crop Production* 157, 157–187.

Bouain, N., Krouk, G., Lacombe, B., and Rouached, H. (2019). Getting to the root of plant mineral nutrition: combinatorial nutrient stresses reveal emergent properties. *Trends Plant Sci.* 24, 542–552. doi: 10.1016/j.tplants.2019.03.008

Bouguyon, E., Brun, F., Meynard, D., Kubeš, M., Pervent, M., Leran, S., et al. (2015). Multiple mechanisms of nitrate sensing by arabidopsis nitrate transceptor NRT1. 1. *Nat. Plants* 1, 1–8. doi: 10.1038/nplants.2015.15

Brauer, E. K., Rochon, A., Bi, Y. M., Bozzo, G. G., Rothstein, S. J., and Shelp, B. J. (2011). Reappraisal of nitrogen use efficiency in rice overexpressing glutamine synthetase1. *Physiol Plant* 141(4), 361–372. doi: 10.1111/j.1399-3054.2011.01443.x

Caba, J. M., Centeno, M. L., Fernández, B., Gresshoff, P. M., and Ligero, F. (2000). Inoculation and nitrate alter phytohormone levels in soybean roots: Differences between a supernodulating mutant and the wild type. *Planta* 211, 98–104. doi: 10.1007/s004250000265

Camanes, G., Pastor, V., Cerezo, M., Garcia-Agustin, P., and Flors Herrero, V. (2012). A deletion in the nitrate high affinity transporter NRT2.1 alters metabolomic and transcriptomic responses to pseudomonas syringae. *Plant Signal Behav.* 7, 619–622. doi: 10.4161/psb.20430

Canales, J., Contreras-López, O., Álvarez, J. M., and Gutiérrez, R. A. (2017). Nitrate induction of root hair density is mediated by TGA 1/TGA 4 and CPC transcription factors in arabidopsis thaliana. *Plant J.* 92, 305–316. doi: 10.1111/tpj.13656

Cañas, R. A., Yesbergenova-Cuny, Z., Belanger, L., Rouster, J., Brulé, L., Gilard, F., et al. (2020). NADH-GOGAT overexpression does not improve maize (Zea mays l.) performance even when pyramiding with NAD-IDH, GDH and GS. *Plants* 9, 130. doi: 10.3390/plants9020130

Cao, H., Qi, S., Sun, M., Li, Z., Yang, Y., Crawford, N. M., et al. (2017). Overexpression of the maize ZmNLP6 and ZmNLP8 can complement the arabidopsis nitrate regulatory mutant nlp7 by restoring nitrate signaling and assimilation. *Front. Plant Sci.* 8, 1703. doi: 10.3389/fpls.2017.01703

Chao, H., He, J., Cai, Q., Zhao, W., Fu, H., Hua, Y., et al. (2021). The expression characteristics of NPF genes and their response to vernalization and nitrogen deficiency in rapeseed. *Int. J. Mol. Sci.* 22, 4944. doi: 10.3390/ijms22094944

Chen, K.-E., Chen, H.-Y., Tseng, C.-S., and Tsay, Y.-F. (2020b). Improving nitrogen use efficiency by manipulating nitrate remobilization in plants. *Nat. Plants* 6, 1126–1135. doi: 10.1038/s41477-020-00758-0

Chen, J., Liu, X., Liu, S., Fan, X., Zhao, L. , Song, M., et al. (2020a). Co-Overexpression of OsNAR2. 1 and OsNRT2. 3a increased agronomic nitrogen use efficiency in transgenic rice plants. *Front. Plant Sci.* 11, 1245. doi: 10.3389/fpls.2020.01245

Chen, C.-Z., Lv, X.-F., Li, J.-Y., Yi, H.-Y., and Gong, J.-M. (2012). Arabidopsis NRT1. 5 is another essential component in the regulation of nitrate reallocation and stress tolerance. *Plant Physiol.* 159, 1582–1590. doi: 10.1104/pp.112.199257

Chen, J., Qi, T., Hu, Z., Fan, X., Zhu, L., Iqbal, M. F., et al. (2019). OsNAR2. 1 positively regulates drought tolerance and grain yield under drought stress conditions in rice. *Front. Plant Sci.* 10, 197. doi: 10.3389/fpls.2019.00197

Chen, Y., Yang, M., Ding, W., Zhao, Y., Li, X., and Xiao, K. (2017). Wheat ZFP gene TaZFP593; l mediates the n-starvation adaptation of plants through regulating n acquisition and the ROS metabolism. *Plant Cell Tissue Organ Culture (PCTOC)* 129, 271–288. doi: 10.1007/s11240-017-1176-9

Chen, J., Zhang, Y., Tan, Y., Zhang, M., Zhu, L., Xu, G., et al. (2016). Agronomic nitrogen-use efficiency of rice can be increased by driving os NRT 2.1 expression with the os NAR 2.1 promoter. *Plant Biotechnol. J.* 14, 1705–1715. doi: 10.1111/pbi.12531

Chiu, C.-C., Lin, C.-S., Hsia, A.-P., Su, R.-C., Lin, H.-L., and Tsay, Y.-F. (2004). Mutation of a nitrate transporter, AtNRT1: 4, results in a reduced petiole nitrate content and altered leaf development. *Plant Cell Physiol.* 45, 1139–1148. doi: 10.1093/pcp/pch143

Chopin, F., Orsel, M., Dorbe, M.-F., Chardon, F., Truong, H.-N., Miller, A. J., et al. (2007). The arabidopsis ATNRT2. 7 nitrate transporter controls nitrate content in seeds. *Plant Cell* 19, 1590–1602. doi: 10.1105/tpc.107.050542

David, L. C., Dechorgnat, J., Berquin, P., Routaboul, J. M., Debeaujon, I., Daniel-Vedele, F., et al. (2014). Proanthocyanidin oxidation of arabidopsis seeds is altered in mutant of the high-affinity nitrate transporter NRT2. 7. *J. Exp. Bot.* 65, 885–893. doi: 10.1093/jxb/ert481

De Magalhães, J., Alves, V., De Novais, R., Mosquim, P., Magalhães, J., Filho, A. B., et al. (1998). Nitrate uptake by corn under increasing periods of phosphorus starvation. *J. Plant Nutr.* 21, 1753–1763. doi: 10.1080/01904169809365520

Devanna, B. N., Jaswal, R., Singh, P. K., Kapoor, R., Jain, P., Kumar, G., et al. (2021). Role of transporters in plant disease resistance. *Physiologia Plantarum* 171, 849–867. doi: 10.1111/ppl.13377

Du Toit, Y., Coles, D. W., Mewalal, R., Christie, N., and Naidoo, S. (2020). eCALIBRATOR: a comparative tool to identify key genes and pathways for eucalyptus defense against biotic stressors. *Front. Microbiol.* 11, 216. doi: 10.3389/fmicb.2020.00216

Du, X.-Q., Wang, F.-L., Li, H., Jing, S., Yu, M., Li, J., et al. (2019). The transcription factor MYB59 regulates K+/NO3− translocation in the arabidopsis response to low k+ stress. *Plant Cell* 31, 699–714. doi: 10.1105/tpc.18.00674

Fagard, M., Launay, A., Clément, G., Courtial, J., Dellagi, A., Farjad, M., et al. (2014). Nitrogen metabolism meets phytopathology. *J. Exp. Bot.* 65, 5643–5656. doi: 10.1093/jxb/eru323

Fan, X., Feng, H., Tan, Y., Xu, Y., Miao, Q., and Xu, G. (2016a). A putative 6-transmembrane nitrate transporter OsNRT1. 1b plays a key role in rice under low nitrogen. *J. Integr. Plant Biol.* 58, 590–599. doi: 10.1111/jipb.12382

Fang, Z., Xia, K., Yang, X., Grotemeyer, M. S., Meier, S., Rentsch, D., et al. (2013). Altered expression of the PTR/NRT 1 homologue os PTR 9 affects nitrogen utilization efficiency, growth and grain yield in rice. *Plant Biotechnol. J.* 11, 446–458. doi: 10.1111/pbi.12031

Fan, S.-C., Lin, C.-S., Hsu, P.-K., Lin, S.-H., and Tsay, Y.-F. (2009). The arabidopsis nitrate transporter NRT1. 7, expressed in phloem, is responsible for source-to-sink remobilization of nitrate. *Plant Cell* 21, 2750–2761. doi: 10.1105/tpc.109.067603

Fan, X., Naz, M., Fan, X., Xuan, W., Miller, A. J., and Xu, G. (2017). Plant nitrate transporters: from gene function to application. *J. Exp. Bot.* 68, 2463–2475. doi: 10.1093/jxb/erx011

Fan, X., Tang, Z., Tan, Y., Zhang, Y., Luo, B., Yang, M., et al. (2016b). Overexpression of a pH-sensitive nitrate transporter in rice increases crop yields. *Proc. Natl. Acad. Sci.* 113, 7118–7123. doi: 10.1073/pnas.1525184113

Fan, X., Xie, D., Chen, J., Lu, H., Xu, Y., Ma, C., et al. (2014). Over-expression of OsPTR6 in rice increased plant growth at different nitrogen supplies but decreased nitrogen use efficiency at high ammonium supply. *Plant Sci.* 227, 1–11. doi: 10.1016/j.plantsci.2014.05.013

Ferreira, S., Moreira, E., Amorim, I., Santos, C., and Melo, P. (2019). Arabidopsis thaliana mutants devoid of chloroplast glutamine synthetase (GS2) have non-lethal phenotype under photorespiratory conditions. *Plant Physiol. Biochem.* 144, 365–374. doi: 10.1016/j.plaphy.2019.10.009

Finnegan, P. M., and Chen, W. (2012). Arsenic toxicity: the effects on plant metabolism. *Front. Physiol.* 3, 182. doi: 10.3389/fphys.2012.00182

Fu, Y., Yi, H., Bao, J., and Gong, J. (2015). LeNRT2. 3 functions in nitrate acquisition and long-distance transport in tomato. *FEBS Lett.* 589, 1072–1079. doi: 10.1016/j.febslet.2015.03.016

Gan, Y., Bernreiter, A., Filleur, S., Abram, S., and Forde, B. G. (2012). Overexpressing the ANR1 MADS-Box Gene in Transgenic Plants Provides New Insights into its Role in the Nitrate Regulation of Root Development. *Plant Cell Physiol* 53(6), 1003–1016. doi: 10.1093/pcp/pcs050

Gao, Y., De Bang, T. C., and Schjoerring, J. K. (2019a). Cisgenic overexpression of cytosolic glutamine synthetase improves nitrogen utilization efficiency in barley and prevents grain protein decline under elevated CO2. *Plant Biotechnol. J.* 17, 1209–1221. doi: 10.1111/pbi.13046

Gao, S., Guo, C., Zhang, Y., Zhang, F., Du, X., Gu, J., et al. (2016). Wheat microRNA member TaMIR444a is nitrogen deprivation-responsive and involves plant adaptation to the nitrogen-starvation stress. *Plant Mol. Biol. Rep.* 34, 931–946. doi: 10.1007/s11105-016-0973-3

Gao, Z., Wang, Y., Chen, G., Zhang, A., Yang, S., Shang, L., et al. (2019b). The indica nitrate reductase gene OsNR2 allele enhances rice yield potential and nitrogen use efficiency. *Nat. Commun.* 10, 1–10. doi: 10.1038/s41467-019-13110-8

Ge, L., Dou, Y., Li, M., Qu, P., He, Z., Liu, Y., et al. (2019). SiMYB3 in foxtail millet (Setaria italica) confers tolerance to low-nitrogen stress by regulating root growth in transgenic plants. *Int. J. Mol. Sci.* 20, 5741. doi: 10.3390/ijms20225741

Ge, M., Wang, Y., Liu, Y., Jiang, L., He, B., Ning, L., et al. (2020). The NIN-like protein 5 (ZmNLP5) transcription factor is involved in modulating the nitrogen response in maize. *Plant J.* 102, 353–368. doi: 10.1111/tpj.14628

Good, A. G., Shrawat, A. K., and Muench, D. G. (2004). Can less yield more? is reducing nutrient input into the environment compatible with maintaining crop production? *Trends Plant Sci.* 9, 597–605. doi: 10.1016/j.tplants.2004.10.008

Guan, Y., Liu, D.-F., Qiu, J., Liu, Z.-J., He, Y.-N., Fang, Z.-J., et al. (2022). The nitrate transporter OsNPF7. 9 mediates nitrate allocation and the divergent nitrate use efficiency between indica and japonica rice. *Plant Physiol* 189 (1), 215–229. doi: 10.1093/plphys/kiac044

Guan, P., Ripoll, J.-J., Wang, R., Vuong, L., Bailey-Steinitz, L. J., Ye, D., et al. (2017). Interacting TCP and NLP transcription factors control plant responses to nitrate availability. *Proc. Natl. Acad. Sci.* 114, 2419–2424. doi: 10.1073/pnas.1615676114

Guo, T., Xuan, H., Yang, Y., Wang, L., Wei, L., Wang, Y., et al. (2014). Transcription analysis of genes encoding the wheat root transporter NRT1 and NRT2 families during nitrogen starvation. *J. Plant Growth Regul.* 33, 837–848. doi: 10.1007/s00344-014-9435-z

Guo, S., Zhou, Y., Shen, Q., and Zhang, F. (2007). Effect of ammonium and nitrate nutrition on some physiological processes in higher plants-growth, photosynthesis, photorespiration, and water relations. *Plant Biol.* 9, 21–29. doi: 10.1055/s-2006-924541

Hasnain, A., Irfan, M., Bashir, A., Maqbool, A., and Malik, K. A. (2020). Transcription factor TaDof1 improves nitrogen and carbon assimilation under low-nitrogen conditions in wheat. *Plant Mol. Biol. Rep.* 38, 441–451. doi: 10.1007/s11105-020-01208-z

He, X., Qu, B., Li, W., Zhao, X., Teng, W., Ma, W., et al. (2015). The nitrate-inducible NAC transcription factor TaNAC2-5A controls nitrate response and increases wheat yield. *Plant Physiol.* 169, 1991–2005. doi: 10.1104/pp.15.00568

Hernandez, L., Garate, A., and Carpena-Ruiz, R. (1997). Effects of cadmium on the uptake, distribution and assimilation of nitrate in pisum sativum. *Plant Soil* 189, 97–106. doi: 10.1023/A:1004252816355

Hou, M., Wu, D., Li, Y., Tao, W., Chao, L., and Zhang, Y. (2021). The role of auxin in nitrogen-modulated shoot branching. *Plant Signal Behav.* 16, 1885888. doi: 10.1080/15592324.2021.1885888

Hsu, P.-K., and Tsay, Y.-F. (2013). Two phloem nitrate transporters, NRT1. 11 and NRT1. 12, are important for redistributing xylem-borne nitrate to enhance plant growth. *Plant Physiol.* 163, 844–856. doi: 10.1104/pp.113.226563

Huang, S., Liang, Z., Chen, S., Sun, H., Fan, X., Wang, C., et al. (2019). A transcription factor, OsMADS57, regulates long-distance nitrate transport and root elongation. *Plant Physiol.* 180, 882–895. doi: 10.1104/pp.19.00142

Huang, N.-C., Liu, K.-H., Lo, H.-J., and Tsay, Y.-F. (1999). Cloning and functional characterization of an arabidopsis nitrate transporter gene that encodes a constitutive component of low-affinity uptake. *Plant Cell* 11, 1381–1392. doi: 10.1105/tpc.11.8.1381

Hu, B., Wang, W., Ou, S., Tang, J., Li, H., Che, R., et al. (2015). Variation in NRT1. 1B contributes to nitrate-use divergence between rice subspecies. *Nat. Genet.* 47, 834–838. doi: 10.1038/ng.3337

Hu, M., Zhao, X., Liu, Q., Hong, X., Zhang, W., Zhang, Y., et al. (2018). Transgenic expression of plastidic glutamine synthetase increases nitrogen uptake and yield in wheat. *Plant Biotechnol. J.* 16, 1858–1867. doi: 10.1111/pbi.12921

Iqbal, A., Qiang, D., Alamzeb, M., Xiangru, W., Huiping, G., Hengheng, Z., et al. (2020). Untangling the molecular mechanisms and functions of nitrate to improve nitrogen use efficiency. *J. Sci. Food Agric.* 100, 904–914. doi: 10.1002/jsfa.10085

Ito, Y., Nishizawa-Yokoi, A., Endo, M., Mikami, M., and Toki, S. (2015). CRISPR/Cas9-mediated mutagenesis of the RIN locus that regulates tomato fruit ripening. *Biochem. Biophys. Res. Commun.* 467, 76–82. doi: 10.1016/j.bbrc.2015.09.117

Iwamoto, M., and Tagiri, A. (2016). Micro RNA-targeted transcription factor gene RDD 1 promotes nutrient ion uptake and accumulation in rice. *Plant J.* 85, 466–477. doi: 10.1111/tpj.13117

Jian, S., Luo, J., Liao, Q., Liu, Q., Guan, C., and Zhang, Z. (2019). NRT1. 1 regulates nitrate allocation and cadmium tolerance in arabidopsis. *Front. Plant Sci.* 10, 384. doi: 10.3389/fpls.2019.00384

Jin, Z., Zhu, Y., Li, X., Dong, Y., and An, Z. (2015). Soil n retention and nitrate leaching in three types of dunes in the mu us desert of China. *Sci. Rep.* 5, 1–8. doi: 10.1038/srep14222

Jonassen, E. M., Sévin, D. C., and Lillo, C. (2009). The bZIP transcription factors HY5 and HYH are positive regulators of the main nitrate reductase gene in arabidopsis leaves, NIA2, but negative regulators of the nitrate uptake gene NRT1. 1. *J. Plant Physiol.* 166, 2071–2076. doi: 10.1016/j.jplph.2009.05.010

Kant, S. (2018). Understanding nitrate uptake, signaling and remobilisation for improving plant nitrogen use efficiency. *Semin. Cell Dev. Biol.* 74, 89–96. doi: 10.1016/j.semcdb.2017.08.034

Kant, S., Bi, Y.-M., and Rothstein, S. J. (2011a). Understanding plant response to nitrogen limitation for the improvement of crop nitrogen use efficiency. *J. Exp. Bot.* 62, 1499–1509. doi: 10.1093/jxb/erq297

Kant, S., Peng, M., and Rothstein, S. J. (2011b). Genetic regulation by NLA and microRNA827 for maintaining nitrate-dependent phosphate homeostasis in arabidopsis. *PloS Genet.* 7, e1002021. doi: 10.1371/journal.pgen.1002021

Kechid, M., Desbrosses, G., Rokhsi, W., Varoquaux, F., Djekoun, A., and Touraine, B. (2013). The NRT2.5 and NRT2.6 genes are involved in growth promotion of arabidopsis by the plant growth-promoting rhizobacterium (PGPR) strain phyllobacterium brassicacearum STM196. *New Phytol.* 198, 514–524. doi: 10.1111/nph.12158

Kendall, A., Wallsgrove, R., Hall, N., Turner, J., and Lea, P. (1986). Carbon and nitrogen metabolism in barley (Hordeum vulgare l.) mutants lacking ferredoxin-dependent glutamate synthase. *Planta* 168, 316–323. doi: 10.1007/BF00392355

Korte, A., and Farlow, A. (2013). The advantages and limitations of trait analysis with GWAS: a review. *Plant Methods* 9, 1–9. doi: 10.1186/1746-4811-9-29

Kumar, A., Sandhu, N., Kumar, P., Pruthi, G., Singh, J., Kaur, S., et al. (2022). Genome-wide identification and in silico analysis of NPF, NRT2, CLC and SLAC1/SLAH nitrate transporters in hexaploid wheat (Triticum aestivum). *Sci. Rep.* 12, 1–20. doi: 10.1038/s41598-022-15202-w

Kurai, T., Wakayama, M., Abiko, T., Yanagisawa, S., Aoki, N., and Ohsugi, R. (2011). Introduction of the ZmDof1 gene into rice enhances carbon and nitrogen assimilation under low-nitrogen conditions. *Plant Biotechnol. J.* 9, 826–837. doi: 10.1111/j.1467-7652.2011.00592.x

Lam, H. M., Wong, P., Chan, H. K., Yam, K. M., Chen, L., Chow, C. M., et al. (2003). Overexpression of the ASN1 gene enhances nitrogen status in seeds of Arabidopsis. *Plant Physiol* 132(2), 926–935. doi: 10.1104/pp.103.020123

Lee, R. (1982). Selectivity and kinetics of ion uptake by barley plants following nutrient deficiency. *Ann. Bot.* 50, 429–449. doi: 10.1093/oxfordjournals.aob.a086383

Lee, S., Marmagne, A., Park, J., Fabien, C., Yim, Y., Kim, S. J., et al. (2020). Concurrent activation of OsAMT1; 2 and OsGOGAT1 in rice leads to enhanced nitrogen use efficiency under nitrogen limitation. *Plant J.* 103, 7–20. doi: 10.1111/tpj.14794

Léran, S., Garg, B., Boursiac, Y., Corratgé-Faillie, C., Brachet, C., Tillard, P., et al. (2015). AtNPF5. 5, a nitrate transporter affecting nitrogen accumulation in arabidopsis embryo. *Sci. Rep.* 5, 1–7. doi: 10.1038/srep07962

Léran, S., Varala, K., Boyer, J.-C., Chiurazzi, M., Crawford, N., Daniel-Vedele, F., et al. (2014). A unified nomenclature of NITRATE TRANSPORTER 1/PEPTIDE TRANSPORTER family members in plants. *Trends Plant Sci.* 19, 5–9. doi: 10.1016/j.tplants.2013.08.008

Liang, Q., Dong, M., Gu, M., Zhang, P., Ma, Q., and He, B. (2022). MeNPF4. 5 improves cassava nitrogen use efficiency and yield by regulating nitrogen uptake and allocation. *Front. Plant Sci.* 13. doi: 10.3389/fpls.2022.866855

Li, J.-Y., Fu, Y.-L., Pike, S. M., Bao, J., Tian, W., Zhang, Y., et al. (2010). The arabidopsis nitrate transporter NRT1. 8 functions in nitrate removal from the xylem sap and mediates cadmium tolerance. *Plant Cell* 22, 1633–1646. doi: 10.1105/tpc.110.075242

Li, H., Hu, B., and Chu, C. (2017a). Nitrogen use efficiency in crops: Lessons from arabidopsis and rice. *J. Exp. Bot.* 68, 2477–2488. doi: 10.1093/jxb/erx101

Lin, S.-H., Kuo, H.-F., Canivenc, G., Lin, C.-S., Lepetit, M., Hsu, P.-K., et al. (2008). Mutation of the arabidopsis NRT1. 5 nitrate transporter causes defective root-to-shoot nitrate transport. *Plant Cell* 20, 2514–2528. doi: 10.1105/tpc.108.060244

Li, Y., Ouyang, J., Wang, Y.-Y., Hu, R., Xia, K., Duan, J., et al. (2015). Disruption of the rice nitrate transporter OsNPF2. 2 hinders root-to-shoot nitrate transport and vascular development. *Sci. Rep.* 5, 1–10. doi: 10.1038/srep09635

Li, H., Peng, Z., Yang, X., Wang, W., Fu, J., Wang, J., et al. (2013). Genome-wide association study dissects the genetic architecture of oil biosynthesis in maize kernels. *Nat. Genet.* 45, 43–50. doi: 10.1038/ng.2484

Li, S., Tian, Y., Wu, K., Ye, Y., Yu, J., Zhang, J., et al. (2018). Modulating plant growth–metabolism coordination for sustainable agriculture. *Nature* 560, 595–600. doi: 10.1038/s41586-018-0415-5

Li, G., Tillard, P., Gojon, A., and Maurel, C. (2016a). Dual regulation of root hydraulic conductivity and plasma membrane aquaporins by plant nitrate accumulation and high-affinity nitrate transporter NRT2. 1. *Plant Cell Physiol.* 57, 733–742. doi: 10.1093/pcp/pcw022

Liu, K.-H., Huang, C.-Y., and Tsay, Y.-F. (1999). CHL1 is a dual-affinity nitrate transporter of arabidopsis involved in multiple phases of nitrate uptake. *Plant Cell* 11, 865–874. doi: 10.1105/tpc.11.5.865

Liu, Y., Jia, Z., Li, X., Wang, Z., Chen, F., Mi, G., et al. (2020). Involvement of a truncated MADS-box transcription factor ZmTMM1 in root nitrate foraging. *J. Exp. Bot.* 71, 4547–4561. doi: 10.1093/jxb/eraa116

Liu, K.-H., and Tsay, Y.-F. (2003). Switching between the two action modes of the dual-affinity nitrate transporter CHL1 by phosphorylation. *EMBO J.* 22, 1005–1013. doi: 10.1093/emboj/cdg118

Li, W., Wang, Y., Okamoto, M., Crawford, N. M., Siddiqi, M. Y., and Glass, A. D. (2007). Dissection of the AtNRT2. 1: AtNRT2. 2 inducible high-affinity nitrate transporter gene cluster. *Plant Physiol.* 143, 425–433. doi: 10.1104/pp.106.091223

Li, X., Xia, K., Liang, Z., Chen, K., Gao, C., and Zhang, M. (2016b). MicroRNA393 is involved in nitrogen-promoted rice tillering through regulation of auxin signal transduction in axillary buds. *Sci. Rep.* 6, 1–12. doi: 10.1038/srep32158

Li, M., Xu, J., Gao, Z., Tian, H., Gao, Y., and Kariman, K. (2020). Genetically modified crops are superior in their nitrogen use efficiency-a meta-analysis of three major cereals. *Sci. Rep.* 10, 1–9. doi: 10.1038/s41598-020-65684-9

Li, H., Yu, M., Du, X.-Q., Wang, Z.-F., Wu, W.-H., Quintero, F. J., et al. (2017b). NRT1. 5/NPF7. 3 functions as a proton-coupled H+/K+ antiporter for k+ loading into the xylem in arabidopsis. *Plant Cell* 29, 2016–2026. doi: 10.1105/tpc.16.00972

Maeda, Y., Konishi, M., Kiba, T., Sakuraba, Y., Sawaki, N., Kurai, T., et al. (2018). A NIGT1-centred transcriptional cascade regulates nitrate signalling and incorporates phosphorus starvation signals in arabidopsis. *Nat. Commun.* 9, 1376. doi: 10.1038/s41467-018-03832-6

Maghiaoui, A., Bouguyon, E., Cuesta, C., Perrine-Walker, F., Alcon, C., Krouk, G., et al. (2020). The arabidopsis NRT1. 1 transceptor coordinately controls auxin biosynthesis and transport to regulate root branching in response to nitrate. *J. Exp. Bot.* 71, 4480–4494. doi: 10.1093/jxb/eraa242

Maierhofer, T., Lind, C., Hüttl, S., Scherzer, S., Papenfuß, M., Simon, J., et al. (2014). A single-pore residue renders the arabidopsis root anion channel SLAH2 highly nitrate selective. *Plant Cell* 26, 2554–2567. doi: 10.1105/tpc.114.125849

Mao, Q. Q., Guan, M. Y., Lu, K. X., Du, S. T., Fan, S. K., Ye, Y. Q., et al. (2014). Inhibition of nitrate transporter 1.1-controlled nitrate uptake reduces cadmium uptake in arabidopsis. *Plant Physiol.* 166, 934–944. doi: 10.1104/pp.114.243766

Marín, I. C., Loef, I., Bartetzko, L., Searle, I., Coupland, G., Stitt, M., et al. (2011). Nitrate regulates floral induction in arabidopsis, acting independently of light, gibberellin and autonomous pathways. *Planta* 233, 539–552. doi: 10.1007/s00425-010-1316-5

Martin, A., Lee, J., Kichey, T., Gerentes, G., Zivy, M., Tatout, C., et al. (2006). Two Cytosolic Glutamine Synthetase Isoforms of Maize Are Specifically Involved in the Control of Grain Production. *Plant Cell*. 18(11), 3252–3274. doi: 10.1105/tpc.106.042689

Ma, X., Zhang, Q., Zhu, Q., Liu, W., Chen, Y., Qiu, R., et al. (2015). A robust CRISPR/Cas9 system for convenient, high-efficiency multiplex genome editing in monocot and dicot plants. *Mol. Plant* 8, 1274–1284. doi: 10.1016/j.molp.2015.04.007

Medici, A., Marshall-Colon, A., Ronzier, E., Szponarski, W., Wang, R., Gojon, A., et al. (2015). AtNIGT1/HRS1 integrates nitrate and phosphate signals at the arabidopsis root tip. *Nat. Commun.* 6, 1–11. doi: 10.1038/ncomms7274

Medici, A., Szponarski, W., Dangeville, P., Safi, A., Dissanayake, I. M., Saenchai, C., et al. (2019). Identification of molecular integrators shows that nitrogen actively controls the phosphate starvation response in plants. *Plant Cell* 31, 1171–1184. doi: 10.1105/tpc.18.00656

Meng, S., Peng, J.-S., He, Y.-N., Zhang, G.-B., Yi, H.-Y., Fu, Y.-L., et al. (2016). Arabidopsis NRT1. 5 mediates the suppression of nitrate starvation-induced leaf senescence by modulating foliar potassium level. *Mol. Plant* 9, 461–470. doi: 10.1016/j.molp.2015.12.015

Miflin, B. J., and Habash, D. Z. (2002). The role of glutamine synthetase and glutamate dehydrogenase in nitrogen assimilation and possibilities for improvement in the nitrogen utilization of crops. *J. Exp. Bot.* 53, 979–987. doi: 10.1093/jexbot/53.370.979

Migocka, M., Warzybok, A., and Kłobus, G. (2013). The genomic organization and transcriptional pattern of genes encoding nitrate transporters 1 (NRT1) in cucumber. *Plant Soil* 364, 245–260. doi: 10.1007/s11104-012-1345-x

Mohanty, S., Swain, C. K., Kumar, A., and Nayak, A. (2020). "Nitrogen footprint: a useful indicator of agricultural sustainability," in *Nutrient dynamics for sustainable crop production* (Springer Singapore: Springer), 135–156.

Noguero, M., Leran, S., Bouguyon, E., Brachet, C., Tillard, P., Nacry, P., et al. (2018). *Revisiting the functional properties of NPF6. 3/NRT1. 1/CHL1 in xenopus oocytes*. hal-01777543.

O'brien, J. A., Vega, A., Bouguyon, E., Krouk, G., Gojon, A., Coruzzi, G., et al. (2016). Nitrate transport, sensing, and responses in plants. *Mol. Plant* 9, 837–856. doi: 10.1016/j.molp.2016.05.004

Ogura, T., and Busch, W. (2015). From phenotypes to causal sequences: using genome wide association studies to dissect the sequence basis for variation of plant development. *Curr. Opin. Plant Biol.* 23, 98–108. doi: 10.1016/j.pbi.2014.11.008

Pan, W., You, Y., Weng, Y. N., Shentu, J. L., Lu, Q., Xu, Q. R., et al. (2020). Zn stress facilitates nitrate transporter 1.1-mediated nitrate uptake aggravating zn accumulation in arabidopsis plants. *Ecotoxicol Environ. Saf.* 190, 110104. doi: 10.1016/j.ecoenv.2019.110104

Peña, P. A., Quach, T., Sato, S., Ge, Z., Nersesian, N., Changa, T., et al. (2017). Expression of the maize Dof1 transcription factor in wheat and sorghum. *Front. Plant Sci.* 8, 434. doi: 10.3389/fpls.2017.00434

Pike, S., Gao, F., Kim, M. J., Kim, S. H., Schachtman, D. P., and Gassmann, W. (2014). Members of the NPF3 transporter subfamily encode pathogen-inducible nitrate/nitrite transporters in grapevine and arabidopsis. *Plant Cell Physiol.* 55, 162–170. doi: 10.1093/pcp/pct167

Qiao, Q., Wang, X., Yang, M., Zhao, Y., Gu, J., and Xiao, K. (2018). Wheat miRNA member TaMIR2275 involves plant nitrogen starvation adaptation *via* enhancement of the n acquisition-associated process. *Acta Physiologiae Plantarum* 40, 1–13. doi: 10.1007/s11738-018-2758-9

Qu, B., He, X., Wang, J., Zhao, Y., Teng, W., Shao, A., et al. (2015). A wheat CCAAT box-binding transcription factor increases the grain yield of wheat with less fertilizer input. *Plant Physiol.* 167, 411–423. doi: 10.1104/pp.114.246959

Raddatz, N., Morales De Los Ríos, L., Lindahl, A. M., Quintero, F. J. , and Pardo, J. M. (2020). Coordinated transport of nitrate, potassium and sodium. *Front. Plant Sci.* 11, 247. doi: 10.3389/fpls.2020.00247

Remans, T., Nacry, P., Pervent, M., Filleur, S., Diatloff, E., Mounier, E., et al. (2006). The arabidopsis NRT1. 1 transporter participates in the signaling pathway triggering root colonization of nitrate-rich patches. *Proc. Natl. Acad. Sci.* 103, 19206–19211. doi: 10.1073/pnas.0605275103

Rubin, G., Tohge, T., Matsuda, F., Saito, K., and Scheible, W.-R. D. (2009). Members of the LBD family of transcription factors repress anthocyanin synthesis and affect additional nitrogen responses in arabidopsis. *Plant Cell* 21, 3567–3584. doi: 10.1105/tpc.109.067041

Rufty, T. W.Jr., Mackown, C. T., and Israel, D. W. (1990). Phosphorus stress effects on assimilation of nitrate. *Plant Physiol.* 94, 328–333. doi: 10.1104/pp.94.1.328

Segonzac, C., Boyer, J.-C., Ipotesi, E., Szponarski, W., Tillard, P., Touraine, B., et al. (2007). Nitrate efflux at the root plasma membrane: identification of an arabidopsis excretion transporter. *Plant Cell* 19, 3760–3777. doi: 10.1105/tpc.106.048173

Shin, J. M., Chung, K., Sakamoto, S., Kojima, S., Yeh, C.-M., Ikeda, M., et al. (2017). The chimeric repressor for the GATA4 transcription factor improves tolerance to nitrogen deficiency in arabidopsis. *Plant Biotechnol.* 34, 151–158. doi: 10.5511/plantbiotechnology.17.0727a

Shrawat, A. K., Carroll, R. T., Depauw, M., Taylor, G. J., and Good, A. G. (2008). Genetic engineering of improved nitrogen use efficiency in rice by the tissue-specific expression of alanine aminotransferase. *Plant Biotechnol. J.* 6, 722–732. doi: 10.1111/j.1467-7652.2008.00351.x

Si, L., Chen, J., Huang, X., Gong, H., Luo, J., Hou, Q., et al. (2016). OsSPL13 controls grain size in cultivated rice. *Nat. Genet.* 48, 447–456. doi: 10.1038/ng.3518

Snyder, R., and Tegeder, M. (2021). Targeting nitrogen metabolism and transport processes to improve plant nitrogen use efficiency. *Front. Plant Sci.* 11. doi: 10.3389/fpls.2020.628366

Somerville, C. R., and Ogren, W. L. (1980). Inhibition of photosynthesis in arabidopsis mutants lacking leaf glutamate synthase activity. *Nature* 286, 257–259. doi: 10.1038/286257a0

Sun, H., Qian, Q., Wu, K., Luo, J., Wang, S., Zhang, C., et al. (2014a). Heterotrimeric G proteins regulate nitrogen-use efficiency in rice. *Nat. Genet.* 46, 652–656. doi: 10.1038/ng.2958

Sun, H., Tao, J., Liu, S., Huang, S., Chen, S., Xie, X., et al. (2014b). Strigolactones are involved in phosphate-and nitrate-deficiency-induced root development and auxin transport in rice. *J. Exp. Bot.* 65, 6735–6746. doi: 10.1093/jxb/eru029

Sun, C.-H., Yu, J.-Q., Wen, L.-Z., Guo, Y.-H., Sun, X., Hao, Y.-J., et al. (2018). Chrysanthemum MADS-box transcription factor CmANR1 modulates lateral root development *via* homo-/heterodimerization to influence auxin accumulation in arabidopsis. *Plant Sci.* 266, 27–36. doi: 10.1016/j.plantsci.2017.09.017

Tal, I., Zhang, Y., Jørgensen, M. E., Pisanty, O., Barbosa, I. C., Zourelidou, M., et al. (2016). The arabidopsis NPF3 protein is a GA transporter. *Nat. Commun.* 7, 11486. doi: 10.1038/ncomms11486

Tang, Z., Chen, Y., Chen, F., Ji, Y., and Zhao, F. J. (2017). OsPTR7 (OsNPF8.1), a putative peptide pransporter in rice, is pnvolved in dimethylarsenate accumulation in rice grain. *Plant Cell Physiol.* 58 (5), 904–913. doi: 10.1093/pcp/pcx029

Tang, Z., Fan, X., Li, Q., Feng, H., Miller, A. J., Shen, Q., et al. (2012). Knockdown of a rice stelar nitrate transporter alters long-distance translocation but not root influx. *Plant Physiol.* 160, 2052–2063. doi: 10.1104/pp.112.204461

Tang, W., Ye, J., Yao, X., Zhao, P., Xuan, W., Tian, Y., et al. (2019). Genome-wide associated study identifies NAC42-activated nitrate transporter conferring high nitrogen use efficiency in rice. *Nat. Commun.* 10, 1–11. doi: 10.1038/s41467-019-13187-1

Taochy, C., Gaillard, I., Ipotesi, E., Oomen, R., Leonhardt, N., Zimmermann, S., et al. (2015). The arabidopsis root stele transporter NPF2.3 contributes to nitrate translocation to shoots under salt stress. *Plant J.* 83, 466–479. doi: 10.1111/tpj.12901

Tian, Q., Chen, F., Liu, J., Zhang, F., and Mi, G. (2008). Inhibition of maize root growth by high nitrate supply is correlated with reduced IAA levels in roots. *J. Plant Physiol.* 165, 942–951. doi: 10.1016/j.jplph.2007.02.011

Tiwari, J. K., Buckseth, T., Singh, R. K., Kumar, M., and Kant, S. (2020). Prospects of improving nitrogen use efficiency in potato: lessons from transgenics to genome editing strategies in plants. *Front. Plant Sci.* 11. doi: 10.3389/fpls.2020.597481

Tsay, Y.-F., Schroeder, J. I., Feldmann, K. A., and Crawford, N. M. (1993). The herbicide sensitivity gene CHL1 of arabidopsis encodes a nitrate-inducible nitrate transporter. *Cell* 72, 705–713. doi: 10.1016/0092-8674(93)90399-B

Uauy, C., Distelfeld, A., Fahima, T., Blechl, A., and Dubcovsky, J. (2006). A NAC Gene regulating senescence improves grain protein, zinc, and iron content in wheat. *Sci.* 314 (5803):1298–301. doi: 10.1126/science.1133649

Vidal, E. A., Alvarez, J. M., Araus, V., Riveras, E., Brooks, M. D., Krouk, G., et al. (2020). Nitrate in 2020: thirty years from transport to signaling networks. *Plant Cell* 32, 2094–2119. doi: 10.1105/tpc.19.00748

Von Der Fecht-Bartenbach, J., Bogner, M., Dynowski, M., and Ludewig, U. (2010). CLC-b-mediated NO– 3/H+ exchange across the tonoplast of arabidopsis vacuoles. *Plant Cell Physiol.* 51, 960–968. doi: 10.1093/pcp/pcq062

Von Wittgenstein, N. J., Le, C. H., Hawkins, B. J., and Ehlting, J. (2014). Evolutionary classification of ammonium, nitrate, and peptide transporters in land plants. *BMC evolutionary Biol.* 14, 1–17. doi: 10.1186/1471-2148-14-11

Walch-Liu, P., and Forde, B. G. (2008). Nitrate signalling mediated by the NRT1. 1 nitrate transporter antagonises l-glutamate-induced changes in root architecture. *Plant J.* 54, 820–828. doi: 10.1111/j.1365-313X.2008.03443.x

Walch-Liu, P., Neumann, G., Bangerth, F., and Engels, C. (2000). Rapid effects of nitrogen form on leaf morphogenesis in tobacco. *J. Exp. Bot.* 51, 227–237. doi: 10.1093/jexbot/51.343.227

Wang, X., Cai, X., Xu, C., and Wang, Q. (2021b). Identification and characterization of the NPF, NRT2 and NRT3 in spinach. *Plant Physiol. Biochem.* 158, 297–307. doi: 10.1016/j.plaphy.2020.11.017

Wang, S., Chen, A., Xie, K., Yang, X., Luo, Z., Chen, J., et al. (2020c). Functional analysis of the OsNPF4.5 nitrate transporter reveals a conserved mycorrhizal pathway of nitrogen acquisition in plants. *Proc. Natl. Acad. Sci. United States America* 117 (28), 16649–16659. doi: 10.1073/pnas.2000926117

Wang, Y., Fu, B., Pan, L., Chen, L., Fu, X., and Li, K. (2013). Overexpression of arabidopsis Dof1, GS1 and GS2 enhanced nitrogen assimilation in transgenic tobacco grown under low-nitrogen conditions. *Plant Mol. Biol. Rep.* 31, 886–900. doi: 10.1007/s11105-013-0561-8

Wang, M., Hasegawa, T., Beier, M., Hayashi, M., Ohmori, Y., Yano, K., et al. (2021a). Growth and nitrate reductase activity are impaired in rice osnlp4 mutants supplied with nitrate. *Plant Cell Physiol.* 62, 1156–1167. doi: 10.1093/pcp/pcab035

Wang, W., Hu, B., Yuan, D., Liu, Y., Che, R., Hu, Y., et al. (2018c). Expression of the nitrate transporter gene OsNRT1. 1A/OsNPF6. 3 confers high yield and early maturation in rice. *Plant Cell* 30, 638–651. doi: 10.1105/tpc.17.00809

Wang, R., Liu, D., and Crawford, N. M. (1998). The arabidopsis CHL1 protein plays a major role in high-affinity nitrate uptake. *Proc. Natl. Acad. Sci.* 95, 15134–15139. doi: 10.1073/pnas.95.25.15134

Wang, Q., Liu, C., Dong, Q., Huang, D., Li, C., Li, P., et al. (2018b). Genome-wide identification and analysis of apple NITRATE TRANSPORTER 1/PEPTIDE TRANSPORTER family (NPF) genes reveals MdNPF6. 5 confers high capacity for nitrogen uptake under low-nitrogen conditions. *Int. J. Mol. Sci.* 19, 2761. doi: 10.3390/ijms19092761

Wang, J., Lu, K., Nie, H., Zeng, Q., Wu, B., Qian, J., et al. (2018a). Rice nitrate transporter OsNPF7. 2 positively regulates tiller number and grain yield. *Rice* 11, 1–13. doi: 10.1186/s12284-018-0205-6

Wang, Y.-Y., and Tsay, Y.-F. (2011). Arabidopsis nitrate transporter NRT1. 9 is important in phloem nitrate transport. *Plant Cell* 23, 1945–1957. doi: 10.1105/tpc.111.083618

Wang, X., Wang, H.-F., Chen, Y., Sun, M.-M., Wang, Y., and Chen, Y.-F. (2020b). The transcription factor NIGT1. 2 modulates both phosphate uptake and nitrate influx during phosphate starvation in arabidopsis and maize. *Plant Cell* 32, 3519–3534. doi: 10.1105/tpc.20.00361

Wang, J., Wan, R., Nie, H., Xue, S., and Fang, Z. (2022). OsNPF5. 16, a nitrate transporter gene with natural variation, is essential for rice growth and yield. *Crop J.* 10, 397–406. doi: 10.1016/j.cj.2021.08.005

Wang, D., Xu, T., Yin, Z., Wu, W., Geng, H., Li, L., et al. (2020a). Overexpression of OsMYB305 in rice enhances the nitrogen uptake under low-nitrogen condition. *Front. Plant Sci.* 11, 369. doi: 10.3389/fpls.2020.00369

Wilkinson, J. Q., and Crawford, N. M. (1993). Identification and characterization of a chlorate-resistant mutant of arabidopsis thaliana with mutations in both nitrate reductase structural genes NIA1 and NIA2. *Mol. Gen. Genet. MGG* 239, 289–297. doi: 10.1007/BF00281630

Wu, J., Zhang, Z. S., Xia, J. Q., Alfatih, A., Song, Y., Huang, Y. J., et al. (2021). Rice NIN-LIKE PROTEIN 4 plays a pivotal role in nitrogen use efficiency. *Plant Biotechnol. J.* 19, 448–461. doi: 10.1111/pbi.13475

Xia, X., Fan, X., Wei, J., Feng, H., Qu, H., Xie, D., et al. (2015). Rice nitrate transporter OsNPF2. 4 functions in low-affinity acquisition and long-distance transport. *J. Exp. Bot.* 66, 317–331. doi: 10.1093/jxb/eru425

Xu, G., Fan, X., and Miller, A. J. (2012). Plant nitrogen assimilation and use efficiency. *Annu. Rev. Plant Biol.* 63, 153–182. doi: 10.1146/annurev-arplant-042811-105532

Yamaya, T., Obara, M., Nakajima, H., Sasaki, S., Hayakawa, T., and Sato, T. (2002). Genetic manipulation and quantitative-trait loci mapping for nitrogen recycling in rice. *J. Exp. Bot.* 53, 917–925. doi: 10.1093/jexbot/53.370.917

Yanagisawa, S., Akiyama, A., Kisaka, H., Uchimiya, H., and Miwa, T. (2004). Metabolic engineering with Dof1 transcription factor in plants: Improved nitrogen assimilation and growth under low-nitrogen conditions. *Proc. Natl. Acad. Sci.* 101, 7833–7838. doi: 10.1073/pnas.0402267101

Yang, L., Luo, S., Wu, Z., Rong, X., and Han, Y. (2022). Low nitrogen stress stimulated nitrate uptake rate modulated by auxin in brassica napus l. *J. Soil Sci. Plant Nutr.* 22, 3500–3506. doi: 10.1007/s42729-022-00904-x

Yang, X., Nong, B., Chen, C., Wang, J., Xia, X., Zhang, Z., et al. (2023). OsNPF3. 1, a member of the NRT1/PTR family, increases nitrogen use efficiency and biomass production in rice. *Crop J* 11, 108–118. doi: 10.1016/j.cj.2022.07.001

Yang, J., Wang, M., Li, W., He, X., Teng, W., Ma, W., et al. (2019). Reducing expression of a nitrate-responsive bZIP transcription factor increases grain yield and n use in wheat. *Plant Biotechnol. J.* 17, 1823–1833. doi: 10.1111/pbi.13103

Yang, X., Xia, X., Zeng, Y., Nong, B., Zhang, Z., Wu, Y., et al. (2020). Genome-wide identification of the peptide transporter family in rice and analysis of the PTR expression modulation in two near-isogenic lines with different nitrogen use efficiency. *BMC Plant Biol.* 20, 1–15. doi: 10.1186/s12870-020-02419-y

Yuan, S., Li, Z., Li, D., Yuan, N., Hu, Q., and Luo, H. (2015). Constitutive expression of rice microRNA528 alters plant development and enhances tolerance to salinity stress and nitrogen starvation in creeping bentgrass. *Plant Physiol.* 169, 576–593. doi: 10.1104/pp.15.00899

Yu, C., Liu, Y., Zhang, A., Su, S., Yan, A., Huang, L., et al. (2015). MADS-box transcription factor OsMADS25 regulates root development through affection of nitrate accumulation in rice. *PloS One* 10, e0135196. doi: 10.1371/journal.pone.0135196

Yu, L.-H., Miao, Z.-Q., Qi, G.-F., Wu, J., Cai, X.-T., Mao, J.-L., et al. (2014). MADS-box transcription factor AGL21 regulates lateral root development and responds to multiple external and physiological signals. *Mol. Plant* 7, 1653–1669. doi: 10.1093/mp/ssu088

Yu, L.-H., Wu, J., Tang, H., Yuan, Y., Wang, S.-M., Wang, Y.-P., et al. (2016). Overexpression of arabidopsis NLP7 improves plant growth under both nitrogen-limiting and-sufficient conditions by enhancing nitrogen and carbon assimilation. *Sci. Rep.* 6, 1–13. doi: 10.1038/srep27795

Zeng, D.-D., Qin, R., Li, M., Alamin, M., Jin, X.-L., Liu, Y., et al. (2017). The ferredoxin-dependent glutamate synthase (OsFd-GOGAT) participates in leaf senescence and the nitrogen remobilization in rice. *Mol. Genet. Genomics* 292, 385–395. doi: 10.1007/s00438-016-1275-z

Zhang, J., Fengler, K. A., Van Hemert, J. L., Gupta, R., Mongar, N., Sun, J., et al. (2019). Identification and characterization of a novel stay-green QTL that increases yield in maize. *Plant Biotechnol. J.* 17, 2272–2285. doi: 10.1111/pbi.13139

Zhang, H., and Forde, B. G. (1998). An arabidopsis MADS box gene that controls nutrient-induced changes in root architecture. *Science* 279, 407–409. doi: 10.1126/science.279.5349.407

Zhang, J., Han, Z., Lu, Y., Zhao, Y., Wang, Y., Zhang, J., et al. (2021a). Genome-wide identification, structural and gene expression analysis of the nitrate transporters (NRTs) family in potato (Solanum tuberosum l.). *PloS One* 16, e0257383. doi: 10.1371/journal.pone.0257383

Zhang, H., Li, S., Shi, M., Wang, S., Shi, L., Xu, F., et al. (2020). Genome-wide systematic characterization of the NPF family genes and their transcriptional responses to multiple nutrient stresses in allotetraploid rapeseed. *Int. J. Mol. Sci.* 21, 5947. doi: 10.3390/ijms21175947

Zhang, G.-B., Meng, S., and Gong, J.-M. (2018). The expected and unexpected roles of nitrate transporters in plant abiotic stress resistance and their regulation. *Int. J. Mol. Sci.* 19 (11), 3535. doi: 10.3390/ijms19113535

Zhang, G.-B., Yi, H.-Y., and Gong, J.-M. (2014). The arabidopsis ethylene/jasmonic acid-NRT signaling module coordinates nitrate reallocation and the trade-off between growth and environmental adaptation. *Plant Cell* 26, 3984–3998. doi: 10.1105/tpc.114.129296

Zhang, S., Zhu, L., Shen, C., Ji, Z., Zhang, H., Zhang, T., et al. (2021b). Natural allelic variation in a modulator of auxin homeostasis improves grain yield and nitrogen use efficiency in rice. *Plant Cell* 33, 566–580. doi: 10.1093/plcell/koaa037

Zhao, M., Ding, H., Zhu, J. K., Zhang, F., and Li, W. X. (2011). Involvement of miR169 in the nitrogen-starvation responses in arabidopsis. *New Phytol.* 190, 906–915. doi: 10.1111/j.1469-8137.2011.03647.x

Zhao, M., Tai, H., Sun, S., Zhang, F., Xu, Y., and Li, W.-X. (2012). Cloning and characterization of maize miRNAs involved in responses to nitrogen deficiency. *PloS One* 7, e29669. doi: 10.1371/journal.pone.0029669

Zheng, Y., Drechsler, N., Rausch, C., and Kunze, R. (2016). The arabidopsis nitrate transporter NPF7. 3/NRT1. 5 is involved in lateral root development under potassium deprivation. *Plant Signaling Behav.* 11, 2832–2847. doi: 10.1080/15592324.2016.1176819

Zhong, L., Chen, D., Min, D., Li, W., Xu, Z., Zhou, Y., et al. (2015). AtTGA4, a bZIP transcription factor, confers drought resistance by enhancing nitrate transport and assimilation in arabidopsis thaliana. *Biochem. Biophys. Res. Commun.* 457, 433–439. doi: 10.1016/j.bbrc.2015.01.009

Zhou, Y., Cai, H., Xiao, J., Li, X., Zhang, Q., and Lian, X. (2009). Over-expression of aspartate aminotransferase genes in rice resulted in altered nitrogen metabolism and increased amino acid content in seeds. *Theor. Appl. Genet.* 118, 1381–1390. doi: 10.1007/s00122-009-0988-3

Zhou, X., Khare, T., and Kumar, V. (2020). Recent trends and advances in identification and functional characterization of plant miRNAs. *Acta physiologiae plantarum* 42, 1–21. doi: 10.1007/s11738-020-3013-8

Zuluaga, D. L., and Sonnante, G. (2019). The use of nitrogen and its regulation in cereals: Structural genes, transcription factors, and the role of miRNAs. *Plants* 8, 294. doi: 10.3390/plants8080294

frontiers | Frontiers in Plant Science

TYPE Original Research
PUBLISHED 07 June 2023
DOI 10.3389/fpls.2023.1135675

OPEN ACCESS

EDITED BY
Laura De Gara,
Campus Bio-Medico University, Italy

REVIEWED BY
Carson Andorf,
United States Department of Agriculture (USDA), United States
Anca Macovei,
University of Pavia, Italy

*CORRESPONDENCE
Nandula Raghuram
raghuram@ipu.ac.in

†PRESENT ADDRESS
Narendra Sharma,
Department of Botany, Swami Shraddhanand College, University of Delhi, Delhi, India

RECEIVED 01 January 2023
ACCEPTED 10 May 2023
PUBLISHED 07 June 2023

CITATION
Sharma N, Madan B, Khan MS, Sandhu KS and Raghuram N (2023) Weighted gene co-expression network analysis of nitrogen (N)-responsive genes and the putative role of G-quadruplexes in N use efficiency (NUE) in rice.
Front. Plant Sci. 14:1135675.
doi: 10.3389/fpls.2023.1135675

Weighted gene co-expression network analysis of nitrogen (N)-responsive genes and the putative role of G-quadruplexes in N use efficiency (NUE) in rice

Narendra Sharma[1†], Bhumika Madan[1], M. Suhail Khan[1], Kuljeet S. Sandhu[2] and Nandula Raghuram[1*]

[1]Centre for Sustainable Nitrogen and Nutrient Management, University School of Biotechnology, Guru Gobind Singh Indraprastha University, Dwarka, New Delhi, India, [2]Department of Biological Sciences, Indian Institute of Science Education and Research (IISER) - Mohali, Nagar, Punjab, India

Rice is an important target to improve crop nitrogen (N) use efficiency (NUE), and the identification and shortlisting of the candidate genes are still in progress. We analyzed data from 16 published N-responsive transcriptomes/microarrays to identify, eight datasets that contained the maximum number of 3020 common genes, referred to as N-responsive genes. These include different classes of transcription factors, transporters, miRNA targets, kinases and events of post-translational modifications. A Weighted gene co-expression network analysis (WGCNA) with all the 3020 N-responsive genes revealed 15 co-expression modules and their annotated biological roles. Protein-protein interaction network analysis of the main module revealed the hub genes and their functional annotation revealed their involvement in the ubiquitin process. Further, the occurrences of G-quadruplex sequences were examined, which are known to play important roles in epigenetic regulation but are hitherto unknown in N-response/NUE. Out of the 3020 N-responsive genes studied, 2298 contained G-quadruplex sequences. We compared these N-responsive genes containing G-quadruplex sequences with the 3601 genes we previously identified as NUE-related (for being both N-responsive and yield-associated). This analysis revealed 389 (17%) NUE-related genes containing G-quadruplex sequences. These genes may be involved in the epigenetic regulation of NUE, while the rest of the 83% (1811) genes may regulate NUE through genetic mechanisms and/or other epigenetic means besides G-quadruplexes. A few potentially important genes/processes identified as associated with NUE were experimentally validated in a pair of rice genotypes contrasting for NUE. The results from the WGCNA and G4 sequence analysis of N-responsive genes helped identify and shortlist six genes as candidates to improve NUE. Further, the hitherto unavailable segregation of genetic and epigenetic gene targets could aid in informed interventions through genetic and epigenetic means of crop improvement.

KEYWORDS

WGCNA (weighted gene co-expression network analyses), G-quadruplexes (G4), NUE (nitrogen use efficiency), epigenetic regulation, hub genes, nitrogen, N-responsive genes, rice

Introduction

Nitrogen (N) is quantitatively the most important input for crop production after water. However, excessive or imbalanced use of N fertilizers exacerbated by inadequate biological N-fixation or legume-based crop rotation led to poor N use efficiency (NUE). The predominant contribution of N-fertilizers to pollution, biodiversity loss, and climate change made them a global economic and environmental concern (Sutton et al., 2019; Kanter et al., 2020; Raghuram et al., 2021; Sutton et al., 2021; Winiwarter et al., 2022). While agronomic practices and controlled-release fertilizers have been important, crop improvement for NUE is increasingly being advocated at both global (Udvardi et al., 2021) and national levels (Móring et al., 2021). The biological avenues for crop improvement have been extensively reviewed (Long et al., 2015; Mandal et al., 2018; Sinha et al., 2020; Madan et al., 2022; Raghuram et al., 2022).

Rice is the third most produced and consumed crop in the world which feeds half the global population (Norton et al., 2015). It has the lowest NUE among cereals and therefore, accounts for the highest consumption of N-fertilizer among them. Further, its rich germplasm diversity, genomic and functional genomic resources (Kawahara et al., 2013; Li et al., 2014; Chen et al., 2016; Li et al., 2018; Huang et al., 2019) make it an ideal crop to improve NUE (Sharma et al., 2021). Thousands of N-responsive genes have been reported using transcriptome studies in rice (Kumari et al., 2021 and references cited therein), including subspecies *indica* (Pathak et al., 2020) and *japonica* (Mandal et al., 2022). The delineation of the phenotype for N-response and NUE (Sharma et al., 2018; Sharma et al., 2021) enabled its integration with the fast-growing transcriptomic data (Sharma et al., 2021). The development of nutrient-depleted soil (Sharma et al., 2019) enabled N-form-specific studies on nitrate or urea to understand the implications of different N-fertilizers used in developed and developing countries for NUE improvement in rice.

But distinguishing between genes for N-response/NUE and shortlisting the fewest possible target genes for NUE is a work in progress (Kumari et al., 2021; Sharma et al., 2022) that could benefit from newer means for systematic shortlisting. In the meantime, there have been several attempts to validate the candidate genes with varying success (Madan et al., 2022, Raghuram et al., 2022), indicating further scope for identification and shortlisting of more candidates. Important recent progress in this regard has been in the comparative transcriptomics of contrasting NUE genotypes in rice, which projected some potentially important genes (Neeraja et al., 2021; Sharma et al., 2022; Sharma et al., 2023).

Being a quantitative trait, NUE requires the coordinated action of a large number of N-responsive genes contributing to yield. Co-expression network analysis could be an important method to identify coexpressed gene modules but was never employed to understand their roles in NUE or to identify/shortlist candidate gene targets on that basis. Weighted gene co-expression network analysis (WGCNA) is the most popular systems biology tool to identify the modules associated with specific biological processes (Ruprecht et al., 2017; Zhang et al., 2019; Sun et al., 2020). WGCNA has been used to identify key salt-responsive genes in rice (Zhu et al., 2019) and Arabidopsis (Amrine et al., 2015), the potential regulatory mechanism of carotenoid accumulation in chrysanthemum (Lu et al., 2019), receptor-like protein genes involved in broad-spectrum resistance in pepper (Kang et al., 2022) and in the co-expression analysis of rice and maize genes (Chang et al., 2019; Zheng et al., 2019).

There is also growing recognition of epigenetic transcriptional reprogramming in response to nutrients (Séré and Martin, 2020) and epigenetic regulation of N-response through miRNAs (Nischal et al., 2012; Islam et al., 2022) and chromatin remodeling (Li et al., 2021 and references cited therein). An emerging mode of epigenetic regulation that was never explored for NUE involves a special type of non-canonical structure known as a G4 sequence or G-quadruplex. It is produced by Hoogsteen hydrogen bonding in DNA and RNA sequences that contain four short segments of guanine (Burge et al., 2006, Sengupta et al., 2021). While being spread out across the entire genome, these G4 sequences are often abundant in promoter regions, gene UTRs, and telomeres (Griffin and Bass, 2018) It is well recognized that they contribute significantly to chromatin remodelling, gene control, epigenetic regulation, genomic instability and genetic disorders (Shao et al., 2020; Varshney et al., 2020). Despite such significance, the occurrence and roles of G4 DNA and G4 RNA in plant species have not been well studied, barring a few reports on stress (Kopec and Karlowski, 2019). Genome-wide studies of G-quadruplexes have the potential to accelerate progress toward a thorough understanding of their biological implications and practical applications in plants (Cagirici and Sen, 2020; Li et al., 2022). It is therefore of significant interest to investigate the potential of G4 sequences as a fresh method of crop development for NUE.

In the present study, we compiled the largest number of shared N-responsive genes from 8 out of 16 N-responsive transcriptomic datasets in rice and analyzed them by WGCNA. We identified fifteen functional modules of co-expressed genes and the most relevant module for N-response/NUE and the associated biological processes. We validated some genes/processes linked to NUE phenotype and identified novel candidate genes for improving N-response/NUE in rice. We also identified and catalogued sequences of G4 quadruplexes among NUE-related genes and validated their differential expression in contrasting genotypes. A hypothesis/model integrating genetic and epigenetic regulation of NUE has been proposed.

Materials and methods

Compilation and annotation of N-responsive genes

To identify N-responsive genes in rice, 16 rice N-responsive microarray datasets available at NCBI GEO were examined. A list of over 18,000 N-responsive genes was compiled from these N-responsive datasets using uniform criteria of Log2FC ≥1, p-value <0.05 with default redundancy removal, as described in Kumari et al. (2021). As very few genes were common to all the N-responsive microarray datasets compiled for this study, individual datasets that were mainly responsible for minimal common genes were eliminated progressively. This led to the shortlisting of eight N-responsive datasets (Supplementary Table S1) that had the

maximum number of 3020 common N-responsive genes (Supplementary Table S2). Gene ontology (GO) enrichment analyses for functional annotation of N-responsive genes were performed Expath 2.0 tool (Chien et al., 2015) using default parameters. The biological processes were obtained using AgriGO v2. (http://systemsbiology.cau.edu.cn/agriGOv2/index.php) and visualized using Heatmapper (http://www.heatmapper.ca).

Weighted gene co-expression network construction and module identification

In order to independently identify co-expressed N-responsive genes, we performed Weighted Gene Co-expression Network Analysis (WGCNA), using 3020 common genes (Supplementary Table S2) from eight N-responsive transcriptomic datasets (Supplementary Table S1). We used version 1.69 of the WGCNA software at Bioconductor (http://bioconductor.org/biocLite.R) on the RStudio platform (1.2.5042). The soft threshold method for Pearson correlation analysis of the expression profiles was used to determine the connection strengths and construct a weighted co-expression network among the genes. Average linkage hierarchical clustering was carried out to group the genes based on topological overlap dissimilarity in network connection strengths. To obtain the correct module number and clarify gene interactions, we restricted the minimum gene number to 20 for each module and used a threshold of 0.25. To identify the significant modules related to rice traits, three available experimental criteria in microarray datasets were used as traits including the age of the plant used for tissue sampling, type of tissue (root/shoot/whole plant), and N-treatment. Two approaches were used to identify the significant modules. The first approach used the relationship between the traits and Module eigengenes (MEs), which are the major components for principal component analysis of genes in a module with the same expression profile. The second approach used the relationship between module membership versus gene significance.

Functional annotation of significant modules

All the genes from each of the modules were analyzed separately using Expath 2.0 (Chien et al., 2015) for their functional annotation by gene ontology (GO) to identify biological, cellular, and molecular processes. In order to study the protein-protein interactions, all the genes from the turquoise module (WGCNA) were used for separate searches for their interacting protein partners on the STRING database version 11 (https://string-db.org/cgi/input.pl?sessionId=Xv9nzTk5s6NX&input_page_show_search=on).

Data mining for transporters, transcription factors, kinases, and miRNA targets

N-responsive genes encoding transporters were retrieved from the Rice transporters database (https://ricephylogenomics.ucdavis.edu/transporter/), RAP-DB (https://rapdb.dna.affrc.go.jp/), and Transport DB2.0 (http://www.membranetransport.org/transportDB2/index.html). Similarly, N-responsive genes encoding transcription factors (TFs) were retrieved from the databases PlantPAN2 (http://plantpan2.itps.ncku.edu.tw/TF_list_search.php#results), RAP-DB, STIFDB (http://caps.ncbs.res.in/stifdb/), PlantTFDB (http://planttfdb.cbi.pku.edu.cn/index.php?sp=Osj) and Rice Frend (http://ricefrend.dna.affrc.go.jp/multi-guide-gene.html). Kinases were searched by using iTAKdatabase (http://itak.feilab.net/cgi-bin/itak/index.cgi). Plant microRNA database (PMRD-http://bioinformatics.cau.edu.cn/PMRD/) was used for searching the miRNAs that target N-responsive genes.

Physiological measurements

In order to measure the N-responsive changes in terms of physiological parameters of rice plants, a contrasting pair of rice genotypes namely Nidhi and Panvel1were used for their known low and high NUE respectively (Sharma et al., 2018; Sharma et al., 2021). They were grown in trays filled with nutrient-depleted soil (Sharma et al., 2019) for 21 days. They were fertigated with media (Hoagland and Arnon, 1950) containing urea as the sole source of N at a normal dose of 15mM as control, or a low dose of 1.5mM as a test. These 21 days-old plants were used to measure photosynthesis and transpiration rate using LI-6400XT Portable Photosynthesis System (LI-COR Biosciences, Lincoln, NE, USA). Net photosynthetic rate was measured in terms of CO_2 assimilated as μ mol CO_2/m^2s^1; transpiration was measured in terms of mol $(H_2O)/m^2s^1$. Student's t-test was performed on the test vs. control data. The reference CO_2 concentration was 410 ± 20 μmol mol^{-1} during the measurements. All LI-COR measurements were carried out at the time of maximal photosynthetic activity between 12:00 noon and 5:00 pm IST. All the measurements were done in at least four replicates.

G-quadruplex sequences and post-translational modifications

All the gene IDs carrying G4 sequences in exon, promoter, gene, CDS, and UTRs regions were downloaded from the PlantG4DB database (http://ccbb.jnu.ac.in/PlantG4DB/). After combining them and removing redundant gene IDs, they were searched for the N-responsive genes having G4 sequences. To find out the genes associated with post-translational modifications (PTM), all genes associated with PTMs were retrieved from Plant PTM Viewer (https://www.psb.ugent.be/webtools/ptm-viewer/experiment.php), which contains PTM data collected from published reports (Møller and Kristensen, 2006; Nakagami et al., 2010; Xie et al., 2015; He et al., 2016; Qiu et al., 2016; Xiong et al., 2016; Zhang et al., 2016; Hou et al., 2017; Meng et al., 2017; Qiu et al., 2017; Wang et al., 2017; Ying et al., 2017; Mujahid et al., 2018).

RNA isolation and RT-qPCR analysis

Leaves were harvested from twenty-one days old plants of rice genotypes Nidhi and Panvel1 (contrasting-NUE genotypes) grown in pots with media containing normal or low nitrate levels (15 mM

and 1.5 mM potassium and calcium nitrate) and immediately frozen in liquid nitrogen as 100 mg aliquots. Total RNAs were isolated using RNAiso Plus solution and 5 µg each were reverse transcribed using PrimeScript^{TM}1st strand cDNA synthesis kit as per the instructions of the supplier (Takara, Japan). Exon spanning primers were designed using the Quant Prime tool (https://quantprime.mpimp577golm.mpg.de/?page=about). RT-qPCR was performed using SYBR Green qPCR MasterMix (GBiosciences, USA) and Aria Mx Real-time PCR System (Agilent technologies, Singapore). The relative abundance of transcripts was calculated by the $2^{-\triangle\triangle CT}$ method (Livak and Schmittgen, 2001) using actin gene (LOC_Os01g64630) as an internal control. The data were statistically analyzed using GraphPad Prism 6 software. These experiments were performed using two biological and three technical replicates.

Results

Co-expression analysis of N-responsive genes requires a large enough dataset as well as a large enough number of such datasets. Fortunately, most of the publicly available N-responsive transcriptome datasets (including our own) are available as microarrays, many of which captured thousands of differentially expressed genes. In total, 16 N-responsive microarrays data available at NCBI GEO were used. Venn selections between them revealed that the largest number of 3020 N-responsive DEGs were shared by only 8 transcriptome datasets (Supplementary Figure 1). They were used for the rest of the study and their results are described below.

N-responsive genes associated with NUE-phenotypic traits

In order to find the trait-gene association, we mined for all the traits associated with the 3020 N-responsive genes in the Oryzabase rice database (Kurata and Yamazaki, 2006) yielded 806 genes related to various traits. Among them, 259 genes fell into three phenotypic categories we identified earlier based on lifelong evaluation of 25 traits using six rice genotypes under different N conditions (Sharma et al., 2021). They include133 genes linked to nine vegetative traits (V1-V9), 110 genes linked to 12 reproductive traits (R1-R12), and 16 genes linked to germination (G) rate and ratio (Figure 1; Supplementary Table S3). Six genes across these three categories were associated with all the eight phenotypic traits that we identified earlier for NUE (Sharma et al., 2021). These traits were, germination, flowering, shoot length, fresh and dry biomass, root length, chlorophyll content and total plant height. The six genes associated with all these 8 NUE traits were, Os06g0603000 (Photoperiod-sensitivity-5), Os07g0497100 (Chromatin Remodeling 4), Os08g0162100 (ABERRANT SPIKELET AND PANICLE1), Os04g0498600 (S-adenosylmethionine decarboxylase), Os08g0127100 (Lysine/Histidine transporter 1), and Os03g0669200 (heterotrimeric G protein beta 1 subunit, RGB1). They could be tested on priority for nitrogen use efficiency.

Biological pathways and sub-cellular locations of genes involved in N-response/NUE

Gene Ontology (GO) analysis of all 3020 N-responsive genes using EXPath 2.0 for biological processes based on P values and

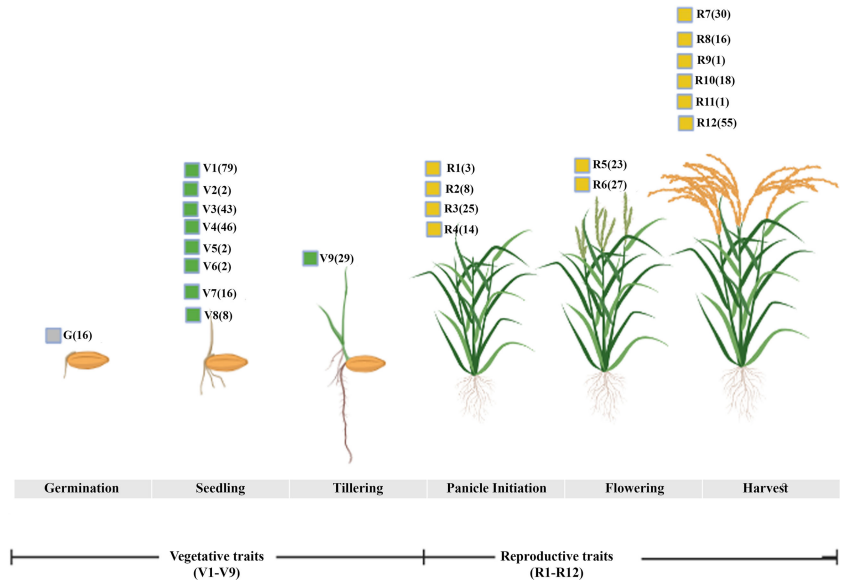

FIGURE 1
NUE traits checked during various growth phases. The mining of N-responsive genes into the rice database identified genes broadly linked to vegetative traits including germination (G, V1-V9) and reproductive stages (R1-R12) linked to NUE-phenotypic traits. The number of genes associated with each corresponding trait is denoted in the bracket.

FDR showed the involvement of translation, salt stress, water deprivation, amino acid biosynthetic process, cold stress, tricarboxylic acid cycle, peptidyl-serine phosphorylation, photosynthesis, mRNA splicing and respiration, among others. The details of GO-enrichment analyses are provided in Supplementary Table S4. The top 20 statistically significant biological processes ($P < 0.05$) were visualized using Heatmapper (Figure 2). Similar processes were also obtained when GO analysis was carried out using AgriGO v2. They include translation, carbohydrate metabolism, hormone, and photosynthesis (Supplementary Table S5). Many DEGs were also mapped to calcium metabolism, amino acid metabolism, ubiquitination, and tricarboxylic acid cycle among others, suggesting crosstalk between these pathways.

Co-expression network analysis reveals coregulated modules of N-responsive genes

Out of the 16 N-responsive microarray datasets considered, only eight of them had the maximum number of shared N-responsive genes (3020) and only these 3020 genes were used for the WGCNA analysis. Prior to analysis, it was verified that the sample dendrogram and corresponding traits of all the 3020 N-responsive genes passed the cutoff thresholds and were suitable for network analysis (Figure 3A). As the soft threshold power value is a critical parameter that affects the independence and average connectivity degree of the co-expression modules, $\beta = 6$ was selected with scale-free $R^2 = 0.928$ for the analysis, based on prior screening for network topology (Figure 3B). The gene co-expression network was constructed using hierarchical clustering of the calculated dissimilarities resulting in fifteen different modules (Figures 3C, D; Supplementary Table S6). We employed eigengenes as indicative patterns and evaluated the similarity of each module by correlating their respective eigengenes (Figure 3E). The turquoise module, which encompasses 29% of the genes, had the highest count of genes with a total of 875 (Figure 3F). The blue module had the next largest number with 479 genes, followed by the brown module with 334 genes, yellow with 270, green with 165, black with 133, and so on.

Significant modules reveal the enrichment of photosynthesis and other processes

To identify the physiological processes involved in N-response/NUE, we examined the correlation between genes from the

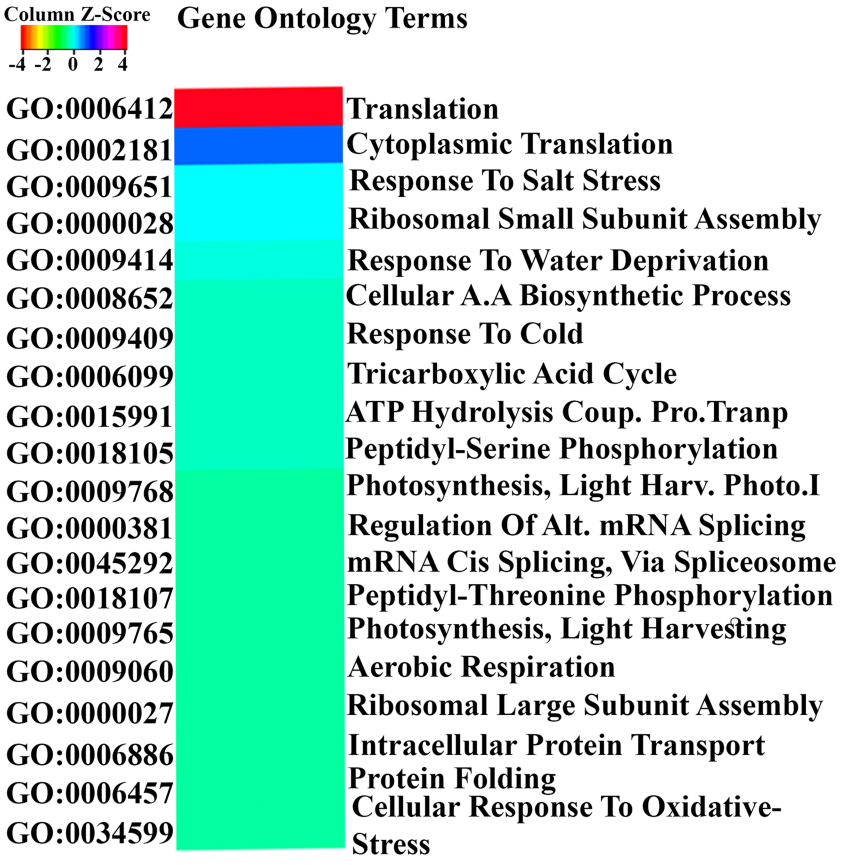

FIGURE 2
Gene Ontology analysis of N-responsive genes. GO analysis of the N-responsive genes performed using Expath for biological processes based on P values and FDR. The top 20 statistically significant biological processes ($P < 0.05$) were visualized using Heatmapper.

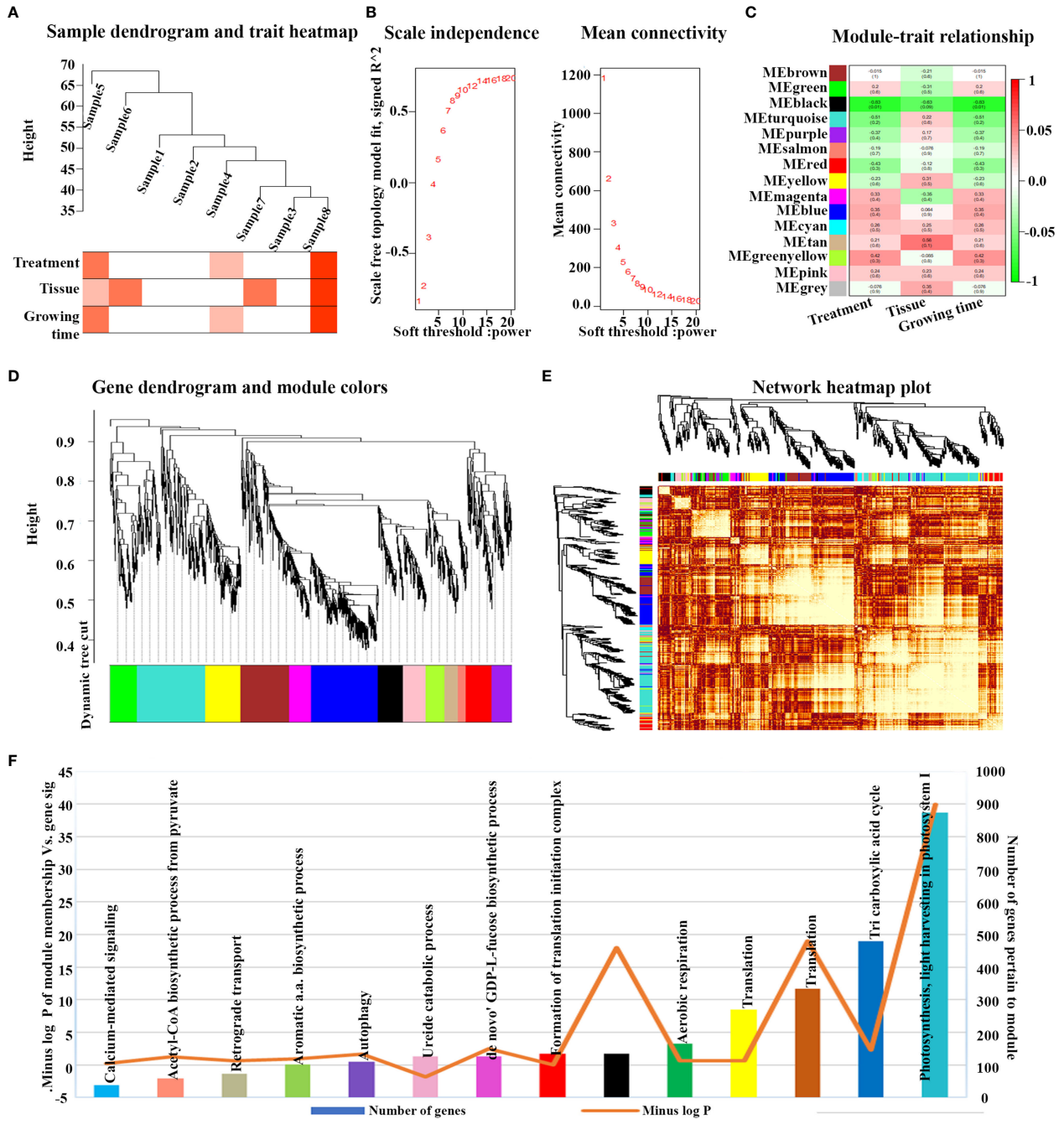

FIGURE 3
Weighted gene co-expression analysis (WGCNA) and module's associated processes of N-responsive genes. **(A)** All eight N-responsive datasets passed the cutoff thresholds, and the sample dendrogram as well as the corresponding traits were deemed suitable for network analysis. **(B)** Topology of the network analyzed for various soft-thresholding powers. On the x-axis, the weight parameter β is represented, while the left figure's y-axis represents the correlation coefficient squared between log(k) and log(p(k)) in the corresponding network. On the right graph's y-axis, the mean of all gene adjacency functions in the corresponding gene module is represented. **(C)** Matrix showing Module-Trait Relationships (MTRs) of 15 different modules under different conditions. The y-axis denotes the module names, while the x-axis denotes the conditions. The numbers in the table correspond to the Pearson correlation coefficients, and the color legend is used to show the correlation level. The heatmap's right side displays the correlation's intensity and direction, with red indicating a positive correlation and green indicating a negative correlation. **(D)** A hierarchical cluster tree of the common genes displaying coexpression modules is shown. The assigned modules are depicted by branches and color bands, while the major tree branches are labeled in distinct colors. Genes are represented by the tips of the branches. **(E)** The interaction between co-expression based on eigengenes as indicative patterns and evaluated the similarity of each module by correlating their respective eigengenes and cluster dendrogram is displayed. The axes' colors indicate their respective modules, and the heatmap's yellow intensity represents the degree of overlap, with darker yellow denoting greater overlap. Indicative patterns and evaluated the similarity of each module by correlating their respective eigengenes. **(F)** Showing the turquoise module, which includes 29% of the genes, had the largest number of genes.

significant co-expression modules with their process annotations. The identification of the modules was based on two criteria: a module-trait relationship with an R2 value greater than 0.5 and a significant p-value for the relationship between module membership and gene significance. Two modules, namely black and turquoise, were identified based on these criteria (Figure 3C). Nevertheless, the turquoise module demonstrated a higher score than any other module according to the second criterion, suggesting its stronger correlation with the NUE traits (Figure 3F). Both modules exhibited a negative correlation with the treatment and age of the plant from which the tissue was sampled. However, a positive correlation was observed in the turquoise module with respect to the type of tissue sampled. These findings suggest that the spatial co-regulation of gene expression in different tissues/organs of the plant may be more significant in N-response/NUE than temporal co-regulation in terms of different stages of development.

Gene ontology analysis of all the modules revealed their involvement in various processes (Supplementary Tables S4, S5), as well as their significance in each module (Figure 3F). It revealed photosynthesis as the most significant process in the turquoise module, TCA cycle in the blue module, translation in the brown/yellow module, respiration in the green module and other physiological processes including proteolysis and defense in the black module (Supplementary Table S7). Other significant processes include jasmonic acid mediated signaling pathway, seed coat development, glutamate metabolic process, response to cold, D-xylose metabolic process, cellular amino acid metabolic process.

PPI network of co-expressed N-responsive genes reveals hub genes

In view of better functional annotation of the co-expressed genes from the turquoise module, this module was chosen for protein-protein interaction (PPI) network analysis. All the interacting partners of the turquoise module were retrieved from the STRING database (Szklarczyk et al., 2015, Supplementary Table S8). They were found to have a highly significant PPI enrichment score (1.0e-16). They were ranked by the experimentally validated protein–protein interaction score and their networks with 518 nodes and 3104 edges were visualized by Cytoscape version 3.91 (Figure 4A) to reveal the interaction modules involved in the associated processes (Supplementary Table S7). Gene Ontology was performed using ExPath2.0 to find out the processes aided by such protein interactions (Supplementary Table S8). It revealed photosynthesis, transport, protein-chromophore linkage, glycolytic process, sterol biosynthetic process, mRNA splicing, chromatin organization and oxidation-reduction among others that need interaction between products of co-expressed N-responsive genes (Supplementary Table S8).

To select the hub genes from the network, firstly CytoHubba plugin was used with the MCC algorithm, which provided the top 10 genes with default parameters. Secondly, the MCODE plugin was used to identify the x highly connected genes among the interactors of these top 10 genes. The CYTOHUBBA and MCODE plugins only provide statistically significant genes or gene clusters by default. Therefore, these x highly connected genes qualify to be called as hub genes (Figure 4B). Their functional annotation revealed their involvement in the ubiquitin process.

Transcription factors and transporters coordinate N-response/NUE

N-response spans thousands of genes and a fraction of those that are additionally associated with yield contribute to NUE as a multi-genic trait (Kumari et al., 2021; Sharma et al., 2021). Identification of the most contributing genes has been a challenge and could be aided by shortlisting them from the functional groups emerging from co-expression analyses, such as transcription factors (TFs), transporters, etc. We searched for the 3020 N-responsive genes among different TF databases and identified 67 classes of TFs encoded by 210 N-responsive genes. They include 26 major classes (≥3 genes) totaling 156 genes and 41 minor classes (¾2 genes)

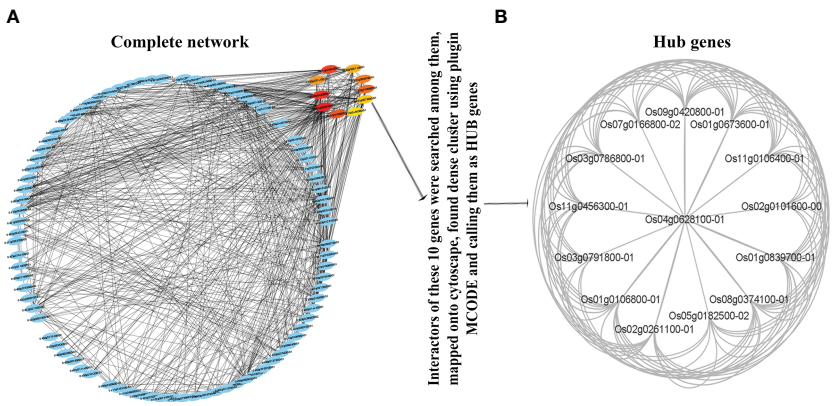

FIGURE 4
Protein-protein interaction (PPI) network and Hub Genes. Network based on functional annotation of the co-expressed genes from the turquoise module. The interactors were identified using STRING database and visualized by Cytoscape based highly significant PPI enrichment score (1.0e-16). **(A)** Interaction modules involved in the associated processes; **(B)** The highly connected genes called as Hub Genes among the interactors of the top 10 genes.

totaling 54 genes (Supplementary Table S9). They are AP2/ERF-ERF, MYB-related, NAC, bZIP, AUX/IAA, PHD, bHLH, C3H, and GRAS among others (Figure 5A; Supplementary Table S9). Among the co-expressed modules, the turquoise module was predominant for transcription factors (55) followed by blue (33), yellow (22), brown (20), pink (16), red (14), and nine others. Gene counts based on Venn analysis of these 210 TFs with predicted NUE-related TFs (Kumari et al., 2021) confirmed 32 of them. Only one of them (Dof1) was previously reported as associated with NUE (Kurai et al., 2011), but our analysis offers many more (31) TFs as candidates to improve N-response/NUE.

N-transporters are important regulators of source-sink dynamics (Tegeder and Masclaux-Daubresse, 2018) and some were indeed associated with NUE (Masclaux-Daubresse et al., 2010; Wang et al., 2018; Wang et al., 2019; Hou et al., 2021, Nazish et al., 2021). We searched for the 3020 N-responsive genes among Rice transporter DB, RAP DB, Transport DB2, and identified 15 major transporter's families (≥3 genes) totaling 92 genes and 32 (≤2 genes) minor transporters families totaling 45 genes (Supplementary Table S10). The top 5 transporter's families are the mitochondrial carrier (MC) family, major facilitator superfamily (MFS), H+- or Na+-translocating F-type, V-type and A-type ATPase (F-ATPase) superfamily, drug/metabolite transporter (DMT) superfamily, ABC transporter superfamily (Figure 5B). Their detailed description has been provided in Supplementary Table S10. Among the coexpressed modules, the turquoise module has maximum transporters followed by blue, brown, pink, black, and others. A Venn analysis comparing these 132 transporters to earlier predicted NUE transporters confirms 17 of them as NUE transporters. Out of the analyzed transporters, AMT1.1 and NRT1.1 were validated in the field for NUE. Thus, our analysis identified several other transporters as potential candidates for improving N-response/NUE.

Protein kinases in N-response/NUE

Protein kinases are known to play an important role in N-response and NUE in crops (Fataftah et al., 2018; Hsieh et al., 2018; Jiang et al., 2018; Perchlik and Tegeder, 2018; Xiong et al., 2019). Here, we identified 98 N-responsive genes encoding 9 kinase families (Figure 5C; Supplementary Table S11) using the database iTak (http://itak.feilab.net/cgi-bin/itak/index.cgi). They are glycogen synthase kinase (GSK) and CDC-like kinase (CLK; CMGC: 27), receptor-like kinases (RLK: 26), Ca2+/calmodulin-dependent protein kinases (CAMK: 22), Tyrosine kinase-like (TKL: 9), casein kinase 1(CK1: 6), AGC (3), serine/threonine protein kinase (STE: 3), a numb-associated family of protein kinases (NAK: 1) and with-no-lysine protein kinases (WNK: 1). Among the coexpressed modules, the turquoise module was predominant for kinases (25) followed by blue (15), brown (11), yellow (10), green (8) and nine others. Venn analysis of these 98 kinases with the previously predicted NUE-related kinases in rice (Kumari et al., 2021) enabled shortlisting of 18 of them as potentially critical for

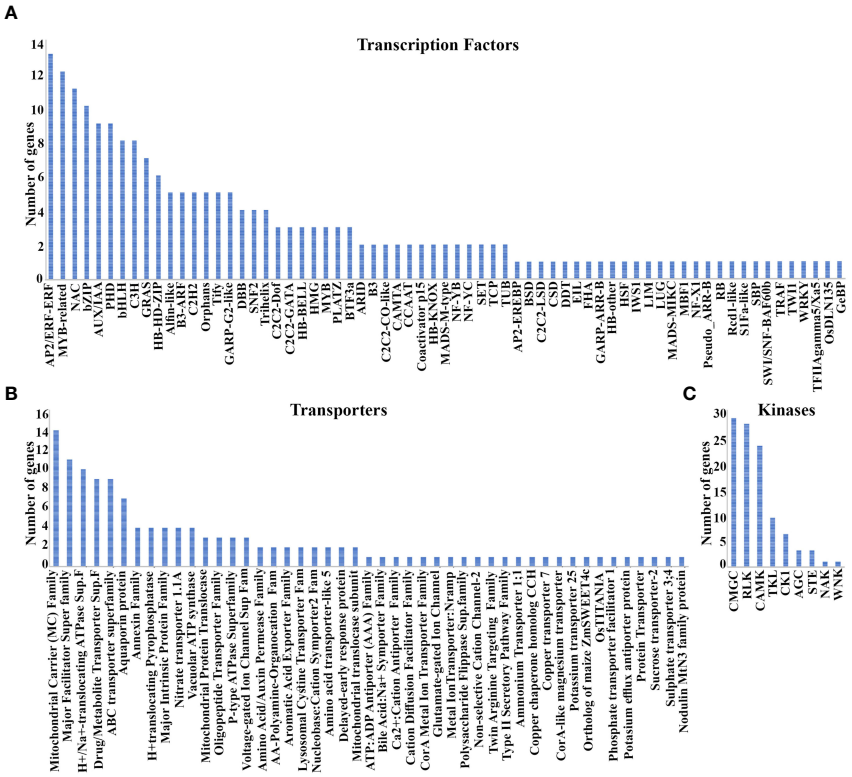

FIGURE 5
Transcription factors, Transporters, and Kinases associated with NUE. **(A)** 67 classes of TFs encoded by 210 N-responsive genes; **(B)** 15 Major and 32 minor transporter gene families identified in 92 and 45 N-responsive genes respectively; **(C)** Nine kinase families identified in 98 N-responsive genes.

NUE. Among them, four kinases namely GUDK, OsBSK3, OSK1, and OSK3 were previously field-validated for yield but not for NUE. Thus, our analysis offers a shortlist of kinases as candidates to improve N-responsive yield and therefore NUE.

miRNAs in N-response/NUE

To understand the role of miRNAs in post-transcriptional regulation of N-response/NUE, targets for miRNAs were searched among the 3020 N-responsive genes using the Plant miRNA database. The search identified 67 unique miRNA targets. The details of their genes and functions along with references are provided in Supplementary Table S12. Their gene ontology analysis by ExPath2.0 revealed the GO terms such as pollen development, splicing, and RNA processing among others (Supplementary Table S12). This indicates the role of these miRNA targets in regulating yield through RNA splicing. Among the coexpressed modules, the turquoise module was predominant for these miRNA targets (15) followed by blue (14), brown (10), magenta (6), and eight others. Venn analysis of these 67 miRNA targets with the previously predicted NUE-related miRNA targets (Kumari et al., 2021) enabled shortlisting of 4 of them as potentially related to NUE. They are, osa-miR1424, osa-miR170a, osa-miR1848 and osa-miR1861. These identified microRNAs have previously been reported to play a role in regulating rice grain development (Lu et al., 2008; Zhu et al., 2008) but not in NUE. Thus, our analysis offers a shortlist of miRNA targets as candidates to improve NUE.

N-regulated post-translational modifications in rice

Initial gene ontology analysis of N-responsive DEGs in Nidhi revealed many terms associated with post-translational modifications (PTM) such as phosphorylation, de-phosphorylation, hydrolase activity, glycosylation, and ubiquitination (Supplementary Table S13). In order to find N-responsive DEG-encoded proteins that can be modified post-translationally, the 3020 N-responsive genes were searched in the PTM viewer database (https://www.psb.ugent.be/webtools/ptm-viewer/experiment.php). We found 1918 gene IDs in the entire WGCNA data, of which the maximum number of PTMs (1056) were found for Lysine 2-Hydroxyisobutyrylation followed by Phosphorylation (651), Lysine Acetylation (102), Carbonylation (71), Ubiquitination (20), N-glycosylation (12), Succinylation (4) and Malonylation (2) (Supplementary Table S13). Gene counts using Venn analyses between these PTM genes and previously predicted NUE-related transcription factor genes in rice (Kumari et al., 2021) shortlisted16 DEGs encoding post-translationally modulated TFsfor NUE. Out of the 16 TFs, 14 (ASD1, DOS, OsbZIP12, OsNAC6, OsHAM2, OsPRR73, OsBIHD1, OsSPL9, OsHDT1, OsABF3, OsARF10, OsFBH1, OsNTL5 and OsMYBS2) underwent post-translational modification by phosphorylation, while the remaining two (OsC3H33 and OsCOL4) were modified by acetylation (Supplementary Table S13).

Similarly, 11 transporters with post-translational modifications were also found. Of these, six (OsLAX1, AMT1.1, OsEIN2, OPT, OsNPF2.4 and OsSUT2(t)) were modified via phosphorylation, while OsPAPST1 and OsABCC1 were modified by 2-Hydroxyisobutyrylation. Additionally, OsBT1-3 and OsABCC13 were modified via acetylation, while OsHT was modified through ubiquitination (Supplementary Table S13). Among the coexpressed modules, the turquoise module was predominant for these PTMs (550) followed by blue (304), brown (233), yellow (169), green (113) and ten others (Supplementary Table S13). Notably, out of these all TFs and transporters identified in this analysis, only one transporter namely AMT1.1 was field-validated for NUE in rice (Ranathunge et al., 2014). This analysis offers many more post-translationally regulated N-responsive genes involved in NUE from coexpression modules.

G-quadruplex sequences could epigenetically regulate N-responsive yield and NUE

To determine the presence of G4 sequences in N-responsive genes, we obtained the complete Oryza sativa G4 sequence data from PlantG4DB. After removing duplicate genes, we identified unique gene IDs that contained G4 sequences and performed Venn Selection with our 3020 N-responsive genes to identify 2298 genes. They were found to be distributed on all 12 chromosomes, though chromosomes 1, 2, and 3 accounted for over 50% of them. A detailed search for G4Q subclasses revealed that 2065 genes contained them in their mRNA/gene region, 1977 in their exons, 1649 in their CDS, 716 in 5'UTRs, 399 in promoters, and 161 in 3'UTR regions (Supplementary Table S14). Their statistical significance was confirmed by Fischer's exact test and the details are provided in Supplementary Table S15. We also found a 17.6% higher occurrence of G4s in the plus/antisense strand compared to the negative/sense strand.

Among the identified WGCNA modules, 674 genes of the turquoise module were found to have G4 sequences followed by blue, brown, and other modules. Their details are presented in Supplementary Table S16. Gene ontology analysis of these N-responsive genes having G4 sequences revealed that they were involved in carbohydrate metabolism, nitrogen transport, signaling, respiration, and water deprivation among others (Supplementary Table S17). As yield association is an important differentiator in N-response and NUE (Sharma et al., 2021), we used a list of 3532 yield related genes compiled from journal literature and online databases as described earlier (Kumari et al., 2021). Their Venn selection with the 2298 genes having G4 sequences revealed 389 genes as both N-responsive and yield associated and therefore NUE-related (Supplementary Table S18). To our knowledge, this is the first shortlisting of G4s genes as important candidates for epigenetic improvement of NUE.

To confirm the differential N-responsiveness of some of these shortlisted genes, we selected 18 NUE-related genes (N-responsive and yield-associated genes) containing different location categories of G4 sequences (5'UTR, 3'UTR, cds, exon, mRNA and promoter)

for further validation by RT-qPCR. The list of primers used in this study is provided in Supplementary Table S19. As negative controls, we used a non-N responsive gene without G4 sequences (Os01g0940000) and a non-N responsive gene with G4 sequences (Os09g0456200). Their expression was nearly unaltered, whether in terms of genotypes or N-treatments (Supplementary Figure 2). In addition, actin was used as an internal housekeeping control for RT-qPCR to test low nitrate response against normal nitrate. Relative to these controls, the expression of 7 test genes was validated for differential expression, either in terms of genotype or nitrate response (Supplementary Figure 2). Interestingly, 4 out of these 7 genes showed contrasting patterns of N-response between contrasting genotypes, while the other 3 showed similar up or downregulation by nitrate in both the genotypes. The genes that showed contrasting patterns were, *OsCYP20-2* (Os05g0103200), *OsGLP2-1* (Os02g0532500), *TubA2* (Os11g0247300) and *OsDXS2* (Os06g0142900), while the other three genes namely *SPDT* (Os06g0143700), OsASNase2 (Os04g0650700) and OsNRT1.1A (Os08g0155400) showed a similar pattern of regulation. These differences in regulation could be of particular interest to further dissect the mechanism of regulation of NUE, or to validate their potential for crop improvement.

G-quadruplex sequences differentiate genes involved in N-response and NUE

G-quadruplex sequences are known in genes that are associated with energy homeostasis, oxidative stress, and signaling pathways such as AMP kinases and TOR kinases (Xu et al., 2010; Robaglia et al., 2012; Dobrenel et al., 2013). TOR kinases have their role in the development of leaf and shoot via the GTPase ROP2 in response to nitrogen (Tulin et al., 2021). Therefore, we propose that nitrogen-responsive genes are important targets for the formation of G-quadruplex sequences and are regulated based on external N-availability. Gene ontology analysis of the N-responsive genes containing G4 sequences reveals their involvement in carbohydrate metabolism, water deprivation, nitrogen transport, respiration, among others (Supplementary Table S17). Interestingly, their Venn selection with the previously reported NUE-related genes revealed that 17% of the N-responsive genes containing G4 sequences are related to yield therefore, NUE. This provides the first ever estimate that upto 17% of the N-responsive genes could participate in NUE through epigenetic regulation mediated by G-quadruplex sequences, subject to further validation. Thus, G4 sequences could provide an effective means for differentiating between N-response and NUE at the gene level. The remaining 83% of them could either use genetic mode of regulation or other forms of epigenetic regulation besides G4Q.

NUE involves better photosynthesis, transpiration, and seed germination in low urea

From the gene ontology (GO) analysis of N-responsive genes containing G4s genes constituting the turquoise co-expression module, photosynthesis transpiration and seed germination were chosen for physiological validation by LICOR, while the genes tested above by RT-qPCR span other processes such as metabolic and abiotic stress processes, apart from chlorophyll and photosynthesis. Using 21 days old potted rice plants, photosynthesis and transpiration were measured on a pair of contrasting rice genotypes namely, Nidhi (low NUE) and Panvel1 (high NUE) using LICOR6400XT as described in materials and methods. Photosynthesis was significantly higher ($P < 0.05$) in low urea (1.5 mM N) over normal urea (15 mM N) for the high NUE genotype Panvel1, while it was lesser in the case of Nidhi (Figure 6A). A similar pattern was also observed for transpiration, though not found to be statistically significant (Figure 6B). In an independent experiment to test N-responsive germination in another high NUE genotype of rice (Vikramarya), surface sterilized and presoaked seeds were grown in Petri plates on moist cotton containing Arnon Hoagland medium (Sharma et al., 2018). The media contained either normal Ndose given as urea (15mM), 50% of normal N (7.5mM), or 10% N (1.5mM). By counting the visibly germinated seeds, it emerged that the highest % germination was found in 10% of normal urea (1.5 mM), followed by 50% N and 100%N (Figure 6C).

Discussion

Several transcriptomic datasets of N-responsive genes are now available in various crops including rice, and they contain a vast amount of valuable information that has yet to be fully utilized. They include the underlying processes, shortlisting of candidate genes, identification of QTLs, miRNAs and their targets (Kumari et al., 2021). Some of them are specific to different sub-species of rice, such as *indica* (Pathak et al., 2020; Sharma et al., 2022), *japonica* (Mandal et al., 2022, others) or different sources of N such as nitrate, ammonium, or urea (Sharma et al., 2021). But together, they span diverse genotypes, N-forms and growth conditions yielding thousands of DEGs and enabling comprehensive meta-analyses. Identification of co-expressed genes/modules by methods such as WGCNA is one of the ways to distill the essence from all these datasets, but so far this was done only with individual N-responsive transcriptomic datasets in rice (Coneva et al., 2014; Zhang et al., 2019; Ueda et al., 2020; Yang et al., 2020b). Therefore, the present study utilized 16 microarray datasets for which the DEGs could be extracted from publicly available datasets and shortlisted 8 of them that shared the largest number of 3020 DEGs for WGCNA and other analyses.

Even though several RNAseq transcriptomes have also been published (SRP253184), very few of them revealed their DEGs and their small number of a few hundred DEGs did not meet the criteria for WGCNA and hence not considered for this study. Our analyses of the 3020 N-responsive DEGs common to 8 transcriptomes included WGCNA for genetic regulation and G-quadruplex sequences and miRNAs for epigenetic regulation to quantify their relative contribution to the NUE trait and to propose a model for its regulation.

Genes with similar expression patterns may participate in similar biological processes or networks. Further, positively coexpressed genes within the same pathway tend to cluster in close proximity within the pathway structure, whereas negatively correlated genes generally occupy more distant positions (Mao

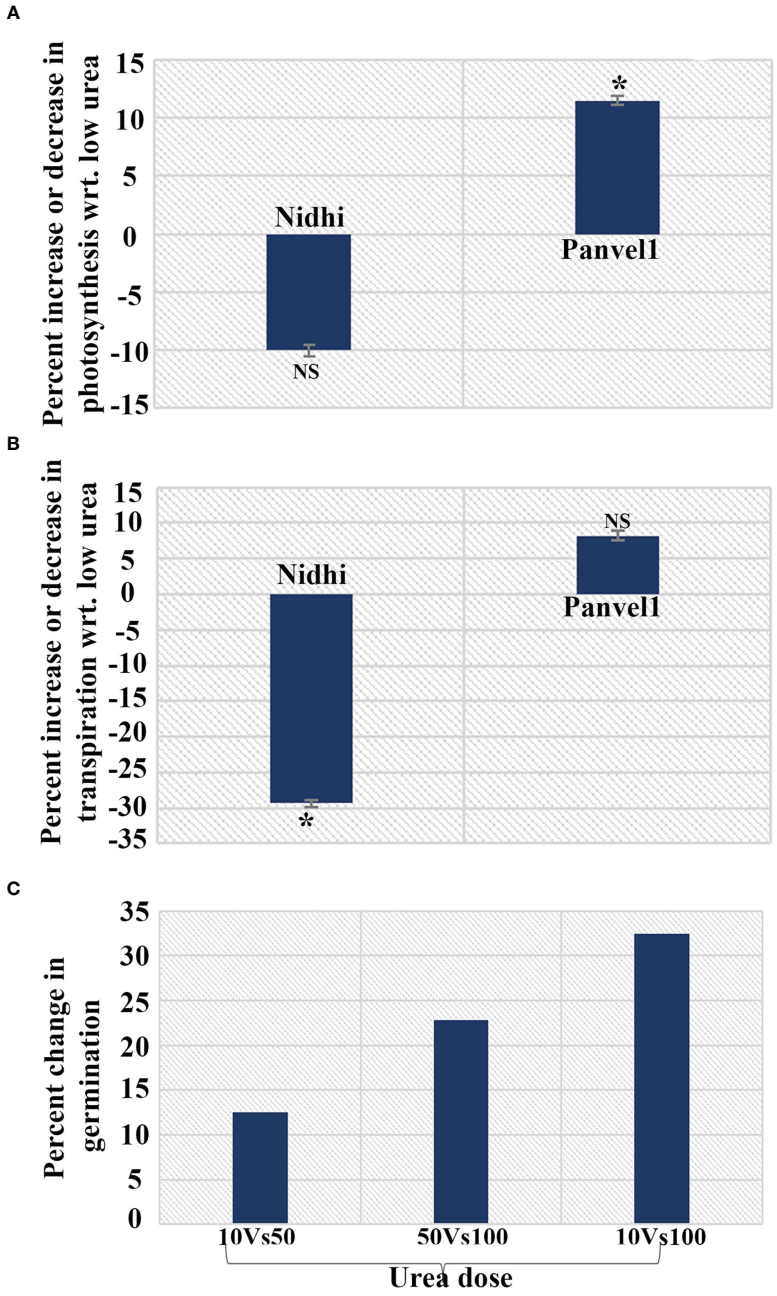

FIGURE 6
N-responsive changes in physiological parameters in a contrasting pair of rice genotypes. Changes measured in **(A)** Photosynthesis; **(B)** Transpiration and **(C)** Germination under low urea and normal conditions in Nidhi (low NUE) and Panvel1 (high NUE) rice genotypes. The test of significance ($P < 0.05$) has been shown as the star, while NS represents non-significance.

et al., 2009). Similar results were found in plants when coexpression networks of 1,330 genes derived from the AraCyc metabolic pathway database of *Arabidopsis thaliana* were analyzed (Wei et al., 2006). Our WGCNA of 3020 N-responsive genes shared by 8 N-responsive microarray datasets yielded 15 modules. The turquoise module had the largest number of 875 genes with the highest significance and proportion of functional categories. Of these, 34% were transporters, 26% TFs, >22% miRNAs, 25.5% kinases, >28% PTMs, and>29% G4 sequences. This module contains the largest number of predicted NUE-related genes by Kumari et al. (2021), apart from the field-validated ammonium transporter and nitrate transporter (OsNPF2.4, Fan et al., 2016). This makes the turquoise module the most suitable one to identify hub genes and important processes for NUE. They include photosynthesis, water transport, and seed germination, which we had earlier shown as important processes for N-response/NUE (Sharma et al., 2018; Kumari et al., 2021; Sharma et al., 2021; Mandal et al., 2022; Sharma et al., 2022).

Gene ontology analyses revealed that biosynthesis and transport of nitrogen, photosynthesis, water deprivation, translation, signal

transduction, respiration and peptide biosynthetic process were prominent biological classes of N-responsive genes (Supplementary Table S4; Figure 2), suggesting the role of nitrogen-responsive genes in respiration, photosynthesis, and water deprivation, etc. These findings extend our experimental observations in *indica* (Sharma et al., 2018; Sharma et al., 2022) Kumari et al. (2021) and *japonica* rice (Mandal et al., 2022), which also indicated the importance of some transcription factors. In this study, we found 210 DEGs encoding transcription factors falling into 67 categories (Supplementary Table S7). A few genes associated with NAC, MYB and GRASS are among the top categories, while DOF and MADS are among the bottom and have been implicated earlier in yield or NUE (Madan et al., 2022). Among them, DOF1 is well-known to improve NUE (Yanagisawa et al., 2004) and ARF4 has been reported to improve yield (Hu et al., 2018). Therefore, it may be attractive to validate the remaining TFs reported here for their role in NUE.

Nitrogen-responsive transporters can uptake either nitrate or ammonium ions, amino acids, or urea through their respective families of transporters for plant growth, development, yield, and NUE (Kumari et al., 2021; Madan et al., 2022; Sharma et al., 2022). In this study, the 132 transporters encoded by urea-responsive genes include 17 that we previously predicted to be involved in NUE (Kumari et al., 2021; Supplementary Table S8). Interestingly, the mitochondrial carrier family tops among the other transporter families and their further characterization, and shortlisting might reveal new targets for NUE.

A common limitation of transcriptomic analyses is that they do not adequately account for the role of post-translational modifications (PTMs) in the response to environmental signals despite their importance in signal transduction. They have also not been explored in N-response till recently (Pei et al., 2019; Wang et al., 2021; Han et al., 2022) and NUE (Sharma et al., 2022). Our bioinformatic analysis revealed 8 types of N-responsive PTMs of 1918 proteins, of which Lysine 2-Hydroxyisobutyrylationemerged as most predominant, followed by phosphorylation for their potential role in N-response/NUE (Supplementary Table S12). Phosphorylation has recently been acknowledged to be a crucial PTM for N response (Han et al., 2022) and NUE (Sharma et al., 2022). Here, we report that the overall targets of PTM in N-response/NUE include 14 transcription factors (Supplementary Table S13) and 6 transporters (Supplementary Table S14).

G4s are considered to act as molecular switches to regulate gene expression in metazoan cells (Eddy and Maizels, 2006). In plants, a few studies have reported the role of G4 sequences, such as in transport and gene expression (Garg et al., 2016), growth and development (Yang et al., 2020b), hydrolase activity (Cagirici et al., 2021), stress response, energy status, and sugar availability (Yadav et al., 2017). Here, we report their role in N-response or NUE for the first time. We found the highest occurrence of G4Q in the turquoise module of N-responsive DEGs in rice. The occurrence of G4s in their mRNAs, exons and CDS suggests their role in the regulation of gene expression (Andorf et al., 2014), while their occurrence in UTRs suggests their role in post-transcriptional regulation (Wang et al., 2015). Among the subtypes of G4s, we found that G2 sequences were >99% in the N-responsive DEGs.

The association of different types of G4s with different genomic regions is considered to suggest their role in different regulatory processes. For example, G2 G4s are implicated in the regulation of transcription and translation (Varshney et al., 2020), while G3 G4s are considered important for promoter regulation (Hegyi, 2015). Gene ontology analysis of all the DEGs containing G4s suggests their involvement in carbohydrate metabolism, nitrogen transport, signaling, respiration, and water deprivation among others (Supplementary Table S17). These observations are in line with the findings of Yadav et al. (2017), who linked G4s with carbohydrate metabolism and water deprivation. Therefore, it is attractive to validate their role in N-response/NUE, for which we provide a prioritized list of 389 G4s-containing genes common to N-response and grain yield (Supplementary Table S18). Further, their regulation needs to be examined in both genetic and epigenetic terms, as G4 sequences are also known to be involved in epigenetic regulation (Cavalieri and Spinelli, 2019; Mukherjee et al., 2019; Reina and Cavalieri, 2020; Wu et al., 2021). Accordingly, the confirmed candidates may be targeted to improve NUE either genetically or epigenetically.

Our RT-qPCR studies validated the nitrate-regulation of seven G4Q harboring genes related to NUE (N-responsive and yield-related) in two Indian rice genotypes (Supplementary Figure 2) that we earlier characterized as contrasting for NUE (Sharma et al., 2018; Sharma et al., 2021). Four of these genes showed contrasting patterns of nitrate regulation between the contrasting genotypes, while the other three genes showed similar up/down regulation between genotypes. These differences in gene expression could be due to genetic and/or epigenetic reasons including G4Q and need further investigation using many more genes in wider germplasm. It also remains to be seen whether post-transcriptional regulation of these genes by G4Qs causes measurable changes in their protein levels and whether they correlate with measurable variation of NUE in the germplasm.

Interestingly, G4 sequences can play a potential role in mitochondria (Falabella et al., 2019) and mitochondrial transporters are emerging as an important class of putative G4s-containing candidates in our study. Further, our earlier findings demonstrated the role of mitochondrial respiration in N-response/NUE (Sharma et al., 2018). Taken together, these two lines of evidence indicate the potentially important role of mitochondria in the epigenetic regulation of N-response/NUE, which was so far attributed only to miRNAs. Further, validation of the role of G4s in mitochondrial regulation of NUE could offer novel means to shortlist candidate genes for crop improvement towards NUE.

Finally, based on our results, we present a model that summarizes the regulatory mechanisms potentially activated by G4 quadruplexes in response to variations in external nitrogen levels (Figure 7). Interestingly, only 17% of the G4s-containing N-responsive genes are found to be related to yield, indicating that only those G4s-containing genes that are both N-responsive and yield-related contribute to NUE. These findings add to our previous

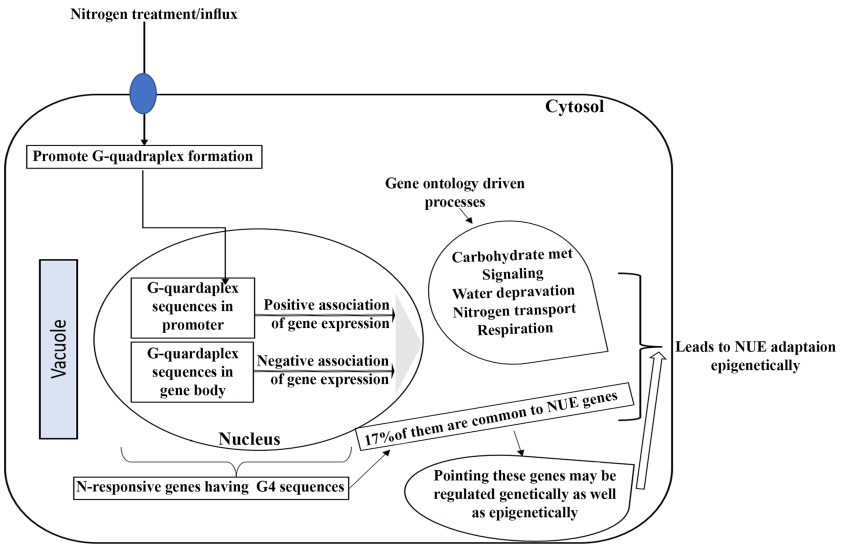

FIGURE 7
A hypothetical model of the underlying regulatory processes that may be triggered by G-quadruplexes in response to change in the availability of external nitrogen.

experimental distinction between N-response at the level of phenotype as well as genotype (Kumari et al., 2021; Sharma et al., 2021; Sharma et al., 2022) and could facilitate the shortlisting of target genes for crop improvement towards NUE as well as to choose between genetic or epigenetic means.

Data availability statement

The original contributions presented in the study are included in the article/Supplementary Material. Further inquiries can be directed to the corresponding author.

Author contributions

NS performed most of the experiments, analyzed the data, and wrote the first draft. BM performed N-responsive gene-trait association and helped in MS drafting. MSK helped in G-quadruplexes experimental design, data analysis, and MS drafting. KS helped WGCNA analysis. NR helped in the planning, mentoring, and supervision of the experiments, data interpretation, editing, and finalizing of the manuscript. All authors read and approved the submitted version.

Funding

We are thankful for research grants from UKRI-GCRF South Asian Nitrogen Hub (SANH) (NE/S009019/1), including a fellowship to NS; GGSIPU FRGS (GGSIPU/DRC/FRGS/2022/1223/14) and CSIR Fellowship to BM {09/806(0038)/2019-EMR-I}. KS acknowledges financial support from the Department of Biotechnology (BT/PR40149/BTIS/137/36/2022).

Conflict of interest

The authors declare that the research was conducted in the absence of any commercial or financial relationships that could be construed as a potential conflict of interest.

Publisher's note

Supplementary material

The Supplementary Material for this article can be found online at: https://www.frontiersin.org/articles/10.3389/fpls.2023.1135675/full#supplementary-material

SUPPLEMENTARY FIGURE 1
Venn selection representing hierarchical shortlisting of N-responsive DEGs used for our WGCNA study.

SUPPLEMENTARY FIGURE 2
RT-qPCR graph showing $\log_2$ fold change values of 7 differentially regulated genes represented as mean± SE in Nidhi and Panvel1 genotypes grown under low-nitrate (1.5 mM) with normal nitrate (15 mM) as control, *OsCYP20-2* (Os05g0103200), *OsGLP2-1* (Os02g0532500), *TubA2* (Os11g0247300), *OsDXS2* (Os06g0142900), *SPDT* (Os06g0143700), *OsASNase2* (Os04g0650700) and *OsNRT1.1A* (Os08g0155400).

References

Amrine, K. C., Blanco-Ulate, B., and Cantu, D. (2015). Discovery of core biotic stress responsive genes in arabidopsis by weighted gene co-expression network analysis. *PloS One* 10 (3), e0118731. doi: 10.1371/journal.pone.0118731

Andorf, C. M., Kopylov, M., Dobbs, D., Koch, K. E., Stroupe, M. E., Lawrence, C. J., et al. (2014). G-Quadruplex (G4) motifs in the maize (Zea mays l.) genome are enriched at specific locations in thousands of genes coupled to energy status, hypoxia, low sugar, and nutrient deprivation. *J. Genet. Genomics* 41 (12), 627–647. doi: 10.1016/j.jgg.2014.10.004

Burge, S., Parkinson, G. N., Hazel, P., Todd, A. K., and Neidle, S. (2006). Quadruplex DNA: sequence, topology and structure. *Nucleic Acids Res.* 34(19), 5402–5415.doi: 10.1093/nar/gkl655

Cagirici, H. B., Budak, H., and Sen, T. Z. (2021). Genome-wide discovery of G-quadruplexes in barley. *Sci. Rep.* 11 (1), 1–15. doi: 10.1038/s41598-021-86838-3

Cagirici, H. B., and Sen, T. Z. (2020). Genome-wide discovery of G-quadruplexes in wheat: distribution and putative functional roles. *G3 (Bethesda Md.)* 10 (6), 2021–2032. doi: 10.1534/g3.120.401288

Cavalieri, V., and Spinelli, G. (2019). "Histone-mediated transgenerational epigenetics," in *Transgenerational epigenetics* (Academic Press, UK), 157–183.

Chang, Y. M., Lin, H. H., Liu, W. Y., Yu, C. P., Chen, H. J., Wartini, P. P., et al. (2019). Comparative transcriptomics method to infer gene coexpression networks and its applications to maize and rice leaf transcriptomes. *Proc. Natl. Acad. Sci.* 116 (8), 3091–3099. doi: 10.1073/pnas.1817621116

Chen, J., Zhang, Y., Tan, Y., Zhang, M., Zhu, L., Xu, G., et al. (2016). Agronomic nitrogen-use efficiency of rice can be increased by driving os NRT 2.1 expression with the os NAR 2.1 promoter. *Plant Biotechnol. J.* 14 (8), 1705–1715. doi: 10.1111/pbi.12531

Chien, C. H., Chow, C. N., Wu, N. Y., Chiang-Hsieh, Y. F., Hou, P. F., and Chang, W. C. (2015). December. EXPath: a database of comparative expression analysis inferring metabolic pathways for plants. in. *BMC Genomics* 16 (2), 1–10. doi: 10.1186/1471-2164-16-S2-S6

Coneva, V., Simopoulos, C., Casaretto, J. A., El-Kereamy, A., Guevara, D. R., Cohn, J., et al. (2014). Metabolic and co-expression network-based analyses associated with nitrate response in rice. *BMC Genomics* 15 (1), 1–14. doi: 10.1186/1471-2164-15-1056

Dobrenel, T., Marchive, C., Azzopardi, M., Clément, G., Moreau, M., Sormani, R., et al. (2013). Sugar metabolism and the plant target of rapamycin kinase: a sweet operaTOR? *Front. Plant Sci.* 4, 93. doi: 10.3389/fpls.2013.00093

Eddy, J., and Maizels, N. (2006). Gene function correlates with potential for G4 DNA formation in the human genome. *Nucleic Acids Res.* 34 (14), 3887–3896. doi: 10.1093/nar/gkl529

Falabella, M., Fernandez, R. J., Johnson, F. B., and Kaufman, B. A. (2019). Potential roles for G-quadruplexes in mitochondria. *Curr. Medicinal Chem.* 26 (16), 2918–2932. doi: 10.2174/0929867325666180228165527

Fan, X., Tang, Z., Tan, Y., Zhang, Y., Luo, B., Yang, M., et al. (2016). Overexpression of a pH-sensitive nitrate transporter in rice increases crop yields. *Proc. Natl. Acad. Sci.* 113 (26), 7118–7123. doi: 10.1073/pnas.1525184113

Fataftah, N., Mohr, C., Hajirezaei, M. R., Wirén, N. V., and Humbeck, K. (2018). Changes in nitrogen availability lead to a reprogramming of pyruvate metabolism. *BMC Plant Biol.* 18 (1), 1–15. doi: 10.1186/s12870-018-1301-x

Garg, R., Aggarwal, J., and Thakkar, B. (2016). Genome-wide discovery of G-quadruplex forming sequences and their functional relevance in plants. *Scientific reports* 6(1), 28211.

Griffin, B. D., and Bass, H. W. (2018). Plant G-quadruplex (G4) motifs in DNA and RNA; abundant, intriguing sequences of unknown function. *Plant Sci.* 269, 143–147. doi: 10.1016/j.plantsci.2018.01.011

Han, R. C., Xu, Z. R., Li, C. Y., Rasheed, A., Pan, X. H., Shi, Q. H., et al. (2022). The removal of nitrate reductase phosphorylation enhances tolerance to ammonium nitrogen deficiency in rice. *J. Integr. Agric.* 21 (3), 631–643. doi: 10.1016/S2095-3119(20)63473-6

He, D., Wang, Q., Li, M., Damaris, R. N., Yi, X., Cheng, Z., et al. (2016). Global proteome analyses of lysine acetylation and succinylation reveal the widespread involvement of both modification in metabolism in the embryo of germinating rice seed. *J. Proteome Res.* 15 (3), 879–890. doi: 10.1021/acs.jproteome.5b00805

Hegyi, H. (2015). Enhancer-promoter interaction facilitated by transiently forming G-quadruplexes. *Sci. Rep.* 5, 9165. doi: 10.1038/srep09165

Hoagland, D. R., and Arnon, D. I. (1950). *The water-culture method for growing plants without soil. circular* Vol. 347 (USA: California agricultural experiment station).

Hou, Y., Qiu, J., Wang, Y., Li, Z., Zhao, J., Tong, X., et al. (2017). A quantitative proteomic analysis of brassinosteroid-induced protein phosphorylation in rice (Oryza sativa l.). *Front. Plant Sci.* 8, 514. doi: 10.3389/fpls.2017.00514

Hou, M., Yu, M., Li, Z., Ai, Z., and Chen, J. (2021). Molecular regulatory networks for improving nitrogen use efficiency in rice. *International Journal of Molecular Sciences* 22(16), 9040.

Hsieh, P. H., Kan, C. C., Wu, H. Y., Yang, H. C., and Hsieh, M. H. (2018). Early molecular events associated with nitrogen deficiency in rice seedling roots. *Sci. Rep.* 8 (1), 1–23. doi: 10.1038/s41598-018-30632-1

Hu, Z., Lu, S. J., Wang, M. J., He, H., Sun, L., Wang, H., et al. (2018). A novel QTL qTGW3 encodes the GSK3/SHAGGY-like kinase OsGSK5/OsSK41 that interacts with OsARF4 to negatively regulate grain size and weight in rice. *Mol. Plant* 11 (5), 736–749. doi: 10.1016/j.molp.2018.03.005

Huang, W., Nie, H., Feng, F., Wang, J., Lu, K., and Fang, Z. (2019). Altered expression of OsNPF7. 1 and OsNPF7. 4 differentially regulates tillering and grain yield in rice. *Plant Sci.* 283, 23–31. doi: 10.1016/j.plantsci.2019.01.019

Islam, W., Tauqeer, A., Waheed, A., and Zeng, F. (2022). MicroRNA mediated plant responses to nutrient stress. *Int. J. Mol. Sci.* 23 (5), 2562. doi: 10.3390/ijms23052562

Jiang, L., Ball, G., Hodgman, C., Coules, A., Zhao, H., and Lu, C. (2018). Analysis of gene regulatory networks of maize in response to nitrogen. *Genes* 9 (3), 151. doi: 10.3390/genes9030151

Kang, W. H., Lee, J., Koo, N., Kwon, J. S., Park, B., Kim, Y. M., et al. (2022). Universal gene co-expression network reveals receptor-like protein genes involved in broad-spectrum resistance in pepper (Capsicum annuum l.). *Horticulture Res.* 9. doi: 10.1093/hr/uhab003

Kanter, D. R., Winiwarter, W., Bodirsky, B. L., Bouwman, L., Boyer, E., Buckle, S., et al. (2020). A framework for nitrogen futures in the shared socioeconomic pathways. *Global Environ. Change* 61, 102029. doi: 10.1016/j.gloenvcha.2019.102029

Kawahara, Y., de la Bastide, M., Hamilton, J. P., Kanamori, H., McCombie, W. R., Ouyang, S., et al. (2013). Improvement of the oryza sativa nipponbare reference genome using next generation sequence and optical map data. *Rice* 6 (1), 1–10. doi: 10.1186/1939-8433-6-4

Kopec, P. M., and Karlowski, W. M. (2019). Sequence dynamics of pre-mRNA G-quadruplexes in plants. *Front. Plant Sci.* 10, 812. doi: 10.3389/fpls.2019.00812

Kumari, S., Sharma, N., and Raghuram, N. (2021). Meta-analysis of yield-related and n-responsive genes reveals chromosomal hotspots, key processes and candidate genes for nitrogen-use efficiency in rice. *Front. Plant Sci.* 12, 627955. doi: 10.3389/fpls.2021.627955

Kurai, T., Wakayama, M., Abiko, T., Yanagisawa, S., Aoki, N., and Ohsugi, R. (2011). Introduction of the ZmDof1 gene into rice enhances carbon and nitrogen assimilation under low-nitrogen conditions. *Plant Biotechnol. J.* 9 (8), 826–837. doi: 10.1111/j.1467-7652.2011.00592.x

Kurata, N., and Yamazaki, Y. (2006). Oryzabase. an integrated biological and genome information database for rice. *Plant Physiol.* 140 (1), 12–17. doi: 10.1104/pp.105.063008

Li, A., Hu, B., and Chu, C. (2021). Epigenetic regulation of nitrogen and phosphorus responses in plants. *J. Plant Physiol.* 258, 153363. doi: 10.1016/j.jplph.2021.153363

Li, M., Tian, R., Monchaud, D., and Zhang, W. (2022). Omics studies of DNA G-/C-quadruplexes in plants. *Trends Genet.* 10, 999–1002. doi: 10.1016/j.tig.2022.06.005

Li, J. Y., Wang, J., and Zeigler, R. S. (2014). The 3,000 rice genomes project: new opportunities and challenges for future rice research. *Gigascience* 3 (1), 2047–217X. doi: 10.1186/2047-217X-3-8

Li, Y., Xiao, J., Chen, L., Huang, X., Cheng, Z., Han, B., et al. (2018). Rice functional genomics research: past decade and future. *Mol. Plant* 11 (3), 359–380. doi: 10.1016/j.molp.2018.01.007

Livak, K. J., and Schmittgen, T. D. (2001). Analysis of relative gene expression data using real-time quantitative PCR and the 2−ΔΔCT method. *Methods* 25, 402–408. doi: 10.1006/meth.2001.1262

Long, S. P., Marshall, A. M., and Zhu, X. G. (2015). Engineering crop photosynthesis and yield potential to meet global food demand of 2050. *Cell* 161, 56–66. doi: 10.1016/j.cell.2015.03.019

Lu, C., Jeong, D. H., Kulkarni, K., Pillay, M., Nobuta, K., German, R., et al. (2008). Genome-wide analysis for discovery of rice microRNAs reveals natural antisense microRNAs (nat-miRNAs). *Proc. Natl. Acad. Sci. U. S. A.* 105, 4951–4956. doi: 10.1073/pnas.0708743105

Lu, C., Pu, Y., Liu, Y., Li, Y., Qu, J., Huang, H., et al. (2019). Comparative transcriptomics and weighted gene co-expression correlation network analysis (WGCNA) reveal potential regulation mechanism of carotenoid accumulation in chrysanthemum× morifolium. *Plant Physiol. Biochem.* 142, 415–428. doi: 10.1016/j.plaphy.2019.07.023

Madan, B., Malik, A., and Raghuram, N. (2022). "Crop nitrogen use efficiency for sustainable food security and climate change mitigation," in *Plant nutrition and food security in the era of climate change* (UK: Academic Press, Elsevier), 47–72.

Mandal, V. K., Jangam, A. P., Chakraborty, N., and Raghuram, N. (2022). Nitrate-responsive transcriptome analysis reveals additional genes/processes and associated traits viz. height, tillering, heading date, stomatal density and yield in japonica rice. *Planta* 255 (2), 1–19. doi: 10.1007/s00425-021-03816-9

Mandal, V. K., Sharma, N., and Raghuram, N. (2018). "Molecular targets for improvement of crop nitrogen use efficiency: current and emerging options," in *Engineering nitrogen utilization in crop plants* (Cham: Springer), 77–93.

Mao, L., Van Hemert, J. L., Dash, S., and Dickerson, J. A. (2009). Arabidopsis gene co-expression network and its functional modules. *BMC Bioinformatics*. 10, 346. doi: 10.1186/1471-2105-10-346

Masclaux-Daubresse, C., Daniel-Vedele, F., Dechorgnat, J., Chardon, F., Gaufichon, L., and Suzuki, A. (2010). Nitrogen uptake, assimilation and remobilization in plants:

challenges for sustainable and productive agriculture. *Ann. Bot.* 105 (7), 1141–1157. doi: 10.1093/aob/mcq028

Meng, X., Xing, S., Perez, L. M., Peng, X., Zhao, Q., Redoña, E. D., et al. (2017). Proteome-wide analysis of lysine 2-hydroxyisobutyrylation in developing rice (*Oryza sativa*) seeds. *Sci. Rep.* 7 (1), 1–11. doi: 10.1038/s41598-017-17756-6

Møller, I. M., and Kristensen, B. K. (2006). Protein oxidation in plant mitochondria detected as oxidized tryptophan. *Free Radical Biol. Med.* 40 (3), 430–435. doi: 10.1016/j.freeradbiomed.2005.08.036

Móring, A., Hooda, S., Raghuram, N., Adhya, T. K., Ahmad, A., Bandyopadhyay, S. K., et al. (2021). Nitrogen challenges and opportunities for agricultural and environmental science in India. *Front. Sustain. Food Syst.* 5, 505347. doi: 10.3389/fsufs.2021.505347

Mujahid, H., Meng, X., Xing, S., Peng, X., Wang, C., and Peng, Z. (2018). Malonylome analysis in developing rice (Oryza sativa) seeds suggesting that protein lysine malonylation is well-conserved and overlaps with acetylation and succinylation substantially. *J. Proteomics* 170, 88–98. doi: 10.1016/j.jprot.2017.08.021

Mukherjee, A. K., Sharma, S., and Chowdhury, S. (2019). Non-duplex G-quadruplex structures emerge as mediators of epigenetic modifications. *Trends Genet.* 35 (2), 129–144. doi: 10.1016/j.tig.2018.11.001

Nakagami, H., Sugiyama, N., Mochida, K., Daudi, A., Yoshida, Y., Toyoda, T., et al. (2010). Large-Scale comparative phosphoproteomics identifies conserved phosphorylation sites in plants. *Plant Physiol.* 153 (3), 1161–1174. doi: 10.1104/pp.110.157347

Nazish, T., Arshad, M., Jan, S. U., Javaid, A., Khan, M. H., Naeem, M. A., et al. (2021). Transporters and transcription factors gene families involved in improving nitrogen use efficiency (NUE) and assimilation in rice (Oryza sativa L.). *Transgenic Research*. 31(1), 23–42. doi: 10.1007/s11248-021-00284-5

Neeraja, C. N., Barbadikar, K. M., Krishnakanth, T., Bej, S., Rao, I. S., Srikanth, B., et al. (2021). Down regulation of transcripts involved in selective metabolic pathways as an acclimation strategy in nitrogen use efficient genotypes of rice under low nitrogen. *3 Biotech.* 11 (2), 1–15. doi: 10.1007/s13205-020-02631-5

Nischal, L., Mohsin, M., Khan, I., Kardam, H., Wadhwa, A., Abrol, Y. P., et al. (2012). Identification and comparative analysis of microRNAs associated with low-n tolerance in rice genotypes. *PloS One* 7 (12), e50261. doi: 10.1371/journal.pone.0050261

Norton, R., Davidson, E., and Roberts, T. (2015). Nitrogen use efficiency and nutrient performance indicators. *Global Partnership Nutrient Manage.* 14. Available at: https://wedocs.unep.org/20.500.11822/10750

Pathak, R. R., Jangam, A. P., Malik, A., Sharma, N., Jaiswal, D. K., and Raghuram, N. (2020). Transcriptomic and network analyses reveal distinct nitrate responses in light and dark in rice leaves (*Oryza sativa* indica var. Panvel1). *Sci. Rep.* 10 (1), 1–17. doi: 10.1038/s41598-020-68917-z

Pei, W., Jain, A., Ai, H., Liu, X., Feng, B., Wang, X., et al. (2019). OsSIZ2 regulates nitrogen homeostasis and some of the reproductive traits in rice. *J. Plant Physiol.* 232, 51–60. doi: 10.1016/j.jplph.2018.11.020

Perchlik, M., and Tegeder, M. (2018). Leaf amino acid supply affects photosynthetic and plant nitrogen use efficiency under nitrogen stress. *Plant Physiol.* 178 (1), 174–188. doi: 10.1104/pp.18.00597

Qiu, J., Hou, Y., Tong, X., Wang, Y., Lin, H., Liu, Q., et al. (2016). Quantitative phosphoproteomic analysis of early seed development in rice (Oryza sativa l.). *Plant Mol. Biol.* 90 (3), 249–265. doi: 10.1007/s11103-015-0410-2

Qiu, J., Hou, Y., Wang, Y., Li, Z., Zhao, J., Tong, X., et al. (2017). A comprehensive proteomic survey of ABA-induced protein phosphorylation in rice (Oryza sativa l.). *Int. J. Mol. Sci.* 18 (1), 60. doi: 10.3390/ijms18010060

Raghuram, N., Aziz, T., Kant, S., Zhou, J., and Schmidt, S. (2022). Nitrogen use efficiency and sustainable nitrogen management in crop plants. *Front. Plant Sci.* 13. doi: 10.3389/978-2-88974-284-4

Raghuram, N., Sutton, M. A., Jeffery, R., Ramachandran, R., and Adhya, T. K. (2021). From south Asia to the world: embracing the challenge of global sustainable nitrogen management. *One Earth* 4 (1), 22–27. doi: 10.1016/j.oneear.2020.12.017

Ranathunge, K., El-Kereamy, A., Gidda, S., Bi, Y. M., and Rothstein, S. J. (2014). AMT1;1 transgenic rice plants with enhanced NH4 + permeability show superior growth and higher yield under optimal and suboptimal NH4+ conditions. *J. Exp. Bot.* 65, 965–979. doi: 10.1093/jxb/ert458

Reina, C., and Cavalieri, V. (2020). Epigenetic modulation of chromatin states and gene expression by G-quadruplex structures. *Int. J. Mol. Sci.* 21 (11), 4172. doi: 10.3390/ijms21114172

Robaglia, C., Thomas, M., and Meyer, C. (2012). Sensing nutrient and energy status by SnRK1 and TOR kinases. *Curr. Opin. Plant Biol.* 15 (3), 301–307. doi: 10.1016/j.pbi.2012.01.012

Ruprecht, C., Vaid, N., Proost, S., Persson, S., and Mutwil, M. (2017). Beyond genomics: studying evolution with gene coexpression networks. *Trends Plant Sci.* 22 (4), 298–307. doi: 10.1016/j.tplants.2016.12.011

Sengupta, A., Roy, S. S., and Chowdhury, S. (2021). Non-duplex G-quadruplex DNA structure: a developing story from predicted sequences to DNA structure-dependent epigenetics and beyond. *Accounts Chem. Res.* 54 (1), 46–56. doi: 10.1021/acs.accounts.0c00431

Séré, D., and Martin, A. (2020). Epigenetic regulation: another layer in plant nutrition. *Plant Signal Behav.* 15 (1), 1–6. doi: 10.1080/15592324.2019.1686236

Shao, X., Zhang, W., Umar, M. I., Wong, H. Y., Seng, Z., Xie, Y., et al. (2020). RNA G-Quadruplex structures mediate gene regulation in bacteria. *mBio* 11 (1), e02926–e02919. doi: 10.1128/mBio.02926-19

Sharma, N., Jaiswal, D. K., Kumari, S., Dash, G. K., Panda, S., Anandan, A., et al. (2023). Genomewide urea response in rice genotypes contrasting for nitrogen use efficiency. *Int. J. Mol. Sci.* 24 (7), 6080. doi: 10.3390/ijms24076080

Sharma, N., Kuchi, S., Singh, V., and Raghuram, N. (2019). Method for preparation of nutrient-depleted soil for determination of plant nutrient requirements. *Commun. Soil Sci. Plant Anal.* 50 (15), 1878–1886. doi: 10.1080/00103624.2019.1648492

Sharma, N., Kumari, S., Jaiswal, D. K., and Raghuram, N. (2022). Comparative transcriptomic analyses of nitrate-response in rice genotypes with contrasting nitrogen use efficiency reveals common and genotype-specific processes, molecular targets and nitrogen use efficiency-candidates. *Front. Plant Sci.* 13. doi: 10.3389/fpls.2022.881204

Sharma, N., Sinha, V. B., Gupta, N., Rajpal, S., Kuchi, S., Sitaramam, V., et al. (2018). Phenotyping for nitrogen use efficiency: rice genotypes differ in n-responsive germination, oxygen consumption, seed urease activities, root growth, crop duration, and yield at low n. *Front. Plant Sci.* 9, 1452. doi: 10.3389/fpls.2018.01452

Sharma, N., Sinha, V. B., Prem Kumar, N. A., Subrahmanyam, D., Neeraja, C. N., Kuchi, S., et al. (2021). Nitrogen use efficiency phenotype and associated genes: roles of germination, flowering, root/shoot length and biomass. *Front. Plant Sci.* 11, 587464. doi: 10.3389/fpls.2020.587464

Sinha, V. B., Jangam, A. P., and Raghuram, N. (2020). "Biological determinants of crop nitrogen use efficiency and biotechnological avenues for improvement," in *Just enough nitrogen* (Cham: Springer), 157–171.

Sun, B., Zhou, X., Chen, C., Chen, C., Chen, K., Chen, M., et al. (2020). Coexpression network analysis reveals an MYB transcriptional activator involved in capsaicinoid biosynthesis in hot peppers. *Horticulture Res.* 7. doi: 10.1038/s41438-020-00381-2

Sutton, M. A., Howard, C. M., Kanter, D. R., Lassaletta, L., Móring, A., Raghuram, N., et al. (2021). The nitrogen decade: mobilizing global action on nitrogen to 2030 and beyond. *One Earth* (Nairobi:UNEP) 4 (1), 10–14. doi: 10.1016/j.oneear.2020.12.016

Sutton, M., Raghuram, N., Adhya, T. K., Baron, J., Cox, C., de Vries, W., et al. (2019). "The nitrogen fix: from nitrogen cycle pollution to nitrogen circular economy-frontiers 2018/19: emerging issues of environmental concern chapter 4," in *Frontiers 2018/19: emerging issues of environmental concern*. (UNEP, Nairobi)

Szklarczyk, D., Franceschini, A., Wyder, S., Forslund, K., Heller, D., Huerta-Cepas, J., et al. (2015). STRING v10: protein-protein interaction networks, integrated over the tree of life. *Nucleic Acids Res.* 43, D447–52. doi: 10.1093/nar/gku1003

Tegeder, M., and Masclaux-Daubresse, C. (2018). Source and sink mechanisms of nitrogen transport and use. *New Phytol.* 217(1), 35–53.

Tulin, F., Zhang, Z., and Wang, Z. Y. (2021). Activation of TOR signaling by diverse nitrogen signals in plants. *Dev. Cell* 56 (9), 1213–1214. doi: 10.1016/j.devcel.2021.04.014

Udvardi, M., Below, F. E., Castellano, M. J., Eagle, A. J., Giller, K. E., Ladha, J. K., et al. (2021). A research road map for responsible use of agricultural nitrogen. *Front. Sustain. Food Syst.* 5, 660155. doi: 10.3389/fsufs.2021.660155

Ueda, Y., Ohtsuki, N., Kadota, K., Tezuka, A., Nagano, A. J., Kadowaki, T., et al. (2020). Gene regulatory network and its constituent transcription factors that control nitrogen-deficiency responses in rice. *New Phytol.* 227 (5), 1434–1452. doi: 10.1111/nph.16627

Varshney, D., Spiege, J., Zyner, K., Tannahill, D., and Balasubramanian, S. (2020). The regulation and functions of DNA and RNA G-quadruplexes. *Nat. Rev. Mol. Cell Biol.* 21 (8), 459–474. doi: 10.1038/s41580-020-0236-x

Wang, Y., Hou, Y., Qiu, J., Li, Z., Zhao, J., Tong, X., et al. (2017). A quantitative acetylomic analysis of early seed development in rice (Oryza sativa l.). *Int. J. Mol. Sci.* 18 (7), 1376. doi: 10.3390/ijms18071376

Wang, W., Hu, B., Yuan, D., Liu, Y., Che, R., Hu, Y., et al. (2018). Expression of the nitrate transporter gene OsNRT1. 1A/OsNPF6. 3 confers high yield and early maturation in rice. *Plant Cell* 30 (3), 638–651. doi: 10.1105/tpc.17.00809

Wang, W., Li, A., Zhang, Z., and Chu, C. (2021). Posttranslational modifications: regulation of nitrogen utilization and signaling. *Plant Cell Physiol.* 62 (4), 543–552. doi: 10.1093/pcp/pcab008

Wang, J., Wu, B., Lu, K., Wei, Q., Qian, J., Chen, Y., et al. (2019). The amino acid permease 5 (OsAAP5) regulates tiller number and grain yield in rice. *Plant Physiol.* 180 (2), 1031–1045. doi: 10.1104/pp.19.00034

Wang, Y., Zhao, M., Zhang, Q., Zhu, G. F., Li, F. F., and Du, L. F. (2015). Genomic distribution and possible functional roles of putative G-quadruplex motifs in two subspecies of oryza sativa. *Comput. Biol. Chem.* 56, 122–130. doi: 10.1016/j.compbiolchem.2015.04.009

Wei, H., Persson, S., Mehta, T., Srinivasasainagendra, V., Chen, L., Page, G. P., et al. (2006). Transcriptional coordination of the metabolic network in arabidopsis. *Plant Physiol.* 142 (2), 762–774. doi: 10.1104/pp.106.080358

Winiwarter, W., Amon, B., Bodirsky, B. L., Friege, H., Geupel, M., Lassaletta, L., et al. (2022). Focus on reactive nitrogen and the UN sustainable development goals. *Environ. Res. Lett.* 17 (5), 050401. doi: 10.1088/1748-9326/ac6226

Wu, F., Niu, K., Cui, Y., Li, C., Lyu, M., Ren, Y., et al. (2021). Genome-wide analysis of DNA G-quadruplex motifs across 37 species provides insights into G4 evolution. *Commun. Biol.* 4, 98. doi: 10.1038/s42003-020-01643-4

Xie, X., Kang, H., Liu, W., and Wang, G. L. (2015). Comprehensive profiling of the rice ubiquitome reveals the significance of lysine ubiquitination in young leaves. *J. Proteome Res.* 14 (5), 2017–2025. doi: 10.1021/pr5009724

Xiong, H., Guo, H., Zhou, C., Guo, X., Xie, Y., Zhao, L., et al. (2019). A combined association mapping and t-test analysis of SNP loci and candidate genes involving in resistance to low nitrogen traits by a wheat mutant population. *PloS One* 14 (1), e0211492. doi: 10.1371/journal.pone.0211492

Xiong, Y., Peng, X., Cheng, Z., Liu, W., and Wang, G. L. (2016). A comprehensive catalog of the lysine-acetylation targets in rice (Oryza sativa) based on proteomic analyses. *J. Proteomics* 138, 20–29. doi: 10.1016/j.jprot.2016.01.019

Xu, X. M., Lin, H., Maple, J., Björkblom, B., Alves, G., Larsen, J. P., et al. (2010). The arabidopsis DJ-1a protein confers stress protection through cytosolic SOD activation. *J. Cell Sci.* 123 (10), 1644–1651. doi: 10.1242/jcs.063222

Yadav, V., Kim, N., Tuteja, N., and Yadav, P. (2017). G Quadruplex in plants: a ubiquitous regulatory element and its biological relevance. *Front. Plant Sci.* 8, 1163. doi: 10.3389/fpls.2017.01163

Yanagisawa, S., Akiyama, A., Kisaka, H., and Miwa, T. (2004). Metabolic engineering with Dof1 transcription factor in plants: Improved nitrogen assimilation and growth under low-nitrogen conditions. *Proc. Natl. Acad. Sci.*. 101(20), 7833–7838. doi: 10.1073/pnas.040226710

Yang, X., Cheema, J., Zhang, Y., Deng, H., Duncan, S., Umar, M. I., et al. (2020b). RNA G-Quadruplex structures exist and function *in vivo* in plants. *Genome Biol.* 21 (1), 1–23. doi: 10.1186/s13059-020-02142-9

Yang, X., Xia, X., Zeng, Y., Nong, B., Zhang, Z., Wu, Y., et al. (2020a). Genome-wide identification of the peptide transporter family in rice and analysis of the PTR expression modulation in two near-isogenic lines with different nitrogen use efficiency. *BMC Plant Biol.* 20 (1), 1–15. doi: 10.1186/s12870-020-02419-y

Ying, J., Zhao, J., Hou, Y., Wang, Y., Qiu, J., Li, Z., et al. (2017). Mapping the n-linked glycosites of rice (Oryza sativa l.) germinating embryos. *PloS One* 12 (3), e0173853. doi: 10.1371/journal.pone.0173853

Zhang, H., He, D., Yu, J., Li, M., Damaris, R. N., Gupta, R., et al. (2016). Analysis of dynamic protein carbonylation in rice embryo during germination through AP-SWATH. *Proteomics* 16 (6), 989–1000. doi: 10.1002/pmic.201500248

Zhang, X., Zhou, J., Huang, N., Mo, L., Lv, M., Gao, Y., et al. (2019). Transcriptomic and co-expression network profiling of shoot apical meristem reveal contrasting response to nitrogen rate between indica and japonica rice subspecies. *Int. J. Mol. Sci.* 20 (23), 5922. doi: 10.3390/ijms20235922

Zheng, J., He, C., Qin, Y., Lin, G., Park, W. D., Sun, M., et al. (2019). Co-Expression analysis aids in the identification of genes in the cuticular wax pathway in maize. *Plant J.* 97 (3), 530–542. doi: 10.1111/tpj.14140

Zhu, Q. H., Spriggs, A., Matthew, L., Fan, L., Kennedy, G., Gubler, F., et al. (2008). A diverse set of microRNAs and microRNA-like small RNAs in developing rice grains. *Genome Res.* 18 (9), 1456–1465. doi: 10.1101/gr.075572.107

Zhu, M., Xie, H., Wei, X., Dossa, K., Yu, Y., Hui, S., et al. (2019). WGCNA analysis of salt-responsive core transcriptome identifies novel hub genes in rice. *Genes* 10 (9), 719. doi: 10.3390/genes10090719

frontiers | Frontiers in Plant Science

TYPE Original Research
PUBLISHED 20 November 2023
DOI 10.3389/fpls.2023.1268739

OPEN ACCESS

EDITED BY
Surya Kant,
La Trobe University, Australia

REVIEWED BY
Yousef Alhaj Hamoud,
Hohai University, China
Mohammad Abu Saleque,
Bangladesh Rice Research Institute, Bangladesh

*CORRESPONDENCE
Chirravuri Naga Neeraja
cnneeraja@gmail.com

RECEIVED 28 July 2023
ACCEPTED 05 October 2023
PUBLISHED 20 November 2023

CITATION
Srikanth B, Subrahmanyam D, Sanjeeva Rao D, Narender Reddy S, Supriya K, Raghuveer Rao P, Surekha K, Sundaram RM and Neeraja CN (2023) Promising physiological traits associated with nitrogen use efficiency in rice under reduced N application. *Front. Plant Sci.* 14:1268739. doi: 10.3389/fpls.2023.1268739

Promising physiological traits associated with nitrogen use efficiency in rice under reduced N application

Bathula Srikanth[1,2], Desiraju Subrahmanyam[1], Durbha Sanjeeva Rao[1], Sadu Narender Reddy[2], Kallakuri Supriya[2], Puskur Raghuveer Rao[1], Kuchi Surekha[1], Raman Meenakshi Sundaram[1] and Chirravuri Naga Neeraja[1]*

[1]ICAR-Indian Institute of Rice Research, Hyderabad, India, [2]Professor Jayashankar Telangana State Agricultural University, Hyderabad, India

Higher grain yield in high-yielding rice varieties is mostly driven by nitrogen (N) fertilizer applied in abundant amounts leading to increased production cost and environmental pollution. This has fueled the studies on nitrogen use efficiency (NUE) to decrease the N fertilizer application in rice to the possible extent. NUE is a complex physiological trait controlled by multiple genes, but yet to be completely deciphered in rice. With an objective of identifying the promising physiological traits associated with NUE in rice, the performance of 14 rice genotypes was assessed at N0, N50, N100, and N150 for four (two wet and two dry) seasons using agro-morphological, grain yield, flag leaf traits, photosynthetic pigment content, flag leaf gas exchange traits, and chlorophyll fluorescence traits. Furthermore, the data were used to derive various NUE indices to identify the most appropriate indices useful to screen rice genotypes at N50. Results indicate that with the increase in N application, cumulative grain yield increased significantly up to N100 (5.02 t ha^{-1}); however, the increment in grain yield was marginal at N150 (5.09 t ha^{-1}). The mean reduction of grain yield was only 26.66% at N50 ranging from 15.0% to 34.2%. The significant finding of the study is the identification of flag leaf chlorophyll fluorescence traits (F_v/F_m, ΦPSII, ETR, and qP) and C_i associated with grain yield under N50, which can be used to screen N use efficient genotypes in rice under reduced N application. Out of nine NUE indices assessed, NUpE, NUtE, and NUE_{yield} were able to delineate the high-yielding genotypes at N50 and were useful to screen rice under reduced N conditions. Birupa emerged as one of the high yielders under N50, even though it is a moderate yielder at N100 and infers the possibility of cultivating some of the released rice varieties under reduced N inputs. The study indicates the possibility of the existence of promising genetic variability for grain yield under reduced N, the potential of flag leaf chlorophyll fluorescence, and gas exchange traits as physiological markers and best suitable NUE indices to be deployed in rice breeding programs.

KEYWORDS

maximum quantum yield of PSII, actual quantum yield of PSII, electron transport rate, nitrogen use efficiency, nitrogen, rice

Introduction

Rice, a grain crop, is the prime source of food for more than half of the global population (Ogawa et al., 2016; Lee, 2021). Owing to the development of high-yielding cultivars, and the application of chemical fertilizers, rice production has been continuously improved during the last 50 years, keeping pace with the increasing global population (FAO, 2018). Nitrogen (N) is one of the key nutrient elements required for growth and development of rice. However, soil N content in agricultural land cannot sustain the higher yields of improved rice varieties. Hence, the application of N fertilizer has become unavoidable to enhance rice yield (Wang et al., 2022). However, most of the fertilizers applied in agriculture is the main source of environmental losses of reactive N compounds contributing to N pollution globally (Sutton et al., 2013) as well as in South Asia (Raghuram et al., 2021). Global N fertilizer consumption has already exceeded 110 million tons per year (Hu et al., 2023). The excess application of N fertilizers is more intense in China and India, which account for nearly 50% of the global rice production and consumption (Muthayya et al., 2014).

In India, from 1961 to 2013, the percentage N fertilizer application in total N input in production of cereal crops enhanced from 8%–10% to 71%–75% (Sapkota et al., 2023). As price of fertilizers are at record levels and may remain elevated, there has been a huge burden on the country's economy. In parallel to the higher N fertilizer application, nitrogen use efficiency (NUE) has also been observed to be decreasing continuously and is evolving to be a major problem in restraining production of rice. In 2013, NUE was in the range of 20%–24% (except 32% for wheat) due to several-fold increase in the use of N fertilizers and imbalanced usage of fertilizer nutrients (Sapkota et al., 2023). In China, the average application rate of N fertilizer has reached 180 kg/hm^2, which is 75% higher than the world average. However, the NUE is only 28%–35%, which is 15%–20% lower than that of the global average NUE (Liu et al., 2013; Han et al., 2015). It is projected that only 30% to 50% of the applied N fertilizer is utilized by rice (Ladha et al., 2020), thus resulting in enormous N leaching, and increased soil acidification and water eutrophication, leading to N-related environmental pollution, which is also a concern for climate change. In addition to the crop production practices targeting NUE, developing N efficient rice varieties to reduce the global climate change impacts should be one of the major research objectives (Neeraja et al., 2016). Reducing the cost of production and minimizing the environmental pollution through loss of N in field by using rice cultivars having higher NUE that can reduce the application of N fertilizers without a greater reduction in grain yield to feed the ever-increasing global population are need of the hour (Ciampitti and Vyn, 2011; Sharma and Bali, 2017).

India faces a dual challenge with N in terms of both food and the environment. On the one hand, India consumes 17 million tons of N fertilizer each year, which represents 14% of the global total. On the other hand, since the green revolution in 1970, the use of N fertilizer has increased at an annual rate of approximately 6% (Sutton et al., 2017). In 2022–2023, the Government of India allocated US$7.6 billion for urea subsidies. India loses US$10 billion worth of reactive N each year as fertilizer value. India is second only to China in terms of N production and consumption (Tewatia and Chanda, 2017). Studies on NUE in India began two to three decades ago in order to achieve sustainable agriculture (Abrol et al., 2007; Abrol et al., 2008; Galloway et al., 2008). As most of the genetic potential to enhance NUE lies unutilized in the germplasm of agricultural crops, focus should be on screening and utilizing them to improve NUE rather than for N-responsive yield alone (Metson et al., 2021). At the Indian Council of Agricultural Research-Indian Institute of Rice Research (ICAR-IIRR), screening of indigenous and exotic rice germplasm, varieties, landraces, and advanced breeding lines at various N levels was carried out as part of National Innovations on Climate Resilient Agriculture (NICRA), Newton-Bhabha Virtual Centre on Nitrogen Efficiency of Whole-cropping Systems for improved performance and resilience in agriculture (NEWS India-UK) and South Asian Nitrogen Hub (SANH) projects. Donors with promising performance at 50% of the recommended N level were identified and mapping populations were established (Subrahmanyam et al., 2019). Some promising breeding lines for NUE were tested under All India Coordinated Rice Improvement Project (AICRIP) across multiple locations from 2018 and identified for NUE in rice.

NUE can be enhanced agronomically up to a certain level, beyond which biological crop improvement alone can break the barrier for further improvement (Chakraborty and Raghuram, 2011). Based on this insight, research on the biological basis of N-response and NUE in diverse crops gained momentum (Raghuram and Sharma, 2019). Understanding physiological processes of the plant controlling N utilization under various N management practices is vital to improve NUE (Ciampitti and Vyn, 2011; Sharma and Bali, 2017). NUE is a multigenic quantitative trait, involving various N-responsive mechanisms that are yet to be fully characterized (Mandal et al., 2022). Earlier studies have documented the association between N application rate on crop photosynthetic traits, NUE, and yield (Makino et al., 2003; Paponov and Engels, 2003; Yang et al., 2010; Kong et al., 2016; Liu et al., 2019; Ochieng' et al., 2021; Shah et al., 2021). Photosynthesis is the plant's most crucial process for growth, biomass production, and yield (Chen et al., 2018). Two of the key traits to determine photosynthetic capacity are specific leaf area and leaf N content (Hikosaka, 2004; Poorter et al., 2009), which enhances chlorophyll content, enzyme content, and enzyme activity, and ultimately improves photosynthetic efficiency (Giersch and Robinson, 1987; Nasar et al., 2020; Noor Shah et al., 2021; Ochieng' et al., 2021). Chlorophyll is highly sensitive to variations in the N content in the soil as a great part (70% of leaf N) of N was reported to part of the pigment's composition (Paul, 1990; Kopsell et al., 2004; Fathi and Zeidali, 2021; Moenirad et al., 2021).

Photosynthetic rate (Pn) and photosynthetic nitrogen use efficiency (PNUE), which is the ratio of Pn to leaf N content, are the two primary attributes affecting the photosynthesis and nutrient utilization by plant leaves (Nasar et al., 2022). Furthermore, PNUE also reflects the N allocation and the overall photosynthesis of the plant (Zhong et al., 2019; Nasar et al., 2021). The greater the photosynthetic rate, the higher the PNUE and the leaf N utilization rate of the plant (Ghannoum et al., 2005). Therefore, studying the photosynthesis and PNUE of the plant is a crucial way

to reveal its effect on NUE of the crops. The reduced quantum yield under N deficiency situations can be ascribed to the reduced photosynthetic capacity of the plant, which is due to the reduction of the production of key enzymes like Rubisco in the photosynthesis process (Qi et al., 2013). In contrast, sufficient N in the plant enhances quantum yield through enhancing leaf area index and photosynthetic electron transfer chain (Qi et al., 2013; Moenirad et al., 2021). Hence, plant breeding programs should emphasize on improving the N uptake, utilization, and remobilization of plant-available N (Laperche et al., 2006).

In rice, the relationship between leaf traits and NUE is yet to be characterized (Xin et al., 2022). Similarly, plant traits associated with N-efficient varieties have not been completely explored (Zhu et al., 2022). In order to identify the physiological traits associated with NUE in rice under reduced application, a set of 14 genotypes with varying yield potential were assessed under four graded levels of N (N0, N50, N100, and N150) for four seasons by deploying agro-morphological, grain yield, flag leaf traits, photosynthetic pigment content, flag leaf gas exchange traits, chlorophyll fluorescence traits, and NUE indices as criteria.

Materials and methods

Plant materials and seasons

Based on studies conducted earlier under NEWS project, genotypes with varying yield potential, *viz*., Anjali, Birupa, Daya, Heera, Indira, Nidhi, N22, Tella Hamsa, VL Dhan 209, Vasumati, IR64, GQ25, Varadhan, and MTU 1010, were selected for characterization of their physiological traits. Details of rice genotypes used in the study are given in Table 1. The trial was conducted at ICAR-IIRR farm during four seasons [Kharif-2020 (wet), Rabi-2021 (dry), Kharif-2021 (wet), and Rabi-2022 (dry)]. For the two wet seasons, seeds were sown in the month of June and seedlings were transplanted in the month of July. For the two dry seasons, seeds were sown in the month of December and seedlings were transplanted in the month of January. N was applied in the form of urea in three equal splits at the basal stage, maximum vegetative stage, and panicle initiation stage. Crop was cultivated by following the standard package of practices of crop production and crop protection.

Meteorological data

Important weather parameters recorded during the crop growing period is given in Table 2. During wet season 2020, mean maximum temperature was 30.7°C while mean minimum temperature was 21.9°C. The mean relative humidity was 93.4%, with a total rainfall of 1,375.6 mm and mean bright sunshine hours was 4.8 h day^{-1}. During dry season 2021, mean maximum temperature was 32.4°C while mean minimum temperature was 16.1°C. The mean relative humidity was 87.5%, with a total rainfall of 16.8 mm and mean bright sunshine hours was 7.9 h day^{-1}. During wet season 2021, mean maximum temperature was 30.7°C while mean minimum temperature was 22.6°C. The mean relative humidity was 93.9%, with a total rainfall of 823.8 mm and mean

TABLE 1 Details of rice genotypes included in the study.

S. No.	Name	Parentage	Year of release	Duration	Ecosystem
1.	Anjali (IET-16430)	PR-19-2 x RR-149-1129	2002	90-95	Rain fed Direct Seeded
2.	Birupa (IET-8620)	ADT-27 x IR-8 x Annapurna	1994	130-135	Irrigated Medium and Rain fed Lands
3.	Daya (OR-131-13-13)	Kumar x CR-57-49	1985	120-125	Irrigated Medium
4.	Heera (IET-10973)	CR-404-48 x Cr-289-1208	1989	65-68	Rainfed Upland
5.	Indira CR MUT587-4 (IET2412)	Tainan 3 mutant	1980	125	Irrigated
6.	Nidhi (IET-9994)	Sona x ARC-14529	1997	120-125	Irrigated Early
7	N22 (Nagina-22)	A selection from Rajbhog	1978	85-102	Promising germplasm identified with tolerance to biotic and abiotic stresses
8	Tella Hamsa	HR-12 x T(N)1	1975	110-115	Irrigated
9	IR64 (IET-9671)	IR-5857-33- 2-1 x IR-2061-465- 1-5-5	1991	115-120	Irrigated
10	GQ25 (INGR20001) Restorer line	(Samba Mahsuri/SC5126-3-2-4)	2011	130-135	Irrigated
11	Varadhan	Swarna x 9314)/BR 827-35	2008	125	Irrigated
12	MTU 1010 (IET-15644)	Krishnaveni x IR-64	2000	120	Irrigated Medium Lands
13	Vasumati (IET 15391 RP3135-17-12-8-8)	PR-109/Pakistani Basmati selection from local collection	2002	135	Irrigated
14	VL Dhan 209	Himdhan/K39 / VL Dhan 211	2006	160- 165	Rainfed

TABLE 2 Important weather parameters recorded during crop growing period at IIRR, Hyderabad.

Weather Parameter	2020-21		2021-22	
	Kharif (Wet)	Rabi (dry)	Kharif (Wet)	Rabi (dry)
Mean Max.Temperature (°C)	30.7	32.4	30.7	32.5
Mean Min.Temperature (°C)	21.9	16.1	22.6	17.3
Mean Relative Humidity (%)	93.4	87.5	93.9	84.4
Total Rainfall (mm)	1375.6	16.8	823.8	14.0
Mean Sunshine duration (h day^{-1})	4.8	7.9	5.0	7.5

bright sunshine hours was 5.0 h day^{-1}. During dry season 2022, mean maximum temperature was 32.5°C while mean minimum temperature was 17.3°C. The mean relative humidity was 84.4%, a total rainfall of 14.0 mm was received, and mean bright sunshine hours was 7.5 h day^{-1}.

Soil analysis and experimental design

The experimental plot soil was clay in texture, slightly alkaline (pH 8.25), non-saline (EC - 0.76 dS/m), and medium in organic carbon content (0.53%). Soil available nitrogen was low (213 kg/ha) with high available phosphorus (92 kg/ha) and potassium (641 kg/ha). Experiments were arranged in a split-plot design with nitrogen application rates as the main plot and genotypes as the subplot with three replications. The size of each plot was 15 m^2 (5.0 m long, 3.0 m wide, and 12 rows with a 25-cm row spacing). Four graded levels of N, *viz.*, N150 [150% recommended dose of N (RDN)—150 kg N ha^{-1}], N100 (100% RDN—100 kg N ha^{-1}), N50 (50% RDN—50 kg N ha^{-1}) and N0 (0% RDN—0 kg N ha^{-1}), were used.

Morpho-physiological traits and grain yield

The number of days taken for 50% of plants to flower in each genotype and each treatment was noted as days to 50% flowering and was expressed in days. The number of days taken from sowing to physiological maturity was recorded and was expressed in days. The flag leaf traits along with SLA and SLW were measured from five randomly selected leaves per plot in three replications during 50% flowering stage (Kumar et al., 2021). Flag leaf length was measured from top to bottom of leaf and width was measured at the widest leaf part using ruler and flag leaf area was calculated using the formula given by (Quarrie and Jones, 1979).

$$\text{Flag leaf area} = \text{Flag leaf length} \times \text{Flag leaf width} \times 0.75$$

Flag leaf thickness is measured using a digital caliper and expressed in millimeters (mm). The flag leaves were oven dried after measuring length, width, and thickness for 3 days at 80°C and flag leaf dry weight was recorded using an electronic balance (Sartorius, Germany). Specific leaf area (SLA) was calculated by dividing leaf area with leaf dry weight, employing the formula of Kvet (1971), and expressed in cm^2 g^{-1}. Specific leaf weight (SLW) was determined by dividing leaf dry weight with leaf area, using the formula of Pearce (1968) and expressed in mg cm^{-2}.

At physiological maturity, plots of 1 m^2 area were harvested and threshed grain weight was determined after drying to 14% moisture content and converted to t ha^{-1} and straw weight was also recorded for the same (Kumar et al., 2021). Total dry matter was calculated as sum of the dry weights of the plant components and converted to t ha^{-1} (Amanullah and Inamullah, 2016).

Photosynthetic pigment content

For the quantitative determination of leaf chlorophyll content, at 50% flowering stage, five plants were randomly chosen in each plot and the flag leaf was labeled to investigate gas exchange traits and photosynthetic pigment content. For the determination of pigment content, leaf tissue of each sample was cut into small pieces with a sharp razor blade and 25 mg of cut leaf pieces was placed into 10-mL tubes containing 10 mL of 80% acetone and stored in the dark for 48 h to ensure complete extraction of leaf chlorophyll pigment. The absorbance of the chlorophyll solution was measured by using a UV-VIS double beam spectrophotometer (Evolution 201, Thermo Scientific, USA). Chlorophyll a, chlorophyll b, and carotenoids were measured at 663.2, 646.8, and 470.0 nm, respectively, and expressed in mg g^{-1} fresh weight (fw). The content of chlorophyll a, chlorophyll b, total chlorophyll, and carotenoids were calculated as per the formulas given by Lichtenthaler and Wellburn (1983).

Flag leaf gas exchange traits

Gas exchange traits in flag leaf such as photosynthetic rate (Pn), stomatal conductance (g_s), transpiration rate (E), and internal CO_2 concentration (C_i) were recorded at 50% flowering stage by using the Infra-Red Gas Analyzer portable photosynthesis measurement system (6400XT, LICOR, USA) attached to a leaf chamber fluorometer, which was used as the light source. During measurements, the photosynthetically active radiation (PAR) was kept at 1,200 µmol m^{-2} s^{-1}. The CO_2 concentration was maintained at 387 ± 6 ppm. These measurements were made between 10:00 a.m. and 12.00 noon at all the sampling dates. Pn was expressed in µmol (CO_2) m^{-2} s^{-1}, g_s was expressed in mol (H_2O) m^{-2} s^{-1}, E was

expressed in mmol (H_2O) m^{-2} s^{-1}, and C_i was expressed in ppm. PNUE was calculated as given by Ye et al. (2019a).

Chlorophyll fluorescence characteristics

Chlorophyll fluorescence traits were measured with MINI PAM-II Photosynthesis Yield Analyzer (Heinz Walz GmbH, Germany) during 50% flowering stage. The instrument was connected to a desktop PC with WinControl-3 software. The flag leaves were dark-adapted for 30 min before recording fluorescence traits and the following fluorescence traits were calculated: the maximum quantum yield of PSII (F_v/F_m), actual quantum yield of PSII (ΦPSII), electron transport rate (ETR), coefficient of photochemical quenching (qP), and coefficient of non-photochemical quenching (qN) (Maxwell and Johnson, 2000).

Nitrogen content estimation and NUE indices

Flag leaf samples collected at 50% flowering stage were used to determine flag leaf N content, and grain and straw samples were collected from 1 m^2 area at harvest. Samples were dried under shade and then in hot air oven at 60°C. Oven-dried samples were ground to fine powder using a grinder and stored in butter paper covers for estimating N concentration. The samples were digested in sulfuric acid (H_2SO_4) using block digestion unit and analyzed for their total N content by the micro Kjeldahl distillation method using automatic N analyzer (Kjeltec 8400 Analyzer FOSS, Denmark) with steam distillation and the N content was expressed as percentage. NUE indices such as nitrogen uptake efficiency (NUpE), nitrogen utilization efficiency (NUtE), nitrogen use efficiency$_{yield}$ (NUE_{yield}), agronomic efficiency (AE), physiology efficiency (PE), partial factor productivity (PFP), apparent nitrogen recovery efficiency (ANRE), and nitrogen harvest index (NHI) were calculated as per formulas given in Congreves et al. (2021) and nitrogen utilization index (NUI) was calculated as per the formula given in Huang et al. (2018).

$$NUpE = \frac{Plant\ \ N}{Fertilizer\ \ N + Soil\ \ N}\ x\ \ 100$$

$$NUtE = \frac{Yield}{Plant\ \ N}$$

$$NUE_{yield} = NUpE\ \ x\ \ NUtE$$

$$AE = \frac{Yield_f - Yield_0}{Fertilizer\ \ N}$$

$$PE = \frac{Yield_f - Yield_0}{Plant\ \ N_f - Plant\ \ N_0}$$

$$PFP = \frac{Yield_f}{Fertilizer\ \ N}$$

$$ANRE = \frac{Plant\ \ N_f - Plant\ \ N_0}{Fertilizer\ \ N}\ x\ \ 100$$

$$NHI = \frac{Yield\ \ N}{Plant\ \ N}\ x\ \ 100$$

$$NUI = \frac{Total\ \ dry\ \ matter}{Plant\ \ N}$$

where Plant N is the amount of N in a plant, Yield N is the amount of grain N in a plant, Plant N_f is the amount of N in a fertilized plant, Plant N_0 is the amount of N in a non-fertilized plant, $Yield_f$ is the grain yield of a fertilized plant, and $Yield_0$ is the grain yield of a non-fertilized plant.

Statistical analysis

Two-way analysis of variance (ANOVA) was performed using an open source software R (R Core Team, 2012) with Agricolae package (de Mendiburu, 2012). Statistical significance of the parameters means was determined by performing Fisher's LSD test to test the statistical significance.

Results

ANOVA indicates that 29 morpho-physiological traits including grain yield and N uptake traits noted significant variation with treatment and among the genotypes (Table 3). Interaction between treatment and genotypes was significant except for E, chlorophyll a, total chlorophyll, and carotenoids. Season × genotypes was significant except for flag leaf thickness, SLA, SLW, and F_v/F_m. Season × treatment was significant for Pn, g_s, E, days to 50% flowering, days to physiological maturity, chlorophyll a, total chlorophyll, carotenoids, PNUE, total dry matter, grain N uptake, straw N uptake, and total N uptake. Season × treatment × genotypes was significant for g_s, E, days to physiological maturity, and photosynthetic pigments. Among the NUE indices, ANOVA showed significant effect of treatment and variation among genotypes and interaction between treatment and genotypes. Three indices (NUtE, NUE_{yield}, and NUI) noted significant interaction for season × treatment and six indices (ANRE, NUpE, NUtE, NUE_{yield}, NUI, and NHI) noted significant interaction for season × genotypes. Significant interaction was not observed in any of the indices for season × treatment × genotypes.

Cumulative data of four seasons

Morpho-physiological traits and grain yield

The genotype-wise values of all the measured traits of the study are presented in Tables 4–7. The range and mean values of morpho-physiological traits along with grain yield and NUE indices at various grades of N fertilizer application are presented in Table 8. Mean grain yield significantly increased from 2.82 to 5.09 t ha^{-1} and

TABLE 3 ANOVA for morpho-physiological parameters, grain yield and nitrogen use efficiency indices.

		Grain Yield			Total dry matter			Days to 50% Flowering			Days to maturity			Flag leaf length			Flag leaf width		
EFFECT	Df	Mean Sq	F value	Pr(>F)	Mean Sq	F value	Pr(>F)	Mean Sq	F value	Pr(>F)	Mean Sq	F value	Pr(>F)	Mean Sq	F value	Pr(>F)	Mean Sq	F value	Pr(>F)
Season (S)	3	1.381			8.982			779.26			351.34			150.23			0.703		
Rep x Season	6	0.054			0.369			0.34			0.43			1.2			0.002		
Treatment (T)	3	204.141	1479.63	0.0000**	451.062	185.28	0.0000**	670.04	392.33	0.0000**	677.41	104.74	0.0000**	2527.06	1152.8	0.0000**	2.225	688.36	0.0000**
S x T	9	0.138	1.95	0.0922	2.434	9.86	0.0000**	1.71	2.37	0.0442*	6.47	3.28	0.0095**	2.19	2.14	0.066	0.003	1.47	0.2163
Error (T)	24	0.071			0.247			0.72			1.97			1.02			0.002		
Genotypes (G)	13	15.432	73.51	0.0000**	56.804	49.06	0.0000**	4420.04	90.3	0.0000**	2951.57	41.17	0.0000**	342.23	46.44	0.0000**	0.295	15.22	0.0000**
S x G	39	0.21	2.46	0.0000**	1.158	3.56	0.0000**	48.61	53.35	0.0000**	71.69	53.78	0.0000**	7.37	2.58	0.0000**	0.019	1.69	0.0074**
T x G	39	0.83	13.37	0.0000**	3.146	11.26	0.0000**	1.42	2.51	0.0001**	2.73	1.57	0.0333*	13.12	12.06	0.0000**	0.014	3	0.0000**
S x T x G	117	0.062	0.73	0.9802	0.279	0.86	0.8379	0.56	0.62	0.9989	1.73	1.3	0.0332*	1.09	0.38	1	0.005	0.41	1
Residual	416	0.085			0.325			0.91			1.33			2.86			0.011		
Total	671	1.348			3.707			95.74			67.4			21.86			0.029		
CV (%)		6.41			5.27			0.86			1.1			3.28			3.31		

		Flag leaf area			Flag leaf thickness			Flag leaf dry weight			Specific leaf area			Specific leaf weight			Chlorophyll a content		
EFFECT	Df	Mean Sq	F value	Pr(>F)	Mean Sq	F value	Pr(>F)	Mean Sq	F value	Pr(>F)	Mean Sq	F value	Pr(>F)	Mean Sq	F value	Pr(>F)	Mean Sq	F value	Pr(>F)
Season (S)	3	524.51			0.0074			0.00786			1177.8			0.414			16.367		
Rep x Season	6	3.08			0.0003			0.00002			50.7			0.022			0.019		
Treatment (T)	3	7787.13	2133.39	0.0000**	0.2696	1069.59	0.0000**	0.07705	1826.99	0.0000**	31447.6	249.38	0.0000**	12.431	270.42	0.0000**	46.847	248.79	0.0000**
S x T	9	3.65	2.12	0.0687	0.0003	0.8	0.6211	0.00004	1.07	0.4177	126.1	2.04	0.0787	0.046	1.7	0.1449	0.188	4.38	0.0018**
Error (T)	24	1.72			0.0003			0.00004			61.8			0.027			0.043		
Genotypes (G)	13	767.81	31.48	0.0000**	0.02	278.07	0.0000**	0.01483	47.29	0.0000**	244.7	2.49	0.0141*	0.095	2.58	0.0111*	0.907	6.9	0.0000**
S x G	39	24.39	2.39	0.0000**	0.0001	0.41	0.9994	0.00031	2.12	0.0002**	98.4	1.24	0.1572	0.037	1.16	0.2377	0.132	3.31	0.0000**
T x G	39	25.25	5.55	0.0000**	0.0009	4.32	0.0000**	0.0004	7.34	0.0000**	229.8	3.72	0.0000**	0.091	3.9	0.0000**	0.077	1.41	0.0837
S x T x G	117	4.55	0.45	1	0.0002	1.16	0.1455	0.00005	0.37	1	61.7	0.78	0.9469	0.023	0.74	0.9761	0.054	1.37	0.0136*
Residual	416	10.19			0.0002			0.00015			79.2			0.032			0.04		
Total	671	62.18			0.0018			0.00081			234.2			0.092			0.351		
CV (%)		3.96			5.43			4.28			3.5			3.68			8.81		

		Chlorophyll b content			Total chlorophyll content			Carotenoid content			Photosynthetic rate			Stomatal conductance			Transpiration rate		
EFFECT	Df	Mean Sq	F value	Pr(>F)	Mean Sq	F value	Pr(>F)	Mean Sq	F value	Pr(>F)	Mean Sq	F value	Pr(>F)	Mean Sq	F value	Pr(>F)	Mean Sq	F value	Pr(>F)
Season (S)	3	2.414			30.508			1.305			112.17			0.2295			16.14		
Rep x Season	6	0.009			0.052			0.002			0.83			0.0026			0.19		
Treatment (T)	3	6.379	357.74	0.0000**	87.79	373.5	0.0000**	2.799	111.1	0.0000**	3233.33	260.81	0.0000**	6.088	135.99	0.0000**	401.41	148.61	0.0000**
S x T	9	0.018	1.74	0.1345	0.235	2.79	0.0216*	0.025	4.86	0.0009**	12.4	9.36	0.0000**	0.0448	10.35	0.0000**	2.7	6.67	0.0000**
Error (T)	24	0.01			0.084			0.005			1.33			0.0043			0.4		

(Continued)

10.3389/fpls.2023.1268739

TABLE 3 Continued

		Chlorophyll b content			Total chlorophyll content			Carotenoid content			Photosynthetic rate			Stomatal conductance			Transpiration rate		
EFFECT	Df	Mean Sq	F value	Pr(>F)	Mean Sq	F value	Pr(>F)	Mean Sq	F value	Pr(>F)	Mean Sq	F value	Pr(>F)	Mean Sq	F value	Pr(>F)	Mean Sq	F value	Pr(>F)
Genotypes (G)	13	0.176	6.24	0.0000**	1.738	7.97	0.0000**	0.062	2.91	0.0049**	33.89	5.84	0.0000**	0.0576	2.83	0.0060**	5.43	2.33	0.0207*
S x G	39	0.028	3.54	0.0000**	0.218	3.06	0.0000**	0.021	4.99	0.0000**	5.8	3.82	0.0000**	0.0204	3.94	0.0000**	2.33	3.83	0.0000**
T x G	39	0.03	1.53	0.0439*	0.14	1.45	0.06835	0.012	1.35	0.1108	2.67	1.53	0.0429*	0.0125	1.6	0.0282*	1.03	1.31	0.1352
S x T x G	117	0.02	2.47	0.0000**	0.097	1.36	0.0158*	0.009	2.16	0.0000**	1.75	1.15	0.1632	0.0078	1.5	0.0019**	0.79	1.29	0.0349*
Residual	416	0.008			0.071			0.004			1.52			0.0052			0.61		
Total	671	0.055			0.651			0.026			17.58			0.0366			2.74		
CV (%)		14.13			9.45			10.71			5.48			12.63			9.29		
		Internal CO_2 concentration			Flag leaf N content			Photosynthetic NUE			Maximum quantum yield of PSII			Actual quantum yield of PSII			Electron transport rate		
EFFECT	Df	Mean Sq	F value	Pr(>F)	Mean Sq	F value	Pr(>F)	Mean Sq	F value	Pr(>F)	Mean Sq	F value	Pr(>F)	Mean Sq	F value	Pr(>F)	Mean Sq	F value	Pr(>F)
Season (S)	3	3014.2			4.685			423.85			0.01104			0.1293			96.24		
Rep x Season	6	74.6			0.014			1.19			0.00006			0.0014			2.78		
Treatment (T)	3	17442.3	38.61	0.0000**	18.603	90.53	0.0000**	1170	73.9	0.0000**	0.02683	372.77	0.0000**	0.2283	227.85	0.0000**	1259.42	276.28	0.0000**
S x T	9	451.8	0.72	0.6887	0.205	5.66	0.0003**	15.83	4.88	0.0009**	0.00007	0.86	0.5706	0.001	0.73	0.6801	4.56	1.34	0.2672
Error (T)	24	630.2			0.036			3.24			0.00008			0.0014			3.39		
Genotypes (G)	13	4995.8	2.45	0.0153*	1.142	3.58	0.0010**	81.2	3.4	0.0015**	0.00097	9.27	0.0000**	0.0056	2.45	0.0156*	19.07	1.75	0.0892
S x G	39	2036.8	3.14	0.0000**	0.32	7.02	0.0000**	23.85	5.37	0.0000**	0.00011	0.84	0.7385	0.0023	2.14	0.0001**	10.92	2.85	0.0000**
T x G	39	723.8	1.61	0.0269*	0.035	2.12	0.0011**	4.77	1.77	0.0101*	0.00016	4.01	0.0000**	0.0011	2.57	0.0000**	5.04	3.29	0.0000**
S x T x G	117	449.4	0.69	0.9911	0.016	0.36	1	2.69	0.61	0.9993	0.00004	0.33	1	0.0004	0.38	1	1.54	0.4	1
Residual	416	649.4			0.046			4.44			0.00012			0.0011			3.83		
Total	671	868.4			0.182			13.94			0.00029			0.0027			10.22		
CV (%)		9.42			7.47			9.65			1.13			10.55			7.43		
		Coefficient of photochemical quenching			Coefficient of non- photochemical quenching			Grain N Uptake			Straw N Uptake			Total N Uptake			Agronomic efficiency			Physiological efficiency		
EFFECT	Df	Mean Sq	F value	Pr(>F)	Mean Sq	F value	Pr(>F)	Mean Sq	F value	Pr(>F)	Mean Sq	F value	Pr(>F)	Mean Sq	F value	Pr(>F)	Mean Sq	F value	Pr(>F)	Mean Sq	F value	Pr(>F)
Season (S)	3	0.0220			0.0546			1415.0			161.1			1540.9			103.26			2319.5		
Rep x Season	6	0.0009			0.0008			28.0			18.6			66.8			11.14			212.9		
Treatment (T)	3	0.5712	89.75	0.0000**	0.1891	163.98	0.0000**	56077.3	655.70	0.0000**	9446.8	236.09	0.0000**	111305.3	860.55	0.0000**	2148.02	151.60	0.0000**	1122.9	34.30	0.0005**
S x T	9	0.0064	2.03	0.0807	0.0012	0.65	0.7474	85.5	2.87	0.0189*	40.0	3.30	0.0093**	129.3	2.51	0.0349*	14.17	1.54	0.2292	32.7	0.18	0.9787
Error (T)	24	0.0031			0.0018			29.8			12.1			51.6			9.22			183.2		
Genotypes (G)	13	0.0161	2.33	0.0210*	0.0080	2.97	0.0043**	2764.9	27.74	0.0000**	558.2	8.10	0.0000**	5508.5	21.31	0.0000**	744.46	40.63	0.0000**	511.1	3.98	0.0004**
S x G	39	0.0069	2.63	0.0000**	0.0027	1.98	0.0006**	99.7	3.31	0.0000**	68.9	5.32	0.0000**	258.5	4.74	0.0000**	18.32	1.05	0.3879	128.3	0.81	0.7792
T x G	39	0.0019	1.64	0.0231*	0.0012	3.05	0.0000**	168.7	10.38	0.0000**	62.2	5.69	0.0000**	350.9	8.73	0.0000**	126.98	14.52	0.0000**	98.9	2.56	0.0008**
S x T x G	117	0.0012	0.44	1	0.0004	0.30	1	16.3	0.54	0.9999	10.9	0.84	0.8654	40.2	0.74	0.9756	8.74	0.50	0.9998	38.7	0.25	1
Residual	416	0.0026			0.0014			30.1			13.0			54.5			17.38			157.7		

(Continued)

10.3389/fpls.2023.1268739

TABLE 3 Continued

		Coefficient of photochemical quenching			Coefficient of non- photochemical quenching			Grain N Uptake			Straw N Uptake			Total N Uptake			Agronomic efficiency			Physiological efficiency		
EFFECT	Df	Mean Sq	F value	Pr(>F)	Mean Sq	F value	Pr(>F)	Mean Sq	F value	Pr(>F)	Mean Sq	F value	Pr(>F)	Mean Sq	F value	Pr(>F)	Mean Sq	F value	Pr(>F)	Mean Sq	F value	Pr(>F)
Total	671	0.0055			0.0025			350.2			72.6			692.0			49.21			160.4		
CV (%)		9.91			11.05			10.42			10.39			8.36			16.83			30.40		
		Partial factor productivity			Apparent nitrogen recovery efficiency			Nitrogen Uptake Efficiency			Nitrogen Utilization Efficiency			Nitrogen Use Efficiency			Nitrogen Utilization Index			Nitrogen Harvest Index		
EFFECT	Df	Mean Sq	F value	Pr(>F)	Mean Sq	F value	Pr(>F)	Mean Sq	F value	Pr(>F)	Mean Sq	F value	Pr(>F)	Mean Sq	F value	Pr(>F)	Mean Sq	F value	Pr(>F)	Mean Sq	F value	Pr(>F)
Season (S)	3	201.15			464.5			192.30			847.09			17.33			5073.5			0.0400		
Rep x Season	6	4.53			112.0			4.85			8.19			0.48			70.4			0.0007		
Treatment (T)	3	65881.17	2243.47	0.0000**	6666.6	81.23	0.0000**	454.84	38.28	0.0000**	776.85	34.69	0.0000**	144.09	54.35	0.0000**	46627.2	116.81	0.0000**	0.2128	156.81	0.0000**
S x T	9	29.37	2.19	0.0979	82.1	1.43	0.2639	11.88	1.62	0.1643	22.40	3.73	0.0047**	2.65	2.36	0.0450*	399.2	11.40	0.0000**	0.0014	2.23	0.0568
Error (T)	24	13.38			57.4			7.31			6.00			1.12			35.0			0.0006		
Genotypes (G)	13	1867.45	96.68	0.0000**	3434.8	15.04	0.0000**	682.03	22.54	0.0000**	221.28	4.14	0.0003**	189.68	76.20	0.0000**	1068.1	4.71	0.0001**	0.0184	6.87	0.0000**
S x G	39	19.32	1.27	0.1414	228.3	1.81	0.0034**	30.26	4.81	0.0000**	53.46	6.06	0.0000**	2.49	2.48	0.0000**	226.8	4.71	0.0000**	0.0027	3.13	0.0000**
T x G	39	155.53	21.12	0.0000**	351.3	6.69	0.0000**	47.42	10.65	0.0000**	23.30	5.98	0.0000**	9.94	14.78	0.0000**	74.0	3.47	0.0000**	0.0023	6.22	0.0000**
S x T x G	117	7.36	0.48	0.9999	52.5	0.42	0.9999	4.45	0.71	0.9871	3.90	0.44	1	0.67	0.67	0.9949	21.4	0.44	1	0.0004	0.43	1
Residual	416	15.25			126.5			6.29			8.82			1.00			48.1			0.0009		
Total	671	332.55			244.7			25.80			22.75			5.95			310.1			0.0024		
CV (%)		6.97			18.33			9.08			5.01			7.31			5.18			4.11		

10.3389/fpls.2023.1268739

TABLE 4 Cumulative mean values of morpho-physiological traits along with grain yield and NUE indices at N0 in different genotypes.

Genotype	Anjali	Birupa	Daya	Heera	Indira	Nidhi	N22	Tella Hamsa	V L Dhan 209	Vasumati	IR64	GQ25	Varadhan	MTU 1010	Mean
GY	2.54	2.91	2.72	3.34	2.98	2.39	1.88	2.30	3.37	2.86	3.36	2.63	2.75	3.43	2.82
TDM	6.96	7.74	7.10	8.49	7.67	6.46	5.29	6.41	8.64	7.44	8.56	6.98	7.17	9.18	7.43
DFF	81	109	108	81	102	100	87	84	99	107	99	99	93	92	96
DPM	112	136	135	115	129	128	118	115	129	134	130	129	125	123	125
FLL	26.8	28.8	25.9	24.4	31.0	25.1	26.2	23.7	28.8	26.0	23.8	25.3	28.1	24.6	26.3
FLW	1.29	1.28	1.30	1.44	1.36	1.28	1.21	1.19	1.38	1.21	1.16	1.34	1.24	1.26	1.28
FLA	26.1	27.5	25.1	26.5	31.6	24.1	23.7	21.2	29.8	23.7	20.8	25.4	26.3	23.3	25.4
FLT	0.268	0.329	0.277	0.297	0.271	0.257	0.298	0.246	0.295	0.286	0.311	0.238	0.260	0.301	0.281
FLDW	0.123	0.129	0.120	0.127	0.154	0.118	0.119	0.102	0.141	0.113	0.098	0.122	0.124	0.108	0.121
SLA	212.1	213.0	208.6	208.9	205.5	203.3	198.2	207.4	212.1	210.0	212.4	208.4	210.7	215.3	209.0
SLW	4.72	4.70	4.80	4.80	4.87	4.92	5.05	4.84	4.72	4.77	4.73	4.80	4.75	4.66	4.80
CHLa	1.53	1.74	1.74	1.84	1.69	1.59	1.59	1.55	1.69	1.82	1.81	1.71	1.82	1.89	1.71
CHLb	0.428	0.511	0.478	0.447	0.486	0.499	0.370	0.421	0.513	0.503	0.453	0.502	0.552	0.527	0.478
TCHL	1.96	2.25	2.22	2.28	2.17	2.09	1.96	1.97	2.20	2.32	2.26	2.22	2.37	2.41	2.19
CAR	0.462	0.511	0.508	0.582	0.514	0.484	0.517	0.457	0.481	0.532	0.547	0.489	0.512	0.544	0.510
Pn	15.1	16.4	15.2	15.9	15.4	14.6	14.4	14.6	16.3	16.3	15.9	16.1	16.3	16.7	15.7
gs	0.277	0.322	0.272	0.296	0.285	0.246	0.238	0.248	0.292	0.287	0.256	0.295	0.306	0.317	0.281
E	4.64	5.07	4.72	4.94	4.91	4.65	4.15	4.96	5.00	5.39	5.08	4.90	5.50	5.28	4.94
Ci	287.9	288.9	287.7	273.0	275.2	269.0	263.1	273.4	282.7	282.4	275.5	280.2	289.5	306.4	281.1
FLN	2.29	2.01	1.92	2.25	1.98	2.04	1.95	2.32	2.00	2.09	2.35	2.15	2.15	2.08	2.11
PNUE	14.1	17.5	16.9	15.0	16.4	14.9	14.8	13.3	17.6	16.6	14.6	15.8	16.1	17.4	15.8
F_v/F_m	0.792	0.799	0.786	0.796	0.792	0.791	0.780	0.781	0.789	0.799	0.794	0.795	0.794	0.807	0.792
ϕPSII	0.320	0.318	0.288	0.305	0.303	0.292	0.306	0.319	0.297	0.313	0.319	0.298	0.316	0.338	0.309
ETR	22.7	21.2	20.5	21.4	21.1	20.3	21.6	21.9	21.2	21.7	22.1	20.5	22.4	23.2	21.5
qP	0.513	0.496	0.474	0.497	0.487	0.484	0.489	0.508	0.498	0.512	0.514	0.488	0.517	0.505	0.499
qN	0.425	0.408	0.414	0.443	0.391	0.464	0.435	0.438	0.422	0.424	0.407	0.447	0.436	0.410	0.426
GNU	27.6	30.5	27.7	38.1	31.1	26.1	20.3	24.6	36.5	30.8	35.3	28.7	29.5	41.4	30.6

(Continued)

10.3389/fpls.2023.1268739

10.3389/fpls.2023.1268739

TABLE 4 Continued

Genotype	Anjali	Birupa	Daya	Heera	Indira	Nidhi	N22	Tella Hamsa	V L Dhan 209	Vasumati	IR64	GQ25	Varadhan	MTU 1010	Mean
SNU	24.3	21.9	22.4	26.5	22.6	22.2	17.9	25.6	28.7	20.0	30.9	24.2	22.2	34.3	24.5
TNU	51.9	52.4	50.1	64.6	53.8	48.2	38.2	50.2	65.2	50.8	66.2	52.9	51.7	75.7	55.1
NUpE	27.1	27.4	26.2	33.7	28.1	25.2	19.9	26.2	34.0	26.5	34.6	27.6	27.0	39.5	28.8
NUtE	49.3	55.7	54.8	52.0	56.0	49.8	49.4	45.7	52.0	56.4	51.0	49.9	53.1	45.3	51.5
NUE_{yield}	13.3	15.2	14.2	17.5	15.5	12.5	9.8	12.0	17.6	14.9	17.5	13.7	14.3	17.9	14.7
NUI	134.9	148.3	142.9	131.9	143.9	134.6	138.7	128.0	133.3	146.6	130.0	132.3	138.9	121.3	136.1
NHI	53.4	58.5	55.5	59.0	57.9	53.9	53.0	49.0	55.9	60.6	53.4	54.3	57.1	54.7	55.4

Where, GY, Grain yield (t ha^{-1}); TDM, Total dry matter (t ha^{-1}); DFF, Days to 50% flowering; DPM, Days to physiological maturity; FLL, Flag leaf length (cm); FLW, Flag leaf width (cm); FLA, Flag leaf area (cm^2); FLT, Flag leaf thickness (mm); FLDW, Flag leaf dry weight (g); SLA, Specific leaf area (cm^2 g^{-1}); SLW, Specific leaf weight (mg cm^{-2}); CHLa, Chlorophyll a (mg g^{-1} fw); CHLb, Chlorophyll b (mg g^{-1} fw); TCHL, Total chlorophyll (mg g^{-1} fw); CAR, Carotenoids (mg g^{-1} fw); Pn, Photosynthetic rate (µmol $[CO_2]$ m^{-2} s^{-1}); gs, Stomatal conductance (mol $[H_2O]$ m^{-2} s^{-1}); E, Transpiration rate (mmol $[H_2O]$ m^{-2} s^{-1}); Ci, Internal CO_2 concentration (ppm); FLN, Flag leaf N content (%); PNUE, Photosynthetic nitrogen use efficiency (µmol $[CO_2]$ g^{-1} $[N]$ s^{-1}); F_v/F_m, Maximum quantum yield of PSII; ΦPSII, Actual quantum yield of PSII; ETR, Electron transport rate; qP, Coefficient of photochemical quenching; qN, Coefficient of non-photochemical quenching; GNU, Grain N uptake (kg N ha^{-1}); SNU, Straw N uptake (kg N ha^{-1}); TNU, Total plant N uptake (kg N ha^{-1}); NUpE, Nitrogen uptake efficiency; NUtE, Nitrogen utilization efficiency; NUE_{yield}, Nitrogen use $efficiency_{yield}$; NUI, Nitrogen utilization index; NHI,Nitrogen harvest index.

total dry matter significantly increased from 7.43 to 10.89 t ha^{-1} with the increase in N fertilizer application among the treatments (from N0 to N50, N100, and N150). Among the genotypes, Vasumati at N50 and MTU 1010 at N100 recorded the highest grain yield (4.22 and 5.84 t ha^{-1}), while N22 recorded the lowest (2.46 and 3.28 t ha^{-1}) at N50 and N100. The highest total dry matter was recorded in Varadhan (9.87 and 12.08 t ha^{-1}) whereas N22 recorded the lowest (6.29 and 7.37 t ha^{-1}) at N50 and N100. With increased N application from N0 to N150, mean days to 50% flowering and physiological maturity significantly increased from 96 to 101 days and 125 to 130 days. Among the genotypes, days to 50% flowering ranged from 83 (Anjali) to 111 days (Birupa) at N50 and 84 (Anjali) to 112 days (Birupa) at N100. Days to maturity ranged from 114 (Anjali) to 137 days (Daya) at N50 and 114 (Anjali) to 138 days (Birupa) at N100.

Flag leaf length, width, area, thickness, and dry weight increased significantly with increased application of N. From N0 to N150, mean values of flag leaf length increased from 26.3 to 35.2 cm, flag leaf width increased from 1.28 to 1.55 cm, flag leaf area increased from 25.4 to 41.1 cm^2, flag leaf thickness increased from 0.281 to 0.374 mm, and flag leaf dry weight increased from 0.121 to 0.170 g. Among the genotypes, Indira exhibited the highest flag leaf length (34.8 and 37.2 cm), area (39.2 and 43.0 cm^2), and dry weight (0.177 and 0.185 g), while the lowest flag leaf length (24.6 and 27.8 cm), area (24.3 and 28.3 cm^2), and dry weight (0.111 and 0.123 g) were observed in IR64, at N50 and N100. The highest flag leaf width (1.52 and 1.60 cm) was noticed in Heera at N50 and N100, whereas MTU 1010 exhibited the lowest values (1.28 and 1.35 cm). Flag leaf thickness was the highest (0.347 mm) in Birupa and the lowest in GQ25 (0.280 mm) at N50, and the highest (0.371 mm) in N22 and the lowest (0.312 mm) in Varadhan at N100. SLA increased significantly with increased application of N whereas significant reduction in SLW is observed. From N0 to N150, mean values of SLA increased from 209.0 to 241.1 cm^2 g^{-1} and SLW decreased from 4.80 to 4.15 mg cm^{-2}. Among the genotypes, SLA ranged from 213.5 (Heera) to 223.5 cm^2 g^{-1} (Tella Hamsa) at N50, and from 220.7 (N22) to 236.0 cm^2 g^{-1} (Nidhi) at N100. SLW ranged from 4.48 (Tella Hamsa) to 4.69 mg cm^{-2} (Heera) at N50, and from 4.25 (Nidhi) to 4.54 mg cm^{-2} (N22) at N100.

Photosynthetic pigment content

Among the treatments, mean contents of chlorophyll a increased significantly from 1.71 to 2.91 mg g^{-1} fw, chlorophyll b increased significantly from 0.478 to 0.921 mg g^{-1} fw, total chlorophyll increased significantly from 2.19 to 3.83 mg g^{-1} fw, and carotenoid increased significantly from 0.510 to 0.802 mg g^{-1} fw with the increase in N application from N0 to N150. Among the genotypes, the highest chlorophyll a content (2.34 and 3.03 mg g^{-1} fw) was recorded in Heera at N50 and Varadhan at N100 while the lowest content (1.81 and 2.32 mg g^{-1} fw) was recorded in N22 at N50 and N100. IR64 at N50 and Varadhan at N100 recorded the highest contents of chlorophyll b (0.756 and 0.939 mg g^{-1} fw), whereas N22 at N50 and Heera at N100 recorded the lowest contents (0.512 and 0.675 mg g^{-1} fw). Total chlorophyll content was the lowest (2.33 and 3.01 mg g^{-1} fw) in N22 at N50 and N100 and the highest (3.03 and 3.97 mg g^{-1} fw) in MTU 1010 at N50 and

TABLE 5 Cumulative mean values of morpho-physiological traits along with grain yield and NUE indices at N50 in different genotypes.

Genotype	Anjali	Birupa	Daya	Heera	Indira	Nidhi	N22	Tella Hamsa	V L Dhan 209	Vasumati	IR64	GQ25	Varadhan	MTU 1010	Mean
GY	3.18	4.08	3.49	3.92	4.04	3.42	2.46	2.96	3.71	4.22	3.74	3.79	4.20	4.12	3.67
TDM	7.77	9.59	8.44	9.26	9.49	8.17	6.29	7.38	8.87	9.86	8.86	8.92	9.87	9.63	8.74
DFF	83	111	109	83	105	103	89	87	102	108	101	101	95	93	98
DPM	114	137	137	116	131	131	120	117	131	135	133	131	127	124	127
FLL	29.8	31.9	28.7	26.5	34.8	27.0	30.8	28.3	33.0	28.4	24.6	27.5	31.5	25.8	29.2
FLW	1.37	1.35	1.40	1.52	1.51	1.34	1.34	1.30	1.47	1.34	1.32	1.43	1.33	1.28	1.38
FLA	30.5	32.3	30.0	30.1	39.2	27.0	31.1	27.6	36.3	28.6	24.3	29.6	31.4	24.6	30.2
FLT	0.297	0.347	0.318	0.329	0.303	0.309	0.338	0.298	0.318	0.309	0.329	0.280	0.283	0.310	0.312
FLDW	0.142	0.148	0.134	0.141	0.177	0.126	0.142	0.123	0.166	0.128	0.111	0.135	0.141	0.115	0.138
SLA	215.6	218.3	222.9	213.5	221.0	214.1	219.7	223.5	218.4	223.0	218.1	219.4	223.0	215.0	219.0
SLW	4.64	4.59	4.49	4.69	4.53	4.68	4.56	4.48	4.58	4.49	4.59	4.56	4.49	4.66	4.57
CHLa	2.03	2.28	2.17	2.34	2.23	1.99	1.81	2.05	2.15	2.21	2.15	2.15	2.26	2.32	2.15
CHLb	0.674	0.731	0.568	0.654	0.705	0.621	0.512	0.588	0.673	0.731	0.756	0.536	0.629	0.703	0.649
TCHL	2.70	3.01	2.74	2.99	2.93	2.61	2.33	2.64	2.83	2.94	2.91	2.69	2.89	3.03	2.80
CAR	0.568	0.661	0.644	0.701	0.648	0.569	0.554	0.636	0.601	0.624	0.589	0.676	0.710	0.656	0.631
Pn	18.1	19.9	18.9	19.7	19.1	18.1	18.8	17.9	20.0	19.8	19.3	19.6	19.4	21.3	19.3
gs	0.400	0.519	0.370	0.425	0.456	0.422	0.419	0.537	0.446	0.466	0.401	0.506	0.517	0.550	0.460
Ci	268.6	282.6	296.5	265.7	273.1	242.4	255.4	271.3	277.4	268.4	266.2	264.6	281.1	285.0	271.3
E	6.28	6.43	5.57	6.37	6.16	6.15	5.29	6.67	6.46	6.49	6.06	6.80	6.30	7.24	6.30
FLN	2.63	2.28	2.23	2.67	2.48	2.49	2.32	2.68	2.44	2.47	2.63	2.49	2.62	2.39	2.49
PNUE	14.9	19.3	19.3	15.9	17.4	15.8	17.9	15.0	18.2	18.1	16.2	17.5	16.6	19.4	17.3
F_v/F_m	0.799	0.812	0.792	0.805	0.804	0.794	0.799	0.803	0.799	0.804	0.803	0.802	0.801	0.814	0.802
ϕPSII	0.339	0.336	0.311	0.328	0.336	0.297	0.339	0.336	0.351	0.339	0.338	0.329	0.338	0.354	0.334
ETR	24.1	22.5	22.2	23.4	23.9	21.8	23.6	23.0	23.9	24.1	23.7	23.4	24.7	25.1	23.5
qP	0.546	0.519	0.527	0.514	0.541	0.474	0.527	0.537	0.564	0.563	0.544	0.545	0.555	0.563	0.537
qN	0.387	0.371	0.382	0.399	0.361	0.393	0.394	0.386	0.384	0.391	0.394	0.414	0.412	0.383	0.389
GNU	38.4	47.4	39.8	48.4	48.7	41.6	28.8	36.2	44.0	51.6	44.0	46.8	49.6	52.3	44.1
SNU	28.2	29.7	28.9	31.6	30.8	29.2	22.5	30.0	31.8	29.9	32.3	31.0	32.2	37.6	30.4

(Continued)

10.3389/fpls.2023.1268739

TABLE 5 Continued

Genotype	Anjali	Birupa	Daya	Heera	Indira	Nidhi	N22	Tella Hamsa	V L Dhan 209	Vasumati	IR64	GQ25	Varadhan	MTU 1010	Mean
TNU	66.6	77.1	68.7	80.0	79.5	70.8	51.4	66.2	75.7	81.5	76.3	77.8	81.8	89.8	74.5
AE	12.7	23.4	15.4	11.4	21.1	20.5	11.6	13.2	6.8	27.3	7.5	23.3	29.2	13.9	17.0
PE	49.0	50.6	46.9	42.5	44.0	45.4	46.4	41.0	31.5	45.6	42.9	49.0	50.1	57.7	45.9
PFP	63.6	81.6	69.9	78.3	80.7	68.4	49.3	59.1	74.2	84.5	74.7	75.8	84.1	82.4	73.3
ANRE	29.3	49.3	37.2	30.7	51.5	45.2	26.4	31.9	21.1	61.4	20.2	49.8	60.3	28.1	38.7
NUpE	25.9	30.0	26.8	31.2	31.0	27.6	20.0	25.8	29.5	31.8	29.7	30.3	31.9	35.0	29.0
NUtE	47.9	53.4	51.1	49.0	51.3	48.4	48.2	44.9	49.0	52.2	49.1	49.2	51.6	46.0	49.4
NUE_{yield}	12.4	15.9	13.6	15.3	15.7	13.3	9.6	11.5	14.5	16.5	14.6	14.8	16.4	16.1	14.3
NUI	116.8	125.4	123.2	115.8	120.3	115.7	123.1	111.9	117.3	121.9	116.6	115.7	121.4	107.5	118.0
NHI	57.7	61.6	58.2	60.5	61.3	58.8	56.0	54.7	58.0	63.0	57.6	60.0	60.8	58.2	59.0

Where, GY, Grain yield (t ha^{-1}), TDM, Total dry matter (t ha^{-1}); DFF, Days to 50% flowering; DPM, Days to physiological maturity; FLL, Flag leaf length (cm); FLW, Flag leaf width (cm); FLA, Flag leaf area (cm^2); FLT, Flag leaf thickness (mm); FLDW, Flag leaf dry weight (g); SLA, Specific leaf area (cm^2 g^{-1}); SLW, Specific leaf weight (mg cm^{-2}); CHLa, Chlorophyll a (mg g^{-1} fw); CHLb, Chlorophyll b (mg g^{-1} fw); TCHL,Total chlorophyll (mg g^{-1} fw); CAR, Carotenoids (mg g^{-1} fw); Pn, Photosynthetic rate (µmol [CO_2] m^{-2} s^{-1}); gs, Stomatal conductance (mol [H_2O] m^{-2} s^{-1}); E, Transpiration rate (mmol [H_2O] m^{-2} s^{-1}); Ci, Internal CO_2 concentration (ppm); FLN, Flag leaf N content (%); PNUE, Photosynthetic nitrogen use efficiency (µmol [CO_2] g^{-1} [N] s^{-1}); F_v/F_m, Maximum quantum yield of PSII; ΦPSII, Actual quantum yield of PSII; ETR, Electron transport rate, qP-Coefficient of photochemical quenching; qN, Coefficient of non-photochemical quenching; GNU, Grain N uptake (kg N ha^{-1}); SNU, Straw N uptake (kg N ha^{-1}); TNU, Total plant N uptake (kg N ha^{-1}); AE, Agronomic efficiency; PE, Physiological efficiency; PFP, Partial factor productivity; ANRE, Apparent nitrogen recovery efficiency; NUpE, Nitrogen uptake efficiency; NUtE, Nitrogen utilization efficiency; NUE_{yield}, Nitrogen use efficiency$_{yield}$; NUI, Nitrogen utilization index; NHI, Nitrogen harvest index.

TABLE 6 Cumulative mean values of morpho-physiological traits along with grain yield and NUE indices at N100 in different genotypes.

Genotype	Anjali	Birupa	Daya	Heera	Indira	Nidhi	N22	Tella Hamsa	V L Dhan 209	Vasumati	IR64	GQ25	Varadhan	MTU 1010	Mean
GY	4.80	4.82	5.31	5.13	5.73	4.86	3.28	3.74	5.49	5.45	5.10	5.08	5.66	5.84	5.02
TDM	10.00	10.51	11.11	10.99	11.86	10.34	7.37	8.36	11.73	11.65	10.61	10.90	12.08	11.55	10.65
DFF	84	112	111	85	107	104	91	88	103	110	102	103	97	94	99
DPM	114	138	138	118	133	133	122	119	133	137	135	132	128	125	129
FLL	34.8	34.5	30.7	30.7	37.2	29.4	34.2	32.7	35.7	32.2	27.8	31.1	35.7	27.9	32.5
FLW	1.43	1.53	1.44	1.60	1.54	1.48	1.44	1.37	1.58	1.46	1.36	1.55	1.41	1.35	1.47
FLA	37.4	39.5	33.0	36.8	43.0	32.6	37.1	33.5	42.2	35.4	28.3	36.2	37.9	28.4	35.8
FLT	0.320	0.370	0.351	0.350	0.334	0.339	0.371	0.338	0.345	0.346	0.359	0.323	0.312	0.340	0.342
FLDW	0.168	0.175	0.146	0.160	0.185	0.138	0.168	0.149	0.185	0.153	0.123	0.153	0.166	0.126	0.157
SLA	222.0	225.0	226.1	230.6	232.1	236.0	220.7	226.2	228.6	230.5	229.5	235.7	227.6	225.8	228.3
SLW	4.51	4.45	4.43	4.34	4.31	4.25	4.54	4.43	4.38	4.35	4.37	4.25	4.40	4.44	4.39
CHLa	2.36	2.67	2.55	2.68	2.75	2.43	2.32	2.52	2.64	2.78	2.77	2.67	3.03	2.82	2.64
CHLb	0.692	0.925	0.697	0.675	0.890	0.776	0.691	0.750	0.811	0.918	0.925	0.850	0.939	0.928	0.819

(Continued)

10.3389/fpls.2023.1268739

TABLE 6 Continued

Genotype	Anjali	Birupa	Daya	Heera	Indira	Nidhi	N22	Tella Hamsa	V L Dhan 209	Vasumati	IR64	GQ25	Varadhan	MTU 1010	Mean
TCHL	3.05	3.60	3.24	3.35	3.64	3.20	3.01	3.27	3.45	3.70	3.69	3.52	3.97	3.75	3.46
CAR	0.695	0.722	0.734	0.834	0.774	0.681	0.673	0.714	0.743	0.766	0.731	0.736	0.833	0.782	0.744
Pn	23.5	23.6	23.4	23.8	24.1	22.1	22.0	23.3	23.8	23.7	23.8	24.0	24.5	26.0	23.7
gs	0.595	0.645	0.615	0.651	0.649	0.596	0.607	0.581	0.647	0.648	0.641	0.642	0.636	0.750	0.636
Ci	256.0	268.5	238.1	256.9	264.6	246.6	250.0	287.7	275.4	283.3	256.6	268.1	267.6	281.6	264.4
E	7.30	7.38	7.99	7.95	7.67	7.16	7.45	7.33	8.01	7.54	7.75	8.14	7.94	8.47	7.72
FLN	2.93	2.51	2.43	2.91	2.67	2.79	2.43	2.91	2.76	2.82	2.96	2.79	2.93	2.60	2.75
PNUE	18.0	21.4	22.3	19.0	21.9	18.9	20.1	18.2	19.9	19.5	18.6	20.3	19.2	22.6	20.0
F_v/F_m	0.813	0.820	0.814	0.818	0.811	0.819	0.805	0.817	0.815	0.812	0.811	0.817	0.817	0.823	0.815
ϕPSII	0.376	0.365	0.381	0.366	0.373	0.335	0.373	0.388	0.384	0.376	0.384	0.378	0.372	0.386	0.374
ETR	26.0	25.3	27.0	26.5	27.2	25.4	26.0	27.4	26.9	26.2	26.7	26.8	27.3	26.5	26.5
qP	0.588	0.585	0.608	0.580	0.579	0.553	0.593	0.596	0.617	0.615	0.616	0.618	0.608	0.622	0.598
qN	0.366	0.356	0.370	0.343	0.341	0.366	0.377	0.357	0.361	0.361	0.373	0.396	0.391	0.363	0.366
GNU	62.3	60.2	67.7	69.6	74.3	65.0	41.8	50.2	70.9	72.5	65.8	67.1	72.5	80.5	65.7
SNU	34.6	36.1	37.4	40.3	38.1	38.4	26.5	34.3	42.6	40.6	40.0	40.2	42.0	40.1	37.9
TNU	96.9	96.3	105.1	109.9	112.4	103.4	68.3	84.5	113.5	113.1	105.8	107.3	114.5	120.5	103.7
AE	22.6	19.1	25.9	17.9	27.6	24.7	14.0	14.4	21.3	25.9	17.4	24.5	29.1	24.2	22.0
PE	52.2	44.5	48.8	40.3	47.5	46.5	46.3	40.8	44.6	42.5	44.6	45.7	47.2	54.5	46.1
PFP	48.0	48.2	53.1	51.3	57.3	48.6	32.8	37.4	54.9	54.5	51.0	50.8	56.6	58.4	50.2
ANRE	44.9	43.9	55.0	45.3	58.6	55.2	30.1	34.2	48.4	62.3	39.5	54.3	62.9	44.8	48.5
NUpE	30.1	29.9	32.7	34.2	34.9	32.2	21.2	26.3	35.3	35.2	32.9	33.3	35.6	37.5	32.2
NUtE	49.8	50.2	50.8	46.8	51.4	47.4	48.0	44.1	48.6	48.6	48.5	47.7	49.7	48.5	48.6
NUE_{yield}	14.9	15.0	16.5	16.0	17.8	15.1	10.2	11.6	17.1	16.9	15.9	15.8	17.6	18.2	15.6
NUI	104.0	109.5	106.2	100.5	106.4	101.0	107.8	98.8	103.8	104.2	101.1	102.4	106.1	96.0	103.4
NHI	64.3	62.5	64.5	63.3	66.0	62.7	61.1	59.3	62.4	64.1	62.0	62.4	63.4	66.7	63.2

Where, GY, Grain yield (t ha^{-1}); TDM, Total dry matter (t ha^{-1}); DFF, Days to 50% flowering; DPM, Days to physiological maturity; FLL, Flag leaf length (cm); FLW, Flag leaf width (cm); FLA, Flag leaf area (cm^2); FLT, Flag leaf thickness (mm); FLDW, Flag leaf dry weight (g); SLA, Specific leaf area (cm^2 g^{-1}); SLW, Specific leaf weight (mg cm^{-2}); CHLa, Chlorophyll a (mg g^{-1} fw); CHLb, Chlorophyll b (mg g^{-1} fw); TCHL, Total chlorophyll (mg g^{-1} fw); CAR, Carotenoids (mg g^{-1} fw); Pn, Photosynthetic rate (µmol [CO_2] m^{-2} s^{-1}); gs, Stomatal conductance (mol [H_2O] m^{-2} s^{-1}); E, Transpiration rate (mmol [H_2O] m^{-2} s^{-1}); Ci, Internal CO_2 concentration (ppm); FLN, Flag leaf N content (%); PNUE, Photosynthetic nitrogen use efficiency (µmol [CO_2] g^{-1} [N] s^{-1}); F_v/F_m, Maximum quantum yield of PSII; ΦPSII, Actual quantum yield of PSII; ETR, Electron transport rate; qP, Coefficient of photochemical quenching; qN, Coefficient of non-photochemical quenching; GNU, Grain N uptake (kg N ha^{-1}); SNU, Straw N uptake (kg N ha^{-1}); TNU, Total plant N uptake (kg N ha^{-1}); AE, Agronomic efficiency; PE, Physiological efficiency; PFP, Partial factor productivity; ANRE, Apparent nitrogen recovery efficiency; NUpE, Nitrogen uptake efficiency; NUtE, Nitrogen utilization efficiency; NUE_{yield}, Nitrogen use efficiency$_{yield}$; NUI, Nitrogen utilization index; NHI, Nitrogen harvest index.

10.3389/fpls.2023.1268739

TABLE 7 Cumulative mean values of morpho-physiological traits along with grain yield and NUE indices at N150 in different genotypes.

Genotype	Anjali	Birupa	Daya	Heera	Indira	Nidhi	N22	Tella Hamsa	V L Dhan 209	Vasumati	IR64	GQ25	Varadhan	MTU 1010	Mean
GY	4.91	5.16	5.24	5.00	5.83	4.64	3.48	3.88	5.30	5.66	5.47	5.12	5.72	5.81	5.09
TDM	10.56	11.26	11.08	10.86	11.98	10.32	7.89	8.75	11.39	12.02	11.23	11.15	12.48	11.43	10.89
DFF	86	113	112	86	108	105	92	89	105	111	104	105	98	95	101
DPM	116	140	140	119	134	134	123	120	134	138	135	134	129	127	130
FLL	39.3	35.1	32.3	34.7	39.5	31.6	37.3	34.3	39.0	35.2	30.8	33.6	38.9	31.5	35.2
FLW	1.54	1.60	1.50	1.61	1.72	1.59	1.48	1.43	1.67	1.52	1.46	1.70	1.45	1.44	1.55
FLA	45.4	42.1	36.2	41.9	50.9	37.7	41.4	36.8	48.8	40.2	33.8	42.9	42.5	34.2	41.1
FLT	0.348	0.420	0.377	0.393	0.377	0.354	0.382	0.352	0.393	0.381	0.400	0.338	0.351	0.374	0.374
FLDW	0.190	0.179	0.152	0.173	0.211	0.151	0.172	0.157	0.202	0.167	0.139	0.172	0.171	0.147	0.170
SLA	239.3	235.7	237.6	241.7	241.7	248.8	240.1	235.3	242.0	240.1	243.3	248.7	248.9	232.5	241.1
SLW	4.19	4.25	4.21	4.14	4.14	4.03	4.17	4.25	4.13	4.17	4.12	4.03	4.02	4.30	4.15
CHLa	2.86	3.01	2.74	2.84	2.99	2.74	2.66	2.68	3.05	3.06	3.04	2.91	2.99	3.13	2.91
CHLb	0.921	0.943	0.855	0.921	1.019	0.945	0.768	0.890	0.951	0.945	0.954	0.912	0.930	0.943	0.921
TCHL	3.78	3.95	3.60	3.76	4.01	3.68	3.43	3.57	4.00	4.00	3.99	3.82	3.92	4.07	3.83
CAR	0.785	0.821	0.730	0.791	0.813	0.729	0.774	0.757	0.846	0.857	0.808	0.792	0.831	0.893	0.802
Pn	25.8	25.1	24.4	25.6	26.1	23.2	23.8	25.5	25.6	25.2	25.1	25.8	26.6	27.3	25.4
gs	0.655	0.667	0.693	0.741	0.680	0.625	0.671	0.710	0.679	0.720	0.717	0.771	0.790	0.767	0.706
E	8.65	8.53	8.21	8.39	8.29	7.44	7.62	8.57	8.56	8.92	8.80	8.92	8.04	8.95	8.42
Ci	247.5	251.5	242.1	257.4	246.2	253.3	228.7	264.8	269.4	256.8	268.8	269.0	273.7	273.2	257.3
FLN	3.03	2.67	2.63	3.03	2.82	2.92	2.54	2.96	2.81	2.91	3.07	2.92	3.02	2.75	2.86
PNUE	20.7	22.4	22.6	20.6	22.9	19.9	22.8	20.4	22.3	21.0	20.0	22.0	22.2	23.2	21.6
F_v/F_m	0.822	0.821	0.821	0.819	0.819	0.821	0.813	0.823	0.819	0.819	0.814	0.820	0.821	0.832	0.820
ϕPSII	0.394	0.376	0.404	0.386	0.405	0.363	0.380	0.392	0.409	0.384	0.395	0.390	0.380	0.401	0.390
ETR	26.7	26.1	28.1	28.2	29.0	26.3	26.6	28.4	28.3	26.7	27.7	27.4	28.4	27.4	27.5
qP	0.617	0.609	0.649	0.615	0.607	0.557	0.629	0.636	0.634	0.643	0.649	0.639	0.648	0.655	0.628
qN	0.362	0.334	0.356	0.328	0.329	0.349	0.352	0.351	0.344	0.349	0.358	0.368	0.362	0.333	0.348
GNU	66.5	67.5	69.4	70.3	78.0	63.3	45.9	54.3	69.3	79.1	72.7	69.8	78.0	83.4	69.1
SNU	40.0	42.1	40.6	42.2	42.0	40.8	29.6	37.8	42.6	43.4	42.7	42.5	47.1	43.2	41.2
TNU	106.5	109.6	110.0	112.5	120.0	104.1	75.6	92.1	111.9	122.5	115.4	112.3	125.1	126.6	110.3
AE	15.8	15.0	16.8	11.1	19.0	15.0	10.6	10.6	12.9	18.7	14.1	16.6	19.8	15.9	15.1

(Continued)

10.3389/fpls.2023.1268739

10.3389/fpls.2023.1268739

TABLE 7 Continued

Genotype	Anjali	Birupa	Daya	Heera	Indira	Nidhi	N22	Tella Hamsa	V L Dhan 209	Vasumati	IR64	GQ25	Varadhan	MTU 1010	Mean
PE	43.8	40.9	42.9	35.1	43.9	40.6	42.5	37.0	40.6	39.6	43.2	42.4	41.8	47.1	41.5
PFP	32.7	34.4	35.0	33.4	38.9	30.9	23.2	25.9	35.3	37.7	36.5	34.1	38.1	38.8	33.9
ANRE	36.4	38.1	39.9	31.9	44.2	37.3	24.9	27.9	31.2	47.8	32.8	39.6	49.0	33.9	36.8
NUpE	28.0	28.8	28.9	29.6	31.6	27.4	19.9	24.2	29.4	32.2	30.4	29.5	32.9	33.3	29.0
NUtE	46.1	47.5	47.8	44.7	49.0	44.7	46.0	42.2	47.4	46.5	47.6	45.8	46.1	45.9	46.2
NUE_{yield}	12.9	13.6	13.8	13.2	15.3	12.2	9.1	10.2	13.9	14.9	14.4	13.5	15.1	15.3	13.4
NUI	99.1	103.7	101.2	97.0	100.8	99.6	104.3	95.0	102.1	99.1	98.3	99.7	100.5	90.3	99.3
NHI	62.5	61.6	63.0	62.6	65.0	60.7	60.8	59.0	61.8	64.6	62.7	62.1	62.5	65.8	62.5

Where, GY, Grain yield (t ha^{-1}); TDM, Total dry matter (t ha^{-1}); DFF, Days to 50% flowering; DPM, Days to physiological maturity; FLL, Flag leaf length (cm); FLW, Flag leaf width (cm); FLA, Flag leaf area (cm^2); FLT, Flag leaf thickness (mm); FLDW, Flag leaf dry weight (g); SLA, Specific leaf area (cm^2 g^{-1}); SLW, Specific leaf weight (mg cm^{-2}); CHLa, Chlorophyll a (mg g^{-1} fw); CHLb, Chlorophyll b (mg g^{-1} fw); TCHL, Total chlorophyll (mg g^{-1} fw); CAR, Carotenoids (mg g^{-1} fw); Pn, Photosynthetic rate (µmol $[CO_2]$ m^{-2} s^{-1}); gs, Stomatal conductance (mol $[H_2O]$ m^{-2} s^{-1}); E, Transpiration rate (mmol $[H_2O]$ m^{-2} s^{-1}); Ci, Internal CO_2 concentration (ppm); FLN, Flag leaf N content (%); PNUE, Photosynthetic nitrogen use efficiency (µmol $[CO_2]$ g^{-1} [N] s^{-1}); F_v/F_m, Maximum quantum yield of PSII; ΦPSII, Actual quantum yield of PSII; ETR, Electron transport rate; qP, Coefficient of photochemical quenching; qN, Coefficient of non-photochemical quenching; GNU, Grain N uptake (kg N ha^{-1}); SNU, Straw N uptake (kg N ha^{-1}); TNU, Total plant N uptake (kg N ha^{-1}); AE, Agronomic efficiency; PE, Physiological efficiency; PFP, Partial factor productivity; ANRE, Apparent nitrogen recovery efficiency; NUpE, Nitrogen uptake efficiency; NUtE, Nitrogen utilization efficiency; NUE_{yield}, Nitrogen use efficiency; NUI, Nitrogen utilization index; NHI, Nitrogen harvest index.

Varadhan at N100. Carotenoid content was the highest (0.710 and 0.834 mg g^{-1} fw) in Varadhan at N50 and Heera at N100 and the lowest (0.554 and 0.673 mg g^{-1} fw) in N22 at N50 and N100.

Flag leaf N content and gas exchange traits

Mean Pn increased significantly from 15.7 to 25.4 µmol (CO_2) m^{-2} s^{-1}, g_s increased significantly from 0.281 to 0.706 mol (H_2O) m^{-2} s^{-1}, and E increased significantly from 4.94 to 8.42 mmol (H_2O) m^{-2} s^{-1} while C_i decreased significantly from 279.6 to 256.5 ppm with an increase in N application from N0 to N150. MTU 1010 exhibited the highest Pn [1.3 and 26.0 µmol (CO_2) m^{-2} s^{-1}], g_s [0.550 and 0.750 mol (H_2O) m^{-2} s^{-1}], and E [7.24 and 8.47 mmol (H_2O) m^{-2} s^{-1}], and the highest C_i (296.5 and 287.7 ppm) was observed in Daya at N50 and Tella Hamsa at N100, while the lowest Pn [17.9 and 22.0 µmol (CO_2) m^{-2} s^{-1}] was observed in Tella Hamsa at N50 and N22 at N100, the lowest g_s [0.370 and 0.581 mol (H_2O) m^{-2} s^{-1}] was recorded in Daya at N50 and Tella Hamsa at N100, the lowest E [5.29 and 7.16 mmol (H_2O) m^{-2} s^{-1}] was noticed in N22 at N50 and Nidhi at N100, and the lowest C_i (242.4 and 238.1 ppm) was recorded in Nidhi at N50 and Daya at N100. Among the treatments, mean flag leaf N content increased significantly from 2.11% to 2.86% and mean PNUE increased significantly from 15.8 to 21.6 µmol (CO_2) g^{-1} N s^{-1} with an increase in N application from N0 to N150. Flag leaf N content was the highest (2.68% and 2.96%) in Tella Hamsa at N50 and IR64 at N100 and the lowest (2.23% and 2.43%) in Daya at N50 and N100. MTU 1010 exhibited the highest PNUE [19.4 and 22.6 µmol (CO_2) g^{-1} N s^{-1}] at N50 and N100 whereas Anjali exhibited the lowest [14.9 and 18.0 µmol (CO_2) g^{-1} N s^{-1}].

Chlorophyll fluorescence traits

F_v/F_m, ΦPSII, ETR, and qP have increased significantly with an increase in application of N, whereas qN has significantly decreased. Mean values of F_v/F_m increased from 0.792 to 0.820, ΦPSII increased from 0.309 to 0.390, ETR increased from 21.5 to 27.5, qP increased from 0.499 to 0.628, and qN decreased from 0.426 to 0.348 with increased N application from N0 to N150. Among the genotypes, MTU 1010 recorded the highest F_v/F_m (0.814 and 0.823) at N50 and N100, whereas Daya at N50 and N22 at N100 recorded the lowest (0.792 and 0.805). ΦPSII was the highest (0.354 and 0.388) in MTU 1010 at N50 and Tella Hamsa at N100 and the lowest (0.297 and 0.335) in Nidhi at N50 and N100. MTU 1010 at N50 and Tella Hamsa at N100 recorded the highest ETR (25.1 and 27.4) whereas Nidhi at N50 and Birupa at N100 recorded the lowest (21.8 and 25.3). qP was the highest (0.564 and 0.622) in VL Dhan 209 at N50 and MTU 1010 at N100 and the lowest (0.474 and 0.553) in Nidhi at N50 and N100. GQ25 exhibited the highest qN (0.414 and 0.396) at N50 and N100 whereas Indira exhibited the lowest qN (0.361 and 0.341).

Nitrogen uptake and NUE indices

Increased N application from N0 to N150 resulted in a significant increase in mean grain N uptake from 30.6 to 69.1 kg N ha^{-1}, mean straw N uptake from 24.5 to 41.2 kg N ha^{-1}, and as total plant from 55.1 to 110.3 kg N ha^{-1}. Grain N uptake ranged from 28.8 (N22) to 52.3 kg N ha^{-1} (MTU 1010) at N50, and from

10.3389/fpls.2023.1268739

TABLE 8 Range and mean values of morpho-physiological traits along with grain yield and NUE indices at graded N application for cumulative data of four seasons.

Trait	N0			N50			N100			N150		
	Min	Max	Mean	Min	Max	Mean	Min	Max	Mean	Min	Max	Mean
Grain yield (g m^{-2})	1.88	3.43	2.82	2.46	4.22	3.67	3.28	5.84	5.02	3.48	5.83	5.09
Total dry matter (g m^{-2})	5.29	9.18	7.43	6.29	9.87	8.74	7.37	12.08	10.65	7.89	12.48	10.89
Days to 50% flowering	81	109	96	83	111	98	84	112	99	86	113	101
Days to maturity	112	136	125	114	137	127	114	138	129	116	140	130
Flag leaf length (cm)	23.7	31.0	26.3	24.6	34.8	29.2	27.8	37.2	32.5	30.8	39.5	35.2
Flag leaf width (cm)	1.16	1.44	1.28	1.28	1.52	1.38	1.35	1.60	1.47	1.43	1.72	1.55
Flag leaf area (cm^2)	20.8	31.6	25.4	24.3	39.2	30.2	28.3	43.0	35.8	33.8	50.9	41.1
Flag leaf thickness (mm)	0.238	0.329	0.281	0.280	0.347	0.312	0.312	0.371	0.342	0.338	0.420	0.374
Flag leaf dry weight (g)	0.098	0.154	0.121	0.111	0.177	0.138	0.123	0.185	0.157	0.139	0.211	0.170
Specific leaf area (cm^2 g^{-1})	198.2	215.3	209.0	213.5	223.5	219.0	220.7	236.0	228.3	232.5	248.9	241.1
Specific leaf weight (mg cm^{-2})	4.66	5.05	4.80	4.48	4.69	4.57	4.25	4.54	4.39	4.02	4.30	4.15
Chlorophyll a content (mg g^{-1} fw)	1.53	1.89	1.71	1.81	2.34	2.15	2.32	3.03	2.64	2.66	3.13	2.91
Chlorophyll b content (mg g^{-1} fw)	0.370	0.552	0.478	0.512	0.756	0.649	0.675	0.939	0.819	0.768	1.019	0.921
Total Chlorophyll content (mg g^{-1} fw)	1.96	2.41	2.19	2.33	3.03	2.80	3.01	3.97	3.46	3.43	4.07	3.83
Carotenoid content (mg g^{-1} fw)	0.457	0.582	0.510	0.554	0.710	0.631	0.673	0.834	0.744	0.729	0.893	0.802
Photosynthetic rate (µmol [CO_2] m^{-2} s^{-1})	14.4	16.7	15.7	17.9	21.3	19.3	22.0	26.0	23.7	23.2	27.3	25.4
Stomatal conductance (mol [H_2O] m^{-2} s^{-1})	0.238	0.322	0.281	0.370	0.550	0.460	0.581	0.750	0.636	0.625	0.790	0.706
Transpiration rate (mmol [H_2O] m^{-2} s^{-1})	4.15	5.50	4.94	5.29	7.24	6.30	7.16	8.47	7.72	7.44	8.95	8.42
Internal CO_2 concentration (ppm)	263.1	306.4	281.1	242.4	296.5	271.3	238.1	287.7	264.4	228.7	273.7	257.3
Flag leaf N (%) content	1.92	2.35	2.11	2.23	2.68	2.49	2.43	2.96	2.75	2.54	3.07	2.86
Photosynthetic nitrogen use efficiency (µmol [CO_2] g^{-1} [N] s^{-1})	13.3	17.6	15.8	14.9	19.4	17.3	18.0	22.6	20.0	19.9	23.2	21.6
Maximum quantum yield of PSII	0.780	0.807	0.792	0.792	0.814	0.802	0.805	0.823	0.815	0.813	0.832	0.820
Actual quantum yield of PSII	0.288	0.338	0.309	0.297	0.354	0.334	0.335	0.388	0.374	0.363	0.409	0.390
Electron transport rate	20.3	23.2	21.5	21.8	25.1	23.5	25.3	27.4	26.5	26.1	29.0	27.5
Coefficient of photochemical quenching	0.474	0.517	0.499	0.474	0.564	0.537	0.553	0.622	0.598	0.557	0.655	0.628
Coefficient of non-photochemical quenching	0.391	0.464	0.426	0.361	0.414	0.389	0.341	0.396	0.366	0.328	0.368	0.348
Grain N uptake (kg N ha^{-1})	20.3	41.4	30.6	28.8	52.3	44.1	41.8	80.5	65.7	45.9	83.4	69.1
Straw N uptake (kg N ha^{-1})	17.9	34.3	24.5	22.5	37.6	30.4	26.5	42.6	37.9	29.6	47.1	41.2
Total plant N uptake (kg N ha^{-1})	38.2	75.7	55.1	51.4	89.8	74.5	68.3	120.5	103.7	75.6	126.6	110.3
Agronomic efficiency	-	–	-	6.8	29.2	17.0	14.0	29.1	22.0	10.6	19.8	15.1
Physiological efficiency	-	–	-	31.5	57.7	45.9	40.3	54.5	46.1	35.1	47.1	41.5
Partial factor productivity	-	–	-	49.3	84.5	73.3	32.8	58.4	50.2	23.2	38.9	33.9
Apparent nitrogen recovery efficiency	-	–	-	20.2	61.4	38.7	30.1	62.9	48.5	24.9	49.0	36.8
Nitrogen uptake efficiency	19.9	39.5	28.8	20.0	35.0	29.0	21.2	37.5	32.2	19.9	33.3	29.0
Nitrogen utilization efficiency	45.3	56.4	51.5	44.9	53.4	49.4	44.1	51.4	48.6	42.2	49.0	46.2
Nitrogen use efficiency	9.8	17.9	14.7	9.6	16.5	14.3	10.2	18.2	15.6	9.1	15.3	13.4
Nitrogen utilization index	121.3	148.3	136.1	107.5	125.4	118.0	96.0	109.5	103.4	90.3	104.3	99.3
Nitrogen harvest index	49.0	60.6	55.4	54.7	63.0	59.0	59.3	66.7	63.2	59.0	65.8	62.5

41.8 (N22) to 80.5 kg N ha^{-1} (MTU 1010) at N100. Straw N uptake ranged from 22.5 (N22) to 37.6 kg N ha^{-1} (MTU 1010) at N50, and from 26.5 (N22) to 42.6 kg N ha^{-1} (VL Dhan 209) at N100. Total N uptake ranged from 51.4 (N22) to 89.8 kg N ha^{-1} (MTU 1010) at N50, and from 68.3 (N22) to 120.5 kg N ha^{-1} (MTU 1010) at N100.

Multiple correlation analysis

Multiple correlation analysis (Figures 1, 2) of morpho-physiological traits along with grain yield separately at N50 and N100 indicates that several traits were highly significantly correlated with grain yield in both N treatments. Interestingly, the correlations of F_v/F_m, ΦPSII, ETR, qP, and C_i with grain yield were only significant at N50. Furthermore, ΦPSII, ETR, and qP showed a significant negative correlation and qN noted a non-significant positive correlation with flag leaf nitrogen (FLN) at N100. In contrast, ΦPSII, ETR, qP, and qN noted a significant positive correlation with FLN at N50.

Correlation of grain yield with NUE indices

As it is inevitable to reduce N fertilizer application by 50% in agriculture for environmental sustainability, in addition to the above traits, various NUE indices were also calculated to identify their applicability to assess the genotypes. Grain yield value is not required to derive NUpE, ANRE, NUI, and NHI. Therefore, these four indices along with other indices were compared with grain yield to assess their suitability to identify promising genotypes at reduced N cultivation conditions. NUpE was highly significantly positively (R^2 > 0.8) correlated with grain yield at all the N levels and seasons (Figure 3). MTU 1010 (14), IR64 (11), VL Dhan 209 (9), and Heera (4) exhibited higher NUpE and grain yield at N0. MTU 1010 (14), Vasumati (10), Varadhan (13), Heera (4), Indira (5), and Birupa (2) showed maximum NUpE along with grain yield at N50. MTU 1010 (14), Vasumati (10), Varadhan (13), VL Dhan 209 (9), and Indira (5) recorded higher NUpE and grain yield at both N100 and N150 [except VL Dhan 209 (9)]. N22 (7) noted the least NUpE and grain yield at all the N levels. ANRE noted a significant ($R^2 \geq 0.5$) or highly significant ($R^2 \geq 0.7$) positive correlation with grain yield at all the N levels and seasons (Figure 4). Varadhan (13), Vasumati (10), and Indira (5) exhibited maximum ANRE along with grain yield at all the N levels whereas N22 (7) and Tella Hamsa (8) showed the least ANRE as well as grain yield. Although non-significant, NUI noted a negative relationship with grain yield at all other grades of N

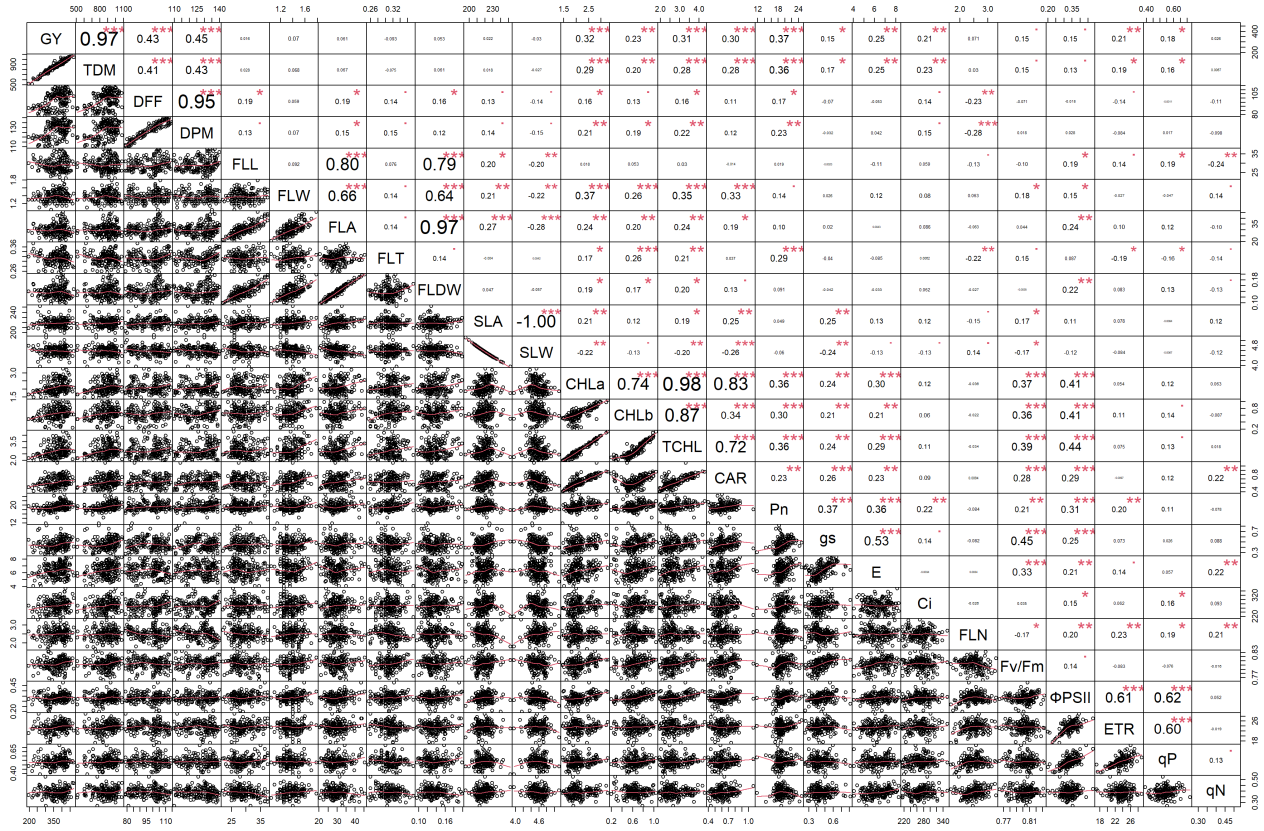

FIGURE 1
Correlation among the morpho-physiological parameters along with grain yield at N50. GY, Grain yield; TDM, Total dry matter; DFF, Days to 50% flowering; DPM, Days to physiological maturity; FLL, Flag leaf length; FLW, Flag leaf width; FLA, Flag leaf area; FLT, Flag leaf thickness; FLDW, Flag leaf dry weight; SLA, Specific leaf area; SLW, Specific leaf weight; CHLa, Chlorophyll a; CHLb, Chlorophyll b; TCHL, Total chlorophyll; CAR, Carotenoids; Pn, Photosynthetic rate; g_s, Stomatal conductance; E, Transpiration rate; C_i, Internal CO_2 concentration; FLN, Flag leaf N content; PNUE, Photosynthetic nitrogen use efficiency; F_v/F_m, Maximum quantum yield of PSII; ΦPSII, Actual quantum yield of PSII; ETR, Electron transport rate; qP, Coefficient of photochemical quenching; qN, Coefficient of non-photochemical quenching. *** - p≤ 0.001, **- p≤ 0.01, *- p≤ 0.05, • - p≤ 0.1.

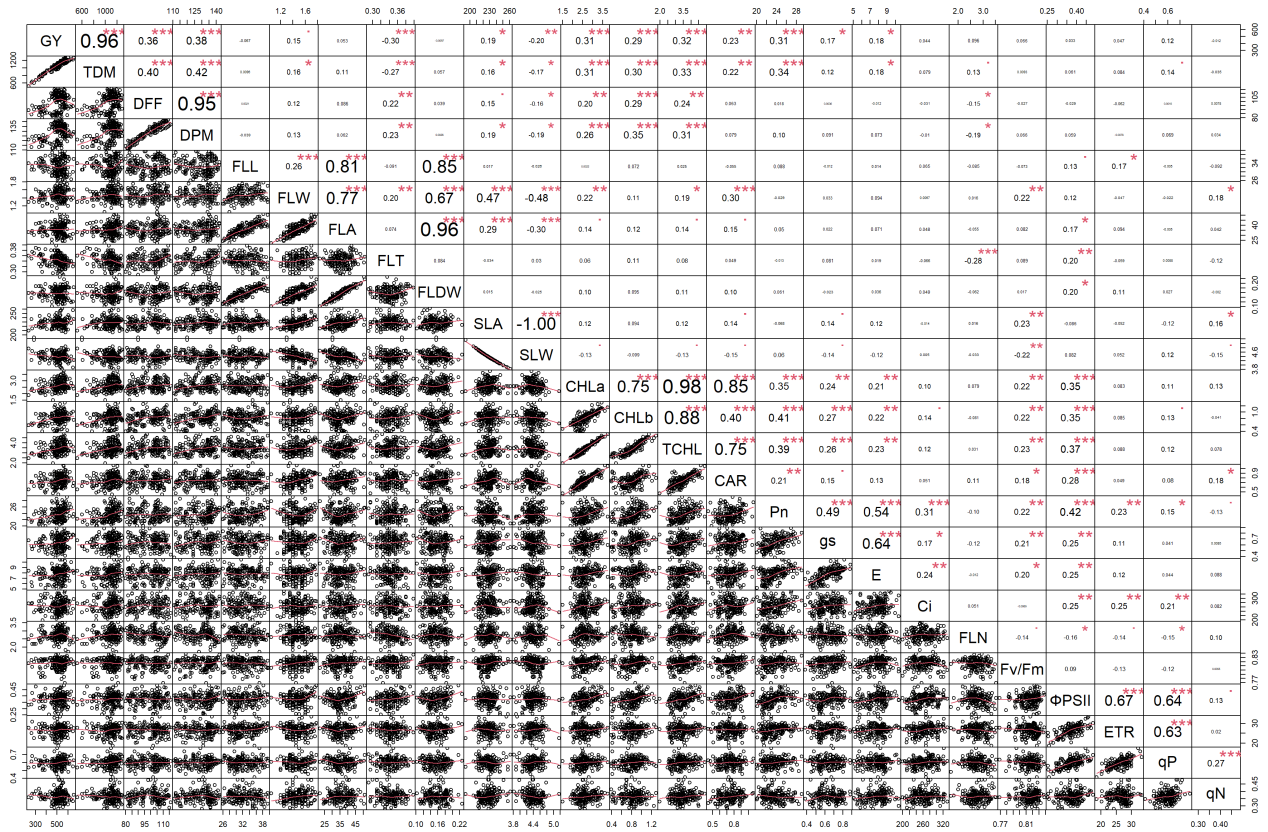

FIGURE 2
Correlation among the morpho-physiological parameters along with grain yield at N100. GY, Grain yield; TDM, Total dry matter; DFF, Days to 50% flowering; DPM, Days to physiological maturity; FLL, Flag leaf length; FLW, Flag leaf width; FLA, Flag leaf area; FLT, Flag leaf thickness; FLDW, Flag leaf dry weight; SLA, Specific leaf area; SLW, Specific leaf weight; CHLa, Chlorophyll a; CHLb, Chlorophyll b; TCHL, Total chlorophyll; CAR, Carotenoids; Pn, Photosynthetic rate; g_s, Stomatal conductance; E, Transpiration rate; C_i, Internal CO_2 concentration; FLN, Flag leaf N content; PNUE, Photosynthetic nitrogen use efficiency; F_v/F_m, Maximum quantum yield of PSII; ΦPSII, Actual quantum yield of PSII; ETR, Electron transport rate; qP, Coefficient of photochemical quenching; qN, Coefficient of non-photochemical quenching. *** - p≤ 0.001, **- p≤ 0.01, *- p≤ 0.05, • - p≤ 0.1.

content in both wet and dry seasons, except for both the dry seasons at N50 and the dry season (2021) at N150 (Figure 5). NHI noted a significant ($R^2 \geq 0.5$) or non-significant ($R^2 < 0.5$) positive correlation with grain yield at all the N levels and seasons (Figure 6). Vasumati (10), Birupa (2), Indira (5), and Heera (4) noted a higher NHI along with grain yield N0 and N50 [also Varadhan (13)]. MTU 1010 (14), Vasumati (10), Varadhan (13), and Indira (5) showed higher grain yield and NHI at both N100 and N150. N22 (7) and Tella Hamsa (8) showed the least NHI along with grain yield at all the N levels.

NUtE was positively correlated with grain yield at all the N levels (Supplementary Figure 1). However, the correlation was significant only in the dry seasons from N50 to N150. Birupa (2), Varadhan (13), Vasumati (10), and Indira (5) have shown higher NUtE and grain yield at N50. Indira (5), VL Dhan 209 (9), Vasumati (10), and Varadhan (13) exhibited higher NUtE along with grain yield at N100 and N150 [except VL Dhan 209 (9)]. Tella Hamsa (8) noted the least NUtE along with grain yield at most of the N levels. NUE_{yield} noted a significant positive correlation ($R^2 = 1$) with grain yield at all N levels and seasons (Supplementary Figure 2). MTU 1010 (14), VL Dhan 209 (9), IR64 (11), and Heera (4) showed higher NUE_{yield} along with grain yield at N0. Vasumati (10), Birupa (2), MTU 1010 (14), Varadhan (13), and Indira (5) have exhibited maximum NUE_{yield} and grain yield at N50. At N100 and N150, MTU 1010 (14), Vasumati (10), Varadhan (13), Indira (5), and VL Dhan 209 (9) have shown higher grain yield and NUE_{yield}. N22 (7) and Tella Hamsa (8) have shown the least NUE_{yield} and grain yield at all N levels. AE showed significantly positive correlation with grain yield at all N levels and seasons except for wet season 2021 at N0 (Supplementary Figure 3). Vasumati (10), Varadhan (13), and Birupa (2) exhibited higher AE along with grain yield at N50. At this N level, VL Dhan 209 (9) and IR64 (11) were good in grain yield and least in AE, while N22 (7) and Tella Hamsa (8) were better than VL Dhan 209 (9) and IR64 (11) in AE but poor in grain yield. At N100 and N150, Varadhan (13), MTU 1010 (14), Vasumati (10), and Indira (5) noted maximum AE and grain yield whereas N22(7) and Tella Hamsa (8) noted the least AE and grain yield. PE noted a non-significant positive correlation with grain yield at all N levels in most of the seasons while it noted a non-significant negative correlation at N100 and N150 levels in wet season 2020 (Supplementary Figure 4). MTU 1010 noted higher PE along with grain yield at all N levels. Moreover, all the tested genotypes noted similar PE values at both N100 and N150 and differed in yield. PFP noted a highly significant positive correlation ($R^2 = 1$) with grain yield at all N levels and seasons (Supplementary Figure 5). Vasumati (10), Varadhan (13),

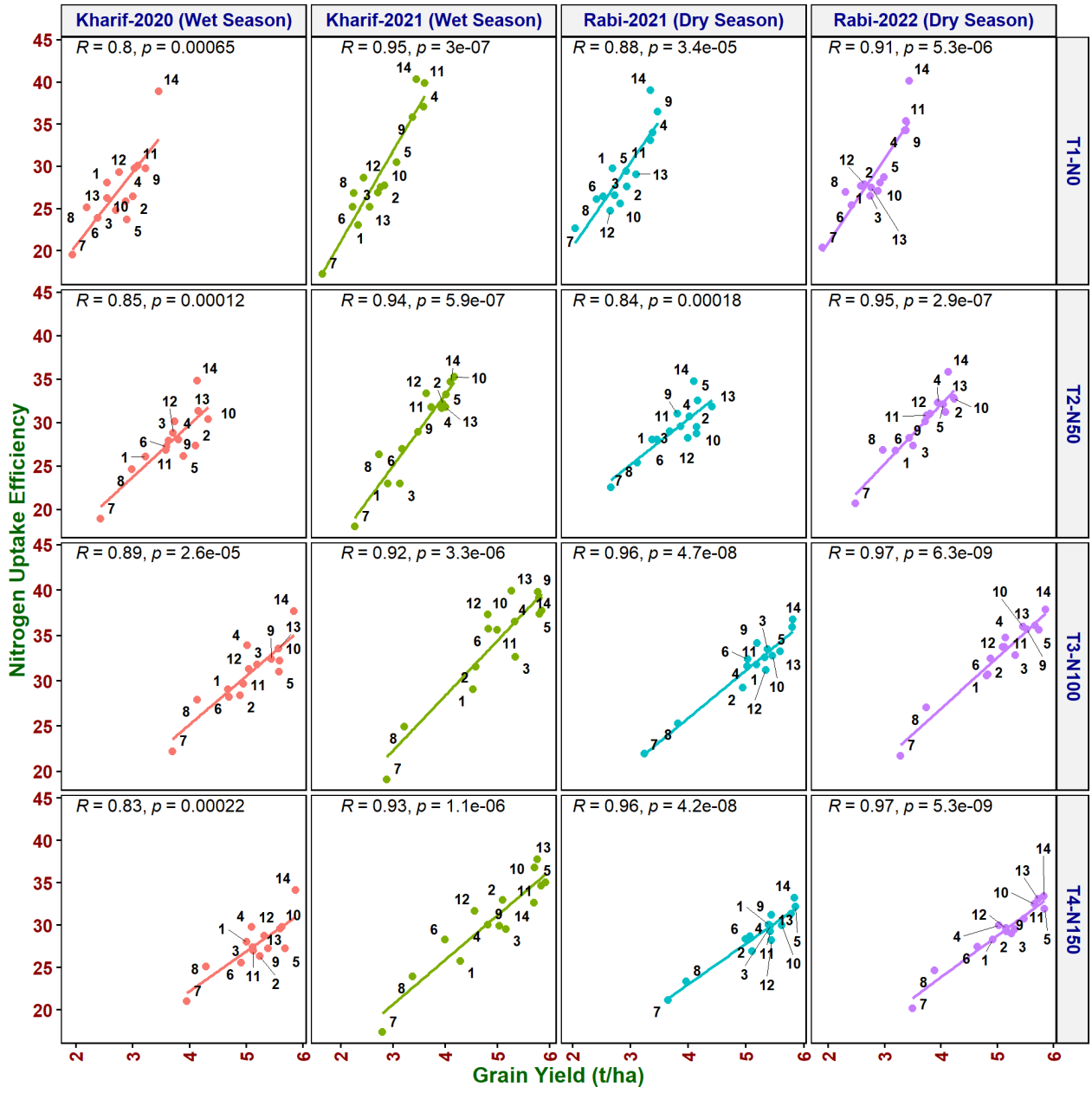

FIGURE 3
Relationship between nitrogen uptake efficiency (NUpE) and grain yield of rice genotypes at different N levels and seasons. 1, Anjali; 2, Birupa; 3, Daya; 4, Heera; 5, Indira; 6, Nidhi; 7, N22; 8, Tella Hamsa; 9, VL Dhan 209; 10, Vasumati; 11, IR64; 12, GQ25; 13, Varadhan; and 14, MTU 1010.

MTU 1010 (14), and Indira (5) noted higher PFP along with grain yield at all the N levels whereas N22 (7) and Tella Hamsa (8) were the least.

Discussion

Nitrogen (N) is an essential nutrient for the growth, development, and maintenance of rice (Wang et al., 2022). As soil N fertilizer alone is not adequate for increase in rice production, farmers add higher amounts of N fertilizer expecting that increased application of N fertilizer will result in the enhanced yields (West et al., 2014; Wang et al., 2022). Higher N fertilizer inputs are leading to serious environmental problems and low production efficiency (Wang et al., 2022). As only 30 to 50% of applied N is reported to be utilized by rice, reduction of N fertilizer application by 50% of the recommended N was chosen as the current target for NUE in rice (Ladha et al., 2020). Variation in rice varietal response to graded N application, especially 50% of recommended N, has been studied (Singh et al., 1998; Singh et al., 2014; Vijayalakshmi et al., 2015). Application of N fertilizer without considering the NUE of a particular variety leads to not only reduced use efficiency but also

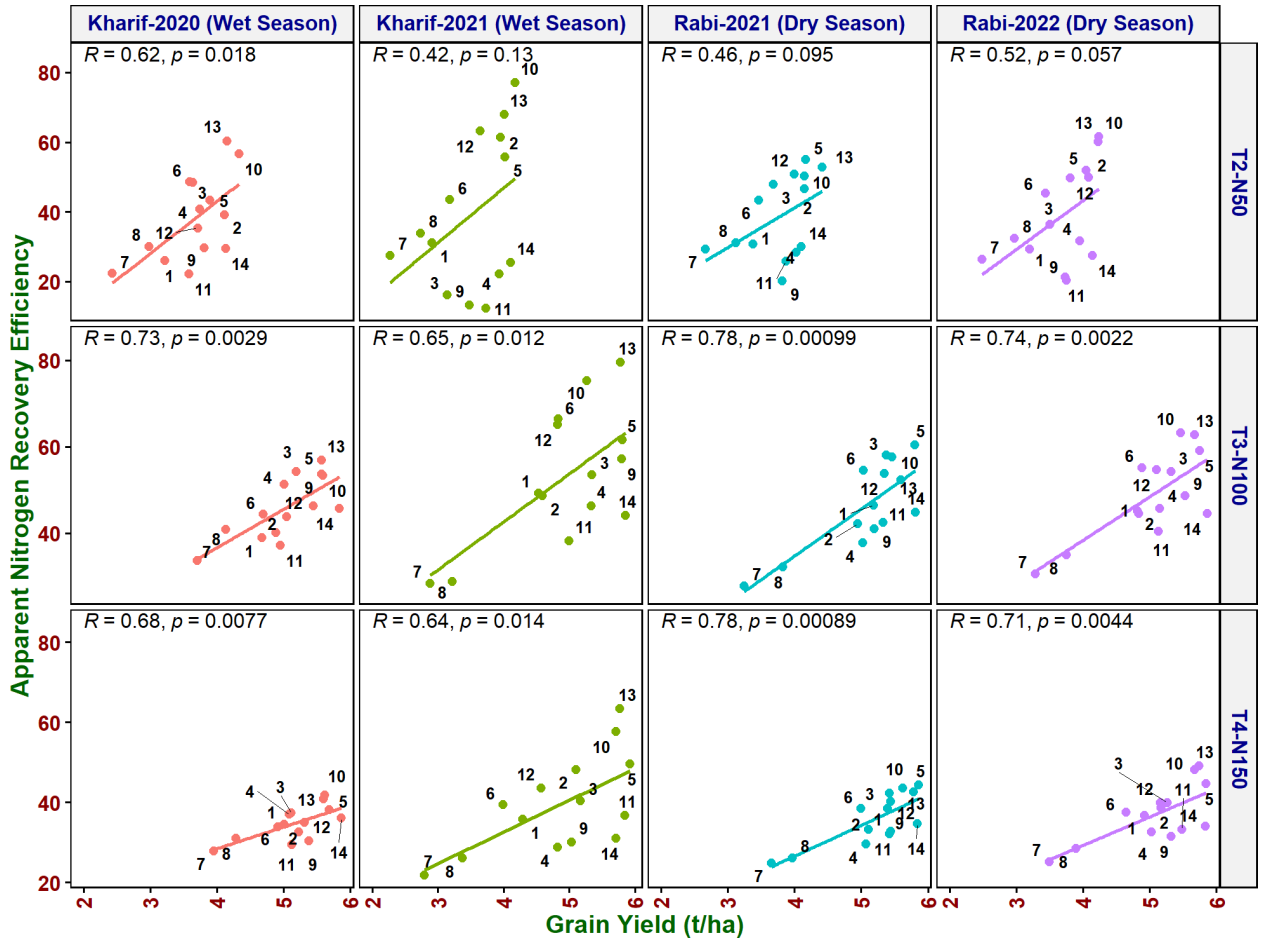

FIGURE 4
Relationship between apparent nitrogen recovery efficiency (ANRE) and grain yield of rice genotypes at different N levels and seasons. 1, Anjali; 2, Birupa; 3, Daya; 4, Heera; 5, Indira; 6, Nidhi; 7, N22; 8, Tella Hamsa; 9, VL Dhan 209; 10, Vasumati; 11, IR64; 12, GQ25; 13, Varadhan; and 14, MTU 1010.

environmental pollution and increased cost of cultivation. In the present study, to evaluate the genotype response with varying yield potential to graded N application, 14 rice genotypes were assessed at four levels of N fertilizer. To identify physiological traits associated with grain yield in selecting promising genotypes at reduced N application (50% of the recommended N), flag leaf characteristics (including N content), photosynthetic pigment content, gas exchange traits, and chlorophyll fluorescence characteristics were studied. In addition, NUE indices were also estimated for their suitability to select N efficient genotypes under reduced N application.

Under N50, a reduction of 26.99% of grain yield in comparison with N100 was observed while 43.88% reduction was observed under N0. However, only marginal increment in grain yield (1.31%) was observed from N100 to N150 (Figure 7). Birupa exhibited the least reduction (15.31%) in grain yield at N50 compared to N100 whereas Daya exhibited the highest reduction (34.20%). Genotypic differences were earlier reported for grain yield of rice at different N levels (Singh et al., 1998). Thus, to achieve the reduction of N fertilizer application, the selection of genotypes is crucial because of their inherent response for N. With the increased N application, previous studies also reported increase in grain yield, which is attributed to increased tillering, number of panicles, and grains (Devika et al., 2018; Zhang et al., 2020; Bama et al., 2021; Karmakar et al., 2021; Liang et al., 2021; Xin et al., 2022; Zhu et al., 2022) and increase in total dry matter accumulation (Pan et al., 2012; Singh et al., 2014; Jyothi Swaroopa and Lakshmi, 2015; Zhang et al., 2020). Days to 50% flowering and days to physiological maturity also increased significantly with increased N application due to increased vegetative growth phase (Mahajan et al., 2011; Rajesh et al., 2017; Wani et al., 2017; Ghoneim and Osman, 2018; Bv et al., 2019; Ye et al., 2019b; Mandal et al., 2022) and increased tillering (Wang et al., 2016).

As expected, six flag leaf traits (FLL, FLW, FLA, FLT, FLDW, and SLA) have shown a significant increase and specific leaf weight (SLW) has shown a significant decrease with increased N application in the present study. Earlier studies have also reported a significant increase in length and width of flag leaf (Bahmaniar and Ranjbar, 2007), an increase in leaf area and leaf thickness with increased N application (Vijayalakshmi et al., 2015), a significant increase in leaf thickness from 0.31 mm at N0 to 0.54 mm at N150 (Devika et al., 2018), and a significant and the highest increase in leaf thickness and leaf dry mass at N270 (Hou et al., 2020) in rice. Similarly, reduction in SLW of rice with increased N application

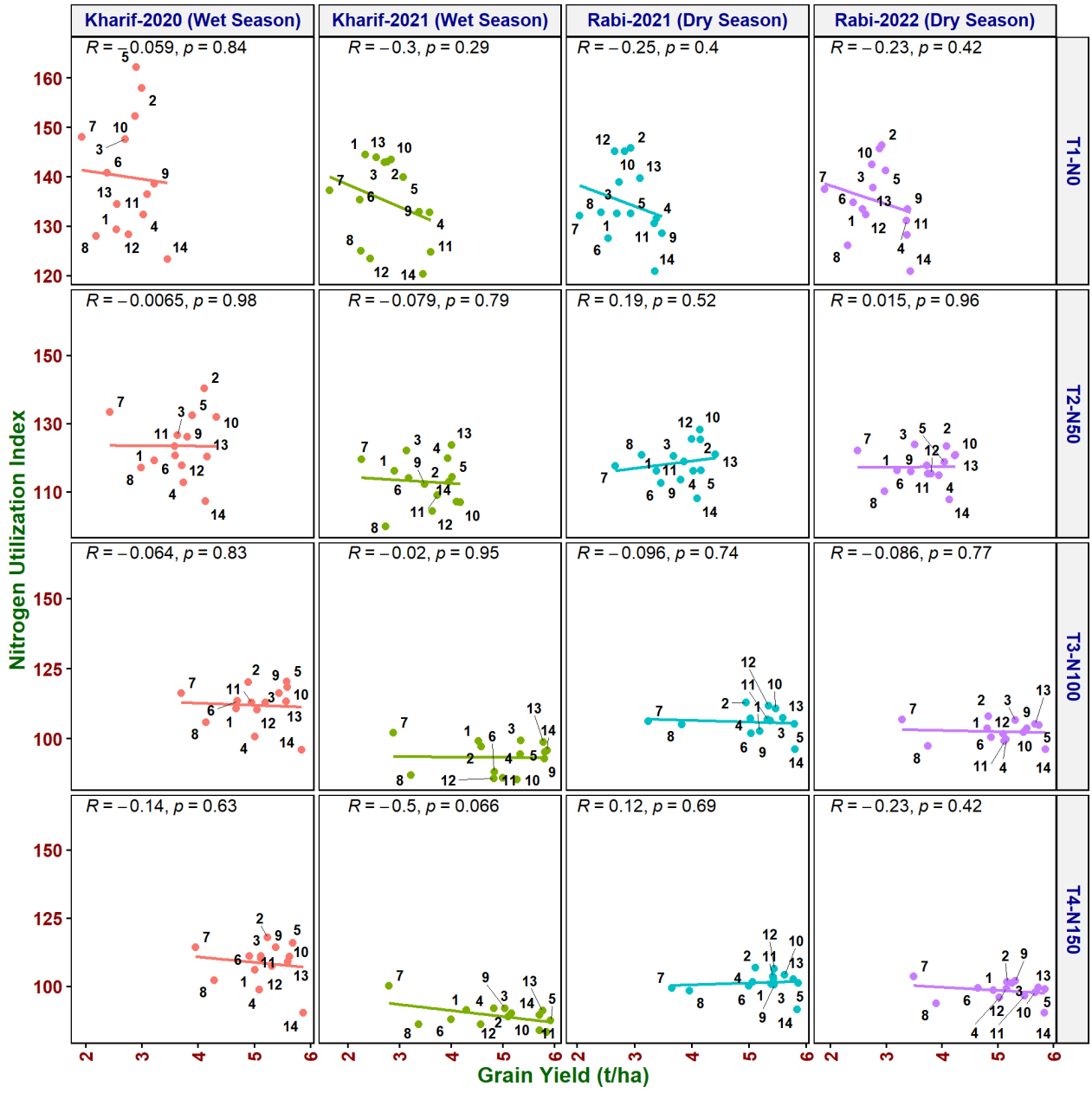

FIGURE 5
Relationship between nitrogen utilization index (NUI) and grain yield of rice genotypes at different N levels and seasons. 1, Anjali; 2, Birupa; 3, Daya; 4, Heera; 5, Indira; 6, Nidhi; 7, N22; 8, Tella Hamsa; 9, VL Dhan 209; 10, Vasumati; 11, IR64; 12, GQ25; 13, Varadhan; and 14, MTU 1010.

(Yang et al., 2003; Huang et al., 2008), under sufficient N compared to low N treatment in inbred *indica* rice cultivars (Liu and Li, 2016) and 2.9% to 11.1% reduction as the N application levels gradually increased from N0 to N270 (Hou et al., 2020), was reported, supporting our observations. Likewise, SLA increase was also reported with increase in N application at crown root initiation stage in wheat (Alam, 2014).

In congruence with our results, the photosynthetic pigment contents were elevated (Jinwen et al., 2009; Cisse et al., 2020; Hou et al., 2020) or showed an upward trend in *indica* hybrid rice (Peng et al., 2021) and *japonica* rice (Gong et al., 2022) with the increase in N application rates. Appropriate N application was shown to improve the enzyme and chlorophyll content of plant leaves, thereby improving the photosynthetic activities of the plant (Giersch and Robinson, 1987; Nduwimana, 2020).

Pn and E are the crucial physiological processes for NUE and Pn was significantly higher for the higher NUE genotypes, relative to the lower NUE genotypes (Kumari et al., 2021). Increased amounts of nitrate supply significantly enhanced Pn, g_s, and E (Mandal et al., 2022). As noted in this study, with the increase in N application level from 0 to 200 kg ha^{-1}, Pn, g_s, and E were also increased gradually, while C_i values were decreased (Gong et al., 2022). Increased N application increased the Pn that noted a positive correlation with leaf N content (Fallah, 2012; Rajesh et al., 2017; Bv

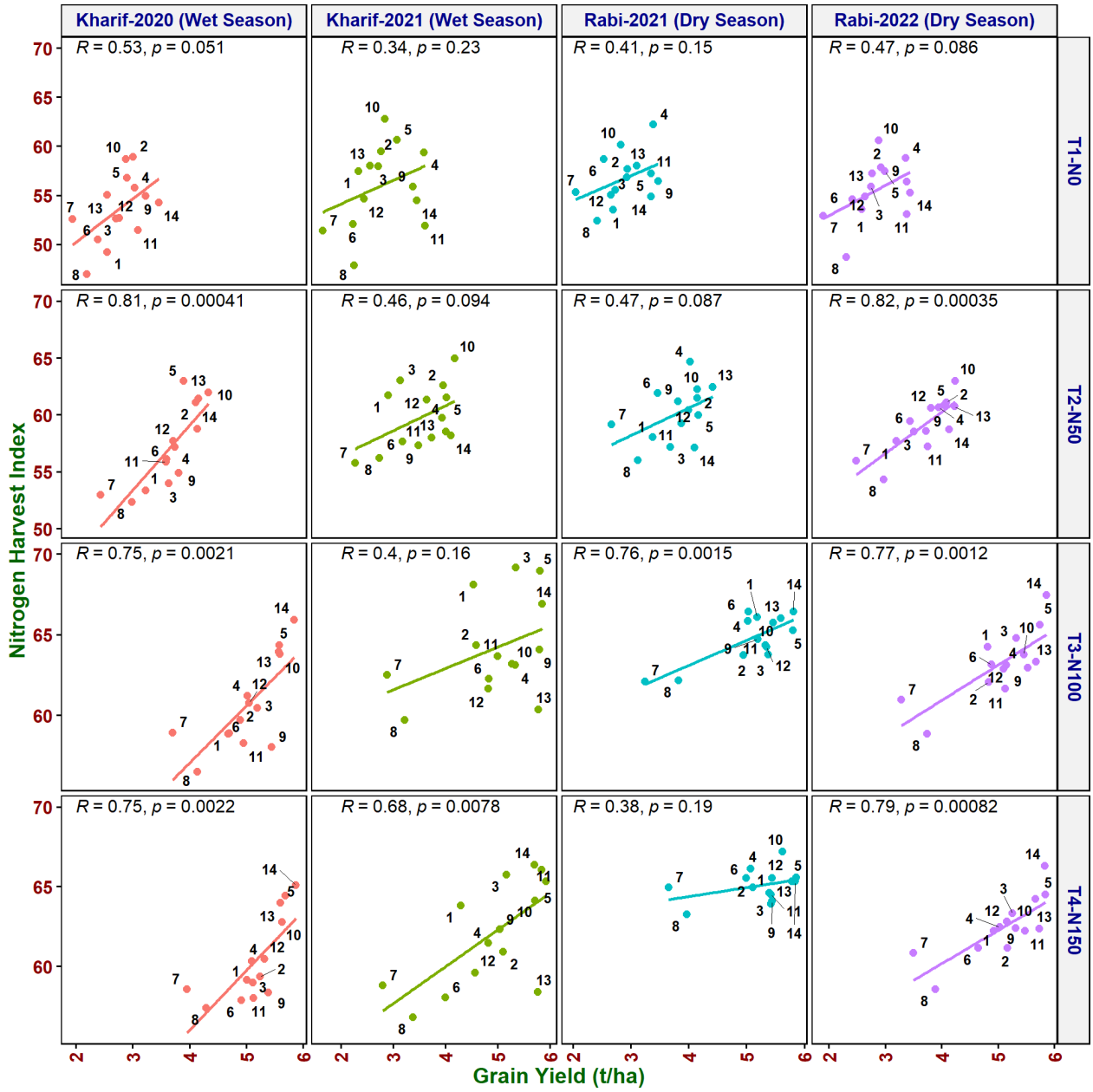

FIGURE 6
Relationship between nitrogen harvest index (NHI) and grain yield of rice genotypes at different N levels and seasons. 1, Anjali; 2, Birupa; 3, Daya; 4, Heera; 5, Indira; 6, Nidhi; 7, N22; 8, Tella Hamsa; 9, VL Dhan 209; 10, Vasumati; 11, IR64; 12, GQ25; 13, Varadhan; and 14, MTU 1010.

et al., 2019; Zhang et al., 2020), increased the E (Zhang et al., 2020), and increased the g_s at the vegetative stage (Roy Chowdhury et al., 2014). Significantly higher values were recorded for g_s and E with N100 compared to N0 (Vijayalakshmi et al., 2015). Compared with low N (0 kg N ha^{-1}), Pn, g_s, and E were significantly higher under medium (120 kg N ha^{-1}) and high N (180 kg N ha^{-1}) levels (Pan et al., 2016). A significantly higher Pn of 29.52 µmol (CO_2) m^{-2} s^{-1} at 150% of RDN was noted compared with a Pn of 17.41 µmol (CO_2) m^{-2} s^{-1} at 0% of RDN (Devika et al., 2018). Flag leaf N content increased significantly with increased N application and is in accordance with the earlier findings (Swarna et al., 2017; Cisse et al., 2020; Hou et al., 2020). Leaf N plays a crucial role in photosynthesis, which ultimately affects biomass production (Ladha et al., 1998). PNUE is the photosynthetic capacity per unit leaf N. PNUE is a key component of NUE and an indicator of the relationship between leaf N and Pn. In the current investigation, PNUE increased with an increase in rate of N application. The higher the PNUE, the higher the crop N utilization rate (Mugo et al., 2021). Leaf N allocation is an important factor influencing PNUE. Suitable N application can improve the leaf photosynthetic rate, which helps to increase the PNUE, which, in turn, enhances the crop yield (Zhao et al., 2013).

Among the chlorophyll fluorescence traits, F_v/F_m, ΦPSII, ETR, and qP showed an increasing trend, while qN decreased as the N

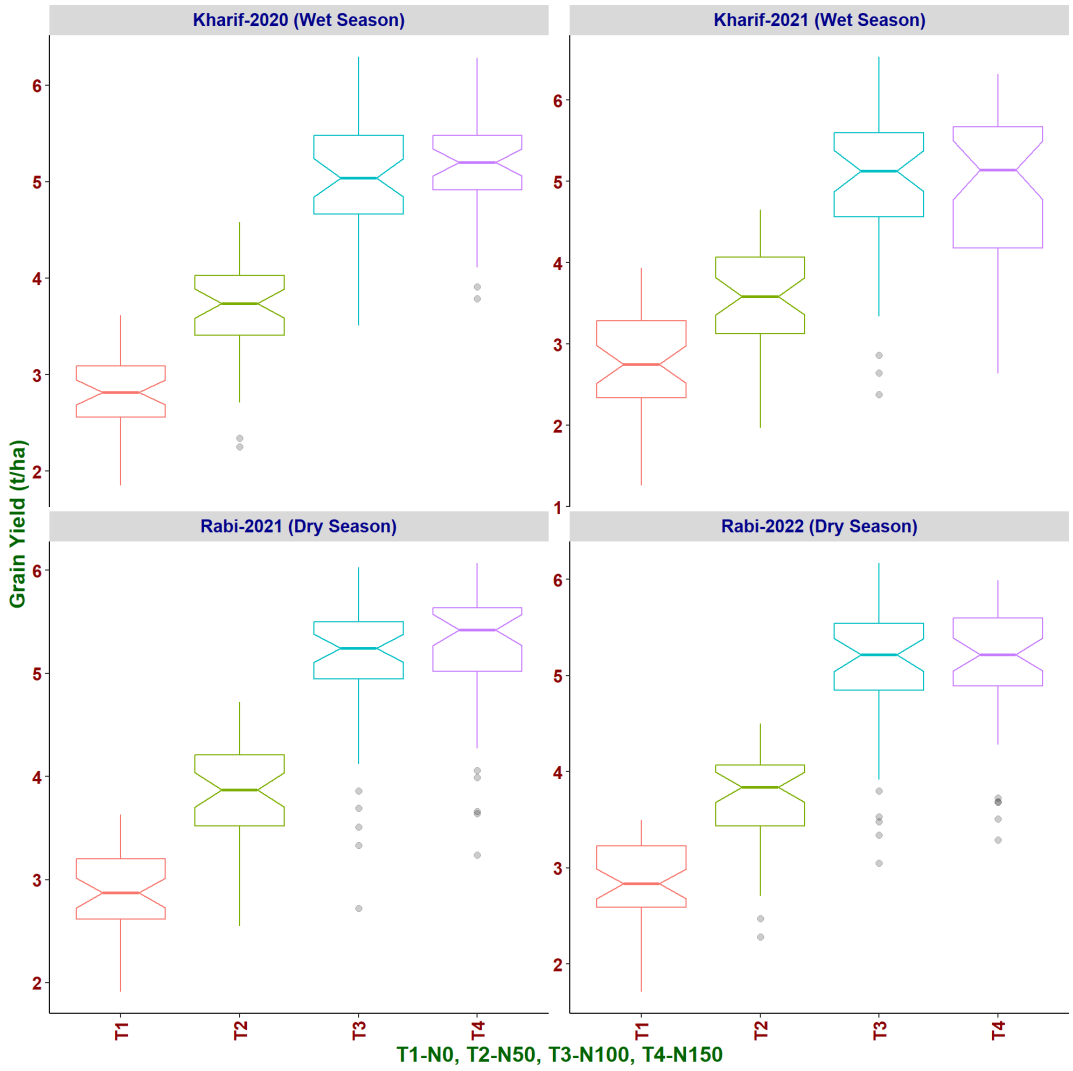

FIGURE 7
Effect of increased levels of N application on grain yield of rice genotypes in different seasons.

rate increased as reported in hybrid rice (Peng et al., 2021). The application of the appropriate amount of N could increase the solar energy conversion efficiency in the PSII reaction center of rice leaves by improving the electron transfer efficiency and enhancing electron flow (Zhang et al., 2017; Fu et al., 2021). Among the total traits of the study, in comparison with N100, most of the chlorophyll fluorescence traits (F_v/F_m, ΦPSII, ETR, and qP) and C_i among the gas exchange traits were significantly correlated with grain yield at N50. As these traits were measured using flag leaf, the correlation of these traits with FLN revealed significant differences between N50 and N100. Hence, flag leaf at 50% flowering can be a good source to assess chlorophyll fluorescence traits under reduced N conditions and can differentiate rice genotypes varying in yield and NUE. In photosystem II of light reaction, F_v/F_m explains the maximum photochemical conversion (quantum yield), ΦPSII explains the effective photochemical conversion, ETR explains the amount of electron transfer at the reaction center in PSII, and qP represents the functional or open proportion of PSII involved in photochemical conversion. The available literature indicates that N-deficient conditions like N50 can result in improper formation and function of PSII affecting photochemical conversion followed by yield (Jin et al., 2012) and reduce carboxylation efficiency (Huang et al., 2004), whereas proper or optimum availability of N improves the function of PSII, quantum efficiency, and grain yield (Liu and Xu, 2018). Hence, results obtained in the current investigation suggest the usage of these physiological traits (F_v/F_m, ΦPSII, ETR, qP, and C_i) to screen genotypes under N50 with known low-yielding and high-yielding genotypes as checks. As optimum N can show the highest quantum efficiency followed by yield and genotype-specific optimum N requirement is unknown, Birupa, a moderate yielder at N100, emerged as one of the top five yielders at N50 and *vice versa* in the case of VL Dhan 209. It indicates differential response of the genotypes for yield potential with varied levels of N.

Increase in grain, straw, and total N uptake with increased N application as observed in the present study is in concurrence with the earlier findings (Tayefe et al., 2011; Swarna et al., 2017; Bama et al., 2021). AE, PE, ANRE, and PFP are indices for NUE proposed

by Dobermann (2007). AE represents the contribution of fertilizer N towards yield in comparison to a non-fertilized control and is helpful to assess the contribution of added N fertilizer in enhancing the yield. PE represents the contribution of fertilizer N from the plant tissues to increase yield and is useful to identify plants that have a superior ability in producing yield per unit of available N. ANRE is the percentage of fertilizer N that is taken up by the plant and it aids in studying crop response to the applied N fertilizer. Both PE and ANRE account for background (available) soil N (Congreves et al., 2021). N application rate showed a significant effect on AE, PE, and ANRE and was maximum with N100 followed by N50 and minimum with N150. Among the treatments, cumulative mean values of AE ranged from 15.1 at N150 to 22.0 at N100, PE ranged from 41.5 at N150 to 46.1 at N100, and ANRE ranged from 36.8 at N150 to 48.5 at N100. AE and ANRE of rice were decreased with increasing N application over N100 and indicated that the capability of increase in yield per kilogram of applied N declined remarkably with increasing N application greater than N100. PE also decreased with increasing N application over N100 and showed that yield increased per kilogram N accumulated in rice plant was decreased with increasing N application greater than N100. AE was 16–36 in Boro rice (Islam et al., 2015) and 0.52–17 in T. Aman rice (Hussain et al., 2016). AE significantly increased with increasing N levels up to 165 kg N ha^{-1} and decreased with further uplift in N application in some recently released Egyptian rice varieties (Ghoneim and Osman, 2018). AE decreased at N120 and N150 (Mboyerwa et al., 2022). Similarly, ANRE increased at first, reached the maximum under optimum N application, and thereafter declined significantly under higher N levels (Ye et al., 2007) and at N160 (Katuwal et al., 2021). PE also decreased significantly at N150 (Kumar et al., 2015). The diminishing trend of PE at higher N rates pointed out that rice plants are unable to absorb or utilize N at higher rates of N application or the rate of N uptake by plant cannot keep pace with the loss of N. AE, PE, and ANRE decreased gradually with an increase in N rate from 3.5 to 14 g m^{-2} in nerica-4 (Yesuf and Balcha, 2014). Partial factor productivity (PFP) is the simplest form of NUE efficiency and is calculated as yield per applied N. It is a convenient index for comparing management practices on a single crop type. Mean values of PFP decreased significantly with increase in N application from 73.3 at N0 to 33.9 at N150 in the present study and is in accordance with previous findings (Pan et al., 2017; Rea et al., 2019). Similar results were also reported by other researchers in their studies (Ye et al., 2007; Cheng et al., 2011; Tayefe et al., 2011).

NUpE is the percentage of available soil N taken up by the plant (Moll et al., 1982) and is useful for sustainable cultivation of rice. The cumulative mean NUpE values increased with an increase in N application from 28.8 at N0 to 32.2 at N100 and declined to 29.0 at N150. NUtE is the contribution of plant N towards yield (Moll et al., 1982). NUtE decreased with increased N application and mean NUtE ranged from 51.5 (N0) to 46.2 (N150). Similarly, higher NUtE was recorded at 0% RDN, and the lower value was recorded at 150% RDN (Devika et al., 2018). Three rice cultivars with similar growth periods tested under different N levels had dissimilar grain yield, N absorption, and utilization rates (Xin et al., 2022). They also found that at low N, rice yield was mainly limited by NUpE, while at high N, yield was mainly limited by NUtE. Increased flag leaf N content and delayed leaf senescence could improve NUtE (Vijayalakshmi et al., 2013). Hence, to maintain stable grain yield at different N levels, both N uptake and utilization efficiencies should be simultaneously improved. In low N conditions, NUpE is more important than NUtE (Witcombe et al., 2008; Khan et al., 2017). NUE_{yield} indicates the contribution of available N towards grain yield (Novoa and Loomis, 1981) and enables comparison of yield potential among genotypes. Among the treatments, mean NUE_{yield} increased from 14.7 at N0 to 15.6 at N100 and decreased to 13.4 at N150. It is indicated that NUE_{yield} did not increase linearly with the amount of N application (Kunta and Thatikunta, 2020). Likewise, NUE_{yield} increased up to 100% RDN and decreased with a further increase in N levels up to 150% RDN and also concluded that the application of excess N was not effectively utilized by the crop and the production rate per unit of N applied was low (Kumar et al., 2008). Lower PE under high N supply results in lower NUE_{yield} (Li et al., 2012). With the increase in N application rates (0, 160, 210, 260, 315, and 420 kg N ha^{-1}), NUE_{yield} increased up to 210 kg N ha^{-1} and then decreased (Liang et al., 2021). NUI is the contribution of plant N towards accumulation of plant biomass (Huang et al., 2018). NUI decreased significantly with increased application of N and mean NUI decreased from 136.1 at N0 to 99.3 at N150. NHI is the amount of plant N present in the yield component (grain in the case of rice) (Moll et al., 1982) and can be used to identify plants with greater N translocation efficiency to the economic part. NHI increased with increase in N application rate from N0 (55.4) up to N100 (63.2) and slightly decreased with N150 (62.5). The increase in NHI up to N100 may be due to the increase in grain yield, and the transfer of N to the grain is greater than the increase in total plant N. Although NHI of rice decreased with increasing N application over N100, N ratio in straw enhanced over grain. NHI may be useful in selecting crop genotypes for higher grain yield (Fageria and Baligar, 2005). Out of nine NUE indices assessed in 14 genotypes under graded N levels, NUpE, NUtE, and NUE_{yield} delineated the best-performing genotypes under N50.

Screening of 14 genotypes under four graded N levels across four seasons revealed wide genotypic variation in their response in terms of grain yield. An increase of agro-morphological traits, photosynthetic pigments, and flag leaf traits (except SLW) was observed with an increase of N fertilizer application. At N50, F_v/F_m, ΦPSII, ETR, qP, and C_i of flag leaf at flowering noted significant association with grain yield. Of the 14 genotypes, the top 5 (MTU 1010, Indira, Varadhan, VL Dhan 209, and Vasumati) grain yielders at N100 were identified as promising genotypes for efficient use of N by NUpE, NUtE, and NUE_{yield} indices at N50. Moreover, NUE_{yield} is the product of NUpE and NUtE. Hence, among the nine indices, these three (NUpE, NUtE, and NUE_{yield}) can be further used to identify promising genotypes at N50.

Conclusion

The present study has clearly demonstrated the existence of genetic variability among the rice genotypes through N response

under graded N levels. The grain yield penalty ranged only from 15% to 34.2% at N50 across the 14 genotypes in comparison with N100, suggesting the possibility of reduction of N fertilizer application. Most importantly, through the evaluation of flag leaf physiological traits at the flowering stage, chlorophyll fluorescence traits (F_v/F_m, ΦPSII, ETR, and qP) and C_i were identified to be associated with grain yield under N50, which could be deployed in the breeding for NUE in rice. Among the tested genotypes, Birupa, which is a relative moderate yielder at N100, emerged as a high yielder under N50, which indicates the potential of the moderate-yielding genotypes at N100 to produce better grain yield at N50. Therefore, this study recommends the evaluation of the released rice varieties at N50 to determine their suitability under low N input conditions. Among the nine NUE indices studied, NUpE, NUtE, and NUE_{yield} are useful to identify promising genotypes at N50.

Data availability statement

The original contributions presented in the study are included in the article/Supplementary Material. Further inquiries can be directed to the corresponding author.

Author contributions

BS: Data curation, Formal analysis, Investigation, Methodology, Writing – original draft. DS: Conceptualization, Funding acquisition, Project administration, Resources, Supervision, Writing – review & editing. DSR: Data curation, Software, Visualization, Writing – review & editing. SR: Methodology, Writing – review & editing. KaS: Software, Writing – review & editing. PR: Resources, Writing – review & editing. KuS: Methodology, Writing – review & editing. RS: Resources, Writing – review & editing. CN: Conceptualization, Supervision, Writing – review & editing.

Funding

The author(s) declare financial support was received for the research, authorship, and/or publication of this article. We are thankful for research grants from UKRI-GCRF South Asian Nitrogen Hub (SANH) (NE/S009019/1), including a fellowship to BS.

Conflict of interest

The authors declare that the research was conducted in the absence of any commercial or financial relationships that could be construed as a potential conflict of interest.

Publisher's note

Supplementary material

The Supplementary Material for this article can be found online at: https://www.frontiersin.org/articles/10.3389/fpls.2023.1268739/full#supplementary-material

SUPPLEMENTARY FIGURE 1
Relationship between nitrogen utilization efficiency (NUtE) and grain yield of rice genotypes at different N levels and seasons. 1, Anjali; 2, Birupa; 3, Daya; 4, Heera; 5, Indira; 6, Nidhi; 7, N22; 8, Tella Hamsa; 9, VL Dhan 209; 10, Vasumati; 11, IR64; 12, GQ25; 13, Varadhan and 14, MTU 1010.

SUPPLEMENTARY FIGURE 2
Relationship between nitrogen use efficiency$_{yield}$ (NUE_{yield}) and grain yield of rice genotypes at different N levels and seasons. 1, Anjali; 2, Birupa; 3, Daya; 4, Heera; 5, Indira; 6, Nidhi; 7, N22; 8, Tella Hamsa; 9, VL Dhan 209; 10, Vasumati; 11, IR64; 12, GQ25; 13, Varadhan and 14, MTU 1010.

SUPPLEMENTARY FIGURE 3
Relationship between agronomic efficiency (AE) and grain yield of rice genotypes at different N levels and seasons. 1, Anjali; 2, Birupa; 3, Daya; 4, Heera; 5, Indira; 6, Nidhi; 7, N22; 8, Tella Hamsa; 9, VL Dhan 209; 10, Vasumati; 11, IR64; 12, GQ25; 13, Varadhan and 14, MTU 1010.

SUPPLEMENTARY FIGURE 4
Relationship between physiological efficiency (PE) and grain yield of rice genotypes at different N levels and seasons. 1, Anjali; 2, Birupa; 3, Daya; 4, Heera; 5, Indira; 6, Nidhi; 7, N22; 8, Tella Hamsa; 9, VL Dhan 209; 10, Vasumati; 11, IR64; 12, GQ25; 13, Varadhan and 14, MTU 1010.

SUPPLEMENTARY FIGURE 5
Relationship between partial factor productivity (PFP) and grain yield of rice genotypes at different N levels and seasons. 1, Anjali; 2, Birupa; 3, Daya; 4, Heera; 5, Indira; 6, Nidhi; 7, N22; 8, Tella Hamsa; 9, VL Dhan 209; 10, Vasumati; 11, IR64; 12, GQ25; 13, Varadhan and 14, MTU 1010.

References

Abrol, Y., Raghuram, N., and Hoysall, C. (2008). Reactive nitrogen in agriculture, environment and health. *Curr. Sci.* 1343–1344.

Abrol, Y. P., Raghuram, N., and Sachdev, M. S. (2007). *Agricultural nitrogen use and its environmental implications* (IK International Pvt Ltd), 1–6.

Alam, M. S. (2014). Physiological traits of wheat as affected by nitrogen fertilization and pattern of planting. *Int. J. Agric. For.* 4, 100–105. doi: 10.5923/j.ijaf.20140402.09

Amanullah and Inamullah, (2016). Dry matter partitioning and harvest index differ in rice genotypes with variable rates of phosphorus and zinc nutrition. *Rice Sci.* 23, 78–87. doi: 10.1016/j.rsci.2015.09.006

Bahmaniar, M. A., and Ranjbar, G. A. (2007). Response of rice cultivars to rates of nitrogen and potassium application in field and pot conditions. *Pakistan J. Biol. Sci.* 10, 1430–1437. doi: 10.3923/pjbs.2007.1430.1437

Bama, K. S., Babu, K. R., Sharmila, R., and Anuradha, A. (2021). Influence of nitrogen application on direct seeded rice in old and new Cauvery Delta zone of Tamil Nadu, India. *J. Appl. Nat. Sci.* 13, 1462–1469. doi: 10.31018/jans.v13i4.3095

Bv, N., Thatikunta, R., Reddy, S. N., Krishna, L., and Supriya, K. (2019). Study on morpho-physiological, yield attributes and quality parameters of rice varieties under different nitrogen levels and zinc application. ~ *586* ~ *Int. J. Chem. Stud.* 7, 586–591.

Chakraborty, N., and Raghuram, N. (2011). *Nitrate sensing and signaling in genome wide plant N response. Nitrogen Use Efficiency in Plants* (New Delhi: V. Jain New India Publishing Agency). P. A.

Chen, Z., Tao, X., Khan, A., Tan, D. K. Y., and Luo, H. (2018). Biomass accumulation, photosynthetic traits and root development of cotton as affected by irrigation and nitrogen-fertilization. *Front. Plant Sci.* 9. doi: 10.3389/fpls.2018.00173

Cheng, J.f., Jiang, H.y., Liu, Y.b., Dai, T., and Cao, W.x. (2011). Methods on identification and screening of rice genotypes with high nitrogen efficiency. *Rice Sci.* 18, 127–135. doi: 10.1016/S1672-6308(11)60018-8

Ciampitti, I. A., and Vyn, T. J. (2011). A comprehensive study of plant density consequences on nitrogen uptake dynamics of maize plants from vegetative to reproductive stages. *F. Crop Res.* 121, 2–18. doi: 10.1016/j.fcr.2010.10.009

Cisse, A., Zhao, X., Fu, W., Kim, R. E. R., Chen, T., Tao, L., et al. (2020). Non-photochemical quenching involved in the regulation of photosynthesis of rice leaves under high nitrogen conditions. *Int. J. Mol. Sci.* 21, 1–17. doi: 10.3390/ijms21062115

Congreves, K. A., Otchere, O., Ferland, D., Farzadfar, S., Williams, S., and Arcand, M. M. (2021). Nitrogen use efficiency definitions of today and tomorrow. *Front. Plant Sci.* 12. doi: 10.3389/fpls.2021.637108

de Mendiburu, F. (2012). *Agricolae: Statistical Procedures for Agricultural Research. – R package version 1.1-2*. Available at: http://CRAN.R-project.org/package=agricolae.

Devika, S., Ravichandran, V., and Boominathan, P. (2018). Physiological analyses of nitrogen use efficiency and yield traits of rice genotypes. *Indian J. Plant Physiol.* 23, 100–110. doi: 10.1007/s40502-018-0358-8

Dobermann, A. (2007). "Nutrient use efficiency—measurement and management," in *Fertilizer Best Management Practices: General Principles, Strategy for Their Adoption and Voluntary Initiatives Versus Regulations*. Eds. A. Krauss, K. Isherwood and P. Heffer (Paris, Fr.: Int. Fertil. Ind. Assoc), 1–28.

Fageria, N. K., and Baligar, V. C. (2005). Enhancing nitrogen use efficiency in crop plants. *Adv. Agron.* 88, 97–185. doi: 10.1016/S0065-2113(05)88004-6

Fallah, A. (2012). Study of silicon and nitrogen effects on some physiological characters of rice. *Int. J. Agric. Crop Sci.* 4, 238–241.

FAO (2018). *Rice Market Monitor* (Roma, Italy: FAO).

Fathi, A., and Zeidali, E. (2021). Conservation tillage and nitrogen fertilizer: a review of corn growth, yield and weed management. *Cent. Asian J. Plant Sci. Innov.* 1, 121–142. doi: 10.22034/CAJPSI.2021.03.01

Fu, H., Cui, D., and Shen, H. (2021). Effects of nitrogen forms and application rates on nitrogen uptake, photosynthetic characteristics and yield of double-cropping rice in South China. *Agronomy* 10 (11), 1–16. doi: 10.3390/agronomy

Galloway, J., Raghuram, N., and Abrol, Y. P. (2008). A perspective on reactive nitrogen in a global, Asian and Indian context. *Curr. Sci.* 94, 1375–1381.

Ghannoum, O., Evans, J. R., Chow, W. S., Andrews, T. J., Conroy, J. P., and von Caemmerer, S. (2005). Faster rubisco is the key to superior nitrogen-use efficiency in NADP-malic enzyme relative to NAD-malic enzyme C4 grasses. *Plant Physiol.* 137, 638–650. doi: 10.1104/pp.104.054759

Ghoneim, A. M., and Osman, M. M. A. (2018). Effects of nitrogen levels on growth, yield and nitrogen use efficiency of some newly released Egyptian rice genotypes. *Open Agric.* 3, 310–318. doi: 10.1515/opag-2018-0034

Giersch, C., and Robinson, S. P. (1987). Regulation of photosynthetic carbon metabolism during phosphate limitation of photosynthesis in isolated spinach chloroplasts. *Photosynth. Res.* 14, 211–227. doi: 10.1007/BF00032706

Gong, Y. L., Lei, Y., Zhang, X. P., Yan, B. C., Ju, X. T., Cheng, X. Y., et al. (2022). Nitrogen rate and plant density interaction enhances grain yield by regulating the grain distribution of secondary branches on the panicle axis and photosynthesis in japonica rice. *Photosynthetica* 60, 179–189. doi: 10.32615/ps.2022.002

Han, M., Okamoto, M., Beatty, P. H., Rothstein, S. J., and Good, A. G. (2015). The genetics of nitrogen use efficiency in crop plants. *Annu. Rev. Genet.* 49, 269–289. doi: 10.1146/annurev-genet-112414-055037

Hikosaka, K. (2004). Interspecific difference in the photosynthesis?nitrogen relationship: patterns, physiological causes, and ecological importance. *J. Plant Res.* 117, 481–494. doi: 10.1007/s10265-004-0174-2

Hou, W., Tränkner, M., Lu, J., Yan, J., Huang, S., Ren, T., et al. (2020). Diagnosis of nitrogen nutrition in rice leaves influenced by potassium levels. *Front. Plant Sci.* 11. doi: 10.3389/fpls.2020.00165

Hu, B., Wang, W., Chen, J., Liu, Y., and Chu, C. (2023). Genetic improvement toward nitrogen-use efficiency in rice: Lessons and perspectives. *Mol. Plant* 16, 64–74. doi: 10.1016/j.molp.2022.11.007

Huang, J., He, F., Cui, K., Buresh, R. J., Xu, B., Gong, W., et al. (2008). Determination of optimal nitrogen rate for rice varieties using a chlorophyll meter. *F. Crop Res.* 105, 70–80. doi: 10.1016/j.fcr.2007.07.006

Huang, Z.-A., Jiang, D.-A., Yang, Y., Sun, J.-W., and Jin, S.-H. (2004). Effects of nitrogen deficiency on gas exchange, chlorophyll fluorescence, and antioxidant enzymes in leaves of rice plants. *Photosynthetica* 42, 357–364.

Huang, S., Zhao, C., Zhang, Y., and Wang, C. (2018). "Nitrogen use efficiency in rice," in *Nitrogen in Agriculture - Updates* (London, UK: IntechOpen Limited), 187–208. doi: 10.5772/intechopen.69052

Hussain, J., Siddique, M. A., Mia, M. M., Hasan, G. N., Seajuti, A. S., Mallik, M. R., et al. (2016). Effect of different doses of nitrogen fertilizer on t. Aman rice. *Int. J. BUSINESS Soc Sci. Res.* 4, 328–332.

Islam, S., Khatun, A., Rahman, F., Hossain, A. S., Naher, U., and Saleque, M. (2015). Rice response to nitrogen in tidal flooded non-saline soil. *Bangladesh Rice J.* 19, 65–70. doi: 10.3329/brj.v19i2.28166

Jin, W. W., Wang, Y., Zhang, H. H., and Sun, G. (2012). Effects of different nitrogen rate on the functions of flue-cured tobacco seedlings photosystem PSII under drought stress. *J. Nanjing Agric. Univ.* 35, 21–26.

Jinwen, L., Jingping, Y., Pinpin, F., Junlan, S., Dongsheng, L., Changshui, G., et al. (2009). Responses of rice leaf thickness, SPAD readings and chlorophyll a/b ratios to different nitrogen supply rates in paddy field. *F. Crop Res.* 114, 426–432. doi: 10.1016/j.fcr.2009.09.009

Jyothi Swaroopa, V., and Lakshmi, M. B. (2015). Effect of nitrogen and foliar fertilization on yield components and quality parameters of machine transplanted rice. *Curr. Biot.* 9, 230–238.

Karmakar, B., Haefele, S. M., Henry, A., Kabir, M. H., Islam, A., and Biswas, J. C. (2021). In quest of nitrogen use-efficient rice genotypes for drought-prone rainfed ecosystems. *Front. Agron.* 2. doi: 10.3389/fagro.2020.607792

Katuwal, Y., Marahatta, S., Sah, S. K., and Dhakal, S. (2021). Nitrogen uptake and nitrogen use efficiencies of improved and hybrid rice varieties at different levels. *Adv. Crop Sci. Technol.* 9, 1–5.

Khan, A., Tan, D. K. Y., Afridi, M. Z., Luo, H., Tung, S. A., Ajab, M., et al. (2017). Nitrogen fertility and abiotic stresses management in cotton crop: a review. *Environ. Sci. Pollut. Res.* 24, 14551–14566. doi: 10.1007/s11356-017-8920-x

Kong, D.-X., Li, Y.-Q., Wang, M.-L., Bai, M., Zou, R., Tang, H., et al. (2016). Effects of light intensity on leaf photosynthetic characteristics, chloroplast structure, and alkaloid content of Mahonia bodinieri (Gagnep.) Laferr. *Acta Physiol. Plant* 38, 120. doi: 10.1007/s11738-016-2147-1

Kopsell, D. A., Kopsell, D. E., Lefsrud, M. G., Curran-Celentano, J., and Dukach, L. E. (2004). Variation in Lutein, β-carotene, and Chlorophyll Concentrations among Brassica oleracea Cultigens and Seasons. *HortScience* 39, 361–364. doi: 10.21273/HORTSCI.39.2.361

Kumar, N., Mathpal, B., Sharma, A., Shukla, A., Shankhdhar, D., and Shankhdhar, S. C. (2015). Physiological evaluation of nitrogen use efficiency and yield attributes in rice (Oryza sativa L.) genotypes under different nitrogen levels. *Cereal Res. Commun.* 43, 166–177. doi: 10.1556/CRC.2014.0032

Kumar, G. S., Rajarajan, A., Thavapraka, N., Babu, C., and Umashankar, R. (2008). Nitrogen use efficiency of rice (Oryza sativa) in systems of cultivation with varied N levels under 15N tracer technique. *Asian J. Agric. Res.* 2, 37–40. doi: 10.3923/ajar.2008.37.40

Kumar, S., Tripathi, S., Singh, S. P., Prasad, A., Akter, F., Syed, M. A., et al. (2021). Rice breeding for yield under drought has selected for longer flag leaves and lower stomatal density. *J. Exp. Bot.* 72, 4981–4992. doi: 10.1093/jxb/erab160

Kumari, S., Sharma, N., and Raghuram, N. (2021). Meta-analysis of yield-related and N-responsive genes reveals chromosomal hotspots, key processes and candidate genes for nitrogen-use efficiency in rice. *Front. Plant Sci.* 12. doi: 10.3389/fpls.2021.627955

Kunta, R., and Thatikunta, R. (2020). Influence of nitrogen levels on physiological response, nitrogen use efficiency and yield of rice (Oryza sativa L.) genotypes. *Curr. J. Appl. Sci. Technol.*, 145–152. doi: 10.9734/cjast/2020/v39i4831211

Kvet, J. (1971). Methods of growth analysis. *Plant Photosynth. Prod. Man. Methods*, 343–391.

Ladha, J. K., Jat, M. L., Stirling, C. M., Chakraborty, D., Pradhan, P., Krupnik, T. J., et al. (2020). *Achieving the sustainable development goals in agriculture: The crucial role of nitrogen in cereal-based systems. Advances in Agronomy* (Academic Press), 163; 39–116. doi: 10.1016/bs.agron.2020.05.006

Ladha, J. K., Kirk, G. J. D., Bennett, J., Peng, S., Reddy, C. K., Reddy, P. M., et al. (1998). Opportunities for increased nitrogen-use efficiency from improved lowland rice germplasm. *F. Crop Res.* 56, 41–71. doi: 10.1016/S0378-4290(97)00123-8

Laperche, A., Devienne-Barret, F., Maury, O., Le Gouis, J., and Ney, B. (2006). A simplified conceptual model of carbon/nitrogen functioning for QTL analysis of winter wheat adaptation to nitrogen deficiency. *Theor. Appl. Genet.* 113, 1131–1146. doi: 10.1007/s00122-006-0373-4

Lee, S. (2021). Recent advances on nitrogen use efficiency in rice. *Agronomy* 11, 1–17. doi: 10.3390/agronomy11040753

Li, Y., Yang, X., Ren, B., Shen, Q., and Guo, S. (2012). Why nitrogen use efficiency decreases under high nitrogen supply in rice (Oryza sativa L.) seedlings. *J. Plant Growth Regul.* 31, 47–52. doi: 10.1007/s00344-011-9218-8

Liang, H., Gao, S., Ma, J., Zhang, T., Wang, T., Zhang, S., et al. (2021). Effect of nitrogen application rates on the nitrogen utilization, yield and quality of rice. *Food Nutr. Sci.* 12, 13–27. doi: 10.4236/fns.2021.121002

Lichtenthaler, H. K., and Wellburn, A. R. (1983). Determinations of total carotenoids and chlorophylls a and *b* of leaf extracts in different solvents. *Biochem. Soc Trans.* 11, 591–592. doi: 10.1042/bst0110591

Liu, Z., Gao, F., Yang, J., Zhen, X., Li, Y., Zhao, J., et al. (2019). Photosynthetic characteristics and uptake and translocation of nitrogen in peanut in a wheat–peanut rotation system under different fertilizer management regimes. *Front. Plant Sci.* 10. doi: 10.3389/fpls.2019.00086

Liu, X., and Li, Y. (2016). Varietal difference in the correlation between leaf nitrogen content and photosynthesis in rice (Oryza sativa L.) plants is related to specific leaf weight. *J. Integr. Agric.* 15, 2002–2011. doi: 10.1016/S2095-3119(15)61262-X

Liu, Q. F., and Xu, S. Q. (2018). Response of fluorescence parameters and photosynthetic traits of rice to different nitrogen application under sufficient irrigation. *J. Irrig. Drainage.* 37, 6–12.

Liu, X., Zhang, Y., Han, W., Tang, A., Shen, J., Cui, Z., et al. (2013). Enhanced nitrogen deposition over China. *Nature* 494, 459–462. doi: 10.1038/nature11917

Mahajan, G., Chauhan, B. S., and Gill, M. S. (2011). Optimal nitrogen fertilization timing and rate in dry-seeded rice in northwest India. *Agron. J.* 103, 1676–1682. doi: 10.2134/agronj2011.0184

Makino, A., Sakuma, H., Sudo, E., and Mae, T. (2003). Differences between maize and rice in N-use efficiency for photosynthesis and protein allocation. *Plant Cell Physiol.* 44, 952–956. doi: 10.1093/pcp/pcg113

Mandal, V. K., Jangam, A. P., Chakraborty, N., and Raghuram, N. (2022). Nitrate-responsive transcriptome analysis reveals additional genes/processes and associated traits viz. height, tillering, heading date, stomatal density and yield in japonica rice. *Planta* 255. doi: 10.1007/s00425-021-03816-9

Maxwell, K., and Johnson, G. N. (2000). Chlorophyll fluorescence—a practical guide. *J. Exp. Bot.* 51, 659–668. doi: 10.1093/jexbot/51.345.659

Mboyerwa, P. A., Kibret, K., Mtakwa, P., and Aschalew, A. (2022). Rice yield and nitrogen use efficiency with system of rice intensification and conventional management practices in mkindo irrigation scheme, Tanzania. *Front. Sustain. Food Syst.* 6. doi: 10.3389/fsufs.2022.802267

Metson, G. S., Chaudhary, A., Zhang, X., Houlton, B., Oita, A., Raghuram, N., et al. (2021). Nitrogen and the food system. *One Earth* 4, 3–7. doi: 10.1016/j.oneear.2020.12.018

Moenirad, A., Zeinali, E., Galeshi, S., Soltani, A., and Eganepour, F. (2021). Investigation of fluorescence chlorophyll sensitivity, chlorophyll index, rate ofChlorophyll (a, b), nitrogen concentration and nitrogen nutrition index under under nitrogen and phosphorus nutrition in wheat. *J. Crop Prod.* 14, 1–18. doi: 10.22069/ejcp.2021.12259.1947

Moll, R. H., Kamprath, E. J., and Jackson, W. A. (1982). Analysis and interpretation of factors which contribute to efficiency of nitrogen utilization [1]. *Agron. J.* 74, 562–564. doi: 10.2134/agronj1982.00021962007400030037x

Mugo, J. N., Karanja, N. N., Gachene, C. K., Dittert, K., Gitari, H. I., and Schulte-Geldermann, E. (2021). Response of potato crop to selected nutrients in central and eastern highlands of Kenya. *Cogent Food Agric.* 7, 1–19. doi: 10.1080/23311932.2021.1898762

Muthayya, S., Sugimoto, J. D., Montgomery, S., and Maberly, G. F. (2014). An overview of global rice production, supply, trade, and consumption. *Ann. N. Y. Acad. Sci.* 1324, 7–14. doi: 10.1111/nyas.12540

Nasar, J., Khan, W., Khan, M. Z., Gitari, H. I., Gbolayori, J. F., Moussa, A. A., et al. (2021). Photosynthetic activities and photosynthetic nitrogen use efficiency of maize crop under different planting patterns and nitrogen fertilization. *J. Soil Sci. Plant Nutr.* 21, 2274–2284. doi: 10.1007/s42729-021-00520-1

Nasar, J., Shao, Z., Arshad, A., Jones, F. G., Liu, S., Li, C., et al. (2020). The effect of maize–alfalfa intercropping on the physiological characteristics, nitrogen uptake and yield of maize. *Plant Biol.* 22, 1140–1149. doi: 10.1111/plb.13157

Nasar, J., Wang, G. Y., Ahmad, S., Muhammad, I., Zeeshan, M., Gitari, H., et al. (2022). Nitrogen fertilization coupled with iron foliar application improves the photosynthetic characteristics, photosynthetic nitrogen use efficiency, and the related enzymes of maize crops under different planting patterns. *Front. Plant Sci.* 13. doi: 10.3389/fpls.2022.988055

Nduwimana, D. (2020). Optimizing nitrogen use efficiency and maize yield under varying fertilizer rates in Kenya. *Int. J. Bioresour. Sci.* 7, 63–73. doi: 10.30954/2347-9655.02.2020.4

Neeraja, C. N., Subramanyam, D., Surekha, K., Rao, P. R., Rao, L. V. S., Babu, M. B. B. P., et al. (2016). Advances in genetic basis of nitrogen use efficiency of rice. *Indian J. Plant Physiol.* 21, 504–513. doi: 10.1007/s40502-016-0254-z

Noor Shah, A., Wu, Y., Iqbal, J., Tanveer, M., Bashir, S., Ur Rahman, S., et al. (2021). Nitrogen and plant density effects on growth, yield performance of two different cotton cultivars from different origin. *J. King Saud Univ. - Sci.* 33, 101512. doi: 10.1016/j.jksus.2021.101512

Novoa, R., and Loomis, R. S. (1981). Nitrogen and plant production. *Plant Soil* 58, 177–204. doi: 10.1007/BF02180053

Ochieng', I. O., Gitari, H. I., Mochoge, B., Rezaei-Chiyaneh, E., and Gweyi-Onyango, J. P. (2021). Optimizing maize yield, nitrogen efficacy and grain protein content under different N forms and rates. *J. Soil Sci. Plant Nutr.* 21, 1867–1880. doi: 10.1007/s42729-021-00486-0

Ogawa, T., Oikawa, S., and Hirose, T. (2016). Nitrogen-utilization efficiency in rice: an analysis at leaf, shoot, and whole-plant level. *Plant Soil* 404, 321–344. doi: 10.1007/s11104-016-2832-2

Pan, S., Huang, S., Zhai, J., Wang, J., Cao, C., Cai, M., et al. (2012). Effects of N management on yield and N uptake of rice in central China. *J. Integr. Agric.* 11, 1993–2000. doi: 10.1016/S2095-3119(12)60456-0

Pan, S., Liu, H., Mo, Z., Patterson, B., Duan, M., Tian, H., et al. (2016). Effects of nitrogen and shading on root morphologies, nutrient accumulation, and photosynthetic parameters in different rice genotypes. *Sci. Rep.* 6, 32148. doi: 10.1038/srep32148

Pan, J., Liu, Y., Zhong, X., Lampayan, R. M., Singleton, G. R., Huang, N., et al. (2017). Grain yield, water productivity and nitrogen use efficiency of rice under different water management and fertilizer-N inputs in South China. *Agric. Water Manage.* 184, 191–200. doi: 10.1016/j.agwat.2017.01.013

Paponov, I. A., and Engels, C. (2003). Effect of nitrogen supply on leaf traits related to photosynthesis during grain filling in two maize genotypes with different N efficiency. *J. Plant Nutr. Soil Sci.* 166, 756–763. doi: 10.1002/jpln.200320339

Paul, N. K. (1990). Physiological analysis of nitrogen response in rape and turnip. II. Photosynthesis, respiration and leaf anatomy. *Acta Agron. Hungarica* 39, 37–42.

Pearce, T. H. (1968). A contribution to the theory of variation diagrams. *Contrib. to Mineral. Petrol.* 19, 142–157. doi: 10.1007/BF00635485

Peng, J., Feng, Y., Wang, X., Li, J., Xu, G., Phonenasay, S., et al. (2021). Effects of nitrogen application rate on the photosynthetic pigment, leaf fluorescence characteristics, and yield of indica hybrid rice and their interrelations. *Sci. Rep.* 11, 1–10. doi: 10.1038/s41598-021-86858-z

Poorter, H., Niinemets, Ü., Poorter, L., Wright, I. J., and Villar, R. (2009). Causes and consequences of variation in leaf mass per area (LMA): a meta-analysis. *New Phytol.* 182, 565–588. doi: 10.1111/j.1469-8137.2009.02830.x

Qi, H., Wang, J., and Wang, Z. (2013). A comparative study of the sensitivity of F v/F m to phosphorus limitation on four marine algae. *J. Ocean Univ. China* 12, 77–84. doi: 10.1007/s11802-011-1975-5

Quarrie, S. A., and Jones, H. G. (1979). Genotypic variation in leaf water potential, stomatal conductance and abscisic acid concentration in spring wheat subjected to artificial drought stress. *Ann. Bot.* 44, 323–332. doi: 10.1093/oxfordjournals.aob.a085736

R Core Team. (2012). *R: A Language and Environment for Statistical Computing*. R Foundation for Statistical Computing, Vienna, Austria. Available at: http://www.r-project.org/.

Raghuram, N., and Sharma, N. (2019). *Improving crop nitrogen use efficiency. Comprehensive Biotechnology. 3rd ed* (ElsevierPergamon) 4, 2011–220.

Raghuram, N., Sutton, M. A., Jeffery, R., Ramachandran, R., and Adhya, T. K. (2021). From South Asia to the world: embracing the challenge of global sustainable nitrogen management. *One Earth* 4, 22–27. doi: 10.1016/j.oneear.2020.12.017

Rajesh, K., Thatikunta, R., Naik, D. S., and Arunakumari, J. (2017). Effect of different nitrogen levels on morpho physiological and yield parameters in rice (Oryza sativa L.). *Int. J. Curr. Microbiol. Appl. Sci.* 6, 2227–2240. doi: 10.20546/ijcmas.2017.608.262

Rea, R., Islam, M., Rahman, M., and Mix, K. (2019). Study of nitrogen use efficiency and yield of rice influenced by deep placement of nitrogen fertilizers. *SAARC J. Agric.* 17, 93–103. doi: 10.3329/sja.v17i1.42764

Roy Chowdhury, S., Brahmanand, P. S., Kundu, D. K., Thakur, A. K., and Kumar, A. (2014). Influence of seedling age and nitrogen application on photosynthesis and yield of rice (Oryza sativa) grown under waterlogged condition. *Indian J. Plant Physiol.* 19, 83–86. doi: 10.1007/s40502-014-0082-y

Sapkota, T. B., Bijay-Singh,, and Takele, R. (2023). Chapter Five - Improving nitrogen use efficiency and reducing nitrogen surplus through best fertilizer nitrogen management in cereal production: The case of India and China. *Advances in Agronomy* (Academic Press) 178, 233–294. doi: 10.1016/bs.agron.2022.11.006

Shah, A. N., Wu, Y., Tanveer, M., Hafeez, A., Tung, S. A., Ali, S., et al. (2021). Interactive effect of nitrogen fertilizer and plant density on photosynthetic and agronomical traits of cotton at different growth stages. *Saudi J. Biol. Sci.* 28, 3578–3584. doi: 10.1016/j.sjbs.2021.03.034

Sharma, L., and Bali, S. (2017). A review of methods to improve nitrogen use efficiency in agriculture. *Sustainability* 10, 51. doi: 10.3390/su10010051

Singh, U., Ladha, J., Castillo, E., Punzalan, G., Tirol-Padre, A., and Duqueza, M. (1998). Genotypic variation in nitrogen use efficiency in medium- and long-duration rice. *F. Crop Res.* 58, 35–53. doi: 10.1016/S0378-4290(98)00084-7

Singh, H., Verma, A., Ansari, M. W., and Shukla, A. (2014). Physiological response of rice (Oryza sativa L.) genotypes to elevated nitrogen applied under field conditions. *Plant Signal. Behav.* 9, 1–8. doi: 10.4161/psb.29015

Subrahmanyam, D., Raghuveer Rao, P., Neeraja, C. N., and Voleti, S. R. (2019). *Research highlights of NICRA on rice, (2011-2019). Technical bulletin no. 107/2019* (India: ICAR- Indian Institute of Rice Research Rajendranagar, Hyderabad-500030), 71.

Sutton, M. A., Bleeker, A., Howard, C. M., Erisman, J. W., Abrol, Y. P., Bekunda, M., et al. (2013). *Our nutrient world : the challenge to produce more food and energy with less pollution* (Centre for Ecology & Hydrology on behalf of the Global Partnership on Nutrient Management (GPNM) and the International Nitrogen Initiative (INI), 1–128.

Sutton, M. A., Drewer, J., Moring, A., Adhya, T. K., Ahmed, A., Bhatia, A., et al. (2017). "The Indian nitrogen challenge in a global perspective," in *The Indian Nitrogen Assessment* (Elsevier), 9–28. doi: 10.1016/B978-0-12-811836-8.00002-1

Swarna, R., Leela Rani, P., Sreenivas, G., Raji Reddy, D., and Madhavi, A. (2017). Growth performance and radiation use efficiency of transplanted rice under varied plant densities and nitrogen levels. *Int. J. Curr. Microbiol. Appl. Sci.* 6, 1429–1437. doi: 10.20546/ijcmas.2017.605.156

Tayefe, M., Gerayzade, A., Amiri, E., and Zade, A. N. (2011). "Effect of nitrogen fertilizer on nitrogen uptake, nitrogen use efficiency of rice," in *International Proceedings of Chemical, Biological and Environmental Engineering (IPCBEE)*. (Dubai, United Arab Emirates: International Association of Computer Science and Information Technology) 24, 470–473.

Tewatia, R. K., and Chanda, T. K. (2017). Trends in fertilizer nitrogen production and consumption in India. *Indian Nitrogen Assess. Sources React. Nitrogen Environ. Clim. Eff. Manage. Options Policies*, 45–56. doi: 10.1016/B978-0-12-811836-8.00004-5

Vijayalakshmi, P., Kiran, T. V., Rao, Y. V., Srikanth, B., Rao, I. S., Sailaja, B., et al. (2013). Physiological approaches for increasing nitrogen use efficiency in rice. *Indian J. Plant Physiol.* 18, 208–222. doi: 10.1007/s40502-013-0042-y

Vijayalakshmi, P., Vishnukiran, T., Ramana Kumari, B., Srikanth, B., Subhakar Rao, I., Swamy, K. N., et al. (2015). Biochemical and physiological characterization for nitrogen use efficiency in aromatic rice genotypes. *F. Crop Res.* 179, 132–143. doi: 10.1016/j.fcr.2015.04.012

Wang, Y., Ren, T., Lu, J., Ming, R., Li, P., Hussain, S., et al. (2016). Heterogeneity in rice tillers yield associated with tillers formation and nitrogen fertilizer. *Agron. J.* 108, 1717–1725. doi: 10.2134/agronj2015.0587

Wang, B., Zhou, G., Guo, S., Li, X., Yuan, J., and Hu, A. (2022). Improving nitrogen use efficiency in rice for sustainable agriculture: strategies and future perspectives. *Life* 12, 1–13. doi: 10.3390/life12101653

Wani, S. A., Qayoom, S., Bhat, M. A., and Sheikh, A. A. (2017). *Effect of Varying Sowing Dates and Nitrogen Levels on Growth and Physiology of Scented Rice Gramin krishi mausam seva View project weed management and nutrient management View project*. Available at: https://www.researchgate.net/publication/319087729.

West, P. C., Gerber, J. S., Engstrom, P. M., Mueller, N. D., Brauman, K. A., Carlson, K. M., et al. (2014). Leverage points for improving global food security and the environment. *Sci. (80-.).* 345, 325–328. doi: 10.1126/science.1246067

Witcombe, J., Hollington, P., Howarth, C., Reader, S., and Steele, K. (2008). Breeding for abiotic stresses for sustainable agriculture. *Philos. Trans. R. Soc. B Biol. Sci.* 363, 703–716. doi: 10.1098/rstb.2007.2179

Xin, W., Zhang, L., Zhang, W., Gao, J., Yi, J., Zhen, X., et al. (2022). Morphological and physiological characteristics of rice cultivars with higher yield and nitrogen use efficiency at various nitrogen rates. *Agronomy* 12, 1–15. doi: 10.3390/agronomy12020358

Yang, W.-H., Peng, S., Huang, J., Sanico, A. L., Buresh, R. J., and Witt, C. (2003). Using leaf color charts to estimate leaf nitrogen status of rice. *Agron. J.* 95, 212–217. doi: 10.2134/agronj2003.2120

Yang, L., Yan, J., and Cai, Z. (2010). Effects of N-applications and photosynthesis of maize (Zea mays L.) on soil respiration and its diurnal variation. *Front. Agric. China* 4, 42–49. doi: 10.1007/s11703-009-0088-9

Ye, T., Li, Y., Zhang, J., Hou, W., Zhou, W., Lu, J., et al. (2019b). Nitrogen, phosphorus, and potassium fertilization affects the flowering time of rice (Oryza sativa L.). *Glob. Ecol. Conserv.* 20, 311–319. doi: 10.1016/j.gecco.2019.e00753

Ye, M., Peng, S. B., and Li, Y. (2019a). Intraspecific variation in photosynthetic nitrogen-use efficiency is positively related to photosynthetic rate in rice (Oryza sativa L.) plants. *Photosynthetica* 57, 311–319. doi: 10.32615/ps.2019.011

Ye, Q., Zhang, H., Wei, H., Zhang, Y., Wang, B., Xia, K., et al. (2007). Effects of nitrogen fertilizer on nitrogen use efficiency and yield of rice under different soil conditions. *Front. Agric. China* 1, 30–36. doi: 10.1007/s11703-007-0005-z

Yesuf, E., and Balcha, A. (2014). Effect of nitrogen application on grain yield and nitrogen efficiency of rice (Oryza sativa L.). *Asian J. Crop Sci.* 6, 273–280. doi: 10.3923/ajcs.2014.273.280

Zhang, J., Tong, T., Potcho, P. M., Huang, S., Ma, L., and Tang, X. (2020). Nitrogen effects on yield, quality and physiological characteristics of giant rice. *Agronomy* 10, 1–16. doi: 10.3390/agronomy10111816

Zhang, Z. X., Zheng, E. N., Wang, C. M., and Fu, N. H. (2017). Effect of different water and nitrogen levels on chlorophyll fluorescence parameters and photosynthetic characteristics of rice. *Trans. Chin. Soc Agric. Mach.* 48, 176–183.

Zhao, B., Dong, S., Zhang, J., and Liu, P. (2013). Effects of controlled-release fertiliser on nitrogen use efficiency in summer maize. *PLoS One* 8, e70569. doi: 10.1371/journal.pone.0070569

Zhong, C., Jian, S.-F., Huang, J., Jin, Q.-Y., and Cao, X.-C. (2019). Trade-off of within-leaf nitrogen allocation between photosynthetic nitrogen-use efficiency and water deficit stress acclimation in rice (Oryza sativa L.). *Plant Physiol. Biochem.* 135, 41–50. doi: 10.1016/j.plaphy.2018.11.021

Zhu, K., Yan, J.q., Shen, Y., Zhang, W.y., Xu, Y., Wang, Z.q., et al. (2022). Deciphering the morpho–physiological traits for high yield potential in nitrogen efficient varieties (NEVs): A japonica rice case study. *J. Integr. Agric.* 21, 947–963. doi: 10.1016/S2095-3119(20)63600-0

frontiers | Frontiers in Plant Science

TYPE Original Research
PUBLISHED 22 January 2024
DOI 10.3389/fpls.2023.1281495

OPEN ACCESS

EDITED BY
Nigel G. Halford,
Rothamsted Research, United Kingdom

REVIEWED BY
Dietmar Funck,
University of Konstanz, Germany
Joseph Oddy,
University of Oxford, United Kingdom

*CORRESPONDENCE
Céline Masclaux-Daubresse
celine.masclaux-daubresse@inrae.fr
Fabien Chardon
fabien.chardon@inrae.fr

†These authors have contributed equally to this work and share last authorship

RECEIVED 22 August 2023
ACCEPTED 01 December 2023
PUBLISHED 22 January 2024

CITATION
Lardos M, Marmagne A, Bonadé Bottino N, Caris Q, Béal B, Chardon F and Masclaux-Daubresse C (2024) Discovery of the biostimulant effect of asparagine and glutamine on plant growth in *Arabidopsis thaliana*. *Front. Plant Sci.* 14:1281495. doi: 10.3389/fpls.2023.1281495

Discovery of the biostimulant effect of asparagine and glutamine on plant growth in *Arabidopsis thaliana*

Manon Lardos[1,2], Anne Marmagne[1], Nolwenn Bonadé Bottino[1,2], Quentin Caris[1,2], Bernard Béal[2], Fabien Chardon[1*†] and Céline Masclaux-Daubresse[1*†]

[1]Université Paris-Saclay, INRAE, AgroParisTech, Institut Jean-Pierre Bourgin (IJPB), Versailles, France, [2]NOVAEM, Aigrefeuille d'Aunis, France

Protein hydrolysates have gained interest as plant biostimulants due to their positive effects on plant performances. They are mainly composed of amino acids, but there is no evidence of the role of individual of amino acids as biostimulants. In this study we carried out *in vitro* experiments to monitor the development of Arabidopsis seedlings on amino acid containing media in order to analyze the biostimulant properties of the twenty individual proteinogenic amino acids. We demonstrated that proteinogenic amino acids are not good nitrogen sources as compared to nitrate for plant growth. Biostimulant analyses were based on leaf area measurements as a proxy of plant growth. We developed the Amino Acid Use Efficiency index to quantify the biostimulating effect of individual amino acids in the presence of nitrate. This index allowed us to classify amino acids into three groups, characterized by their inhibiting, neutral, and beneficial effects regarding leaf area. Glutamine and asparagine demonstrated the most significant effects in promoting leaf area in the presence of nitrate supply. The stimulating effect was confirmed by using the L and D enantiomeric forms. Both L-glutamine and L-asparagine stimulated leaf area at low concentrations, emphasizing their biostimulating properties. Our plant growth design and AAUE index pave the way for the identification of other bioactive molecules in protein hydrolysates and for the comparison of biostimulant performances.

KEYWORDS

protein hydrolysate, *in vitro* experiment, amino acid enantiomer, amino acid use efficiency, *Arabidopsis thaliana*

Introduction

In a context where the world's population is estimated to be about 9.3 billion people by 2050 (Department of Economic and Social Affairs, 2022), agriculture must face the twin challenges of assuring food security and reducing pressure on the environment and natural resources (Searchinger et al., 2013). To date, the use of fertilizers essentially in the form of ammonium nitrate assures the stability of agricultural crop yield. However, in many countries, the overuse of those fertilizers is responsible for nitrogen leaching in groundwater (Sun et al., 2019) and for nitrous oxide emission (Billen et al., 2013). In addition, the synthesis of ammonium nitrate fertilizers through the Haber Bosch process is costly and fossil energy-consuming. To tackle these-substantial negative environmental consequences, it is crucial to identify and characterize sustainable inputs that can improve the plant nitrogen use efficiency.

Biostimulants constitute a suitable answer to this challenge. They are a novel category of agricultural inputs recently defined by the European Parliament. They stimulate nutrient use efficiency, tolerance to abiotic stress, quality trait, or availability of confined nutrients in the soil or rhizosphere independently of the product's nutrient content (Regulation EU, 2019). Moreover, they participate in a circular economy allowing upcycling of by-products or waste from other industries (Baglieri et al., 2014; Colla et al., 2015). There are 7 classes of biostimulants; among them protein hydrolysates (PHs) are produced from strong acid or alkaline hydrolysis of plants, vegetable by-products, or animal sources (i.e. leather, viscera, feather, blood) (Colla et al., 2015; du Jardin, 2015; Xu and Geelen, 2018). Due to their mode of production PHs mostly contain amino acids (AAs) and small peptides. Their foliar or root application can promote the growth and yield of crops. For instance, PHs could enhance the yield of soybean and pepper by 32% and 22% respectively (Paradiković et al., 2011; Kocira, 2019). They could also enhance the root growth and fruit weight of tomatoes and the fresh biomass of lettuce (Cerdán et al., 2013; Rouphael et al., 2017; Malécange et al., 2022). The above positive effects might be associated with the stimulation of leaf sugar accumulation and nitrogen assimilation (Schiavon et al., 2008; Ertani et al., 2013). Nevertheless, despite plenty of examples of their positive effects and because of the diversity and inconsistency of source materials used for these products, the identity of the bioactive molecules of PHs remains to be determined.

In PHs from animal or vegetable sources, total amino acids can represent 27% to 68.5% of the total nitrogen content and individual amino acids vary from 2% to 18% of the total product depending on the sources of materials used to produce them (Calvo et al., 2014; Colla et al., 2014; Lucini et al., 2015; Ambrosini et al., 2021). It is well known that amino acids are essential molecules in plants as building blocks of proteins. They are also involved as precursors of tremendous specialized metabolites for plant adaptation to environmental stresses (Zhao, 2010; Maeda and Dudareva, 2012; Hildebrandt et al., 2015). Soil can contain free amino acids and plant roots possess transporters on plasma membranes for their absorption (Näsholm et al., 2009; Tegeder and Rentsch, 2010; Tegeder and Masclaux-Daubresse, 2018; Yang et al., 2020; Yao et al., 2020). Amino acid transporters described in literature belong to families as AAP (Amino acids permease), LHT (Lysine Histidine like transporter) and ProT (Proline transporter). Once they are absorbed by the plant, amino acids can be directly used for root growth or loaded to xylem to be transported to the aerial parts and contribute to general plant growth (Tegeder, 2014). Several publications report that amino acids alone are not efficient sources of nitrogen for plant growth. For example, Forsum et al. (2008) demonstrated that when *Arabidopsis thaliana* (Arabidopsis) seedlings were grown on amino acids, only six [Glutamine (Gln); Asparagine (Asn), Aspartate (Asp), Glycine (Gly), Alanine (Ala) and Arginine (Arg)] over the ten tested supported plant growth. However at equivalent supply of nitrogen, amino acids were weaker to promote growth compared to nitrate (Forsum et al., 2008). Nutritive effect of amino acids on plant growth is also dependent of their enantiomeric forms. Even if the L and D forms can be both absorbed by roots (Forsum et al., 2008), it seems that plants lack the capacity to metabolize the D-form in contrast to microbes (Bollard, 1966; Forsum, 2016). At the concentration of use described in literature, the positive effects of PHs cannot be explained by the nutritive effect of the amino acids they contain. Thus, we can hypothesize that the amino acids composing PHs display biostimulant effects.

In this study we examined the individual effects of the 20 proteinogenic amino acids on the growth of Arabidopsis seedlings. To discriminate biostimulant effect from nutritive effect, we first monitored leaf area when amino acids were provided as sole source of nitrogen. Next, we analyzed the positive, neutral or inhibitory effects of individual amino acids on plant growth, when provided in addition of a sufficient nitrate supply (KNO_3). We then developed a new index AAUE (Amino acids use efficiency) as an indicator of the biostimulating effect of individual amino acids. The biostimulant activities of amino acids were then confirmed by decreasing the concentrations of amino acids supplied into the plant growth medium, and by using enantiomeric forms.

Materials and methods

Plant material and growth conditions

Seeds of the *Arabidopsis thaliana* Columbia wild type (*Col-0*) have been provided by the Versailles Resource center (INRA Versailles France, http://dbsgap.versailles.inra.fr/vnat/). *In vitro* culture was carried out using surface-sterilized seeds on horizontal agar plates. Using toothpick, seeds were sown on 0.8% agar medium with 1% sucrose, 2.5 mM KH_2PO_4, 2 mM $MgSO_4$, 5 mM KCl, 2 mM $CaCl_2$, 0.015 mM bromocresol purple (pH 5.8), 3.6 mM MES, 0.014 mM Fe-EDTA, supplemented with 1X microelements (Estelle and Somerville, 1987) and Morel and Wetmore vitamins. The concentrations of KNO_3 and/or amino acids supplied in the media are indicated in the legends of the figures. All solutions had a pH of 5.8. After sowing, agar plates were

incubated in a cold dark room at 4°C for 48 h for seed stratification and then transferred to a climate chamber (12 m^2) under long day conditions (16/8 h photoperiod at 90 µmol photons m^{-2} s^{-1} with OSRAM LUMINUX COOL DAYLIGHT fluorescent lamps (L36W/865), 21°C day temperature and 18°C night temperature, relative humidity of 63%. Despite the global control of all the environmental parameters, there were still local uncontrolled variations due to the size of the chamber. To minimize related stochastic variation, the location of the plates in the growth chamber was changed regularly and all the experiments were repeated several times. Depending on experiments, the seed density was 16, 40, or 100 seeds per plate and is indicated in the legends of the figures. The culture duration was 12 days for high seed density and 14 days for low seed density.

Leaf area imaging

All agar plates were imaged 12 or 14 days after sowing. Images were obtained using Gel doc Systems (Biorad®) with white trays. Then leaf area was determined using ImageJ software. (Version 1.53C).

Determination of amino acid use efficiency

The contribution of an amino acid to plant growth was obtained by comparing the leaf area of the plants grown on plates containing amino acid and nitrate [AA + KNO_3], nitrate alone [KNO_3] or no nitrogen [0N]. To estimate contribution of individual amino acids to plant growth, we developed the AAUE index (Amino Acid Use Efficiency), that calculates the gain of growth in the presence of AA and nitrate compared to the gain in the presence of nitrate only, according to the equation below:

$$AAUE = \frac{Area_{(AA+3N)} - \overline{Area}_{(Ctrl\ 0N)}}{\overline{Area}_{(Ctrl\ 3N)} - \overline{Area}_{(Ctrl\ 0N)}} \quad (1)$$

with $Area_{(AA+3N)}$ is the leaf area of plants grown with amino acid and 3 mM nitrate in one plate, $\overline{Area}_{(Ctrl\,0N)}$ is the mean of leaf area of plants grown without nitrogen, $\overline{Area}_{(Ctrl\,3N)}$ is the mean of leaf area of plants grown with 3 mM nitrate only.

For plates corresponding to the control conditions (3 mM KNO_3; Ctrl 3N) and (5 mM KNO_3; Ctrl 5N), AAUE was calculated using the (Equation 2, 3):

$$AAUE = \frac{Area_{(3N)} - \overline{Area}_{(Ctrl\ 0N)}}{\overline{Area}_{(Ctrl\ 3N)} - \overline{Area}_{(Ctrl\ 0N)}} \quad (2)$$

and

$$AAUE = \frac{Area_{(5N)} - \overline{Area}_{(Ctrl\ 0N)}}{\overline{Area}_{(Ctrl\ 3N)} - \overline{Area}_{(Ctrl\ 0N)}} \quad (3)$$

where $Area_{(3N)}$ and $Area_{(5N)}$ are the leaf area of plants grown with 3 mM KNO_3; or with 5 mM KNO_3 respectively.

In each experiment, 2 to 8 plates were prepared for each growth medium. On each plate, leaf area was estimated as the ratio of the total green area in the plate divided by the number of plants. We then calculated the mean of leaf areas for all the control conditions and computed the AAUE index by plate using the (Equations 1–3).

Statistical analyses

Two-way ANOVA (R software package) was used to assess the effects of experiment (Exp), media (Med) and their interaction factors (Med×Exp) on the trait variation. Med is the media tested in the plates (different nitrogen sources), Exp is a batch of plates tested on the same date and Med×Exp is an interaction between the two main factors. Before statistical analysis, the homogeneity of variance and normality of distribution of data were tested. For Figures 1, 2, these data did not fulfil the normality and homoscedasticity hypotheses, thus we used a log(x) and log(x+1) transformation respectively of data before running ANOVA with the *lm* function. Each contrast between the control condition and the other media conditions was tested by using marginal means with the function *contrast* of the R package "emmeans". Bar plots and curves were generated in R (R version 4.2.1). Pairwise differences between conditions were carried out by t-test using Bonferroni correction to adjust multiple comparisons (p value< 0.05, with n the total number of values per condition).

Results

Amino acids as nitrogen source for plant growth are less efficient than nitrate

To investigate amino acids as nitrogen sources for plant growth, we measured leaf area on seedlings grown for 12 days *in vitro* on agar media containing either 5 mM of one of the twenty proteinogenic amino acids, or 5 mM of KNO_3 as a control condition (Ctrl 5N). The use of amino acids as nitrogen source to sustain plant growth and metabolism is complex. It depends on the capacity of each amino acid to be absorbed at root level, mobilized in the plant tissue and then catabolized or use by amino-transferases. We then decided to start our study by providing each amino acid at equal molarity without considering their nitrogen stoichiometries.

We observed that the growth of the Arabidopsis seedlings was significantly reduced on amino acid containing media compared to Ctrl 5N, except in the case of glutamine (Gln), as illustrated by Figure 1A. In our experimental conditions, Gln was the only amino acid to promote plant growth to the same level as Ctrl 5N (Figure 1B). Leaf area was reduced by 52% compared with Ctrl 5N when the only nitrogen sources were glutamate (Glu) or alanine (Ala). With asparagine (Asn), aspartate (Asp), glycine (Gly), arginine (Arg), cysteine (Cys) and proline (Pro), the reduction of leaf area ranged between 69% to 88% of Ctrl 5N. Isoleucine (Ile), histidine (His), serine (Ser), and threonine (Thr) were the worst nitrogen sources as leaf area was reduced by at least 99% compared to Ctrl 5N. Seedlings barely developed after seed germination on media containing tyrosine (Tyr), valine (Val), methionine (Met), tryptophan (Trp), lysine (Lys), leucine (Leu) or phenylalanine (Phe) (Figure 1B). Altogether results show that except for glutamine, all the other amino acids are not a good source of nitrogen for the Arabidopsis seedling growth. The growth on amino acid media is independent of the N stoichiometry. For example, growth on Arginine, which has four

10.3389/fpls.2023.1281495

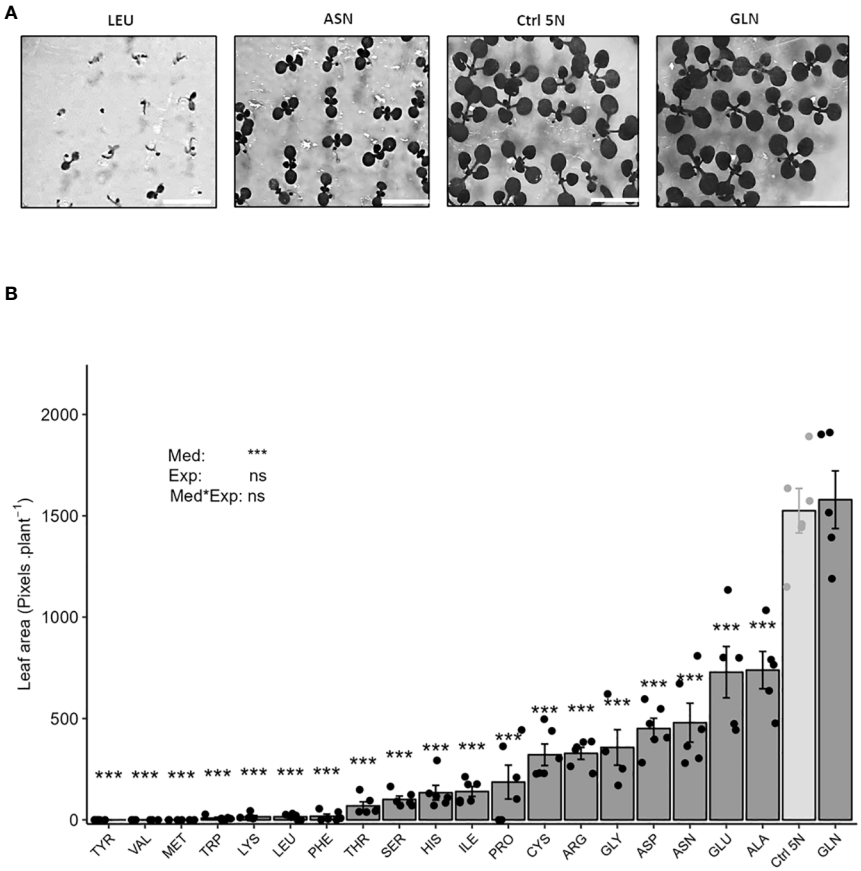

FIGURE 1
Glutamine and KNO_3 are the best nitrogen sources for *in vitro* plant growth. Representative pictures of mediocre, weak and optimal plant growth phenotypes **(A)**, scale = 0.80 cm. Plant growth was determined measuring leaf area **(B)**. Seedlings (100 per plate) of the Col-0 accession were grown for 12 days on agar media containing 1% sucrose and 5 mM of one of the twenty proteinogenic amino acids. Media also contained 0.1 mM KNO_3 to relieve dormancy and permit homogenous germination (Alboresi et al., 2005). The growth of the seedlings was determined by analyzing leaf area expressed in pixels per plant. The control consists of an agar medium containing 1% sucrose and 5 mM KNO_3 (Ctrl 5N, light grey). Data represent mean values obtained in 3 independent experiments containing 0-2 repeats. Error bars indicate the standard error of the mean. Stars indicate significant differences with Ctrl 5N (t-test, n= 4-6), and levels of significance for media (Med), experiment (Exp) and their interaction (Med*Exp) effects from ANOVA (full ANOVA results are shown in Supplementary Table 1); ns p-value >0.05, ***p-value< 0.001.

nitrogen atoms per molecule, was 44% of that obtained with alanine that provides only one nitrogen atom per molecule.

Detecting inhibitory, neutral, and beneficial effects of amino acid supplies on plant growth in the presence of nitrate using amino acid use efficiency indicator

Since we found that none of the twenty amino acids were as good nitrogen sources as nitrate for plant growth, we then questioned about the potential stimulating effects of individual amino acids on growth when nitrate is sufficient in growth medium. To test how amino acids could interfere with plant growth, we used a new agar medium that combined each amino acid (2 mM) with KNO_3 (3 mM). Contrasted growth rates were then observed depending on the nature of the amino acid. For example, Figure 2A illustrates the opposite effects of leucine and glutamine on plant growth by comparison to KNO_3 (3 mM; Ctrl 3N). Leaf areas were measured like in Figure 1, and we defined the "Amino acid use efficiency" (AAUE) index as the indicator of the relative plant growth on [nitrate plus amino acid] relative to [nitrate alone] [see Material and Methods, Equations 1–3)]. AAUE determined for each media allowed us to distinguish three different groups of amino acids (Figure 2B). Group 1 gathers the majority of the amino acids (12 in total) with AAUE significantly lower than 1. Growths on Group 1 media were decreased by 23% for Arg up to 100% for Tyr compared to Ctrl 3N (Figure 2B). Group 2 contains the three amino acids Pro, Gly, and Ala, and is characterized by an AAUE equivalent to 1, meaning that the presence of these amino acids in the growth medium was neutral and did not improve or reduce plant growth compared to Ctrl 3N (Figure 2B). The presence of amino acids from Group 3 (Asp, Glu, Cys, Asn, and Gln) is beneficial to plant growth relative to Ctrl 3N, as shown by their AAUE significantly higher than 1 (Figure 2B). AAUE was increased by 19% for Asp and up to 46% for Gln relative to Ctrl 3N. As Groups 1 and 2 amino acids did not stimulate plant growth under our conditions, by contrast with group 3, we decided to focus on the characterization of group 3 amino acids.

To better evaluate AAUE of the potential beneficial AA (group 3), we introduced Ctrl 5N (5 mM KNO_3) as a new nitrate control

10.3389/fpls.2023.1281495

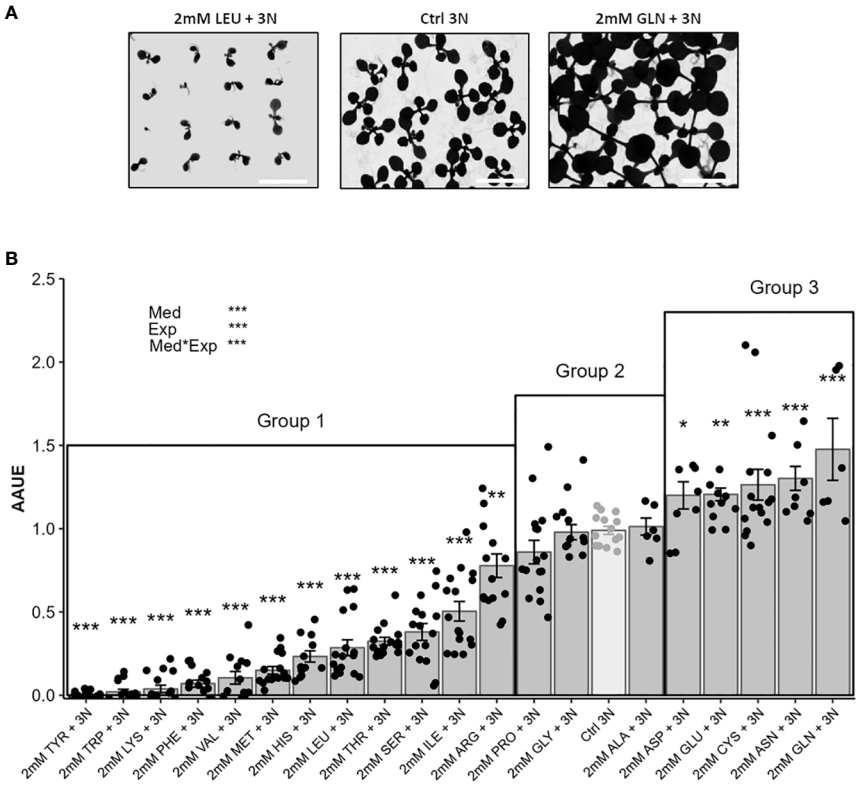

FIGURE 2
The new index "Amino acid use efficiency" (AAUE) distinguish inhibitory, neutral and beneficial amino acid nitrogen sources according to plant growth. Eighty seedlings of the Col-0 accession were grown for 12 days on an agar medium containing 1% sucrose, 3 mM KNO_3, and 2 mM of one of the 20 proteinogenic amino acids. The controls consisted of agar medium containing 1% sucrose with 3 mM KNO_3 (Ctrl 3N, light grey). Representative illustration of growth phenotypes for two amino acids presenting inhibitory or stimulating effects **(A)**, scale = 1.3 cm. AAUE were calculated from the leaf areas of plants grown on the different amino acid containing media according to Materiel and Methods **(B)**. Data are mean values obtained in 8 independent experiments containing 0-2 repeats. Error bars indicate the standard error of the mean. AAUE classifies amino acids into three groups: Group 1 (AAUE<1); group 2 (AAUE= 1); group 3 (AAUE> 1). Stars indicate significant differences with the Ctrl 3N (t-test, n= 6-16), and levels of significance for media (Med), experiment (Exp) and their interaction (Med*Exp) effects from ANOVA (full ANOVA results are shown in Supplementary Table 1); *p-value<0.05, **p-value<0.01, ***p-value<0.001.

condition and decreased the density of plants. Ctrl 5N provided the same nitrogen concentration (stoichiometry) as the [2 mM amino acid + 3 mM nitrate] condition when using Asp, Glu and Cys. Comparing the AAUE of the group 3 amino acids to the AAUE of Ctrl 5N, we found that only AAUE of Asn and Gln were significantly higher than the AAUE of Ctrl 5N (20% and 28% increase respectively; Supplementary Figures S1A, B). We concluded that Asp, Glu, Cys had no biostimulant effect in our experimental design.

Bio-stimulating effects of asparagine and glutamine on plant growth are independent of enantiomeric forms and can be observed at low concentrations

To investigate the potential bio-stimulating effects of Asn and Gln on plant growth, we decided to (i) compare the enantiomeric L and D forms and (ii) to decrease the concentrations of Asn and Gln in growth media. In the experiment testing enantiomeric forms, the concentrations of the Gln and Asn were decreased to 1 mM to reach the same nitrogen stoichiometry as Ctrl 5N. The AAUE of the Asn (1 mM) and Gln (1 mM) L and D enantiomeric forms were then compared to Ctrl 5N. The AAUE of L-Asn, D-Asn, L-Gln and D-Gln were all significantly higher than the AAUE of Ctrl 5N (Figures 3A, B). This indicated that the bio-stimulant action of Asn and Gln was independent of the enantiomeric forms and thus independent of the possible assimilation and use in plant metabolism of these molecules. An experiment using lower concentration of L-Asn and L-Gln showed that adding 0.25 mM of one of these amino acids ($1/12^{th}$ of the nitrate concentration) was enough to provide a positive effect on plant growth compared to the N equivalent control (Figure 4). This emphasizes the potential of Asn and Gln as bio-stimulants of leaf area development.

Discussion

PHs have been described in the literature to promote plant growth and plant fitness of crops in the field (Ertani et al., 2013; Santi et al., 2017). In this study, we aimed at deciphering the role of each proteinogenic amino acid as a bioactive molecule that could

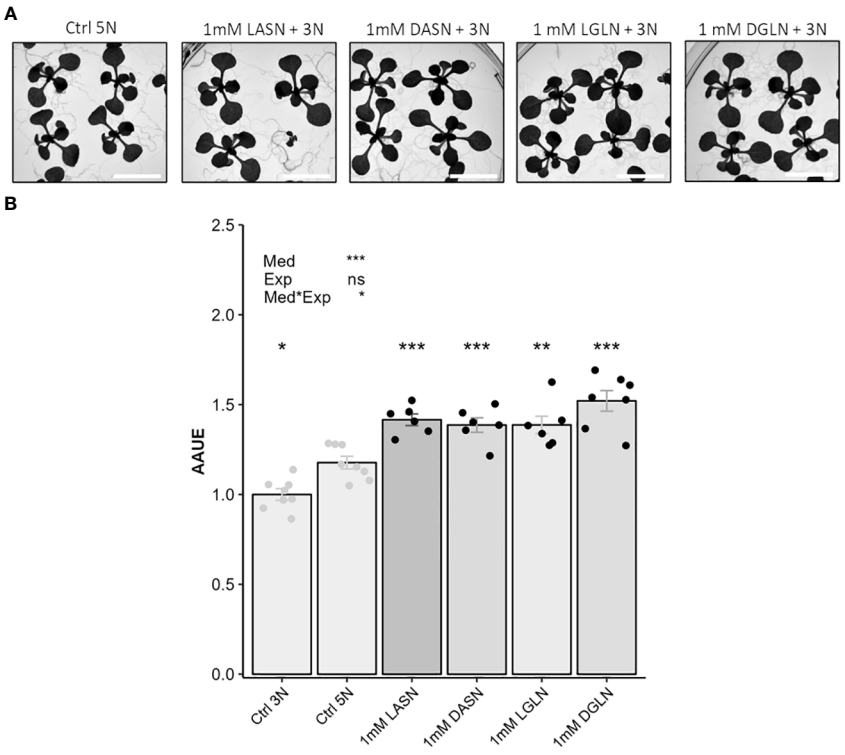

FIGURE 3
Both L and D enantiomers of asparagine and glutamine stimulate plant growth in presence of KNO_3. Scale = 1.3 cm. In this experiment 16 seedlings of Col-0 accession were grown for 14 days on an agar medium containing 1% sucrose, 3 mM KNO_3 and 1 mM of asparagine or glutamine. Control consists of an agar medium containing 1% sucrose and 3 mM (Ctrl 3N, light grey) or 5 mM of KNO_3 (Ctrl 5N, light grey). Note that adding 1 mM of Asn or Gln to 3 mM nitrate medium results in 5N nitrogen stoichiometry as found in the 5 mM nitrate control. Representative pictures of plant growth **(A)**. Plant growth estimated using AAUE index **(B)**. Data represent mean values obtained in 2 independent experiments containing 3 or 4 repeats. Error bars indicate the standard error of the mean. Stars indicate significant differences with the Ctrl 5N (t-test, n= 6-8), and levels of significance for media (Med), experiment (Exp) and their interaction (Med*Exp) effects from ANOVA (full ANOVA results are shown in Supplementary Table 1); ns p-value > 0.05, *p-value<0.01, **p-value<0.01, ***p-value<0.001.

stimulate plant growth and contribute to the PHs biostimulating effects. In our experimental condition, none of the twenty proteinogenic amino acids could better satisfy seedling nitrogen demand than nitrate, when used as the sole source of nitrogen. Our results were consistent with Forsum et al. in 2008, who tested ten amino acids as the sole source of nitrogen and showed that none of them were as effective as nitrate. To evaluate whether proteinogenic amino acids could have different effects on plant growth in the presence of nitrate, we then developed a new index called Amino acid use efficiency (AAUE) that was based on leaf area measurements.

AAUE facilitated the identification of amino acids providing inhibiting, neutral or stimulating effects on seedling growth when added to media containing nitrate. Among the twenty proteinogenic amino acids, we identified twelve amino acids that behaved as growth inhibitors, and three amino acids with neutral effect on plant growth, according to our experimental design. Inhibiting effects of several amino acids have already been identified, as for example in the case of branched chain amino acids, which inhibit plant growth as they have negative feedback on the synthesis of the other branched chain amino acids (Binder, 2010; Xing and Last, 2017). The feedback-inhibition of aspartate kinase by Lys, which is blocking the entrance enzyme into the Asp pathway, may also explain the negative effect of lysine on plant growth (Yang and Ludewig, 2014). Basic-, hydroxyl- and sulfur-containing amino acids were shown to severely block primary root growth at least when provided as sole source of nitrogen (Yang and Ludewig, 2014).

Regarding neutral effect, it was not surprising to find proline, that was a mediocre nitrogen source in our first experiment (Figure 1). More unexpected was the neutral effect of alanine that was one of the best nitrogen sources in Figure 1. Besides inhibitory and neutral amino acids, the five candidates (Glu, Asp, Cys, Asn, and Gln) displaying positive effects on plant growth were considered for better characterization. Taking into account nitrogen stoichiometry, determination of AAUE eliminated Glu, Asp and Cys from the potential biostimulating amino acids and led us to focus on Asn and Gln. The biostimulant properties of Gln and Asn were then completed showing that both amino acids can stimulate plant growth at low concentrations (0.25 mM; 1/12th of the nitrate supply) (Figure 4) thus independently of a potential carbon bonus effect. The absence of potential carbon bonus effect in our experiment was supported by the lack of growth stimulation by Asp and Glu that are built on the same carbon backbone as Gln and Asn.

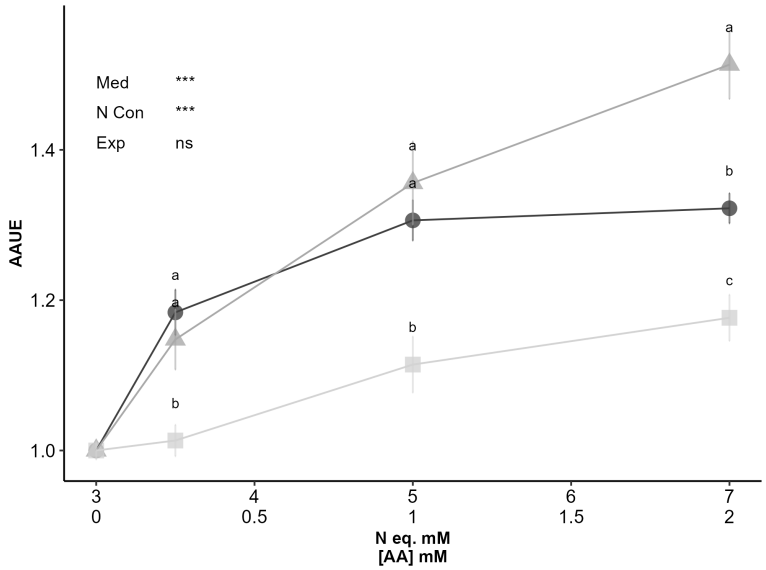

FIGURE 4
Asn and Gln stimulate plant growth at lower concentration. In this experiment, 16 seedlings of Col-0 accession were grown for 14 days on an agar medium containing 1% sucrose, 3 mM KNO_3 and 0.00, 0.25, 1.00 or 2.00 mM asparagine (dark grey circle) or glutamine (grey triangle). N equivalent controls consisted in 1% sucrose media with 3.00, 3.50, 5.00 and 7.00 mM of KNO_3 (light grey square). Both total N concentrations (top) and Asn and Gln concentrations (down) are presented on the X axis. Data represent the AAUE mean values obtained in 2 independent experiments containing 5-8 repeats. Error bars indicate the standard error of the mean. Different letters indicate significant differences between the AAUE obtained on the three media with equivalent N concentration (p-value<0.05, t.test, n=10-16). Stars indicate levels of significance for media (Med), N concentration (N Conc) and experiment (Exp) effects from ANOVA (full ANOVA results are shown in Supplementary Table 1); ns p-value>0.05, *** p-value<0.001.

In plants, amino acids are mainly present as L- enantiomeric forms. Several reports show that plants can uptake D- enantiomeric forms when available in the soil or growth medium (Bollard, 1966; Forsum, 2016). However, if and how plants utilize the D-amino acid forms remains debated and largely unclear. Gördes et al. (2011) and Gördes et al. (2013) showed that most of the D-amino acids can be absorbed by Arabidopsis seedlings. Whether racemisation of D amino acid occurs *in planta* remained unclear, but authors showed that most of the D-AAs could be metabolized and form D-Glu and D-Ala. The fact that L and D enantiomeric forms of Asn and Gln could stimulate plant growth to the same level in presence of nitrate (Figure 3) led us to conclude to their biostimulant properties.

Positive effects of Asn and Gln on plant growth have already been reported but without considering explicitly biostimulant effects. For instance, it was shown that supplying asparagine and glutamine at 1 mM could increase shoot length of *Phaseolus vulgaris* (Haroun et al., 2010). Glutamine application was reported to increase maize shoot dry weight by 7% (Hassan et al., 2020).

Processes for PHs production through chemical hydrolysis leads to the total conversion of asparagine and glutamine into Asp and Glu (Rouphael et al., 2020). While several of the inhibiting amino acids identified in our study are present in PHs, the fact that PHs can enhance plant growth suggests that mixtures of inhibitory, neutral and stimulating amino acid can mitigate the effects of inhibitory amino acids and possibly facilitate the expression of biostimulant effects that are independent from Asn and Gln. Accordingly, Bonner et al. (1992) demonstrated that the combination of amino acids could overcome amino acid inhibition. For instance, the inhibition of plant growth by glycine, alanine, proline and asparagine were partially antagonized by glutamine in woodland tobacco (Bonner et al., 1992). Correlative studies comparing PHs amino acid composition and biostimulant efficiency would be interesting to study and improve commercialized PHs. Such studies should also consider the supplementation of PHs with Gln and Asn regarding the biostimulant properties demonstrated here. In that context new sourcing of raw materials rich in these two amino acids has to be discovered. One other issue of PHs study is the racemisation of amino acids and the role of enantiomeric forms (Cavani et al., 2003). In the case of Gln and Asn, our study nicely shows that both the L and D enantiomeric forms display biostimulating effects.

In conclusion our study shows stimulating effect on Arabidopsis only for Gln and Asn. We could not identify biostimulating effect for any other amino acids composing protein hydrolysates. Then, our study cannot explain the biostimulating effect of protein hydrolysates on plant growth by the property of only one of the individual amino acids from their formula. Nevertheless, our *in vitro* system and AAUE index offer a new tool to estimate quantitatively the biostimulating effects of any kind of compounds. It would be now of interest to test amino acid mixtures. How our experimental design and index can be adapted to different plant species is also an interesting development. It would elucidate the biostimulant × plant species interaction, which

is crucial for selecting the best combinations of amino acids depending on crops.

Data availability statement

The raw data supporting the conclusions of this article will be made available by the authors, without undue reservation.

Author contributions

ML: Conceptualization, Methodology, Formal analysis, Investigation, Writing – original draft. AM: Conceptualization, Methodology, Project administration, Validation, Writing – review & editing. NB-B: Writing – review & editing, Investigation. QC: Funding acquisition, Project administration, Supervision, Writing – review & editing, Conceptualization, Investigation, Methodology, Validation, Visualization. BB: Writing – review & editing, Funding acquisition, Project administration, Resources, Supervision. FC: Conceptualization, Funding acquisition, Investigation, Methodology, Project administration, Supervision, Validation, Visualization, Writing – review & editing, Formal analysis, Resources. CM-D: Conceptualization, Funding acquisition, Investigation, Methodology, Project administration, Supervision, Validation, Visualization, Writing – review & editing.

Funding

The author(s) declare financial support was received for the research, authorship, and/or publication of this article. This work has benefited from the support of IJPB's Plant Observatory technological platforms. The IJPB benefits from the support of Saclay Plant Sciences-SPS (ANR-17-EUR-0007).

Acknowledgments

We will thank you Luc Bachelet for technical assistance. This work has benefited from the support of IJPB's Plant Observatory technological platforms. The IJPB benefits from the support of Saclay Plant Sciences-SPS (ANR-17-EUR-0007).

Conflict of interest

Authors ML, QC, NB-B and BB are employed by NOVAEM.

The remaining authors declare that the research was conducted in the absence of any commercial or financial relationships that could be construed as a potential conflict of interest.

The author(s) declared that they were an editorial board member of Frontiers, at the time of submission. This had no impact on the peer review process and the final decision.

Publisher's note

Supplementary material

The Supplementary Material for this article can be found online at: https://www.frontiersin.org/articles/10.3389/fpls.2023.1281495/full#supplementary-material

References

Alboresi, A., Gestin, C., Leydecker, M. T., Bedu, M., Meyer, C., and Truong, H. N. (2005). Nitrate, a signal relieving seed dormancy in Arabidopsis. *Plant Cell Environ.* 28, 500–512. doi: 10.1111/j.13653040.2005.01292.x

Ambrosini, S., Sega, D., Santi, C., Zamboni, A., Varanini, Z., and Pandolfini, T. (2021). Evaluation of the potential use of a collagen-based protein hydrolysate as a plant multi-stress protectant. *Front. Plant Sci.* 12. doi: 10.3389/fpls.2021.600623

Baglieri, A., Cadili, V., Mozzetti Monterumici, C., Gennari, M., Tabasso, S., Montoneri, E., et al. (2014). Fertilization of bean plants with tomato plants hydrolysates. Effect on biomass production, chlorophyll content and N assimilation. *Sci. Hortic. (Amsterdam).* 176, 194–199. doi: 10.1016/j.scienta.2014.07.002

Billen, G., Garnier, J., and Lassaletta, L. (2013). The nitrogen cascade from agricultural soils to the sea: Modelling nitrogen transfers at regional watershed and global scales. *Philos. Trans. R. Soc B Biol. Sci.* 368. doi: 10.1098/rstb.2013.0123

Binder, S. (2010). Branched-chain amino acid metabolism in arabidopsis thaliana. *Arabidopsis book* 8, 1–14, e0137. doi: 10.1199/tab.0137

Bollard, E. G. (1966). A comparative study of the ability of organic nitrogenous compounds to serve as sole sources of nitrogen for the growth of plants. *Plant Soil* 25, 153–166. doi: 10.1007/BF01347815

Bonner, C. A., Rodrigues, A. M., Miller, J. A., and Jensen, R. A. (1992). Amino acids are general growth inhibitors of Nicotiana silvestris in tissue culture. *Physiol. Plant* 84, 319–328. doi: 10.1111/j.1399-3054.1992.tb04671.x

Calvo, P., Nelson, L., and Kloepper, J. W. (2014). Agricultural uses of plant biostimulants. *Plant Soil* 383, 3–41. doi: 10.1007/s11104-014-2131-8

Cavani, L., Ciavatta, C., and Gessa, C. (2003). Determination of free L- and D-alanine in hydrolysed protein fertilisers by capillary electrophoresis. *J. Chromatogr. A* 985, 463–469. doi: 10.1016/S0021-9673(02)01733-8

Cerdán, M., Sánchez-Sánchez, A., Jordá, J. D., Juárez, M., and Sánchez-Andreu, J. (2013). Effect of commercial amino acids on iron nutrition of tomato plants grown under lime-induced iron deficiency. *J. Plant Nutr. Soil Sci.* 176, 859–866. doi: 10.1002/jpln.201200525

Colla, G., Nardi, S., Cardarelli, M., Ertani, A., Lucini, L., Canaguier, R., et al. (2015). Protein hydrolysates as biostimulants in horticulture. *Sci. Hortic. (Amsterdam).* 196, 28–38. doi: 10.1016/j.scienta.2015.08.037

Colla, G., Rouphael, Y., Canaguier, R., Svecova, E., and Cardarelli, M. (2014). Biostimulant action of a plant-derived protein hydrolysate produced through enzymatic hydrolysis. *Front. Plant Sci.* 5. doi: 10.3389/fpls.2014.00448

Department of Economic and Social Affairs, P. D. (2022). *World population prospects 2022*. Available at: https://www.un.org/development/desa/pd/sites/www.un.org.development.desa.pd/files/wpp2022_summary_of_results.pdf (Accessed October 6, 2023).

du Jardin, P. (2015). Plant biostimulants: Definition, concept, main categories and regulation. *Sci. Hortic. (Amsterdam).* 196, 3–14. doi: 10.1016/j.scienta.2015.09.021

Ertani, A., Schiavon, M., Muscolo, A., and Nardi, S. (2013). Alfalfa plant-derived biostimulant stimulate short-term growth of salt stressed Zea mays L. plants. *Plant Soil* 364, 145–158. doi: 10.1007/s11104-012-1335-z

Estelle, M. A., and Somerville, C. (1987). Auxin-resistant mutants of Arabidopsis thaliana with an altered morphology. *Mol. Gen. Genet.* 206, 200–206. doi: doi : 10.1007/BF00333575

Forsum, O. (2016). On plant responses to D-amino acids. Features of growth, root behavior and selection for plant transformation [doctoral thesis] (Faculty of Forest Science Department of Forest Ecology and Management Umeå).

Forsum, O., Svennerstam, H., Ganeteg, U., and Näsholm, T. (2008). Capacities and constraints of amino acid utilization in *Arabidopsis*. *New Phytol.* 179, 1058–1069. doi: 10.1111/j.1469-8137.2008.02546.x

Gördes, D., Koch, G., Thurow, K., and Kolukisaoglu, Ü. (2013). Analyses of Arabidopsis ecotypes reveal metabolic diversity to convert D-amino acids. *Springerplus* 2, 1–11. doi: 10.1186/2193-1801-2-559

Gördes, D., Kolukisaoglu, Ü., and Thurow, K. (2011). Uptake and conversion of D-amino acids in Arabidopsis thaliana. *Amino Acids* 40, 553–563. doi: 10.1007/s00726-010-0674-4

Haroun, S. A., Shukry, W. M., and El-Sawy, O. (2010). Effect of asparagine or glutamine on growth and metabolic changes in phaseolus vulgaris under in *vitro* conditions. *Biosci. Res.* 7, 1–21.

Hassan, M. U., Islam, M. M., Wang, R., Guo, J., Luo, H., Chen, F., et al. (2020). Glutamine application promotes nitrogen and biomass accumulation in the shoot of seedlings of the maize hybrid ZD958. *Planta* 251, 1–15. doi: 10.1007/s00425-020-03363-9

Hildebrandt, T. M., Nunes Nesi, A., Araújo, W. L., and Braun, H. P. (2015). Amino acid catabolism in plants. *Mol. Plant* 8, 1563–1579. doi: 10.1016/j.molp.2015.09.005

Kocira, S. (2019). Effect of amino acid biostimulant on the yield and nutraceutical potential of soybean. *Chil. J. Agric. Res.* 79, 17–25. doi: 10.4067/S0718-58392019000100017

Lucini, L., Rouphael, Y., Cardarelli, M., Canaguier, R., Kumar, P., and Colla, G. (2015). The effect of a plant-derived biostimulant on metabolic profiling and crop performance of lettuce grown under saline conditions. *Sci. Hortic. (Amsterdam).* 182, 124–133. doi: 10.1016/j.scienta.2014.11.022

Maeda, H., and Dudareva, N. (2012). The shikimate pathway and aromatic amino acid biosynthesis in plants. *Annu. Rev. Plant Biol.* 63, 73–105. doi: 10.1146/annurev-arplant-042811-105439

Malécange, M., Pérez-Garcia, M. D., Citerne, S., Sergheraert, R., Lalande, J., Teulat, B., et al. (2022). Leafamine ®, a free amino acid-rich biostimulant, promotes growth performance of deficit-irrigated lettuce. *Int. J. Mol. Sci.* 23, 7338. doi: 10.33.90/ijms23137338

Näsholm, T., Kielland, K., and Ganeteg, U. (2009). Uptake of organic nitrogen by plants. *New Phytol.* 182, 31–48. doi: 10.1111/j.14698137.2008.02751.x

Paradiković, N., Vinković, T., Vinković Vrček, I., Žuntar, I., Bojić, M., and Medić-Šarić, M. (2011). Effect of natural biostimulants on yield and nutritional quality: An example of sweet yellow pepper (Capsicum annuum L.) plants. *J. Sci. Food Agric.* 91, 2146–2152. doi: 10.1002/jsfa.4431

Regulation EU (2019). Regulation of the european parliament and of the council laying down rules on the making available on the market of EU fertilising products and amending Regulations (EC) No 1069/2009 and (EC) No 1107/2009 and repealing Regulation (EC) No 2003/2003. *Off. J. Eur. Union* 2019, 114.

Rouphael, Y., Colla, G., Giordano, M., El-Nakhel, C., Kyriacou, M. C., and De Pascale, S. (2017). Foliar applications of a legume-derived protein hydrolysate elicit dose-dependent increases of growth, leaf mineral composition, yield and fruit quality in two greenhouse tomato cultivars. *Sci. Hortic. (Amsterdam).* 226, 353–360. doi: 10.1016/j.scienta.2017.09.007

Rouphael, Y., du Jardin, P., Brown, P., De Pascale, S., and Colla, G. (2020). *Biostimulants for sustainable crop production*. Cambridge: Burleigh dodds science publishing. doi: 10.1016/B978-0-323-85579-2.00004-6

Santi, C., Zamboni, A., Varanini, Z., and Pandolfini, T. (2017). Growth stimulatory effects and genome-wide transcriptional changes produced by protein hydrolysates in maize seedlings. *Front. Plant Sci.* 8. doi: 10.3389/fpls.2017.00433

Schiavon, M., Ertani, A., and Nardi, S. (2008). Effects of an alfalfa protein hydrolysate on the gene expression and activity of enzymes of the tricarboxylic acid (TCA) cycle and nitrogen metabolism in Zea mays L. *J. Agric. Food Chem.* 56, 11800–11808. doi: 10.1021/jf802362g

Searchinger, T., Hanson, C., Ranganathan, J., Lipinski, B., Waite, R., Winterbottom, R., et al. (2013). *"The great balancing act." Working paper, installment 1 of creating a sustainable food future* (Washington, DC: World Resources Institute). Available at: https://files.wri.org/d8/s3fs-public/great_balancing_act.pdf (Accessed October 6, 2023).

Sun, Y., Zhang, J., Wang, H., Wang, L., and Li, H. (2019). Identifying optimal water and nitrogen inputs for high efficiency and low environment impacts of a greenhouse summer cucumber with a model method. *Agric. Water Manage.* 212, 23–34. doi: 10.1016/j.agwat.2018.08.028

Tegeder, M. (2014). Transporters involved in source to sink partitioning of amino acids and ureides: Opportunities for crop improvement. *J. Exp. Bot.* 65, 1865–1878. doi: 10.1093/jxb/eru012

Tegeder, M., and Masclaux-Daubresse, C. (2018). Source and sink mechanisms of nitrogen transport and use. *New Phytol.* 217, 35–53. doi: 10.1111/nph.14876

Tegeder, M., and Rentsch, D. (2010). Uptake and partitioning of amino acids and peptides. *Mol. Plant* 3, 997–1011. doi: 10.1093/mp/ssq047

Xing, A., and Last, R. L. (2017). A regulatory hierarchy of the arabidopsis branched-chain amino acid metabolic network. *Plant Cell* 29, 1480–1499. doi: 10.1105/tpc.17.00186

Xu, L., and Geelen, D. (2018). Developing biostimulants from agro-food and industrial by-products. *Front. Plant Sci.* 871. doi: 10.3389/fpls.2018.01567

Yang, H., and Ludewig, U. (2014). Lysine catabolism, amino acid transport, and systemic acquired resistance: What is the link? *Plant Signal. Behav.* 9. doi: 10.4161/psb.28933

Yang, G., Wei, Q., Huang, H., and Xia, J. (2020). Amino acid transporters in plant cells. *Plants* 9, 967. doi: 10.3390/plants9080967

Yao, X., Nie, J., Bai, R., and Sui, X. (2020). Amino acid transporters in plants: Identification and function. *Plants* 9, 1–17. doi: 10.3390/plants9080972

Zhao, Y. (2010). Auxin biosynthesis and its role in plant development. *Annu. Rev. Plant Biol.* 61, 49–64. doi: 10.1146/annurev-arplant-042809-112308

Frontiers in
Plant Science

Cultivates the science of plant biology and its applications

The most cited plant science journal, which advances our understanding of plant biology for sustainable food security, functional ecosystems and human health.

Discover the latest Research Topics

See more →

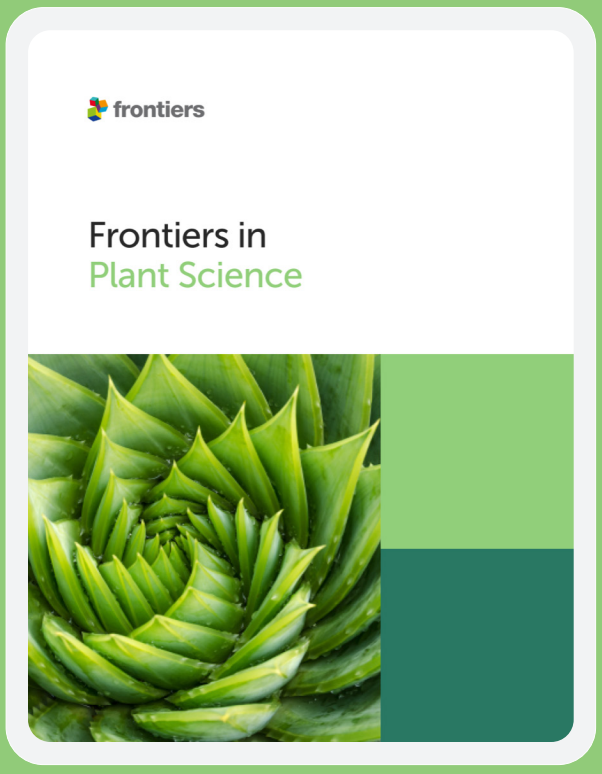

Frontiers

Avenue du Tribunal-Fédéral 34
1005 Lausanne, Switzerland
frontiersin.org

Contact us

+41 (0)21 510 17 00
frontiersin.org/about/contact